

Cell Press Selections

Reprint Compendium

Immune Checkpoints in Cancer Therapy

How Co-receptors Shape the Immune Response to Cancer

CellPress
www.cell.com

CPSIMUNECAN2018

BETHYL
LABORATORIES, INC
Improving Lives by Supporting Scientific Discovery

Light your way.

Get the full picture with trusted tumor immune response results from our in-house validated antibodies.

When it comes to your tumor immune response research, blind spots are unacceptable. Independent testing has demonstrated that 75% of antibodies in today's market are non-specific or simply do not work at all.* But at Bethyl, we've manufactured and validated every antibody we make on site to ensure target specificity and sensitivity. All to guarantee our antibodies will function as designed in your assay 100% of the time. More than 10,000 independent citations over the past 15 years have proven that, at Bethyl, we put a lot in every drop.

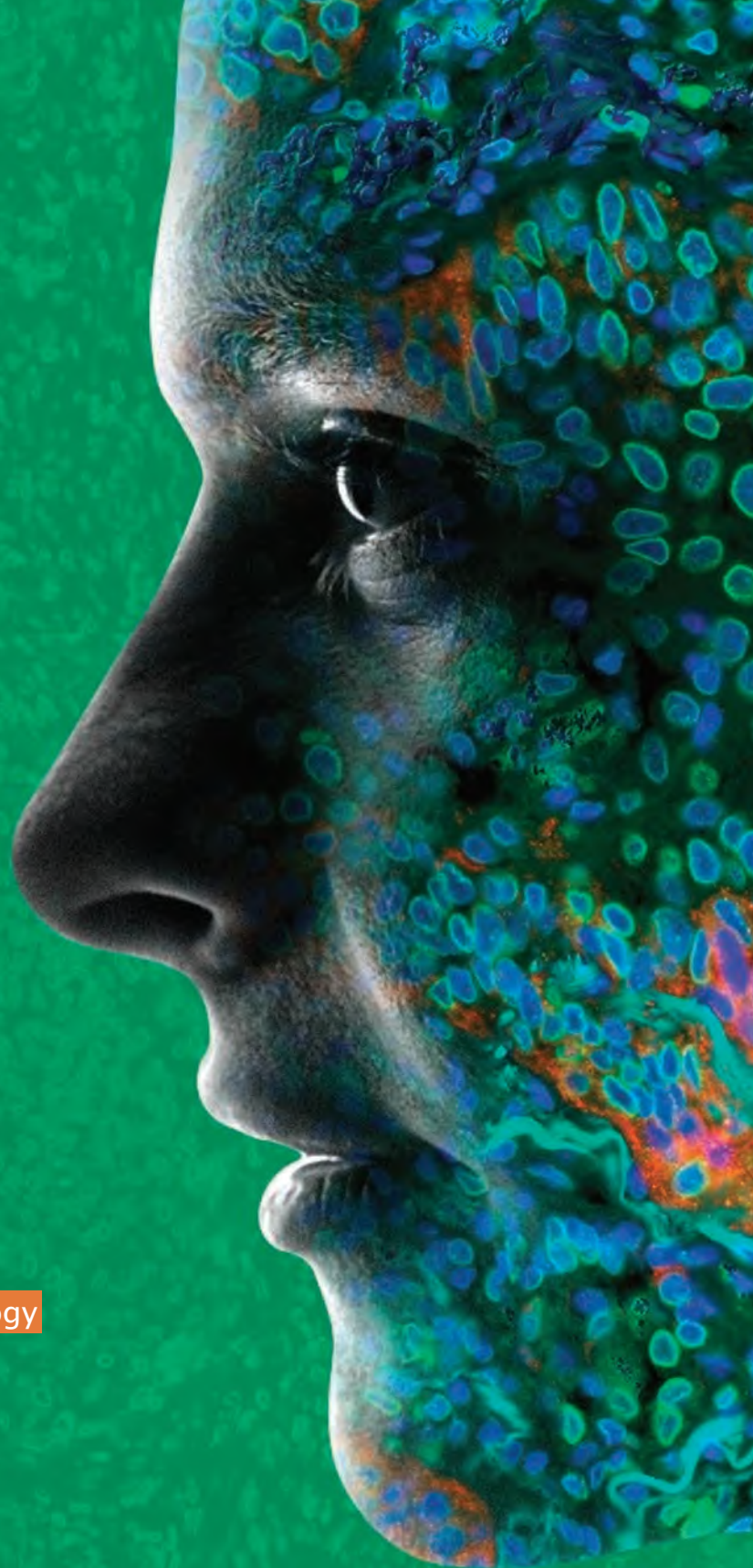
See our data at bethyl.com/immuno-oncology

**Weller, MG, Analytical Chemistry Insights:11, 21-27 (2016).*

Antibodies shown: Rabbit anti-PD-L1 (red, A700-020) & Lamin-A/C (green, A303-430A) in FFPE lung.
©2018 Bethyl Laboratories, Inc. All rights reserved.

BETHYL
LABORATORIES, INC

Really Good Antibodies



ARE YOUR ANTIBODIES WORKING HARD, OR HARDLY WORKING?

75%

OF MANUFACTURED
ANTIBODIES ARE
NON-SPECIFIC OR DID
NOT WORK AT ALL*

\$350

MILLION

IS WASTED ANNUALLY ON
BIOMEDICAL RESEARCH
BECAUSE POOR QUALITY
MATERIALS LEAD TO
FALSE RESULTS**



EVERY ANTIBODY THAT
BETHYL SELLS IS
MANUFACTURED TO
EXACTING STANDARDS
ON SITE IN
MONTGOMERY, TX



QUALIFIED
ANTIBODIES
MADE IN THE USA
VALIDATED IN THE USA

TARGETING OVER

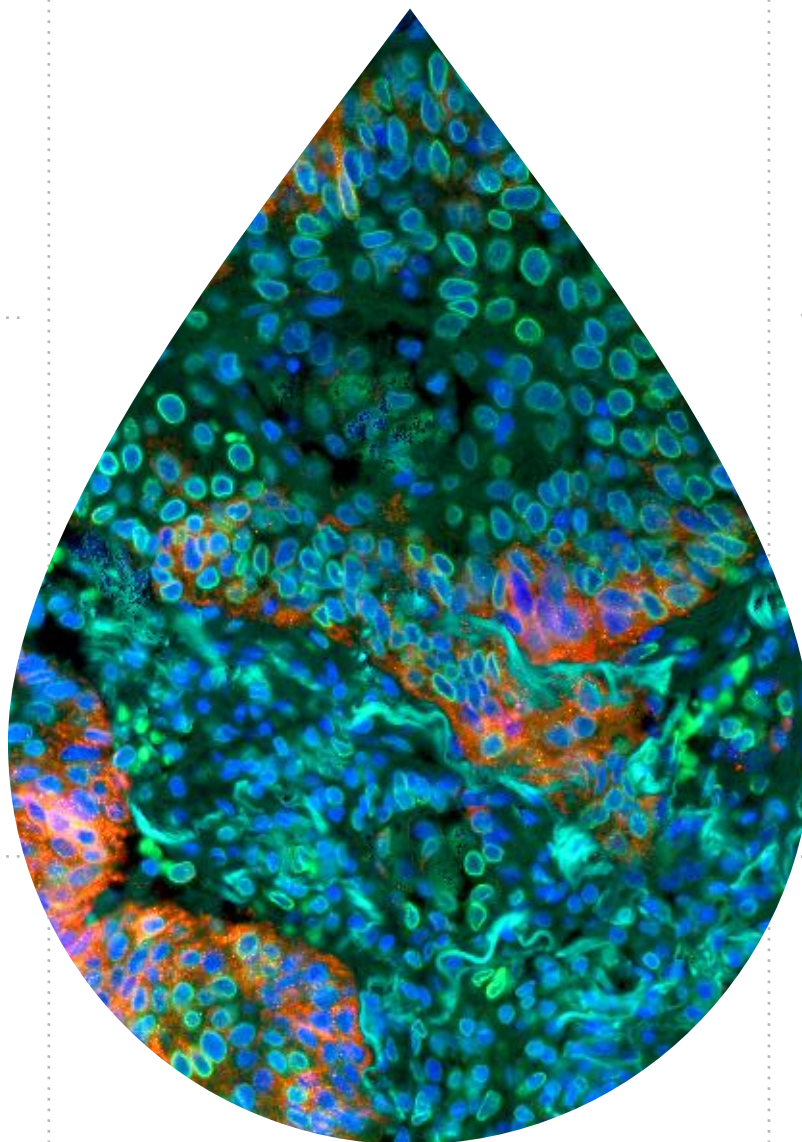
3,300

PROTEINS AND 1,300
SECONDARY ANTIBODIES

40+

YEARS OF
EXPERIENCE

OF CATALOG &
CUSTOM ANTIBODY
PRODUCTION SERVICES



Bethyl is dedicated to improving lives by supporting scientific discovery through its qualified polyclonal and recombinant rabbit monoclonal antibody products and ELISA kits. Our antibodies have been manufactured and validated on-site by our scientists to ensure target specificity and sensitivity. If a product doesn't meet our standards, it doesn't leave our facility and every antibody sold is backed with a 100% guarantee to provide confidence in your results. We put a lot in every drop.

BETHYL
LABORATORIES, INC

Really Good Antibodies

FIND OUT MORE AT [BETHYL.COM/VALIDATION](https://www.bethyl.com/validation)

Ignite your breakthrough.

Ensure reproducible results with antibodies that are 100% guaranteed to work.

Every great discovery requires a bold approach and reliable tools. With each cell-labeling experiment, you can trust in our more than 40 years of experience in antibody manufacturing and on site validation. You need antibodies with performance that exceeds the 50% failure rate common in the industry.* That's why, from polyclonals to recombinant rabbit monoclonal abs, we guarantee 100% target specificity and sensitivity to help you continue moving toward your next breakthrough. Our antibodies have been trusted in over 10,000 independent citations in the last 15 years. Because at Bethyl, we put a lot in every drop.

See our data at bethyl.com/breakthrough

**Weller, MG, Analytical Chemistry Insights:11, 21-27 (2016).*

Antibodies shown: Rabbit anti-CD3e recombinant monoclonal (yellow, A700-016) & mouse anti-CD23 monoclonal (red, A500-017A) in FFPE lymphnode.
©2018 Bethyl Laboratories, Inc. All rights reserved.

BETHYL
LABORATORIES, INC

Really Good Antibodies



Foreword

The success of immune checkpoint blockade therapies in the treatment of multiple types of cancers has changed the way we treat cancer and how we think about the immune response to tumors. These therapies are built on basic research that has identified co-receptors on T cells and defined their functional impact in the immune response. Basic and clinical research in this area has advanced in lockstep, with observations in the clinic informing basic research and findings in the lab guiding new therapeutic approaches. The reviews and research in this *Cell Press Selection* offer a snapshot of the latest advances in this rapidly evolving field.

Despite the promise of immune checkpoint blockade therapies in the treatment of cancer, there is a great need to better understand the mechanisms underlying an effective response and resistance—both primary and emerging—in response to therapy. Studies in both model organisms and human patients are now shedding light on the cellular players that enable a productive response, as well as those cells and pathways that facilitate immune suppression. This, in turn, is guiding combination therapy approaches aimed at potentiating the effects of immune checkpoint blockade. Moreover, it's becoming clear that much remains to be explored in terms of co-receptors, both co-stimulatory and co-inhibitory, that can be targeted for immunotherapy. The articles compiled in this reprint collection showcase the current progress in these areas: from genomic and proteomic approaches that are providing a view into the responses to checkpoint blockade therapies to mechanistic studies that are defining the biochemical pathways that mediate an active response or resistance.

These articles represent only a small portion of the exciting research Cell Press has published on immune checkpoint blockade approaches and the basic biology underlying how these therapies impact the anti-tumor immune response. We hope you'll visit www.cell.com on a regular basis to keep up with the latest cancer biology and tumor immunology news.

Finally, we are grateful for the support of Bethyl Labs, who made the publication of this collection possible.

Fabiola Rivas
Senior Scientific Editor, *Immunity*

For more information about Cell Press Selections:
Gordon Sheffield
Program Director, Cell Press Selections
g.sheffield@cell.com
617-386-2189



Set your sights ablaze.

Track groundbreaking proteins with our in-house validated custom & contract antibodies.

Your discoveries are crucial to blazing new trails. That's why our custom and contract production antibody services are held to rigorous standards to ensure reliable results. We validate all custom and contract recombinant rabbit monoclonal antibodies in-house to ensure that they will work in your desired application. It's about providing you with the affinity and consistency necessary to generate a more trustworthy and complete tumor immune response result without extra work. At Bethyl, we put a lot in every drop.

Is a partnership with Bethyl right for you?
Learn more at bethyl.com/customabs

Antibodies shown: Rabbit anti-recombinant monoclonal BRD4 (yellow, A700-004) & mouse anti-Cytokeratin monoclonal (red, A500-019A) in FFPE gastric carcinoma.
©2018 Bethyl Laboratories, Inc. All rights reserved.

Immune Checkpoints in Cancer Therapy

How Co-receptors Shape the Immune Response to Cancer

Reviews

Coinhibitory Pathways in the B7-CD28 Ligand-Receptor Family

Frank A. Schildberg, Sarah R. Klein, Gordon J. Freeman, and Arlene H. Sharpe

Lag-3, Tim-3, and TIGIT: Co-inhibitory Receptors with Specialized Functions in Immune Regulation

Ana C. Anderson, Nicole Joller, and Vijay K. Kuchroo

Primary, Adaptive, and Acquired Resistance to Cancer Immunotherapy

Padmanee Sharma, Siwen Hu-Lieskovan, Jennifer A. Wargo, and Antoni Ribas

Reports and Articles

Fc-Optimized Anti-CD25 Depletes Tumor-Infiltrating Regulatory T Cells and Synergizes with PD-1 Blockade to Eradicate Established Tumors

Frederick Arce Vargas, Andrew J.S. Furness, Isabelle Solomon, Kroopa Joshi, Lella Mekkaoui, Marta H. Lesko, Enrique Miranda Rota, Rony Dahan, Andrew Georgiou, Anna Sledzinska, Assma Ben Aissa, Dafne Franz, Mariana Werner Sunderland, Yien Ning Sophia Wong, Jake Y. Henry, Tim O'Brien, David Nicol, Ben Challacombe, Stephen A. Beers, Melanoma TRACERx Consortium, Renal TRACERx Consortium, Lung TRACERx Consortium, Samra Turajlic, Martin Gore, James Larkin, Charles Swanton, Kerry A. Chester, Martin Pule, Jeffrey V. Ravetch, Teresa Marafioti, Karl S. Peggs, and Sergio A. Quezada

Immunogenic Chemotherapy Sensitizes Tumors to Checkpoint Blockade Therapy

Christina Pfirschke, Camilla Engblom, Steffen Rickelt, Virna Cortez-Retamozo, Christopher Garris, Ferdinando Pucci, Takahiro Yamazaki, Vichnou Poirier-Colame, Andita Newton, Younes Redouane, Yi-Jang Lin, Gregory Wojtkiewicz, Yoshiko Iwamoto, Mari Mino-Kenudson, Tiffany G. Huynh, Richard O. Hynes, Gordon J. Freeman, Guido Kroemer, Laurence Zitvogel, Ralph Weissleder, and Mikael J. Pittet

Facilitating T Cell Infiltration in Tumor Microenvironment Overcomes Resistance to PD-L1 Blockade

Haidong Tang, Yang Wang, Lukasz K. Chlewicki, Yuan Zhang, Jingya Guo, Wei Liang, Jieyi Wang, Xiaoxiao Wang, and Yang-Xin Fu

(continued on next page)

Oncogenic RAS Signaling Promotes Tumor Immuno-resistance by Stabilizing PD-L1 mRNA

Matthew A. Coelho, Sophie de Carné Trécesson, Sareena Rana, Davide Zecchin, Christopher Moore, Miriam Molina-Arcas, Philip East, Bradley Spencer-Dene, Emma Nye, Karin Barnouin, Ambrosius P. Snijders, Wi S. Lai, Perry J. Blackshear, and Julian Downward

Distinct Cellular Mechanisms Underlie Anti-CTLA-4 and Anti-PD-1 Checkpoint Blockade

Spencer C. Wei, Jacob H. Levine, Alexandria P. Cogdill, Yang Zhao, Nana-Ama A.S. Anang, Miles C. Andrews, Padmanee Sharma, Jing Wang, Jennifer A. Wargo, Dana Pe'er, and James P. Allison

Tumor and Microenvironment Evolution during Immunotherapy with Nivolumab

Nadeem Riaz, Jonathan J. Havel, Vladimir Makarov, Alexis Desrichard, Walter J. Urba, Jennifer S. Sims, F. Stephen Hodi, Salvador Martín-Algarra, Rajarsi Mandal, William H. Sharfman, Shailender Bhatia, Wen-Jen Hwu, Thomas F. Gajewski, Craig L. Slingluff, Jr., Diego Chowell, Sviatoslav M. Kendall, Han Chang, Rachna Shah, Fengshen Kuo, Luc G.T. Morris, John-William Sidhom, Jonathan P. Schneck, Christine E. Horak, Nils Weinhold, and Timothy A. Chan

Inactivation of Interferon Receptor Promotes the Establishment of Immune Privileged Tumor Microenvironment

Kanstantsin V. Katlinski, Jun Gui, Yuliya V. Katlinskaya, Angelica Ortiz, Riddhita Chakraborty, Sabyasachi Bhattacharya, Christopher J. Carbone, Daniel P. Beiting, Melanie A. Gironde, Amy R. Peck, Ellen Puré, Priya Chatterji, Anil K. Rustgi, J. Alan Diehl, Constantinos Koumenis, Hallgeir Rui, and Serge Y. Fuchs



On the cover: Immune checkpoint blockade therapies have revolutionized cancer treatment. These therapies target co-receptors on T cells, halting pathways that would normally function to suppress an ongoing immune response and mediate the return to homeostasis. In cancer, however, these pathways inhibit potentially curative anti-tumor immune responses. The cover image depicts these pathways as falling dominoes, with a hand actively blocking the progression of the domino cascade. Image by Oatawa/iStock. Cover design by Yvonne Blanco.



Make your big idea bright.

Use our bulk antibody manufacturing & processing services to deliver consistent results on a larger scale.

When your ideas are big, it's important that your antibodies consistently perform. For more than 40 years, we've focused on manufacturing high quality antibodies in bulk. From antiserum generation to large-scale conjugation, preparative work to the final product, you can count on our big bulk capabilities to elevate big discoveries. At Bethyl, we put a lot in every drop.

Find your reliable bulk partner
at [bethyl.com/bulkabs](https://www.bethyl.com/bulkabs)

Antibody shown: Rabbit anti-KIF14 (IHC-00475)
in formaldehyde-fixed HeLa cells.
©2018 Bethyl Laboratories, Inc. All rights reserved.

Go figure

With author-narrated animations



Introducing Figure360, an author-narrated animation of select figures in Cell Press primary research and review journals.

A short, digestible synopsis puts the figure in context and helps you zoom in on the most important take-home message in a matter of minutes. Why go it alone when the author can help you figure it out in less than half the time?

Check it out at www.cell.com/figure360

Figure360

CellPress

Coinhibitory Pathways in the B7-CD28 Ligand-Receptor Family

Frank A. Schildberg,¹ Sarah R. Klein,² Gordon J. Freeman,² and Arlene H. Sharpe^{1,*}

¹Department of Microbiology and Immunobiology, and Evergrande Center for Immunologic Diseases, Harvard Medical School, Boston, MA 02115, USA

²Department of Medical Oncology, Dana-Farber Cancer Institute, Harvard Medical School, Boston, MA 02115, USA

*Correspondence: arlene_sharpe@hms.harvard.edu

<http://dx.doi.org/10.1016/j.immuni.2016.05.002>

Immune responses need to be controlled for optimal protective immunity and tolerance. Coinhibitory pathways in the B7-CD28 family provide critical inhibitory signals that regulate immune homeostasis and defense and protect tissue integrity. These coinhibitory signals limit the strength and duration of immune responses, thereby curbing immune-mediated tissue damage, regulating resolution of inflammation, and maintaining tolerance to prevent autoimmunity. Tumors and microbes that cause chronic infections can exploit these coinhibitory pathways to establish an immunosuppressive microenvironment, hindering their eradication. Advances in understanding T cell coinhibitory pathways have stimulated a new era of immunotherapy with effective drugs to treat cancer, autoimmune and infectious diseases, and transplant rejection. In this review we discuss the current knowledge of the mechanisms underlying the coinhibitory functions of pathways in the B7-CD28 family, the diverse functional consequences of these inhibitory signals on immune responses, and the overlapping and unique functions of these key immunoregulatory pathways.

Introduction

The immune system is capable of defending against diverse microbial pathogens and early malignant cells, yet maintains tolerance to self. T cell costimulation plays a pivotal role in this exquisite regulation of immune responses to promote protective immunity and prevent autoimmunity. Our understanding of costimulation has evolved substantially from the two-signal model proposed by Lafferty and Cunningham to explain the activation of naive T cells (Bretscher and Cohn, 1970; Cunningham and Lafferty, 1977; Lafferty and Cunningham, 1975). Although T cell costimulatory pathways were envisioned as stimulators of T cell responses, it is now clear that there are both stimulatory (costimulatory) and inhibitory (coinhibitory) second signals that modulate T cell receptor (TCR)-mediated T cell activation. The “co-” in coinhibitory and costimulatory refers to how these antigen-independent second signals modify the first signal, provided by interaction of antigenic peptide-MHC complex with the TCR, which confers specificity to the response. Furthermore, although T cell costimulation was envisaged to control initial activation of naive T cells, T cell costimulatory and coinhibitory pathways have much broader immunoregulatory functions, controlling effector, memory, and regulatory T cells, as well as naive T cells. These pathways are key regulators of T cell activation, tolerance, and T cell exhaustion, and therapeutic modulation of costimulatory and coinhibitory pathways is translating to effective new strategies for treating cancer, autoimmune and infectious diseases, and transplant rejection.

We now know a large number of costimulatory and coinhibitory pathways. The first costimulatory receptor CD28 and the first coinhibitory receptor CTLA-4 and their shared ligands CD80 (B7-1) and CD86 (B7-2) constitute the best-characterized pathway, which serves as a paradigm for other costimulatory (see also Esensten et al., 2016, this issue) and coinhibitory pathways. These pathways fall into two major families: the Ig

superfamily, which includes the B7-CD28, TIM, and CD226-TIGIT-CD96 (see Anderson et al., 2016, this issue) families as well as LAG-3, and the TNF-TNF receptor superfamily (see Ward-Kavanagh et al., 2016, this issue). Reviews in this special issue of *Immunity* discuss the functions of costimulatory and coinhibitory pathways within all of these families. These articles review the current understanding of costimulation on the fundamental level and discuss the roles of these pathways in the pathogenesis of autoimmunity (Zhang and Vignali, 2016, this issue), graft rejection (Ford, 2016, this issue), cancer (Callahan et al., 2016, this issue), and infectious diseases (Attanasio and Wherry, 2016, this issue), as well as the therapeutic opportunities and challenges of targeting these costimulatory and coinhibitory pathways.

In this review we will focus on recent advances in our understanding of coinhibitory pathways in the B7-CD28 family (Figure 1). We first will discuss the current understanding of the mechanisms underlying the coinhibitory effects of the two most clinically relevant pathways thus far, the PD-1 and CTLA-4 pathways. Next, we will review other inhibitory pathways in the B7-CD28 family. We then will consider overlapping and unique functions of these pathways. Finally, we will discuss how this progress is changing our view of the functions of T cell costimulation and important areas for future inquiry.

Cytotoxic T Lymphocyte-Associated Antigen-4 CTLA-4 Gene Structure, Splice Variants, and Polymorphisms

The CD28 family shares a common protein architecture of a single extracellular IgV, stalk, transmembrane (TM), and a cytoplasmic domain with one or more tyrosine signaling motifs. The core of the CD28 gene family is composed of CD28, cytotoxic T lymphocyte-associated antigen-4 (CTLA-4, also known as CD152), and ICOS, which share a cysteine in the stalk region

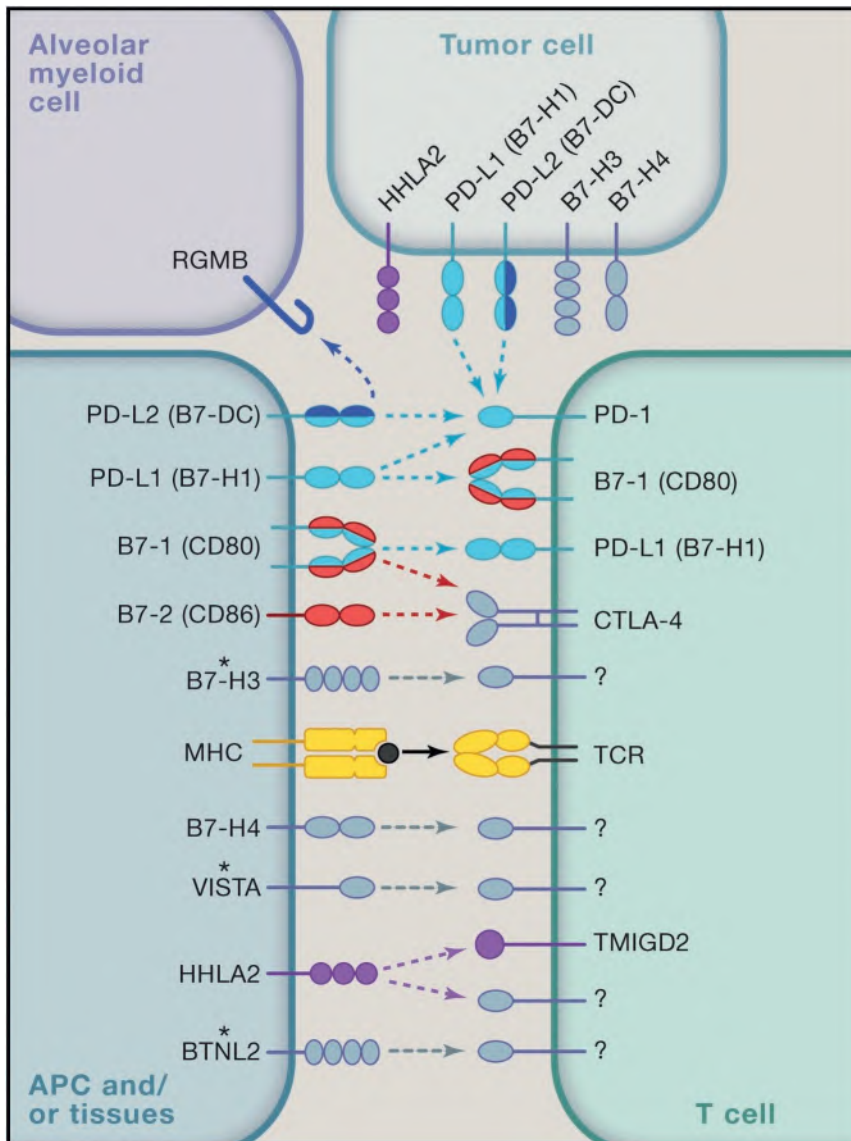


Figure 1. Coinhibitory Pathways in the B7-CD28 Family

T cell activation is initiated by recognition of peptide antigens presented by APCs to the TCR-CD3 complex and T cell costimulatory signals provided by CD28 interactions with CD80 and CD86. Upon T cell activation, many coinhibitory pathways are upregulated and can attenuate TCR and costimulatory signals. Coinhibitory pathways in the B7-CD28 family control responses of naive, effector, regulatory, memory, and exhausted T cells. These receptors are expressed on T cells and some are also expressed on other hematopoietic cells, as described in the text. Their ligands can be expressed on APCs, non-hematopoietic cells, and in tumors; some molecules are expressed on both APCs and T cells (indicated by asterisk). Binding partners for B7-H3, B7-H4, VISTA, and BTNL2 have not yet been identified.

gene can undergo alternative splicing, and four splice variants of CTLA-4 have been described. Full-length mRNA (fICTLA-4) has all four exons and possesses an extracellular IgV-like domain that contains the MYPPPY motif involved in binding B7-1 or B7-2, a TM, and a cytoplasmic tail (Brunet et al., 1987; Daria-vach et al., 1988; Lindsten et al., 1993; Linsley et al., 1995; Metzler et al., 1997; Ostrov et al., 2000). The soluble CTLA-4 (sCTLA-4) transcript lacks the TM region due to splicing out of exon 3 (Magistrelli et al., 1999), and a transcript encoding only exons 1 and 4 lacks the ligand binding and TM domains (1/4CTLA-4) (Brunet et al., 1987; Magistrelli et al., 1999; Oaks et al., 2000; Ueda et al., 2003; Vijayakrishnan et al., 2004). fICTLA-4 is upregulated quickly after T cell activation and becomes the predominant transcript, whereas expression of sCTLA-4 has been detected mainly in resting T cells, with mRNA levels similar to those of fICTLA-4

that mediates homodimerization and a ligand binding site with an FG loop containing a PPP motif in *cis-trans-cis* configuration that gives the geometric complementarity for B7 ligand binding. The inhibitory receptor CTLA-4 is a structural homolog of the costimulatory receptor CD28 and shares with CD28 the same binding partners B7-1 (CD80) and B7-2 (CD86), but binds with greater avidity and affinity (Collins et al., 2002). CTLA-4 is a covalent homodimer (Lindsten et al., 1993; Linsley et al., 1995); its higher avidity for B7 ligands results from the binding of each CTLA-4 homodimer to two divalent B7 molecules, leading to the formation of a stable CTLA-4-B7 structure on the cell surface. This contrasts with the monovalent binding of B7 molecules by CD28.

Highly conserved across species, *Ctla4* consists of four exons: exon 1 encodes the signal peptide sequence; exon 2, an IgV-like domain comprising the B7 binding domain; exon 3, the TM region; and exon 4, the cytoplasmic tail. The CTLA-4

(Magistrelli et al., 1999; Oaks et al., 2000; Pérez-García et al., 2013; Ueda et al., 2003; Wicker et al., 2004). It is thought that sCTLA-4 plays an inhibitory role in regulatory T (Treg) cell function (Gerold et al., 2011; Oaks et al., 2000), and sCTLA-4 polymorphisms have been implicated in human autoimmune diseases including familial Grave's disease, type 1 diabetes, and Hashimoto's thyroiditis. Genetic overexpression of the 1/4CTLA-4 transcript shows that this isoform can promote T cell activation and autoimmunity *in vivo* (Liu et al., 2012). The fourth CTLA-4 transcript, ligand-independent CTLA-4 (liCTLA-4), lacks exon 2 and thus the ligand binding domain (Ueda et al., 2003; Vijayakrishnan et al., 2004). The liCTLA-4 isoform has a potent inhibitory function in mice but has not yet been found in humans (Araki et al., 2009; Vijayakrishnan et al., 2004). Recent studies also found a gene fusion between *CTLA4* and *CD28* that occurs in T cell lymphomas. The fusion gene consists of the extracellular domain of CTLA-4 and the intracellular

Table 1. Comparison of CD28 and CD28-like Receptors

	Percent Identity (with CD28 Extracellular Domain)	Chromosome		Structure		Expression	
		Human	Mouse	Ligand- Binding Motif	Cytoplasmic Tyrosine Signaling Motifs	Cell Type	Ligand
CD28	100%	2q33.2	1qC2	MYPPPY	PI3K motif, PP2A	T, plasma cell, NK, NKT	B7-1, B7-2, ICOSL (only human)
CTLA-4 (CD152)	26.9%	2q33.2	1qC2	MYPPPY	PI3K motif, PP2A, SHP2, PKC- η	T, B, NK, NKT, DC	B7-1, B7-2
ICOS (CD278)	24.1%	2q33.2	1qC2	FDPPPF	PI3K	T, B (only human)	ICOSL
PD-1 (CD279)	15.6%	2q37.3	1qD		ITIM, ITSM, SHP1, SHP2	T, B, NK, NKT, DC, myeloid	PD-L1, PD-L2
TMIGD2 (IGPR1)	22.8%	19p13.3	absent		Y192 and Y222	only human: T, APC	HHLA2

domain of CD28, transforming inhibitory signals into stimulatory signals (Sekulic et al., 2015; Ungewickell et al., 2015; Yoo et al., 2016).

Polymorphisms in *CTLA4* are associated with human autoimmune diseases (Scalapino and Daikh, 2008), consistent with the critical role of CTLA-4 inhibitory signals in tolerance. The rapid development in *Ctla4*^{-/-} mice of a fatal multi-organ inflammatory disease (Linsley et al., 1991; Tivol et al., 1995; Waterhouse et al., 1995) within 2–4 weeks after birth resembled systemic autoimmune disease and first demonstrated the key role of CTLA-4 in tolerance. Similarly, severe immune dysregulation occurs in people heterozygous for mutations that result in reduced CTLA-4 mRNA and protein levels (Kuehn et al., 2014). Several SNPs have been identified in the regulatory or promoter and signal sequence regions of human CTLA-4 (Deichmann et al., 1996; Donner et al., 1997; Kristiansen et al., 2000; Nisticò et al., 1996; Wang et al., 2002b). The polymorphism at A49G is the only polymorphism that changes the primary amino acid sequence of CTLA-4. In vitro studies of A49G CTLA-4 have shown that this variant is aberrantly processed in the endoplasmic reticulum, leading to reduced surface expression (Anjos et al., 2002). Different polymorphisms can favor particular splice variants, which are associated with autoimmunity. In mice, the expression of liCTLA-4 depends on a SNP at base 77 of exon 2 and affects diabetes susceptibility in NOD mice. In humans, autoimmunity is associated with two SNPs (CT60 and +49G>A) that both favor the generation of sCTLA-4 over the full-length protein (Ueda et al., 2003; Wang et al., 2012b). In summary, CTLA-4 polymorphisms can regulate autoimmunity in several ways, leading to altered expression of different CTLA-4 transcripts and/or changes in CTLA-4 expression levels, which might affect CTLA-4 intracellular trafficking, surface expression, dimerization, or additional functions. Further work is required to determine how CTLA-4 polymorphisms affect CTLA-4 function and T cell responses.

Regulation of CTLA-4 Expression

CTLA-4 is induced after activation on CD4⁺Foxp3⁻ and CD8⁺Foxp3⁻ conventional T cells (Freeman et al., 1992; Linsley et al., 1992; Walunas et al., 1996) but is constitutively expressed by CD4⁺Foxp3⁺ Treg cells (Harper et al., 1991; Lindsten et al., 1993; Takahashi et al., 2000). Notably, CTLA-4 expression is not restricted to T cells. CTLA-4 expression also has been reported in B cells, dendritic cells (DCs), monocytes, granulocytes, CD34⁺ stem cells, placental fibroblasts, mouse embryonic cells,

pituitary gland, and embryoid bodies (Table 1; Kaufman et al., 1999; Ling et al., 1998; Pioli et al., 2000; Pistillo et al., 2003; Wang et al., 2002a).

CTLA-4 expression is regulated transcriptionally and post-transcriptionally. Foxp3 and NFAT are two important transcriptional regulators of *Ctla4* (Finn et al., 1997; Gibson et al., 2007; Miller et al., 2002; Wu et al., 2006; Zheng et al., 2007). Post-transcriptionally, the stability and translational efficiency of CTLA-4 mRNA (Finn et al., 1997) are defined through the 3' UTR (Malquori et al., 2008). Also, microRNAs (miR-145 and miR-155) regulate expression of CTLA-4. Alterations in expression of microRNAs or variations in the 3' UTR region, which are responsible for differential binding of several microRNAs, correlate with autoimmune diseases (de Jong et al., 2013; Sonkoly et al., 2010).

The localization of CTLA-4 protein is dynamically regulated within T cells depending on the tyrosine phosphorylation status of its cytoplasmic domain (Figure 2A). Only a small proportion of CTLA-4 can be detected on the cell surface of resting T cells; the majority of CTLA-4 molecules are localized in the intracellular compartments of perinuclear Golgi vesicles, endosomes, and lysosomes (Alegre et al., 1996; Iida et al., 2000; Linsley et al., 1996; Schneider et al., 1999), and cycle continuously to the cell surface, followed by rapid internalization of CTLA-4 molecules with unphosphorylated cytoplasmic domains and either recycling to the plasma membrane or lysosomal degradation (Qureshi et al., 2012). CTLA-4 intracellular trafficking is mediated in part by the association of the CTLA-4 cytoplasmic domain with clathrin-associated adaptor proteins AP-1 and AP-2, which are involved in the selective recognition and recruitment of proteins into coated pits (Kristiansen et al., 2000; Schneider et al., 1999; Ueda et al., 2003). CTLA-4 internalization is regulated by the opposing effects of phosphorylation and clathrin adaptor protein-2 (AP-2) binding. The unphosphorylated CTLA-4 cytoplasmic domain binds to AP-2, which promotes rapid internalization, whereas tyrosine phosphorylation of the CTLA-4 cytoplasmic domain delays internalization. Association of CTLA-4 with adaptor protein-1 (AP-1) mediates shuttling from the trans golgi network (TGN) to lysosomal compartments for degradation, a mechanism that controls the overall abundance of CTLA-4 in the TGN. Upon T cell activation, CTLA-4-containing endosomes are recycled to the cell surface, which is regulated by lipopolysaccharide-responsive and beige-like anchor protein (LRBA). A recent study has shown that mutations in the LRBA

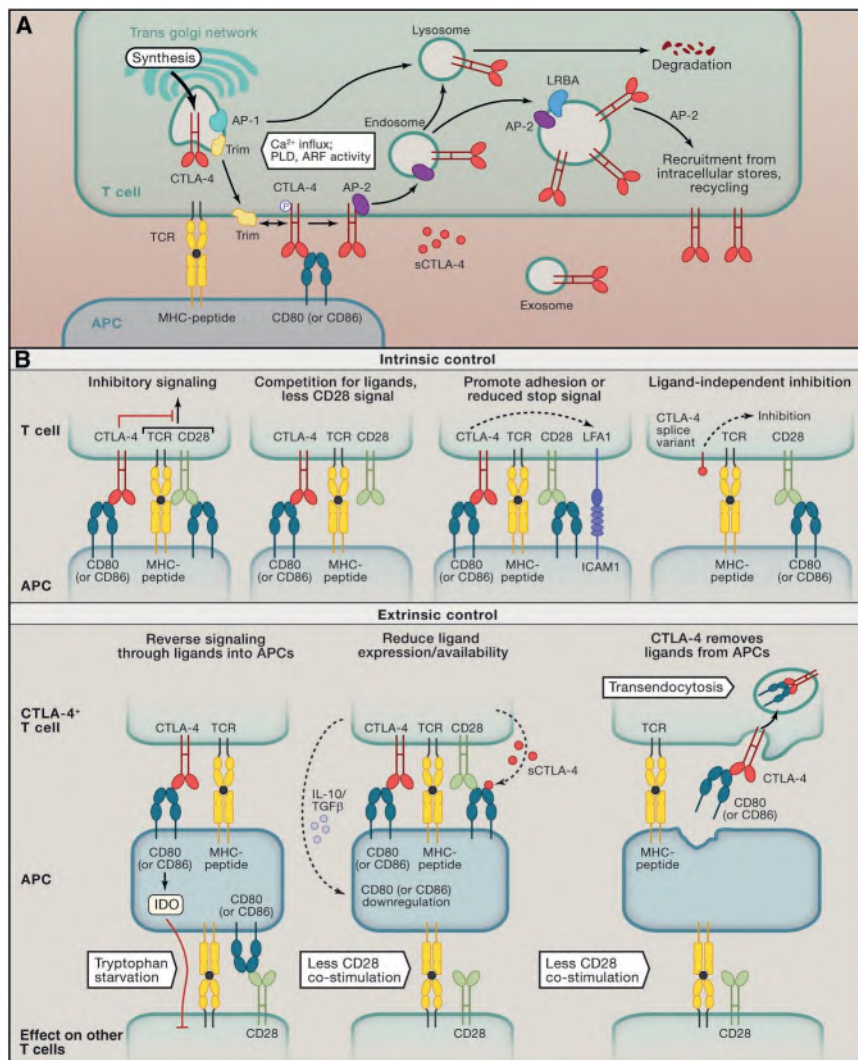


Figure 2. Regulation of CTLA-4 Expression and Functional Effects of CTLA-4

(A) Dynamics of CTLA-4 expression and membrane cycling. After synthesis in the trans Golgi network (TGN), CTLA-4 binds to T cell receptor-interacting molecule (TRIM), promoting formation of CTLA-4-containing vesicles. TCR signaling-mediated calcium influx induces CTLA-4 release from the vesicles to the cell surface, and CTLA-4 and TRIM no longer associate. CTLA-4 externalization also depends on phospholipase D (PLD) and GTPase adenosine diphosphate ribosylation factor 1 (ARF-1). Unphosphorylated CTLA-4 cytoplasmic domain binds to the clathrin adaptor protein 2 (AP-2), which promotes rapid internalization to endosomes and lysosomes. Tyrosine phosphorylation of the CTLA-4 cytoplasmic domain retards internalization. Upon T cell activation, CTLA-4-containing endosomes are recycled to the cell surface; this is regulated by lipopolysaccharide-responsive and beige-like anchor protein (LRBA). Association of CTLA-4 with adaptor protein 1 (AP-1) mediates shuttling from the TGN to lysosomal compartments for degradation, a mechanism that controls the overall abundance of CTLA-4 in the TGN.

(B) CTLA-4 can exert T-cell-intrinsic and T-cell-extrinsic functions. Intrinsic control is provided by the following: (1) Inhibitory signaling. Signals through CTLA-4 can interfere with proximal signaling by the T cell receptor (TCR) and CD28. (2) Competition for ligands. CTLA-4 is the higher-affinity receptor than CD28 for CD80/CD86 and can outcompete CD28 for CD80/CD86 binding. (3) Promote adhesion or reduced stop signal. CTLA-4 can increase T cell/APC adhesion through a pathway mediated by LFA1 and decrease duration of APC/T cell interactions by inhibiting the TCR-mediated stop signal, resulting in reduced T cell activation. (4) Ligand-independent inhibition. A CTLA-4 splice variant that cannot bind to ligands can inhibit T cell activation through a similar signaling pathway as full-length CTLA-4. Extrinsic control is provided by the following: (1) Reverse signaling through ligands into APCs. CTLA-4 can reverse signal through CD80 and CD86 into APCs, leading to IDO production and suppression of T cell effector responses. (2) Reduce ligand expression/availability. Secreted factors such as

IL-10, TGF- β , or soluble splice variants of CTLA-4 reduce ligand expression or availability. (3) CTLA-4 removes ligands from APCs. CTLA-4 binding to CD80 or CD86 can result in transendocytosis of the ligands from the APC, resulting in lower levels of ligands on the surface of APCs.

protein result in impaired CTLA-4 surface expression on T effectors and Treg cells due to an increase in degradation of CTLA-4 in lysosomes (Lo et al., 2015). This interaction between CTLA-4 and LRBA appears to occur in recycling endosomes, suggesting that LRBA rescues CTLA-4 from entering the lysosomal pathway.

Upon TCR stimulation, CTLA-4 is released to the cell surface (Linsley et al., 1996; Schneider et al., 1999) and localizes to the immune synapse, a process that is still under investigation. Expression of CTLA-4 on the cell surface and localization to the immune synapse are proportional to the strength of TCR stimulus, which might provide feedback to inhibit activation of T cells receiving a stronger stimulus, thereby promoting diversity of the T cell response. A multimeric complex composed of TRIM, LAX, and Rab8 in cooperation with processes involving the GTPase ADP ribosylation factor-1 (ARF-1) and phospholipase D (PLD) might facilitate release of CTLA-4 to the cell surface (Mead et al., 2005; Valk et al., 2006). In addition, T cells secrete

nano-sized microvesicles or exosomes that contain fCTLA-4; but whether CTLA-4 in these microvesicles or exosomes is functional is not yet clear (Esposito et al., 2014). These studies highlight the finely balanced and quantitative nature of CTLA-4 expression, which is regulated not only on the transcriptional level, but also by vesicle transport, endocytosis, and recycling. This dynamic regulation provides spatial and temporal control of CTLA-4-mediated inhibitory signals during T cell activation.

Inhibitory Functions of CTLA-4

The critical role of CTLA-4 in controlling T cell activation and tolerance is well established, but many mechanistic questions remain about how CTLA-4 exerts its inhibitory effects. CTLA-4 inhibits T cell proliferation, cell cycle progression, and IL-2 production (Walunas et al., 1994, 1996) and influences naive CD4⁺ T cell differentiation. Both antibody blockade of CTLA-4 and genetic deletion of CTLA-4 result in increased Th2 cell differentiation (Bour-Jordan et al., 2003) and favor the induction of Th17 cells (Ying et al., 2010). In addition to its role during T cell

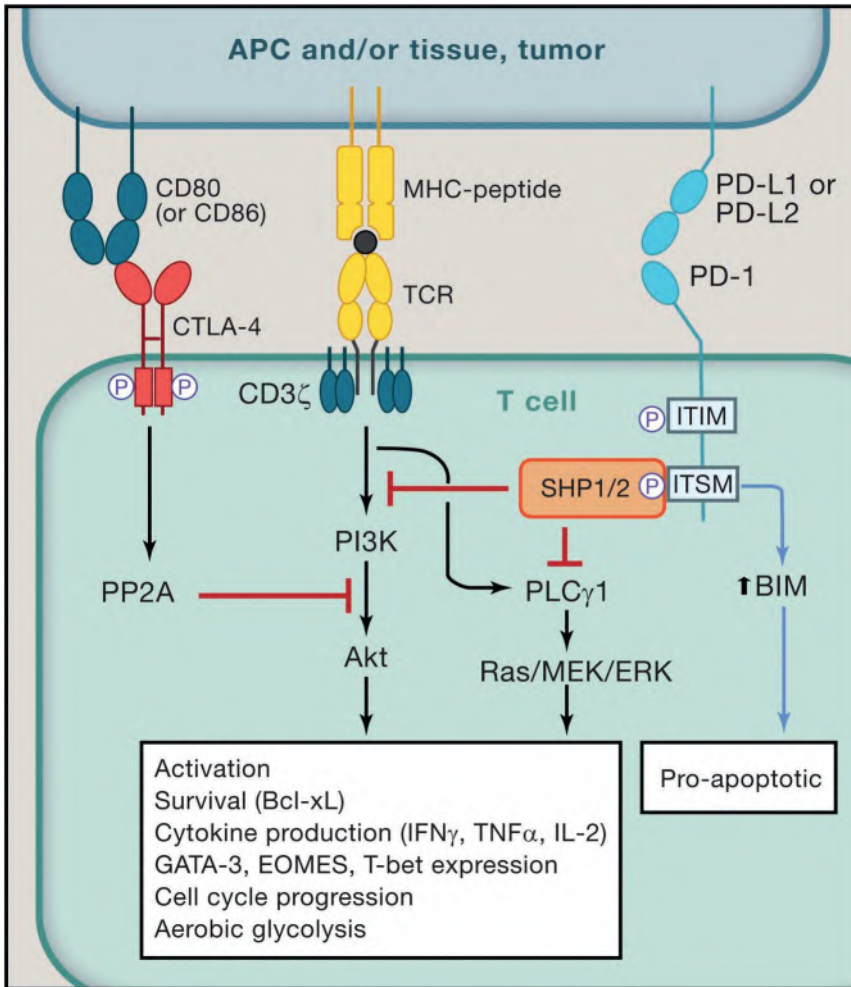


Figure 3. Comparison of Intracellular Signaling by CTLA-4 and PD-1

PD-1 and CTLA-4 both inhibit Akt activation, but they target different signaling molecules. CTLA-4 engagement by its ligands CD80 and CD86 activates the serine/threonine phosphatase PP2A, which directly inhibits the TCR/CD28-mediated activation of Akt, but preserves PI3K activity, and therefore expression of Bcl-xL. PD-1 ligation by PD-L1 or PD-L2 leads to phosphorylation of ITSM/ITIM motifs in the PD-1 cytoplasmic domain, which results in recruitment of the tyrosine phosphatases SHP-1 and SHP-2 and inhibition of PI3K activity and therefore reduced expression of Bcl-xL. PD-1 ligation also inhibits PLC γ 1 and downstream Ras-MEK-ERK signaling and leads to upregulation of the pro-apoptotic molecule BIM. In contrast to PD-1, CTLA-4 does not inhibit Ras-MEK-ERK and PLC γ 1 signaling.

in controlling T cell repertoire development in the thymus in the neonatal period.

CTLA-4 is thought to inhibit T cell responses in two ways, by cell-intrinsic and cell-extrinsic mechanisms (Figure 2B; Corse and Allison, 2012; Walunas et al., 1996; Wang et al., 2012a). Antibody-mediated crosslinking of CTLA-4 inhibits CD3- and CD28-induced T cell stimulation and argues for a cell-intrinsic role. CTLA-4-expressing cells can inhibit their own activation intrinsically by locally out-competing CD28 for ligand binding due to preferential binding of B7 molecules by CTLA-4. In addition, the tyrosine-phosphorylated cytoplasmic domain of CTLA-4 can interact with phosphatases SHP-2 and PP2A, which might inhibit

signaling downstream of the TCR and CD28, respectively (Figures 2B and 3; Chuang et al., 2000). However, SHP-2 can also transmit a positive signal in T cells so further work is needed to elucidate the role of PP2A in CTLA-4 signaling. The biological significance of CTLA-4 as a specific inhibitor of CD28 is demonstrated by studies showing that CD28 signaling is necessary for the phenotype of *Ctla4*^{-/-} mice; a single-point mutation in the CD28 cytoplasmic domain that affects Lck binding can abrogate the phenotype (Tai et al., 2007). Within Treg cells, the cytoplasmic domain of CTLA-4 can bind the kinase PKC- η (Kong et al., 2014) and thereby modulate Treg cell function.

activation, CTLA-4 can control T cell effector functions. Recent studies demonstrate that CTLA-4 controls B cell responses by regulating function of T follicular helper cells and T follicular regulatory cells (Sage et al., 2014; Wing et al., 2014). CTLA-4 is a transcriptional target of Foxp3 and Foxp3⁺ Treg cells constitutively express CTLA-4 (Gibson et al., 2007; Wu et al., 2006; Zheng et al., 2007). The important function of CTLA-4 on Treg cells is illustrated by the phenotype of mice lacking CTLA-4 only on Treg cells, either constitutively or inducibly. Foxp3Cre CTLA-4^{fl/fl} mice in which CTLA-4 is deleted in Foxp3⁺ Treg cells constitutively develop a lymphoproliferative disease and multiorgan autoimmunity, similar to *Ctla4*^{-/-} mice, but with delayed kinetics (Wing et al., 2008). Treg cells are expanded in these mice but do not suppress as effectively. In contrast, inducible deletion of CTLA-4 on all cells or only on Foxp3⁺ Treg cells in adult mice does not result in fatal systemic inflammation. Treg cells are expanded in these mice and have more potent suppressive functions (Paterson et al., 2015). IL-10 might be one potential mechanism by which CTLA-4-deleted Treg cells could promote effector T cell dysfunction (Paterson et al., 2015; Sakuishi et al., 2013). These findings point to different roles for CTLA-4 during the neonatal period versus adulthood, and suggest that CTLA-4 might play a critical role

Experiments with mixed bone marrow chimeras of wild-type and *Ctla4*^{-/-} donor cells first suggested that CTLA-4 also can exert cell-extrinsic effects because these bone marrow chimeras did not develop signs of autoimmunity (Bachmann et al., 1999; Ise et al., 2010). The mechanism of CTLA-4 cell-extrinsic effects might be to reduce CD80 and CD86 expression on antigen-presenting cells (APCs) by either an indirect mechanism (through B7 down-modulating cytokines such as IL-10 or TGF- β) or a direct mechanism involving transendocytosis (CTLA-4-mediated transfer of B7 molecules from the surface of the APC to inside the T cell), which reduces B7 availability on the APCs thereby reducing CD28 costimulatory signals (Qureshi et al., 2011;

Wing et al., 2008). The longevity of this effect is not clear, because CD80 and CD86 molecules are re-expressed within a relatively short time frame. Another possibility could be that CTLA-4 molecules on T cells simply compete or occupy CD80 and CD86 on APCs (Linsley et al., 1991; Walunas et al., 1994). CTLA-4 also can engage B7 ligands on DCs and induce the production of indoleamine 2,3-dioxygenase (IDO) (Fallarino et al., 2003; Grohmann et al., 2002), which catabolizes tryptophan, an essential amino acid for T cell proliferation (Munn et al., 1999). Localized tryptophan depletion resulting from IDO action limits T cell proliferation. Several other mechanisms have also been reported, including inhibition of microclusters and activation of E3 ligases (Chattopadhyay and Shevach, 2013; Schneider et al., 2008). Further work is needed to gain a better understanding of the mechanisms by which CTLA-4 regulates immune responses.

The functional significance of CTLA-4 expression on B cells and DCs is not yet clear. Germline and *Foxp3*-specific deletion of CTLA-4 results in increased antibody concentrations, suggesting an essential role for CTLA-4 on Treg cells in limiting B cell responses (Bour-Jordan et al., 2003; Wing et al., 2008). People heterozygous for CTLA-4 mutations (Kuehn et al., 2014) have an increased frequency of CD21^{lo} B cells but further work is needed to understand the mechanism. CTLA-4 on DCs might exert immune modulatory effects and define a subset of regulatory DCs (Han et al., 2014; Laurent et al., 2010). CTLA-4 might regulate DC maturation and/or function by interacting with B7 ligands on DCs either by reverse signaling into DCs (Kowalczyk et al., 2014) or reducing B7 ligand expression on DCs indirectly or directly by transendocytosis (Qureshi et al., 2011). In addition, CTLA-4 might modulate differentiation or cytokine production of monocytes (Wang et al., 2002a) or NK cells (Stojanovic et al., 2014). Moreover, there are reports that different progenitor or stromal cells can express CTLA-4.

Together, these studies indicate that CTLA-4 uses multiple mechanisms to exert its critical inhibitory functions on Treg and conventional T (Tconv) cells. The clinical success of anti-CTLA-4 antibodies for cancer immunotherapy (Hodi et al., 2010; Robert et al., 2011) motivates further investigation of CTLA-4 function. Notably, the efficacy of CTLA-4 mAbs for cancer immunotherapy can depend on their ADCC-mediated depletion of intratumoral Treg cells that express much higher amounts of cell surface CTLA-4 than other T cells (Selby et al., 2013). A deeper knowledge of CTLA-4 biology is necessary for developing effective combination therapies for cancer and therapies for other immune-mediated diseases.

Programmed Death 1

PD-1, PD-L1, and PD-L2 Gene Structure, Splice Variants, and Polymorphisms

Programmed death-1 (PD-1, CD279) has two ligands, programmed death-ligand 1 (PD-L1, also called B7-H1; CD274) and programmed death-ligand 2 (PD-L2, also called B7-DC; CD273) (Zhang et al., 2004). PD-L1 and PD-L2 differ in their affinities for PD-1: PD-L2 has approximately 3-fold higher affinity for PD-1 than does PD-L1. Each ligand has an additional unique binding partner. B7-1 binds to PD-L1 but *not* PD-L2, whereas RGMb (repulsive guidance molecule b) binds to PD-L2 but *not* PD-L1 (Butte et al., 2007; Xiao et al., 2014).

In both humans and mice, the gene encoding PD-1 consists of five exons: exon 1 encodes a signal sequence, exon 2, an IgV-like domain, exon 3, a stalk and TM domain. Exons 4 and 5 encode the cytoplasmic domain that contains an immunoreceptor tyrosine-based inhibitory motif (ITIM) and an immunoreceptor tyrosine-based switch motif (ITSM) (exon 5) (Ishida et al., 1992; Shinohara et al., 1994). Four splice variants of PD-1 are expressed in human PBMCs. These splice variants lack exon 2, exon 3, exons 2 and 3, or exons 2 through 4 (Nielsen et al., 2005). Expression of all PD-1 splice variants is induced by *in vitro* stimulation of T cells with anti-CD3 and anti-CD28. The functions of many of these splice variants remain unclear, but the splice variant lacking exon 3 (PD-1 Δ ex3) encodes a soluble form of PD-1 due to lack of the TM region and resembles the soluble form of CTLA-4, which has been implicated in human autoimmune diseases (Nielsen et al., 2005; Ueda et al., 2003). Soluble PD-1 (sPD-1) is detected in inflammatory and autoimmune diseases, and sPD-1 levels might serve as a biomarker. For example, in rheumatoid arthritis, sPD-1 is present in the synovial fluid and sera (Wan et al., 2006) and increased levels correlate with disease activity. The inclusion of this sPD-1 in a vaccine vector improves vaccine efficacy, presumably by binding to PD-L1 and PD-L2 and reducing the PD-1 signal (Zhou et al., 2013b). There is also a splice variant that splices out 42 bp within the IgV exon 2 (Δ 42PD-1). This splice variant does not bind PD-L1 or PD-L2 but induces proinflammatory cytokine production and increases vaccine efficacy in infectious or tumor models, when included in a vaccine vector (Zhou et al., 2013a).

The PD-1 ligands are structurally similar and closely linked in the genome, separated by only 23 kb in mice and 42 kb in humans. The 30 aa PD-L1 intracellular domain is well conserved across species but has no known function. There is a splice variant of PD-L1 that lacks the IgV domain required for binding to PD-1 but its function is unknown (He et al., 2005). In addition, there is a soluble form of PD-L1 that can be produced by cleavage of cell surface PD-L1 from DCs by a metalloproteinase and detected in serum, but this form is not the result of alternative splicing (Frigola et al., 2011). A soluble form of PD-L2 can be generated by tumors and immune cells, but further work is needed to understand how it is generated and its function. Three PD-L2 splice variants have been identified lacking only IgV, only IgC, or both IgC and TM domains, the latter potentially representing a soluble ligand for PD-1.

Polymorphisms in *PDCD1* are associated with autoimmune disorders, cancers, and viral pathogenesis, and the functional effects of several SNPs have been characterized. A regulatory G7146A SNP, PD-1.3 (rs11568821) located within the fourth intron of the *PDCD1* gene, disrupts binding of runt-related transcription factor 1 (Runx1) to the intronic enhancer region and thereby alters the regulation of *PDCD1* gene expression (Prokunina et al., 2002) and has been associated with susceptibility to systemic lupus erythematosus (Prokunina et al., 2002). In multiple sclerosis patients, the PD-1.3 SNP had no effect on PD-1 expression but resulted in impaired PD-1-mediated inhibition of T cell activation and cytokine secretion (Kroner et al., 2005). A C7209T SNP (rs41386349) within intron 4 creates a negative *cis*-element for *PDCD1* gene transcription that is significantly associated with lower hepatitis B viral burden in patients with chronic hepatitis B viral infection (Zheng et al., 2010). An

A-to-G SNP located in the 3' untranslated regions of *PDCD1* (rs10204525) allows miR-4717 to bind to PD-1 mRNA, thereby suppressing PD-1 protein expression (Zhang et al., 2015) and has been associated with lower chronic HBV susceptibility and disease progression (Zhang et al., 2010a).

Regulation of PD-1 Expression

PD-1 is inducibly expressed on CD4⁺ and CD8⁺ T cells, NK, NKT, B cells, macrophages, and some DC subsets during immune activation and chronic inflammation (Table 1; Chang et al., 2008; Liu et al., 2009; Nishimura et al., 1996; Petrovas et al., 2006). TCR signaling and cytokines (common γ chain family cytokines IL-2, IL-7, IL-15, IL-21, and type I IFNs) can induce PD-1 expression on T cells (Terawaki et al., 2011). PD-1 can be detected on the surface of naive T cells by 24 hr after activation but expression is transient, declining when antigen is cleared. When T cells are continually stimulated by antigen (during viral chronic infection or cancer), PD-1 expression remains high and T cells enter into a dysfunctional state termed "exhaustion." T cell metabolism also regulates PD-1 expression in T cells; activated CD4⁺ T cells undergoing aerobic glycolysis exhibited reduced expression of PD-1 compared to T cells undergoing oxidative phosphorylation (Chang et al., 2013), suggesting that metabolic constraints in addition to antigen might influence PD-1 expression. In B cells, BCR signaling induces PD-1, but LPS, CpG oligonucleotides, IFN- γ , and IL-4 inhibit BCR-induced PD-1 upregulation (Zhong et al., 2004). In macrophages, cytokines (IFN- α , TNF- α , IL-1 β , or IL-6), LPS, and TLR ligands induce PD-1 expression (Cho et al., 2008). Estrogen can also induce PD-1 on T cells and APCs (Polanczyk et al., 2006).

Mechanisms that regulate the transient nature of PD-1 expression are best understood in CD8⁺ T cells. PD-1 expression inversely correlates with DNA methylation of the gene encoding PD-1 in mice and humans, which represses transcriptional activation (Youngblood et al., 2011). When PD-1 expression is upregulated during initial CD8⁺ T cell activation after acute LCMV infection, there is transient loss of DNA methylation at the *Pdcd1* locus; remethylation occurs during generation of functional memory cells in which PD-1 expression is reduced. During initial CD8⁺ T cell activation, NFATc1 (NFAT2) binds to a conserved region in the *Pdcd1* promoter (CR-C) and leads to short-lived PD-1 expression. Cytokines that signal through STAT transcription factors (Austin et al., 2014; Terawaki et al., 2011), as well as activation-driven c-Fos (Cho et al., 2008; Xiao et al., 2012), can augment this process. c-Fos binds to another conserved region (CR-B) in the PD-1 promoter. STAT transcription factors can bind to DNA-hypersensitive sites upstream or downstream of the transcriptional start site. An interferon-stimulated regulatory element (ISRE), located in CR-C, also can prolong PD-1 transcription upon T cell activation through IRF9, and also during macrophage activation (Agata et al., 1996; Cho et al., 2008). In addition, the intracellular domain of Notch (NICD) binds to the PD-1 promoter and promotes PD-1 transcription during CD8⁺ T cell activation (Mathieu et al., 2013). During the later phases of an acute response when PD-1 is downregulated, Blimp-1 is expressed and serves as a transcriptional repressor of PD-1 expression (Lu et al., 2014). Blimp-1 binds to a sequence between CR-B and CR-C and inhibits PD-1 transcription directly. Blimp-1 also represses expression

of the PD-1 activator NFATc1 and displaces NFAT from the CR-C site where it controls PD-1 expression.

During chronic LCMV expression, exhausted CD8⁺ T cells, which highly express PD-1, are hypomethylated at the CR-B and CR-C sites (Youngblood et al., 2011). FoxO1 binds to the CR-C site and promotes PD-1 expression and the formation of more terminally exhausted PD-1^{hi}Eomes^{hi} CD8⁺ T cells (Staron et al., 2014). T-bet is another transcriptional repressor of PD-1 expression, and high PD-1 expression on exhausted CD8⁺ T cells is due in part to reduced T-bet expression (Kao et al., 2011).

In macrophages, NFAT also is a critical activator of PD-1 expression. In B cells and CD4⁺ T cells, the NF- κ B p65 subunit binds to the CR-C region, inducing PD-1 expression (Bally et al., 2015; Oestreich et al., 2008).

Regulation of PD-L1 and PD-L2 Expression

The PD-1 ligands are distinctly expressed, with PD-L1 being more widely expressed than PD-L2 (Dong et al., 2002; Hamanishi et al., 2007; Nomi et al., 2007; Ohigashi et al., 2005; Yamazaki et al., 2002). PD-L1 can be expressed by a variety of hematopoietic and non-hematopoietic cells, whereas PD-L2 is expressed mainly by dendritic cells and macrophages and non-hematopoietic cells in the lung (Tables 1 and 2). The expression of PD-1 ligands in tissues enables this pathway to regulate T cell responses locally in tissues. Proinflammatory stimuli induce PD-L1 and PD-L2 expression, which might serve as a negative feedback mechanism to downregulate T cell responses in tissues, protecting tissues from immune-mediated damage or tumors from immune attack. PD-L1 can be induced by type I and II IFNs, TNF- α , IL-10, and common γ chain cytokines (Eppihimer et al., 2002). IL-4 and GM-CSF are the most potent stimuli for PD-L2 expression (Loke and Allison, 2003; Yamazaki et al., 2002), but IFNs and γ chain cytokines also can induce PD-L2. Complement c5a also promotes PD-L1 and PD-L2 expression.

Relatively little is known about the transcriptional regulation of PD-L1 or PD-L2. The human PD-L1 promoter contains a STAT3 binding site required for PD-L1 expression, two IFN regulatory factor-1 (IRF-1) binding sites, which regulate both constitutive and inducible PD-L1 expression, and an NF- κ B binding site that regulates LPS-induced PD-L1 expression in human monocytes. The transcription factor FoxA1, which is induced by IFN- β , binds to the *cd274* promoter and induces PD-L1 expression on a novel FoxA1⁺ regulatory T cell population (Liu et al., 2014). MicroRNAs also regulate PD-L1 expression. miR-513 and miR-200 target the 3' UTR of PD-L1 and inhibit PD-L1 expression. miR-513 is downregulated by IFN- γ and might contribute to IFN-induced expression of PD-L1 (Gong et al., 2009). miR-200 regulates EMT transition and is repressed in tumor cells, resulting in increased PD-L1 expression (Chen et al., 2014). PD-L2 has NF- κ B binding sites upstream of the transcriptional start site and PD-L2 induction by IFN- γ depends in part on NF- κ B. There is an intronic promoter between PD-L2 exons 1 and 2 that binds Octamer binding proteins 1 and 2 and is responsible for constitutive expression of PD-L2 in B-1 cells (Kaku and Rothstein, 2010).

The JAK-STAT, MAP kinase, and PI3K-Akt pathways mediate IFN signaling, and these pathways regulate IFN-induced PD-L1 expression. PD-L1 expression in cell lines is decreased when MyD88, TRAF6, and MEK are inhibited. In tumor cells, multiple

Table 2. Comparison of B7 Family of Costimulatory Molecules

	Percent Identity (with CD80 extracellular domain)	Chromosome		Expression		
		Human	Mouse	Lymphoid	Non-lymphoid	Receptor
B7-1 (CD80)	100%	3q13.33	16qB4	T, B, DC, mo, mac, mast cells	rare; podocyte, fibroblast, osteoblast	CD28, CTLA-4, PD-L1
B7-2 (CD86)	27%	3q13.33	16qB4	T, B, DC, mo, mac, mast cells	rare	CD28, CTLA-4
ICOSL (CD275; B7-H2, B7h, B7RP-1, LICOS)	27%	21p12	10qC1	T, B, DC, mo, mac, mast cells	endothelial, epithelial, fibroblast, osteoblast	ICOS
PD-L1 (CD274; B7-H1)	25%	9p24.1	19qC1	DC, mo, mac, mast cells, T, B, NK	endothelial, epithelial, fibroblast, msc, pancreas islet, syncytiotrophoblast, stroma, tumor	PD-1, B7-1
PD-L2 (CD273; B7-DC)	23%	9p24.1	19qC1	DC, B, Th2, mo, mac, mast cells	endothelial, lung epithelia, tumor	PD-1, RGMB
B7-H3 (CD276)	29%	15q24.1	9qB4	only mouse: APC; only human: T, NK, DC, mo, mac	rare, epithelial, fibroblast, tumor, osteoblast	?
B7-H4 (B7x, B7S1, Vtcn1)	21%	1q13.1	3qF2.2	DC, mo, mac	MSC, stroma, tumor	?
VISTA (PD-1H, Vsir, DD1a, Dies1, Gi24, SISP1, C10orf54)	24%	10q22.1	10qB4	T, DC, mo, mac	stroma, tumor	?
BTNL2 (BTL-II)	24%	6p21.32	17qB1	mo, mac; act. T, B	intestinal epithelial	?
HHLA2 (B7-H6, B7-H7)	10%	3q13.13	–	only human: B, mo, mac	only human: endothelial, epithelial, stroma, syncytiotrophoblast, tumor	TMIGD2

Abbreviations are as follows: act., activated (cell type); B, B cell; DC, dendritic cell; mac, macrophage; mo, monocyte; MSC, mesenchymal stem cells; NK, natural killer cell; NKT, natural killer cell T cell; T, T cell.

reinforcing mechanisms stimulate PD-L1 and PD-L2 expression, including cytokines, chromosomal copy gain, Epstein Barr virus LMP protein, and mutations in microRNA binding sites. The region on human chromosome 9p24.1 encoding PD-L1, PD-L2, and Jak2 is often amplified in certain tumors including mediastinal large B cell lymphoma and Hodgkin lymphoma, leading to high constitutive expression and responsiveness to PD-1 blockade (Ansell et al., 2015). Loss of phosphatase and tensin homolog (PTEN) increases PD-L1 expression in tumors by a post-transcriptional mechanism. Loss or inhibition of PTEN, a cellular phosphatase that modifies phosphatidylinositol 3-kinase (PI3K) and Akt signaling, is one of the most frequent alterations in cancer and might contribute to constitutive tumor expression of PD-L1. Inhibition of PI3K or Akt decreases PD-L1 expression in tumor cells.

Inhibitory Functions of PD-1

PD-1 was cloned from a T cell hybridoma undergoing TCR activation-induced cell death—hence its name “programmed death-1.” However, PD-1 does not directly activate caspases or a cell death pathway. PD-1 signals regulate T cell responses in several ways. Despite early *in vitro* studies pointing to a possible costimulatory role for PD-L1 (B7-H1), further *in vivo* investigations using blocking antibodies, Fab, and knockout mice have since demonstrated that PD-1 ligation reduces signals downstream of TCR stimulation, resulting in decreased activation and cytokine production. Upon PD-L1 or PD-L2 binding, PD-1 is phosphorylated on its ITIM (Y223) and ITSM (Y248) tyrosine motifs, leading to recruitment of Src homology region 2

domain-containing phosphatases (primarily SHP-2 but also SHP-1) and downregulation of TCR (or BCR) signaling through dephosphorylation of signaling intermediates such as CD3 ζ , ZAP70, and PKC θ in T cells (and Syk and PI3K in B cells) (Chemnitz et al., 2004; Okazaki et al., 2001; Sheppard et al., 2004). SHP-2 binding to the ITSM of PD-1 appears to be key for PD-1-mediated inhibition (Chemnitz et al., 2004; Parry et al., 2005). PD-1 inhibitory function is lost when the ITSM alone is mutated, demonstrating that this tyrosine plays a primary functional role in PD-1 action (Chemnitz et al., 2004; Okazaki et al., 2001). Similarly, SHP-2 recruitment to the ITSM tyrosine of PD-1 is required for inhibition of B cell receptor (BCR)-mediated calcium mobilization and phosphorylation of Ig β , Syk, PLC γ 2, and Erk1/2 (Okazaki et al., 2001). Moreover, in live cell imaging studies, SHP-2, but not SHP-1, interacts with the ITSM of PD-1 in dynamic central supramolecular activation clusters (c-SMAC). PD-1 recruitment to c-SMACs was required for the PD-1-SHP-2 association and correlated with dephosphorylation of TCR proximal signaling molecules within the PD-1-TCR microclusters and consequent inhibition of T cell activation (Yokosuka et al., 2012). Although the coinhibitory function of PD-1 is well established, further work is needed to cement our understanding of how the intracellular domain of PD-1 implements reduced TCR-CD28 signaling.

PD-1 ligation inhibits two important pathways: PI3K-Akt and Ras-MEK-ERK signaling. Although PD-1 and CTLA-4 both inhibit Akt activation, they target different signaling molecules (Figure 3). PD-1 inhibits PI3K activation, which is required for Akt activation,

and leads to increased PTEN phosphatase activity, effectively inhibiting the PI3K-Akt pathway (Patsoukis et al., 2013). In contrast, CTLA-4 preserves PI3K activity and expression of certain molecules such as Bcl-xL and inhibits Akt directly via the PP2A phosphatase (Parry et al., 2005). PD-1 ligation also inhibits Ras-MEK-ERK pathway signaling, possibly via SHP-2 dephosphorylation of PLC γ 1 (Patsoukis et al., 2012). PD-1-mediated inhibition of the PI3K-Akt and Ras-MEK-ERK pathways inhibits cell cycle progression, ultimately through inhibiting cyclin-dependent kinase-2 (Cdk2) activation (Patsoukis et al., 2012). Moreover, due to the wide variety of Cdk2 substrates involved in transcription, PD-1 can regulate other T cell properties and function by reprogramming transcriptional and epigenetic events independently of its effects as an inhibitor of cell cycle progression (Wells, 2007).

Further downstream, PD-1 modulates T cell effector function by reducing expression of cytokines and transcription factors associated with effector cell function (GATA-3, Tbet, and Eomes) (Nurieva et al., 2006). In addition, PD-1-mediated upregulation of the transcription factor Batf (basic leucine zipper transcription factor ATF-like) can impair T cell proliferation and cytokine production. PD-1 signaling also can decrease the production of cytotoxic effector molecules by T cells, reducing their killing capacity. T cell effector functions are not all equally inhibited, but are inhibited in a PD-1 dose-dependent fashion with a hierarchy of IL-2, TNF- α , and proliferation being most readily inhibited, followed by cytotoxicity and IFN- γ , and finally MIP-1 β (Wei et al., 2013). PD-1 signals also modulate T cell motility and length of interaction with DCs and target cells (Fife et al., 2009). Furthermore, signaling through PD-1 can promote the induction and maintenance of inducible regulatory T cells from naive or Th cells (Francisco et al., 2009), by downregulating phospho-Akt, mTOR, S6, and ERK2 and upregulating PTEN, all of which are key signaling molecules for iTreg cell development. PD-1 signaling inhibits aerobic glycolysis, which is required for T cell effector function and Th1 and Th17 cell differentiation (Chang et al., 2013) and metabolically reprograms T cells from aerobic glycolysis to fatty acid oxidation (Chang et al., 2015; Patsoukis et al., 2015), a program that promotes the generation of regulatory T cells (Michalek et al., 2011). Thus, PD-1 signaling can alter T cells in many ways that work in concert to inhibit immune responses.

PD-1 inhibitory signals have key functions in regulating the threshold for T cell activation and limiting effector T cell responses, as well as controlling T cell tolerance, resolution of inflammation, and T cell exhaustion. PD-L1 and PD-L2 expression in tissues dampens local immune responses, controls tissue injury, and maintains tissue tolerance. PD-L1 interactions with CD80 also inhibit T cells (Butte et al., 2007). PD-L2 interactions with RGMB (repulsive guidance molecule b) play an important role in respiratory tolerance (Xiao et al., 2014). Tumors and microbes that cause chronic infection exploit the PD-1 pathway to inhibit their eradication. PD-1 pathway antagonists aim to reverse T cell dysfunction. In multiple pre-clinical models, PD-1-PD-L1 blockade has enhanced anti-viral and anti-tumor immunity. This has been translated to therapy. Blockade of the PD-1-PD-L1 inhibitory pathway has led to striking clinical trial results with 10%–87% overall response rates, typically about 20%, across a range of cancers, and resulted in FDA approval

of anti-PD-1 mAb drugs for advanced melanoma, non-small cell lung cancer (NSCLC), and kidney cancer.

B7-H3

B7-H3 (also known as CD276) has several isoforms (Chapoval et al., 2001). Differential splicing of human B7-H3 leads to 4lg domain (VCVC) and 2lg domain transcripts (V1C2). The 4lg domain transcript is the predominantly expressed isoform and appears to result from exon duplication with a tandem repeat of the IgV and IgC domains (VCVC) (Sun et al., 2002). The functional relevance of the different isoforms of B7-H3 is not known. Mice express only one form of B7-H3 with a single VC domain. In addition, B7-H3 can be shed from the cell surface, resulting in a soluble version (Sun et al., 2011).

B7-H3 mRNA is broadly expressed in both lymphoid and non-lymphoid organs, but protein expression is limited and maintained at low levels. B7-H3 is constitutively expressed on murine APCs (Collins et al., 2005), but inducibly expressed on human T cells, NK cells, DCs, macrophages, and monocytes (Chapoval et al., 2001; Prasad et al., 2004; Steinberger et al., 2004; Suh et al., 2003). B7-H3 can also be expressed on non-hematopoietic cells (Table 2; Loos et al., 2010). Elevated B7-H3 levels are correlated with several cancers, sepsis, and meningitis (Chen et al., 2009; Zhang et al., 2008, 2010b). The discrepancy between the ubiquitous expression of B7-H3 transcripts in a wide spectrum of tissues and differential B7-H3 expression at the protein level argues for posttranscriptional regulation, but molecular mechanisms are not yet clear. miR-29 levels are inversely correlated with B7-H3 protein expression (Xu et al., 2009), suggesting a microRNA-related mechanism involved in regulation.

There are data to support both costimulatory (Chapoval et al., 2001; Luo et al., 2004; Sun et al., 2003; Wang et al., 2005) and coinhibitory (Leitner et al., 2009; Prasad et al., 2004; Suh et al., 2003) functions for B7-H3. The role of B7-H3 seems to be dependent on the context of expression and disease model. Because the binding partner(s) for B7-H3 are not known, it is difficult to interpret studies with B7-H3 mAb. TLT-2 (TREML2) was suggested as a binding partner for B7-H3 (Hashiguchi et al., 2008), but other studies did not confirm this interaction (Leitner et al., 2009).

B7-H4

B7-H4 (also known as B7S1, B7x, and Vtcn1) has an IgV-IgC extracellular domain and is linked to the cell surface by a glycosyl phosphatidylinositol anchor (Sica et al., 2003). Differential splicing of exon 6 results in two transcripts, a full-length and truncated B7-H4 transcript (Choi et al., 2003). The truncated splice variant appears to have a similar function as full-length B7-H4 due to the location of the truncation in the 3' UTR.

B7-H4 transcripts are ubiquitously expressed in lymphoid and non-lymphoid tissues, but B7-H4 protein expression is extremely limited in normal tissues, suggesting tight post-transcriptional regulation (Table 2; Choi et al., 2003; Sica et al., 2003). B7-H4 can be expressed on the cell surface, in the cytoplasm and in nucleus of cancer cells. A nuclear localization sequence motif mediates nuclear localization, which promotes cell cycle progression and proliferation (via upregulation of Cyclin D1 and Cyclin E) (Zhang et al., 2013) in tumor cell lines.

B7-H4 expression can be induced in monocytes, macrophages, and myeloid DCs by IL-6 and IL-10 (Kryczek et al., 2006a) and inhibited by GM-CSF and IL-4 (Kryczek et al., 2006b). B7-H4 is expressed in many cancers, including breast, kidney, ovarian, pancreas, brain, and lung cancers (Cheng et al., 2009; Choi et al., 2003; Krambeck et al., 2006; Salceda et al., 2005; Yao et al., 2008; Zhang et al., 2013), and higher expression correlates with poor prognosis and decreased survival. A soluble form of B7-H4 has been found in sera of patients with rheumatoid arthritis and ovarian cancer, and in mice soluble B7-H4 increases with disease severity in autoimmune models. The receptor for B7-H4 is not known, but the putative receptor appears to be upregulated on T cells after in vitro activation and myeloid-derived suppressor cells, because soluble B7-H4 binds to both (Abadi et al., 2013; Sica et al., 2003).

Studies of B7-H4-deficient (*Vtcn1*^{-/-}) mice, B7-H4 overexpression, and B7-H4 Ig fusion proteins are all consistent with an inhibitory function for B7-H4. A number of in vitro and in vivo studies indicate that B7-H4 can inhibit T cell responses. *Vtcn1*^{-/-} mice do not display spontaneous autoimmunity or disruption of immune homeostasis (Suh et al., 2006; Zhu et al., 2009). However, B7-H4 deficiency increased incidence and severity of EAE and collagen-induced arthritis (CIA). Overexpression of B7-H4 in pancreatic islets ameliorated autoimmunity and prolonged islet allograft survival in mice. Similarly, administration of B7-H4 Ig delayed the onset of NOD diabetes and CIA and was associated with reduced Th17 cell and increased IFN- γ production, suggesting the B7-H4 might regulate the generation of Th17 cells. Consistent with these findings, *Vtcn1*^{-/-} mice exhibit elevated Th1 cell responses to *Leishmania major* and experimental autoimmune diseases (Suh et al., 2006). However, *Vtcn1*^{-/-} mice do not show altered responses in Th1-cell-driven airway inflammation or contact hypersensitivity models or CTL responses to acute viral infections, suggesting that B7-H4 is not a dominant inhibitory molecule, but rather a fine tuner of immune responses.

Studies of infection indicate that B7-H4 also might regulate innate as well as adaptive immunity. *Vtcn1*^{-/-} mice have increased neutrophil-mediated resistance to infection with *Listeria monocytogenes* (Zhu et al., 2009) independent of adaptive immunity. B7-H4 deficiency leads to increased proliferation of bone marrow Gr-1⁺CD11b⁺ neutrophil progenitors. Thus, B7-H4 might negatively regulate neutrophil responses.

B7-H4 also can exert a cell-intrinsic effect on tumor cells. siRNA B7-H4 knockdown increased caspase-mediated tumor cell apoptosis, whereas overexpression of B7-H4 expression in a ovarian tumor cell line protected from cell death in vitro and increased tumor formation in SCID mice.

V-Domain Ig Suppressor of T Cell Activation

The extracellular domain of V-domain Ig suppressor of T cell activation (VISTA) has some similarities with the PD-L1 IgV domain. However, VISTA shares only weak homology with B7-CD28 family members (Wang et al., 2011) because it contains an unusual single IgV domain with three additional cysteine residues, which differs structurally from the other B7 family members (Ceeraz et al., 2013; Wang et al., 2011). No signaling motifs have been identified in the VISTA cytoplasmic domain.

There are two potential isoforms of VISTA, one with a 60 aa deletion, the other with an alternative start site. Once expressed at the cell surface, VISTA can potentially undergo proteolytic cleavage by MMP14, resulting in a soluble extracellular fragment and a membrane-bound fragment (Sakr et al., 2010). The binding partner for VISTA is not yet known, but several studies suggest that VISTA can function as ligand (Lines et al., 2014; Wang et al., 2011) and as a receptor (Flies et al., 2014) and form homophilic interactions. VISTA can control BMP4 signaling in mouse ES cells by binding a component in the BMP4 receptor complex (Aloia et al., 2010; Sakr et al., 2010).

VISTA is predominantly expressed on hematopoietic cells (Table 2) in both mice (encoded by *Vsir*) and humans (encoded by *C10orf54*) (Lines et al., 2014; Wang et al., 2011). VISTA is most highly expressed on myeloid and granulocytic cells, expressed at lower levels on T cells but not present on B cells (Flies et al., 2011; Wang et al., 2011). VISTA is induced on T cells and myeloid cell populations upon activation or immunization, suggesting that inflammation induces its expression (Wang et al., 2011).

VISTA inhibits T cell responses and regulates T cell tolerance. VISTA-Fc fusion protein or full-length VISTA expressed on APCs can inhibit T cell activation, proliferation, and cytokine production (Lines et al., 2014; Wang et al., 2011). Similar to PD-L1, VISTA can induce Foxp3 expression in CD4⁺ T cells. On T cells themselves, VISTA also can act as an inhibitory receptor and suppress activation (Flies et al., 2014). *Vsir*^{-/-} mice have increased numbers of activated T cells and an age-related multi-organ proinflammatory phenotype but no signs of spontaneous autoimmunity (Flies et al., 2014). However, *Vsir*^{-/-} mice develop more severe experimental autoimmune encephalitis (EAE) compared to controls, and VISTA on T cells and APCs contribute to exacerbated EAE (Wang et al., 2014). Likewise, administration of anti-VISTA mAb results in exacerbated EAE (Wang et al., 2011). However, further work is needed to understand the effects of VISTA antibodies, as another study saw a potentially inhibitory effect in graft-versus-host-disease (Flies et al., 2011).

VISTA appears to have inhibitory functions that are non-redundant with PD-1 and PD-L1 (Liu et al., 2015). PD-1 and VISTA double-deficient mice exhibited accelerated onset and severity of EAE compared to PD-1 and VISTA single-deficient mice. Similarly, anti-VISTA and anti-PD-L1 synergized to promote anti-tumor immunity in the CT26 mouse tumor model (Liu et al., 2015).

HHLA2

Human endogenous retrovirus-H long terminal repeat-associated protein 2 (HHLA2, also known as B7-H7) is the most recently characterized member of the B7 family. HHLA2 is located on chromosome 3 near *CD80* and *CD86* (Zhao et al., 2013). Unlike other B7 family members, HHLA2 contains 3Ig-like domains (VCV) (Mager et al., 1999). HHLA2 orthologs are present in a wide variety of vertebrates including monkeys and humans but not in rodents. HHLA2 polymorphisms have been associated with autism spectrum disorders.

HHLA2 protein is constitutively expressed on human monocytes and macrophages and further upregulated by inflammatory stimuli including LPS, IFN- γ , and poly(I:C). HHLA2 is not expressed on resting T or B cells, but induced on activated

B cells, but not T cells (Table 2; Zhao et al., 2013). HHLA2 mRNA is highly expressed in the gut, kidney, and lung (Janakiram et al., 2015), whereas its protein expression is limited in normal tissues. HHLA2 is highly expressed in many cancers. In triple-negative breast cancer, high HHLA2 expression is related to gene amplification and associated with higher risk of metastasis and more invasive disease (Janakiram et al., 2015). Studies using HHLA2 Ig fusion proteins have identified putative receptors expressed constitutively on CD4⁺ and CD8⁺ T cells, B cells, NK cells, monocytes, and DCs. TM and immunoglobulin domain containing 2 (TMIGD2; also known as CD28H) protein has been identified as a receptor for HHLA2. TMIGD2 is expressed on naive T cells and NK cells and can function as a costimulatory receptor for naive T cells. Unusually, TMIGD2 expression declines with T cell activation and is not on activated T cells, Treg cells, B cells, or APCs (Xiao and Freeman, 2015; Zhao et al., 2013; Zhu et al., 2013). TMIGD2 also is expressed on endothelial and epithelial cells, suggesting the possibility for additional immunoregulatory functions in tissue microenvironments.

Data support both T cell costimulatory and coinhibitory functions for HHLA2. In two studies, plate-bound HHLA2 Ig fusion inhibited CD4⁺ and CD8⁺ T cell proliferation and cytokine production (including IFN- γ , TNF- α , IL-5, IL-10, IL-13, IL-17A, and IL-22) (Zhao et al., 2013). In another study, plate-bound HHLA2 Ig enhanced CD4⁺ T cell proliferation, cytokine production (IL-2, IFN- γ , TNF, and IL-10), and Akt phosphorylation (Zhu et al., 2013). An anti-HHLA2 mAb that blocked the interaction between HHLA2 and TMIGD2 reduced allogeneic T cell proliferation in vivo in a human xenograft model of GVHD, consistent with a costimulatory function for HHLA2 via TMIGD2 (Zhu et al., 2013). The immunoinhibitory capacity of HHLA2-Ig suggests there might be an additional HHLA2 receptor.

Butyrophilin-like 2

Butyrophilin-like 2 (BTNL2) shares considerable sequence homology with the butyrophilin family of proteins and is located in the MHC class II gene locus in both mice and humans. Unlike most other butyrophilin family members, BTNL2 lacks the prototypical B30.2 ring domain in the cytoplasmic tail (Arnett et al., 2007). Although the sequence homology between the B7 family and BTNL2 is low, the domain structure is conserved. Human BTNL2 has two TM splice variants that remove the C-terminal IgC domain. BTNL2 genetic polymorphisms have been identified in humans and are associated in multiple studies with risk for inflammatory and autoimmune diseases including sarcoidosis, inflammatory bowel disease, and rheumatoid arthritis, as well as risk for both familial and sporadic prostate cancer. Sarcoidosis-associated polymorphism rs2076530 is predicted to lead to a soluble form of BTNL2 due to a premature stop codon that deprives BTNL2 of its IgC, TM, and cytoplasmic domains, thereby disrupting the membrane localization of BTNL2 (Valentonyte et al., 2005). The impact of other polymorphisms on BTNL2 is not yet clear.

Murine BTNL2 mRNA and protein are expressed primarily in the gut and lymphoid tissues, most abundantly by epithelial cells in the small intestine and on DCs in lymphoid organs (Arnett et al., 2007; Nguyen et al., 2006). BTNL2 is markedly upregulated in mouse models of inflammatory bowel disease. In the immune system, T cells, B cells, and macrophages express BTNL2

(Table 2). The receptor for BTNL2 remains unknown, but studies have excluded CD28, CTLA4, ICOS, and PD-1 (Arnett et al., 2007). The putative BTNL2 receptor is constitutively expressed on B cells and is upregulated on activated T cells.

BTNL2 Ig fusion proteins can inhibit CD4⁺ T cell proliferation and cytokine production (IL-2, TNF- α , GM-CSF, IL-10, IL-4, IL-6, IL-17, and IFN- γ) in vitro (Nguyen et al., 2006). BTNL2 Ig can inhibit cytokine production induced by CD28 and ICOSL costimulation in a dose-dependent manner (Arnett et al., 2007). Underlying mechanisms are challenging to define with fusion proteins, because they can function as agonists or antagonists. Moreover, recombinant BTNL2 induced differentiation of naive T cells into Treg cells similarly to PD-L1 and PD-L2 (Swanson et al., 2013). Given the high level of expression in the gut, its role in T cell inhibition, and its association with inflammatory disorders such as inflammatory bowel disease, BTNL2 might play a role in mucosal immunity and tolerance. However, further work is needed to elucidate the immunoregulatory functions of BTNL2.

Overlapping and Unique Functions of Coinhibitory Pathways in the B7-CD28 Family

Characterization of coinhibitory pathways in the B7-CD28 family has revealed mechanisms by which coinhibitory signals can limit the strength and duration of T cell responses, as well as the diverse functional consequences of these inhibitory signals on immune responses. Studies of CTLA-4 indicate that coinhibitory pathways might exert their immunoregulatory effects through both cell-intrinsic and -extrinsic mechanisms.

The dramatic phenotype of *Ctla4*^{-/-} mice provided the first indication that coinhibitory signals could regulate T cell tolerance. Further work has revealed that coinhibitory pathways can control T cell tolerance in a variety of ways. Coinhibitory pathways can regulate both the induction and maintenance of tolerance, restraining initial activation of naive self-reactive T cells and responses of potentially pathogenic effector cells. Different pathways might exert their effects at different stages (generation of T cell repertoire in the thymus, induction and maintenance of peripheral T cell tolerance) or at different sites (lymphoid versus target organs), depending on expression of the ligands and receptors.

Coinhibitory ligands can be expressed on hematopoietic and non-hematopoietic cells either constitutively or inducibly (in response to inflammatory cues), and differential expression in distinct tissue microenvironments provides a means for selective roles in tolerance. For example, CTLA-4 primarily affects early T cell priming in lymphoid organs since its B7 ligands are expressed mostly in lymphoid tissues, whereas PD-1 also can control primed T cells at a later time point in tissues where its ligands are expressed (such as pancreatic islet cells) and mediate tissue tolerance. The identification of functions for PD-L1 on non-hematopoietic cells serves as a paradigm for other B7 family members expressed on non-hematopoietic cells (Mueller et al., 2010). BTNL2, with its high expression levels in the gut, might play a role in mucosal immunity and tolerance. Understanding the tissue distribution of coinhibitory ligands has important therapeutic implications, suggesting which pathways might be modulated during different disease settings and in specific tissues during infection, cancer, or autoimmunity.

Coinhibitory pathways also can influence tolerance by controlling the generation and function of regulatory T cells. For example, CTLA-4 inhibits Treg cell expansion but also is an important mediator of Treg-cell-suppressive function. PD-1 inhibits the differentiation of T follicular regulatory cells from thymic-derived Treg cells. PD-1 limits the function of this specialized Treg cell subset that functions to inhibit T follicular helper cells, B cells, and antibody production. In addition, PD-L1, PD-L2, VISTA, and BTNL2 can induce naive T cells to become Treg cells and sustain their suppressive function. Thus, coinhibitory signals also can control T cell differentiation and cell fate.

Coinhibitory signals in B7-CD28 pathways act to limit immune-mediated tissue damage, promote resolution of inflammation, and maintain tissue integrity. The expression of coinhibitory molecules on professional APCs and non-hematopoietic cells allows fine-tuning of immune responses and regulation of immune responses locally in tissue microenvironments. For example, PD-L1 regulates the extent of inflammation and immunopathology during infectious and autoimmune diseases.

Tumors and microbes that cause chronic infections have exploited these coinhibitory pathways to evade immune defenses. Blockade of CTLA-4 and PD-1 is a promising therapeutic strategy for cancer, and agents targeting other coinhibitory pathways will soon enter the clinic. Given the roles of these pathways in T cell tolerance, this approach carries the risk of autoimmune adverse events. Combination therapies that target two coinhibitory pathways such as PD-1 and CTLA-4 can increase anti-tumor responses, but raise the likelihood of inflammatory and autoimmune adverse events, given the synergistic roles of some of these coinhibitory pathways.

The differential regulation of expression of coinhibitory molecules on different cell types within different tissue microenvironments might allow context-dependent control of immune responses and argues for a hierarchy of coinhibitory molecules that regulate different phases of the immune response. Studies of blockade of inhibitory pathways and mice lacking coinhibitory receptors or their ligands are beginning to reveal the relative roles these pathways play in controlling inflammation and tolerance. In contrast to *Ctla4*^{-/-} mice, mice lacking PD-1 or its ligands do not spontaneously develop a fatal inflammatory disease. *Vsir*^{-/-} mice develop spontaneous T cell activation and multi-organ chronic inflammation but not overt autoimmunity. However, deficiency or blockade of either PD-1 or VISTA can intensify inflammation and exacerbate autoimmunity. Combined CTLA-4 and PD-1 pathway blockade reveals that CTLA-4 and PD-1 have non-redundant functions. Similarly, studies of VISTA-PD-1 and VISTA-PD-L1 double-deficient mice reveal non-redundant roles for these pathways in regulating T cell tolerance. These findings suggest a hierarchy in which CTLA-4 has a dominant role within lymphoid organs but PD-1, VISTA, and other coinhibitory pathways have non-redundant functions in peripheral tissues. These multiple pathways orchestrate inhibitory signals that, together, fine tune T cells in different phases of protective and pathogenic immune responses.

Future Directions and Concluding Remarks

In summary, coinhibitory signals provided by pathways in the B7-CD28 family are vital for optimal immune homeostasis, pro-

TECTIVE immunity, and tolerance. These inhibitory pathways not only control the initial activation of naive T cells, but also regulate the differentiation and function of effector, memory, and regulatory T cells. These coinhibitory signals are needed to promote tolerance and resolve inflammation but can contribute to the immunosuppressive microenvironment in tumors and chronic viral infections. Advances in understanding T cell coinhibitory pathways have stimulated a new era of immunotherapy. In particular, the clinical success of checkpoint blockade with the CTLA-4 antibody Ipilimumab and the PD-1 antibodies Nivolumab and Pembrolizumab is changing cancer therapy.

Although significant progress has been made in the understanding of the immunoregulatory functions of coinhibitory pathways in the B7-CD28 family, many important questions still remain. (1) Why are there so many coinhibitory pathways? Further work is needed to understand the biological necessity for so many coinhibitory signals. Examination of the evolutionary selection of costimulatory ligands and receptors has identified “hotspots” of positive selection that confer a selective advantage to infectious challenges and mediate a balance between immune responsiveness and autoimmunity. These hotspots include the CD28 TM domain, the CD80 IgV domain, the CD86 IgC, stalk, and TM domains, and the PD-L1 and PDL2 stalk domains (Forni et al., 2013; Jones and Freeman, 2013). However, the functional significance of changes in some of these domains, such as the stalk, remains to be determined. Also important is to determine the extent to which coinhibitory pathways provide redundant or unique functions and whether there is a hierarchy in the orchestration of these signals. In particular, a better understanding of the molecular pathways triggered by coinhibitory receptors is needed to determine shared and unique signaling nodes, as well as mechanisms of synergy between coinhibitory pathways, because multiple coinhibitory receptors can be co-expressed on T cells. Therapeutic synergy could result from co-blockade on the same cell or different cells. (2) What are the functions of coinhibitory molecules in non-lymphoid organs? PD-L1, PD-L2, B7-H3, B7-H4, and HHLA-2 can be expressed on non-hematopoietic cells and tumors. Despite coexpression on hematopoietic and non-hematopoietic cells, coinhibitory ligands can be distinctly expressed in different tissue microenvironments. Temporal as well as spatial differences in ligand expression might contribute to distinct immunoregulatory functions. PD-L1 on non-hematopoietic cells can regulate tissue tolerance and PD-L1 on tumor cells can thwart anti-tumor immunity, giving impetus to studies of other B7 family members on non-hematopoietic cells in controlling pathogenic and protective immune responses in different tissue microenvironments in health and disease. (3) What are the functions of coinhibitory receptors on non-T cells? Some coinhibitory molecules, such as PD-L1 and PD-L2, have receptors on non-T cells, suggesting that these molecules might have broader immunoregulatory roles. Moreover, although coinhibitory ligands are mainly thought to exert their effects by engaging coinhibitory receptors on T cells, some receptor ligand interactions might result in bidirectional signaling with important consequences for the non T cell partner. (4) Why do the receptors for so many B7 family members remain to be identified? There are still many orphan B7 family molecules whose unidentified receptors are the key to understanding their functions. The identification of phosphatidyserine as a ligand for

TIM-1, TIM-3, and TIM-4 reminds us that not all binding partners will be proteins. In addition, it is possible that the receptors might be multi protein complexes, a potential reason why conventional approaches for identifying these receptors might not be successful. The therapeutic potential of additional understanding of T cell costimulatory pathways is underscored by the FDA approval of CTLA-4Ig for rheumatoid arthritis (Abatacept) and kidney transplant rejection (Belatacept) and of anti-CTLA-4 (Ipilimumab) and anti-PD-1 (Nivolumab and Pembrolizumab) for cancer immunotherapy.

ACKNOWLEDGMENTS

The authors would like to thank their colleagues for critical discussions. This work was supported by grants from NIH (P01AI056299 and P50CA101942 to A.H.S. and G.J.F.). G.J.F. has patents/pending royalties on the PD-1 pathway from Bristol-Myers-Squibb, Roche, Merck, EMD-Serono, Boehringer-Ingelheim, AstraZeneca, and Novartis. A.H.S. has received sponsored research support from Novartis and Roche. She has patents/pending royalties from Roche and Novartis. Because of space restrictions, we were able to cite only a fraction of the relevant literature and apologize to colleagues whose contributions might not be appropriately acknowledged in this review.

REFERENCES

Abadi, Y.M., Jeon, H., Ohaegbulam, K.C., Scanduzzi, L., Ghosh, K., Hofmeyer, K.A., Lee, J.S., Ray, A., Gravekamp, C., and Zang, X. (2013). Host b7x promotes pulmonary metastasis of breast cancer. *J. Immunol.* *190*, 3806–3814.

Agata, Y., Kawasaki, A., Nishimura, H., Ishida, Y., Tsubata, T., Yagita, H., and Honjo, T. (1996). Expression of the PD-1 antigen on the surface of stimulated mouse T and B lymphocytes. *Int. Immunol.* *8*, 765–772.

Alegre, M.L., Noel, P.J., Eisfelder, B.J., Chuang, E., Clark, M.R., Reiner, S.L., and Thompson, C.B. (1996). Regulation of surface and intracellular expression of CTLA-4 on mouse T cells. *J. Immunol.* *157*, 4762–4770.

Aloia, L., Parisi, S., Fusco, L., Pastore, L., and Russo, T. (2010). Differentiation of embryonic stem cells 1 (Dies1) is a component of bone morphogenetic protein 4 (BMP4) signaling pathway required for proper differentiation of mouse embryonic stem cells. *J. Biol. Chem.* *285*, 7776–7783.

Anderson, A., Joller, N., and Kuchroo, V. (2016). Lag-3, Tim-3, and TIGIT co-inhibitory receptors with specialized functions in immune regulation. *Immunity* *44*, this issue, 989–1004.

Anjos, S., Nguyen, A., Ounissi-Benkhalha, H., Tessier, M.C., and Polychronakos, C. (2002). A common autoimmunity predisposing signal peptide variant of the cytotoxic T-lymphocyte antigen 4 results in inefficient glycosylation of the susceptibility allele. *J. Biol. Chem.* *277*, 46478–46486.

Ansell, S.M., Lesokhin, A.M., Borrello, I., Halwani, A., Scott, E.C., Gutierrez, M., Schuster, S.J., Millenson, M.M., Cattry, D., Freeman, G.J., et al. (2015). PD-1 blockade with nivolumab in relapsed or refractory Hodgkin's lymphoma. *N. Engl. J. Med.* *372*, 311–319.

Araki, M., Chung, D., Liu, S., Rainbow, D.B., Chamberlain, G., Garner, V., Hunter, K.M., Vijaykrishnan, L., Peterson, L.B., Oukka, M., et al. (2009). Genetic evidence that the differential expression of the ligand-independent isoform of CTLA-4 is the molecular basis of the Idd5.1 type 1 diabetes region in nonobese diabetic mice. *J. Immunol.* *183*, 5146–5157.

Arnett, H.A., Escobar, S.S., Gonzalez-Suarez, E., Budelsky, A.L., Steffen, L.A., Bojani, N., Zhang, M., Siu, G., Brewer, A.W., and Viney, J.L. (2007). BTNL2, a butyrophilin/B7-like molecule, is a negative costimulatory molecule modulated in intestinal inflammation. *J. Immunol.* *178*, 1523–1533.

Attanasio, J., and Wherry, E.J. (2016). Costimulatory and coinhibitory receptor pathways in infectious disease. *Immunity* *44*, this issue, 1052–1068.

Austin, J.W., Lu, P., Majumder, P., Ahmed, R., and Boss, J.M. (2014). STAT3, STAT4, NFATc1, and CTCF regulate PD-1 through multiple novel regulatory regions in murine T cells. *J. Immunol.* *192*, 4876–4886.

Bachmann, M.F., Köhler, G., Ecabert, B., Mak, T.W., and Kopf, M. (1999). Cutting edge: lymphoproliferative disease in the absence of CTLA-4 is not T cell autonomous. *J. Immunol.* *163*, 1128–1131.

Bally, A.P., Lu, P., Tang, Y., Austin, J.W., Scharer, C.D., Ahmed, R., and Boss, J.M. (2015). NF- κ B regulates PD-1 expression in macrophages. *J. Immunol.* *194*, 4545–4554.

Bour-Jordan, H., Grogan, J.L., Tang, Q., Auger, J.A., Locksley, R.M., and Bluestone, J.A. (2003). CTLA-4 regulates the requirement for cytokine-induced signals in T(H)2 lineage commitment. *Nat. Immunol.* *4*, 182–188.

Bretscher, P., and Cohn, M. (1970). A theory of self-nonself discrimination. *Science* *169*, 1042–1049.

Brunet, J.F., Denizot, F., Luciani, M.F., Roux-Dosseto, M., Suzan, M., Mattei, M.G., and Golstein, P. (1987). A new member of the immunoglobulin superfamily—CTLA-4. *Nature* *328*, 267–270.

Butte, M.J., Keir, M.E., Phamduy, T.B., Sharpe, A.H., and Freeman, G.J. (2007). Programmed death-1 ligand 1 interacts specifically with the B7-1 costimulatory molecule to inhibit T cell responses. *Immunity* *27*, 111–122.

Callahan, M.K., Postow, M.A., and Wolchok, J.D. (2016). Targeting T cell co-receptors for cancer therapy. *Immunity* *44*, this issue, 1069–1078.

Ceeraz, S., Nowak, E.C., and Noelle, R.J. (2013). B7 family checkpoint regulators in immune regulation and disease. *Trends Immunol.* *34*, 556–563.

Chang, W.S., Kim, J.Y., Kim, Y.J., Kim, Y.S., Lee, J.M., Azuma, M., Yagita, H., and Kang, C.Y. (2008). Cutting edge: Programmed death-1/programmed death ligand 1 interaction regulates the induction and maintenance of invariant NKT cell anergy. *J. Immunol.* *181*, 6707–6710.

Chang, C.H., Curtis, J.D., Maggi, L.B., Jr., Faubert, B., Villarino, A.V., O'Sullivan, D., Huang, S.C., van der Windt, G.J., Blagih, J., Qiu, J., et al. (2013). Posttranscriptional control of T cell effector function by aerobic glycolysis. *Cell* *153*, 1239–1251.

Chang, C.H., Qiu, J., O'Sullivan, D., Buck, M.D., Noguchi, T., Curtis, J.D., Chen, Q., Gindin, M., Gubin, M.M., van der Windt, G.J., et al. (2015). Metabolic competition in the tumor microenvironment is a driver of cancer progression. *Cell* *162*, 1229–1241.

Chapoval, A.I., Ni, J., Lau, J.S., Wilcox, R.A., Flies, D.B., Liu, D., Dong, H., Sica, G.L., Zhu, G., Tamada, K., and Chen, L. (2001). B7-H3: a costimulatory molecule for T cell activation and IFN- γ production. *Nat. Immunol.* *2*, 269–274.

Chattopadhyay, G., and Shevach, E.M. (2013). Antigen-specific induced T regulatory cells impair dendritic cell function via an IL-10/MARCH1-dependent mechanism. *J. Immunol.* *191*, 5875–5884.

Chemnitz, J.M., Parry, R.V., Nichols, K.E., June, C.H., and Riley, J.L. (2004). SHP-1 and SHP-2 associate with immunoreceptor tyrosine-based switch motif of programmed death 1 upon primary human T cell stimulation, but only receptor ligation prevents T cell activation. *J. Immunol.* *173*, 945–954.

Chen, X., Zhang, G., Li, Y., Feng, X., Wan, F., Zhang, L., Wang, J., and Zhang, X. (2009). Circulating B7-H3(CD276) elevations in cerebrospinal fluid and plasma of children with bacterial meningitis. *J. Mol. Neurosci.* *37*, 86–94.

Chen, L., Gibbons, D.L., Goswami, S., Cortez, M.A., Ahn, Y.H., Byers, L.A., Zhang, X., Yi, X., Dwyer, D., Lin, W., et al. (2014). Metastasis is regulated via microRNA-200/ZEB1 axis control of tumour cell PD-L1 expression and intratumoral immunosuppression. *Nat. Commun.* *5*, 5241.

Cheng, L., Jiang, J., Gao, R., Wei, S., Nan, F., Li, S., and Kong, B. (2009). B7-H4 expression promotes tumorigenesis in ovarian cancer. *Int. J. Gynecol. Cancer* *19*, 1481–1486.

Cho, H.Y., Lee, S.W., Seo, S.K., Choi, I.W., Choi, I., and Lee, S.W. (2008). Interferon-sensitive response element (ISRE) is mainly responsible for IFN- α -induced upregulation of programmed death-1 (PD-1) in macrophages. *Biochim. Biophys. Acta* *1779*, 811–819.

Choi, I.H., Zhu, G., Sica, G.L., Strome, S.E., Cheville, J.C., Lau, J.S., Zhu, Y., Flies, D.B., Tamada, K., and Chen, L. (2003). Genomic organization and expression analysis of B7-H4, an immune inhibitory molecule of the B7 family. *J. Immunol.* *171*, 4650–4654.

Chuang, E., Fisher, T.S., Morgan, R.W., Robbins, M.D., Duerr, J.M., Vander Heiden, M.G., Gardner, J.P., Hambor, J.E., Neveu, M.J., and Thompson,

- C.B. (2000). The CD28 and CTLA-4 receptors associate with the serine/threonine phosphatase PP2A. *Immunity* 13, 313–322.
- Collins, A.V., Brodie, D.W., Gilbert, R.J., Iaboni, A., Manso-Sancho, R., Walse, B., Stuart, D.I., van der Merwe, P.A., and Davis, S.J. (2002). The interaction properties of costimulatory molecules revisited. *Immunity* 17, 201–210.
- Collins, M., Ling, V., and Carreno, B.M. (2005). The B7 family of immune-regulatory ligands. *Genome Biol.* 6, 223.
- Corse, E., and Allison, J.P. (2012). Cutting edge: CTLA-4 on effector T cells inhibits in trans. *J. Immunol.* 189, 1123–1127.
- Cunningham, A.J., and Lafferty, K.J. (1977). A simple conservative explanation of the H-2 restriction of interactions between lymphocytes. *Scand. J. Immunol.* 6, 1–6.
- Dariavach, P., Mattéi, M.G., Golstein, P., and Lefranc, M.P. (1988). Human Ig superfamily CTLA-4 gene: chromosomal localization and identity of protein sequence between murine and human CTLA-4 cytoplasmic domains. *Eur. J. Immunol.* 18, 1901–1905.
- de Jong, V.M., Zaldumbide, A., van der Slik, A.R., Persengiev, S.P., Roep, B.O., and Koeleman, B.P. (2013). Post-transcriptional control of candidate risk genes for type 1 diabetes by rare genetic variants. *Genes Immun.* 14, 58–61.
- Deichmann, K., Heinzmann, A., Brüngenolte, E., Forster, J., and Kuehr, J. (1996). An Mse I RFLP in the human CTLA4 promoter. *Biochem. Biophys. Res. Commun.* 225, 817–818.
- Dong, H., Strome, S.E., Salomao, D.R., Tamura, H., Hirano, F., Flies, D.B., Roche, P.C., Lu, J., Zhu, G., Tamada, K., et al. (2002). Tumor-associated B7-H1 promotes T-cell apoptosis: a potential mechanism of immune evasion. *Nat. Med.* 8, 793–800.
- Donner, H., Rau, H., Walfish, P.G., Braun, J., Siegmund, T., Finke, R., Herwig, J., Usadel, K.H., and Badenhop, K. (1997). CTLA4 alanine-17 confers genetic susceptibility to Graves' disease and to type 1 diabetes mellitus. *J. Clin. Endocrinol. Metab.* 82, 143–146.
- Eppihimer, M.J., Gunn, J., Freeman, G.J., Greenfield, E.A., Chernova, T., Erickson, J., and Leonard, J.P. (2002). Expression and regulation of the PD-L1 immunoinhibitory molecule on microvascular endothelial cells. *Microcirculation* 9, 133–145.
- Esensten, J.H., Helou, Y.A., Chopra, G., Weiss, A., and Bluestone, J.A. (2016). CD28 costimulation: from mechanism to therapy. *Immunity* 44, this issue, 973–988.
- Esposito, L., Hunter, K.M., Clark, J., Rainbow, D.B., Stevens, H., Denesha, J., Duley, S., Dawson, S., Coleman, G., Nutland, S., et al. (2014). Investigation of soluble and transmembrane CTLA-4 isoforms in serum and microvesicles. *J. Immunol.* 193, 889–900.
- Fallarino, F., Grohmann, U., Hwang, K.W., Orabona, C., Vacca, C., Bianchi, R., Belladonna, M.L., Fioretti, M.C., Alegre, M.L., and Puccetti, P. (2003). Modulation of tryptophan catabolism by regulatory T cells. *Nat. Immunol.* 4, 1206–1212.
- Fife, B.T., Pauken, K.E., Eagar, T.N., Obu, T., Wu, J., Tang, Q., Azuma, M., Krummel, M.F., and Bluestone, J.A. (2009). Interactions between PD-1 and PD-L1 promote tolerance by blocking the TCR-induced stop signal. *Nat. Immunol.* 10, 1185–1192.
- Finn, P.W., He, H., Wang, Y., Wang, Z., Guan, G., Listman, J., and Perkins, D.L. (1997). Synergistic induction of CTLA-4 expression by costimulation with TCR plus CD28 signals mediated by increased transcription and messenger ribonucleic acid stability. *J. Immunol.* 158, 4074–4081.
- Flies, D.B., Wang, S., Xu, H., and Chen, L. (2011). Cutting edge: A monoclonal antibody specific for the programmed death-1 homolog prevents graft-versus-host disease in mouse models. *J. Immunol.* 187, 1537–1541.
- Flies, D.B., Han, X., Higuchi, T., Zheng, L., Sun, J., Ye, J.J., and Chen, L. (2014). Coinhibitory receptor PD-1H preferentially suppresses CD4⁺ T cell-mediated immunity. *J. Clin. Invest.* 124, 1966–1975.
- Ford, M.L. (2016). T cell cosignaling molecules in transplantation. *Immunity* 44, this issue, 1020–1033.
- Forni, D., Cagliani, R., Pozzoli, U., Colleoni, M., Riva, S., Biasin, M., Filippi, G., De Gioia, L., Gnudi, F., Comi, G.P., et al. (2013). A 175 million year history of T cell regulatory molecules reveals widespread selection, with adaptive evolution of disease alleles. *Immunity* 38, 1129–1141.
- Francisco, L.M., Salinas, V.H., Brown, K.E., Vanguri, V.K., Freeman, G.J., Kuchroo, V.K., and Sharpe, A.H. (2009). PD-L1 regulates the development, maintenance, and function of induced regulatory T cells. *J. Exp. Med.* 206, 3015–3029.
- Freeman, G.J., Lombard, D.B., Gimmi, C.D., Brod, S.A., Lee, K., Laning, J.C., Hafler, D.A., Dorf, M.E., Gray, G.S., Reiser, H., et al. (1992). CTLA-4 and CD28 mRNA are coexpressed in most T cells after activation. Expression of CTLA-4 and CD28 mRNA does not correlate with the pattern of lymphokine production. *J. Immunol.* 149, 3795–3801.
- Frigola, X., Inman, B.A., Lohse, C.M., Krco, C.J., Chevillat, J.C., Thompson, R.H., Leibovich, B., Blute, M.L., Dong, H., and Kwon, E.D. (2011). Identification of a soluble form of B7-H1 that retains immunosuppressive activity and is associated with aggressive renal cell carcinoma. *Clin. Cancer Res.* 17, 1915–1923.
- Gerold, K.D., Zheng, P., Rainbow, D.B., Zernecke, A., Wicker, L.S., and Kissler, S. (2011). The soluble CTLA-4 splice variant protects from type 1 diabetes and potentiates regulatory T-cell function. *Diabetes* 60, 1955–1963.
- Gibson, H.M., Hedgcock, C.J., Aufiero, B.M., Wilson, A.J., Hafner, M.S., Tsokos, G.C., and Wong, H.K. (2007). Induction of the CTLA-4 gene in human lymphocytes is dependent on NFAT binding the proximal promoter. *J. Immunol.* 179, 3831–3840.
- Gong, A.Y., Zhou, R., Hu, G., Li, X., Splinter, P.L., O'Hara, S.P., LaRusso, N.F., Soukup, G.A., Dong, H., and Chen, X.M. (2009). MicroRNA-513 regulates B7-H1 translation and is involved in IFN- γ -induced B7-H1 expression in cholangiocytes. *J. Immunol.* 182, 1325–1333.
- Grohmann, U., Orabona, C., Fallarino, F., Vacca, C., Calcinaro, F., Falorni, A., Candeloro, P., Belladonna, M.L., Bianchi, R., Fioretti, M.C., and Puccetti, P. (2002). CTLA-4-Ig regulates tryptophan catabolism in vivo. *Nat. Immunol.* 3, 1097–1101.
- Hamanishi, J., Mandai, M., Iwasaki, M., Okazaki, T., Tanaka, Y., Yamaguchi, K., Higuchi, T., Yagi, H., Takakura, K., Minato, N., et al. (2007). Programmed cell death 1 ligand 1 and tumor-infiltrating CD8⁺ T lymphocytes are prognostic factors of human ovarian cancer. *Proc. Natl. Acad. Sci. USA* 104, 3360–3365.
- Han, Y., Chen, Z., Yang, Y., Jiang, Z., Gu, Y., Liu, Y., Lin, C., Pan, Z., Yu, Y., Jiang, M., et al. (2014). Human CD14⁺ CTLA-4⁺ regulatory dendritic cells suppress T-cell response by cytotoxic T-lymphocyte antigen-4-dependent IL-10 and indoleamine-2,3-dioxygenase production in hepatocellular carcinoma. *Hepatology* 59, 567–579.
- Harper, K., Balzano, C., Rouvier, E., Mattéi, M.G., Luciani, M.F., and Golstein, P. (1991). CTLA-4 and CD28 activated lymphocyte molecules are closely related in both mouse and human as to sequence, message expression, gene structure, and chromosomal location. *J. Immunol.* 147, 1037–1044.
- Hashiguchi, M., Kobori, H., Ritprajak, P., Kamimura, Y., Kozono, H., and Azuma, M. (2008). Triggering receptor expressed on myeloid cell-like transcript 2 (TLT-2) is a counter-receptor for B7-H3 and enhances T cell responses. *Proc. Natl. Acad. Sci. USA* 105, 10495–10500.
- He, X.H., Xu, L.H., and Liu, Y. (2005). Identification of a novel splice variant of human PD-L1 mRNA encoding an isoform-lacking IgV-like domain. *Acta Pharmacol. Sin.* 26, 462–468.
- Hodi, F.S., O'Day, S.J., McDermott, D.F., Weber, R.W., Sosman, J.A., Haanen, J.B., Gonzalez, R., Robert, C., Schadendorf, D., Hassel, J.C., et al. (2010). Improved survival with ipilimumab in patients with metastatic melanoma. *N. Engl. J. Med.* 363, 711–723.
- Iida, T., Ohno, H., Nakaseko, C., Sakuma, M., Takeda-Ezaki, M., Arase, H., Komiyama, E., Fujisawa, T., and Saito, T. (2000). Regulation of cell surface expression of CTLA-4 by secretion of CTLA-4-containing lysosomes upon activation of CD4⁺ T cells. *J. Immunol.* 165, 5062–5068.
- Ise, W., Kohyama, M., Nutsch, K.M., Lee, H.M., Suri, A., Unanue, E.R., Murphy, T.L., and Murphy, K.M. (2010). CTLA-4 suppresses the pathogenicity of self antigen-specific T cells by cell-intrinsic and cell-extrinsic mechanisms. *Nat. Immunol.* 11, 129–135.
- Ishida, Y., Agata, Y., Shibahara, K., and Honjo, T. (1992). Induced expression of PD-1, a novel member of the immunoglobulin gene superfamily, upon programmed cell death. *EMBO J.* 11, 3887–3895.

- Janakiram, M., Chinai, J.M., Fineberg, S., Fiser, A., Montagna, C., Medavaram, R., Castano, E., Jeon, H., Ohaegbulam, K.C., Zhao, R., et al. (2015). Expression, clinical significance, and receptor identification of the newest B7 family member HHLA2 protein. *Clin. Cancer Res.* *21*, 2359–2366.
- Jones, J.C., and Freeman, G.J. (2013). Costimulatory genes: hotspots of conflict between host defense and autoimmunity. *Immunity* *38*, 1083–1085.
- Kaku, H., and Rothstein, T.L. (2010). Octamer binding protein 2 (Oct2) regulates PD-L2 gene expression in B-1 cells through lineage-specific activity of a unique, intronic promoter. *Genes Immun.* *11*, 55–66.
- Kao, C., Oestreich, K.J., Paley, M.A., Crawford, A., Angelosanto, J.M., Ali, M.A., Intlekofer, A.M., Boss, J.M., Reiner, S.L., Weinmann, A.S., and Wherry, E.J. (2011). Transcription factor T-bet represses expression of the inhibitory receptor PD-1 and sustains virus-specific CD8+ T cell responses during chronic infection. *Nat. Immunol.* *12*, 663–671.
- Kaufman, K.A., Bowen, J.A., Tsai, A.F., Bluestone, J.A., Hunt, J.S., and Ober, C. (1999). The CTLA-4 gene is expressed in placental fibroblasts. *Mol. Hum. Reprod.* *5*, 84–87.
- Kong, K.F., Fu, G., Zhang, Y., Yokosuka, T., Casas, J., Canonigo-Balancio, A.J., Becart, S., Kim, G., Yates, J.R., 3rd, Kronenberg, M., et al. (2014). Protein kinase C- η controls CTLA-4-mediated regulatory T cell function. *Nat. Immunol.* *15*, 465–472.
- Kowalczyk, A., D'Souza, C.A., and Zhang, L. (2014). Cell-extrinsic CTLA4-mediated regulation of dendritic cell maturation depends on STAT3. *Eur. J. Immunol.* *44*, 1143–1155.
- Krambeck, A.E., Thompson, R.H., Dong, H., Lohse, C.M., Park, E.S., Kuntz, S.M., Leibovich, B.C., Blute, M.L., Cheville, J.C., and Kwon, E.D. (2006). B7-H4 expression in renal cell carcinoma and tumor vasculature: associations with cancer progression and survival. *Proc. Natl. Acad. Sci. USA* *103*, 10391–10396.
- Kristiansen, O.P., Larsen, Z.M., and Pociot, F. (2000). CTLA-4 in autoimmune diseases—a general susceptibility gene to autoimmunity? *Genes Immun.* *1*, 170–184.
- Kroner, A., Mehling, M., Hemmer, B., Rieckmann, P., Toyka, K.V., Mäurer, M., and Wiendl, H. (2005). A PD-1 polymorphism is associated with disease progression in multiple sclerosis. *Ann. Neurol.* *58*, 50–57.
- Kryczek, I., Wei, S., Zou, L., Zhu, G., Mottram, P., Xu, H., Chen, L., and Zou, W. (2006a). Cutting edge: induction of B7-H4 on APCs through IL-10: novel suppressive mode for regulatory T cells. *J. Immunol.* *177*, 40–44.
- Kryczek, I., Zou, L., Rodriguez, P., Zhu, G., Wei, S., Mottram, P., Brumlik, M., Cheng, P., Curiel, T., Myers, L., et al. (2006b). B7-H4 expression identifies a novel suppressive macrophage population in human ovarian carcinoma. *J. Exp. Med.* *203*, 871–881.
- Kuehn, H.S., Ouyang, W., Lo, B., Deenick, E.K., Niemela, J.E., Avery, D.T., Schickel, J.N., Tran, D.Q., Stoddard, J., Zhang, Y., et al. (2014). Immune dysregulation in human subjects with heterozygous germline mutations in CTLA4. *Science* *345*, 1623–1627.
- Lafferty, K.J., and Cunningham, A.J. (1975). A new analysis of allogeneic interactions. *Aust. J. Exp. Biol. Med. Sci.* *53*, 27–42.
- Laurent, S., Carrega, P., Saverino, D., Piccioli, P., Camoriano, M., Morabito, A., Dozin, B., Fontana, V., Simone, R., Mortara, L., et al. (2010). CTLA-4 is expressed by human monocyte-derived dendritic cells and regulates their functions. *Hum. Immunol.* *71*, 934–941.
- Leitner, J., Klauser, C., Pickl, W.F., Stöckl, J., Majdic, O., Bardet, A.F., Kreil, D.P., Dong, C., Yamazaki, T., Zlabinger, G., et al. (2009). B7-H3 is a potent inhibitor of human T-cell activation: No evidence for B7-H3 and TREM2 interaction. *Eur. J. Immunol.* *39*, 1754–1764.
- Lindsten, T., Lee, K.P., Harris, E.S., Petryniak, B., Craighead, N., Reynolds, P.J., Lombard, D.B., Freeman, G.J., Nadler, L.M., Gray, G.S., et al. (1993). Characterization of CTLA-4 structure and expression on human T cells. *J. Immunol.* *151*, 3489–3499.
- Lines, J.L., Pantazi, E., Mak, J., Sempere, L.F., Wang, L., O'Connell, S., Ceeraz, S., Suriawinata, A.A., Yan, S., Ernstoff, M.S., and Noelle, R. (2014). VISTA is an immune checkpoint molecule for human T cells. *Cancer Res.* *74*, 1924–1932.
- Ling, V., Munroe, R.C., Murphy, E.A., and Gray, G.S. (1998). Embryonic stem cells and embryoid bodies express lymphocyte costimulatory molecules. *Exp. Cell Res.* *247*, 55–65.
- Linsley, P.S., Brady, W., Urnes, M., Grosmaire, L.S., Damle, N.K., and Ledbetter, J.A. (1991). CTLA-4 is a second receptor for the B cell activation antigen B7. *J. Exp. Med.* *174*, 561–569.
- Linsley, P.S., Greene, J.L., Tan, P., Bradshaw, J., Ledbetter, J.A., Anasetti, C., and Damle, N.K. (1992). Coexpression and functional cooperation of CTLA-4 and CD28 on activated T lymphocytes. *J. Exp. Med.* *176*, 1595–1604.
- Linsley, P.S., Nadler, S.G., Bajorath, J., Peach, R., Leung, H.T., Rogers, J., Bradshaw, J., Stebbins, M., Leytze, G., Brady, W., et al. (1995). Binding stoichiometry of the cytotoxic T lymphocyte-associated molecule-4 (CTLA-4). A disulfide-linked homodimer binds two CD86 molecules. *J. Biol. Chem.* *270*, 15417–15424.
- Linsley, P.S., Bradshaw, J., Greene, J., Peach, R., Bennett, K.L., and Mittler, R.S. (1996). Intracellular trafficking of CTLA-4 and focal localization towards sites of TCR engagement. *Immunity* *4*, 535–543.
- Liu, Y., Yu, Y., Yang, S., Zeng, B., Zhang, Z., Jiao, G., Zhang, Y., Cai, L., and Yang, R. (2009). Regulation of arginase I activity and expression by both PD-1 and CTLA-4 on the myeloid-derived suppressor cells. *Cancer Immunol. Immunother.* *58*, 687–697.
- Liu, S.M., Sutherland, A.P., Zhang, Z., Rainbow, D.B., Quintana, F.J., Patterson, A.M., Sharpe, A.H., Oukka, M., Wicker, L.S., and Kuchroo, V.K. (2012). Overexpression of the Ctl α -4 isoform lacking exons 2 and 3 causes autoimmunity. *J. Immunol.* *188*, 155–162.
- Liu, Y., Carlsson, R., Comabella, M., Wang, J., Kosicki, M., Carrion, B., Hasan, M., Wu, X., Montalban, X., Dziegiel, M.H., et al. (2014). FoxA1 directs the lineage and immunosuppressive properties of a novel regulatory T cell population in EAE and MS. *Nat. Med.* *20*, 272–282.
- Liu, J., Yuan, Y., Chen, W., Putra, J., Suriawinata, A.A., Schenk, A.D., Miller, H.E., Guleria, I., Barth, R.J., Huang, Y.H., and Wang, L. (2015). Immune-checkpoint proteins VISTA and PD-1 nonredundantly regulate murine T-cell responses. *Proc. Natl. Acad. Sci. USA* *112*, 6682–6687.
- Lo, B., Zhang, K., Lu, W., Zheng, L., Zhang, Q., Kanellopoulou, C., Zhang, Y., Liu, Z., Fritz, J.M., Marsh, R., et al. (2015). AUTOIMMUNE DISEASE. Patients with LRBA deficiency show CTLA4 loss and immune dysregulation responsive to abatacept therapy. *Science* *349*, 436–440.
- Loke, P., and Allison, J.P. (2003). PD-L1 and PD-L2 are differentially regulated by Th1 and Th2 cells. *Proc. Natl. Acad. Sci. USA* *100*, 5336–5341.
- Loos, M., Hedderich, D.M., Friess, H., and Kleeff, J. (2010). B7-h3 and its role in antitumor immunity. *Clin. Dev. Immunol.* *2010*, 683875.
- Lu, P., Youngblood, B.A., Austin, J.W., Mohammed, A.U., Butler, R., Ahmed, R., and Boss, J.M. (2014). Blimp-1 represses CD8 T cell expression of PD-1 using a feed-forward transcriptional circuit during acute viral infection. *J. Exp. Med.* *211*, 515–527.
- Luo, L., Chapoval, A.I., Flies, D.B., Zhu, G., Hirano, F., Wang, S., Lau, J.S., Dong, H., Tamada, K., Flies, A.S., et al. (2004). B7-H3 enhances tumor immunity in vivo by costimulating rapid clonal expansion of antigen-specific CD8+ cytolytic T cells. *J. Immunol.* *173*, 5445–5450.
- Mager, D.L., Hunter, D.G., Schertzer, M., and Freeman, J.D. (1999). Endogenous retroviruses provide the primary polyadenylation signal for two new human genes (HHLA2 and HHLA3). *Genomics* *59*, 255–263.
- Magistrelli, G., Jeannin, P., Herbault, N., Benoit De Coignac, A., Gauchat, J.F., Bonnefoy, J.Y., and Delneste, Y. (1999). A soluble form of CTLA-4 generated by alternative splicing is expressed by nonstimulated human T cells. *Eur. J. Immunol.* *29*, 3596–3602.
- Malquori, L., Carsetti, L., and Ruberti, G. (2008). The 3' UTR of the human CTLA4 mRNA can regulate mRNA stability and translational efficiency. *Biochim. Biophys. Acta* *1779*, 60–65.
- Mathieu, M., Cotta-Grand, N., Daudelin, J.F., Thébaud, P., and Labrecque, N. (2013). Notch signaling regulates PD-1 expression during CD8(+) T-cell activation. *Immunol. Cell Biol.* *91*, 82–88.
- Mead, K.I., Zheng, Y., Manzotti, C.N., Perry, L.C., Liu, M.K., Burke, F., Powner, D.J., Wakelam, M.J., and Sansom, D.M. (2005). Exocytosis of CTLA-4 is

- dependent on phospholipase D and ADP ribosylation factor-1 and stimulated during activation of regulatory T cells. *J. Immunol.* **174**, 4803–4811.
- Metzler, W.J., Bajorath, J., Fenderson, W., Shaw, S.Y., Constantine, K.L., Naemura, J., Leytze, G., Peach, R.J., Lavoie, T.B., Mueller, L., and Linsley, P.S. (1997). Solution structure of human CTLA-4 and delineation of a CD80/CD86 binding site conserved in CD28. *Nat. Struct. Biol.* **4**, 527–531.
- Michalek, R.D., Gerriets, V.A., Jacobs, S.R., Macintyre, A.N., MacIver, N.J., Mason, E.F., Sullivan, S.A., Nichols, A.G., and Rathmell, J.C. (2011). Cutting edge: distinct glycolytic and lipid oxidative metabolic programs are essential for effector and regulatory CD4+ T cell subsets. *J. Immunol.* **186**, 3299–3303.
- Miller, R.E., Fayen, J.D., Mohammad, S.F., Stein, K., Kadereit, S., Woods, K.D., Sramkoski, R.M., Jacobberger, J.W., Templeton, D., Shurin, S.B., and Laughlin, M.J. (2002). Reduced CTLA-4 protein and messenger RNA expression in umbilical cord blood T lymphocytes. *Exp. Hematol.* **30**, 738–744.
- Mueller, S.N., Vanguri, V.K., Ha, S.J., West, E.E., Keir, M.E., Glickman, J.N., Sharpe, A.H., and Ahmed, R. (2010). PD-L1 has distinct functions in hematopoietic and nonhematopoietic cells in regulating T cell responses during chronic infection in mice. *J. Clin. Invest.* **120**, 2508–2515.
- Munn, D.H., Shafiqzadeh, E., Attwood, J.T., Bondarev, I., Pashine, A., and Mellor, A.L. (1999). Inhibition of T cell proliferation by macrophage tryptophan catabolism. *J. Exp. Med.* **189**, 1363–1372.
- Nguyen, T., Liu, X.K., Zhang, Y., and Dong, C. (2006). BTNL2, a butyrophilin-like molecule that functions to inhibit T cell activation. *J. Immunol.* **176**, 7354–7360.
- Nielsen, C., Ohm-Laursen, L., Barington, T., Husby, S., and Lillevang, S.T. (2005). Alternative splice variants of the human PD-1 gene. *Cell. Immunol.* **235**, 109–116.
- Nishimura, H., Agata, Y., Kawasaki, A., Sato, M., Imamura, S., Minato, N., Yagita, H., Nakano, T., and Honjo, T. (1996). Developmentally regulated expression of the PD-1 protein on the surface of double-negative (CD4-CD8-) thymocytes. *Int. Immunol.* **8**, 773–780.
- Nisticò, L., Buzzetti, R., Pritchard, L.E., Van der Auwera, B., Giovannini, C., Bosi, E., Larrad, M.T., Rios, M.S., Chow, C.C., Cockram, C.S., et al. (1996). The CTLA-4 gene region of chromosome 2q33 is linked to, and associated with, type 1 diabetes. *Belgian Diabetes Registry. Hum. Mol. Genet.* **5**, 1075–1080.
- Nomi, T., Sho, M., Akahori, T., Hamada, K., Kubo, A., Kanehiro, H., Nakamura, S., Enomoto, K., Yagita, H., Azuma, M., and Nakajima, Y. (2007). Clinical significance and therapeutic potential of the programmed death-1 ligand/programmed death-1 pathway in human pancreatic cancer. *Clin. Cancer Res.* **13**, 2151–2157.
- Nurieva, R., Thomas, S., Nguyen, T., Martin-Orozco, N., Wang, Y., Kaja, M.K., Yu, X.Z., and Dong, C. (2006). T-cell tolerance or function is determined by combinatorial costimulatory signals. *EMBO J.* **25**, 2623–2633.
- Oaks, M.K., Hallett, K.M., Penwell, R.T., Stauber, E.C., Warren, S.J., and Tector, A.J. (2000). A native soluble form of CTLA-4. *Cell. Immunol.* **207**, 144–153.
- Oestreich, K.J., Yoon, H., Ahmed, R., and Boss, J.M. (2008). NFATc1 regulates PD-1 expression upon T cell activation. *J. Immunol.* **181**, 4832–4839.
- Ohigashi, Y., Sho, M., Yamada, Y., Tsurui, Y., Hamada, K., Ikeda, N., Mizuno, T., Yoriki, R., Kashizuka, H., Yane, K., et al. (2005). Clinical significance of programmed death-1 ligand-1 and programmed death-1 ligand-2 expression in human esophageal cancer. *Clin. Cancer Res.* **11**, 2947–2953.
- Okazaki, T., Maeda, A., Nishimura, H., Kurosaki, T., and Honjo, T. (2001). PD-1 immunoreceptor inhibits B cell receptor-mediated signaling by recruiting src homology 2-domain-containing tyrosine phosphatase 2 to phosphotyrosine. *Proc. Natl. Acad. Sci. USA* **98**, 13866–13871.
- Ostrov, D.A., Shi, W., Schwartz, J.C., Almo, S.C., and Nathenson, S.G. (2000). Structure of murine CTLA-4 and its role in modulating T cell responsiveness. *Science* **290**, 816–819.
- Parry, R.V., Chemnitz, J.M., Frauwirth, K.A., Lanfranco, A.R., Braunstein, I., Kobayashi, S.V., Linsley, P.S., Thompson, C.B., and Riley, J.L. (2005). CTLA-4 and PD-1 receptors inhibit T-cell activation by distinct mechanisms. *Mol. Cell. Biol.* **25**, 9543–9553.
- Paterson, A.M., Lovitch, S.B., Sage, P.T., Juneja, V.R., Lee, Y., Trombly, J.D., Arancibia-Carcamo, C.V., Sobel, R.A., Rudensky, A.Y., Kuchroo, V.K., et al. (2015). Deletion of CTLA-4 on regulatory T cells during adulthood leads to resistance to autoimmunity. *J. Exp. Med.* **212**, 1603–1621.
- Patsoukis, N., Brown, J., Petkova, V., Liu, F., Li, L., and Boussiotis, V.A. (2012). Selective effects of PD-1 on Akt and Ras pathways regulate molecular components of the cell cycle and inhibit T cell proliferation. *Sci. Signal.* **5**, ra46.
- Patsoukis, N., Li, L., Sari, D., Petkova, V., and Boussiotis, V.A. (2013). PD-1 increases PTEN phosphatase activity while decreasing PTEN protein stability by inhibiting casein kinase 2. *Mol. Cell. Biol.* **33**, 3091–3098.
- Patsoukis, N., Bardhan, K., Chatterjee, P., Sari, D., Liu, B., Bell, L.N., Karoly, E.D., Freeman, G.J., Petkova, V., Seth, P., et al. (2015). PD-1 alters T-cell metabolic reprogramming by inhibiting glycolysis and promoting lipolysis and fatty acid oxidation. *Nat. Commun.* **6**, 6692.
- Pérez-García, A., Osca, G., Bosch-Vizcaya, A., Kelleher, N., Santos, N.Y., Rodríguez, R., González, Y., Roncero, J.M., Coll, R., Serrando, M., et al. (2013). Kinetics of the CTLA-4 isoforms expression after T-lymphocyte activation and role of the promoter polymorphisms on CTLA-4 gene transcription. *Hum. Immunol.* **74**, 1219–1224.
- Petrovas, C., Casazza, J.P., Brenchley, J.M., Price, D.A., Gostick, E., Adams, W.C., Precopio, M.L., Schacker, T., Roederer, M., Douek, D.C., and Koup, R.A. (2006). PD-1 is a regulator of virus-specific CD8+ T cell survival in HIV infection. *J. Exp. Med.* **203**, 2281–2292.
- Pioli, C., Gatta, L., Ubaldi, V., and Doria, G. (2000). Inhibition of IgG1 and IgE production by stimulation of the B cell CTLA-4 receptor. *J. Immunol.* **165**, 5530–5536.
- Pistillo, M.P., Tazzari, P.L., Palmisano, G.L., Pierri, I., Bolognesi, A., Ferlito, F., Capanni, P., Polito, L., Ratta, M., Pileri, S., et al. (2003). CTLA-4 is not restricted to the lymphoid cell lineage and can function as a target molecule for apoptosis induction of leukemic cells. *Blood* **101**, 202–209.
- Polanczyk, M.J., Hopke, C., Vandenbark, A.A., and Offner, H. (2006). Estrogen-mediated immunomodulation involves reduced activation of effector T cells, potentiation of Treg cells, and enhanced expression of the PD-1 costimulatory pathway. *J. Neurosci. Res.* **84**, 370–378.
- Prasad, D.V., Nguyen, T., Li, Z., Yang, Y., Duong, J., Wang, Y., and Dong, C. (2004). Murine B7-H3 is a negative regulator of T cells. *J. Immunol.* **173**, 2500–2506.
- Prokunina, L., Castillejo-López, C., Oberg, F., Gunnarsson, I., Berg, L., Magnusson, V., Brookes, A.J., Tentler, D., Kristjansdóttir, H., Gröndal, G., et al. (2002). A regulatory polymorphism in PDCD1 is associated with susceptibility to systemic lupus erythematosus in humans. *Nat. Genet.* **32**, 666–669.
- Qureshi, O.S., Zheng, Y., Nakamura, K., Attridge, K., Manzotti, C., Schmidt, E.M., Baker, J., Jeffery, L.E., Kaur, S., Briggs, Z., et al. (2011). Trans-endocytosis of CD80 and CD86: a molecular basis for the cell-extrinsic function of CTLA-4. *Science* **332**, 600–603.
- Qureshi, O.S., Kaur, S., Hou, T.Z., Jeffery, L.E., Poulter, N.S., Briggs, Z., Kenefick, R., Wilcox, A.K., Royle, S.J., Rappoport, J.Z., and Sansom, D.M. (2012). Constitutive clathrin-mediated endocytosis of CTLA-4 persists during T cell activation. *J. Biol. Chem.* **287**, 9429–9440.
- Robert, C., Thomas, L., Bondarenko, I., O'Day, S., Weber, J., Garbe, C., Lebbe, C., Baurain, J.F., Testori, A., Grob, J.J., et al. (2011). Ipilimumab plus dacarbazine for previously untreated metastatic melanoma. *N. Engl. J. Med.* **364**, 2517–2526.
- Sage, P.T., Paterson, A.M., Lovitch, S.B., and Sharpe, A.H. (2014). The coinhibitory receptor CTLA-4 controls B cell responses by modulating T follicular helper, T follicular regulatory, and T regulatory cells. *Immunity* **41**, 1026–1039.
- Sakr, M.A., Takino, T., Domoto, T., Nakano, H., Wong, R.W., Sasaki, M., Nakanuma, Y., and Sato, H. (2010). Gl24 enhances tumor invasiveness by regulating cell surface membrane-type 1 matrix metalloproteinase. *Cancer Sci.* **101**, 2368–2374.
- Sakuishi, K., Ngiew, S.F., Sullivan, J.M., Teng, M.W., Kuchroo, V.K., Smyth, M.J., and Anderson, A.C. (2013). TIM3(+)FOXP3(+) regulatory T cells are tissue-specific promoters of T-cell dysfunction in cancer. *Oncolmmunology* **2**, e23849.
- Salceda, S., Tang, T., Kmet, M., Munteanu, A., Ghosh, M., Macina, R., Liu, W., Pilkington, G., and Papkoff, J. (2005). The immunomodulatory protein B7-H4 is overexpressed in breast and ovarian cancers and promotes epithelial cell transformation. *Exp. Cell Res.* **306**, 128–141.

- Scalapino, K.J., and Daikh, D.I. (2008). CTLA-4: a key regulatory point in the control of autoimmune disease. *Immunol. Rev.* **223**, 143–155.
- Schneider, H., Martin, M., Agarraberes, F.A., Yin, L., Rapoport, I., Kirchhausen, T., and Rudd, C.E. (1999). Cytolytic T lymphocyte-associated antigen-4 and the TCR zeta/CD3 complex, but not CD28, interact with clathrin adaptor complexes AP-1 and AP-2. *J. Immunol.* **163**, 1868–1879.
- Schneider, H., Smith, X., Liu, H., Bismuth, G., and Rudd, C.E. (2008). CTLA-4 disrupts ZAP70 microcluster formation with reduced T cell/APC dwell times and calcium mobilization. *Eur. J. Immunol.* **38**, 40–47.
- Sekulic, A., Liang, W.S., Tembe, W., Izatt, T., Kruglyak, S., Kiefer, J.A., Cuyugan, L., Zismann, V., Legendre, C., Pittelkow, M.R., et al. (2015). Personalized treatment of Sézary syndrome by targeting a novel CTLA4:CD28 fusion. *Mol. Genet. Genomic Med.* **3**, 130–136.
- Selby, M.J., Engelhardt, J.J., Quigley, M., Henning, K.A., Chen, T., Srinivasan, M., and Korman, A.J. (2013). Anti-CTLA-4 antibodies of IgG2a isotype enhance antitumor activity through reduction of intratumoral regulatory T cells. *Cancer Immunol. Res.* **1**, 32–42.
- Sheppard, K.A., Fitz, L.J., Lee, J.M., Benander, C., George, J.A., Wooters, J., Qiu, Y., Jussif, J.M., Carter, L.L., Wood, C.R., and Chaudhary, D. (2004). PD-1 inhibits T-cell receptor induced phosphorylation of the ZAP70/CD3zeta signalosome and downstream signaling to PKC θ . *FEBS Lett.* **574**, 37–41.
- Shinohara, T., Taniwaki, M., Ishida, Y., Kawauchi, M., and Honjo, T. (1994). Structure and chromosomal localization of the human PD-1 gene (PDCD1). *Genomics* **23**, 704–706.
- Sica, G.L., Choi, I.H., Zhu, G., Tamada, K., Wang, S.D., Tamura, H., Chapoval, A.I., Flies, D.B., Bajorath, J., and Chen, L. (2003). B7-H4, a molecule of the B7 family, negatively regulates T cell immunity. *Immunity* **18**, 849–861.
- Sonkoly, E., Janson, P., Majuri, M.L., Savinko, T., Fyhrquist, N., Eidsmo, L., Xu, N., Meisgen, F., Wei, T., Bradley, M., et al. (2010). MiR-155 is overexpressed in patients with atopic dermatitis and modulates T-cell proliferative responses by targeting cytotoxic T lymphocyte-associated antigen 4. *J. Allergy Clin. Immunol.* **126**, 581–9.e1, 20.
- Staron, M.M., Gray, S.M., Marshall, H.D., Parish, I.A., Chen, J.H., Perry, C.J., Cui, G., Li, M.O., and Kaech, S.M. (2014). The transcription factor FoxO1 sustains expression of the inhibitory receptor PD-1 and survival of antiviral CD8(+) T cells during chronic infection. *Immunity* **41**, 802–814.
- Steinberger, P., Majdic, O., Derdak, S.V., Pfistershammer, K., Kirchberger, S., Klausner, C., Zlabinger, G., Pickl, W.F., Stöckl, J., and Knapp, W. (2004). Molecular characterization of human 4Ig-B7-H3, a member of the B7 family with four Ig-like domains. *J. Immunol.* **172**, 2352–2359.
- Stojanovic, A., Fiegler, N., Brunner-Weinzierl, M., and Cerwenka, A. (2014). CTLA-4 is expressed by activated mouse NK cells and inhibits NK cell IFN- γ production in response to mature dendritic cells. *J. Immunol.* **192**, 4184–4191.
- Suh, W.K., Gajewska, B.U., Okada, H., Gronski, M.A., Bertram, E.M., Dawicki, W., Duncan, G.S., Bukczynski, J., Plyte, S., Elia, A., et al. (2003). The B7 family member B7-H3 preferentially down-regulates T helper type 1-mediated immune responses. *Nat. Immunol.* **4**, 899–906.
- Suh, W.K., Wang, S., Duncan, G.S., Miyazaki, Y., Cates, E., Walker, T., Gajewska, B.U., Deenick, E., Dawicki, W., Okada, H., et al. (2006). Generation and characterization of B7-H4/B7S1/B7x-deficient mice. *Mol. Cell. Biol.* **26**, 6403–6411.
- Sun, M., Richards, S., Prasad, D.V., Mai, X.M., Rudensky, A., and Dong, C. (2002). Characterization of mouse and human B7-H3 genes. *J. Immunol.* **168**, 6294–6297.
- Sun, X., Vale, M., Leung, E., Kanwar, J.R., Gupta, R., and Krissansen, G.W. (2003). Mouse B7-H3 induces antitumor immunity. *Gene Ther.* **10**, 1728–1734.
- Sun, J., Fu, F., Gu, W., Yan, R., Zhang, G., Shen, Z., Zhou, Y., Wang, H., Shen, B., and Zhang, X. (2011). Origination of new immunological functions in the costimulatory molecule B7-H3: the role of exon duplication in evolution of the immune system. *PLoS ONE* **6**, e24751.
- Swanson, R.M., Gavin, M.A., Escobar, S.S., Rottman, J.B., Lipsky, B.P., Dube, S., Li, L., Bigler, J., Wolfson, M., Arnett, H.A., and Viney, J.L. (2013). Butyrophilin-like 2 modulates B7 costimulation to induce Foxp3 expression and regulatory T cell development in mature T cells. *J. Immunol.* **190**, 2027–2035.
- Tai, X., Van Laethem, F., Sharpe, A.H., and Singer, A. (2007). Induction of autoimmune disease in CTLA-4^{-/-} mice depends on a specific CD28 motif that is required for in vivo costimulation. *Proc. Natl. Acad. Sci. USA* **104**, 13756–13761.
- Takahashi, T., Tagami, T., Yamazaki, S., Uede, T., Shimizu, J., Sakaguchi, N., Mak, T.W., and Sakaguchi, S. (2000). Immunologic self-tolerance maintained by CD25(+)CD4(+) regulatory T cells constitutively expressing cytotoxic T lymphocyte-associated antigen 4. *J. Exp. Med.* **192**, 303–310.
- Terawaki, S., Chikuma, S., Shibayama, S., Hayashi, T., Yoshida, T., Okazaki, T., and Honjo, T. (2011). IFN- α directly promotes programmed cell death-1 transcription and limits the duration of T cell-mediated immunity. *J. Immunol.* **186**, 2772–2779.
- Tivol, E.A., Borriello, F., Schweitzer, A.N., Lynch, W.P., Bluestone, J.A., and Sharpe, A.H. (1995). Loss of CTLA-4 leads to massive lymphoproliferation and fatal multiorgan tissue destruction, revealing a critical negative regulatory role of CTLA-4. *Immunity* **3**, 541–547.
- Ueda, H., Howson, J.M., Esposito, L., Heward, J., Snook, H., Chamberlain, G., Rainbow, D.B., Hunter, K.M., Smith, A.N., Di Genova, G., et al. (2003). Association of the T-cell regulatory gene CTLA4 with susceptibility to autoimmune disease. *Nature* **423**, 506–511.
- Ungewickell, A., Bhaduri, A., Rios, E., Reuter, J., Lee, C.S., Mah, A., Zehnder, A., Ohgami, R., Kulkarni, S., Armstrong, R., et al. (2015). Genomic analysis of mycosis fungoides and Sézary syndrome identifies recurrent alterations in TNFR2. *Nat. Genet.* **47**, 1056–1060.
- Valentonyte, R., Hampe, J., Huse, K., Rosenstiel, P., Albrecht, M., Stenzel, A., Nagy, M., Gaede, K.I., Franke, A., Haesler, R., et al. (2005). Sarcoidosis is associated with a truncating splice site mutation in BTLN2. *Nat. Genet.* **37**, 357–364.
- Valk, E., Leung, R., Kang, H., Kaneko, K., Rudd, C.E., and Schneider, H. (2006). T cell receptor-interacting molecule acts as a chaperone to modulate surface expression of the CTLA-4 coreceptor. *Immunity* **25**, 807–821.
- Vijaykrishnan, L., Slavik, J.M., Illés, Z., Greenwald, R.J., Rainbow, D., Greve, B., Peterson, L.B., Hafler, D.A., Freeman, G.J., Sharpe, A.H., et al. (2004). An autoimmune disease-associated CTLA-4 splice variant lacking the B7 binding domain signals negatively in T cells. *Immunity* **20**, 563–575.
- Walunas, T.L., Lenschow, D.J., Bakker, C.Y., Linsley, P.S., Freeman, G.J., Green, J.M., Thompson, C.B., and Bluestone, J.A. (1994). CTLA-4 can function as a negative regulator of T cell activation. *Immunity* **1**, 405–413.
- Walunas, T.L., Bakker, C.Y., and Bluestone, J.A. (1996). CTLA-4 ligation blocks CD28-dependent T cell activation. *J. Exp. Med.* **183**, 2541–2550.
- Wan, B., Nie, H., Liu, A., Feng, G., He, D., Xu, R., Zhang, Q., Dong, C., and Zhang, J.Z. (2006). Aberrant regulation of synovial T cell activation by soluble costimulatory molecules in rheumatoid arthritis. *J. Immunol.* **177**, 8844–8850.
- Wang, X.B., Giscombe, R., Yan, Z., Heiden, T., Xu, D., and Lefvert, A.K. (2002a). Expression of CTLA-4 by human monocytes. *Scand. J. Immunol.* **55**, 53–60.
- Wang, X.B., Zhao, X., Giscombe, R., and Lefvert, A.K. (2002b). A CTLA-4 gene polymorphism at position -318 in the promoter region affects the expression of protein. *Genes Immun.* **3**, 233–234.
- Wang, L., Fraser, C.C., Kiky, K., Wells, A.D., Han, R., Coyle, A.J., Chen, L., and Hancock, W.W. (2005). B7-H3 promotes acute and chronic allograft rejection. *Eur. J. Immunol.* **35**, 428–438.
- Wang, L., Rubinstein, R., Lines, J.L., Wasiuk, A., Ahonen, C., Guo, Y., Lu, L.F., Gondek, D., Wang, Y., Fava, R.A., et al. (2011). VISTA, a novel mouse Ig superfamily ligand that negatively regulates T cell responses. *J. Exp. Med.* **208**, 577–592.
- Wang, C.J., Kenefeck, R., Wardzinski, L., Attridge, K., Manzotti, C., Schmidt, E.M., Qureshi, O.S., Sansom, D.M., and Walker, L.S. (2012a). Cutting edge: cell-extrinsic immune regulation by CTLA-4 expressed on conventional T cells. *J. Immunol.* **189**, 1118–1122.
- Wang, H., Wang, K., Zhong, X., Dai, Y., Wu, A., Li, Y., and Hu, X. (2012b). Plasma sCD28, sCTLA-4 levels in neuromyelitis optica and multiple sclerosis during relapse. *J. Neuroimmunol.* **243**, 52–55.

- Wang, L., Le Mercier, I., Putra, J., Chen, W., Liu, J., Schenk, A.D., Nowak, E.C., Suriawinata, A.A., Li, J., and Noelle, R.J. (2014). Disruption of the immune-checkpoint VISTA gene imparts a proinflammatory phenotype with predisposition to the development of autoimmunity. *Proc. Natl. Acad. Sci. USA* *111*, 14846–14851.
- Ward-Kavanagh, L.K., Lin, W.W., Šedý, J.R., and Ware, C.F. (2016). The TNF receptor superfamily in co-stimulating and co-inhibitory responses. *Immunity* *44*, this issue, 1005–1019.
- Waterhouse, P., Penninger, J.M., Timms, E., Wakeham, A., Shahinian, A., Lee, K.P., Thompson, C.B., Griesser, H., and Mak, T.W. (1995). Lymphoproliferative disorders with early lethality in mice deficient in Ctl4-4. *Science* *270*, 985–988.
- Wei, F., Zhong, S., Ma, Z., Kong, H., Medvec, A., Ahmed, R., Freeman, G.J., Krogsgaard, M., and Riley, J.L. (2013). Strength of PD-1 signaling differentially affects T-cell effector functions. *Proc. Natl. Acad. Sci. USA* *110*, E2480–E2489.
- Wells, A.D. (2007). Cyclin-dependent kinases: molecular switches controlling energy and potential therapeutic targets for tolerance. *Semin. Immunol.* *19*, 173–179.
- Wicker, L.S., Chamberlain, G., Hunter, K., Rainbow, D., Howlett, S., Tiffen, P., Clark, J., Gonzalez-Munoz, A., Cumiskey, A.M., Rosa, R.L., et al. (2004). Fine mapping, gene content, comparative sequencing, and expression analyses support Ctl4 and Nramp1 as candidates for Idd5.1 and Idd5.2 in the nonobese diabetic mouse. *J. Immunol.* *173*, 164–173.
- Wing, K., Onishi, Y., Prieto-Martin, P., Yamaguchi, T., Miyara, M., Fehervari, Z., Nomura, T., and Sakaguchi, S. (2008). CTLA-4 control over Foxp3+ regulatory T cell function. *Science* *322*, 271–275.
- Wing, J.B., Ise, W., Kurosaki, T., and Sakaguchi, S. (2014). Regulatory T cells control antigen-specific expansion of T_H cell number and humoral immune responses via the coreceptor CTLA-4. *Immunity* *41*, 1013–1025.
- Wu, Y., Borde, M., Heissmeyer, V., Feuerer, M., Lapan, A.D., Stroud, J.C., Bates, D.L., Guo, L., Han, A., Ziegler, S.F., et al. (2006). FOXP3 controls regulatory T cell function through cooperation with NFAT. *Cell* *126*, 375–387.
- Xiao, Y., and Freeman, G.J. (2015). A new B7:CD28 family checkpoint target for cancer immunotherapy: HHLA2. *Clin. Cancer Res.* *21*, 2201–2203.
- Xiao, G., Deng, A., Liu, H., Ge, G., and Liu, X. (2012). Activator protein 1 suppresses antitumor T-cell function via the induction of programmed death 1. *Proc. Natl. Acad. Sci. USA* *109*, 15419–15424.
- Xiao, Y., Yu, S., Zhu, B., Bedoret, D., Bu, X., Francisco, L.M., Hua, P., Duke-Cohan, J.S., Umetsu, D.T., Sharpe, A.H., et al. (2014). RGMB is a novel binding partner for PD-L2 and its engagement with PD-L2 promotes respiratory tolerance. *J. Exp. Med.* *211*, 943–959.
- Xu, H., Cheung, I.Y., Guo, H.F., and Cheung, N.K. (2009). MicroRNA miR-29 modulates expression of immunoinhibitory molecule B7-H3: potential implications for immune based therapy of human solid tumors. *Cancer Res.* *69*, 6275–6281.
- Yamazaki, T., Akiba, H., Iwai, H., Matsuda, H., Aoki, M., Tanno, Y., Shin, T., Tsuchiya, H., Pardoll, D.M., Okumura, K., et al. (2002). Expression of programmed death 1 ligands by murine T cells and APC. *J. Immunol.* *169*, 5538–5545.
- Yao, Y., Wang, X., Jin, K., Zhu, J., Wang, Y., Xiong, S., Mao, Y., and Zhou, L. (2008). B7-H4 is preferentially expressed in non-dividing brain tumor cells and in a subset of brain tumor stem-like cells. *J. Neurooncol.* *89*, 121–129.
- Ying, H., Yang, L., Qiao, G., Li, Z., Zhang, L., Yin, F., Xie, D., and Zhang, J. (2010). Cutting edge: CTLA-4–B7 interaction suppresses Th17 cell differentiation. *J. Immunol.* *185*, 1375–1378.
- Yokosuka, T., Takamatsu, M., Kobayashi-Imanishi, W., Hashimoto-Tane, A., Azuma, M., and Saito, T. (2012). Programmed cell death 1 forms negative costimulatory microclusters that directly inhibit T cell receptor signaling by recruiting phosphatase SHP2. *J. Exp. Med.* *209*, 1201–1217.
- Yoo, H.Y., Kim, P., Kim, W.S., Lee, S.H., Kim, S., Kang, S.Y., Jang, H.Y., Lee, J.E., Kim, J., Kim, S.J., et al. (2016). Frequent CTLA4-CD28 gene fusion in diverse types of T cell lymphoma. *Haematologica*. Published online January 27, 2016. [haematol.2015.139253](https://doi.org/10.1182/haematol.2015.139253).
- Youngblood, B., Oestreich, K.J., Ha, S.J., Duraiswamy, J., Akondy, R.S., West, E.E., Wei, Z., Lu, P., Austin, J.W., Riley, J.L., et al. (2011). Chronic virus infection enforces demethylation of the locus that encodes PD-1 in antigen-specific CD8(+) T cells. *Immunity* *35*, 400–412.
- Zhang, Q., and Vignali, D.A.A. (2016). Co-stimulatory and co-inhibitory pathways in autoimmunity. *Immunity* *44*, this issue, 1034–1051.
- Zhang, X., Schwartz, J.C., Guo, X., Bhatia, S., Cao, E., Lorenz, M., Cammer, M., Chen, L., Zhang, Z.Y., Edidin, M.A., et al. (2004). Structural and functional analysis of the costimulatory receptor programmed death-1. *Immunity* *20*, 337–347.
- Zhang, G., Hou, J., Shi, J., Yu, G., Lu, B., and Zhang, X. (2008). Soluble CD276 (B7-H3) is released from monocytes, dendritic cells and activated T cells and is detectable in normal human serum. *Immunology* *123*, 538–546.
- Zhang, G., Liu, Z., Duan, S., Han, Q., Li, Z., Lv, Y., Chen, J., Lou, S., and Li, N. (2010a). Association of polymorphisms of programmed cell death-1 gene with chronic hepatitis B virus infection. *Hum. Immunol.* *71*, 1209–1213.
- Zhang, G., Wang, J., Kelly, J., Gu, G., Hou, J., Zhou, Y., Redmond, H.P., Wang, J.H., and Zhang, X. (2010b). B7-H3 augments the inflammatory response and is associated with human sepsis. *J. Immunol.* *185*, 3677–3684.
- Zhang, L., Wu, H., Lu, D., Li, G., Sun, C., Song, H., Li, J., Zhai, T., Huang, L., Hou, C., et al. (2013). The costimulatory molecule B7-H4 promote tumor progression and cell proliferation through translocating into nucleus. *Oncogene* *32*, 5347–5358.
- Zhang, G., Li, N., Li, Z., Zhu, Q., Li, F., Yang, C., Han, Q., Lv, Y., Zhou, Z., and Liu, Z. (2015). microRNA-4717 differentially interacts with its polymorphic target in the PD1 3' untranslated region: A mechanism for regulating PD-1 expression and function in HBV-associated liver diseases. *Oncotarget* *6*, 18933–18944.
- Zhao, R., Chinai, J.M., Buhl, S., Scanduzzi, L., Ray, A., Jeon, H., Ohaegbulam, K.C., Ghosh, K., Zhao, A., Scharff, M.D., and Zang, X. (2013). HHLA2 is a member of the B7 family and inhibits human CD4 and CD8 T-cell function. *Proc. Natl. Acad. Sci. USA* *110*, 9879–9884.
- Zheng, Y., Josefowicz, S.Z., Kas, A., Chu, T.T., Gavin, M.A., and Rudensky, A.Y. (2007). Genome-wide analysis of Foxp3 target genes in developing and mature regulatory T cells. *Nature* *445*, 936–940.
- Zheng, L., Li, D., Wang, F., Wu, H., Li, X., Fu, J., Chen, X., Wang, L., Liu, Y., and Wang, S. (2010). Association between hepatitis B viral burden in chronic infection and a functional single nucleotide polymorphism of the PDCD1 gene. *J. Clin. Immunol.* *30*, 855–860.
- Zhong, X., Bai, C., Gao, W., Strom, T.B., and Rothstein, T.L. (2004). Suppression of expression and function of negative immune regulator PD-1 by certain pattern recognition and cytokine receptor signals associated with immune system danger. *Int. Immunol.* *16*, 1181–1188.
- Zhou, J., Cheung, A.K., Liu, H., Tan, Z., Tang, X., Kang, Y., Du, Y., Wang, H., Liu, L., and Chen, Z. (2013a). Potentiating functional antigen-specific CD8⁺ T cell immunity by a novel PD1 isoform-based fusion DNA vaccine. *Mol. Ther.* *21*, 1445–1455.
- Zhou, J., Cheung, A.K., Tan, Z., Wang, H., Yu, W., Du, Y., Kang, Y., Lu, X., Liu, L., Yuen, K.Y., and Chen, Z. (2013b). PD1-based DNA vaccine amplifies HIV-1 GAG-specific CD8⁺ T cells in mice. *J. Clin. Invest.* *123*, 2629–2642.
- Zhu, G., Augustine, M.M., Azuma, T., Luo, L., Yao, S., Anand, S., Rietz, A.C., Huang, J., Xu, H., Flies, A.S., et al. (2009). B7-H4-deficient mice display augmented neutrophil-mediated innate immunity. *Blood* *113*, 1759–1767.
- Zhu, Y., Yao, S., Iliopoulou, B.P., Han, X., Augustine, M.M., Xu, H., Phenicie, R.T., Flies, S.J., Broadwater, M., Ruff, W., et al. (2013). B7-H5 costimulates human T cells via CD28H. *Nat. Commun.* *4*, 2043.

Lag-3, Tim-3, and TIGIT: Co-inhibitory Receptors with Specialized Functions in Immune Regulation

Ana C. Anderson,¹ Nicole Joller,² and Vijay K. Kuchroo^{1,*}

¹Evergrande Center for Immunologic Diseases and Ann Romney Center for Neurologic Diseases, Brigham and Women's Hospital and Harvard Medical School, Boston, MA 02115, USA

²Institute of Experimental Immunology, University of Zürich, Zürich 8057, Switzerland

*Correspondence: vkuchroo@evergrande.hms.harvard.edu

<http://dx.doi.org/10.1016/j.immuni.2016.05.001>

Co-inhibitory receptors, such as CTLA-4 and PD-1, have an important role in regulating T cell responses and have proven to be effective targets in the setting of chronic diseases where constitutive co-inhibitory receptor expression on T cells dampens effector T cell responses. Unfortunately, many patients still fail to respond to therapies that target CTLA-4 and PD-1. The next wave of co-inhibitory receptor targets that are being explored in clinical trials include Lag-3, Tim-3, and TIGIT. These receptors, although they belong to the same class of receptors as PD-1 and CTLA-4, exhibit unique functions, especially at tissue sites where they regulate distinct aspects of immunity. Increased understanding of the specialized functions of these receptors will inform the rational application of therapies that target these receptors to the clinic.

Introduction

Co-inhibitory or immune checkpoint receptors have a critical role in the maintenance of immune homeostasis: their expression on effector T cells ensures the proper contraction of effector T cell responses and their expression on regulatory T (Treg) cells guarantees the proper function of Treg cells to control effector T cells. Co-inhibitory receptors play a central role in regulating autoimmune disease. Indeed, many co-inhibitory receptors have been genetically linked to autoimmune diseases (Kasagi et al., 2011; Qu et al., 2009; Song et al., 2011; Wang et al., 2014; Zhang and Vignali, 2016 [this issue]). Accordingly, their function in regulating pro-inflammatory T cell responses and the maintenance of self-tolerance has been most widely studied in this context. More recently, the role of co-inhibitory receptors has come to the forefront in cancer (Callahan et al., 2016, this issue) and chronic viral infection (Attanasio and Wherry, 2016, this issue) where these receptors are highly expressed and are being targeted clinically to improve anti-tumor and anti-viral T cell responses (Mahoney et al., 2015; Pauken and Wherry, 2015). Although current immunotherapies directed against the co-inhibitory receptors CTLA-4 and PD-1 are exhibiting unprecedented efficacy in several cancer indications and in some chronic viral infections, there are still many patients that do not respond to these therapeutic approaches and some tumor types remain largely refractory to these therapies. This has prompted intense investigation into the targeting of other co-inhibitory receptors in order to broaden the therapeutic repertoire. Lag-3, Tim-3, and TIGIT comprise the next generation of co-inhibitory receptors to be translated to the clinic. This review will highlight the unique aspects of each of these molecules in regulating immune responses, specifically at tissue sites.

Lag-3

Discovery, Ligands, and Function

Lymphocyte activation gene-3 (Lag-3) was discovered 25 years ago as a molecule that is upregulated on activated CD4⁺ and CD8⁺ T cells and a subset of natural killer (NK) cells (Table 1; Trie-

bel et al., 1990). Lag-3 structurally resembles the CD4 co-receptor and, indeed, binds to MHC class II with a higher affinity than CD4 (Figure 1A; Huard et al., 1995). The fact that Lag-3 impacts the function of CD8⁺ T cells and NK cells, neither of which interact with MHC class II, has led to speculation about the existence of alternate ligands for Lag-3. In this regard, it has been suggested that LSEctin, a member of the DC-SIGN family of molecules, is another ligand for Lag-3 (Xu et al., 2014). LSEctin is expressed in the liver and also on many tumors (Xu et al., 2014), thus providing a potential mechanism by which Lag-3-expressing CD8⁺ T cells and NK cells can be regulated in these tissues (Figure 1A).

Although initial examination of Lag-3-deficient mice revealed no T cell defects (Miyazaki et al., 1996), subsequent careful examination both in vitro and in vivo revealed that Lag-3-deficient T cells exhibit defects consistent with Lag-3 being a negative regulator of T cell expansion (Workman et al., 2004; Workman and Vignali, 2003). Administration of the superantigen Staphylococcal enterotoxin B (SEB) in Lag-3-deficient mice was shown to result in uncontrolled expansion of V β 8⁺ T cells and splenomegaly. Similarly, OVA-specific Lag-3-deficient CD4⁺ T cells were shown to exhibit uncontrolled expansion after immunization with OVA.

In addition to effector CD4⁺ T cells, Lag-3 is also expressed on CD4⁺ T cells that have regulatory functions. Lag-3 is expressed on both activated natural Treg (nTreg) and induced CD4⁺FoxP3⁺ Treg (iTreg) cells (Table 1), where expression levels are higher than that observed on activated effector CD4⁺ T cells (Huang et al., 2004). Blockade of Lag-3 on Treg cells abrogates Treg cell suppressor function whereas ectopic expression of Lag-3 in non-Treg CD4⁺ T cells confers suppressive activity. In addition, Lag-3 is required for Treg-cell-mediated control of T cell homeostasis (Workman and Vignali, 2005). Together, these data support a functional role for Lag-3 in Treg cell function. Lag-3 is further expressed on CD4⁺FoxP3⁻ IL-10-secreting type 1 regulatory (Tr1) T cells. Indeed, Tr1 cells can be identified in both humans and mice by expression of Lag-3 together with CD49b

Table 1. Comparison of Lag-3, Tim-3, and TIGIT

	Lag-3	Tim-3	TIGIT
Expression			
CD4 ^a	Tr1, nTreg, iTreg	Th1, Tr1, nTreg ^b	Tr1, Tfh, nTreg ^c
CD8 ^a	dysfunctional T cells	Tc1, dysfunctional T cells	dysfunctional T cells
Natural killer cells	+	+	+
Dendritic cells	–	+	–
Monocytes/macrophages	–	+/- ^d	–
Signaling motifs	KIEELE	tyrosine ^e	ITT/ITIM
Ligands	MHC II, LSECtin	Galectin-9, Ceacam-1, HMGB-1, phosphatidyl serine	CD112, CD155

^aLag-3, Tim-3, and TIGIT are transiently upregulated on activated CD4⁺ and CD8⁺ T cells.

^bIn both mouse and human, Tim-3 is either not expressed or expressed on a very small fraction of CD4⁺Foxp3⁺ Treg cells in the normal circulation but is highly expressed on Treg cells at sites of tissue inflammation.

^cIn both mouse and human, TIGIT is expressed on about one-third of CD4⁺FoxP3⁺ Treg cells in the normal circulation and is highly upregulated on Treg cells at sites of tissue inflammation.

^dIn the mouse, Tim-3 is expressed on monocytes/macrophages only in inflammatory conditions. In humans, Tim-3 is expressed on peripheral blood monocytes and on macrophages.

^eTim-3 has five tyrosines in its cytoplasmic tail but no known signaling motif.

(Gagliani et al., 2013); however, whether Lag-3 is required for Tr1-cell-mediated suppression of immune responses has not been addressed.

Signaling

The association of Lag-3 with inhibition of effector T cells and promotion of Treg-cell-mediated suppression raises the important question of how Lag-3 signals in these different T cell subsets to achieve its inhibitory effects. To date, most of what we know about Lag-3 signaling addresses its role in effector T cells where Lag-3 has been shown to associate with CD3 and crosslinking of Lag-3 together with CD3 inhibits T cell proliferation, cytokine production, and calcium flux (Hannier et al., 1998). The signaling pathway downstream of Lag-3 responsible for these effects is still not clear. In fact, the cytoplasmic tail of Lag-3 is unique among all known immune receptors. The Lag-3 cytoplasmic tail has three regions that are conserved between human and mouse. The first region contains a serine-phosphorylation site, the second region contains a unique KIEELE motif, and the third region contains glutamic acid-proline (EP) repeats (Workman et al., 2002). Of these three regions, the KIEELE motif has been shown to be essential for the inhibitory function of Lag-3 in effector CD4⁺ T cells (Workman et al., 2002); however, the intracellular proteins that bind to this motif have not been identified. Moreover, whether this motif is required for the effects of Lag-3 in Treg cells is not known.

Role in Disease

The association of Lag-3 with T cell regulation via its roles in effector T cells, Treg cells, and potentially Tr1 cells position Lag-3 as a potential target for modulating T cell responses in disease (Figures 2A and 3). Indeed, current data support that modulating Lag-3 can impact autoimmunity, cancer, chronic viral infection, and parasitic infection. The role of Lag-3 in these different disease contexts will be discussed below.

Autoimmunity. Deficiency in co-inhibitory receptor expression can promote autoimmunity. This is most notable for CTLA-4 deficiency and PD-1 deficiency, both of which result in the development of spontaneous autoimmunity even on genetic backgrounds that normally don't develop disease (Nishimura et al.,

1999, 2001; Tivol et al., 1995; Waterhouse et al., 1995). In this regard, Lag-3 deficiency alone does not predispose toward autoimmunity unless the mice are on a permissive genetic background. Lag-3 deficiency on the NOD background results in accelerated type 1 diabetes with 100% of Lag-3-deficient mice developing diabetes before age-matched wild-type controls (Bettini et al., 2011; Okazaki et al., 2011). In wild-type NOD mice, administration of blocking anti-Lag-3 antibody also accelerates type 1 diabetes (Bettini et al., 2011). Furthermore, Lag-3 deficiency on the B6.SJL background results in increased susceptibility to Hg-induced autoimmunity and defects in antigen-specific tolerance induction (Jha et al., 2014). The importance of Lag-3 for antigen-specific tolerance and its impact on autoimmunity indicated by the aforementioned studies is further reinforced by a recent study showing that auto-antigen-specific tolerance drives the generation of regulatory T cells that express Lag-3 together with PD-1, Tim-3, TIGIT, and the immunosuppressive cytokine IL-10 (Burton et al., 2014). This last observation points to the co-operative function of Lag-3 with other co-inhibitory molecules for achieving optimal T cell regulation.

Cancer and Chronic Viral Infections. Co-inhibitory receptors are highly expressed on the dysfunctional or exhausted T cells that develop in chronic diseases such as chronic viral infections and cancer. Dysfunctional or exhausted T cells are characterized by variable deficits in their ability to proliferate and elicit effector functions (cytotoxicity, cytokine production) upon stimulation through the TCR (Wherry and Kurachi, 2015). Chronic infection with the clone 13 strain of LCMV is the gold standard experimental model for studies of T cell dysfunction or exhaustion. In this model, Lag-3 expression was shown to correlate strongly with the severity of infection (Blackburn et al., 2009) and to be co-expressed with PD-1 on dysfunctional or exhausted virus-specific CD8⁺ T cells (Richter et al., 2010). Interestingly, although blockade of Lag-3 alone had little effect (Blackburn et al., 2009; Richter et al., 2010), blockade of Lag-3 synergized with blockade of PD-L1 to improve CD8⁺ T cell responses and reduce viral load (Blackburn et al., 2009). Similarly, Lag-3 is expressed on

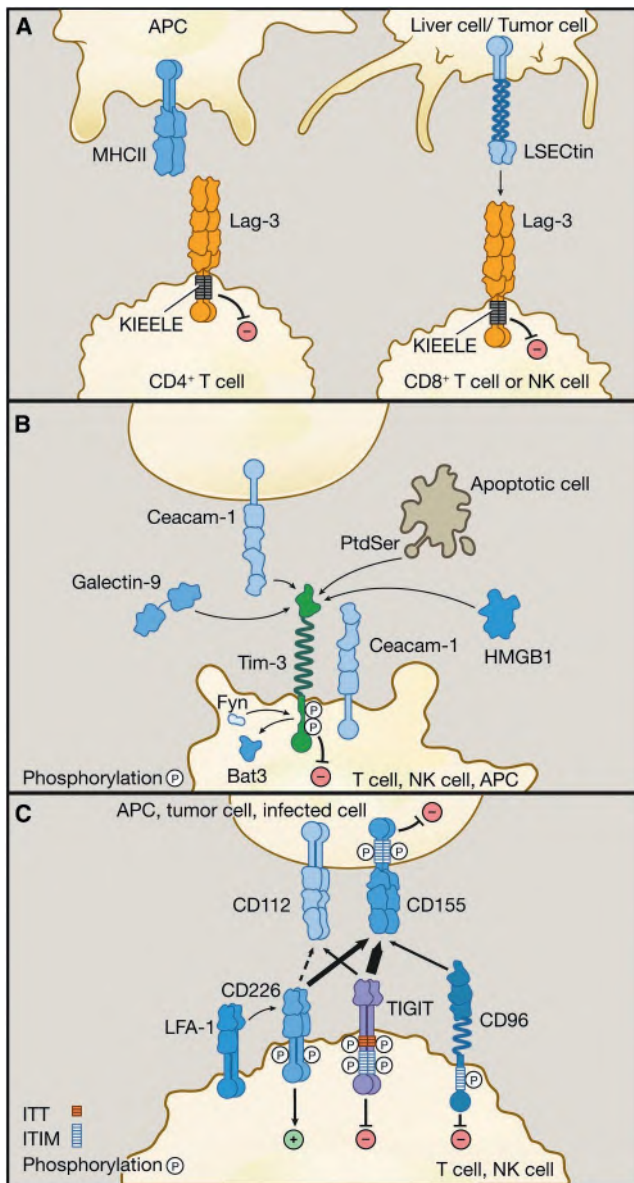


Figure 1. Co-inhibitory Receptor Pathways

(A) The Lag-3 pathway. Left: Lag-3 is expressed on CD4⁺ T cells and binds to MHC class II on antigen-presenting cells. Right: Lag-3 is expressed on CD8⁺ T cells and NK cells and binds to L-SECtin on tumor cells or liver cells. The cytoplasmic tail of Lag-3 contains a unique KIEELE motif that is essential for the inhibitory function of Lag-3.

(B) The Tim-3 pathway. Tim-3 is expressed on T cells, NK cells, and some APCs. Tim-3 ligands include soluble ligands (galectin-9 and HMGB1) and cell surface ligands (Ceacam-1 and Phosphatidyl serine [PtdSer]). Bat-3 and Fyn bind to the same region on the cytoplasmic tail of Tim-3. Ligand binding triggers the dissociation of Bat-3 from the cytoplasmic tail of Tim-3, thus allowing Fyn to bind and promote the inhibitory function of Tim-3.

(C) The CD226/TIGIT pathway. CD226, TIGIT, and CD96 are expressed on T cells and NK cells and share the ligands CD112 and CD155, which are expressed on APCs and other cells such as tumor cells. CD226 associates with the integrin LFA-1 and delivers a positive signal. TIGIT, CD96, and CD155 contain ITIM motifs in their cytoplasmic tails and can deliver inhibitory signals. TIGIT further contains an ITT-like motif. CD155 and TIGIT exist as homodimers on the cell surface, and dimerization is essential for their proper function.

dysfunctional or exhausted parasite-specific CD4⁺ T cells during malaria infection and Lag-3 blockade synergizes with PD-L1 blockade to improve CD4⁺ T cell function and parasite clearance (Butler et al., 2012).

Cancer and chronic infections share common features, notably chronic exposure to antigen and the development of dysfunctional or exhausted effector T cells. Indeed, Lag-3 and PD-1 are co-expressed on both CD4⁺ and CD8⁺ tumor infiltrating lymphocytes (TILs) in several pre-clinical murine models of cancer and co-blockade of the Lag-3 and PD-1 pathways has been shown to synergize to improve anti-tumor CD8⁺ T cell responses (Woo et al., 2012). Lag-3 blockade has also been shown to synergize with anti-tumor vaccination to improve tumor-specific CD8⁺ T cell activation. Interestingly, this effect did not require CD4⁺ T cells, thus supporting a direct role for Lag-3 in regulating CD8⁺ T cells (Grosso et al., 2007). In humans, Lag-3 and PD-1 co-expression has been noted to mark dysfunctional or exhausted CD8⁺ T cells in ovarian cancer and, as observed in pre-clinical cancer models, Lag-3 and PD-1 co-blockade improved the proliferation and cytokine production of tumor-antigen-specific CD8⁺ T cells (Matsuzaki et al., 2010). Thus, in both chronic infections and cancer, Lag-3 and PD-1 signaling functionally cooperate to dampen T cell responses (Figure 3).

As mentioned above, Lag-3 is highly expressed on Treg cells. Lag-3⁺FoxP3⁺ Treg cells have been shown to be expanded in the PBMC, tumor-infiltrated lymph node, and tumor tissue of both melanoma and colorectal cancer patients (Gamisaschi et al., 2010). These Lag-3⁺ Treg cells exhibit an activated phenotype, producing high IL-10 and TGF-β1. Lastly, the presence of Lag-3⁺CD49b⁺IL-10-producing Tr1 cells has been associated with poor prognosis in colorectal cancer (Chen and Chen, 2014). Together these data support a role for Lag-3 in suppressing immunity via its role in Treg cells.

Lag-3 has thus been shown to be an important immune regulator in autoimmunity, chronic viral infection, parasitic infection, and cancer; however, whether Lag-3-driven regulation in these different disease contexts stems from its function in modulating effector T cell, regulatory T cell (Treg and/or Tr1), or NK cell responses has not been determined. Resolution of this important issue will require careful examination of mice harboring conditional deletion of Lag-3 in different immune cell subsets. Furthermore, which ligand (MHC class II or LSECtin) is operational in promoting T cell inhibition via Lag-3 has not been addressed.

Clinical Trials

The potential for Lag-3-driven regulation of immune responses is now being explored in clinical trials for cancer. Early trials have focused on using a soluble Lag-3-Ig and are based on the observation that administration of soluble Lag-3-Ig together with irradiated wild-type tumor cells inhibits the growth of established tumors (Prigent et al., 1999). Phase I studies of soluble Lag-3-Ig (IMP321) have been completed in advanced renal cell carcinoma (Brignone et al., 2009) and advanced pancreatic adenocarcinoma, where IMP321 was combined with the chemotherapeutic gemcitabine (Wang-Gillam et al., 2013). In both trials, IMP321 was well tolerated with no treatment-related adverse events. In renal cell carcinoma, tumor growth reduction and stable disease were observed at high treatment doses. In pancreatic adenocarcinoma, lack of activity was attributed to sub-optimal dosing.

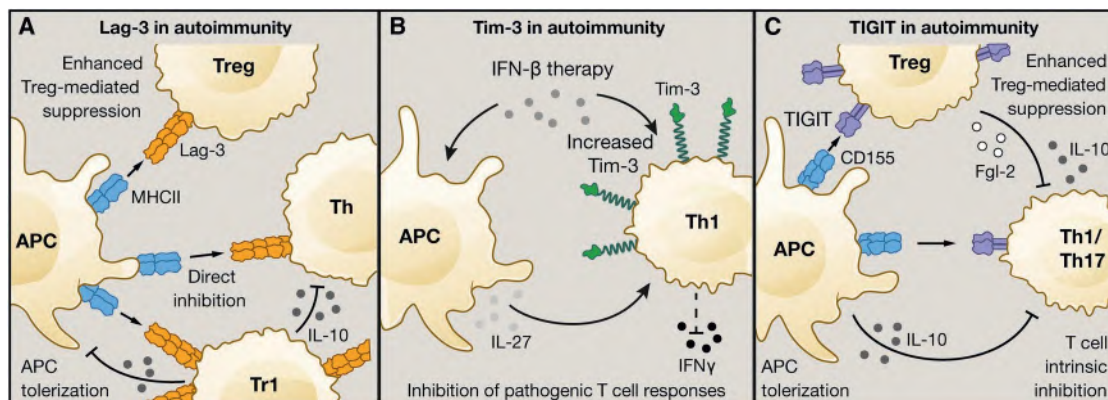


Figure 2. The Lag-3, Tim-3, and TIGIT Pathways in Autoimmunity

(A) Lag-3 plays a protective role in autoimmunity by dampening T helper (Th) cell responses directly through engagement of MHCII. In addition, Lag-3 indirectly inhibits effector T cell responses via promotion of Treg-cell- and Tr1-cell-mediated suppression. (B) In autoimmune diseases such as MS, Tim-3 is under-expressed on pathogenic Th1 cells. IFN- β therapy can increase Tim-3 on antigen-specific T cells directly or indirectly via promotion of IL-27 production from local antigen-presenting cells. Increased expression of Tim-3 is associated with reduction in disease relapses. (C) TIGIT inhibits auto-pathogenic Th1/Th17 T cell responses through three different pathways: (1) TIGIT directly inhibits T cell activation and expansion; (2) TIGIT-expressing effector and regulatory T cells engage CD155 on APCs thereby inducing tolerogenic APCs that secrete IL-10; (3) TIGIT promotes Treg-cell-mediated suppression through the induction of IL-10 and Fgl2, which potently and selectively suppress Th1 and Th17 cell responses.

IMP321 has also been tested in combination with MART-1 peptide vaccination in advanced melanoma in a phase I trial (Romano et al., 2014). Although positive responses were not observed as per RECIST (response evaluation criteria in solid tumors) criteria, increased frequencies of MART-1-reactive CD8⁺ T cells along with decreased frequencies of Treg cells were observed, thus supporting further exploration of IMP321. Lastly, a phase I/II trial of IMP321 in combination with the chemotherapeutic paclitaxel in metastatic breast carcinoma has shown an objective response rate of 50% (Brignone et al., 2010).

Although Lag-3-Ig has shown some efficacy in the clinic, the mechanism by which Lag-3-Ig modulates anti-tumor responses remains unclear. IMP321 was initially described as an activator of antigen-presenting cells (APCs); however, MHC class II cross-linking by Lag-3 in dendritic cells (DCs) has been shown to suppress the maturation and antigen-presenting function of DCs (Liang et al., 2008). Moreover, IMP321 has a human IgG1 tail and thus can mediate Fc-dependent functions.

In contrast to Lag-3-Ig, the targeting of Lag-3 with antibodies is more straightforward. Antibodies that block Lag-3 binding to MHC class II are now being explored in the clinic. These trials are exploring the use of anti-Lag-3 antibodies either alone or in combination with anti-PD-1 in both solid and hematologic cancers. These trials are still recruiting patients and thus it will be some time before trial data are available.

Tim-3

Discovery, Ligands, and Function

T cell immunoglobulin-3 (Tim-3) was identified 13 years ago as a cell surface molecule selectively expressed on IFN- γ -producing CD4⁺ T helper 1 (Th1) and CD8⁺ T cytotoxic 1 (Tc1) T cells (Figure 1B; Table 1; Monney et al., 2002). In addition to its expression on T cells, Tim-3 has now been identified on Treg cells and on innate immune cells (DCs, NK cells, monocytes). The discovery of Tim-3 led to the identification of the Tim family of genes, which is encoded both in mice and in humans in

loci that have been repeatedly associated with immune-mediated diseases such as asthma, allergy, and atopy (Meyers et al., 2005). In the mouse there are eight Tim genes; however, only three of these, *Havcr1* (Tim-1), *Havcr2* (Tim-3), and *Timd4* (Tim-4), are conserved in humans.

Initial examination of Tim-3 function suggested that Tim-3 is a negative regulator of type 1 immunity. Anti-Tim-3 antibody was shown to exacerbate experimental autoimmune encephalomyelitis (EAE) (Monney et al., 2002), a T-cell-mediated autoimmune disease of the central nervous system that serves as an animal model for multiple sclerosis (MS). Subsequent studies with Tim-3-deficient mice and wild-type mice treated with Tim-3-Ig fusion protein showed that Tim-3 signaling is required for the induction of antigen-specific tolerance and that Tim-3 blockade enhances the development of spontaneous autoimmunity (Sabatos et al., 2003; Sánchez-Fueyo et al., 2003). The C-type lectin galectin-9 was later discovered as a Tim-3 ligand (Zhu et al., 2005). This discovery solidified the inhibitory function of Tim-3 as galectin-9-triggering of Tim-3 was shown to induce cell death in Tim-3⁺ Th1 cells and ameliorate EAE.

In addition to galectin-9, several other ligands have been subsequently identified for Tim-3 (Figure 1B; Table 1), some of which primarily have a role in innate immune cells. One of these, phosphatidyl serine (PtdSer), is not a unique ligand for Tim-3, as shown by the fact that Tim-1, Tim-3, and Tim-4 all bind to PtdSer (Cao et al., 2007; Santiago et al., 2007a, 2007b). The binding of Tim-3 to PtdSer is rather weak (at least 5-fold lower) relative to the binding of Tim-1 and Tim-4 to PtdSer (DeKruyff et al., 2010). The binding of Tim-3 to PtdSer has been implicated in the uptake of apoptotic cells and cross-presentation of antigen by dendritic cells, which constitutively express high levels of Tim-3 (Nakayama et al., 2009); however, this is not a mechanism that would be operative in T cells, which are not phagocytic.

Another Tim-3 ligand that impacts on innate immune responses is high mobility group protein B1 (HMGB1) (Chiba et al., 2012). HMGB1 binding to Tim-3 was identified by examination of the

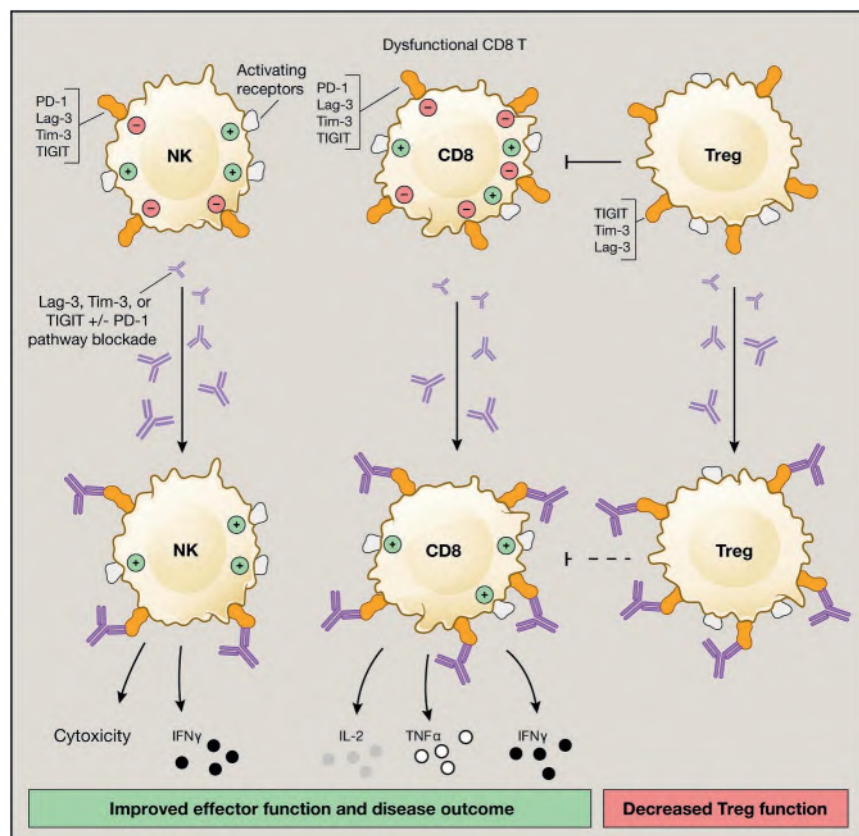


Figure 3. The Lag-3, Tim-3, and TIGIT Pathways in Chronic Diseases

Lag-3, Tim-3, and TIGIT are highly expressed on dysfunctional or exhausted T cells in chronic diseases such as chronic viral infection and cancer. In these diseases, combinatorial receptor blockade has strong synergistic effects, resulting in improved effector CD8⁺ T cell and NK cell function as well as decreased Treg-cell-mediated suppression. These combined actions improve disease outcome.

five conserved tyrosine residues among which Y256 and Y263 can be phosphorylated by either Src kinases (Lee et al., 2011) or ITK (van de Weyer et al., 2006). Y256 and Y263 are involved in the binding of Bat3 (HLA-B associated transcript 3), p85 PI3K, Fyn, and Lck to the C-terminal tail of Tim-3 (Lee et al., 2011; Rangachari et al., 2012). In the absence of ligand-mediated Tim-3 signaling, Bat3 is bound to Tim-3 and blocks SH2 domain-binding sites in the Tim-3 tail. In this state, Bat3 recruits the catalytically active form of Lck, thereby forming an intracellular molecular complex with Tim-3 that preserves and potentially promotes T cell signaling (Rangachari et al., 2012). In contrast, Bat3-deficient T cells exhibit elevated pY505 Lck, the catalytically

mechanisms underlying the defective responses of Tim-3⁺ DCs to nucleic acid stimulation. HMGB1 binds DNA released from dying cells and facilitates delivery to innate cells via binding to receptor for advanced glycation end products (RAGE) and Toll-like receptors (TLRs) (2, 4, and 9), thereby triggering innate cell activation and production of pro-inflammatory cytokines. The binding of Tim-3 to HMGB1 can interfere with this process, thus suppressing activation of the innate immune response.

Most recently, Ceacam-1 was identified as a novel cell surface ligand for Tim-3 (Huang et al., 2015). Ceacam-1 co-immunoprecipitates with Tim-3 and is co-expressed with Tim-3 on CD4⁺ T cells upon tolerance induction and on CD8⁺ TILs that exhibit dysfunctional/exhausted phenotype. Importantly, the negative regulatory function of Tim-3 is defective in the absence of Ceacam-1, suggesting a requirement for Ceacam-1:Tim-3 interaction for proper Tim-3 function. Notably, Ceacam-1 binds to Tim-3 in both *cis* and *trans*, where the *cis* interaction promotes the stability of mature Tim-3 glycoprotein on the cell surface and both the *cis* and *trans* interactions drive the inhibitory function of Tim-3. Whether triggering of Tim-3 by Ceacam-1, galectin-9, or both ligands together differentially impacts on Tim-3 function remains to be determined.

Signaling

That Tim-3 is a key regulator of effector T cell function underscores the importance of elucidating the signaling pathway downstream of Tim-3. Similar to Lag-3, Tim-3 does not have a classical signaling motif in its cytoplasmic tail (Table 1). Rather, the cytoplasmic tails of both mouse and human Tim-3 contain

inactive form of Lck (Rangachari et al., 2012). Galectin-9 and Ceacam-1 binding to Tim-3 leads to phosphorylation of Y256 and Y263 and release of Bat-3 from the Tim-3 tail, thereby promoting Tim-3-mediated T cell inhibition by allowing binding of SH2 domain-containing Src kinases and subsequent regulation of TCR signaling (Figure 1B; Huang et al., 2015; Rangachari et al., 2012). Interestingly, Fyn binds to the same region on the Tim-3 tail as Bat3. Fyn has been implicated in the induction of T cell anergy (Davidson et al., 2007) and is known to be a key kinase to activate phosphoprotein associated with glycosphingolipid microdomains (PAG), which recruits Csk to suppress Lck function (Salmond et al., 2009; Smida et al., 2007). Because Fyn and Bat3 bind to the same domain in the Tim-3 cytoplasmic tail, it is possible that a switch between Tim-3-Bat3 and Tim-3-Fyn might trigger the switch of Tim-3 function from being permissive to TCR signaling to inhibition of upstream TCR signaling. In line with these data, loss of Bat-3 has been shown to result in dephosphorylation and degradation of TCR ζ (Rangachari et al., 2012).

Overall, current data show that the Tim-3 cytoplasmic tail has the potential to interact with multiple components of the TCR complex and that the balance of Bat-3 versus Fyn bound to the Tim-3 intracellular tail might be a key determinant of Tim-3 function. Because Tim-3 has many ligands, it will be important to determine how different ligands affect the binding of Bat-3 versus Fyn to the Tim-3 tail. This will be crucial to unraveling how Tim-3 functions to determine effector T cell responses.

Role of Tim-3 in Disease

The role of Tim-3 was initially investigated in autoimmunity where highly activated and uncontrolled responses directed to self-antigens are key drivers of disease. More recently, Tim-3 function has been examined in two diseases that serve as good counterpoints to autoimmunity, namely chronic viral infection and cancer. Indeed, Tim-3 can be protective in autoimmunity but is often poorly expressed (Figure 2B), whereas in both cancer and chronic viral infection, Tim-3 is highly expressed and contributes to the dampening of protective immunity (Figure 3). The function of Tim-3 in these different settings will be discussed below.

Autoimmunity. Because Th1 cells predominantly express Tim-3 (Monney et al., 2002) and Th1 cells are considered to be an important player in tissue-specific autoimmunity, the function of Tim-3 was initially probed in models of autoimmunity and tolerance. Animals treated with anti-Tim-3 antibody were shown to develop hyper-acute EAE accompanied by uncontrolled macrophage activation (Monney et al., 2002). Furthermore, administration of soluble Tim-3-Ig resulted in T cell hyperactivation, IFN- γ production, and loss of high-dose tolerance (Sabatos et al., 2003). These data gave the first indication that Tim-3 might function as an inhibitory molecule that serves to contract IFN- γ -driven inflammation. Indeed, it was later shown that administration of galectin-9 ameliorated EAE while knock-down of galectin-9 in vivo with siRNA exacerbated disease (Zhu et al., 2005). In keeping with its expression on IFN- γ -secreting Th1 T cells, Tim-3 deficiency regulates Th1- but not Th17-cell-driven EAE (Lee and Goverman, 2013). Collectively, these observations suggested that Tim-3 expression is an important determinant of autoimmunity. Indeed, in humans, Tim-3 expression is low on T cells in the peripheral blood and cerebrospinal fluid of patients with MS (Koguchi et al., 2006; Yang et al., 2008), in the peripheral blood of patients with rheumatoid arthritis (RA) (Liu et al., 2010), and in the peripheral blood of patients with psoriasis (Kanai et al., 2012). Importantly, Tim-3 expression is regained in MS patients that exhibit stable disease and reduced relapses after IFN- β therapy (Figure 2B; Yang et al., 2008). Moreover, preliminary genome-wide analysis of mRNA expression data from the peripheral blood of MS patients show that Tim-3 is significantly induced in responders to IFN- β therapy whereas non-responders show lower or no Tim-3 induction (Ottoboni et al., 2012).

The promotion of Tim-3 expression in MS patients after IFN- β therapy is in line with a recent study showing that IL-27, which is potentially induced by IFN- β , promotes not only Tim-3 but also IL-10 expression on murine T cells (Zhu et al., 2015). In addition, a recent study shows that IFN- β can induce Tim-3 directly on murine Th1 cells (Boivin et al., 2015). Thus, IFN- β can promote Tim-3 expression both directly and indirectly. Similarly, increased Tim-3 expression on peripheral blood T cells is also associated with responsiveness to treatment (Methotrexate or Tocilizumab [anti-IL6R]) and decreased disease activity in RA (Liu et al., 2010), although the mechanism underlying the increased Tim-3 expression in this setting has not been elucidated.

Cancer and Chronic Viral Infections. In recent years, the role of Tim-3 in the T cell dysfunction that arises in chronic viral infection and cancer has been heavily investigated. In the LCMV chronic infection model, Tim-3 marks virus-specific CD8⁺ T cells that

exhibit the biggest defects in pro-inflammatory cytokine (IL-2, TNF- α , IFN- γ) production (Jin et al., 2010). All virus-specific CD8⁺Tim-3⁺ T cells co-express PD-1 and co-blockade of Tim-3 and PD-1 is more effective at restoring anti-viral immunity than blockade of either receptor alone (Figure 3; Table 1). In humans, Tim-3 is similarly expressed on dysfunctional or exhausted CD8⁺ T cells during chronic viral infection. In HIV, Tim-3 marks virus-specific CD8⁺ T cells in the peripheral blood that exhibit dysfunctional/exhausted phenotype and Tim-3 blockade restores proliferation in response to stimulation with HIV-1 peptides (Jones et al., 2008). Tim-3⁺ T cells that exhibit dysfunctional or exhausted phenotype are also found in the peripheral blood and liver of patients chronically infected with hepatitis C virus (HCV) and in the peripheral blood of patients with hepatitis B virus (HBV). Importantly, blockade of Tim-3 restores effector function in T cells in these chronic viral infections (Golden-Mason et al., 2009; McMahan et al., 2010; Nebbia et al., 2012; Wu et al., 2012). Interestingly, increased frequencies of Tim-3⁺ T cells in HIV, HCV, and HBV patients positively correlate with increasing viral load and disease progression while reduced frequencies of Tim-3⁺ T cells correlate with anti-viral treatment and resolution of viral infection (Jones et al., 2008; McMahan et al., 2010; Wu et al., 2011). The positive correlation of Tim-3 with disease in chronic viral infections is diametrically opposed to the negative correlation of Tim-3 with disease activity in autoimmunity discussed above. Together these observations support the value of Tim-3 as a prognostic indicator of disease course in both chronic viral infections and autoimmunity.

The observation that CD8⁺Tim-3⁺ T cells exhibit dysfunctional or exhausted phenotype in chronic viral infection has called into question the reliability of using PD-1 expression as the sole hallmark for identifying dysfunctional or exhausted CD8⁺ T cells in chronic disease. Indeed, in HIV-infection, Tim-3 is found on dysfunctional/exhausted T cells that lack PD-1 expression (Jones et al., 2008). Moreover, Tim-3 expression marks the most dysfunctional/exhausted population within CD8⁺PD-1⁺ T cells in multiple chronic viral infections in humans (HCV, HBV) and also in experimental models of chronic viral infections (LCMV, HBV, Friend virus) (Jin et al., 2010; Ju et al., 2009; McMahan et al., 2010; Takamura et al., 2010). Importantly, co-blockade of the Tim-3 and PD-1 pathways results in greater restoration of T cell responses in HCV, HBV, and LCMV than PD-1 pathway blockade alone (Figure 3; Jin et al., 2010; McMahan et al., 2010; Nebbia et al., 2012). Collectively, these observations underscore the importance of the Tim-3 pathway in promoting T cell dysfunction and suggest that Tim-3 and PD-1 have non-redundant and synergistic functions in inhibiting effector T cell responses.

Tim-3 also marks dysfunctional or exhausted CD8⁺ T cells in cancer (Figure 3). Indeed, it was first shown here that expression of Tim-3 and PD-1 could be used to stratify populations of CD8⁺ TILs that exhibit different functional phenotypes (Sakuishi et al., 2010). Specifically, CD8⁺Tim-3⁺PD-1⁺ double-positive TILs exhibit severe dysfunctional or exhausted phenotype and CD8⁺Tim-3⁻PD-1⁺ single-positive TILs exhibit weak dysfunction/exhaustion and CD8⁺Tim-3⁻PD-1⁻ double-negative TILs exhibit good effector function. In line with these observations, co-blockade of the Tim-3 and PD-1 pathways is superior to

PD-1 pathway blockade alone at improving anti-tumor effector function and suppressing tumor growth in preclinical models of both solid and hematologic cancer (Figure 3; Ngiow et al., 2011; Sakuishi et al., 2010; Zhou et al., 2011). Importantly, in patients with advanced metastatic melanoma (Fourcade et al., 2010), non-small cell lung cancer (NSCLC) (Gao et al., 2012), or follicular B cell non-Hodgkin lymphoma (FL) (Yang et al., 2012), Tim-3 expression also marks dysfunctional/exhausted T cells and Tim-3 blockade improves function with Tim-3/PD-1 co-blockade showing greater effects (Fourcade et al., 2010; Yang et al., 2012). Notably, as observed in HIV, HBV, and HCV, the frequency of Tim-3⁺ T cells positively correlates with cancer severity and poor prognosis in both NSCLC (Gao et al., 2012) and FL (Yang et al., 2012). Interestingly, in FL, the frequency of PD-1⁺ T cells in tumors does not correlate with disease even though Tim-3 and PD-1 expression are correlated (Yang et al., 2012). This is probably due to the presence of PD-1 on other T cells that might not be dysfunctional and again underscores the value of Tim-3 expression as a marker for T cell dysfunction/exhaustion and the presence of Tim-3⁺ cells as a prognostic indicator of disease course.

In addition to its role in regulating effector T cell responses, Tim-3 might also have a role in regulating the function of FoxP3⁺ Treg cells. Tim-3 is upregulated on the FoxP3⁺ Treg cells that are present at tissue sites in different pathological settings (Table 1). In a model of allograft rejection, up to 40% of graft-infiltrating FoxP3⁺ cells express Tim-3 (Gupta et al., 2012). In cancer, Tim-3⁺ Treg cells constitute the majority (>50%) of Treg cells present in tumor tissue in both experimental tumor models and human tumors (Gao et al., 2012; Sakuishi et al., 2013; Yan et al., 2013). Notably, Tim-3⁺ Treg cells are infrequent in the peripheral blood and in peripheral lymphoid tissues. These observations suggest that Tim-3 marks tissue Treg cells and that Tim-3⁺ Treg cells might have a specialized role in suppressing immune responses at peripheral tissue sites. Although the Tim-3⁺ Treg cells in tissue allografts appear to be short-lived (Gupta et al., 2012), several lines of data show that Tim-3⁺ Treg cells have superior suppressive function when compared to Tim-3⁻ Treg cells. Tim-3⁺ Treg cells have higher expression of known Treg cell effector molecules such as IL-10, granzymes, and perforin as well as higher FoxP3 compared to Tim-3⁻ Treg cells. Furthermore, Tim-3⁺ Treg cells exhibit superior suppressor function *in vitro* relative to Tim-3⁻ Treg cells (Gautron et al., 2014; Gupta et al., 2012; Sakuishi et al., 2013). Lastly, the presence of Tim-3⁺ Treg cells has been found to correlate with poor clinical parameters such as the presence of nodal metastases and advanced disease stage in lung cancer (Gao et al., 2012), further supporting the value of Tim-3 as a prognostic indicator of disease course.

IL-27, a heterodimeric immunosuppressive cytokine, is a potent inducer of Tr1 cells (Awasthi et al., 2007) and, as mentioned above, also drives the expression of Tim-3 on CD4⁺ T cells (Zhu et al., 2015). Given that Tr1 cells also express Lag-3 (Gagliani et al., 2013), these observations raise the possibility that Tim-3, Lag-3, and potentially other co-inhibitory receptors have an important regulatory role in Tr1 cells and are in line with the demonstrated role of IL-27 in promoting resolution of autoimmune tissue inflammation (Fitzgerald et al., 2007a, 2007b) and suppressing anti-tumor immunity (Zhu et al., 2015).

Thus, Tim-3 functions in both effector and regulatory T lymphocyte subsets to regulate immune responses at sites of tissue inflammation.

Tim-3 in Innate Immunity

Recent studies have shown that Tim-3 is expressed on mature resting CD56^{dim} NK cells and is further upregulated upon activation in response to cytokine stimulation (Gleason et al., 2012; Ndhlovu et al., 2012). High expression of Tim-3 marks effector NK that are producing IFN- γ and are undergoing degranulation (Ndhlovu et al., 2012). However, in the context of metastatic melanoma, Tim-3 marks NK cells that exhibit a functional phenotype reminiscent of T cell dysfunction or exhaustion and Tim-3 blockade similarly restores function (da Silva et al., 2014). Furthermore, the level of Tim-3 expression on NK cells correlates with disease stage and poor prognostic factors. These observations extend the co-inhibitory function of Tim-3 to NK cells and further underscore the prognostic value of Tim-3 in cancer.

As mentioned above, Tim-3 can inhibit DC activation by acting as a molecular sink for HMGB1 (Chiba et al., 2012). Although this mechanism can inhibit DC responses, it is not known whether it depends on the ability of Tim-3 to signal into DC. Examination of the role of Tim-3 in mice bearing conditional deletion of Tim-3 in DCs will help resolve this important issue.

In recent years, it has further been discovered that Tim-3 has a role in regulating monocyte and/or macrophage function in both humans and mice (Yang et al., 2013; Zhang et al., 2012). Down-modulation of Tim-3 signaling either by Tim-3 antibody blockade or by Tim-3 knock-down with small-interfering RNA in monocytes and macrophages increases the production of IL-1 β , IL-6, IL-10, IL-12, TNF- α , and HMGB1 in response to activation via TLRs (Yang et al., 2013; Zhang et al., 2012). The modulation of responses to TLR stimulation by Tim-3 has important implications for sepsis where Tim-3 expression has been shown to be upregulated on PBMCs in patients with acute sepsis but suppressed in patients with severe sepsis (Yang et al., 2013). These observations are consistent with a model where during acute sepsis Tim-3 is upregulated on macrophages in order to attenuate the massive inflammatory response and prevent unwanted tissue pathology but that during the progression of sepsis the expression of Tim-3 becomes downregulated, thereby resulting in uncontrolled macrophage activation. The fact that Tim-3 expression is dynamically regulated in response to LPS, initially increasing and then decreasing after either prolonged stimulation with LPS or stimulation with increasing doses of LPS, supports this model (Yang et al., 2013). Indeed, Tim-3 might have a specialized role in regulating the response to LPS through TLR4 because Tim-3 blockade exacerbates sepsis after cecal ligation and puncture in wild-type but not *Tlr4*^{-/-} mice. Collectively, these data support the fact that Tim-3 is an inhibitory receptor on monocytes/macrophages and that increasing Tim-3 signals might be of therapeutic value in treating severe sepsis.

Tim-3: Promotion of Myeloid-Derived Suppressor Cells

Tim-3 can also suppress the immune response indirectly via its promotion of myeloid-derived suppressor cells (MDSCs). MDSCs are a heterogeneous population of immature myeloid cells that exhibit features of both granulocytes and monocytes and are important suppressors of the T cell response in many pathologic conditions but most notably in cancer where they expand to large numbers (reviewed in Gabrilovich and Nagaraj,

Table 2. Ligand Binding Affinities for TIGIT, CD226, and CD96

Receptor	Affinity (nM)	
	CD155	CD112
TIGIT	1–3	not measurable
CD226	114–199	8,790
CD96	37.6	not tested

2009). In mice, MDSCs express CD11b and high levels of the granulocyte marker Gr-1. Transgenic overexpression of Tim-3 on T cells promotes expansion of CD11b⁺Gr-1⁺ cells (Dardalhon et al., 2010). Accordingly, Tim-3 transgenic mice exhibit accelerated tumor growth and decreased autoimmunity (Dardalhon et al., 2010). The Tim-3-galectin-9 interaction drives expansion of MDSCs as shown by the fact that galectin-9 transgenic mice also exhibit expansion of MDSCs and introduction of Tim-3 deficiency reverses this expansion. Together, these observations indicate that Tim-3 can suppress the adaptive immune response indirectly via promotion of MDSCs.

It is important to note that therapeutic blockade of Tim-3 in order to enhance immune responses will affect multiple targets including CD4⁺ T cells, CD8⁺ T cells, FoxP3⁺ Treg cells, FoxP3⁻ Tr1 cells, NK cells, DCs, and MDSCs and that in all of these cell types Tim-3 acts to inhibit immune responses and promote tolerance.

TIGIT

Discovery, Ligands, and Function

TIGIT (T cell immunoglobulin and ITIM domain) was first identified by bioinformatic algorithm as a novel member of the CD28 family and was given the HUGO designation Vsig9, which was later changed to Vstm3 and then to TIGIT. A number of groups simultaneously identified the molecule to be expressed on NK cells, effector, and memory T cells and Treg cells and each group gave it a different name including Vstm3 (Levin et al., 2011), TIGIT (Stanietsky et al., 2009; Yu et al., 2009), and WUCAM (Boles et al., 2009). TIGIT is a receptor of the Ig superfamily that is specifically expressed in immune cells where it functions as a co-inhibitory receptor (Boles et al., 2009; Stanietsky et al., 2009; Yu et al., 2009). TIGIT is expressed on activated T cells and is also found on NK cells, memory T cells, a subset of Treg cells as well as follicular T helper (T_{fh}) cells (Boles et al., 2009; Joller et al., 2011, 2014; Levin et al., 2011; Stanietsky et al., 2009; Yu et al., 2009). TIGIT binds two ligands, CD155 (PVR) and CD112 (PVRL2, nectin-2), which are expressed on APCs, T cells, and a variety of non-hematopoietic cell types including tumor cells (Casado et al., 2009; Levin et al., 2011; Mendelsohn et al., 1989; Stanietsky et al., 2009; Yu et al., 2009). However, TIGIT binds with much higher affinity to CD155 than to CD112 (Table 2) and whether the TIGIT:CD112 interaction has functional relevance in mediating inhibitory functions still needs to be addressed. CD226 (DNAM-1) and CD96 (Tactile) bind to the same ligands and together with TIGIT form a pathway in which CD226 delivers a positive co-stimulatory signal (Bottino et al., 2003), while CD96 and TIGIT deliver inhibitory signals (Figure 1C; Chan et al., 2014).

The pathway formed by CD226, TIGIT, and their ligands is reminiscent of the B7-CD28-CTLA-4 pathway in that both pathways are formed by a positive and negative receptor expressed

on T and NK cells that share ligands expressed on APCs. Like CTLA-4, TIGIT binds its ligands with much higher affinity than CD226 (Figure 1C; Table 2) and can inhibit the interaction between CD226 and CD155 in a dose-dependent manner in competition assays (Levin et al., 2011; Stanietsky et al., 2009; Yu et al., 2009). A recent study suggests that TIGIT not only competes with CD226 for its ligands but that it can also directly bind to CD226 *in cis* and disrupt its homodimerization and hence its co-stimulatory function (Johnston et al., 2014). However, to what degree TIGIT and CD226 are co-expressed on T cells at inflamed tissue sites is unclear. Thus, a careful examination of CD226 and TIGIT co-expression together with visualization of CD226 homodimers in disease settings is needed to determine whether this mechanism is operative *in vivo*.

In addition to directly acting on T and NK cells, TIGIT also indirectly suppresses immune responses through the triggering of CD155 on DCs. TIGIT engagement of CD155, which itself contains an immunoreceptor tyrosine-based inhibitory motif (ITIM) in its cytoplasmic tail, inhibits IL-12p40 production and instead induces IL-10 from treated DCs, rendering them tolerogenic (Yu et al., 2009). Why the engagement of CD155 by CD226 or CD96 would not similarly induce tolerance is not completely understood. TIGIT binds to its ligand CD155 by forming a heterotetramer with a core TIGIT homodimer (Stengel et al., 2012), reminiscent of what was observed with the CTLA-4/B7-1 crystal structure (Stamper et al., 2001). This clustering of TIGIT is essential for the observed back signaling into DCs as disruption of the TIGIT-TIGIT interface abrogates CD155 phosphorylation (Stengel et al., 2012). The differential ability of TIGIT versus CD226 and CD96 to induce a tolerizing signal in DCs could therefore be linked to their ability to induce CD155 clustering.

Signaling

TIGIT shares structural similarities with the larger PVR-nectin family of molecules and is composed of an extracellular IgV domain, a type 1 transmembrane region, and a cytoplasmic tail containing an ITIM and an immunoglobulin tail tyrosine (ITT)-like motif, which are highly conserved between mouse and human (Figure 1C; Table 1; Boles et al., 2009; Levin et al., 2011; Stanietsky et al., 2009; Stengel et al., 2012; Yu et al., 2009). However, which of the two motifs is important for the inhibitory function of TIGIT seems to differ between the species. Biochemical aspects of TIGIT signaling have only been studied in NK cells, where in mice, the function of the two motifs seems redundant. Phosphorylation of the tyrosine residue in either the ITIM motif (Y233) or the ITT-like motif (Y227) is sufficient for signal transduction and the inhibitory activity of TIGIT is lost only when both residues are mutated (Stanietsky et al., 2013). In human NK cells, different groups have reported an essential role for the phosphorylation of the tyrosine residue in either the ITIM motif (Y231) (Stanietsky et al., 2009) or the ITT-like motif (Y225) (Li et al., 2014; Liu et al., 2013). Hence, the contribution of the ITIM versus ITT-like motif in mediating the inhibitory signal of human TIGIT remains unclear. These studies were performed in cell lines overexpressing TIGIT, so investigating the role of the ITIM versus ITT-like motifs in primary cells might bring more clarity.

Engagement of TIGIT through CD155 induces its phosphorylation through Fyn and Lck and the recruitment of SHIP1 (SH2 domain-containing inositol-5-phosphatase 1) through the cytosolic adaptor Grb2 (growth factor receptor-bound protein 2)

(Liu et al., 2013). Recruitment of SHIP1 to the TIGIT tail blocks signal transduction through the PI3K (phosphoinositide 3-kinase) and MAPK (mitogen-activated protein kinase) pathways and results in NK cell inhibition (Li et al., 2014; Liu et al., 2013). In addition, upon phosphorylation, the ITT-like motif of TIGIT binds β -arrestin 2 and recruits SHIP1 to limit NF- κ B (nuclear factor- κ B) signaling (Li et al., 2014; Liu et al., 2013). The combined effects of TIGIT on these three signaling pathways leads to a strong reduction of NK cytotoxicity, granule polarization, and cytokine secretion in NK cells (Li et al., 2014; Liu et al., 2013; Stanietsky et al., 2009). Although the inhibitory effects of TIGIT on T cell responses were initially believed to be indirect via CD155 ligation on DCs, we (Joller et al., 2011) and others (Levin et al., 2011) later showed that TIGIT also directly induces T cell inhibition in a cell-intrinsic manner. In T cells, TIGIT blocks productive T cell activation, proliferation, and acquisition of effector functions by targeting molecules in the TCR signaling pathway. TIGIT engagement downregulates components of the TCR complex itself (e.g., TCR α , CD3 ϵ) as well as central regulators of the TCR signaling cascade such as PLC γ (Joller et al., 2011). At the same time, however, TIGIT engagement induces anti-apoptotic molecules such as Bcl-xL as well as upregulation of the receptors for IL-2, IL-7, and IL-15, which promote T cell survival. Thus, although TIGIT inhibits T cell activation, it also actively contributes to their maintenance and ensures that the T cells that have been functionally inhibited are not deleted from the repertoire.

Role of TIGIT in Disease

Autoimmunity. Genome-wide association studies have linked a SNP in the positive regulator CD226 (Gly307Ser) of the TIGIT-CD226 pathway to multiple autoimmune diseases in humans including type 1 diabetes, multiple sclerosis, and rheumatoid arthritis (Hafler et al., 2009; Maiti et al., 2010). As a consequence, the function of TIGIT was initially investigated in models of autoimmunity and tolerance (Figure 2C). Although TIGIT-deficient mice do not develop spontaneous autoimmunity, they display augmented T cell responses upon immunization (Joller et al., 2011). A series of EAE experiments demonstrated that TIGIT has an inhibitory function in regulating CNS autoimmunity. As observed for Tim-3, blocking of TIGIT exacerbates autoimmune disease (Levin et al., 2011). TIGIT-deficient mice were shown to be highly susceptible to EAE with higher frequencies of encephalitogenic T cells and elevated levels of pro-inflammatory cytokines relative to wild-type controls (Joller et al., 2011). Furthermore, when crossed to MOG_{35–55}-specific TCR transgenic 2D2 mice, TIGIT-deficient mice developed spontaneous atypical EAE that was marked by signs of neurologic dysfunction reminiscent of Th17-cell-driven disease (Jäger et al., 2009; Joller et al., 2011). In addition to EAE, TIGIT also plays a protective role in collagen-induced arthritis (CIA) and graft versus host disease (GvHD). In both models, blocking of TIGIT resulted in an exacerbation of the disease driven by enhanced pro-inflammatory T cell responses (Levin et al., 2011). Collectively, these data suggest that TIGIT plays an important role in maintaining peripheral tolerance by dampening T cell activation.

In addition to its direct inhibitory role in NK and effector T cells, TIGIT also inhibits immune responses through promoting Treg cell function (Figure 2C). TIGIT is a direct target gene of Foxp3, the master transcription factor in Treg cells (Zhang et al.,

2013). In Treg cells, TIGIT expression correlates with markers for natural, rather than peripherally induced Treg cells and TIGIT⁺ Treg cells show enhanced demethylation in Treg-cell-specific demethylated regions compared to their TIGIT⁻ Treg cell counterparts, leading to higher lineage stability (Fuhrman et al., 2015; Joller et al., 2014). TIGIT⁺ Treg cells further express higher levels of Treg cell signature genes, such as Foxp3, CD25, and CTLA-4, and engagement of TIGIT on Treg cells leads to an upregulation of the suppressive mediator Fgl2, which confers superior suppressive function to TIGIT⁺ Treg cells (Joller et al., 2014). Importantly, TIGIT-dependent induction of Fgl2 results in selective sparing of Th2 cell responses, while potently suppressing pro-inflammatory Th1 and Th17 cell responses, which are the dominant responses driving autoimmune tissue inflammation. Thus, TIGIT⁺ Treg cells inhibit autoreactive T cells not only by suppressing their proliferation, but also by shifting the cytokine balance away from a Th1- and Th17-cell-dominated response and toward a Th2 cell-like response.

Cancer and Chronic Viral Infections. In addition to its protective role in autoimmune diseases, TIGIT has also gained attention in the context of cancer and chronic infections (Figure 3). The TIGIT ligands CD155 and CD112 are widely expressed on tumor cells. CD226, the positive counterpart of this costimulatory pathway, promotes cytotoxicity and enhances anti-tumor responses (Gilfillan et al., 2008; Iguchi-Manaka et al., 2008). In contrast, TIGIT negatively regulates anti-tumor responses, as indicated by the fact that TIGIT-deficient mice show significantly delayed tumor growth in two different tumor models (Kurtulus et al., 2015). Interestingly, TIGIT does not seem to affect metastasis formation, as shown by the fact that the number of lung nodules found after intravenous injection of B16 melanoma cells was comparable in TIGIT-deficient and in wild-type mice (Chan et al., 2014; Kurtulus et al., 2015). The suppressive function of TIGIT is also exploited by *Fusobacterium nucleatum*, a bacterium often found within the tumor microenvironment, to inhibit protective immune responses (Gur et al., 2015). TIGIT directly binds to the Fap2 protein of *F. nucleatum* and its engagement inhibits NK cell cytotoxicity in vitro.

Within the tumor microenvironment, TIGIT is highly expressed on human and murine TILs across a broad range of tumors (Chauvin et al., 2015; Johnston et al., 2014; Kurtulus et al., 2015). In murine tumors, CD8⁺TIGIT⁺ TILs co-express PD-1, Tim-3, and Lag3 and exhibit the most dysfunctional phenotype among CD8⁺ TILs (Kurtulus et al., 2015). TIGIT further marks tumor tissue Treg cells. Importantly, TIGIT expression is relatively poor in the peripheral lymphoid organs of tumor-bearing mice but highly enriched in tumor tissue, indicating a specialized role for TIGIT in regulating immune responses in tumor tissue (Kurtulus et al., 2015).

As has been mentioned earlier, blockade of the PD-1-PD-L1 pathway is able to restore function in exhausted CD8⁺ T cells and co-blockade with Tim-3 is able to further enhance this effect (Ngiow et al., 2011; Sakuishi et al., 2010; Zhou et al., 2011). A number of recent publications indicate that TIGIT might have similar effects. In CD8⁺ TILs from melanoma patients, co-blockade of TIGIT with PD-1 additively improved proliferation, cytokine production, and degranulation (Chauvin et al., 2015). Similarly, co-blockade of TIGIT with PDL1 showed synergistic effects in the murine CT26 tumor model, leading to enhanced CTL

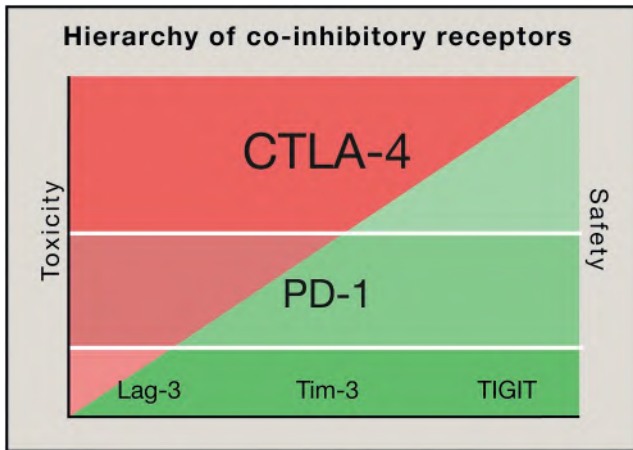


Figure 4. Hierarchy of Co-inhibitory Receptors

Co-inhibitory receptors are ranked from top to bottom according to their impact on the maintenance of self-tolerance. The impact of a given co-inhibitory receptor on self-tolerance is directly proportional to the amount of autoimmune toxicity observed when the receptor is deficient as a result of either genetic loss or therapeutic modulation. Genetic and/or therapeutic modulation of co-inhibitory receptors at the top of the hierarchy (tier 1; PD-1, CTLA-4) is predicted to be associated with more autoimmune-like toxicity than modulation of co-inhibitory receptors at the bottom of the hierarchy (tier 2; Lag-3, Tim-3, TIGIT). Accordingly, tier 2 co-inhibitory receptors are predicted to have a better safety profile in the clinic.

effector function and reversal of CD8⁺ T cell exhaustion. Combined treatment resulted in complete tumor rejection and induced tumor-antigen-specific protective memory responses

(Johnston et al., 2014). Interestingly, TIGIT synergizes not only with PD-1 but also with Tim-3 in impairing protective anti-tumor responses (Kurtulus et al., 2015). Therefore, co-blockade of either TIGIT with PD-1 or TIGIT with Tim-3 promotes anti-tumor immunity and induces tumor regression. Collectively, these data indicate that TIGIT synergizes with other co-inhibitory molecules to dampen effector T cell responses and promote T cell dysfunction.

As mentioned above, TIGIT is highly enriched on tumor-infiltrating Treg cells. The TIGIT⁺ Treg cells in tumor tissue exhibit a highly active and suppressive Treg cell phenotype. Importantly, dissection of the functional role of TIGIT in CD8⁺ T cells and Treg cells suggests that TIGIT plays a key role in driving suppression in the tumor environment via its function in Treg cells (Kurtulus et al., 2015). Thus, TIGIT can suppress anti-tumor immunity by multiple mechanisms that include direct suppression of effector CD8⁺ T cell function and indirect suppression via promotion of Treg cell function.

The chronic exposure to antigen and the functional exhaustion of effector T cells are hallmarks of both cancer and chronic infections. Similar to its role in anti-tumor responses, CD226 was shown to enhance CTL and NK functions during persistent viral infection and thus promote viral clearance (Nabekura et al., 2014; Welch et al., 2012). Recent data showed that exhausted CD8⁺ T cells induced in chronic LCMV infection also co-express TIGIT with PD-1, Tim-3, and Lag-3 (Figure 3; Doering et al., 2012; Johnston et al., 2014). Parallel to its role in TILs, co-blockade of TIGIT with PDL1 restored cytokine production in exhausted CD8⁺ T cells in chronic LCMV infection (Johnston et al., 2014). Whether in this context TIGIT also has

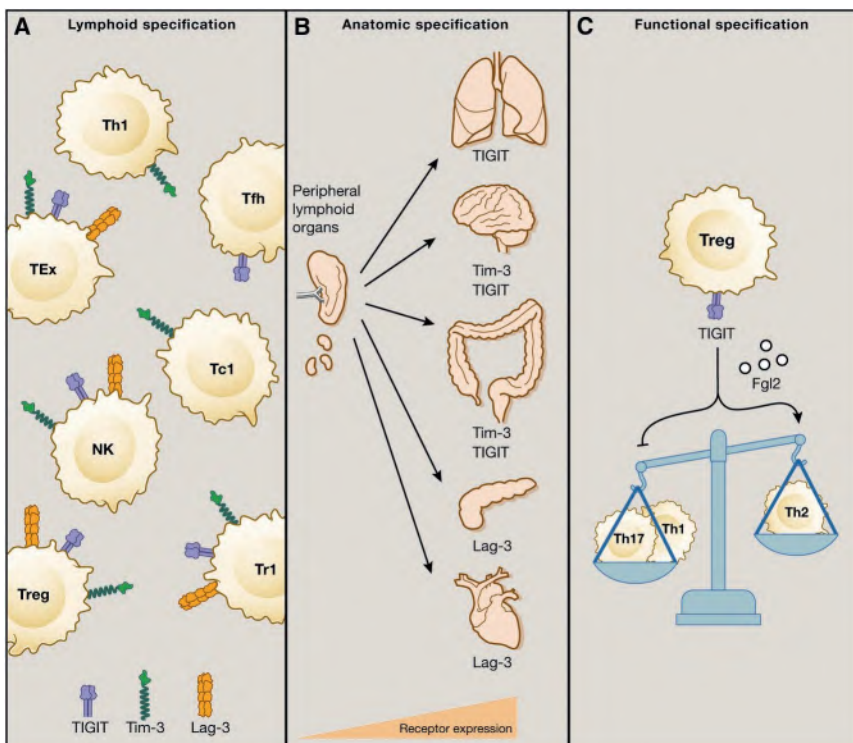


Figure 5. Specification of Checkpoint-Receptor Pathways

(A) Lymphoid specification. Some co-inhibitory receptors are preferentially expressed on distinct lymphocyte subsets.

(B) Anatomic specification. Some co-inhibitory receptor pathways may dominate in different tissue sites where ligands and/or receptors are highly expressed.

(C) Functional specification. Some co-inhibitory receptors may regulate distinct aspects of immunity such as the regulation of the balance between type 1/type 17 immunity and type 2 immunity by TIGIT.

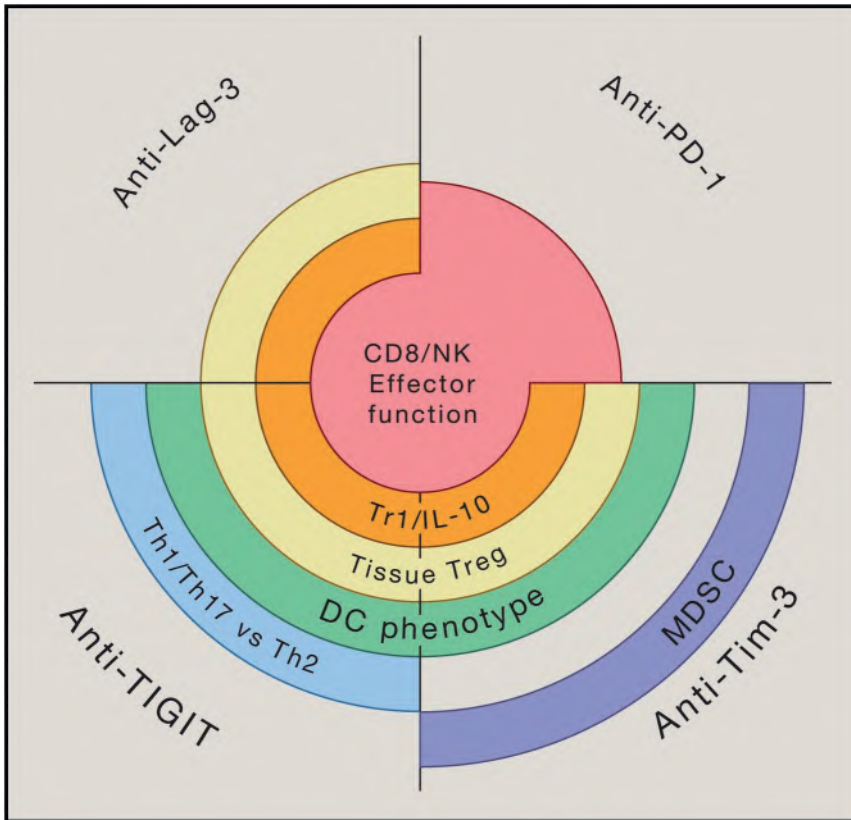


Figure 6. Immunological Effects of Checkpoint Receptor Blockades

Schematic representation showing the effects of PD-1, Lag-3, Tim-3, and TIGIT blockades on the immune response. Although all checkpoint receptor blockades have some effect on CD8⁺ T cell and NK cell effector function, the effect of PD-1 blockade is proportionally larger than that of Lag-3, Tim-3, or TIGIT blockade alone. Lag-3, Tim-3, and TIGIT blockades will preferentially affect tumor tissue Treg cells and IL-10-producing Tr1 cells. Tim-3 and TIGIT blockades will additionally affect DC phenotype. A unique effect of TIGIT blockade is shifting the balance in favor of type 1/17 immunity versus type 2 immunity while a unique effect of Tim-3 blockade is to dampen MDSCs. Thus, different checkpoint receptor blockades can be combined to achieve distinct effects on the immune response.

synergistic effects with Tim-3, as seen in cancer, remains to be determined.

TIGIT Shifts the Cytokine Balance

As observed for all co-inhibitory receptors, TIGIT has a general dampening effect on the immune response as exemplified by the hyperproliferative phenotype of T cells from TIGIT-deficient mice (Joller et al., 2011; Levin et al., 2011). In addition to this general regulatory role, TIGIT and its costimulatory counterpart CD226 have differential effects on the cytokine environment elicited after immunization. In mouse and human effector T cells, CD226 is expressed on Th1 and Th17, but not on Th2, cells and promotes IFN- γ and IL-17 production (Dardalhon et al., 2005; Lozano et al., 2013). In contrast, TIGIT inhibits production of IFN- γ and IL-17 while enhancing Th2 cell cytokines and IL-10 (Burton et al., 2014; Joller et al., 2011, 2014; Lozano et al., 2012; Yu et al., 2009). Thus, TIGIT shifts the balance away from type 1 and type 17 immunity toward type 2 immunity and IL-10.

TIGIT mediates this shift in the cytokine balance by targeting the immune response at multiple levels, namely through its action on APCs, effector T cells, and Treg cells. In DCs, TIGIT ligation of CD155 inhibits IL-12p40 production and instead induces IL-10 production, thus generating tolerogenic DCs that suppress T cell proliferation and IFN- γ production from responding T cells (Yu et al., 2009). Hence, TIGIT dampens type 1 immunity indirectly via its interaction with APCs.

TIGIT further acts directly in effector T cells to induce a shift from a type-1- or type-17-dominated to an IL-10-dominated immune response. TIGIT-deficient mice exhibit increased frequencies of IFN- γ ⁺ and IL-17⁺CD4⁺ T cells while simultaneously

showing a near complete loss in IL-10 production after immunization with antigen in complete Freund's adjuvant (Joller et al., 2011). Importantly, this further holds true for human effector T cells, where TIGIT knock down results in upregulation of T-bet and IFN- γ with a concomitant decrease in IL-10 (Lozano et al., 2012). In addition, in a model of antigen-specific tolerance induction, where reduction in IFN- γ ⁺ T cells goes along with an increase in IL-10⁺Foxp3⁻ Tr1

cells, IL-10 expression is correlated with TIGIT expression (Burton et al., 2014). Therefore, the direct action of TIGIT on effector T cells further contributes to shift the cytokine balance by inhibiting pro-inflammatory type 1 and type 17 immunity while favoring IL-10 induction.

In Foxp3⁺ Treg cells, TIGIT expression marks a functionally distinct subset that selectively suppresses pro-inflammatory type 1 and type 17 responses (Joller et al., 2014). TIGIT ligation in Treg cells directly induces the suppressive mediator Fgl2 in a CEBP α -dependent manner. Fgl2 inhibits differentiation of IFN- γ -secreting Th1 cells but promotes secretion of IL-4 and IL-10 (Chan et al., 2003). Co-culture of TIGIT⁺ Treg cells with effector T cells stimulated under polarizing conditions suppresses Th1 and Th17 cell differentiation but not Th2 cell differentiation. This effect is entirely dependent on Fgl2 because loss of Fgl2 in TIGIT⁺ Treg cells restores their ability to suppress Th2 cell responses. Importantly, this differential suppression can also be recapitulated in vivo as TIGIT⁺ Treg cells are capable of inhibiting Th1 or Th17 cell responses elicited upon immunization with peptide in complete Freund's adjuvant. In contrast, TIGIT⁺ Treg cells are unable to suppress disease in a Th2-cell-driven asthma model (Joller et al., 2014). In addition, TIGIT ligation in Treg cells directly induces IL-10 and IL-10⁺ Treg cells are almost exclusively found within the TIGIT⁺ Treg cell subset. Thus, TIGIT⁺ Treg cells shift the cytokine balance by selectively suppressing type 1 and type 17 immunity while favoring type 2 immunity and secretion of IL-10. TIGIT therefore targets different players in the immune response that work together to dampen pro-inflammatory type 1 and type 17 immunity and instead shift the

cytokine balance toward an IL-10-dominated or type-2-immunity-dominated environment.

Conclusion

The current landscape of co-inhibitory receptor pathways has expanded from CTLA-4 and PD-1 to include Lag-3, Tim-3, and most recently, TIGIT. This growing landscape of co-inhibitory receptor pathways raises the important question of why there are so many pathways that seemingly perform the same function. A simplistic answer would be that the immune system has built in a high order of functional redundancy to ensure the preservation of immune homeostasis and self-tolerance in the event that one or more co-inhibitory receptor pathways are compromised. Although this may be true, it seems that such an immune fail safe could be achieved with fewer pathways. We propose an alternative model, namely that CTLA-4 and PD-1 represent a first tier of co-inhibitory receptors that are primarily responsible for maintaining self-tolerance and restricting T cell clonotypes in lymphoid organs and that Lag-3, Tim-3, and TIGIT represent a second tier of co-inhibitory molecules that has distinct and specific roles in regulating immune responses, particularly at sites of tissue inflammation. Indeed, although Lag-3, Tim-3, and TIGIT have partially overlapping expression patterns (Table 1), their unique signaling tails provide a basis for both their unique regulatory functions as well as for the synergistic effects of therapies targeting these molecules in disease (Figure 3).

Our proposed model fits with the dominant function of CTLA-4 and then PD-1 in maintaining self-tolerance relative to Tim-3, Lag-3, and TIGIT (Figure 4). Indeed, the first and second tier co-inhibitory receptors can be ranked in a hierarchy. CTLA-4 sits at the top of this hierarchy given its critical role in maintaining self-tolerance as demonstrated by the massive lymphoproliferation and early lethality that occurs in mice deficient in CTLA-4 (Tivol et al., 1995; Waterhouse et al., 1995). In line with these observations, CTLA-4 blockade in cancer patients has been shown to result in significant grade 3–5 autoimmune-like toxicities in a fraction of treated patients (Hodi et al., 2010; Robert et al., 2015). PD-1 ranks second in the hierarchy. Mice deficient in PD-1 develop spontaneous autoimmunity but with lower penetrance and at a much later age than CTLA-4-deficient mice (Nishimura et al., 1999, 2001). Indeed, cancer patients undergoing anti-PD-1 immunotherapy exhibit less toxicity than patients treated with anti-CTLA-4 (Robert et al., 2015). Based on current data, Tim-3, Lag-3, and TIGIT would equally rank next in the hierarchy. Mice deficient in these molecules do not develop spontaneous autoimmunity and their inhibitory function becomes evident only in susceptible backgrounds or upon active induction of disease. Accordingly, interference with these pathways would be predicted to be associated with less toxicity than has been observed with either CTLA-4 or PD-1.

According to our model, the second tier of co-inhibitory receptors provides specificity to the regulation of immune responses in tissue, where their ligands may be expressed and function to maintain tissue tolerance and inhibit immunopathology (Figure 5). This concept of specification can operate at multiple levels. The first is at the level of the lymphocyte and is exemplified by the expression of different co-inhibitory receptors on distinct lymphocyte subsets. One example is the preferential expression of Tim-3 on IFN- γ -secreting effector T cells that infiltrate in-

flamed tissues (Monney et al., 2002). Another example is the specific upregulation of Tim-3 and TIGIT on tissue Treg cells (Figure 5A; Kurtulus et al., 2015; Sakuishi et al., 2013). Anatomic specification operates at the level of tissue sites. One example is the Tim-3 pathway. Two of the known ligands for Tim-3, galectin-9 and Ceacam-1, are highly expressed in the gut, thus positioning the Tim-3 pathway as having a dominant role in regulating immune responses in the gut. Other pathways might have dominant roles in other organs (Figure 5B). Functional specification holds that some pathways might regulate distinct features of the immune response. Here, the TIGIT pathway seems to have evolved to shift the cytokine balance and specifically suppress type 1 and type 17 immunity while sparing or even promoting type 2 immunity (Figure 5C; Joller et al., 2014).

As therapies that target Lag-3, Tim-3, and TIGIT move forward in clinical development, it is important to deepen our understanding of the specialized roles of each of these molecules in regulating the immune response and their tissue-specific functions. The insight gained into the specialized functions of these molecules will inform as to how to best apply therapies that interfere with these pathways in the clinic, particularly in the context of combinatorial strategies with existing therapies (Figure 6).

CONFLICTS OF INTEREST

V.K.K. is a founder and member of the scientific advisory board for Potenza Therapeutics and Tizona Therapeutics. A.C.A. is a member of the scientific advisory board for Potenza Therapeutics and Tizona Therapeutics.

ACKNOWLEDGMENTS

Research in the authors' laboratories was supported by grants from the NIH (P01 AI073748, P01 NS076410, P01 AI039671, and R01 NS045937 to V.K.K. and R01 CA187975 to A.C.A.), from the Melanoma Research Alliance (to A.C.A.), from the Melanoma Research Foundation (to A.C.A.), and from the American Cancer Society (RSG-11-057-01-LIB to A.C.A.).

REFERENCES

- Attanasio, J., and Wherry, E.J. (2016). Costimulatory and coinhibitory receptor pathways in infectious disease. *Immunity* 44, this issue, 1052–1068.
- Awasthi, A., Carrier, Y., Peron, J.P., Bettelli, E., Kamanaka, M., Flavell, R.A., Kuchroo, V.K., Oukka, M., and Weiner, H.L. (2007). A dominant function for interleukin 27 in generating interleukin 10-producing anti-inflammatory T cells. *Nat. Immunol.* 8, 1380–1389.
- Bettini, M., Szymczak-Workman, A.L., Forbes, K., Castellaw, A.H., Selby, M., Pan, X., Drake, C.G., Korman, A.J., and Vignali, D.A. (2011). Cutting edge: accelerated autoimmune diabetes in the absence of LAG-3. *J. Immunol.* 187, 3493–3498.
- Blackburn, S.D., Shin, H., Haining, W.N., Zou, T., Workman, C.J., Polley, A., Betts, M.R., Freeman, G.J., Vignali, D.A., and Wherry, E.J. (2009). Coregulation of CD8+ T cell exhaustion by multiple inhibitory receptors during chronic viral infection. *Nat. Immunol.* 10, 29–37.
- Boivin, N., Baillargeon, J., Doss, P.M., Roy, A.P., and Rangachari, M. (2015). Interferon- β suppresses murine Th1 cell function in the absence of antigen-presenting cells. *PLoS ONE* 10, e0124802.
- Boles, K.S., Vermi, W., Facchetti, F., Fuchs, A., Wilson, T.J., Diacovo, T.G., Cella, M., and Colonna, M. (2009). A novel molecular interaction for the adhesion of follicular CD4 T cells to follicular DC. *Eur. J. Immunol.* 39, 695–703.
- Bottino, C., Castriconi, R., Pende, D., Rivera, P., Nanni, M., Carnemolla, B., Cantoni, C., Grassi, J., Marcenaro, S., Reymond, N., et al. (2003). Identification of PV9 (CD155) and Nectin-2 (CD112) as cell surface ligands for the human DNAM-1 (CD226) activating molecule. *J. Exp. Med.* 198, 557–567.

- Brignone, C., Escudier, B., Grygar, C., Marcu, M., and Triebel, F. (2009). A phase I pharmacokinetic and biological correlative study of IMP321, a novel MHC class II agonist, in patients with advanced renal cell carcinoma. *Clin. Cancer Res.* **15**, 6225–6231.
- Brignone, C., Gutierrez, M., Mefti, F., Brain, E., Jarcau, R., Cvitkovic, F., Bousetta, N., Medioni, J., Gligorov, J., Grygar, C., et al. (2010). First-line chemioimmunotherapy in metastatic breast carcinoma: combination of paclitaxel and IMP321 (LAG-3lg) enhances immune responses and antitumor activity. *J. Transl. Med.* **8**, 71.
- Burton, B.R., Britton, G.J., Fang, H., Verhagen, J., Smithers, B., Sabatos-Peyton, C.A., Carney, L.J., Gough, J., Strobel, S., and Wraith, D.C. (2014). Sequential transcriptional changes dictate safe and effective antigen-specific immunotherapy. *Nat. Commun.* **5**, 4741.
- Butler, N.S., Moebius, J., Pewe, L.L., Traore, B., Doumbo, O.K., Tygrett, L.T., Waldschmidt, T.J., Crompton, P.D., and Harty, J.T. (2012). Therapeutic blockade of PD-L1 and LAG-3 rapidly clears established blood-stage *Plasmodium* infection. *Nat. Immunol.* **13**, 188–195.
- Callahan, M.K., Postow, M.A., and Wolchok, J.D. (2016). Targeting T cell co-receptors for cancer therapy. *Immunity* **44**, this issue, 1069–1078.
- Camisaschi, C., Casati, C., Rini, F., Perego, M., De Filippo, A., Triebel, F., Parmiani, G., Belli, F., Rivoltini, L., and Castelli, C. (2010). LAG-3 expression defines a subset of CD4(+)CD25(high)Foxp3(+) regulatory T cells that are expanded at tumor sites. *J. Immunol.* **184**, 6545–6551.
- Cao, E., Zang, X., Ramagopal, U.A., Mukhopadhyaya, A., Federov, A., Federov, E., Zencheck, W.D., Lary, J.W., Cole, J.L., Deng, H., et al. (2007). T cell immunoglobulin mucin-3 crystal structure reveals a galectin-9-independent ligand binding surface. *Immunity* **26**, 311–321.
- Casado, J.G., Pawelec, G., Morgado, S., Sanchez-Correa, B., Delgado, E., Gayoso, I., Duran, E., Solana, R., and Tarazona, R. (2009). Expression of adhesion molecules and ligands for activating and costimulatory receptors involved in cell-mediated cytotoxicity in a large panel of human melanoma cell lines. *Cancer Immunol. Immunother.* **58**, 1517–1526.
- Chan, C.W., Kay, L.S., Khadaroo, R.G., Chan, M.W., Lakatoo, S., Young, K.J., Zhang, L., Gorczynski, R.M., Catral, M., Rotstein, O., and Levy, G.A. (2003). Soluble fibrinogen-like protein 2/fibroleukin exhibits immunosuppressive properties: suppressing T cell proliferation and inhibiting maturation of bone marrow-derived dendritic cells. *J. Immunol.* **170**, 4036–4044.
- Chan, C.J., Martinet, L., Gilfillan, S., Souza-Fonseca-Guimaraes, F., Chow, M.T., Town, L., Ritchie, D.S., Colonna, M., Andrews, D.M., and Smyth, M.J. (2014). The receptors CD96 and CD226 oppose each other in the regulation of natural killer cell functions. *Nat. Immunol.* **15**, 431–438.
- Chauvin, J.M., Pagliano, O., Fourcade, J., Sun, Z., Wang, H., Sander, C., Kirkwood, J.M., Chen, T.H., Maurer, M., Korman, A.J., and Zarour, H.M. (2015). TIGIT and PD-1 impair tumor antigen-specific CD8⁺ T cells in melanoma patients. *J. Clin. Invest.* **125**, 2046–2058.
- Chen, J., and Chen, Z. (2014). The effect of immune microenvironment on the progression and prognosis of colorectal cancer. *Med. Oncol.* **31**, 82.
- Chiba, S., Baghdadi, M., Akiba, H., Yoshiyama, H., Kinoshita, I., Dosaka-Akita, H., Fujioka, Y., Ohba, Y., Gorman, J.V., Colgan, J.D., et al. (2012). Tumor-infiltrating DCs suppress nucleic acid-mediated innate immune responses through interactions between the receptor TIM-3 and the alarmin HMGB1. *Nat. Immunol.* **13**, 832–842.
- da Silva, I.P., Gallois, A., Jimenez-Baranda, S., Khan, S., Anderson, A.C., Kuchroo, V.K., Osman, I., and Bhardwaj, N. (2014). Reversal of NK-cell exhaustion in advanced melanoma by Tim-3 blockade. *Cancer Immunol. Res.* **2**, 410–422.
- Dardalhon, V., Schubart, A.S., Reddy, J., Meyers, J.H., Monney, L., Sabatos, C.A., Ahuja, R., Nguyen, K., Freeman, G.J., Greenfield, E.A., et al. (2005). CD226 is specifically expressed on the surface of Th1 cells and regulates their expansion and effector functions. *J. Immunol.* **175**, 1558–1565.
- Dardalhon, V., Anderson, A.C., Karman, J., Apetoh, L., Chandwaskar, R., Lee, D.H., Cornejo, M., Nishi, N., Yamauchi, A., Quintana, F.J., et al. (2010). Tim-3/galectin-9 pathway: regulation of Th1 immunity through promotion of CD11b+Ly-6G+ myeloid cells. *J. Immunol.* **185**, 1383–1392.
- Davidson, D., Schraven, B., and Veillette, A. (2007). PAG-associated FynT regulates calcium signaling and promotes energy in T lymphocytes. *Mol. Cell. Biol.* **27**, 1960–1973.
- DeKruyff, R.H., Bu, X., Ballesteros, A., Santiago, C., Chim, Y.L., Lee, H.H., Karisola, P., Pichavant, M., Kaplan, G.G., Umetsu, D.T., et al. (2010). T cell/transmembrane, Ig, and mucin-3 allelic variants differentially recognize phosphatidylserine and mediate phagocytosis of apoptotic cells. *J. Immunol.* **184**, 1918–1930.
- Doering, T.A., Crawford, A., Angelosanto, J.M., Paley, M.A., Ziegler, C.G., and Wherry, E.J. (2012). Network analysis reveals centrally connected genes and pathways involved in CD8⁺ T cell exhaustion versus memory. *Immunity* **37**, 1130–1144.
- Fitzgerald, D.C., Ciric, B., Touil, T., Harle, H., Grammatikopolou, J., Das Sarma, J., Gran, B., Zhang, G.X., and Rostami, A. (2007a). Suppressive effect of IL-27 on encephalitogenic Th17 cells and the effector phase of experimental autoimmune encephalomyelitis. *J. Immunol.* **179**, 3268–3275.
- Fitzgerald, D.C., Zhang, G.X., El-Behi, M., Fonseca-Kelly, Z., Li, H., Yu, S., Saris, C.J., Gran, B., Ciric, B., and Rostami, A. (2007b). Suppression of autoimmune inflammation of the central nervous system by interleukin 10 secreted by interleukin 27-stimulated T cells. *Nat. Immunol.* **8**, 1372–1379.
- Fourcade, J., Sun, Z., Benallaoua, M., Guillaume, P., Luescher, I.F., Sander, C., Kirkwood, J.M., Kuchroo, V., and Zarour, H.M. (2010). Upregulation of Tim-3 and PD-1 expression is associated with tumor antigen-specific CD8⁺ T cell dysfunction in melanoma patients. *J. Exp. Med.* **207**, 2175–2186.
- Fuhrman, C.A., Yeh, W.I., Seay, H.R., Saikumar Lakshmi, P., Chopra, G., Zhang, L., Perry, D.J., McClymont, S.A., Yadav, M., Lopez, M.C., et al. (2015). Divergent phenotypes of human regulatory T cells expressing the receptors TIGIT and CD226. *J. Immunol.* **195**, 145–155.
- Gabrilovich, D.I., and Nagaraj, S. (2009). Myeloid-derived suppressor cells as regulators of the immune system. *Nat. Rev. Immunol.* **9**, 162–174.
- Gagliani, N., Magnani, C.F., Huber, S., Gianolini, M.E., Pala, M., Licona-Limon, P., Guo, B., Herbert, D.R., Bulfone, A., Trentini, F., et al. (2013). Coexpression of CD49b and LAG-3 identifies human and mouse T regulatory type 1 cells. *Nat. Med.* **19**, 739–746.
- Gao, X., Zhu, Y., Li, G., Huang, H., Zhang, G., Wang, F., Sun, J., Yang, Q., Zhang, X., and Lu, B. (2012). TIM-3 expression characterizes regulatory T cells in tumor tissues and is associated with lung cancer progression. *PLoS ONE* **7**, e306676.
- Gautron, A.S., Dominguez-Villar, M., de Marken, M., and Hafler, D.A. (2014). Enhanced suppressor function of TIM-3⁺ FoxP3⁺ regulatory T cells. *Eur. J. Immunol.* **44**, 2703–2711.
- Gilfillan, S., Chan, C.J., Cella, M., Haynes, N.M., Rapaport, A.S., Boles, K.S., Andrews, D.M., Smyth, M.J., and Colonna, M. (2008). DNAM-1 promotes activation of cytotoxic lymphocytes by nonprofessional antigen-presenting cells and tumors. *J. Exp. Med.* **205**, 2965–2973.
- Gleason, M.K., Lenvik, T.R., McCullar, V., Felices, M., O'Brien, M.S., Cooley, S.A., Verneris, M.R., Cichocki, F., Holman, C.J., Panoskaltsis-Mortari, A., et al. (2012). Tim-3 is an inducible human natural killer cell receptor that enhances interferon gamma production in response to galectin-9. *Blood* **119**, 3064–3072.
- Golden-Mason, L., Palmer, B.E., Kassam, N., Townshend-Bulson, L., Livingston, S., McMahon, B.J., Castelblanco, N., Kuchroo, V., Gretch, D.R., and Rosen, H.R. (2009). Negative immune regulator Tim-3 is overexpressed on T cells in hepatitis C virus infection and its blockade rescues dysfunctional CD4⁺ and CD8⁺ T cells. *J. Virol.* **83**, 9122–9130.
- Grosso, J.F., Kelleher, C.C., Harris, T.J., Maris, C.H., Hipkiss, E.L., De Marzo, A., Anders, R., Netto, G., Getnet, D., Bruno, T.C., et al. (2007). LAG-3 regulates CD8⁺ T cell accumulation and effector function in murine self- and tumor-tolerance systems. *J. Clin. Invest.* **117**, 3383–3392.
- Gupta, S., Thornley, T.B., Gao, W., Larocca, R., Turka, L.A., Kuchroo, V.K., and Strom, T.B. (2012). Allograft rejection is restrained by short-lived TIM-3+PD-1+Foxp3+ Tregs. *J. Clin. Invest.* **122**, 2395–2404.
- Gur, C., Ibrahim, Y., Isaacson, B., Yamin, R., Abed, J., Gamliel, M., Enk, J., Bar-On, Y., Stanietsky-Kaynan, N., Copenhagen-Glazer, S., et al. (2015). Binding of the Fap2 protein of *Fusobacterium nucleatum* to human inhibitory

- receptor TIGIT protects tumors from immune cell attack. *Immunity* 42, 344–355.
- Hafler, J.P., Maier, L.M., Cooper, J.D., Plagnol, V., Hinks, A., Simmonds, M.J., Stevens, H.E., Walker, N.M., Healy, B., Howson, J.M., et al.; International Multiple Sclerosis Genetics Consortium (IMSGC) (2009). CD226 Gly307Ser association with multiple autoimmune diseases. *Genes Immun.* 10, 5–10.
- Hannier, S., Tournier, M., Bismuth, G., and Triebel, F. (1998). CD3/TCR complex-associated lymphocyte activation gene-3 molecules inhibit CD3/TCR signaling. *J. Immunol.* 161, 4058–4065.
- Hodi, F.S., O'Day, S.J., McDermott, D.F., Weber, R.W., Sosman, J.A., Haanen, J.B., Gonzalez, R., Robert, C., Schadendorf, D., Hassel, J.C., et al. (2010). Improved survival with ipilimumab in patients with metastatic melanoma. *N. Engl. J. Med.* 363, 711–723.
- Huang, C.T., Workman, C.J., Flies, D., Pan, X., Marson, A.L., Zhou, G., Hipkiss, E.L., Ravi, S., Kowalski, J., Levitsky, H.I., et al. (2004). Role of LAG-3 in regulatory T cells. *Immunity* 21, 503–513.
- Huang, Y.H., Zhu, C., Kondo, Y., Anderson, A.C., Gandhi, A., Russell, A., Dougan, S.K., Petersen, B.S., Melum, E., Pertel, T., et al. (2015). CEACAM1 regulates TIM-3-mediated tolerance and exhaustion. *Nature* 517, 386–390.
- Huard, B., Prigent, P., Tournier, M., Bruniquel, D., and Triebel, F. (1995). CD4/major histocompatibility complex class II interaction analyzed with CD4- and lymphocyte activation gene-3 (LAG-3)-Ig fusion proteins. *Eur. J. Immunol.* 25, 2718–2721.
- Iguchi-Manaka, A., Kai, H., Yamashita, Y., Shibata, K., Tahara-Hanaoka, S., Honda, S., Yasui, T., Kikutani, H., Shibuya, K., and Shibuya, A. (2008). Accelerated tumor growth in mice deficient in DNAM-1 receptor. *J. Exp. Med.* 205, 2959–2964.
- Jäger, A., Dardalhon, V., Sobel, R.A., Bettelli, E., and Kuchroo, V.K. (2009). Th1, Th17, and Th9 effector cells induce experimental autoimmune encephalomyelitis with different pathological phenotypes. *J. Immunol.* 183, 7169–7177.
- Jha, V., Workman, C.J., McGaha, T.L., Li, L., Vas, J., Vignali, D.A., and Monestier, M. (2014). Lymphocyte Activation Gene-3 (LAG-3) negatively regulates environmentally-induced autoimmunity. *PLoS ONE* 9, e104484.
- Jin, H.T., Anderson, A.C., Tan, W.G., West, E.E., Ha, S.J., Araki, K., Freeman, G.J., Kuchroo, V.K., and Ahmed, R. (2010). Cooperation of Tim-3 and PD-1 in CD8 T-cell exhaustion during chronic viral infection. *Proc. Natl. Acad. Sci. USA* 107, 14733–14738.
- Johnston, R.J., Comps-Agrar, L., Hackney, J., Yu, X., Huseni, M., Yang, Y., Park, S., Javinal, V., Chiu, H., Irving, B., et al. (2014). The immunoreceptor TIGIT regulates antitumor and antiviral CD8(+) T cell effector function. *Cancer Cell* 26, 923–937.
- Joller, N., Hafler, J.P., Brynedal, B., Kassam, N., Spoerl, S., Levin, S.D., Sharpe, A.H., and Kuchroo, V.K. (2011). Cutting edge: TIGIT has T cell-intrinsic inhibitory functions. *J. Immunol.* 186, 1338–1342.
- Joller, N., Lozano, E., Burkett, P.R., Patel, B., Xiao, S., Zhu, C., Xia, J., Tan, T.G., Sefik, E., Yajnik, V., et al. (2014). Treg cells expressing the coinhibitory molecule TIGIT selectively inhibit proinflammatory Th1 and Th17 cell responses. *Immunity* 40, 569–581.
- Jones, R.B., Ndhlovu, L.C., Barbour, J.D., Sheth, P.M., Jha, A.R., Long, B.R., Wong, J.C., Satkunarajah, M., Schwenecker, M., Chapman, J.M., et al. (2008). Tim-3 expression defines a novel population of dysfunctional T cells with highly elevated frequencies in progressive HIV-1 infection. *J. Exp. Med.* 205, 2763–2779.
- Ju, Y., Hou, N., Zhang, X.N., Zhao, D., Liu, Y., Wang, J.J., Luan, F., Shi, W., Zhu, F.L., Sun, W.S., et al. (2009). Blockade of Tim-3 pathway ameliorates interferon-gamma production from hepatic CD8+ T cells in a mouse model of hepatitis B virus infection. *Cell. Mol. Immunol.* 6, 35–43.
- Kanai, Y., Satoh, T., Igawa, K., and Yokozeki, H. (2012). Impaired expression of Tim-3 on Th17 and Th1 cells in psoriasis. *Acta Derm. Venereol.* 92, 367–371.
- Kasagi, S., Kawano, S., and Kumagai, S. (2011). PD-1 and autoimmunity. *Crit. Rev. Immunol.* 31, 265–295.
- Koguchi, K., Anderson, D.E., Yang, L., O'Connor, K.C., Kuchroo, V.K., and Hafler, D.A. (2006). Dysregulated T cell expression of TIM3 in multiple sclerosis. *J. Exp. Med.* 203, 1413–1418.
- Kurtulus, S., Sakuishi, K., Ngiew, S.F., Joller, N., Tan, D.J., Teng, M.W.L., Smyth, M.J., Kuchroo, V.K., and Anderson, A.C. (2015). TIGIT predominantly regulates the immune response via regulatory T cells. *J. Clin. Invest.* 125, 4053–4062.
- Lee, S.Y., and Gorman, J.M. (2013). The influence of T cell Ig mucin-3 signaling on central nervous system autoimmune disease is determined by the effector function of the pathogenic T cells. *J. Immunol.* 190, 4991–4999.
- Lee, J., Su, E.W., Zhu, C., Hainline, S., Phuach, J., Moroco, J.A., Smithgall, T.E., Kuchroo, V.K., and Kane, L.P. (2011). Phosphotyrosine-dependent coupling of Tim-3 to T-cell receptor signaling pathways. *Mol. Cell. Biol.* 31, 3963–3974.
- Levin, S.D., Taft, D.W., Brandt, C.S., Bucher, C., Howard, E.D., Chadwick, E.M., Johnston, J., Hammond, A., Bontadelli, K., Ardourel, D., et al. (2011). Vstm3 is a member of the CD28 family and an important modulator of T-cell function. *Eur. J. Immunol.* 41, 902–915.
- Li, M., Xia, P., Du, Y., Liu, S., Huang, G., Chen, J., Zhang, H., Hou, N., Cheng, X., Zhou, L., et al. (2014). T-cell immunoglobulin and ITIM domain (TIGIT) receptor/poliovirus receptor (PVR) ligand engagement suppresses interferon- γ production of natural killer cells via β -arrestin 2-mediated negative signaling. *J. Biol. Chem.* 289, 17647–17657.
- Liang, B., Workman, C., Lee, J., Chew, C., Dale, B.M., Colonna, L., Flores, M., Li, N., Schweighoffer, E., Greenberg, S., et al. (2008). Regulatory T cells inhibit dendritic cells by lymphocyte activation gene-3 engagement of MHC class II. *J. Immunol.* 180, 5916–5926.
- Liu, Y., Shu, Q., Gao, L., Hou, N., Zhao, D., Liu, X., Zhang, X., Xu, L., Yue, X., Zhu, F., et al. (2010). Increased Tim-3 expression on peripheral lymphocytes from patients with rheumatoid arthritis negatively correlates with disease activity. *Clin. Immunol.* 137, 288–295.
- Liu, S., Zhang, H., Li, M., Hu, D., Li, C., Ge, B., Jin, B., and Fan, Z. (2013). Recruitment of Grb2 and SHIP1 by the ITT-like motif of TIGIT suppresses granule polarization and cytotoxicity of NK cells. *Cell Death Differ.* 20, 456–464.
- Lozano, E., Dominguez-Villar, M., Kuchroo, V., and Hafler, D.A. (2012). The TIGIT/CD226 axis regulates human T cell function. *J. Immunol.* 188, 3869–3875.
- Lozano, E., Joller, N., Cao, Y., Kuchroo, V.K., and Hafler, D.A. (2013). The CD226/CD155 interaction regulates the proinflammatory (Th1/Th17)/anti-inflammatory (Th2) balance in humans. *J. Immunol.* 191, 3673–3680.
- Mahoney, K.M., Rennert, P.D., and Freeman, G.J. (2015). Combination cancer immunotherapy and new immunomodulatory targets. *Nat. Rev. Drug Discov.* 14, 561–584.
- Maiti, A.K., Kim-Howard, X., Viswanathan, P., Guillén, L., Qian, X., Rojas-Villarraga, A., Sun, C., Cañas, C., Tobón, G.J., Matsuda, K., et al. (2010). Non-synonymous variant (Gly307Ser) in CD226 is associated with susceptibility to multiple autoimmune diseases. *Rheumatology (Oxford)* 49, 1239–1244.
- Matsuzaki, J., Gnjatich, S., Mhawech-Fauceglia, P., Beck, A., Miller, A., Tsuji, T., Eppolito, C., Qian, F., Lele, S., Shrikant, P., et al. (2010). Tumor-infiltrating NY-ESO-1-specific CD8+ T cells are negatively regulated by LAG-3 and PD-1 in human ovarian cancer. *Proc. Natl. Acad. Sci. USA* 107, 7875–7880.
- McMahan, R.H., Golden-Mason, L., Nishimura, M.I., McMahon, B.J., Kemper, M., Allen, T.M., Gretch, D.R., and Rosen, H.R. (2010). Tim-3 expression on PD-1+ HCV-specific human CTLs is associated with viral persistence, and its blockade restores hepatocyte-directed in vitro cytotoxicity. *J. Clin. Invest.* 120, 4546–4557.
- Mendelsohn, C.L., Wimmer, E., and Racaniello, V.R. (1989). Cellular receptor for poliovirus: molecular cloning, nucleotide sequence, and expression of a new member of the immunoglobulin superfamily. *Cell* 56, 855–865.
- Meyers, J.H., Sabatos, C.A., Chakravarti, S., and Kuchroo, V.K. (2005). The TIM gene family regulates autoimmune and allergic diseases. *Trends Mol. Med.* 11, 362–369.
- Miyazaki, T., Dierich, A., Benoist, C., and Mathis, D. (1996). Independent modes of natural killing distinguished in mice lacking Lag3. *Science* 272, 405–408.
- Monney, L., Sabatos, C.A., Gaglia, J.L., Ryu, A., Waldner, H., Chernova, T., Manning, S., Greenfield, E.A., Coyle, A.J., Sobel, R.A., et al. (2002). Th1-specific cell surface protein Tim-3 regulates macrophage activation and severity of an autoimmune disease. *Nature* 415, 536–541.

- Nabekura, T., Kanaya, M., Shibuya, A., Fu, G., Gascoigne, N.R., and Lanier, L.L. (2014). Costimulatory molecule DNAM-1 is essential for optimal differentiation of memory natural killer cells during mouse cytomegalovirus infection. *Immunity* 40, 225–234.
- Nakayama, M., Akiba, H., Takeda, K., Kojima, Y., Hashiguchi, M., Azuma, M., Yagita, H., and Okumura, K. (2009). Tim-3 mediates phagocytosis of apoptotic cells and cross-presentation. *Blood* 113, 3821–3830.
- Ndhlovu, L.C., Lopez-Vergès, S., Barbour, J.D., Jones, R.B., Jha, A.R., Long, B.R., Schoeffler, E.C., Fujita, T., Nixon, D.F., and Lanier, L.L. (2012). Tim-3 marks human natural killer cell maturation and suppresses cell-mediated cytotoxicity. *Blood* 119, 3734–3743.
- Nebbia, G., Peppas, D., Schurich, A., Khanna, P., Singh, H.D., Cheng, Y., Rosenberg, W., Dusheiko, G., Gilson, R., ChinAleong, J., et al. (2012). Upregulation of the Tim-3/galectin-9 pathway of T cell exhaustion in chronic hepatitis B virus infection. *PLoS ONE* 7, e47648.
- Ngiow, S.F., von Scheidt, B., Akiba, H., Yagita, H., Teng, M.W., and Smyth, M.J. (2011). Anti-TIM3 antibody promotes T cell IFN- γ -mediated antitumor immunity and suppresses established tumors. *Cancer Res.* 71, 3540–3551.
- Nishimura, H., Nose, M., Hiai, H., Minato, N., and Honjo, T. (1999). Development of lupus-like autoimmune diseases by disruption of the PD-1 gene encoding an ITIM motif-carrying immunoreceptor. *Immunity* 11, 141–151.
- Nishimura, H., Okazaki, T., Tanaka, Y., Nakatani, K., Hara, M., Matsumori, A., Sasayama, S., Mizoguchi, A., Hiai, H., Minato, N., and Honjo, T. (2001). Auto-immune dilated cardiomyopathy in PD-1 receptor-deficient mice. *Science* 291, 319–322.
- Okazaki, T., Okazaki, I.M., Wang, J., Sugiura, D., Nakaki, F., Yoshida, T., Kato, Y., Fagarasan, S., Muramatsu, M., Eto, T., et al. (2011). PD-1 and LAG-3 inhibitory co-receptors act synergistically to prevent autoimmunity in mice. *J. Exp. Med.* 208, 395–407.
- Ottoboni, L., Keenan, B.T., Tamayo, P., Kuchroo, M., Mesirov, J.P., Buckle, G.J., Khoury, S.J., Hafler, D.A., Weiner, H.L., and De Jager, P.L. (2012). An RNA profile identifies two subsets of multiple sclerosis patients differing in disease activity. *Sci. Transl. Med.* 4, 153ra131.
- Pauken, K.E., and Wherry, E.J. (2015). Overcoming T cell exhaustion in infection and cancer. *Trends Immunol.* 36, 265–276.
- Prigent, P., El Mir, S., Dréano, M., and Triebel, F. (1999). Lymphocyte activation gene-3 induces tumor regression and antitumor immune responses. *Eur. J. Immunol.* 29, 3867–3876.
- Qu, H.Q., Bradfield, J.P., Grant, S.F., Hakonarson, H., and Polychronakos, C.; Type 1 Diabetes Genetics Consortium (2009). Remapping the type 1 diabetes association of the CTLA4 locus. *Genes Immun.* 10 (Suppl 1), S27–S32.
- Rangachari, M., Zhu, C., Sakuishi, K., Xiao, S., Karman, J., Chen, A., Angin, M., Wakeham, A., Greenfield, E.A., Sobel, R.A., et al. (2012). Bat3 promotes T cell responses and autoimmunity by repressing Tim-3-mediated cell death and exhaustion. *Nat. Med.* 18, 1394–1400.
- Richter, K., Agnelli, P., and Oxenius, A. (2010). On the role of the inhibitory receptor LAG-3 in acute and chronic LCMV infection. *Int. Immunol.* 22, 13–23.
- Robert, C., Schachter, J., Long, G.V., Arance, A., Grob, J.J., Mortier, L., Daud, A., Carlino, M.S., McNeil, C., Lotem, M., et al.; KEYNOTE-006 investigators (2015). Pembrolizumab versus ipilimumab in advanced melanoma. *N. Engl. J. Med.* 372, 2521–2532.
- Romano, E., Michielin, O., Voelter, V., Laurent, J., Bichat, H., Stravodimou, A., Romero, P., Speiser, D.E., Triebel, F., Leyvraz, S., and Harari, A. (2014). MART-1 peptide vaccination plus IMP321 (LAG-3lg fusion protein) in patients receiving autologous PBMCs after lymphodepletion: results of a Phase I trial. *J. Transl. Med.* 12, 97.
- Sabatos, C.A., Chakravarti, S., Cha, E., Schubart, A., Sánchez-Fueyo, A., Zheng, X.X., Coyle, A.J., Strom, T.B., Freeman, G.J., and Kuchroo, V.K. (2003). Interaction of Tim-3 and Tim-3 ligand regulates T helper type 1 responses and induction of peripheral tolerance. *Nat. Immunol.* 4, 1102–1110.
- Sakuishi, K., Apetoh, L., Sullivan, J.M., Blazar, B.R., Kuchroo, V.K., and Anderson, A.C. (2010). Targeting Tim-3 and PD-1 pathways to reverse T cell exhaustion and restore anti-tumor immunity. *J. Exp. Med.* 207, 2187–2194.
- Sakuishi, K., Ngiow, S.F., Sullivan, J.M., Teng, M.W.L., Kuchroo, V.K., Smyth, M.J., and Anderson, A.C. (2013). TIM3⁺FOXP3⁺ regulatory T cells are tissue-specific promoters of T-cell dysfunction in cancer. *Oncol Immunology* 2, e23849.
- Salmond, R.J., Filby, A., Qureshi, I., Caserta, S., and Zamoyska, R. (2009). T-cell receptor proximal signaling via the Src-family kinases, Lck and Fyn, influences T-cell activation, differentiation, and tolerance. *Immunol. Rev.* 228, 9–22.
- Sánchez-Fueyo, A., Tian, J., Picarella, D., Domenig, C., Zheng, X.X., Sabatos, C.A., Manlongat, N., Bender, O., Kamradt, T., Kuchroo, V.K., et al. (2003). Tim-3 inhibits T helper type 1-mediated auto- and alloimmune responses and promotes immunological tolerance. *Nat. Immunol.* 4, 1093–1101.
- Santiago, C., Ballesteros, A., Martínez-Muñoz, L., Mellado, M., Kaplan, G.G., Freeman, G.J., and Casasnovas, J.M. (2007a). Structures of T cell immunoglobulin mucin protein 4 show a metal-ion-dependent ligand binding site where phosphatidylserine binds. *Immunity* 27, 941–951.
- Santiago, C., Ballesteros, A., Tami, C., Martínez-Muñoz, L., Kaplan, G.G., and Casasnovas, J.M. (2007b). Structures of T cell immunoglobulin mucin receptors 1 and 2 reveal mechanisms for regulation of immune responses by the TIM receptor family. *Immunity* 26, 299–310.
- Smida, M., Posevitz-Fejfar, A., Horejsi, V., Schraven, B., and Lindquist, J.A. (2007). A novel negative regulatory function of the phosphoprotein associated with glycosphingolipid-enriched microdomains: blocking Ras activation. *Blood* 110, 596–615.
- Song, Y.W., Im, C.H., Park, J.H., Lee, Y.J., Lee, E.Y., Lee, E.B., and Park, K. (2011). T-cell immunoglobulin and mucin domain 3 genetic polymorphisms are associated with rheumatoid arthritis independent of a shared epitope status. *Hum. Immunol.* 72, 652–655.
- Stamper, C.C., Zhang, Y., Tobin, J.F., Erbe, D.V., Ikemizu, S., Davis, S.J., Stahl, M.L., Seehra, J., Somers, W.S., and Mosyak, L. (2001). Crystal structure of the B7-1/CTLA-4 complex that inhibits human immune responses. *Nature* 410, 608–611.
- Stanietsky, N., Simic, H., Arapovic, J., Toporik, A., Levy, O., Novik, A., Levine, Z., Beiman, M., Dassa, L., Achdout, H., et al. (2009). The interaction of TIGIT with PVR and PVRL2 inhibits human NK cell cytotoxicity. *Proc. Natl. Acad. Sci. USA* 106, 17858–17863.
- Stanietsky, N., Rovis, T.L., Glasner, A., Seidel, E., Tsukerman, P., Yamin, R., Enk, J., Jonjic, S., and Mandelboim, O. (2013). Mouse TIGIT inhibits NK-cell cytotoxicity upon interaction with PVR. *Eur. J. Immunol.* 43, 2138–2150.
- Stengel, K.F., Harden-Bowles, K., Yu, X., Rouge, L., Yin, J., Comps-Agrar, L., Wiesmann, C., Bazan, J.F., Eaton, D.L., and Grogan, J.L. (2012). Structure of TIGIT immunoreceptor bound to poliovirus receptor reveals a cell-cell adhesion and signaling mechanism that requires cis-trans receptor clustering. *Proc. Natl. Acad. Sci. USA* 109, 5399–5404.
- Takamura, S., Tsuji-Kawahara, S., Yagita, H., Akiba, H., Sakamoto, M., Chikaishi, T., Kato, M., and Miyazawa, M. (2010). Premature terminal exhaustion of Friend virus-specific effector CD8⁺ T cells by rapid induction of multiple inhibitory receptors. *J. Immunol.* 184, 4696–4707.
- Tivol, E.A., Borriello, F., Schweitzer, A.N., Lynch, W.P., Bluestone, J.A., and Sharpe, A.H. (1995). Loss of CTLA-4 leads to massive lymphoproliferation and fatal multiorgan tissue destruction, revealing a critical negative regulatory role of CTLA-4. *Immunity* 3, 541–547.
- Triebel, F., Jitsukawa, S., Baixeras, E., Roman-Roman, S., Genevee, C., Viegas-Pequignot, E., and Hercend, T. (1990). LAG-3, a novel lymphocyte activation gene closely related to CD4. *J. Exp. Med.* 171, 1393–1405.
- van de Weyer, P.S., Muehleite, M., Klose, C., Bonventre, J.V., Walz, G., and Kuehn, E.W. (2006). A highly conserved tyrosine of Tim-3 is phosphorylated upon stimulation by its ligand galectin-9. *Biochem. Biophys. Res. Commun.* 351, 571–576.
- Wang, M., Ji, B., Wang, J., Cheng, X., Zhou, Q., Zhou, J., Cao, C., and Guo, Q. (2014). Tim-3 polymorphism downregulates gene expression and is involved in the susceptibility to ankylosing spondylitis. *DNA Cell Biol.* 33, 723–728.
- Wang-Gillam, A., Plambeck-Suess, S., Goedegebuure, P., Simon, P.O., Mitchem, J.B., Hornick, J.R., Sorscher, S., Picus, J., Suresh, R., Lockhart, A.C., et al. (2013). A phase I study of IMP321 and gemcitabine as the frontline therapy in patients with advanced pancreatic adenocarcinoma. *Invest. New Drugs* 31, 707–713.

- Waterhouse, P., Penninger, J.M., Timms, E., Wakeham, A., Shahinian, A., Lee, K.P., Thompson, C.B., Griesser, H., and Mak, T.W. (1995). Lymphoproliferative disorders with early lethality in mice deficient in Ctlα-4. *Science* *270*, 985–988.
- Welch, M.J., Teijaro, J.R., Lewicki, H.A., Colonna, M., and Oldstone, M.B. (2012). CD8 T cell defect of TNF- α and IL-2 in DNAM-1 deficient mice delays clearance in vivo of a persistent virus infection. *Virology* *429*, 163–170.
- Wherry, E.J., and Kurachi, M. (2015). Molecular and cellular insights into T cell exhaustion. *Nat. Rev. Immunol.* *15*, 486–499.
- Woo, S.R., Turnis, M.E., Goldberg, M.V., Bankoti, J., Selby, M., Nirschl, C.J., Bettini, M.L., Gravano, D.M., Vogel, P., Liu, C.L., et al. (2012). Immune inhibitory molecules LAG-3 and PD-1 synergistically regulate T-cell function to promote tumoral immune escape. *Cancer Res.* *72*, 917–927.
- Workman, C.J., and Vignali, D.A. (2003). The CD4-related molecule, LAG-3 (CD223), regulates the expansion of activated T cells. *Eur. J. Immunol.* *33*, 970–979.
- Workman, C.J., and Vignali, D.A. (2005). Negative regulation of T cell homeostasis by lymphocyte activation gene-3 (CD223). *J. Immunol.* *174*, 688–695.
- Workman, C.J., Dugger, K.J., and Vignali, D.A. (2002). Cutting edge: molecular analysis of the negative regulatory function of lymphocyte activation gene-3. *J. Immunol.* *169*, 5392–5395.
- Workman, C.J., Cauley, L.S., Kim, I.J., Blackman, M.A., Woodland, D.L., and Vignali, D.A. (2004). Lymphocyte activation gene-3 (CD223) regulates the size of the expanding T cell population following antigen activation in vivo. *J. Immunol.* *172*, 5450–5455.
- Wu, W., Shi, Y., Li, J., Chen, F., Chen, Z., and Zheng, M. (2011). Tim-3 expression on peripheral T cell subsets correlates with disease progression in hepatitis B infection. *Virology* *422*, 113–118.
- Wu, W., Shi, Y., Li, S., Zhang, Y., Liu, Y., Wu, Y., and Chen, Z. (2012). Blockade of Tim-3 signaling restores the virus-specific CD8⁺ T-cell response in patients with chronic hepatitis B. *Eur. J. Immunol.* *42*, 1180–1191.
- Xu, F., Liu, J., Liu, D., Liu, B., Wang, M., Hu, Z., Du, X., Tang, L., and He, F. (2014). LSECtin expressed on melanoma cells promotes tumor progression by inhibiting antitumor T-cell responses. *Cancer Res.* *74*, 3418–3428.
- Yan, J., Zhang, Y., Zhang, J.P., Liang, J., Li, L., and Zheng, L. (2013). Tim-3 expression defines regulatory T cells in human tumors. *PLoS ONE* *8*, e58006.
- Yang, L., Anderson, D.E., Kuchroo, J., and Hafler, D.A. (2008). Lack of TIM-3 immunoregulation in multiple sclerosis. *J. Immunol.* *180*, 4409–4414.
- Yang, Z.Z., Grote, D.M., Ziesmer, S.C., Niki, T., Hirashima, M., Novak, A.J., Witzig, T.E., and Ansell, S.M. (2012). IL-12 upregulates TIM-3 expression and induces T cell exhaustion in patients with follicular B cell non-Hodgkin lymphoma. *J. Clin. Invest.* *122*, 1271–1282.
- Yang, X., Jiang, X., Chen, G., Xiao, Y., Geng, S., Kang, C., Zhou, T., Li, Y., Guo, X., Xiao, H., et al. (2013). T cell Ig mucin-3 promotes homeostasis of sepsis by negatively regulating the TLR response. *J. Immunol.* *190*, 2068–2079.
- Yu, X., Harden, K., Gonzalez, L.C., Francesco, M., Chiang, E., Irving, B., Tom, I., Ivelja, S., Refino, C.J., Clark, H., et al. (2009). The surface protein TIGIT suppresses T cell activation by promoting the generation of mature immunoregulatory dendritic cells. *Nat. Immunol.* *10*, 48–57.
- Zhang, Q., and Vignali, D.A. (2016). Co-stimulatory and co-inhibitory pathways in autoimmunity. *Immunity* *44*, this issue, 1034–1051.
- Zhang, Y., Ma, C.J., Wang, J.M., Ji, X.J., Wu, X.Y., Moorman, J.P., and Yao, Z.Q. (2012). Tim-3 regulates pro- and anti-inflammatory cytokine expression in human CD14⁺ monocytes. *J. Leukoc. Biol.* *91*, 189–196.
- Zhang, Y., Maksimovic, J., Naselli, G., Qian, J., Chopin, M., Blewitt, M.E., Oshlack, A., and Harrison, L.C. (2013). Genome-wide DNA methylation analysis identifies hypomethylated genes regulated by FOXP3 in human regulatory T cells. *Blood* *122*, 2823–2836.
- Zhou, Q., Munger, M.E., Veenstra, R.G., Weigel, B.J., Hirashima, M., Munn, D.H., Murphy, W.J., Azuma, M., Anderson, A.C., Kuchroo, V.K., and Blazar, B.R. (2011). Coexpression of Tim-3 and PD-1 identifies a CD8⁺ T-cell exhaustion phenotype in mice with disseminated acute myelogenous leukemia. *Blood* *117*, 4501–4510.
- Zhu, C., Anderson, A.C., Schubart, A., Xiong, H., Imitola, J., Khoury, S.J., Zheng, X.X., Strom, T.B., and Kuchroo, V.K. (2005). The Tim-3 ligand galectin-9 negatively regulates T helper type 1 immunity. *Nat. Immunol.* *6*, 1245–1252.
- Zhu, C., Sakuishi, K., Xiao, S., Sun, Z., Zaghoulani, S., Gu, G., Wang, C., Tan, D.J., Wu, C., Rangachari, M., et al. (2015). An IL-27/NFIL3 signalling axis drives Tim-3 and IL-10 expression and T-cell dysfunction. *Nat. Commun.* *6*, 6072.

Primary, Adaptive, and Acquired Resistance to Cancer Immunotherapy

Padmanee Sharma,^{1,*} Siwen Hu-Lieskovan,² Jennifer A. Wargo,³ and Antoni Ribas^{2,*}

¹Department of Genitourinary Medical Oncology and Immunology, The University of Texas MD Anderson Cancer Center, Houston, TX 77030, USA

²Department of Medicine, Division of Hematology-Oncology, University of California, Los Angeles and the Jonsson Comprehensive Cancer Center, Los Angeles, CA 90095, USA

³Department of Melanoma Medical Oncology, The University of Texas MD Anderson Cancer Center, Houston, TX 77030, USA

*Correspondence: padsharma@mdanderson.org (P.S.), aribas@mednet.ucla.edu (A.R.)

<http://dx.doi.org/10.1016/j.cell.2017.01.017>

SUMMARY

Cancer immunotherapy can induce long lasting responses in patients with metastatic cancers of a wide range of histologies. Broadening the clinical applicability of these treatments requires an improved understanding of the mechanisms limiting cancer immunotherapy. The interactions between the immune system and cancer cells are continuous, dynamic, and evolving from the initial establishment of a cancer cell to the development of metastatic disease, which is dependent on immune evasion. As the molecular mechanisms of resistance to immunotherapy are elucidated, actionable strategies to prevent or treat them may be derived to improve clinical outcomes for patients.

Introduction

Metastatic cancers remain an incurable disease for the great majority of patients, as the intrinsic genomic instability common to all cancers facilitates the escape from cytotoxic or targeted therapies. The recent breakthroughs in the understanding of tumor immune biology and the development of newer generation of cancer immunotherapies have opened a brand new chapter in the war against cancer. This change in landscape is based on the discovery of cancer immune checkpoints and the success of checkpoint inhibitors, as well as the advances in technology to generate genetically modified immune cells (Miller and Sadelain, 2015). The focus of treatment has shifted from the tumor itself to the host's immune system, to mobilize immune cells to recognize and eventually eliminate the cancer cells. A hallmark of immunotherapy is the durability of responses, most likely due to the memory of the adaptive immune system, which translates into long-term survival for a subset of patients.

Early efforts to harness the immune system in cancer control, pioneered by Dr. William B. Coley in the 1890s (Coley, 1910), were overlooked due to the lack of consistency in response and were soon overwhelmed by the development of more effective treatments such as radiotherapy and chemotherapy. However, investigations continued to unravel and elucidate the interactions between the immune system and cancer cells. The concept of cancer immunosurveillance, which was proposed by Paul Ehrlich (Ehrlich, 1956) and enriched by Burnet and Thomas (Burnet, 1971) in the 1950s, stated that the emergence of malignant cells is a frequent event but is suppressed by the host's natural immunity, that cancer develops when this immunity is weakened, and that lymphocytes are responsible for this process. Finally, the cancer immune-editing concept was eluci-

dated by Schreiber and colleagues in 2002 (Dunn et al., 2002), recognizing a dual role of the host's immunity, both as an extrinsic tumor suppressor and a facilitator of tumor growth and progression, acting across three sequential phases—elimination, equilibrium and escape—through constant interactions between tumor cells, immune cells, and the tumor microenvironment. Importantly, host immune responses and tumor genomics are tightly related, as illustrated by the notion that neoantigens arising from genomic mutations may shape immune responses (Schumacher and Schreiber, 2015); however, these responses may prove ineffective against a heterogeneous and evolving tumor microenvironment.

The process of T cell activation involves antigen presentation by the major histocompatibility complex (MHC) molecules on the antigen-presenting cells (APCs) to the corresponding T cell receptor (TCR) on naive T cells. The interaction of costimulatory molecules CD28 and B7 is required for full activation, which is tightly regulated by inhibitory checkpoints to avoid collateral damage and autoimmunity. The CTLA-4 receptor on activated effector T cells and regulatory T cells (Tregs) was discovered in the 1980s (Brunet et al., 1987). Seminal work by James Allison and colleagues showed that CTLA-4 competes with CD28 for B7 ligands and inhibits proliferation and IL-2 secretion by T cells (Krummel and Allison, 1995) and that CTLA-4 blocking antibodies could treat tumors in immune competent animal models (Leach et al., 1996). Subsequent clinical testing resulted in the approval of ipilimumab for treatment of advanced melanoma in 2011, the first in class CTLA-4 checkpoint inhibitor approved by the US Food and Drug Administration (FDA) (Hodi et al., 2010; Robert et al., 2011). Pooled data from clinical trials of ipilimumab confirmed durable clinical responses, depicted by a plateau in the survival curve beginning around year 3, that lasted

Table 1. Terminology for Different Resistance Mechanisms to Immunotherapy

Term	Description
primary resistance	A clinical scenario where a cancer does not respond to an immunotherapy strategy. The mechanistic basis of lack of response to immunotherapy may include adaptive immune resistance.
adaptive immune resistance	A mechanism of resistance where a cancer is recognized by the immune system but it protects itself by adapting to the immune attack. Given the evolving nature of the immune/cancer cell interaction, this could clinically manifest as primary resistance, mixed responses or acquired resistance.
acquired resistance	A clinical scenario in which a cancer initially responded to immunotherapy but after a period of time it relapsed and progressed.

10 years or more in a subset of approximately 21% of patients (Schadendorf et al., 2015). In 2015, ipilimumab was also approved by the FDA as adjuvant therapy for locally advanced melanoma. Due to enhanced immune responses, possibly during early stages of T cell activation, significant immune-related toxicities have been observed, but most can be managed by systemic steroid therapy.

Another checkpoint receptor expressed by activated T cells, programmed death 1 (PD-1), was cloned in 1992 (Ishida et al., 1992), and subsequently its ligand PD-L1 was characterized (Dong et al., 1999; Freeman et al., 2000). PD-L1 expression can be constitutive or induced in many tumors to evade immune attack. Since PD-L1 expression can be induced by IFN γ , which is expressed during an active anti-tumor immune response, it has been referred to as a mechanism of adaptive immune resistance (Table 1). Antibodies blocking the PD-1 and PD-L1 inhibitory axis can unleash activated tumor-reactive T cells and have been shown in clinical trials to induce durable anti-tumor responses in increasing numbers of tumor histologies, including the tumor types that are not traditionally considered immunotherapy sensitive (Okazaki et al., 2013; Zou et al., 2016). This led to the approval of two anti-PD1 antibodies (pembrolizumab and nivolumab) and one anti-PD-L1 antibody (atezolimumab) for the treatment of advanced melanoma, non-small-cell lung cancer, renal cell carcinoma, head and neck squamous carcinoma, Hodgkin's lymphoma, and bladder cancer. Currently there are over ten anti-PD-1 and anti-PD-L1 antibodies in various stages of clinical testing in many different tumor types. Interestingly, there have been thousands of patients receiving PD-1 blockade therapy thus far, with similar immune related toxicities as observed for anti-CTLA-4 but with generally lower frequency, possibly because the PD-1 and PD-L1 checkpoint may act later in the T cell response, resulting in a more restricted T cell reactivity toward tumor cells, with the majority of patients tolerating treatment well (Larkin et al., 2015b). Due to the non-overlapping mechanism of action of anti-CTLA4 and anti-PD1 antibodies (Das et al., 2015; Gubin et al., 2014), clinical testing of the combination of these two classes of checkpoint inhibitors showed improved clinical response (up to 60%) in melanoma at the expense of significantly increased frequency of toxicities (Larkin et al., 2015a). The combination of CTLA4 and PD-1 and PD-L1 checkpoint blockade has been approved as front line therapy for advanced melanoma patients and is being tested in other tumor types with different dose levels and intervals of anti-CTLA4 to reduce toxicity.

Cell-based immunotherapy was pioneered by many investigators, including Alex Fefer, Phil Greenberg, Zelig Eshhar, Steven

Rosenberg, and colleagues in the 1980s, inspired by the correlation of the number of tumor infiltrating lymphocytes (TILs) and survival in some cancers. This process required TILs to be isolated from the patient's surgical specimen, expanded *in vitro*, and re-infused back to the lymphocyte-depleted patient. In these studies, sufficient TILs could not be isolated or expanded from tumors of approximately 50%–60% of patients, which limited the number of patients who could be treated. For patients who could be treated with the expanded TILs, the reported response rate was 50% for melanoma, including 20% complete responses, and 95% of these complete responders had more than 5 years of survival (Rosenberg et al., 2011). This approach, however, requires large surgical samples, experienced academic centers, and tumors enriched with anti-tumor T cells, which is a rare event for most tumor types. The recent advance of gene transfer technologies and T cell engineering has enabled more versatile approaches, including adoptive cell transfer (ACT) of the patient's peripheral T cells that are genetically modified to target cancer specific antigens, via physiological TCRs or chimeric antigen receptors (CARs) (Sadelain, 2016; Yang and Rosenberg, 2016). TCRs are usually cloned from TILs that are reactive to specific cancer antigens with no or very limited expression in normal adult tissue but are widely expressed by cancer cells. Such TCRs recognize tumor antigen presented in the context of the MHC. Clinical success has been documented (Yee et al., 2015). The TCR approach allows intracellular antigen targets but is MHC restricted and can be subject to treatment failure for tumors that have downregulated their MHC surface expression. CAR technology was first developed by Eshhar et al., 1993, who genetically engineered T cells with chimeric genes, linking single chain antibodies (scFv) targeting tumor cell surface antigens to intracellular signaling adaptors for TCR: in the first generation, to the T cell specific activating ζ chain of the CD3 complex. Subsequent modification with costimulatory molecules CD28 (second generation) and 4-1BB (third generation) has enabled the expansion of T cells while retaining function upon repeated antigen exposure. CAR T cells do not require MHC restriction and can be engineered to enhance T cell function. Recent clinical success with CD19 targeting CAR to treat CD19+ B cell malignancy has shown great success, with a remarkable 90% complete remission in a cohort of 30 patients with relapsed or refractory pediatric acute lymphoblastic leukemia (ALL), and two thirds of these patients remained in remission after 6 months (Maude et al., 2014). The biggest challenge facing the field of ACT is the identification of target tumor antigens that are not expressed by normal tissues, both to maximize specificity and efficacy and to minimize toxicity (Fesnak

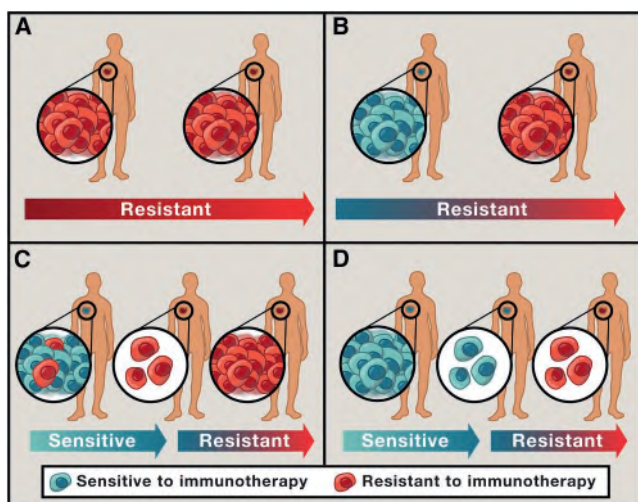


Figure 1. Clinical Scenarios of Primary, Adaptive, and Acquired Resistance to Immunotherapy

- (A) Patient's tumor is resistant to immunotherapy with no active immune response.
 (B) Patient's tumor is resistant to immunotherapy; active anti-tumor immune response, but turned off by checkpoints or other adaptive resistance mechanisms.
 (C) Patient has an initial response to immunotherapy but later progressed; heterogeneous population and selection of resistant clones that were present before treatment started.
 (D) Patient has an initial response to immunotherapy but later progressed; true acquired resistance during the immunotherapy.

et al., 2016). A commonly seen toxicity in ACT therapy is cytokine release syndrome, which can be life-threatening and requires prompt management with steroids and IL-6 receptor antibody (tocilizumab).

Despite the unprecedented durable response rates observed with cancer immunotherapies, the majority of patients do not benefit from the treatment (primary resistance), and some responders relapse after a period of response (acquired resistance). Several common cancer types have shown very low frequency of response (breast, prostate, and colon cancers), and heterogeneous responses have been seen even between distinct tumors within the same patient (Figure 1). For the purposes of this review, we have categorized primary, adaptive, and acquired resistance as described in Table 1, in keeping with the most typical conceptualization for practicing clinicians. However, in considering resistance mechanisms to immune-based therapies, it is important to remember that the immune response is dynamic and constantly evolving in each patient, either as a result of the patient's own environmental and genetic factors or as a result of treatment interventions, including surgery, chemotherapy, radiation therapy, and immunotherapy. Anti-tumor immune responses that are ongoing throughout the course of a patient's disease may be affected by many of these factors, and the establishment of resistance mechanisms relevant to immunotherapeutic failure may pre-date immunotherapy challenge. Without recourse to detailed immune and tumor characterization, these resistance mechanisms can be divided, clinically, into those that prevent a patient from ever responding

Table 2. Mechanisms of Primary and Adaptive Resistance to Immunotherapy

	Mechanism	Examples
tumor cell intrinsic	absence of antigenic proteins	low mutational burden
		lack of viral antigens
	absence of antigen presentation	lack of cancer-testis antigens
		overlapping surface proteins
genetic T cell exclusion	absence of antigen presentation	deletion in TAP
		deletion in B2M
		silenced HLA
insensibility to T cells	genetic T cell exclusion	MAPK oncogenic signaling
		stabilized b-catenin
tumor cell extrinsic	immunosuppressive cells	mesenchymal transcriptome
		oncogenic PD-L1 expression
		mutations in interferon gamma pathway signaling
tumor cell extrinsic	inhibitory immune checkpoints	absence of T cells with tumor antigen-specific TCRs
		VISTA, LAG-3, TIM-3
		TAMs, Tregs

to an immunotherapy or those that facilitate relapse after an initial response. Thus, although resistance to immunotherapies may manifest at different times, in many cases, similar or overlapping mechanisms enable tumor cells to evade anti-tumor immune responses. We discuss known resistance mechanisms and provide rationale for combination therapies to overcome resistance.

Primary and Adaptive Resistance to Immunotherapy

Patients who have primary resistance to checkpoint inhibitors do not respond to the initial therapy. Ongoing studies indicate that both tumor-cell-intrinsic and tumor-cell-extrinsic factors contribute to the resistance mechanisms (Table 2). The most straightforward reason why a tumor would not respond to immune checkpoint therapy or ACT is lack of recognition by T cells because of absence of tumor antigens (Gubin et al., 2014). Alternatively, cancer cells may have tumor antigens but develop mechanisms to avoid presenting them on the surface restricted by MHC, due to alterations in the antigen-presenting machinery (such as proteasome subunits or transporters associated with antigen processing), beta-2-microglobulin (B2M), or MHC itself (Marincola et al., 2000; Sucker et al., 2014). B2M is required for HLA class I folding and transport to the cell surface, and its genetic deficiency leads to lack of CD8 T cell recognition (Figures 2 and 3).

Tumor-Cell-Intrinsic Factors for Primary and Adaptive Resistance

Tumor-cell-intrinsic factors that contribute to immunotherapy resistance include expression or repression of certain genes and pathways in tumor cells that prevent immune cell infiltration or function within the tumor microenvironment. These mechanisms may exist at the time of initial presentation, highlighting primary resistance mechanisms, or these mechanisms may

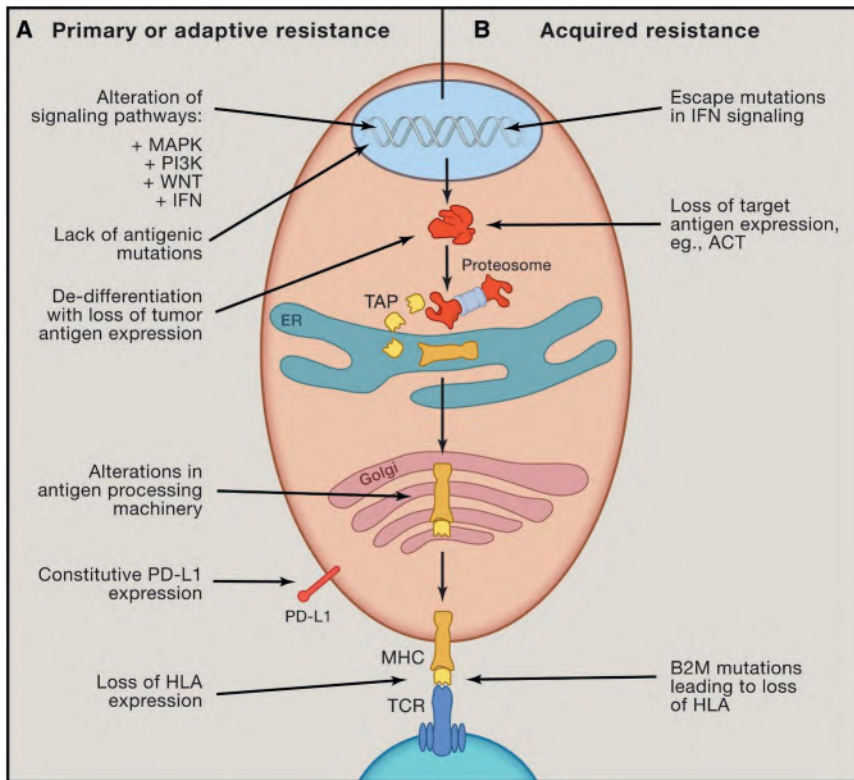


Figure 2. Known Intrinsic Mechanisms of Resistance to Immunotherapy

(A) Intrinsic factors that lead to primary or adaptive resistance including lack of antigenic mutations, loss of tumor antigen expression, loss of HLA expression, alterations in antigen processing machinery, alterations of several signaling pathways (MAPK, PI3K, WNT, IFN), and constitutive PD-L1 expression.

(B) Intrinsic factors that are associated with acquired resistance of cancer, including loss of target antigen, HLA, and altered interferon signaling, as well as loss of T cell functionality.

that attracts CD103⁺ DCs. In addition, murine tumors lacking β -catenin responded effectively to immune checkpoint therapy whereas β -catenin-positive tumors did not. Non-T-cell-inflamed human melanoma tumors, which lacked T cells and CD103⁺ DCs in the tumor microenvironment, had significantly higher expression of tumor intrinsic β -catenin signaling genes.

Cancer cells that constitutively express immunosuppressive cell surface ligands like PD-L1 may actively inhibit anti-tumor T cell responses. A genetic amplification of a locus in chromosome 9 that contains the genes for the two ligands of PD-1 (PD-L1 and PD-L2) and the interferon gamma

evolve later, highlighting adaptive resistance mechanisms. Multiple tumor-intrinsic mechanisms have recently been identified and include (1) signaling through the mitogen-activated protein kinase (MAPK) pathway and/or loss of PTEN expression, which enhances PI3K signaling, (2) expression of the WNT/ β -catenin signaling pathway, (3) loss of interferon-gamma (IFN γ) signaling pathways, and (4) lack of T cell responses as result of loss of tumor antigen expression.

Oncogenic signaling through the MAPK pathway results in the production of VEGF and IL-8, among many other secreted proteins, which have known inhibitory effects on T cell recruitment and function (Liu et al., 2013). Similarly, loss of PTEN, which enhances PI3K signaling and is a common phenomenon across several cancers, including 30% of melanomas, was found to be associated with resistance to immune checkpoint therapy (Peng et al., 2016). PTEN loss in tumors of the Cancer Genome Atlas (TCGA) melanoma dataset correlated with significantly decreased gene expression of IFN γ , granzyme B, and CD8⁺ T cell infiltration; importantly, the frequency of PTEN deletions and mutations was higher in non-T-cell-inflamed tumors as compared to T-cell-inflamed tumors. In a murine model, PTEN-knockout tumors were less susceptible to adoptive cell therapy than PTEN-expressing tumors.

The potential of oncogenic signaling pathways to induce T cell exclusion from cancers has also been described through the stabilization of β -catenin resulting in constitutive WNT signaling (Spranger et al., 2015). In a murine model, tumors with elevated β -catenin lacked a subset of dendritic cells (DCs) known as CD103⁺ DCs, due to decreased expression of CCL4, a chemokine

receptor signaling molecule Janus kinase 2 (JAK2) is termed the PDJ amplicon (Ansell et al., 2015; Green et al., 2010; Rooney et al., 2015). PDJ is amplified in the malignant Reed-Sternberg cells in Hodgkin's disease, and anti-PD-1 therapy results in objective responses in over 80% of patients with chemotherapy-refractory Hodgkin's disease (Ansell et al., 2015). Other mechanisms that have been described as leading to constitutive PD-L1 expression by cancer cells include PTEN deletions or PI3K and/or AKT mutations (Lastwika et al., 2016; Parsa et al., 2007), EGFR mutations (Akbay et al., 2013), MYC overexpression (Casey et al., 2016), CDK5 disruption (Dorand et al., 2016), and an increase in PD-L1 transcripts stabilized by truncation of the 3' UTR of this gene (Kataoka et al., 2016). It is currently unclear whether constitutive PD-L1 expression resulting from these oncogenic signaling processes results in decreased or increased likelihood of responding to anti-PD-1 and PD-L1 therapy, but it may indeed result in lack of response to other cancer immunotherapy strategies by actively inhibiting anti-tumor T cells.

The interferon-gamma pathway is emerging as a key player in primary, adaptive, and acquired resistance to checkpoint blockade therapy (Gao et al., 2016; Pardoll, 2012; Ribas, 2015; Shin et al., 2016; Zaretsky et al., 2016). It has both favorable and detrimental effects on anti-tumor immune responses. Interferon-gamma produced by tumor-specific T cells that have recognized their cognate antigen on cancer cells or APCs induces an effective anti-tumor immune response through (1) enhanced tumor antigen presentation that occurs as a result of increased expression of proteins, such as MHC molecules, involved in antigen presentation, (2) recruitment of other immune

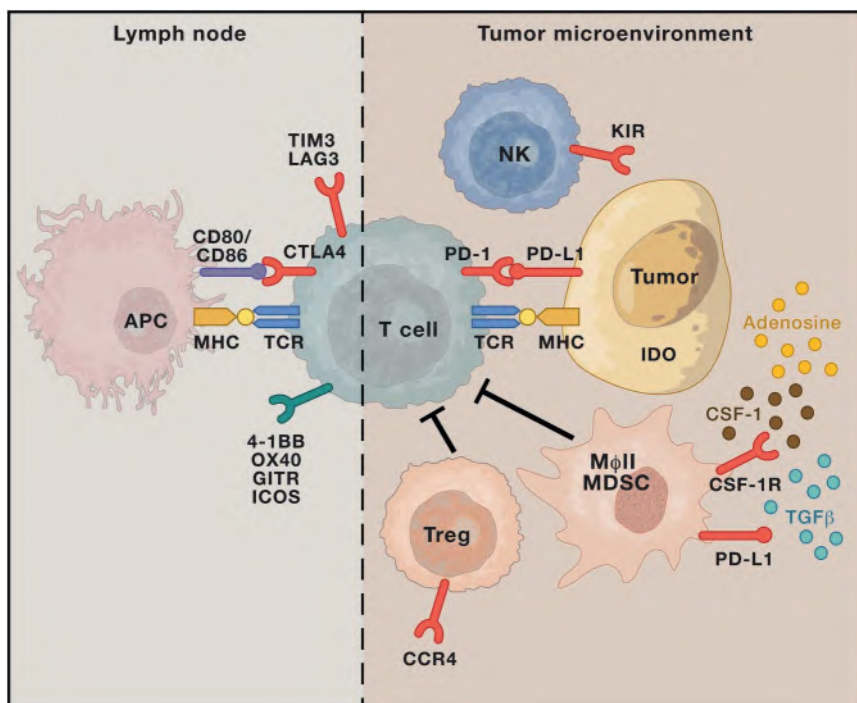


Figure 3. Known Extrinsic Mechanisms of Resistance to Immunotherapy

This includes CTLA-4, PD1, and other immune checkpoints, T cell exhaustion and phenotype change, immune suppressive cell populations (Tregs, MDSC, type II macrophages), and cytokine and metabolite release in the tumor microenvironment (CSF-1, tryptophan metabolites, TGF- β , adenosine). Abbreviations are as follows: APC, antigen-presenting cells; MHC, major histocompatibility complex; TCR, T cell receptor; Treg, regulatory T cell; MDSC, myeloid-derived suppressor cell; M ϕ II, type II macrophage.

who did not respond to anti-PD-1 therapy, termed innate anti-PD-1 resistance signature, or IPRES (Hugo et al., 2016). These genes that lead to lack of response are related to mesenchymal transformation, stemness, and wound healing and are preferentially expressed by cancers that seldom respond to PD-1 blockade therapy, such as pancreatic cancer.

Epigenetic modification of the DNA in cancer cells may lead to changes in gene expression of immune-related genes, which can impact antigen processing,

cells, and (3) direct anti-proliferative and pro-apoptotic effects on tumor cells (Platanias, 2005). But continuous interferon-gamma exposure can lead to immunoediting of cancer cells, resulting in immune escape (Benci et al., 2016; Shankaran et al., 2001). One mechanism by which cancer cells could escape the effects of interferon gamma is by downregulating or mutating molecules involved in the interferon gamma signaling pathway, which goes through the interferon gamma receptor chains JAK1 and/or JAK2 and the signal transducer and activators of transcription (STATs) (Darnell et al., 1994). In cell line and animal models, mutations or epigenetic silencing of molecules in the interferon receptor signaling pathway results in loss of the anti-tumor effects of interferon gamma (Dunn et al., 2005; Kaplan et al., 1998). Analysis of tumors in patients who did not respond to therapy with the anti-CTLA-4 antibody ipilimumab revealed an enriched frequency of mutations in the interferon gamma pathway genes interferon gamma receptor 1 and 2 (IFNGR1 and IFNGR2), JAK2, and interferon regulatory factor 1 (IRF1) (Gao et al., 2016). Any of these mutations would prevent signaling in response to interferon gamma and give an advantage to the tumor cells escaping from T cells, thereby resulting in primary resistance to anti-CTLA-4 therapy. Mutations in this pathway would additionally result in lack of PD-L1 expression upon interferon gamma exposure, thereby resulting in cancer cells that would be genetically negative for inducible PD-L1 expression. In such a scenario, blocking PD-L1 or PD-1 with therapeutic antibodies would not be useful, and these would be patients who are primary resistant to anti-PD-1 therapy (Shin and Ribas, 2015; Shin et al., 2016).

An additional cancer-cell-intrinsic mechanism of primary resistance to immunotherapy is expression of a certain set of genes that were found to be enriched in tumors from patients

processing, presentation, and immune evasion (Karpf and Jones, 2002; Kim and Bae, 2011). Therefore, demethylating agents may enable re-expression of immune related genes, with potential for therapeutic impact, especially in the setting of combination treatment with immunotherapy. (Héninger et al., 2015). Histone deacetylase inhibitors led to increased expression of MHC and tumor-associated antigens, which synergized with ACT therapy to improve anti-tumor responses in a murine melanoma model (Vo et al., 2009). Similarly, in a lymphoma model, hypomethylating agents were found to increase CD80 expression on tumor cells, with concomitant increase in tumor-infiltrating CD8⁺ T cells (Wang et al., 2013). These pre-clinical data indicate the potential to reverse the epigenetic changes in cancer cells, which may enable enhanced immune recognition and response to immunotherapy.

Tumor-Cell-Extrinsic Factors for Primary and Adaptive Resistance

Tumor-cell-extrinsic mechanisms that lead to primary and/or adaptive resistance involve components other than tumor cells within the tumor microenvironment, including Tregs, myeloid derived suppressor cells (MDSCs), M2 macrophages, and other inhibitory immune checkpoints, which may all contribute to inhibition of anti-tumor immune responses.

Tregs, which can be identified by expression of the FoxP3 transcription factor, have a central role in maintaining self-tolerance (Rudensky, 2011). The existence of suppressor T cells that could downregulate immune responses of antigen-specific T cells was first identified nearly four decades ago in thymectomized, lethally irradiated, bone-marrow-reconstituted mice (Gershon and Kondo, 1970). Tregs are known to suppress effector T cell (Teff) responses by secretion of certain

inhibitory cytokines, such as IL-10, IL-35, and TGF- β , or by direct cell contact (Oida et al., 2003; Sakaguchi et al., 2008; Sundstedt et al., 2003). Published data indicate that many human tumors are infiltrated by Tregs (Chaudhary and Elkord, 2016; Ormandy et al., 2005; Woo et al., 2002). A vast number of murine studies have shown that the depletion of Treg cells from the tumor microenvironment can enhance or restore anti-tumor immunity (Linehan and Goedegebuure, 2005; Viehl et al., 2006). In murine models, response to anti-CTLA-4 therapy was shown to be associated with an increase in the ratio of Teffs to Tregs (Quezada et al., 2006). This shift in the ratio of Teffs to Tregs was found to be a result of both an increase in Teffs and depletion of Tregs in a murine tumor model (Simpson et al., 2013). These data suggest that tumors for which immunotherapy is unable to increase Teffs and/or deplete Tregs to increase the ratio of Teffs to Tregs are likely to be resistant to treatment, either initially or during the relapsed disease setting. However, it is possible that tumor-infiltrating Tregs may co-exist with other immune cells, indicating a potentially immune-responsive tumor. A retrospective study of patients treated with anti-CTLA-4 reported that a high baseline expression of FoxP3⁺ Tregs in the tumor was associated with better clinical outcomes (Hamid et al., 2011). Additional studies are ongoing to determine the impact of tumor-infiltrating Tregs on clinical outcomes for patients who receive treatment with immunotherapy agents.

Myeloid-derived suppressor cells (MDSCs) have emerged as major regulators of immune responses in various pathological conditions, including cancer. MDSCs were initially defined in murine models and were characterized by the expression of CD11b (CR3A or integrin α M) and Gr-1 markers (Bronte et al., 1998; Talmadge and Gabrilovich, 2013). Human MDSCs express markers such as CD11b⁺ and CD33⁺ but are mostly negative for HLA-DR and lineage-specific antigens (Lin), including CD3, CD19, and CD57. Monocytic MDSCs are HLA-DR⁻, CD11b⁺, CD33⁺ and CD14⁺ and granulocytic MDSCs are HLA-DR⁻, CD11b⁺, CD33⁺, CD15⁺; however, mature monocytes express HLA-DR (Wesolowski et al., 2013). MDSCs have been implicated in promoting angiogenesis, tumor cell invasion, and metastases (Yang et al., 2004; Yang et al., 2008). Furthermore, clinical findings have shown that the presence of MDSCs correlates with reduced survival in human cancers, including breast cancer and colorectal cancer (Solito et al., 2011). Reports suggest that the presence of MDSCs in the tumor microenvironment correlates with decreased efficacy of immunotherapies, including immune checkpoint therapy (Meyer et al., 2014), adoptive T cell therapy (Kodumudi et al., 2012), and DC vaccination (Laborde et al., 2014). Therefore, eradicating or reprogramming MDSCs could enhance clinical responses to immunotherapy. Indeed, in melanoma, breast cancer, and head and neck murine tumor models, selective inactivation of macrophage PI3K γ synergized with immune checkpoint inhibitors to promote tumor regression and increase survival (De Henau et al., 2016; Kaneda et al., 2016). In one study, the investigators demonstrated that mice lacking PI3K γ or tumor-bearing mice treated with PI3K γ inhibitors (TG100-115 or IPI-549) had reduced tumor growth, which was associated with enhanced expression of pro-inflammatory cytokines and inhibition of immune-suppressive factors in the tu-

mors (Kaneda et al., 2016). Moreover, genes and proteins associated with immune activation were upregulated in macrophages that were treated with PI3K γ inhibitors or those from mice lacking PI3K γ . These data established PI3K γ as a molecular switch that regulates macrophage function. The investigators also demonstrated that a PI3K γ inhibitor (TG100-115) plus anti-PD-1 led to improved tumor rejection and survival of tumor-bearing mice (Kaneda et al., 2016). In a second study, tumor-bearing mice treated with triple-combination therapy, a PI3K γ inhibitor (IPI-549) plus anti-CTLA-4 and anti-PD-1, had improved tumor regression and long-term survival as compared to dual therapy with anti-CTLA-4 plus anti-PD-1 (De Henau et al., 2016). These pre-clinical studies highlight inhibitors of PI3K γ as a therapeutic potential for combination strategies with immune checkpoint therapy in cancer patients.

Tumor-associated macrophages (TAMs) are another subset of cells that seem to affect responses to immunotherapy. TAMs include both M1 macrophages, which are involved in promoting anti-tumor immunity, and the M2 macrophages, which possess pro-tumorigenic properties (Chanmee et al., 2014). M1 and M2 macrophages can be distinguished based on the differential expression of transcription factors and surface molecules and the disparities in their cytokine profile and metabolism (Biswas and Mantovani, 2010; Hu et al., 2016). Clinical studies have shown an association between higher frequencies of TAMs and poor prognosis in human cancers (Hu et al., 2016). In a chemically induced mouse model of lung adenocarcinoma, depletion of TAMs reduced tumor growth as a result of downregulation of M2 and/or TAM recruitment, possibly due to the inactivation of CCL2 and/or CCR2 signaling (Fritz et al., 2014). Likewise, depletion of M2 macrophages in various murine tumor models, including cutaneous T cell lymphoma (Wu et al., 2014), colon cancer, lung cancer, breast cancer (Luo et al., 2006), and melanoma (Ries et al., 2014; Ruffell et al., 2014; Tham et al., 2015), have shown similar results. Several reports have discussed the role of macrophages in mediating therapeutic resistance in cancer (De Palma and Lewis, 2013; Ruffell et al., 2014; Ruffell and Coussens, 2015). Reports suggest that macrophages can directly suppress T cell responses through programmed death-ligand 1 (PD-L1) in hepatocellular carcinoma (Kuang et al., 2009) and B7-H4 in ovarian carcinoma (Kryczek et al., 2006). To overcome the potential resistance mechanism of macrophages, investigators tested blockade of CSF-1R, a receptor for macrophage-colony stimulating growth factor, in a murine model of pancreatic cancer and demonstrated decreased frequencies of TAMs, with subsequent increase in interferon production and restrained tumor progression. Importantly, neither PD-1 nor CTLA-4 blockade could significantly reduce tumor growth in the murine model, results that were similar to findings from single agent studies in patients with pancreatic cancer (Le et al., 2013; Zhu et al., 2014). However, CSF1R blockade in combination with either an antibody against PD-1 or CTLA-4, in addition to gemcitabine, led to improved tumor regression (Zhu et al., 2014). These data suggest that CSF-1R blockade induced reduction of TAMs, which enabled response to immune checkpoint therapy. Similarly, in a melanoma model, CSF-1R inhibitor was shown to synergize with ACT therapy (Mok et al., 2014). Several early phase clinical trials

are underway to test the combination of CSF-1R inhibition with checkpoint inhibitors (Table 3).

The immune response is dynamic and signals that enhance anti-tumor immune responses also tend to turn on inhibitory genes and pathways in order to tightly regulate the immune response. For example, initial T cell activation, via TCR signaling and CD28 co-stimulation, eventually leads to increased expression of the inhibitory CTLA-4 immune checkpoint (Leach et al., 1996). Similarly, effector T cell responses such as increased IFN γ production leads to increased expression of the PD-L1 protein on multiple cell types, including tumor cells, T cells and macrophages, which can engage the PD-1 receptor on T cells to suppress anti-tumor immunity (Chen, 2004; Dong et al., 2002). Apart from this, IFN γ may additionally promote the expression of immunosuppressive molecules such as indoleamine-2, 3-deoxygenase (IDO), a tryptophan-metabolizing enzyme that can contribute to peripheral tolerance and can have a direct negative effect on effector T cell function (Gajewski et al., 2013). Similarly, carcinoembryonic antigen cell adhesion molecule-1 (CEACAM1), seems to be another inhibitory molecule that is induced by IFN γ (Takahashi et al., 1993), (Gray-Owen and Blumberg, 2006). Therapeutic antibodies blocking CEACAM1 (Ortenberg et al., 2012) and TIM-3 have resulted in enhanced anti-tumor immune responses (Pardoll, 2012; Sakuishi et al., 2010). A recent study in an immunocompetent mouse model of lung adenocarcinoma demonstrated that recurrent tumors after anti-PD-1 treatment were due to increased expression of TIM-3 on T cells. Notably, anti-PD-1 plus anti-TIM-3 led to improved responses in the tumor bearing mice. Similarly, two lung cancer patients who developed recurrent disease after anti-PD-1 treatment were found to have increased TIM-3 expression on T cells (Koyama et al., 2016).

Immune suppressive cytokines are often released by tumor or macrophages for local suppression of anti-tumor immune responses. Transforming growth factor β (TGF- β) is a cytokine that plays important roles in angiogenesis and immunosuppression by stimulating Tregs (Lebrun, 2012). Increased levels of TGF- β are associated with poor prognosis in multiple tumor types (Lin and Zhao, 2015; Massagué, 2008). Preclinical models have shown synergy combining TGF- β receptor kinase inhibitor with anti-CTLA-4, which led to anti-tumor responses in a melanoma model (BRAF^{V600E}PTEN^{-/-}) (Hanks et al., 2014). Another pre-clinical study consisting of radiation therapy combined with TGF- β inhibition also demonstrated anti-tumor responses (Vanpouille-Box et al., 2015). Adenosine was shown to inhibit T cell proliferation and cytotoxic function via the A2A receptor on T cells (Zhang et al., 2004) as well as to promote metastasis via the A2B receptor on tumor cells (Mittal et al., 2016). In addition, CD73 is the enzyme that dephosphorylates adenosine monophosphate (AMP) to form adenosine, thus also suppressing immune function and promoting tumor cell metastasis (Stagg et al., 2010), and also stimulates angiogenesis (Allard et al., 2014). High expression of CD73 is associated with poor prognosis in different cancer types (Leclerc et al., 2016; Loi et al., 2013; Turcotte et al., 2015). CD73 is also a potential biomarker for anti-PD-1 therapy, with high expression limiting anti-PD-1 efficacy, which can be rescued by concomitant A2A blockade (Beavis et al., 2015).

Specific chemokines and chemokine receptors are important for trafficking of MDSCs and Tregs to the tumor. For example, tumors secrete ligands CCL5, CCL7, and CXCL8, bind to their receptors CCR1 or CXCR2 expressed on subtypes of MDSCs (Highfill et al., 2014), and attract MDSCs in the tumor microenvironment. Inhibitors of these chemokine receptors could abrogate immune evasion and improve anti-tumor T cell responses. CCR4 is highly expressed by Tregs in the blood and tumors (Sugiyama et al., 2013), and anti-CCR4 inhibits Treg recruitment as well as promotes antibody-dependent cell-mediated cytotoxicity (ADCC), further reducing the Treg population (Chang et al., 2012). CXCR4 is a receptor for the chemokine CXCL12, which has been shown to promote an immunosuppressive tumor microenvironment through several mechanisms, including Treg localization (Gil et al., 2014).

Acquired Resistance to Immunotherapy

A hallmark of cancer immunotherapy has been the induction of long lasting tumor responses. However, with higher activity and broader use of immunotherapies, the denominator of patients with a tumor response has increased and the chances of finding patients who responded for a period of time and then progressed, termed acquired resistance, increases. It is becoming clear that approximately one fourth to one third of patients with metastatic melanoma who have objective responses to checkpoint blockade therapy with anti-CTLA-4 or anti-PD-1 will relapse over time, even despite receiving continued therapy (Schachter et al., 2016). The potential mechanisms of relapse include loss of T cell function, lack of T cell recognition by down-regulation of tumor antigen presentation, and development of escape mutation variants in the cancer (Figures 2 and 3). There is evidence that each of these mechanisms can lead to acquired resistance to checkpoint inhibitor therapy or ACT.

If the anti-tumor T cells change their functional phenotype and stop exerting their cytotoxic activity, then a patient who responded to immunotherapy may develop a tumor relapse even if everything else continues to be the same. Acquired resistance to TCR-engineered ACT is rather frequent, with high initial anti-tumor response followed by a high frequency of tumor relapses within months. This has been evident with the ACT of T cells expressing TCRs to melanosomal antigens (MART-1, gp100) and to cancer testis antigens (NY ESO-1) (Chodon et al., 2014; Morgan et al., 2006; Robbins et al., 2011). By studying how the TCR transgenic T cells change their functionality after ACT to humans, it has been reported that the initial highly cytolytic profile when administered shifts over time to a Th2-type cytokine release and lack of cytotoxic functions in late time points when recovered from patients at the time of tumor relapse (Ma et al., 2013; Ma et al., 2011).

It was already well documented by the 1990s that some patients who initially respond to cancer immunotherapies with IL-2 or TIL ACT might develop acquired resistance through loss of the shared component of all HLA class I molecules, B2M, which leads to absence of surface expression of HLA class I (D'Urso et al., 1991; Restifo et al., 1996). B2M is required for HLA class I folding and transport to the cell surface, and its genetic deficiency would lead to lack of CD8 T cell recognition. This mechanism of acquired resistance has also been

Table 3. Examples of Combination Therapies Being Developed to Overcome Resistance to Cancer Immunotherapy

Broad Approach	Specific Approach	Examples in Clinical Testing
combination checkpoint blockade	anti-PD-1/L1 plus anti-CTLA4	Durvalumab + tremelimumab Nivolumab + ipilimumab Pembrolizumab + ipilimumab
	anti-PD-1 plus anti-PD-L1	MEDI0680 + durvalumab PDR001 + FAZ053
	anti-PD-1/L1 plus anti-TIM 3	Nivolumab + TSR022 PDR001 + MBG453
	anti-PD-1/L1 plus anti-LAG 3	Nivolumab + BMS 986016 PDR001 + LAG525 Pembrolizumab + IMP321 REGN2810 + REGN3767
checkpoint blockade plus immune-stimulatory agents	anti-PD-1/L1 plus anti-41BB/CD137	Avelumab + utomilumab Nivolumab + urelumab Pembrolizumab + utomilumab
	anti-CTLA4 plus anti-OX40	Atezolimumab + MOXR0916 ± bevacizumab
	anti-PD-1/L1 plus anti-OX40	Avelumab + PF-04518600
	anti-CTLA4 plus Anti-PD-1/L1 plus anti-OX40	Durvalumab + MEDI0562
	anti-41BB/CD137 plus anti-OX40	Pembrolizumab + GSK3174998 Tremelimumab + durvalumab + MEDI6469 Tremelimumab + MEDI0562 Utomilumab + PF-04518600
	anti-CTLA4 plus anti-CD40	Atezolimumab + RO7009789
checkpoint blockade plus metabolic modulators	anti-PD-1/L1 plus anti-CD40	Tremelimumab + CP870893
	anti-PD-1/L1 plus anti-GITR	Nivolumab + BMS986156 PDR001 + GWN323
	anti-PD-1/L1 plus anti-ICOS	Nivolumab + JTX-2011
	anti-CTLA-4 plus IDO inhibitors	Atezolizumab + GDC0919
	anti-PD-1/L1 plus IDO inhibitors	Ipilimumab + epacadostat Ipilimumab + indoximid Nivolumab + BMS986205 Pembrolizumab+ epacadostat
	anti-PD-1/L1 plus A2AR inhibitors or anti-CD73	Atezolizumab + CPI-444 Durvalumab + MEDI9447 PDR001+ PBF509
checkpoint blockade plus other immune modulators	anti-PD-1/L1 plus TGFβ inhibitors	Nivolumab + LY2157299 PDR001 + NIS793
	anti-PD-1/L1 plus CXCR4 inhibitors	Nivolumab + ulocuplumab Durvalumab + LY2510924
	anti-PD-1/L1 plus CCR4 inhibitors	Nivolumab + mogamulizumab
	anti-PD-1/L1 plus anti-CD27	Nivolumab + varlilumab Atezolizumab + varlilumab
	anti-PD-1/L1 plus CD122-biased cytokine	Nivolumab + NKTR-214
	anti-PD-1/L1 plus yeast-derived soluble β-glucan	Pembrolizumab + Imprime PGG
	anti-PD-1/L1 plus anti- TRAIL-DR5	Nivolumab + DS-8273a
	anti-PD-1/L1 plus glutaminase inhibitor	Nivolumab + CB839
checkpoint blockade plus macrophage inhibitors	anti-PD-1/L1 plus IAP inhibitor	PDR001 + LCL161
	anti-CTLA4 plus CSF1R inhibitors	Durvalumab + Pexidartinib (PLX3397)
	anti-PD-1/L1 plus CSF1R inhibitors	Durvalumab + LY3022855 Nivolumab + FPA008 Pembrolizumab + Pexidartinib PDR001 + BLZ945 Tremelimumab + LY3022855

(Continued on next page)

Table 3. Continued

Broad Approach	Specific Approach	Examples in Clinical Testing
checkpoint blockade plus injectable therapies	anti-CTLA-4 plus oncolytic viruses anti-PD-1/L1 plus oncolytic viruses	Ipilimumab + Talimogene Laherparepvec Nivolumab + Talimogene Laherparepvec Pembrolizumab + DNX2401 Pembrolizumab + Talimogene Laherparepvec
	anti-CTLA4 plus TLR agonists anti-PD-1/L1 plus TLR agonists	Ipilimumab + MGN1703 Pembrolizumab + CMP001 Pembrolizumab + SD101 Tremelimumab + PF-3512676
checkpoint blockade plus cancer vaccines	anti-CTLA4 plus DC vaccine anti-PD-1/L1 plus DC vaccine anti-PD-1/L1 plus peptide vaccine anti-PD-1/L1 plus neoantigen vaccine	Durvalumab + ADXS11-001 Durvalumab + TPIV200/huFR-1 Ipilimumab + GVAX Nivolumab + GVAX + CRS207 Nivolumab + CIMAvax Nivolumab+ CV301 Nivolumab + NEO-PV-01 Nivolumab + Viagenpumatu cel-L (HS-110) Pembrolizumab + ADXS31-142 Durvalumab ± tremelimumab + IMCgp100
checkpoint blockade plus adoptive cell transfer (ACT)	anti-CTLA4 plus ACT anti-PD-1/L1 plus ACT anti-PD-1/L1 plus anti-CD137 plus ACT	Atezolimumab + KTE-C19 Ipilimumab + NYESO TCR ACT Nivolumab + NYESO TCR ACT Nivolumab + urelumab + TIL ACT Pembrolizumab + TIL ACT Ipilimumab + modified CD8 T cell ACT Pembrolizumab + modified CD8 T cell ACT
checkpoint blockade plus targeted therapies	anti-CTLA4 plus BRAF+MEK inhibitors	Atezolizumab + bevacizumab versus sunitinib
	anti-CTLA4 plus VEGF inhibitors	Atezolizumab + trametinib
	anti-PD-1/L1 plus BRAF+MEK inhibitors	Atezolizumab + vemurafenib ± cobimetinib
	anti-PD-1/L1 plus EGFR inhibitors	Durvalumab + ensartinib (ALK inhibitor)
	anti-PD-1/L1 plus VEGF inhibitors	Durvalumab + gefitinib
	anti-PD-1/L1 plus PI3K delta inhibitor	Durvalumab + trametinib ± dabrafenib Ipilimumab + bevacizumab Ipilimumab + dabrafenib ± trametinib Ipilimumab + vemurafenib Nivolumab + sunitinib or pazopanib Nivolumab + trametinib ± dabrafenib PDR001 + sorafenib Pembrolizumab + dabrafenib + trametinib Pembrolizumab + lenalidomide Pembrolizumab + nintedarnib Pidilizumab + lenalidomide Tremelimumab + sunitinib Nivolumab + SYM004
	anti-PD-1/L1 plus PARP inhibitors	Atezolizumab + Veliparib Durvalumab + olaparib BGB-A317 + BGB-290
	anti-PD-1/L1 plus mTOR inhibitor	PDR001 + everolimus
	anti-PD-1/L1 plus pan RAF inhibitor	PDR001 + LXH254
	anti-PD-1/L1 plus glutaminase inhibitor	Nivolumab + CB839
checkpoint blockade plus radiation therapy (RT)	anti-CTLA4 plus RT anti-PD-1/L1 plus RT anti-CTLA4 plus Anti-PD-1/L1 plus RT	Atezolizumab + stereotactic radiation therapy Pembrolizumab + cisplatin/radiotherapy Pembrolizumab + stereotactic body radiotherapy Pembrolizumab + hypofractionated radiotherapy

(Continued on next page)

Table 3. Continued

Broad Approach	Specific Approach	Examples in Clinical Testing
checkpoint blockade plus chemotherapy	anti-CTLA4 plus chemotherapy anti-PD-1/L1 plus chemotherapy anti-CTLA4 plus Anti-PD-1/L1 plus chemotherapy	Atezolizumab + carboplatin/paclitaxel Atezolizumab + carboplatin/gemcitabine Durvalumab + paclitaxel Ipilimumab + carboplatin/paclitaxel Ipilimumab + dacarbazine Nivolumab + platinum doublets Pembrolizumab + carbo/paclitaxel or carbo/pemetrexed
checkpoint blockade plus epigenetic modifications	anti-PD-1/L1 plus histone deacetylase inhibitors anti-PD-1/L1 plus hypomethylating agents	Azacitidine + entinostat followed by nivolumab Atezolizumab + azacitidine Nivolumab + RRX001 Pembrolizumab + CC486 Pembrolizumab + CC486 + romidepsin Pembrolizumab + romidepsin Pembrolizumab + vorinostat + tamoxifen PDR001 + panobinostat
checkpoint blockade plus NK activation	anti-CTLA4 plus anti-KIR anti-PD-1/L1 plus anti-KIR	Ipilimumab + lirilumab Nivolumab + lirilumab

documented in a case of late acquired resistance to anti-PD-1 therapy, where the resistant cells had a new and homozygous truncating mutation in B2M, leading to lack of surface expression of HLA class I (Zaretsky et al., 2016). In two other cases of tumor relapse, there were copy-number-neutral loss-of-function mutations in *JAK1* or *JAK2*, concurrent with loss of heterozygosity due to deletion of the wild-type allele, which were absent in the baseline biopsies. These mutations allowed the cancer cells to escape from the anti-proliferative effects of interferon gamma (Zaretsky et al., 2016). Additional evidence of loss of antigen-presenting machinery leading to acquired resistance to cancer immunotherapy is provided by a case of a patient with metastatic colorectal carcinoma who responded to TIL ACT. The therapeutic TIL recognized mutated *KRAS G12D* presented by HLA-C*08:02, resulting in an objective tumor response for 9 months, followed by an isolated relapse in a lesion that had lost HLA-C*08:02 in chromosome 6 (Tran et al., 2016). Therefore, acquired resistance to anti-PD-1 therapy and ACT could be mediated through genetic mechanisms that altered antigen-presenting machinery and interferon gamma signaling.

Because anti-tumor T cells are specific for cancer cells that express their cognate antigen, it is possible that cancers may develop acquired resistance through decreased expression or mutations in these tumor antigens. Data suggest that anti-tumor T cells turned on by checkpoint blockade therapy primarily recognize mutational neoantigens (Schumacher and Schreiber, 2015; van Rooij et al., 2013). Therefore, genetic deletions, mutations, or epigenetic changes that would lead to loss of expression of these mutational neoantigens presented by MHC molecules might result in acquired resistance to checkpoint blockade therapy. However, thus far there has not been evidence of such mechanisms in the clinic. CAR T cells are also antigen-specific, but they rely on the whole protein expression on the cancer cell surface. In some cases of patients with ALL who responded initially to CD19 CAR T cell ACT, it has been documented that the epitope in the CD19 protein sequence that is recognized by the CAR can be selectively deleted at pro-

gression (Ruella et al., 2016) and that preexisting alternatively spliced CD19 isoforms might predispose to acquired resistance (Sotillo et al., 2015). Therefore, there is evidence from the clinic that loss of the target of the anti-tumor T cells can result in progression to cancer immunotherapy.

This yin and yang of the immune response, which results in immune editing and eventually immune escape, is clearly a factor as we administer immunotherapeutic agents and attempt to drive anti-tumor immune responses, which may encounter a multitude of inhibitory pathways, either during initial treatment or at the time of relapsed disease. Additional inhibitory immune checkpoints that are often expressed in the tumor microenvironment include LAG-3, TIGIT, VISTA, and many more that are being identified in ongoing studies (Topalian et al., 2015). Several clinical trials are currently underway to test antibodies against these inhibitory pathways, both as monotherapy and combination therapy strategies (Anderson et al., 2016; Sharma and Allison, 2015). To date, the combination of anti-CTLA-4 (ipilimumab) plus anti-PD-1 (nivolumab) has demonstrated improved clinical outcomes as compared to monotherapy, and this combination was recently FDA-approved for patients with metastatic melanoma (Larkin et al., 2015a). We will need data from ongoing and future clinical trials to determine whether combination therapies targeting other inhibitory pathways, either as doublets or triplets in concurrent or sequential treatment strategies, will effectively overcome the resistance mechanisms that act to regulate immune responses and provide additional clinical benefit.

Monitoring Resistance Mechanisms

There are significant efforts underway to identify reliable predictive biomarkers of response and resistance to checkpoint inhibitors in baseline tumor biopsies in patients on immune checkpoint blockade. To date, the best predictive biomarkers identified include total tumor mutational load (Roszik et al., 2016; Snyder et al., 2014), as well as markers of an effective immune infiltrate within a tumor signifying a “hot” tumor

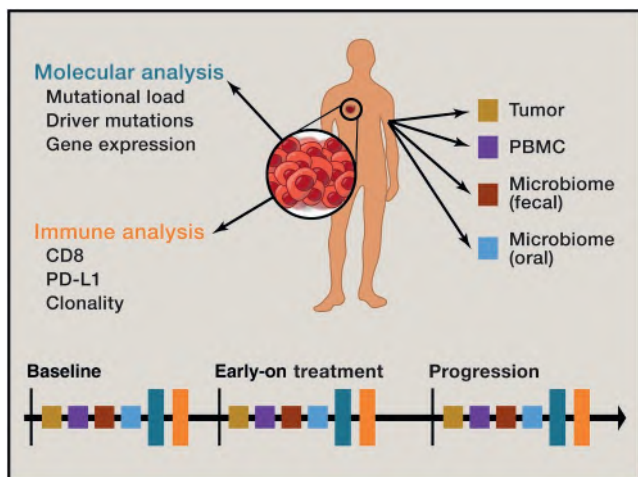


Figure 4. Schema for Analysis of Baseline and Longitudinal Tumor, Blood, and Other Samples

(A) Baseline assessment of the tumor microenvironment typically involves molecular analysis for mutational load, driver mutations, and gene expression, with immune profiling including analysis of CD8⁺ T cells, PD-L1 expression, and T cell clonality.

(B) Longitudinal evaluation of fresh serial human specimens (tumor, blood, serum, and microbiome) during treatment (at pre-treatment, early-on-treatment, and progression time points) allows for deep analysis to unveil potential mechanisms of therapeutic resistance.

microenvironment, typified by an increased number of CD8⁺ cytotoxic T lymphocytes in proximity to PD-L1-positive cells (Taube et al., 2014; Tumeh et al., 2014). Mutational load is highly relevant, given that tumors with a higher mutational load exhibit higher levels of neoantigens capable of inducing anti-tumor immune responses, translating into a higher likelihood of response to immune checkpoint blockade across several cancer types (Rizvi et al., 2015; Snyder et al., 2014; Van Allen et al., 2015). In addition to genomic markers and immune regulatory gene expression profiles (Hugo et al., 2016), immune markers in pre-treatment biopsies, including the density and distribution of CD8⁺ T lymphocytes, PD-L1 expression, and T cell clonality (Taube et al., 2014; Tumeh et al., 2014), have also been associated with differential responses to immune checkpoint blockade, although significant limitations exist when each of these biomarkers is assessed in isolation. Integrative approaches incorporating analysis of several of these features have also been developed, such as the cancer immunogram, which incorporates analysis of seven distinct features within the tumor microenvironment: tumor sensitivity to immune effectors, tumor foreignness, general immune status, immune cell infiltration, absence of checkpoint molecule expression, absence of soluble inhibitors such as interleukin-1 and interleukin-6, and absence of inhibitory tumor metabolism (Blank et al., 2016). These efforts are critical and will ultimately contribute to more personalized treatment strategies for cancer immunotherapy.

An emerging strategy in elucidating mechanisms of response and resistance to immune checkpoint blockade involves the assessment of longitudinal tumor samples throughout the course of treatment. This approach is powerful because it transcends conventional analysis of static time points and seeks to

identify superior predictive biomarkers by assessing dynamic responses to cancer treatment. Such an approach has been employed to better understand response and resistance to immune checkpoint blockade (Chen et al., 2016; Hugo et al., 2016; Madore et al., 2015; Tumeh et al., 2014) and has yielded important information that would not have been elucidated through analysis of static unpaired biopsies. A key example is in a recent report describing immune markers in longitudinal tumor samples of patients on immune checkpoint blockade, demonstrating that although pre-treatment markers were largely non-predictive, immune markers in early-on-treatment samples were highly predictive of treatment response (Chen et al., 2016). In addition to this, resistance mechanisms were identified via pairwise comparison of gene expression profiles in pre- to on-treatment tumor samples of responders versus non-responders, including defects in interferon signaling as well as antigen processing and presentation (Chen et al., 2016). This approach is currently under-utilized but is gaining traction in light of advantages over assessment of static baseline biomarkers (Figure 4), as well as an increasing need to better understand responses to a growing number of immunotherapeutic approaches. However nuances exist with regard to immune monitoring in the tumor microenvironment (Wargo et al., 2016), and an appreciation of the importance of concurrent monitoring in the peripheral blood is growing, though the ideal assays to perform are still being elucidated.

Overcoming Resistance to Immunotherapy

On the basis of insights gained (Hugo et al., 2016; Snyder et al., 2014; Van Allen et al., 2015), efforts are currently underway to derive actionable strategies to combat therapeutic resistance to immunotherapy. This includes fundamental efforts to transform immunologically “cold” tumors into “hot” tumors through the use of several approaches (Corrales et al., 2015; Holmgaard et al., 2013; Tang et al., 2016) and also involves tactics to either enhance endogenous T cell function (Gubin et al., 2014; Hodi et al., 2010; Miller et al., 2002; Redmond et al., 2007; Ribas et al., 2015; Weber et al., 2015) or to adoptively transfer antigen-specific T lymphocytes via ex vivo expansion of tumor-infiltrating lymphocytes (Rosenberg et al., 2011) or via administration of antigen-specific engineered T cells (via transduction with CARs or TCRs) (Beatty et al., 2014; Kalos et al., 2011).

Though some of these approaches involve treatment with drugs as monotherapy (including monoclonal antibodies), the majority of contemporary approaches focus on combination strategies in an effort to overcome resistance associated with treatment with single-pronged efforts (Table 3) (Hicklin et al., 1998; Moon et al., 2014; Ninomiya et al., 2015). A prime example of enhanced efficacy with combination therapy is the use of combined therapy with blocking antibodies against two key immune checkpoints, CTLA-4 and PD-1, which results in significantly higher response rates to therapy and improved survival in patients with metastatic melanoma (Larkin et al., 2015a; Postow et al., 2015; Wolchok et al., 2013). The rationale for this combination approach is several fold, as blocking several checkpoints on anergized tumor-specific T cells has been shown to be more efficacious (Berrien-Elliott et al., 2013; Curran et al., 2010; Redmond et al., 2014; Spranger et al., 2014) and CTLA-4 blockade may itself facilitate the conversion of a tumor

microenvironment from “cold” to “hot” (Simpson et al., 2013). Indeed, each of these checkpoint inhibitors has been shown to have both overlapping and unique effects on tumor-specific T cells (Gubin et al., 2014), substantiating the use of these in combination. Numerous other strategies combining immune modulation of the tumor microenvironment with immune checkpoint inhibitor therapy are currently being tested in clinical trials (Puzanov et al., 2016) (NCT02263508, NCT02626000, NCT02565992, NCT02043665, NCT02501473). Vaccine strategies against identified neoantigen epitopes are also being combined with immunotherapeutic approaches, though mature data are not available regarding efficacy.

Another combination strategy with strong clinical and pre-clinical rationale involves the use of molecularly targeted therapy in conjunction with immunotherapy. The most extensively studied cancer type treated with this strategy is melanoma, though the concept is now being widely extended across solid and liquid tumors. The rationale for combining these treatments is that treatment with molecularly targeted therapy can have a substantial effect on anti-tumor immunity and potential synergy when used with immunotherapy (Homet Moreno et al., 2015; Hu-Lieskovan et al., 2015; Koya et al., 2012). Perhaps most illustrative of this is oncogenic BRAF in melanoma. Though treatment with BRAF-targeted therapy alone provides limited durable disease control (Chapman et al., 2011; Hauschild et al., 2012), it is associated with favorable effects in the tumor microenvironment, including increased antigen (Boni et al., 2010) and HLA expression (Bradley et al., 2015), increased T cell infiltrate, reduced immunosuppressive cytokines (Frederick et al., 2013; Wilmott et al., 2012), and improved T cell function (Comin-Anduix et al., 2010). Thus, treatment with molecularly targeted therapy may indeed help convert a “cold” microenvironment to a “hot” one, with resultant increased expression of PD-L1 via the phenomenon of adaptive resistance (Taube et al., 2012), further supporting a multi-modality treatment approach. Emerging strategies to enhance responses to immunotherapy are being developed based on novel insights into T cell and overall immune function. Examples of this include insights into metabolic reprogramming of T cells to enhance therapeutic responses (Buck et al., 2016; Chang and Pearce, 2016) and via modulation of the gut microbiome to augment responses to cancer immunotherapy (Sivan et al., 2015; Vétizou et al., 2015).

Complexities exist when attempting to validate these combination strategies given that the extent of possible combinations far outnumbers the human and technical resources available. There is an urgent need to test these combinations in appropriate pre-clinical models and expedite clinical translation through novel approaches to clinical trial design. In addition, we need to have a deep understanding of the kinetics of the immune response to each of these agents in isolation as well as in combination in order to narrow the search space of biologically promising and optimal combination strategies. Immune responses to targeted agents may be short-lived (Cooper et al., 2014), thus proper timing and sequence of therapy must be strongly considered.

Conclusions

Great advances have occurred in the field of cancer immunotherapy as a result of elegant research work conducted to eluci-

date the mechanisms that regulate anti-tumor T cell responses, including eventual translation of these concepts to the clinic. This has allowed the rational design and clinical development of treatment strategies that might result in tumor regression and long-term survival for patients with metastatic cancer. However, the benefit, to date, has been limited to a minority of patients with certain cancer types. In addition, as a result of more successful immunotherapy treatments, we now have a significant subset of patients who initially respond but eventually relapse. Bringing clinical benefit to the majority of patients requires a complete understanding of the mechanisms that would lead to an effective anti-tumor response and the different tumor-cell-intrinsic and -extrinsic factors that would result in primary, adaptive, and acquired resistance to immunotherapy. Elucidation of these mechanisms will reveal important clues as to the next steps that need to be taken to potentially overcome resistance to immunotherapy.

ACKNOWLEDGMENTS

This research was supported by the Parker Institute for Cancer Immunotherapy, NIH/NCI grants R01 CA1633793 (P.S.), R35 CA197633, and P01 CA168585 (A.R.), Cancer Prevention Research in Texas (CPRIT) grant RP120108 (P.S.), the Ressler Family Fund, the Garcia-Corsini Family Fund, the Samuels Family Fund, and the Grimaldi Family Fund (A.R.), and a Stand Up To Cancer-Cancer Research Institute Cancer Immunology Dream Team Translational Research Grant (SU2C-AACR-DT1012; P.S. and A.R.). S.H.-L. was supported by a Career Development Award from the American Society of Clinical Oncology (ASCO), a Tower Cancer Research Foundation Grant, a Dr. Charles Coltman Fellowship Award from the Hope Foundation, and a UCLA KL2 Award.

REFERENCES

- Akbay, E.A., Koyama, S., Carretero, J., Altobelli, A., Tchaicha, J.H., Christensen, C.L., Mikse, O.R., Cherniack, A.D., Beauchamp, E.M., Pugh, T.J., et al. (2013). Activation of the PD-1 pathway contributes to immune escape in EGFR-driven lung tumors. *Cancer Discov.* 3, 1355–1363.
- Allard, B., Turcotte, M., Spring, K., Pommey, S., Royal, I., and Stagg, J. (2014). Anti-CD73 therapy impairs tumor angiogenesis. *Int. J. Cancer* 134, 1466–1473.
- Anderson, A.C., Joller, N., and Kuchroo, V.K. (2016). Lag-3, Tim-3, and TIGIT: Co-inhibitory Receptors with Specialized Functions in Immune Regulation. *Immunity* 44, 989–1004.
- Ansell, S.M., Lesokhin, A.M., Borrello, I., Halwani, A., Scott, E.C., Gutierrez, M., Schuster, S.J., Millenson, M.M., Cattray, D., Freeman, G.J., et al. (2015). PD-1 blockade with nivolumab in relapsed or refractory Hodgkin's lymphoma. *N. Engl. J. Med.* 372, 311–319.
- Beatty, G.L., Haas, A.R., Maus, M.V., Torigian, D.A., Soulen, M.C., Plesa, G., Chew, A., Zhao, Y., Levine, B.L., Albelda, S.M., et al. (2014). Mesothelin-specific chimeric antigen receptor mRNA-engineered T cells induce anti-tumor activity in solid malignancies. *Cancer Immunol. Res.* 2, 112–120.
- Beavis, P.A., Slaney, C.Y., Milenkovski, N., Henderson, M.A., Loi, S., Stagg, J., Kershaw, M.H., and Darcy, P.K. (2015). CD73: A potential biomarker for anti-PD-1 therapy. *Oncimmunology* 4, e1046675.
- Benci, J.L., Xu, B., Qiu, Y., Wu, T.J., Dada, H., Twyman-Saint Victor, C., Cucolo, L., Lee, D.S., Pauken, K.E., Huang, A.C., et al. (2016). Tumor interferon signaling regulates a multigenic resistance program to immune checkpoint blockade. *Cell* 167, 1540–1554.
- Berrien-Elliott, M.M., Jackson, S.R., Meyer, J.M., Rouskey, C.J., Nguyen, T.L., Yagita, H., Greenberg, P.D., DiPaolo, R.J., and Teague, R.M. (2013). Durable adoptive immunotherapy for leukemia produced by manipulation of multiple regulatory pathways of CD8+ T-cell tolerance. *Cancer Res.* 73, 605–616.

- Biswas, S.K., and Mantovani, A. (2010). Macrophage plasticity and interaction with lymphocyte subsets: cancer as a paradigm. *Nat. Immunol.* *11*, 889–896.
- Blank, C.U., Haanen, J.B., Ribas, A., and Schumacher, T.N. (2016). Cancer immunology. The “cancer immunogram.” *Science* *352*, 658–660.
- Boni, A., Cogdill, A.P., Dang, P., Udayakumar, D., Njauw, C.N., Sloss, C.M., Ferrone, C.R., Flaherty, K.T., Lawrence, D.P., Fisher, D.E., et al. (2010). Selective BRAFV600E inhibition enhances T-cell recognition of melanoma without affecting lymphocyte function. *Cancer Res.* *70*, 5213–5219.
- Bradley, S.D., Chen, Z., Melendez, B., Talukder, A., Khalili, J.S., Rodriguez-Cruz, T., Liu, S., Whittington, M., Deng, W., Li, F., et al. (2015). BRAFV600E co-opts a conserved MHC class I internalization pathway to diminish antigen presentation and CD8+ T-cell recognition of melanoma. *Cancer Immunol. Res.* *3*, 602–609.
- Bronte, V., Wang, M., Overwijk, W.W., Surman, D.R., Pericle, F., Rosenberg, S.A., and Restifo, N.P. (1998). Apoptotic death of CD8+ T lymphocytes after immunization: induction of a suppressive population of Mac-1+/Gr-1+ cells. *J. Immunol.* *161*, 5313–5320.
- Brunet, J.F., Denizot, F., Luciani, M.F., Roux-Dosseto, M., Suzan, M., Mattei, M.G., and Golstein, P. (1987). A new member of the immunoglobulin superfamily—CTLA-4. *Nature* *328*, 267–270.
- Buck, M.D., O’Sullivan, D., Klein Geltink, R.I., Curtis, J.D., Chang, C.H., Sanin, D.E., Qiu, J., Kretz, O., Braas, D., van der Windt, G.J., et al. (2016). Mitochondrial Dynamics Controls T Cell Fate through Metabolic Programming. *Cell* *166*, 63–76.
- Burnet, F.M. (1971). Immunological surveillance in neoplasia. *Transplant. Rev.* *7*, 3–25.
- Casey, S.C., Tong, L., Li, Y., Do, R., Walz, S., Fitzgerald, K.N., Gouw, A.M., Baylot, V., Gütgemann, I., Eilers, M., and Felsner, D.W. (2016). MYC regulates the antitumor immune response through CD47 and PD-L1. *Science* *352*, 227–231.
- Chang, C.H., and Pearce, E.L. (2016). Emerging concepts of T cell metabolism as a target of immunotherapy. *Nat. Immunol.* *17*, 364–368.
- Chang, D.-K., Sui, J., Geng, S., Muvaffak, A., Bai, M., Fuhlbrigge, R.C., Lo, A., Yammanuru, A., Hubbard, L., Sheehan, J., et al. (2012). Humanization of an anti-CCR4 antibody that kills cutaneous T-cell lymphoma cells and abrogates suppression by T-regulatory cells. *Mol. Cancer Ther.* *11*, 2451–2461.
- Chanmee, T., Ontong, P., Konno, K., and Itano, N. (2014). Tumor-associated macrophages as major players in the tumor microenvironment. *Cancers (Basel)* *6*, 1670–1690.
- Chapman, P.B., Hauschild, A., Robert, C., Haanen, J.B., Ascierto, P., Larkin, J., Dummer, R., Garbe, C., Testori, A., Maio, M., et al.; BRIM-3 Study Group (2011). Improved survival with vemurafenib in melanoma with BRAF V600E mutation. *N. Engl. J. Med.* *364*, 2507–2516.
- Chaudhary, B., and Elkord, E. (2016). Regulatory T Cells in the Tumor Microenvironment and Cancer Progression: Role and Therapeutic Targeting. *Vaccines (Basel)* *4*.
- Chen, L. (2004). Co-inhibitory molecules of the B7-CD28 family in the control of T-cell immunity. *Nat. Rev. Immunol.* *4*, 336–347.
- Chen, P.L., Roh, W., Reuben, A., Cooper, Z.A., Spencer, C.N., Prieto, P.A., Miller, J.P., Bassett, R.L., Gopalakrishnan, V., Wani, K., et al. (2016). Analysis of Immune Signatures in Longitudinal Tumor Samples Yields Insight into Biomarkers of Response and Mechanisms of Resistance to Immune Checkpoint Blockade. *Cancer Discov.* *6*, 827–837.
- Chodon, T., Comin-Anduix, B., Chmielowski, B., Koya, R.C., Wu, Z., Auerbach, M., Ng, C., Avramis, E., Seja, E., Villanueva, A., et al. (2014). Adoptive transfer of MART-1 T-cell receptor transgenic lymphocytes and dendritic cell vaccination in patients with metastatic melanoma. *Clin. Cancer Res.* *20*, 2457–2465.
- Coley, W.B. (1910). The treatment of inoperable sarcoma by bacterial toxins (the mixed toxins of the *Streptococcus erysipelas* and the *Bacillus prodigiosus*). *Proc. R. Soc. Med. 3(Surg Sect)*, 1–48.
- Comin-Anduix, B., Chodon, T., Sazegar, H., Matsunaga, D., Mock, S., Jalil, J., Escuin-Ordinas, H., Chmielowski, B., Koya, R.C., and Ribas, A. (2010). The oncogenic BRAF kinase inhibitor PLX4032/RG7204 does not affect the viability or function of human lymphocytes across a wide range of concentrations. *Clin. Cancer Res.* *16*, 6040–6048.
- Cooper, Z.A., Juneja, V.R., Sage, P.T., Frederick, D.T., Piris, A., Mitra, D., Lo, J.A., Hodi, F.S., Freeman, G.J., Bosenberg, M.W., et al. (2014). Response to BRAF inhibition in melanoma is enhanced when combined with immune checkpoint blockade. *Cancer Immunol. Res.* *2*, 643–654.
- Corrales, L., Glickman, L.H., McWhirter, S.M., Kanne, D.B., Sivick, K.E., Katibah, G.E., Woo, S.R., Lemmens, E., Banda, T., Leong, J.J., et al. (2015). Direct activation of STING in the tumor microenvironment leads to potent and systemic tumor regression and immunity. *Cell Rep.* *11*, 1018–1030.
- Curran, M.A., Montalvo, W., Yagita, H., and Allison, J.P. (2010). PD-1 and CTLA-4 combination blockade expands infiltrating T cells and reduces regulatory T and myeloid cells within B16 melanoma tumors. *Proc. Natl. Acad. Sci. USA* *107*, 4275–4280.
- D’Urso, C.M., Wang, Z.G., Cao, Y., Tataka, R., Zeff, R.A., and Ferrone, S. (1991). Lack of HLA class I antigen expression by cultured melanoma cells FO-1 due to a defect in B2m gene expression. *J. Clin. Invest.* *87*, 284–292.
- Darnell, J.E., Jr., Kerr, I.M., and Stark, G.R. (1994). Jak-STAT pathways and transcriptional activation in response to IFNs and other extracellular signaling proteins. *Science* *264*, 1415–1421.
- Das, R., Verma, R., Sznol, M., Boddupalli, C.S., Gettinger, S.N., Kluger, H., Callahan, M., Wolchok, J.D., Halaban, R., Dhodapkar, M.V., and Dhodapkar, K.M. (2015). Combination therapy with anti-CTLA-4 and anti-PD-1 leads to distinct immunologic changes in vivo. *J. Immunol.* *194*, 950–959.
- De Henau, O., Rausch, M., Winkler, D., Campesato, L.F., Liu, C., Cymerman, D.H., Budhu, S., Ghosh, A., Pink, M., Tchaicha, J., et al. (2016). Overcoming resistance to checkpoint blockade therapy by targeting PI3K γ in myeloid cells. *Nature* *539*, 443–447.
- De Palma, M., and Lewis, C.E. (2013). Macrophage regulation of tumor responses to anticancer therapies. *Cancer Cell* *23*, 277–286.
- Dong, H., Zhu, G., Tamada, K., and Chen, L. (1999). B7-H1, a third member of the B7 family, co-stimulates T-cell proliferation and interleukin-10 secretion. *Nat. Med.* *5*, 1365–1369.
- Dong, H., Strome, S.E., Salomao, D.R., Tamura, H., Hirano, F., Flies, D.B., Roche, P.C., Lu, J., Zhu, G., Tamada, K., et al. (2002). Tumor-associated B7-H1 promotes T-cell apoptosis: a potential mechanism of immune evasion. *Nat. Med.* *8*, 793–800.
- Dorand, R.D., Nthale, J., Myers, J.T., Barkauskas, D.S., Avril, S., Chirieleison, S.M., Pareek, T.K., Abbott, D.W., Stearns, D.S., Letterio, J.J., et al. (2016). Cdk5 disruption attenuates tumor PD-L1 expression and promotes antitumor immunity. *Science* *353*, 399–403.
- Dunn, G.P., Bruce, A.T., Ikeda, H., Old, L.J., and Schreiber, R.D. (2002). Cancer immunoeediting: from immunosurveillance to tumor escape. *Nat. Immunol.* *3*, 991–998.
- Dunn, G.P., Bruce, A.T., Sheehan, K.C., Shankaran, V., Uppaluri, R., Bui, J.D., Diamond, M.S., Koebel, C.M., Arthur, C., White, J.M., and Schreiber, R.D. (2005). A critical function for type I interferons in cancer immunoeediting. *Nat. Immunol.* *6*, 722–729.
- Ehrlich, P. (1956). *Collected Papers in Four Volumes Including A Complete Bibliography* (Pergamon Press).
- Eshhar, Z., Waks, T., Gross, G., and Schindler, D.G. (1993). Specific activation and targeting of cytotoxic lymphocytes through chimeric single chains consisting of antibody-binding domains and the gamma or zeta subunits of the immunoglobulin and T-cell receptors. *Proc. Natl. Acad. Sci. USA* *90*, 720–724.
- Fesnak, A.D., June, C.H., and Levine, B.L. (2016). Engineered T cells: the promise and challenges of cancer immunotherapy. *Nat. Rev. Cancer* *16*, 566–581.
- Frederick, D.T., Piris, A., Cogdill, A.P., Cooper, Z.A., Lezcano, C., Ferrone, C.R., Mitra, D., Boni, A., Newton, L.P., Liu, C., et al. (2013). BRAF inhibition is associated with enhanced melanoma antigen expression and a more favorable tumor microenvironment in patients with metastatic melanoma. *Clin. Cancer Res.* *19*, 1225–1231.

- Freeman, G.J., Long, A.J., Iwai, Y., Bourque, K., Chernova, T., Nishimura, H., Fitz, L.J., Malenkovich, N., Okazaki, T., Byrne, M.C., et al. (2000). Engagement of the PD-1 immunoinhibitory receptor by a novel B7 family member leads to negative regulation of lymphocyte activation. *J. Exp. Med.* *192*, 1027–1034.
- Fritz, J.M., Tennis, M.A., Orlicky, D.J., Lin, H., Ju, C., Redente, E.F., Choo, K.S., Staab, T.A., Bouchard, R.J., Merrick, D.T., et al. (2014). Depletion of tumor-associated macrophages slows the growth of chemically induced mouse lung adenocarcinomas. *Front. Immunol.* *5*, 587.
- Gajewski, T.F., Schreiber, H., and Fu, Y.X. (2013). Innate and adaptive immune cells in the tumor microenvironment. *Nat. Immunol.* *14*, 1014–1022.
- Gao, J., Shi, L.Z., Zhao, H., Chen, J., Xiong, L., He, Q., Chen, T., Roszik, J., Bernatchez, C., Woodman, S.E., et al. (2016). Loss of IFN- γ pathway genes in tumor cells as a mechanism of resistance to anti-CTLA-4 therapy. *Cell* *167*, 397–404.
- Gershon, R.K., and Kondo, K. (1970). Cell interactions in the induction of tolerance: the role of thymic lymphocytes. *Immunology* *18*, 723–737.
- Gil, M., Komorowski, M.P., Seshadri, M., Rokita, H., McGray, A.J., Opyrchal, M., Odunsi, K.O., and Kozbor, D. (2014). CXCL12/CXCR4 blockade by oncolytic virotherapy inhibits ovarian cancer growth by decreasing immunosuppression and targeting cancer-initiating cells. *J. Immunol.* *193*, 5327–5337.
- Gray-Owen, S.D., and Blumberg, R.S. (2006). CEACAM1: contact-dependent control of immunity. *Nat. Rev. Immunol.* *6*, 433–446.
- Green, M.R., Monti, S., Rodig, S.J., Juszczynski, P., Currie, T., O'Donnell, E., Chapuy, B., Takeyama, K., Neuberger, D., Golub, T.R., et al. (2010). Integrative analysis reveals selective 9p24.1 amplification, increased PD-1 ligand expression, and further induction via JAK2 in nodular sclerosing Hodgkin lymphoma and primary mediastinal large B-cell lymphoma. *Blood* *116*, 3268–3277.
- Gubin, M.M., Zhang, X., Schuster, H., Caron, E., Ward, J.P., Noguchi, T., Ivanova, Y., Hundal, J., Arthur, C.D., Krebber, W.J., et al. (2014). Checkpoint blockade cancer immunotherapy targets tumour-specific mutant antigens. *Nature* *515*, 577–581.
- Hamid, O., Schmidt, H., Nissan, A., Ridolfi, L., Aamdal, S., Hansson, J., Guida, M., Hyams, D.M., Gómez, H., Bastholt, L., et al. (2011). A prospective phase II trial exploring the association between tumor microenvironment biomarkers and clinical activity of ipilimumab in advanced melanoma. *J. Transl. Med.* *9*, 204.
- Hanks, B.A., Holtzhausen, A., Evans, K., Heid, M., and Blobe, G.C. (2014). Combinatorial TGF- β signaling blockade and anti-CTLA-4 antibody immunotherapy in a murine BRAFV600E-PTEN-/-transgenic model of melanoma. ASCO Annual Meeting Proceedings.
- Hauschild, A., Grob, J.J., Demidov, L.V., Jouary, T., Gutzmer, R., Millward, M., Rutkowski, P., Blank, C.U., Miller, W.H., Jr., Kaempgen, E., et al. (2012). Dabrafenib in BRAF-mutated metastatic melanoma: a multicentre, open-label, phase 3 randomised controlled trial. *Lancet* *380*, 358–365.
- Héninger, E., Krueger, T.E., and Lang, J.M. (2015). Augmenting antitumor immune responses with epigenetic modifying agents. *Front. Immunol.* *6*, 29.
- Hicklin, D.J., Wang, Z., Arienti, F., Rivoltini, L., Parmiani, G., and Ferrone, S. (1998). beta2-Microglobulin mutations, HLA class I antigen loss, and tumor progression in melanoma. *J. Clin. Invest.* *101*, 2720–2729.
- Highfill, S.L., Cui, Y., Giles, A.J., Smith, J.P., Zhang, H., Morse, E., Kaplan, R.N., and Mackall, C.L. (2014). Disruption of CXCR2-mediated MDSC tumor trafficking enhances anti-PD1 efficacy. *Sci. Transl. Med.* *6*.
- Hodi, F.S., O'Day, S.J., McDermott, D.F., Weber, R.W., Sosman, J.A., Haanen, J.B., Gonzalez, R., Robert, C., Schadendorf, D., Hassel, J.C., et al. (2010). Improved survival with ipilimumab in patients with metastatic melanoma. *N. Engl. J. Med.* *363*, 711–723.
- Holmgaard, R.B., Zamarin, D., Munn, D.H., Wolchok, J.D., and Allison, J.P. (2013). Indoleamine 2,3-dioxygenase is a critical resistance mechanism in anti-tumor T cell immunotherapy targeting CTLA-4. *J. Exp. Med.* *210*, 1389–1402.
- Homet Moreno, B., Mok, S., Comin-Anduix, B., Hu-Lieskovan, S., and Ribas, A. (2015). Combined treatment with dabrafenib and trametinib with immunostimulating antibodies for BRAF mutant melanoma. *Oncol Immunology* *5*, e1052212.
- Hu, W., Li, X., Zhang, C., Yang, Y., Jiang, J., and Wu, C. (2016). Tumor-associated macrophages in cancers. *Clin. Transl. Oncol.* *18*, 251–258.
- Hu-Lieskovan, S., Mok, S., Homet Moreno, B., Tsoi, J., Robert, L., Goedert, L., Pinheiro, E.M., Koya, R.C., Graeber, T.G., Comin-Anduix, B., and Ribas, A. (2015). Improved antitumor activity of immunotherapy with BRAF and MEK inhibitors in BRAF(V600E) melanoma. *Sci. Transl. Med.* *7*, 279ra41.
- Hugo, W., Zaretsky, J.M., Sun, L., Song, C., Moreno, B.H., Hu-Lieskovan, S., Berent-Maoz, B., Pang, J., Chmielowski, B., Cherry, G., et al. (2016). Genomic and Transcriptomic Features of Response to Anti-PD-1 Therapy in Metastatic Melanoma. *Cell* *165*, 35–44.
- Ishida, Y., Agata, Y., Shibahara, K., and Honjo, T. (1992). Induced expression of PD-1, a novel member of the immunoglobulin gene superfamily, upon programmed cell death. *EMBO J.* *11*, 3887–3895.
- Kalos, M., Levine, B.L., Porter, D.L., Katz, S., Grupp, S.A., Bagg, A., and June, C.H. (2011). T cells with chimeric antigen receptors have potent antitumor effects and can establish memory in patients with advanced leukemia. *Sci. Transl. Med.* *3*, 95ra73.
- Kaneda, M.M., Messer, K.S., Ralainirina, N., Li, H., Leem, C.J., Gorjestani, S., Woo, G., Nguyen, A.V., Figueiredo, C.C., Foubert, P., et al. (2016). PI3K γ is a molecular switch that controls immune suppression. *Nature* *539*, 437–442.
- Kaplan, M.H., Wurster, A.L., and Grusby, M.J. (1998). A signal transducer and activator of transcription (Stat)4-independent pathway for the development of T helper type 1 cells. *J. Exp. Med.* *188*, 1191–1196.
- Karpf, A.R., and Jones, D.A. (2002). Reactivating the expression of methylation silenced genes in human cancer. *Oncogene* *21*, 5496–5503.
- Kataoka, K., Shiraishi, Y., Takeda, Y., Sakata, S., Matsumoto, M., Nagano, S., Maeda, T., Nagata, Y., Kitanaka, A., Mizuno, S., et al. (2016). Aberrant PD-L1 expression through 3'-UTR disruption in multiple cancers. *Nature* *534*, 402–406.
- Kim, H.J., and Bae, S.C. (2011). Histone deacetylase inhibitors: molecular mechanisms of action and clinical trials as anti-cancer drugs. *Am. J. Transl. Res.* *3*, 166–179.
- Kodumudi, K.N., Weber, A., Sarnaik, A.A., and Pilon-Thomas, S. (2012). Blockade of myeloid-derived suppressor cells after induction of lymphopenia improves adoptive T cell therapy in a murine model of melanoma. *J. Immunol.* *189*, 5147–5154.
- Koya, R.C., Mok, S., Otte, N., Blacketer, K.J., Comin-Anduix, B., Tumei, P.C., Minasian, A., Graham, N.A., Graeber, T.G., Chodon, T., and Ribas, A. (2012). BRAF inhibitor vemurafenib improves the antitumor activity of adoptive cell immunotherapy. *Cancer Res.* *72*, 3928–3937.
- Koyama, S., Akbay, E.A., Li, Y.Y., Herter-Sprie, G.S., Buczkowski, K.A., Richards, W.G., Gandhi, L., Redig, A.J., Rodig, S.J., Asahina, H., et al. (2016). Adaptive resistance to therapeutic PD-1 blockade is associated with upregulation of alternative immune checkpoints. *Nat. Commun.* *7*, 10501.
- Krummel, M.F., and Allison, J.P. (1995). CD28 and CTLA-4 have opposing effects on the response of T cells to stimulation. *J. Exp. Med.* *182*, 459–465.
- Kryczek, I., Zou, L., Rodriguez, P., Zhu, G., Wei, S., Mottram, P., Brumlik, M., Cheng, P., Curiel, T., Myers, L., et al. (2006). B7-H4 expression identifies a novel suppressive macrophage population in human ovarian carcinoma. *J. Exp. Med.* *203*, 871–881.
- Kuang, D.M., Zhao, Q., Peng, C., Xu, J., Zhang, J.P., Wu, C., and Zheng, L. (2009). Activated monocytes in peritumoral stroma of hepatocellular carcinoma foster immune privilege and disease progression through PD-L1. *J. Exp. Med.* *206*, 1327–1337.
- Laborde, R.R., Lin, Y., Gustafson, M.P., Bulur, P.A., and Dietz, A.B. (2014). Cancer Vaccines in the World of Immune Suppressive Monocytes (CD14(+) HLA-DR(lo/neg) Cells): The Gateway to Improved Responses. *Front. Immunol.* *5*, 147.
- Larkin, J., Chiarion-Sileni, V., Gonzalez, R., Grob, J.J., Cowey, C.L., Lao, C.D., Schadendorf, D., Dummer, R., Smylie, M., Rutkowski, P., et al. (2015a). Combined Nivolumab and Ipilimumab or Monotherapy in Untreated Melanoma. *N. Engl. J. Med.* *373*, 23–34.

- Larkin, J., Lao, C.D., Urba, W.J., McDermott, D.F., Horak, C., Jiang, J., and Wolchok, J.D. (2015b). Efficacy and safety of nivolumab in patients with BRAF V600 mutant and BRAF wild-type advanced melanoma: a pooled analysis of 4 clinical trials. *JAMA Oncol.* *1*, 433–440.
- Lastwika, K.J., Wilson, W., 3rd, Li, Q.K., Norris, J., Xu, H., Ghazarian, S.R., Kitagawa, H., Kawabata, S., Taube, J.M., Yao, S., et al. (2016). Control of PD-L1 expression by oncogenic activation of the AKT-mTOR pathway in non-small cell lung cancer. *Cancer Res.* *76*, 227–238.
- Le, D.T., Lutz, E., Uram, J.N., Sugar, E.A., Onners, B., Solt, S., Zheng, L., Diaz, L.A., Jr., Donehower, R.C., Jaffee, E.M., and Laheru, D.A. (2013). Evaluation of ipilimumab in combination with allogeneic pancreatic tumor cells transfected with a GM-CSF gene in previously treated pancreatic cancer. *J. Immunother.* *36*, 382–389.
- Leach, D.R., Krummel, M.F., and Allison, J.P. (1996). Enhancement of anti-tumor immunity by CTLA-4 blockade. *Science* *271*, 1734–1736.
- Lebrun, J.-J. (2012). The dual role of TGF β in human cancer: from tumor suppression to cancer metastasis. *ISRN Mol. Biol.* *2012*, 381428.
- Leclerc, B.G., Charlebois, R., Chouinard, G., Allard, B., Pommey, S., Saad, F., and Stagg, J. (2016). CD73 expression is an independent prognostic factor in prostate cancer. *Clin. Cancer Res.* *22*, 158–166.
- Lin, R.L., and Zhao, L.J. (2015). Mechanistic basis and clinical relevance of the role of transforming growth factor- β in cancer. *Cancer Biol. Med.* *12*, 385–393.
- Linehan, D.C., and Goedegebuure, P.S. (2005). CD25+ CD4+ regulatory T-cells in cancer. *Immunol. Res.* *32*, 155–168.
- Liu, C., Peng, W., Xu, C., Lou, Y., Zhang, M., Wargo, J.A., Chen, J.Q., Li, H.S., Watowich, S.S., Yang, Y., et al. (2013). BRAF inhibition increases tumor infiltration by T cells and enhances the antitumor activity of adoptive immunotherapy in mice. *Clin. Cancer Res.* *19*, 393–403.
- Loi, S., Pommey, S., Haibe-Kains, B., Beavis, P.A., Darcy, P.K., Smyth, M.J., and Stagg, J. (2013). CD73 promotes anthracycline resistance and poor prognosis in triple negative breast cancer. *Proc. Natl. Acad. Sci. USA* *110*, 11091–11096.
- Luo, Y., Zhou, H., Krueger, J., Kaplan, C., Lee, S.H., Dolman, C., Markowitz, D., Wu, W., Liu, C., Reisfeld, R.A., and Xiang, R. (2006). Targeting tumor-associated macrophages as a novel strategy against breast cancer. *J. Clin. Invest.* *116*, 2132–2141.
- Ma, C., Fan, R., Ahmad, H., Shi, Q., Comin-Anduix, B., Chodon, T., Koya, R.C., Liu, C.C., Kwong, G.A., Radu, C.G., et al. (2011). A clinical microchip for evaluation of single immune cells reveals high functional heterogeneity in phenotypically similar T cells. *Nat. Med.* *17*, 738–743.
- Ma, C., Cheung, A.F., Chodon, T., Koya, R.C., Wu, Z., Ng, C., Avramis, E., Cochran, A.J., Witte, O.N., Baltimore, D., et al. (2013). Multifunctional T-cell analyses to study response and progression in adoptive cell transfer immunotherapy. *Cancer Discov.* *3*, 418–429.
- Madore, J., Vilain, R.E., Menzies, A.M., Kakavand, H., Wilmott, J.S., Hyman, J., Yearley, J.H., Kefford, R.F., Thompson, J.F., Long, G.V., et al. (2015). PD-L1 expression in melanoma shows marked heterogeneity within and between patients: implications for anti-PD-1/PD-L1 clinical trials. *Pigment Cell Melanoma Res.* *28*, 245–253.
- Marincola, F.M., Jaffee, E.M., Hicklin, D.J., and Ferrone, S. (2000). Escape of human solid tumors from T-cell recognition: molecular mechanisms and functional significance. *Adv. Immunol.* *74*, 181–273.
- Massagué, J. (2008). TGF β in Cancer. *Cell* *134*, 215–230.
- Maude, S.L., Frey, N., Shaw, P.A., Aplenc, R., Barrett, D.M., Bunin, N.J., Chew, A., Gonzalez, V.E., Zheng, Z., Lacey, S.F., et al. (2014). Chimeric antigen receptor T cells for sustained remissions in leukemia. *N. Engl. J. Med.* *371*, 1507–1517.
- Meyer, C., Cagnon, L., Costa-Nunes, C.M., Baumgaertner, P., Montandon, N., Leyvraz, L., Michielin, O., Romano, E., and Speiser, D.E. (2014). Frequencies of circulating MDSC correlate with clinical outcome of melanoma patients treated with ipilimumab. *Cancer Immunol. Immunother.* *63*, 247–257.
- Miller, J.F., and Sadelain, M. (2015). The journey from discoveries in fundamental immunology to cancer immunotherapy. *Cancer Cell* *27*, 439–449.
- Miller, R.E., Jones, J., Le, T., Whitmore, J., Boiani, N., Gliniak, B., and Lynch, D.H. (2002). 4-1BB-specific monoclonal antibody promotes the generation of tumor-specific immune responses by direct activation of CD8 T cells in a CD40-dependent manner. *J. Immunol.* *169*, 1792–1800.
- Mittal, D., Sinha, D., Barkauskas, D., Young, A., Kalimutho, M., Stannard, K., Caramia, F., Haibe-Kains, B., Stagg, J., and Khanna, K.K. (2016). Adenosine 2B receptor expression on cancer cells promotes metastasis. *Cancer Res.* *76*.
- Mok, S., Koya, R.C., Tsui, C., Xu, J., Robert, L., Wu, L., Graeber, T.G., West, B.L., Bollag, G., and Ribas, A. (2014). Inhibition of CSF-1 receptor improves the antitumor efficacy of adoptive cell transfer immunotherapy. *Cancer Res.* *74*, 153–161.
- Moon, E.K., Wang, L.C., Dolfi, D.V., Wilson, C.B., Ranganathan, R., Sun, J., Kapoor, V., Scholler, J., Pure, E., Milone, M.C., et al. (2014). Multifactorial T-cell hypofunction that is reversible can limit the efficacy of chimeric antigen receptor-transduced human T cells in solid tumors. *Clin. Cancer Res.* *20*, 4262–4273.
- Morgan, R.A., Dudley, M.E., Wunderlich, J.R., Hughes, M.S., Yang, J.C., Sherry, R.M., Royal, R.E., Topalian, S.L., Kammula, U.S., Restifo, N.P., et al. (2006). Cancer regression in patients after transfer of genetically engineered lymphocytes. *Science* *314*, 126–129.
- Ninomiya, S., Narala, N., Huye, L., Yagyu, S., Savoldo, B., Dotti, G., Heslop, H.E., Brenner, M.K., Rooney, C.M., and Ramos, C.A. (2015). Tumor indoleamine 2,3-dioxygenase (IDO) inhibits CD19-CAR T cells and is downregulated by lymphodepleting drugs. *Blood* *125*, 3905–3916.
- Oida, T., Zhang, X., Goto, M., Hachimura, S., Totsuka, M., Kaminogawa, S., and Weiner, H.L. (2003). CD4+CD25- T cells that express latency-associated peptide on the surface suppress CD4+CD45RBhigh-induced colitis by a TGF- β -dependent mechanism. *J. Immunol.* *170*, 2516–2522.
- Okazaki, T., Chikuma, S., Iwai, Y., Fagarasan, S., and Honjo, T. (2013). A rheostat for immune responses: the unique properties of PD-1 and their advantages for clinical application. *Nat. Immunol.* *14*, 1212–1218.
- Ormandy, L.A., Hilleman, T., Wedemeyer, H., Manns, M.P., Greten, T.F., and Korangy, F. (2005). Increased populations of regulatory T cells in peripheral blood of patients with hepatocellular carcinoma. *Cancer Res.* *65*, 2457–2464.
- Ortenberg, R., Sapir, Y., Raz, L., Hershkovitz, L., Ben Arav, A., Sapoznik, S., Barshack, I., Avivi, C., Berkun, Y., Besser, M.J., et al. (2012). Novel immunotherapy for malignant melanoma with a monoclonal antibody that blocks CEACAM1 homophilic interactions. *Mol. Cancer Ther.* *11*, 1300–1310.
- Pardoll, D.M. (2012). The blockade of immune checkpoints in cancer immunotherapy. *Nat. Rev. Cancer* *12*, 252–264.
- Parsa, A.T., Waldron, J.S., Panner, A., Crane, C.A., Parney, I.F., Barry, J.J., Cachola, K.E., Murray, J.C., Tihan, T., Jensen, M.C., et al. (2007). Loss of tumor suppressor PTEN function increases B7-H1 expression and immunoresistance in glioma. *Nat. Med.* *13*, 84–88.
- Peng, W., Chen, J.Q., Liu, C., Malu, S., Creasy, C., Tetzlaff, M.T., Xu, C., McKenzie, J.A., Zhang, C., Liang, X., et al. (2016). Loss of PTEN promotes resistance to T cell-mediated immunotherapy. *Cancer Discov.* *6*, 202–216.
- Platanias, L.C. (2005). Mechanisms of type-I- and type-II-interferon-mediated signalling. *Nat. Rev. Immunol.* *5*, 375–386.
- Postow, M.A., Chesney, J., Pavlick, A.C., Robert, C., Grossmann, K., McDermott, D., Linette, G.P., Meyer, N., Giguere, J.K., Agarwala, S.S., et al. (2015). Nivolumab and ipilimumab versus ipilimumab in untreated melanoma. *N. Engl. J. Med.* *372*, 2006–2017.
- Puzanov, I., Milhem, M.M., Minor, D., Hamid, O., Li, A., Chen, L., Chastain, M., Gorski, K.S., Anderson, A., Chou, J., et al. (2016). Talmogene Lahereparepvec in Combination With Ipilimumab in Previously Untreated, Unresectable Stage IIIB-IV Melanoma. *J. Clin. Oncol.* *34*, 2619–2626.
- Quezada, S.A., Peggs, K.S., Curran, M.A., and Allison, J.P. (2006). CTLA4 blockade and GM-CSF combination immunotherapy alters the intratumor balance of effector and regulatory T cells. *J. Clin. Invest.* *116*, 1935–1945.
- Redmond, W.L., Gough, M.J., Charbonneau, B., Ratliff, T.L., and Weinberg, A.D. (2007). Defects in the acquisition of CD8 T cell effector function after

- priming with tumor or soluble antigen can be overcome by the addition of an OX40 agonist. *J. Immunol.* **179**, 7244–7253.
- Redmond, W.L., Linch, S.N., and Kasiewicz, M.J. (2014). Combined targeting of costimulatory (OX40) and coinhibitory (CTLA-4) pathways elicits potent effector T cells capable of driving robust antitumor immunity. *Cancer Immunol. Res.* **2**, 142–153.
- Restifo, N.P., Marincola, F.M., Kawakami, Y., Taubenberger, J., Yannelli, J.R., and Rosenberg, S.A. (1996). Loss of functional beta 2-microglobulin in metastatic melanomas from five patients receiving immunotherapy. *J. Natl. Cancer Inst.* **88**, 100–108.
- Ribas, A. (2015). Adaptive Immune Resistance: How Cancer Protects from Immune Attack. *Cancer Discov.* **5**, 915–919.
- Ribas, A., Puzanov, I., Dummer, R., Schadendorf, D., Hamid, O., Robert, C., Hodi, F.S., Schachter, J., Pavlick, A.C., Lewis, K.D., et al. (2015). Pembrolizumab versus investigator-choice chemotherapy for ipilimumab-refractory melanoma (KEYNOTE-002): a randomised, controlled, phase 2 trial. *Lancet Oncol.* **16**, 908–918.
- Ries, C.H., Cannarile, M.A., Hoves, S., Benz, J., Wartha, K., Runza, V., Rey-Giraud, F., Pradel, L.P., Feuerhake, F., Klaman, I., et al. (2014). Targeting tumor-associated macrophages with anti-CSF-1R antibody reveals a strategy for cancer therapy. *Cancer Cell* **25**, 846–859.
- Rizvi, N.A., Hellmann, M.D., Snyder, A., Kvistborg, P., Makarov, V., Havel, J.J., Lee, W., Yuan, J., Wong, P., Ho, T.S., et al. (2015). Cancer immunology. Mutational landscape determines sensitivity to PD-1 blockade in non-small cell lung cancer. *Science* **348**, 124–128.
- Robbins, P.F., Morgan, R.A., Feldman, S.A., Yang, J.C., Sherry, R.M., Dudley, M.E., Wunderlich, J.R., Nahvi, A.V., Helman, L.J., Mackall, C.L., et al. (2011). Tumor regression in patients with metastatic synovial cell sarcoma and melanoma using genetically engineered lymphocytes reactive with NY-ESO-1. *J. Clin. Oncol.* **29**, 917–924.
- Robert, C., Thomas, L., Bondarenko, I., O'Day, S., Weber, J., Garbe, C., Lebbe, C., Baurain, J.F., Testori, A., Grob, J.J., et al. (2011). Ipilimumab plus dacarbazine for previously untreated metastatic melanoma. *N. Engl. J. Med.* **364**, 2517–2526.
- Rooney, M.S., Shukla, S.A., Wu, C.J., Getz, G., and Hacohen, N. (2015). Molecular and genetic properties of tumors associated with local immune cytolytic activity. *Cell* **160**, 48–61.
- Rosenberg, S.A., Yang, J.C., Sherry, R.M., Kammula, U.S., Hughes, M.S., Phan, G.Q., Citrin, D.E., Restifo, N.P., Robbins, P.F., Wunderlich, J.R., et al. (2011). Durable complete responses in heavily pretreated patients with metastatic melanoma using T-cell transfer immunotherapy. *Clin. Cancer Res.* **17**, 4550–4557.
- Roszik, J., Haydu, L.E., Hess, K.R., Oba, J., Joon, A.Y., Siroy, A.E., Karpinets, T.V., Stingo, F.C., Baladandayuthapani, V., Tetzlaff, M.T., et al. (2016). Novel algorithmic approach predicts tumor mutation load and correlates with immunotherapy clinical outcomes using a defined gene mutation set. *BMC Med.* **14**, 168.
- Rudensky, A.Y. (2011). Regulatory T cells and Foxp3. *Immunol. Rev.* **241**, 260–268.
- Ruella, M., Barrett, D.M., Kenderian, S.S., Shestova, O., Hofmann, T.J., Perazzelli, J., Klichinsky, M., Aikawa, V., Nazimuddin, F., Kozlowski, M., et al. (2016). Dual CD19 and CD123 targeting prevents antigen-loss relapses after CD19-directed immunotherapies. *J. Clin. Invest.* **126**, 3814–3826.
- Ruffell, B., and Coussens, L.M. (2015). Macrophages and therapeutic resistance in cancer. *Cancer Cell* **27**, 462–472.
- Ruffell, B., Chang-Strachan, D., Chan, V., Rosenbusch, A., Ho, C.M., Pryer, N., Daniel, D., Hwang, E.S., Rugo, H.S., and Coussens, L.M. (2014). Macrophage IL-10 blocks CD8+ T cell-dependent responses to chemotherapy by suppressing IL-12 expression in intratumoral dendritic cells. *Cancer Cell* **26**, 623–637.
- Sadelain, M. (2016). Chimeric antigen receptors: driving immunology towards synthetic biology. *Curr. Opin. Immunol.* **41**, 68–76.
- Sakaguchi, S., Yamaguchi, T., Nomura, T., and Ono, M. (2008). Regulatory T cells and immune tolerance. *Cell* **133**, 775–787.
- Sakuishi, K., Apetoh, L., Sullivan, J.M., Blazar, B.R., Kuchroo, V.K., and Anderson, A.C. (2010). Targeting Tim-3 and PD-1 pathways to reverse T cell exhaustion and restore anti-tumor immunity. *J. Exp. Med.* **207**, 2187–2194.
- Schachter, J. R.A., Long GV, Arance A, Grob JJ, Mortier L, Daud A, Carlino MS, McNeil CM, Lotem M, Larkin J, Lorigan P, Neyns B, Blank CU, Petrella TM, Hamid O, Zhou H, Ebbinghaus S, Ibrahim N, Robert C (2016). Pembrolizumab versus ipilimumab for advanced melanoma: final overall survival analysis of KEYNOTE-006. *Clin Oncol* **34** (suppl; abstr 9504).
- Schadendorf, D., Hodi, F.S., Robert, C., Weber, J.S., Margolin, K., Hamid, O., Patt, D., Chen, T.-T., Berman, D.M., and Wolchok, J.D. (2015). Pooled analysis of long-term survival data from phase II and phase III trials of ipilimumab in unresectable or metastatic melanoma. *J. Clin. Oncol.* **33**.
- Schumacher, T.N., and Schreiber, R.D. (2015). Neoantigens in cancer immunotherapy. *Science* **348**, 69–74.
- Shankaran, V., Ikeda, H., Bruce, A.T., White, J.M., Swanson, P.E., Old, L.J., and Schreiber, R.D. (2001). IFN γ and lymphocytes prevent primary tumour development and shape tumour immunogenicity. *Nature* **410**, 1107–1111.
- Sharma, P., and Allison, J.P. (2015). Immune checkpoint targeting in cancer therapy: toward combination strategies with curative potential. *Cell* **161**, 205–214.
- Shin, D.S., and Ribas, A. (2015). The evolution of checkpoint blockade as a cancer therapy: what's here, what's next? *Curr. Opin. Immunol.* **33**, 23–35.
- Shin, D.S., Zaretsky, J.M., Escuin-Ordinas, H., Garcia-Diaz, A., Hu-Lieskovan, S., Kalbasi, A., Grasso, C.S., Hugo, W., Sandoval, S., Torrejon, D.Y., et al. (2016). Primary Resistance to PD-1 Blockade Mediated by JAK(1/2) Mutations. *Cancer Discov.*
- Simpson, T.R., Li, F., Montalvo-Ortiz, W., Sepulveda, M.A., Bergerhoff, K., Arce, F., Roddie, C., Henry, J.Y., Yagita, H., Wolchok, J.D., et al. (2013). Fc-dependent depletion of tumor-infiltrating regulatory T cells co-defines the efficacy of anti-CTLA-4 therapy against melanoma. *J. Exp. Med.* **210**, 1695–1710.
- Sivan, A., Corrales, L., Hubert, N., Williams, J.B., Aquino-Michaels, K., Earley, Z.M., Benyamin, F.W., Lei, Y.M., Jabri, B., Alegre, M.L., et al. (2015). Commensal bifidobacterium promotes antitumor immunity and facilitates anti-PD-L1 efficacy. *Science* **350**, 1084–1089.
- Snyder, A., Makarov, V., Merghoub, T., Yuan, J., Zaretsky, J.M., Desrichard, A., Walsh, L.A., Postow, M.A., Wong, P., Ho, T.S., et al. (2014). Genetic basis for clinical response to CTLA-4 blockade in melanoma. *N. Engl. J. Med.* **371**, 2189–2199.
- Solito, S., Falisi, E., Diaz-Montero, C.M., Doni, A., Pinton, L., Rosato, A., Francescato, S., Basso, G., Zanovello, P., Onicescu, G., et al. (2011). A human promyelocytic-like population is responsible for the immune suppression mediated by myeloid-derived suppressor cells. *Blood* **118**, 2254–2265.
- Sotillo, E., Barrett, D.M., Black, K.L., Bagashev, A., Oldridge, D., Wu, G., Sussman, R., Lanauze, C., Ruella, M., Gazzara, M.R., et al. (2015). Convergence of Acquired Mutations and Alternative Splicing of CD19 Enables Resistance to CART-19 Immunotherapy. *Cancer Discov.* **5**, 1282–1295.
- Spranger, S., Koblisch, H.K., Horton, B., Scherle, P.A., Newton, R., and Gajewski, T.F. (2014). Mechanism of tumor rejection with doublets of CTLA-4, PD-1/PD-L1, or IDO blockade involves restored IL-2 production and proliferation of CD8(+) T cells directly within the tumor microenvironment. *J. Immunother. Cancer* **2**, 3.
- Spranger, S., Bao, R., and Gajewski, T.F. (2015). Melanoma-intrinsic β -catenin signalling prevents anti-tumour immunity. *Nature* **523**, 231–235.
- Stagg, J., Divisekera, U., McLaughlin, N., Sharkey, J., Pommey, S., Denoyer, D., Dwyer, K.M., and Smyth, M.J. (2010). Anti-CD73 antibody therapy inhibits breast tumor growth and metastasis. *Proc. Natl. Acad. Sci. USA* **107**, 1547–1552.
- Sucker, A., Zhao, F., Real, B., Heeke, C., Bielefeld, N., Mabetan, S., Horn, S., Moll, I., Maltaner, R., Horn, P.A., et al. (2014). Genetic evolution of T-cell

- resistance in the course of melanoma progression. *Clin. Cancer Res.* 20, 6593–6604.
- Sugiyama, D., Nishikawa, H., Maeda, Y., Nishioka, M., Tanemura, A., Katayama, I., Ezoe, S., Kanakura, Y., Sato, E., Fukumori, Y., et al. (2013). Anti-CCR4 mAb selectively depletes effector-type FoxP3+CD4+ regulatory T cells, evoking antitumor immune responses in humans. *Proc. Natl. Acad. Sci. USA* 110, 17945–17950.
- Sundstedt, A., O'Neill, E.J., Nicolson, K.S., and Wraith, D.C. (2003). Role for IL-10 in suppression mediated by peptide-induced regulatory T cells in vivo. *J. Immunol.* 170, 1240–1248.
- Takahashi, H., Okai, Y., Paxton, R.J., Hefta, L.J., and Shively, J.E. (1993). Differential regulation of carcinoembryonic antigen and biliary glycoprotein by gamma-interferon. *Cancer Res.* 53, 1612–1619.
- Talmadge, J.E., and Gabrilovich, D.I. (2013). History of myeloid-derived suppressor cells. *Nat. Rev. Cancer* 13, 739–752.
- Tang, D.Y., Ellis, R.A., and Lovat, P.E. (2016). Prognostic Impact of Autophagy Biomarkers for Cutaneous Melanoma. *Front. Oncol.* 6, 236.
- Taube, J.M., Anders, R.A., Young, G.D., Xu, H., Sharma, R., McMiller, T.L., Chen, S., Klein, A.P., Pardoll, D.M., Topalian, S.L., and Chen, L. (2012). Colocalization of inflammatory response with B7-h1 expression in human melanocytic lesions supports an adaptive resistance mechanism of immune escape. *Sci. Transl. Med.* 4, 127ra37.
- Taube, J.M., Klein, A., Brahmer, J.R., Xu, H., Pan, X., Kim, J.H., Chen, L., Pardoll, D.M., Topalian, S.L., and Anders, R.A. (2014). Association of PD-1, PD-1 ligands, and other features of the tumor immune microenvironment with response to anti-PD-1 therapy. *Clin. Cancer Res.* 20, 5064–5074.
- Tham, M., Khoo, K., Yeo, K.P., Kato, M., Prevost-Blondel, A., Angeli, V., and Abastado, J.P. (2015). Macrophage depletion reduces postsurgical tumor recurrence and metastatic growth in a spontaneous murine model of melanoma. *Oncotarget* 6, 22857–22868.
- Topalian, S.L., Drake, C.G., and Pardoll, D.M. (2015). Immune checkpoint blockade: a common denominator approach to cancer therapy. *Cancer Cell* 27, 450–461.
- Tran, E., Robbins, P.F., Lu, Y.C., Prickett, T.D., Gartner, J.J., Jia, L., Pasetto, A., Zheng, Z., Ray, S., Groh, E.M., et al. (2016). T-Cell Transfer Therapy Targeting Mutant KRAS in Cancer. *N. Engl. J. Med.* 375, 2255–2262.
- Tumeh, P.C., Harview, C.L., Yearley, J.H., Shintaku, I.P., Taylor, E.J., Robert, L., Chmielowski, B., Spasic, M., Henry, G., Ciobanu, V., et al. (2014). PD-1 blockade induces responses by inhibiting adaptive immune resistance. *Nature* 515, 568–571.
- Turcotte, M., Spring, K., Pommey, S., Chouinard, G., Cousineau, I., George, J., Chen, G.M., Gendoo, D.M., Haibe-Kains, B., Karn, T., et al. (2015). CD73 is associated with poor prognosis in high-grade serous ovarian cancer. *Cancer Res.* 75, 4494–4503.
- Van Allen, E.M., Miao, D., Schilling, B., Shukla, S.A., Blank, C., Zimmer, L., Sucker, A., Hillen, U., Geukes Foppen, M.H., Goldinger, S.M., et al. (2015). Genomic correlates of response to CTLA-4 blockade in metastatic melanoma. *Science* 350, 207–211.
- van Rooij, N., van Buuren, M.M., Philips, D., Velds, A., Toebes, M., Heemskerk, B., van Dijk, L.J., Behjati, S., Hilkmann, H., El Atmioui, D., et al. (2013). Tumor exome analysis reveals neoantigen-specific T-cell reactivity in an ipilimumab-responsive melanoma. *J. Clin. Oncol.* 31, e439–e442.
- Vanpouille-Box, C., Diamond, J.M., Pilonis, K.A., Zavadil, J., Babb, J.S., Formenti, S.C., Barcellos-Hoff, M.H., and Demaria, S. (2015). TGF β is a master regulator of radiation therapy-induced antitumor immunity. *Cancer Res.* 75, 2232–2242.
- Vétizou, M., Pitt, J.M., Daillère, R., Lepage, P., Waldschmitt, N., Flament, C., Rusakiewicz, S., Routy, B., Roberti, M.P., Duong, C.P., et al. (2015). Anticancer immunotherapy by CTLA-4 blockade relies on the gut microbiota. *Science* 350, 1079–1084.
- Viehl, C.T., Moore, T.T., Liyanage, U.K., Frey, D.M., Ehlers, J.P., Eberlein, T.J., Goedegebuure, P.S., and Linehan, D.C. (2006). Depletion of CD4+CD25+ regulatory T cells promotes a tumor-specific immune response in pancreas cancer-bearing mice. *Ann. Surg. Oncol.* 13, 1252–1258.
- Vo, D.D., Prins, R.M., Begley, J.L., Donahue, T.R., Morris, L.F., Bruhn, K.W., de la Rocha, P., Yang, M.-Y., Mok, S., Garban, H.J., et al. (2009). Enhanced anti-tumor activity induced by adoptive T-cell transfer and adjunctive use of the histone deacetylase inhibitor LAQ824. *Cancer Res.* 69, 8693–8699.
- Wang, L.X., Mei, Z.Y., Zhou, J.H., Yao, Y.S., Li, Y.H., Xu, Y.H., Li, J.X., Gao, X.N., Zhou, M.H., Jiang, M.M., et al. (2013). Low dose decitabine treatment induces CD80 expression in cancer cells and stimulates tumor specific cytotoxic T lymphocyte responses. *PLoS ONE* 8, e62924.
- Wargo, J.A., Reddy, S.M., Reuben, A., and Sharma, P. (2016). Monitoring immune responses in the tumor microenvironment. *Curr. Opin. Immunol.* 41, 23–31.
- Weber, J.S., D'Angelo, S.P., Minor, D., Hodi, F.S., Gutzmer, R., Neyns, B., Hoeller, C., Khushalani, N.I., Miller, W.H., Jr., Lao, C.D., et al. (2015). Nivolumab versus chemotherapy in patients with advanced melanoma who progressed after anti-CTLA-4 treatment (CheckMate 037): a randomised, controlled, open-label, phase 3 trial. *Lancet Oncol.* 16, 375–384.
- Wesolowski, R., Markowitz, J., and Carson, W.E., 3rd. (2013). Myeloid derived suppressor cells - a new therapeutic target in the treatment of cancer. *J. Immunother. Cancer* 1, 10.
- Wilmott, J.S., Long, G.V., Howle, J.R., Haydu, L.E., Sharma, R.N., Thompson, J.F., Keefe, R.F., Hersey, P., and Scolyer, R.A. (2012). Selective BRAF inhibitors induce marked T-cell infiltration into human metastatic melanoma. *Clin. Cancer Res.* 18, 1386–1394.
- Wolchok, J.D., Kluger, H., Callahan, M.K., Postow, M.A., Rizvi, N.A., Lesokhin, A.M., Segal, N.H., Ariyan, C.E., Gordon, R.-A., Reed, K., et al. (2013). Nivolumab plus ipilimumab in advanced melanoma. *N. Engl. J. Med.* 369, 122–133.
- Woo, E.Y., Yeh, H., Chu, C.S., Schlienger, K., Carroll, R.G., Riley, J.L., Kaiser, L.R., and June, C.H. (2002). Cutting edge: Regulatory T cells from lung cancer patients directly inhibit autologous T cell proliferation. *J. Immunol.* 168, 4272–4276.
- Wu, X., Schulte, B.C., Zhou, Y., Haribhai, D., Mackinnon, A.C., Plaza, J.A., Williams, C.B., and Hwang, S.T. (2014). Depletion of M2-like tumor-associated macrophages delays cutaneous T-cell lymphoma development in vivo. *J. Invest. Dermatol.* 134, 2814–2822.
- Yang, J.C., and Rosenberg, S.A. (2016). Chapter Seven—Adoptive T-Cell Therapy for Cancer. In *Advances in Immunology*, D.S. Robert, ed. (Academic Press), pp. 279–294.
- Yang, L., DeBusk, L.M., Fukuda, K., Fingleton, B., Green-Jarvis, B., Shyr, Y., Matrisian, L.M., Carbone, D.P., and Lin, P.C. (2004). Expansion of myeloid immune suppressor Gr+CD11b+ cells in tumor-bearing host directly promotes tumor angiogenesis. *Cancer Cell* 6, 409–421.
- Yang, L., Huang, J., Ren, X., Gorska, A.E., Chytil, A., Aakre, M., Carbone, D.P., Matrisian, L.M., Richmond, A., Lin, P.C., and Moses, H.L. (2008). Abrogation of TGF beta signaling in mammary carcinomas recruits Gr-1+CD11b+ myeloid cells that promote metastasis. *Cancer Cell* 13, 23–35.
- Yee, C., Lizee, G., and Schueneman, A.J. (2015). Endogenous T-Cell Therapy: Clinical Experience. *Cancer J.* 21, 492–500.
- Zaretsky, J.M., Garcia-Diaz, A., Shin, D.S., Escuin-Ordinas, H., Hugo, W., Hu-Lieskovan, S., Torrejon, D.Y., Abril-Rodriguez, G., Sandoval, S., Barthly, L., et al. (2016). Mutations Associated with Acquired Resistance to PD-1 Blockade in Melanoma. *N. Engl. J. Med.* 375, 819–829.
- Zhang, H., Conrad, D.M., Butler, J.J., Zhao, C., Blay, J., and Hoskin, D.W. (2004). Adenosine acts through A2 receptors to inhibit IL-2-induced tyrosine phosphorylation of STAT5 in T lymphocytes: role of cyclic adenosine 3',5'-monophosphate and phosphatases. *J. Immunol.* 173, 932–944.
- Zhu, Y., Knolhoff, B.L., Meyer, M.A., Nywening, T.M., West, B.L., Luo, J., Wang-Gillam, A., Goedegebuure, S.P., Linehan, D.C., and DeNardo, D.G. (2014). CSF1/CSF1R blockade reprograms tumor-infiltrating macrophages and improves response to T-cell checkpoint immunotherapy in pancreatic cancer models. *Cancer Res.* 74, 5057–5069.
- Zou, W., Wolchok, J.D., and Chen, L. (2016). PD-L1 (B7-H1) and PD-1 pathway blockade for cancer therapy: Mechanisms, response biomarkers, and combinations. *Sci. Transl. Med.* 8.

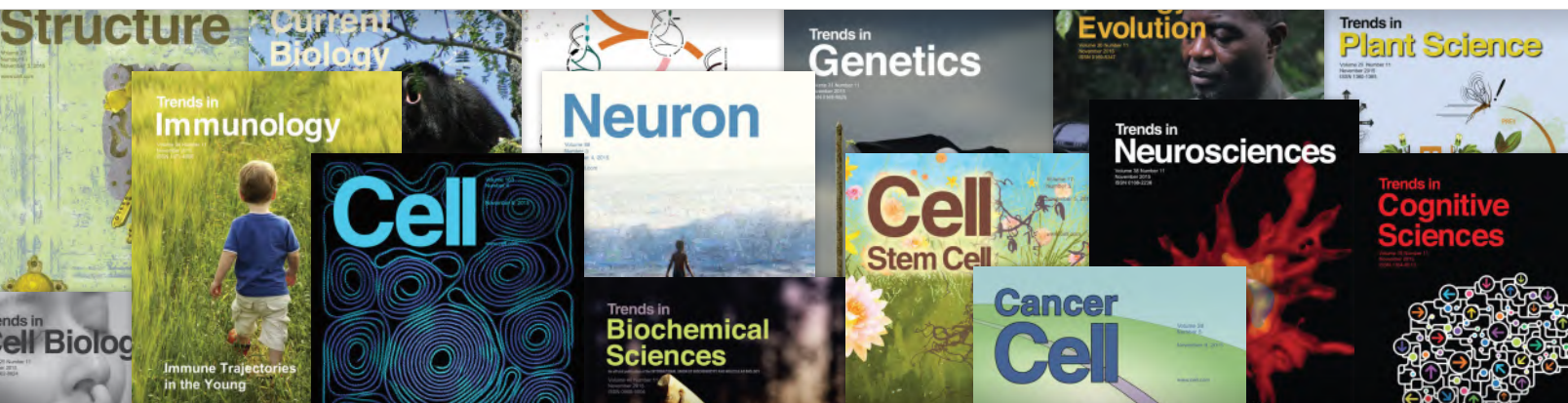


**DON'T BE THE
LAST TO KNOW**

Give your research a boost with alerts from Cell Press. You'll be glad you did.

Get first access with immediate, regular electronic table of contents (eToCs) alerts delivered directly to your desktop, free of charge, that keep you informed of breakthroughs in your field.

Exciting extra features like video abstracts, podcasts, and blog posts give you additional depth and context and you can access news and commentary, normally not accessible online, in advance of publication.



Register today
Visit cell.com/alerts

CellPress

Fc-Optimized Anti-CD25 Depletes Tumor-Infiltrating Regulatory T Cells and Synergizes with PD-1 Blockade to Eradicate Established Tumors

Frederick Arce Vargas,^{1,2,11} Andrew J.S. Furness,^{1,2,3,11} Isabelle Solomon,^{1,2} Kroopa Joshi,^{1,2,3} Leila Mekkaoui,⁴ Marta H. Lesko,^{1,2} Enrique Miranda Rota,⁴ Rony Dahan,⁵ Andrew Georgiou,^{1,2} Anna Sledzinska,^{1,2} Assma Ben Aissa,^{1,2} Dafne Franz,^{1,2} Mariana Werner Sunderland,^{1,2} Yien Ning Sophia Wong,^{1,2} Jake Y. Henry,^{1,2} Tim O'Brien,⁶ David Nicol,³ Ben Challacombe,⁶ Stephen A. Beers,⁷ Melanoma TRACERx Consortium, Renal TRACERx Consortium, Lung TRACERx Consortium, Samra Turajlic,^{3,8} Martin Gore,³ James Larkin,³ Charles Swanton,^{8,9} Kerry A. Chester,⁴ Martin Pule,² Jeffrey V. Ravetch,⁵ Teresa Marafioti,¹⁰ Karl S. Peggs,^{1,2,*} and Sergio A. Quezada^{1,2,12,*}

¹Cancer Immunology Unit, University College London Cancer Institute, London WC1E 6DD, UK

²Research Department of Haematology, UCL Cancer Institute, London WC1E 6DD, UK

³The Royal Marsden NHS Foundation Trust, London SW3 6JJ, UK

⁴Research Department of Oncology, UCL Cancer Institute, London WC1E 6DD, UK

⁵Leonard Wagner Laboratory of Molecular Genetics and Immunology, The Rockefeller University, New York, NY 10065, USA

⁶Guy's and St. Thomas' NHS Foundation Trust, London SE1 9RT, UK

⁷Antibody and Vaccine Group, Cancer Sciences Unit, University of Southampton, Faculty of Medicine, Southampton SO17 1BJ, UK

⁸The Francis Crick Institute, London NW1 1AT, UK

⁹Translational Cancer Therapeutics Laboratory, UCL Cancer Institute, London WC1E 6DD, UK

¹⁰Department of Cellular Pathology, University College London Hospital, London NW1 2BU, UK

¹¹These authors contributed equally

¹²Lead Contact

*Correspondence: k.peggs@ucl.ac.uk (K.S.P.), s.quezada@ucl.ac.uk (S.A.Q.)

<http://dx.doi.org/10.1016/j.immuni.2017.03.013>

SUMMARY

CD25 is expressed at high levels on regulatory T (Treg) cells and was initially proposed as a target for cancer immunotherapy. However, anti-CD25 antibodies have displayed limited activity against established tumors. We demonstrated that CD25 expression is largely restricted to tumor-infiltrating Treg cells in mice and humans. While existing anti-CD25 antibodies were observed to deplete Treg cells in the periphery, upregulation of the inhibitory Fc gamma receptor (Fc γ R) IIb at the tumor site prevented intra-tumoral Treg cell depletion, which may underlie the lack of anti-tumor activity previously observed in pre-clinical models. Use of an anti-CD25 antibody with enhanced binding to activating Fc γ Rs led to effective depletion of tumor-infiltrating Treg cells, increased effector to Treg cell ratios, and improved control of established tumors. Combination with anti-programmed cell death protein-1 antibodies promoted complete tumor rejection, demonstrating the relevance of CD25 as a therapeutic target and promising substrate for future combination approaches in immune-oncology.

INTRODUCTION

Regulatory T (Treg) cells are generally regarded as one of the major obstacles to the successful clinical application of tumor

immunotherapy. It has been consistently demonstrated that Treg cells contribute to the early establishment and progression of tumors in murine models and that their absence results in delay of tumor progression (Elpek et al., 2007; Golgher et al., 2002; Jones et al., 2002; Onizuka et al., 1999; Shimizu et al., 1999). In humans, high tumor infiltration by Treg cells and, more importantly, a low ratio of effector T (Teff) cells to Treg cells, is associated with poor outcomes in multiple solid cancers (Shang et al., 2015). Conversely, a high Teff/Treg cell ratio is associated with favorable responses to immunotherapy in both humans and mice (Hodi et al., 2008; Quezada et al., 2006). To date, most studies support the notion that targeting Treg cells, either by depletion or functional modulation, may offer significant therapeutic benefit, particularly in combination with other immune modulatory interventions such as vaccines and checkpoint blockade (Bos et al., 2013; Goding et al., 2013; Quezada et al., 2008; Suttmuller et al., 2001).

Defining appropriate targets for selective interference with Treg cells is therefore a critical step in the development of effective therapies. In this regard, CD25, also known as the interleukin-2 high-affinity receptor alpha chain (IL-2R α), was the first surface marker used to identify and isolate Treg cells (Sakaguchi et al., 1995) prior to the discovery of their master regulator, transcription factor forkhead box P3 (FoxP3). It is also the most extensively studied target for mediating Treg cell depletion. Whereas CD25 is constitutively expressed on Treg cells and absent on naive Teff cells, transient upregulation has been described upon activation of Teff cells, although these observations derive largely from *in vitro* studies (Boyman and Sprent, 2012).

A number of pre-clinical studies in mice have used the anti-CD25 antibody clone PC-61 (rat IgG1, λ), which partially depletes Treg cells in the blood and peripheral lymphoid organs (Setiady

et al., 2010), inhibits tumor growth, and improves survival when administered before or soon after tumor challenge (Golgher et al., 2002; Jones et al., 2002; Onizuka et al., 1999; Quezada et al., 2008; Shimizu et al., 1999). However, the use of anti-CD25 as a therapeutic intervention against established tumors fails to delay tumor growth or prolong survival (Golgher et al., 2002; Jones et al., 2002; Onizuka et al., 1999; Shimizu et al., 1999). This has been attributed to several factors, including poor T cell infiltration of the tumor (Quezada et al., 2008) and potential depletion of activated effector CD8⁺ and CD4⁺ T cells that upregulate CD25 (Onizuka et al., 1999). Early-phase clinical studies exploring the use of vaccines in combination with daclizumab (a humanized IgG1 anti-human CD25 antibody) (Jacobs et al., 2010; Rech et al., 2012) or denileukin difitox (a recombinant fusion protein combining human IL-2 and a fragment of diphtheria toxin) (Dannull et al., 2005; Luke et al., 2016) demonstrate a variable impact on the number of circulating Treg cells and vaccine-induced immunity. However, the limited indirect data assessing intra-tumoral FoxP3 transcript levels provide no clear evidence that Treg cells in the tumor microenvironment are effectively reduced and anti-tumor activity has appeared disappointing across all studies, with no demonstrable survival benefit.

The modest therapeutic activity in pre-clinical and clinical settings and concern regarding potential depletion of activated T cell subsets has contributed to limited enthusiasm for the further evaluation of anti-CD25 antibodies in combination with novel immunotherapies. However, recent data demonstrate the contribution of intra-tumoral Treg cell depletion to the activity of immune modulatory antibody-based therapies and the relevance of the antibody isotype in this setting (Bulliard et al., 2014; Coe et al., 2010; Selby et al., 2013; Simpson et al., 2013). We therefore re-evaluated CD25 as target for Treg cell depletion and tumor immunotherapy in vivo. We demonstrated that the lack of therapeutic activity of the widely used anti-CD25 antibody (PC-61) against established mouse tumors results from a failure to effectively deplete intra-tumoral Treg cells. Optimizing Fc γ R binding and antibody-dependent cell-mediated cytotoxicity (ADCC) resulted in superior intra-tumoral Treg cell depletion and potent synergy when combined with programmed cell death protein-1 (PD-1) blockade. We demonstrated high levels of CD25 expression on Treg but not T cell subsets in human tumors, highlighting this receptor as a clinical target and anti-CD25 as a promising therapeutic strategy in combination with novel immunotherapies.

RESULTS

CD25 Is Highly Expressed on Murine Tumor-Infiltrating Treg Cells

We sought to evaluate the relative expression of CD25 on individual T lymphocyte subsets within tumors (TILs) and draining lymph nodes (LNs) of mice 10 days after tumor challenge. CD25 expression appeared consistent across multiple models of transplantable tumor cell lines of variable immunogenicity including MCA205 sarcoma, MC38 colon adenocarcinoma, B16 melanoma, and CT26 colorectal carcinoma, with a higher percentage of CD25-expressing CD4⁺FoxP3⁺ Treg cells relative to CD4⁺FoxP3⁻ and CD8⁺ T cell subsets (Figure 1A). In contrast to in vitro studies, minimal expression of CD25 on the

T cell compartment was observed in vivo and the percentage of CD25-expressing T cell subsets (CD8⁺ = 3.08%–8.35%, CD4⁺FoxP3⁻ = 14.11%–26.87%) was significantly lower than on Treg cells (83.66%–90.23%) ($p < 0.001$) (Figure 1B). CD25 expression was also observed on Treg cells present in LNs and blood (data not shown). However, the level of expression, based on mean fluorescence intensity (MFI), was significantly lower than that observed on tumor-infiltrating Treg cells (Figure 1C). Based on these data, CD25 appeared an attractive target for preferential depletion of Treg cells.

Anti-CD25-Mediated Depletion of Treg Cells Is Limited to Lymph Nodes and Blood

Based on evidence demonstrating the contribution of intra-tumoral Treg cell depletion to the activity of immune modulatory antibodies (Bulliard et al., 2014; Coe et al., 2010; Selby et al., 2013; Simpson et al., 2013), we sought to compare the impact of anti-CD25 (clone PC-61 rat IgG1, α CD25-r1) on the frequency of T cell subsets in the blood, LNs, and TILs of mice with established tumors. We focused our analyses on the MCA205 model because of its higher immunogenicity in order to determine any potential negative impact of α CD25 on activated T cell subsets within tumors.

As previously described (Onizuka et al., 1999; Setiady et al., 2010), administration of 200 μ g of α CD25-r1 on days 5 and 7 after tumor challenge resulted in a reduced frequency of CD25⁺ cells in all analyzed sites (Figures 1D and 1E) and a reduction in the frequency of CD4⁺FoxP3⁺ Treg cells in blood and LN (Figure 1F). However, α CD25-r1 failed to deplete tumor-infiltrating Treg cells, which demonstrated a CD4⁺FoxP3⁺ CD25⁻ phenotype after therapy. Their frequency remained comparable to that of untreated mice (Figure 1F), potentially explaining the lack of efficacy observed against established tumors in previous studies despite an apparent reduction in CD25⁺ T cells within the tumor (Golgher et al., 2002; Jones et al., 2002; Onizuka et al., 1999; Quezada et al., 2008; Shimizu et al., 1999).

We next investigated whether an antibody with optimized ADCC activity could efficiently deplete intra-tumoral Treg cells without significant impact on T cell subsets. We replaced the constant regions of the original α CD25 obtained from clone PC-61 with murine IgG2a and κ constant regions (α CD25-m2a), the classical mouse isotype associated with ADCC, and compared its activity to that of α CD25-r1 in vivo. While both antibody variants resulted in reduced expression of CD25 on T cells and a reduction in the number of Treg cells in blood and LNs, only α CD25-m2a resulted in depletion of tumor-infiltrating Treg cells to levels comparable to those observed with anti-cytotoxic T lymphocyte associated protein-4 (α CTLA-4, clone 9H10), which is known to preferentially deplete Treg cells in the tumor but not the periphery (Figures 1D–1F; Selby et al., 2013; Simpson et al., 2013). In keeping with these observations, both α CD25 isotypes resulted in an increased T cell/Treg cell ratio in circulating lymphocytes and LN, but only α CD25-m2a increased the intra-tumoral ratio in a similar manner to α CTLA-4 (Figure 1G). Despite a reduction in the number of circulating and LN-resident Treg cells, no macroscopic, microscopic, or biochemical evidence of toxicity was observed in the skin, lungs, or liver after multiple doses of α CD25-m2a (Figures S1A–S1C).

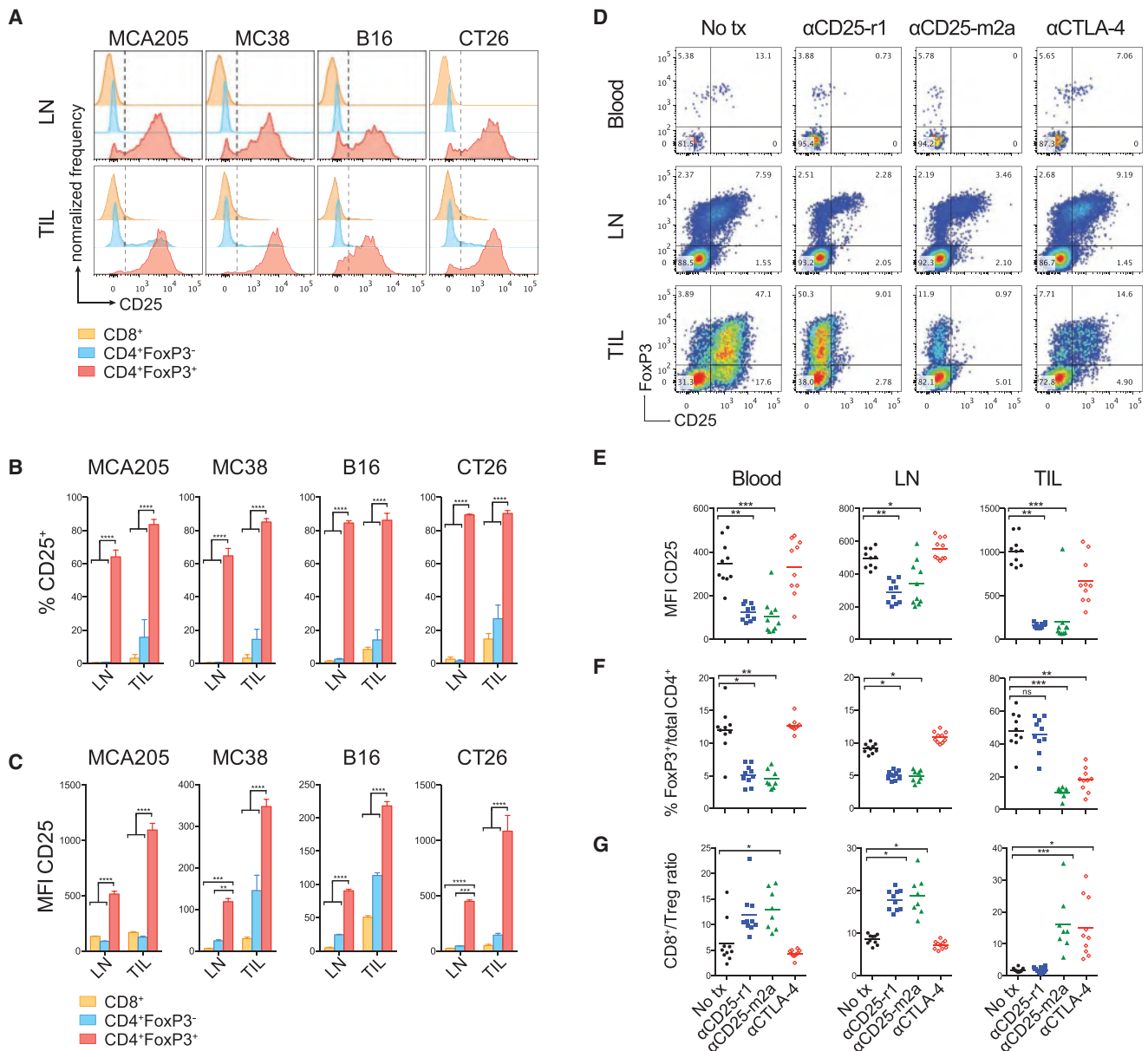


Figure 1. Anti-CD25-r1-Mediated Depletion of CD25⁺ Regulatory T Cells Is Restricted to Blood and Lymph Nodes

(A–C) Mouse LNs and TILs were analyzed by flow cytometry 10 days after MCA205 (n = 10), MC38 (n = 5), B16 (n = 3), or CT26 (n = 3) tumor implantation.

(A) CD25 expression on T cell subsets in representative mice. Dotted lines indicate the gate.

(B and C) Percentage (B) and MFI (C) of CD25 in each T cell subset. Error bars show standard error of the mean (SEM). p values obtained by two-way analysis of variance (ANOVA).

(D–G) Tumor-bearing mice were injected with 200 μ g of α CD25-r1, α CD25-m2a, or α CTLA-4 on days 5 and 7 after MCA205 tumor implantation. Blood, LNs, and TILs were harvested and processed on day 9 for flow cytometry analysis.

(D) Representative plots showing expression of CD25 (detected with antibody clone 7D4) and FoxP3 in CD3⁺CD4⁺ T cells. Numbers show percentage of cells in each quadrant.

(E) MFI of CD25 in CD4⁺FoxP3⁺ Treg cells.

(F) Percentage of FoxP3⁺ Treg cells of total CD3⁺CD4⁺ T cells.

(G) CD8⁺/Treg cell ratios (n = 10). Experiment was repeated three times.

High Expression of Fc γ R1b Inhibits α CD25-r1-Mediated Treg Cell Depletion in the Tumor

Anti-CD25-r1 has been described to deplete circulating Treg cells by Fc γ R1b-mediated ADCC (Setiady et al., 2010). However,

its intra-tumoral activity has not been investigated. To determine this, we characterized the expression of Fc-gamma receptors (Fc γ Rs) on different leukocyte subpopulations in the blood, spleen, LN, and tumor of mice bearing MCA205 tumors

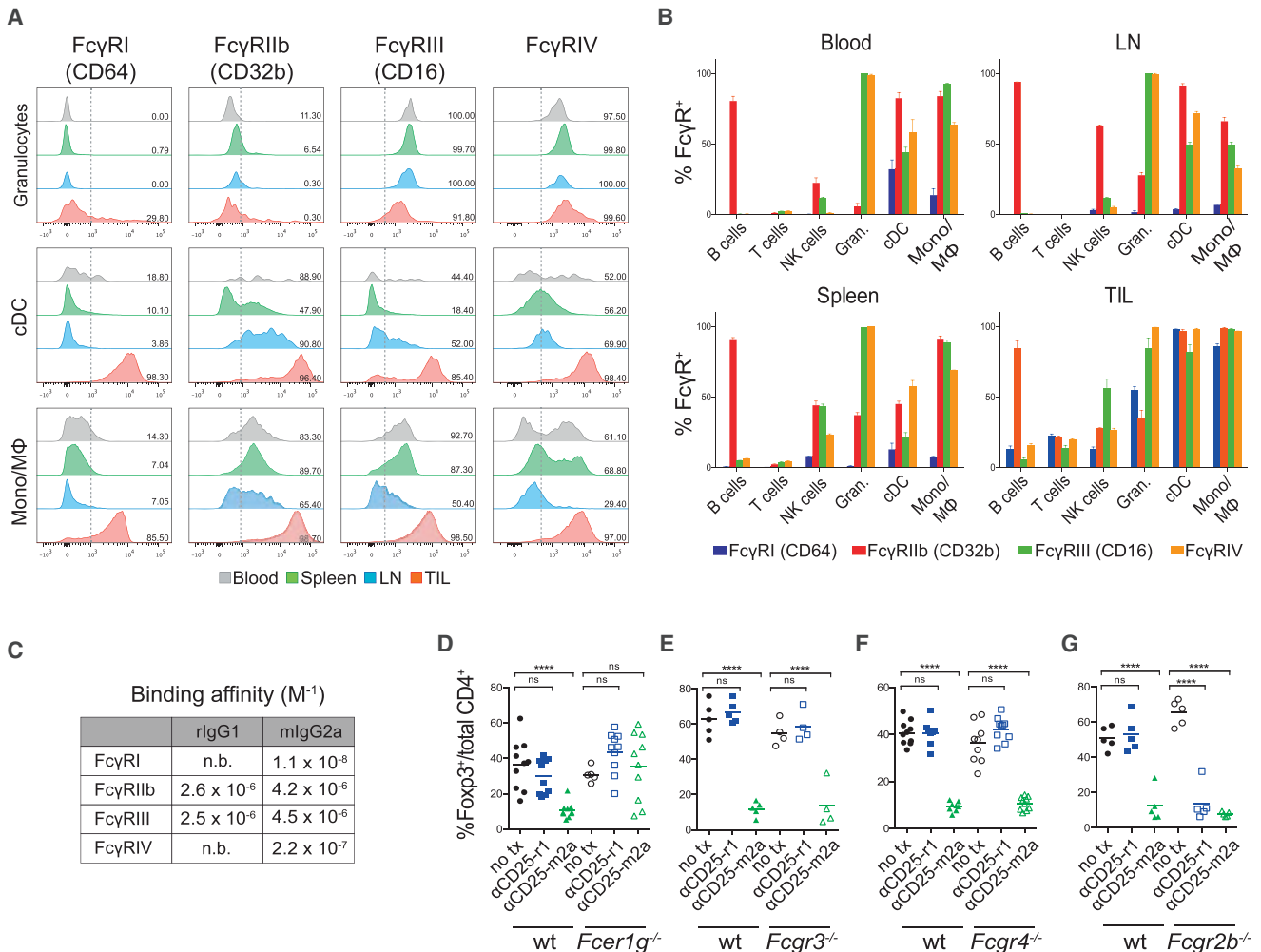


Figure 2. FcγRIIb Inhibits αCD25-r1-Mediated Treg Cell Depletion in Tumors

(A and B) Expression of FcγRs was measured by flow cytometry in leukocytes from blood, spleen, LNs, and MCA205 tumors (TIL) 10 days after tumor implantation.

(A) Expression of FcγRs on granulocytes (CD11b⁺Ly6G⁺), conventional dendritic cells (cDCs) (CD11c^{hi}MHC-II⁺), and monocyte/macrophages (Mono/Mφ) (CD11b⁺Ly6G[−]NK1.1[−]CD11c^{lo/neg}). Dotted lines indicate the gate, numbers show the percentage of positive cells.

(B) Cumulative data of FcγR expression in cell subpopulations (n = 3). Error bars represent SEM; the experiment was repeated three times.

(C) Binding affinity of rat IgG1 and mouse IgG2a isotypes to individual mouse FcγRs as determined by surface plasmon resonance (SPR).

(D–G) Percentage of CD4⁺FoxP3⁺ Treg cells of total CD4⁺ T cells in TILs of wild-type (WT, n = 5–10), *FcγRIIb*^{−/−} (n = 10), *FcγRIII*^{−/−} (n = 5), *FcγRIV*^{−/−} (n = 10), or *FcγRIIb*^{−/−} (n = 5) mice treated as in Figures 1D–1G.

(Figures 2A and S2). The percentage of FcγR-expressing cells appeared higher on tumor-infiltrating myeloid cells (granulocytic cells, dendritic cells, and monocyte/macrophages) relative to all other studied organs (Figures 2A and 2B). We then analyzed the binding affinity of the two Fc variants of αCD25 to FcγRs (Figure 2C). As previously described (Nimmerjahn and Ravetch, 2005), the mlgG2a isotype binds to all FcγR subtypes with a high activatory to inhibitory ratio (A/I). In contrast, the rlgG1 isotype binds with a similar affinity to a single activatory FcγR, FcγRIII, as well as the inhibitory FcγRIIb, resulting in a low A/I ratio (<1) (Figure 2C).

To determine which specific FcγRs were involved in αCD25-mediated Treg cell depletion, we quantified the number of tumor-infiltrating Treg cells in mice lacking expression of different

FcγRs (Figures 2D–2G). Analysis of *FcγRIIb*^{−/−} mice, which lack expression of activating FcγRs (I, III, and IV), demonstrated a complete absence of Treg cell depletion. Treg cell elimination by αCD25-r1 in the periphery and by αCD25-m2a in the periphery and tumor therefore results from FcγR-mediated ADCC and not blocking of IL-2 binding to CD25 (Figure 2D). Depletion by αCD25-m2a was not dependent on any individual activatory FcγR, with Treg cell elimination maintained in both *FcγRIII*^{−/−} and *FcγRIV*^{−/−} mice (Figures 2E and 2F). In keeping with previous studies (Setiady et al., 2010), we confirmed that depletion of peripheral Treg cells by αCD25-r1 depends on FcγRIII (data not shown), but it fails to deplete in the tumor despite high intra-tumoral expression of this receptor (Figure 2E). Intra-tumoral Treg cell depletion was, however, effectively restored in mice

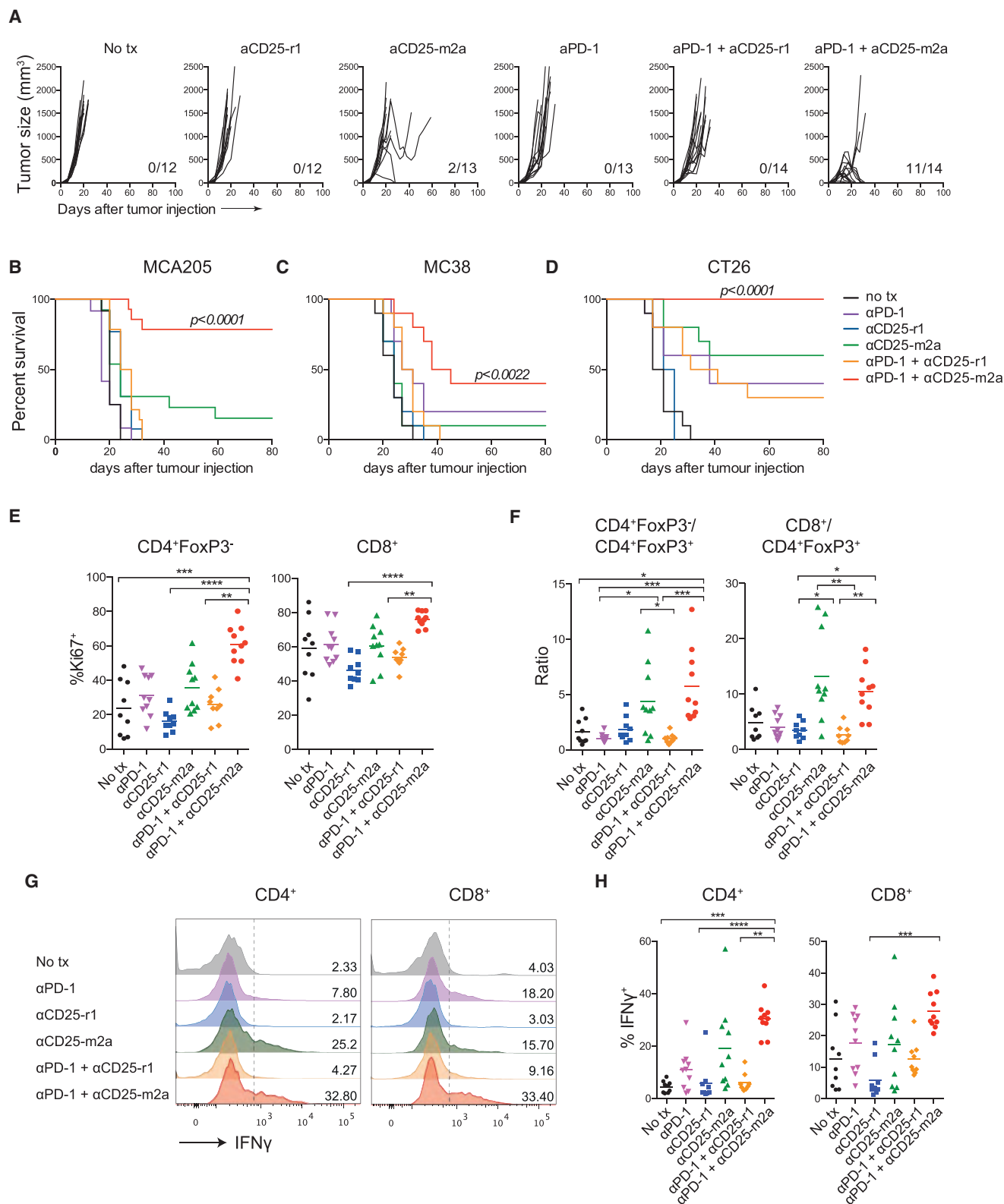


Figure 3. Synergistic Effect of Anti-CD25-m2a and Anti-PD-1 Combination Results in Eradication of Established Tumors

Tumor-bearing mice were treated with 200 μg of αCD25 on day 5 and 100 μg of αPD-1 on days 6, 9, and 12 after tumor implantation.

(A) Growth curves of individual MCA205 tumors, showing the product of three orthogonal tumor diameters. The number of tumor-free survivors is shown in each graph.

(legend continued on next page)

lacking expression of the inhibitory receptor Fc γ R11b. In this setting, intra-tumoral Treg cell depletion was comparable between α CD25-r1 and α CD25-m2a (Figure 2G). Therefore, the lack of Treg cell depletion by α CD25-r1 in the tumor is explained by its low A/I binding ratio and high intra-tumoral expression of Fc γ R11b. Fc γ R11b has been associated with modulation of ADCC in tumors (Clynes et al., 2000), and in this case inhibits ADCC mediated by the single activatory receptor engaged by the α CD25-r1 isotype.

Anti-CD25-m2a Synergizes with Anti-PD-1 to Eradicate Established Tumors

To determine whether the enhanced intra-tumoral Treg cell-depleting activity of α CD25-m2a could improve therapeutic outcomes, we compared the anti-tumor activity of α CD25-m2a and -r1 against established tumors. We administered a single dose of α CD25 5 days after subcutaneous implantation of MCA205 cells, when tumors were established with an average diameter of 4–5 mm. Consistent with the observed lack of capacity to deplete intra-tumoral Treg cells (Figure 1F) and previous studies (Golgher et al., 2002; Jones et al., 2002; Onizuka et al., 1999; Quezada et al., 2008; Shimizu et al., 1999), α CD25-r1 failed to control tumor growth. Conversely, growth delay and long-term survival was observed in a proportion of mice receiving α CD25-m2a (15.4%) (Figures 3A and 3B).

Based on its role in T cell regulation within the tumor microenvironment and the observed clinical activity of agents targeting the PD-1-PD-L1 axis, we hypothesized that depletion of CD25⁺ Treg cells and PD-1 blockade might be synergistic in combination. In the same model, blocking anti-PD-1 antibody (α PD-1, clone RMP1-14) at a dose of 100 μ g every 3 days was ineffective in the treatment of established MCA205 tumors when used as monotherapy or in combination with α CD25-r1 (Figures 3A and 3B). However, a single dose of α CD25-m2a followed by α PD-1 therapy eradicated established tumors in 78.6% of the mice, resulting in long-term survival of more than 100 days (Figures 3A and 3B). This activity was significantly reduced in the absence of CD8⁺ T cells (Figures S3A and S3B), demonstrating that tumor elimination depends on the impact of the α PD-1 and α CD25 combination on both CD8⁺ and Treg cell compartments, and that overall effector T cell responses are not negatively impacted by a depleting α CD25 antibody.

Similar findings were observed in MC38 and CT26 tumor models, where α CD25-m2a had a partial therapeutic effect that synergized with α PD-1 therapy (Figures 3C and 3D). Activity was also observed against the poorly immunogenic B16 melanoma tumor model when α CD25-m2a and α PD-1 were combined with a granulocyte-macrophage colony stimulating factor (GM-CSF)-expressing whole tumor cell vaccine (Gvax). As previously described, in this system, Gvax alone failed to extend survival of tumor-bearing mice (Quezada et al., 2006; van Elsas et al., 2001). Combination therapy

with α CD25-m2a and α PD-1 translated into a modest increase in survival, which was not observed with α CD25-r1 and α PD-1 (Figure S4).

To understand the mechanisms underpinning the observed synergy, we evaluated the phenotype and function of TILs in MCA205 tumors at the end of the treatment protocol, 24 hr after the third dose of α PD-1 (Figures 3E–3H). Monotherapy with α PD-1 did not impact upon Teff cell proliferation (Figure 3E) nor the number infiltrating the tumor, where a persisting high frequency of Treg cells was observed (data not shown), resulting in a low Teff/Treg ratio (Figure 3F) and lack of therapeutic activity. Conversely, intra-tumoral Treg cell depletion with α CD25-m2a resulted in a higher proportion of proliferating and interferon- γ (IFN- γ)-producing CD4⁺ and CD8⁺ T cells in the tumor, corresponding to a high Teff/Treg cell ratio and anti-tumor activity (Figures 3E–3H). This effect was further enhanced in combination with α PD-1, which yielded even higher proliferation and a 1.6-fold increase in the number of IFN- γ -producing CD4⁺ and CD8⁺ T cells compared to α CD25-m2a alone. In contrast, the observed lack of Treg cell depletion with α CD25-r1 resulted in no change in Teff cell proliferation or IFN- γ production, when used as monotherapy or in combination with α PD-1 (Figures 3E–3H). Combination of α CD25 and α PD-1 therefore appeared highly effective at rejecting established tumors, but only when intra-tumoral Treg cells were efficiently depleted by α CD25 of appropriate isotype.

CD25 Expression Profiles in Human Cancers Validate Its Use as Target for Therapeutic Treg Cell Depletion

To validate the translational value of CD25 as a target for Treg cell depletion, we analyzed the expression of CD25 on peripheral blood mononuclear cells (PBMCs) and TILs in patients with advanced melanoma, early-stage non-small cell lung carcinoma (NSCLC), and renal cell carcinoma (RCC) by flow cytometry and multiplex immunohistochemistry (IHC). Despite heterogeneity in clinical characteristics both within and between studied cohorts (Tables S1–S3), CD25 expression remained largely restricted to CD4⁺FoxP3⁺ Treg cells (mean % CD25⁺ = 54.8% of Treg, 7.5% of CD4⁺FoxP3⁻, and 1.9% of CD8⁺; $p < 0.0001$) (Figures 4A and 4B). Similar to murine models, the level of CD25 expression, as assessed by MFI, was significantly higher on CD4⁺FoxP3⁺ Treg cells relative to CD4⁺FoxP3⁻ and CD8⁺ T cells within all studied tumor subtypes (mean MFI Treg = 190.0, CD4⁺FoxP3⁺ = 34.5 and CD8⁺ = 17.9; $p < 0.0001$) (Figure 4C).

We further performed longitudinal assessment of CD25 expression in the context of immune modulation. Core biopsies were performed on the same lesion at baseline and after either four cycles of nivolumab (3 mg/kg Q2W) or two cycles of pembrolizumab (200 mg Q3W) in patients with advanced kidney cancer and melanoma, respectively (Table S4). Despite systemic immune modulation, CD25 expression remained restricted to

(B) Survival of mice shown in (A).

(C and D) Survival of mice with MC38 or CT26 tumors treated as described above ($n = 10$ per condition).

(E) Percentage of Ki67⁺ cells in tumor-infiltrating CD4⁺FoxP3⁻ and CD8⁺ T cells.

(F) CD4⁺FoxP3⁻/CD4⁺FoxP3⁺ and CD8⁺/CD4⁺FoxP3⁺ cell ratios.

(G and H) Representative histograms (G) and percentage (H) of IFN- γ -producing CD4⁺ and CD8⁺ TILs in MCA205 tumors determined by intracellular staining after ex vivo re-stimulation with PMA and ionomycin. Graphs show cumulative data of two separate experiments ($n = 10$).

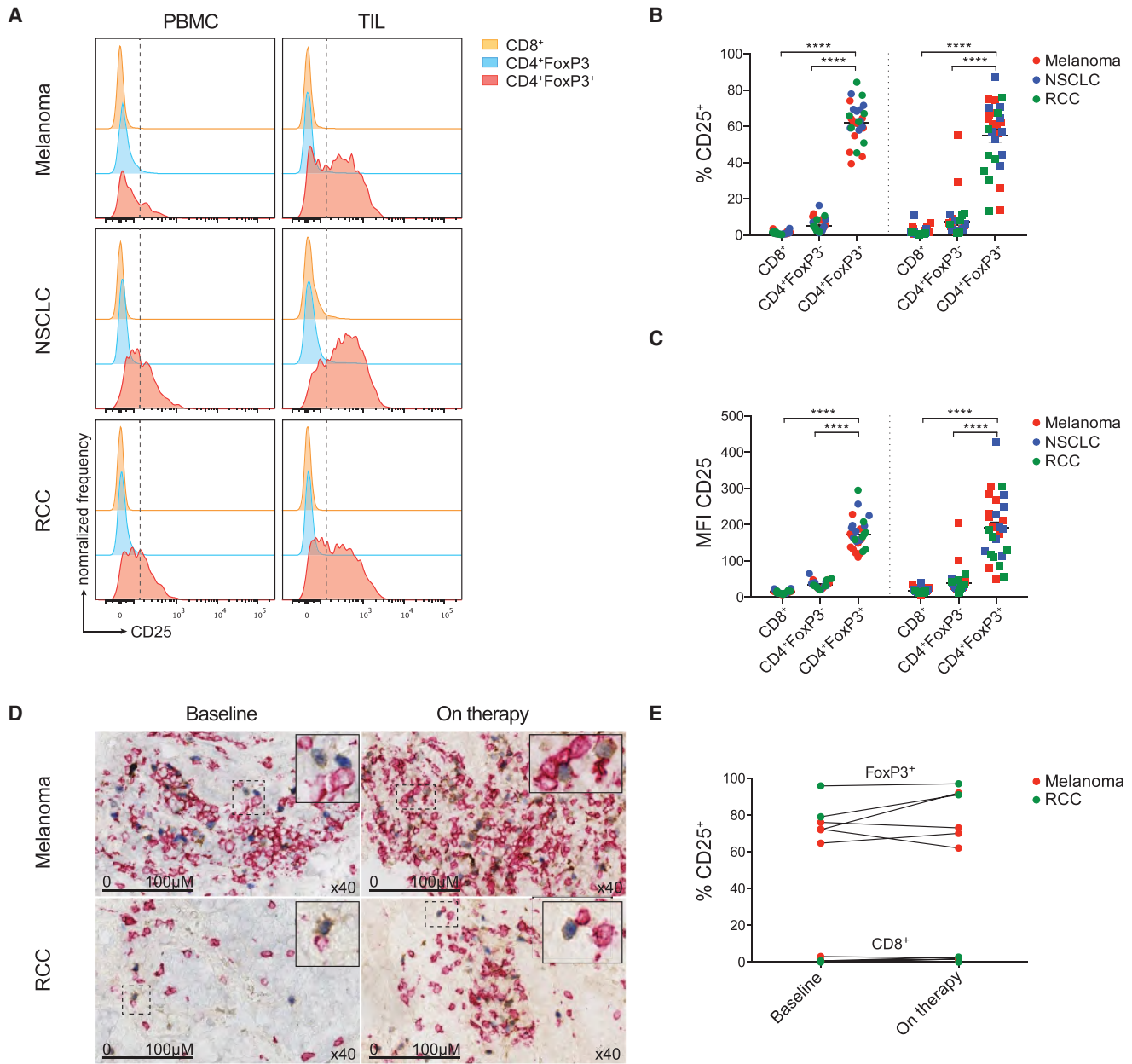


Figure 4. CD25 Is Highly Expressed on Treg Cell Infiltrating Human Tumors

(A) Representative histograms demonstrating CD25 expression on circulating (PBMC) and tumor-infiltrating (TIL) CD8⁺, CD4⁺FoxP3⁻, and CD4⁺FoxP3⁺ T cell subsets. Dotted lines indicate the gate.

(B and C) Quantification of CD25 expression (percentage [B] and MFI [C]) on individual T cell subsets in human melanoma (n = 11), NSCLC (n = 9), and RCC (n = 8). Error bars represent SEM; p values obtained by two-way ANOVA.

(D) Longitudinal analysis of CD25 expression in human melanoma and RCC lesions prior to ("Baseline") and during PD-1 blockade ("On therapy"). CD8 staining is displayed in red, FoxP3 in blue, and CD25 in brown.

(E) Percentage of CD25 expression on CD8⁺ and FoxP3⁺ T cells at baseline and during PD-1 blockade. Plotted values derive from analysis of 10 × 40 high-power fields per patient at each time point.

FoxP3⁺ Treg cells, even in areas of dense CD8⁺ T cell infiltrate evaluated by multiplex immunohistochemistry (Figures 4D and 4E). These findings confirmed the translational value of the described pre-clinical data, lending further support to the concept of selective therapeutic targeting of Treg cells via CD25 in human cancers.

DISCUSSION

We have demonstrated that CD25 is an attractive target for Treg cell depletion owing to its expression profile on tumor-infiltrating T cells in both mice and humans. Contrary to *in vitro* studies, minimal expression of CD25 on the effector

compartment was observed *in vivo*. The efficacy of α CD25 as an anti-tumor therapy depends on Treg cell depletion in the tumor microenvironment, which can be achieved only by using an antibody isotype optimized for engagement of activating Fc γ Rs, capable of inducing ADCC. Our results demonstrated that the limited efficacy observed in pre-clinical studies using the α CD25 PC-61 monoclonal antibody with a rat IgG1 isotype relates to ineffective or suboptimal intra-tumoral Treg cell depletion, a consequence of its low A/I binding ratio and high intra-tumoral expression of inhibitory Fc γ R11b. This may also explain the modest results observed in early clinical trials using the anti-human CD25 antibody daclizumab. However, the impact of α CD25 antibodies of varying IgG subclass remains to be evaluated in humans.

Local depletion of tumor-infiltrating Treg cells by α CD25 monotherapy mediated only partial tumor control, suggesting that further intervention is necessary to increase the intra-tumoral Teff/Treg cell balance and promote effector T cell activity. These data mirror those previously demonstrated for α CTLA-4 antibodies, where targeting solely the Treg cell compartment was ineffective in eradicating established tumors, while targeting both Treg and Teff cell compartments resulted in effective therapeutic synergy (Peggs et al., 2009). Increased regulation of Teff cell responses by co-inhibitory immune checkpoints in the tumor microenvironment might also explain the modest responses observed in early-stage clinical trials evaluating α CD25 antibodies in cancer patients (Jacobs et al., 2010; Rech et al., 2012). Our data suggest that such responses could be enhanced through combination with therapies that address this regulation including immune checkpoint blockade or agonistic antibodies targeting immune co-stimulatory receptors.

Treg cell depletion can be achieved by targeting other molecules highly expressed on Treg cells (Bulliard et al., 2014; Coe et al., 2010; Selby et al., 2013; Simpson et al., 2013). While combined blocking and depleting activity of specific immune modulatory antibodies is effective against certain target molecules, such as CTLA-4, it can also be deleterious owing to simultaneous high expression on Teff cells. Differential expression is therefore critical; for example, in addition to its expression on Treg cells, PD-1 is highly expressed on activated CD8⁺ T cells. Anti-PD-1 antibodies therefore lose anti-tumor activity when a depleting antibody isotype is employed (Dahan et al., 2015).

Anti-PD-1 therapy now forms a key part of the treatment paradigm for multiple solid malignancies, with response rates varying between 20% and 30% when used as monotherapy (Topalian et al., 2015). However, the majority of responses are partial. This could be explained in part by tumor infiltration with CD25⁺FoxP3⁺ Treg cells that are unaffected by non-depleting α PD-1 antibodies. In this setting another target molecule specific to Treg cells is required in order to achieve potential synergy through Treg cell depletion. Combination of α CTLA-4 and α PD-1 therapy has achieved superior response rates to either agent alone in patients with advanced melanoma (Larkin et al., 2015). This may be the result of the cell-intrinsic immune modulatory activity of α CTLA-4 and α PD-1 antibodies and concomitant depletion of Treg cells by α CTLA-4, although this second activity has not been demonstrated *in vivo*. Combi-

nation therapy results in higher immune-related toxicity, underscoring the need for alternative combinations balancing maximal activity with minimal toxicity. We have demonstrated that α CD25 therapy synergizes with blocking α PD-1 therapy, provided Treg cells are depleted locally in the tumor. Combining α PD-1 with α CD25-depleting antibodies might improve the therapeutic window compared to the α CTLA-4 combination, as α CD25 lacks the additional cell-intrinsic immune modulatory activity of α CTLA-4. Such hypotheses are further supported by our model, in which only transient Treg cell depletion was required for effective synergy, with no evidence of immune-related toxicity. These data support further evaluation of Fc-optimized α CD25 as a combination partner in clinical trials.

EXPERIMENTAL PROCEDURES

Antibodies and Antibody Production

The sequence of the variable regions of the heavy and light chains of α CD25 were resolved from the PC-61.5.3 hybridoma by rapid amplification of cDNA ends (RACE), cloned into the constant regions of murine IgG2a and κ chains and expressed in a stable K562 cell line generated by co-transduction with murine leukemia virus-derived retroviral vectors encoding both chains. The antibody was initially purified from supernatants with a protein G HiTrap MabSelect column (GE Healthcare), dialyzed in phosphate-buffered saline (PBS), concentrated, and filter-sterilized. For subsequent experiments, antibody production was outsourced to Evitria AG. Anti-CD25-r1 (PC-61.5.3), α CTLA-4 (9H10), α PD-1 (RMP1-14), and α CD8 (2.43) were supplied by BioXcell. The binding affinity of isotype variants to Fc γ Rs was measured by SPR in the Ravetch laboratory as described before (Nimmerjahn and Ravetch, 2005).

Tumor Experiments

Details of mouse strains, cell lines and flow cytometry antibodies are shown in Supplemental Experimental Procedures. Mice were injected subcutaneously with 5×10^5 MCA205, MC38, or CT26 cells or 5×10^4 B16 cells re-suspended in PBS. Therapeutic antibodies were administered intraperitoneally at the time points and doses shown in figure legends. Cell suspensions for flow cytometry were prepared as described previously (Simpson et al., 2013). Tumors were measured twice weekly and mice were euthanized when any orthogonal tumor diameter reached 150 mm.

Human Study Oversight

Human data derives from three translational studies approved by local institutional review board and Research Ethics Committee (Melanoma, REC no. 11/LO/0003; NSCLC, REC no.13/LO/1546; RCC, REC no. 11/LO/1996). All were conducted in accordance with the provisions of the Declaration of Helsinki and with Good Clinical Practice guidelines as defined by the International Conference on Harmonization. All patients (or their legal representatives) provided written informed consent before enrollment.

Analysis of Human Tissue

For flow cytometry, cell suspensions were prepared with the same protocol employed for mouse tissues (Simpson et al., 2013). Leukocytes were enriched by gradient centrifugation with Ficoll-paque (GE Healthcare). Isolated live cells were frozen at -80°C and stored in liquid nitrogen until analysis.

Histopathology protocols are described in Supplemental Experimental Procedures.

Data Analysis

Flow cytometry data were analyzed with FlowJo v10.0.8 (Tree Star). Statistical analyses were done with Prism 6 (GraphPad Software); p values were calculated using Kruskal-Wallis and Dunn's post hoc tests, unless otherwise indicated (ns = $p > 0.05$; * $p \leq 0.05$; ** $p \leq 0.01$; *** $p \leq 0.001$; **** $p \leq 0.0001$). Kaplan-Meier curves were analyzed with the log-rank test.

SUPPLEMENTAL INFORMATION

Supplemental Information includes four figures, four tables, Supplemental Experimental Procedures, and consortia memberships and can be found with this article online at <http://dx.doi.org/10.1016/j.immuni.2017.03.013>.

AUTHOR CONTRIBUTIONS

S.A.Q. and K.S.P. conceived the project. F.A.V., A.J.S.F., K.S.P., and S.A.Q. designed the experiments, analyzed the data, and wrote the manuscript. F.A.V. and A.J.S.F. performed the experiments. I.S., K.J., L.M., M.H.L., A.G., A.S., A.B.A., D.F., M.W.S., Y.N.S.W., and J.Y.H. contributed experimentally. E.M.R., R.D., S.A.B., K.A.C., M.P., and J.V.R. provided reagents and contributed scientifically. T.M. performed the histology analyses. T.O., D.N., B.C., S.T., M.G., J.L., C.S., and the TRACERx consortia coordinated clinical trials and provided patient samples.

ACKNOWLEDGMENTS

We thank Josep Linares for his technical expertise. S.A.Q. is a Cancer Research U.K. (CRUK) Senior Fellow (C36463/A22246) and is funded by a Cancer Research Institute Investigator Award and a CRUK Biotherapeutic Program Grant (C36463/A20764). K.S.P. receives funding from the NIHR BTRU for Stem Cells and Immunotherapies (167097), of which he is the Scientific Director. None of the animal work described was funded by NIHR. This work was undertaken at UCL Hospitals/UCL with support from the CRUK-UCL Centre (C416/A18088), CRUK's Lung Cancer Centre of Excellence (C5759/A20465), the CRUK and Engineering and Physical Sciences Research Council at King's College London and UCL (C1519/A16463), the Cancer Immunotherapy Accelerator Award (CITA-CRUK) (C33499/A20265), CRUK's Lung TRACERx study (led by C. Swanton) (C11496/A17786), the Sam Keen Foundation/RMH NIHR Biomedical Research Centre, Bloodwise (formerly Leukaemia and Lymphoma Research) (08022/P4664), the Department of Health, and CRUK funding schemes for National Institute for Health Research Biomedical Research Centres and Experimental Cancer Medicine Centres.

Received: August 27, 2016

Revised: January 26, 2017

Accepted: February 9, 2017

Published: April 11, 2017

REFERENCES

- Bos, P.D., Plitas, G., Rudra, D., Lee, S.Y., and Rudensky, A.Y. (2013). Transient regulatory T cell ablation deters oncogene-driven breast cancer and enhances radiotherapy. *J. Exp. Med.* **210**, 2435–2466.
- Boyman, O., and Sprent, J. (2012). The role of interleukin-2 during homeostasis and activation of the immune system. *Nat. Rev. Immunol.* **12**, 180–190.
- Bulliard, Y., Jolicoeur, R., Zhang, J., Dranoff, G., Wilson, N.S., and Brogdon, J.L. (2014). OX40 engagement depletes intratumoral Tregs via activating Fc γ Rs, leading to antitumor efficacy. *Immunol. Cell Biol.* **92**, 475–480.
- Clynes, R.A., Towers, T.L., Presta, L.G., and Ravetch, J.V. (2000). Inhibitory Fc receptors modulate in vivo cytotoxicity against tumor targets. *Nat. Med.* **6**, 443–446.
- Coe, D., Begom, S., Addey, C., White, M., Dyson, J., and Chai, J.G. (2010). Depletion of regulatory T cells by anti-GITR mAb as a novel mechanism for cancer immunotherapy. *Cancer Immunol. Immunother.* **59**, 1367–1377.
- Dahan, R., Sega, E., Engelhardt, J., Selby, M., Korman, A.J., and Ravetch, J.V. (2015). Fc γ Rs modulate the anti-tumor activity of antibodies targeting the PD-1/PD-L1 axis. *Cancer Cell* **28**, 285–295.
- Dannull, J., Su, Z., Rizzieri, D., Yang, B.K., Coleman, D., Yancey, D., Zhang, A., Dahm, P., Chao, N., Gilboa, E., and Vieweg, J. (2005). Enhancement of vaccine-mediated antitumor immunity in cancer patients after depletion of regulatory T cells. *J. Clin. Invest.* **115**, 3623–3633.
- Elpek, K.G., Lacelle, C., Singh, N.P., Yolcu, E.S., and Shirwan, H. (2007). CD4+CD25+ T regulatory cells dominate multiple immune evasion mechanisms in early but not late phases of tumor development in a B cell lymphoma model. *J. Immunol.* **178**, 6840–6848.
- Goding, S.R., Wilson, K.A., Xie, Y., Harris, K.M., Baxi, A., Akpınarlı, A., Fulton, A., Tamada, K., Strome, S.E., and Antony, P.A. (2013). Restoring immune function of tumor-specific CD4+ T cells during recurrence of melanoma. *J. Immunol.* **190**, 4899–4909.
- Golgher, D., Jones, E., Powrie, F., Elliott, T., and Gallimore, A. (2002). Depletion of CD25+ regulatory cells uncovers immune responses to shared murine tumor rejection antigens. *Eur. J. Immunol.* **32**, 3267–3275.
- Hodi, F.S., Butler, M., Oble, D.A., Seiden, M.V., Haluska, F.G., Kruse, A., Macrae, S., Nelson, M., Canning, C., Lowy, I., et al. (2008). Immunologic and clinical effects of antibody blockade of cytotoxic T lymphocyte-associated antigen 4 in previously vaccinated cancer patients. *Proc. Natl. Acad. Sci. USA* **105**, 3005–3010.
- Jacobs, J.F.M., Punt, C.J.A., Lesterhuis, W.J., Suttmuller, R.P.M., Brouwer, H.M.-L.H., Scharenborg, N.M., Klasen, I.S., Hilbrands, L.B., Figdor, C.G., de Vries, I.J.M., and Adema, G.J. (2010). Dendritic cell vaccination in combination with anti-CD25 monoclonal antibody treatment: a phase I/II study in metastatic melanoma patients. *Clin. Cancer Res.* **16**, 5067–5078.
- Jones, E., Dahm-Vicker, M., Simon, A.K., Green, A., Powrie, F., Cerundolo, V., and Gallimore, A. (2002). Depletion of CD25+ regulatory cells results in suppression of melanoma growth and induction of autoreactivity in mice. *Cancer Immunol.* **2**, 1.
- Larkin, J., Chiarion-Sileni, V., Gonzalez, R., Grob, J.J., Cowey, C.L., Lao, C.D., Schadendorf, D., Dummer, R., Smylie, M., Rutkowski, P., et al. (2015). Combined nivolumab and ipilimumab or monotherapy in untreated melanoma. *N. Engl. J. Med.* **373**, 23–34.
- Luke, J.J., Zha, Y., Matijevich, K., and Gajewski, T.F. (2016). Single dose denileukin difitox does not enhance vaccine-induced T cell responses or effectively deplete Tregs in advanced melanoma: immune monitoring and clinical results of a randomized phase II trial. *J. Immunother. Cancer* **4**, 35.
- Nimmerjahn, F., and Ravetch, J.V. (2005). Divergent immunoglobulin g subclass activity through selective Fc receptor binding. *Science* **310**, 1510–1512.
- Onizuka, S., Tawara, I., Shimizu, J., Sakaguchi, S., Fujita, T., and Nakayama, E. (1999). Tumor rejection by in vivo administration of anti-CD25 (interleukin-2 receptor alpha) monoclonal antibody. *Cancer Res.* **59**, 3128–3133.
- Peggs, K.S., Quezada, S.A., Chambers, C.A., Korman, A.J., and Allison, J.P. (2009). Blockade of CTLA-4 on both effector and regulatory T cell compartments contributes to the antitumor activity of anti-CTLA-4 antibodies. *J. Exp. Med.* **206**, 1717–1725.
- Quezada, S.A., Peggs, K.S., Curran, M.A., and Allison, J.P. (2006). CTLA4 blockade and GM-CSF combination immunotherapy alters the intratumor balance of effector and regulatory T cells. *J. Clin. Invest.* **116**, 1935–1945.
- Quezada, S.A., Peggs, K.S., Simpson, T.R., Shen, Y., Littman, D.R., and Allison, J.P. (2008). Limited tumor infiltration by activated T effector cells restricts the therapeutic activity of regulatory T cell depletion against established melanoma. *J. Exp. Med.* **205**, 2125–2138.
- Rech, A.J., Mick, R., Martin, S., Recio, A., Aqui, N.A., Powell, D.J., Jr., Colligon, T.A., Trosko, J.A., Leinbach, L.I., Pletcher, C.H., et al. (2012). CD25 blockade depletes and selectively reprograms regulatory T cells in concert with immunotherapy in cancer patients. *Sci. Transl. Med.* **4**, 134a62.
- Sakaguchi, S., Sakaguchi, N., Asano, M., Itoh, M., and Toda, M. (1995). Immunologic self-tolerance maintained by activated T cells expressing IL-2 receptor alpha-chains (CD25). Breakdown of a single mechanism of self-tolerance causes various autoimmune diseases. *J. Immunol.* **155**, 1151–1164.
- Selby, M.J., Engelhardt, J.J., Quigley, M., Henning, K.A., Chen, T., Srinivasan, M., and Korman, A.J. (2013). Anti-CTLA-4 antibodies of IgG2a isotype enhance antitumor activity through reduction of intratumoral regulatory T cells. *Cancer Immunol. Res.* **1**, 32–42.
- Setiady, Y.Y., Coccia, J.A., and Park, P.U. (2010). In vivo depletion of CD4+FOXP3+ Treg cells by the PC61 anti-CD25 monoclonal antibody is mediated by Fc γ RIII+ phagocytes. *Eur. J. Immunol.* **40**, 780–786.

- Shang, B., Liu, Y., Jiang, S.J., and Liu, Y. (2015). Prognostic value of tumor-infiltrating FoxP3+ regulatory T cells in cancers: a systematic review and meta-analysis. *Sci. Rep.* 5, 15179.
- Shimizu, J., Yamazaki, S., and Sakaguchi, S. (1999). Induction of tumor immunity by removing CD25+CD4+ T cells: a common basis between tumor immunity and autoimmunity. *J. Immunol.* 163, 5211–5218.
- Simpson, T.R., Li, F., Montalvo-Ortiz, W., Sepulveda, M.A., Bergerhoff, K., Arce, F., Roddie, C., Henry, J.Y., Yagita, H., Wolchok, J.D., et al. (2013). Fc-dependent depletion of tumor-infiltrating regulatory T cells co-defines the efficacy of anti-CTLA-4 therapy against melanoma. *J. Exp. Med.* 210, 1695–1710.
- Sutmuller, R.P., van Duivenvoorde, L.M., van Elsas, A., Schumacher, T.N., Wildenberg, M.E., Allison, J.P., Toes, R.E., Offringa, R., and Melief, C.J. (2001). Synergism of cytotoxic T lymphocyte-associated antigen 4 blockade and depletion of CD25(+) regulatory T cells in antitumor therapy reveals alternative pathways for suppression of autoreactive cytotoxic T lymphocyte responses. *J. Exp. Med.* 194, 823–832.
- Topalian, S.L., Drake, C.G., and Pardoll, D.M. (2015). Immune checkpoint blockade: a common denominator approach to cancer therapy. *Cancer Cell* 27, 450–461.
- van Elsas, A., Sutmuller, R.P., Hurwitz, A.A., Ziskin, J., Villasenor, J., Medema, J.P., Overwijk, W.W., Restifo, N.P., Melief, C.J., Offringa, R., and Allison, J.P. (2001). Elucidating the autoimmune and antitumor effector mechanisms of a treatment based on cytotoxic T lymphocyte antigen-4 blockade in combination with a B16 melanoma vaccine: comparison of prophylaxis and therapy. *J. Exp. Med.* 194, 481–489.

Immunogenic Chemotherapy Sensitizes Tumors to Checkpoint Blockade Therapy

Christina Pfirschke,^{1,7} Camilla Engblom,^{1,2,7} Steffen Rickelt,³ Virna Cortez-Retamozo,¹ Christopher Garris,^{1,2} Ferdinando Pucci,¹ Takahiro Yamazaki,⁴ Vichnou Poirier-Colame,⁴ Andita Newton,¹ Younes Redouane,¹ Yi-Jang Lin,¹ Gregory Wojtkiewicz,¹ Yoshiko Iwamoto,¹ Mari Mino-Kenudson,⁵ Tiffany G. Huynh,⁵ Richard O. Hynes,³ Gordon J. Freeman,⁶ Guido Kroemer,⁴ Laurence Zitvogel,⁴ Ralph Weissleder,¹ and Mikael J. Pittet^{1,*}

¹Center for Systems Biology, Massachusetts General Hospital Research Institute and Harvard Medical School, Boston, MA 02114, USA

²Graduate Program in Immunology, Harvard Medical School, Boston, MA 02115, USA

³Koch Institute for Integrative Cancer Research, Massachusetts Institute of Technology, Cambridge, MA 02139, USA

⁴Gustave Roussy Cancer Campus, 94805 Villejuif, France

⁵Department of Pathology, Massachusetts General Hospital, Boston, MA 02114, USA

⁶Department of Medical Oncology, Dana-Farber Cancer Institute, Harvard Medical School, Boston, MA 02115, USA

⁷Co-first author

*Correspondence: mpittet@mgh.harvard.edu

<http://dx.doi.org/10.1016/j.immuni.2015.11.024>

SUMMARY

Checkpoint blockade immunotherapies can be extraordinarily effective, but might benefit only the minority of patients whose tumors are pre-infiltrated by T cells. Here, using lung adenocarcinoma mouse models, including genetic models, we show that autochthonous tumors that lacked T cell infiltration and resisted current treatment options could be successfully sensitized to host antitumor T cell immunity when appropriately selected immunogenic drugs (e.g., oxaliplatin combined with cyclophosphamide for treatment against tumors expressing oncogenic *Kras* and lacking *Trp53*) were used. The antitumor response was triggered by direct drug actions on tumor cells, relied on innate immune sensing through toll-like receptor 4 signaling, and ultimately depended on CD8⁺ T cell antitumor immunity. Furthermore, instigating tumor infiltration by T cells sensitized tumors to checkpoint inhibition and controlled cancer durably. These findings indicate that the proportion of cancers responding to checkpoint therapy can be feasibly and substantially expanded by combining checkpoint blockade with immunogenic drugs.

INTRODUCTION

The ability of the immune system to control tumor cells was proposed more than a century ago, demonstrated during the last decade, and recently harnessed for therapy (Sharma and Allison, 2015; Topalian et al., 2015). A foundational principle of tumor immunology is that cancer cells can be eliminated by host cytotoxic CD8⁺ T cells (Schreiber et al., 2011; Gajewski et al., 2013; Schumacher and Schreiber, 2015; Rooney et al., 2015). Accordingly, CD8⁺ T cell infiltration of various solid tumor types has pos-

itive prognostic value (Fridman et al., 2012), although these cells can be subject to various suppressive mechanisms including inhibition by regulatory T (Treg) cells and induced expression of programmed death-1 (PD-1) and other inhibitory checkpoint receptors, all limiting the antitumor functions of lymphocytes (Sharma and Allison, 2015; Topalian et al., 2015).

Therapies targeting T cell inhibitory checkpoint signaling pathways are redefining cancer therapy because clinical trials show unprecedented rates of durable responses in patients with common cancer types, including lung adenocarcinoma (Topalian et al., 2015). Lung adenocarcinoma was long considered to be nonimmunogenic and is the leading cause of cancer incidence and mortality worldwide, with more than one million deaths per year (Torre et al., 2015). Yet, only a minority of cancer patients respond to checkpoint inhibition and evidence suggests that those patients might preferentially have tumors that have favorable mutational landscapes, express the PD-1 ligand (PD-L1), and/or contain pre-existing tumor-infiltrating CD8⁺ T cells that are inhibited locally, e.g., by PD-1 engagement (Tumeh et al., 2014; Sharma and Allison, 2015; Rizvi et al., 2015; Schumacher and Schreiber, 2015; Herbst et al., 2014; Topalian et al., 2012, 2015). In order to define the proportion of patients who could ultimately benefit from immunotherapies, it appears important to clarify whether strategies can be employed for converting tumor microenvironments lacking T cell infiltration to ones displaying antitumor T cell immunity and then to determine whether this process sensitizes tumors to checkpoint therapy.

One approach to achieving this goal might involve the induction of immunogenic conditions in the tumor microenvironment. For example, some chemotherapeutics and other treatments shape clinical outcome by influencing tumor-host interactions to stimulate T cell immunosurveillance (Zitvogel et al., 2013; Klug et al., 2013; Shalapour et al., 2015). The drugs prescribed today against lung adenocarcinomas increase survival only marginally. Despite their low success rate, these drugs deserve re-consideration for several reasons, especially when combined with immunotherapy: (1) they were originally selected for their capacity to prevent human tumor cell growth in vitro and in

xenotransplanted immunodeficient mouse models without considering the relevance of immune reactions to treatment outcomes; (2) they are generally given indiscriminately even though their impact might vary across individuals and tumor microenvironments; and (3) improved understanding of drug effects *in vivo* might help identify synergistic treatment options.

To address these knowledge gaps, we explored conditional genetic lung adenocarcinoma models (with *Kras* and *Trp53* mutations, referred to as KP), in addition to orthotopic KP lung tumor models. In the genetic models, cancer cells are derived from somatic cells that are transformed in their normal tissue microenvironment and progress to high-grade tumors that lack T cell infiltration and resist prescribed chemo- and immunotherapeutic treatments. These models can also be used to study autochthonous tumors that express model neoantigens, which are important drivers of antitumor T cell immunity (Gubin et al., 2014; Rooney et al., 2015) and targets of checkpoint blockade therapy (Schumacher and Schreiber, 2015). The genetic tumor models we used for this study also avoid the inherent limitations of tumor grafts, including sensitivity to numerous chemotherapeutic agents (Olive et al., 2009).

Here we identified that a combination of clinically approved chemotherapeutic drugs (oxaliplatin-cyclophosphamide [Oxa-Cyc]) elicited immunogenic phenotypes on KP tumor cells. We also found that Oxa-Cyc treatment fostered CD8⁺ T cell infiltration into KP tumors and delayed cancer progression. Tumor control depended on direct drug actions on tumor cells and required both CD8⁺ T cells and TLR4⁺ cells. Importantly, the immunogenic chemotherapeutics successfully sensitized KP lung adenocarcinomas to immune checkpoint blockade. We extended these findings to other tumor types. Consequently, this study suggests that anticancer drugs that are rationally selected for triggering tumor immunogenicity can be used to make resistant tumors sensitive to checkpoint blockade therapy.

RESULTS

KP Lung Adenocarcinomas Resist Current Treatment Options

Kirsten rat sarcoma viral oncogene homolog (*KRAS*) and tumor suppressor p53 (*TP53*) genes are mutated in ~25% and 50%, respectively, of non-small-cell lung cancer (NSCLC) patients. Initially, we examined *Kras*^{LSL-G12D/+}; *Trp53*^{flox/flox} (hereafter KP) mice that express endogenous mutant *Kras* and deleted *Trp53* alleles in lung epithelial cells upon administration of adenovirus expressing Cre recombinase (Cortez-Retamozo et al., 2013). These mice develop lung adenocarcinomas with both pathological and molecular features of the human disease. Evaluation of the lungs of KP tumor-bearing mice revealed the presence of CD3⁺ T cells only within the normal tissue parenchyma and at frequencies comparable to those in tumor-free mice; by contrast, all the KP lung adenoma and adenocarcinoma nodules lacked CD3⁺ T cell infiltration (Figures 1A and S1A–S1C). As anticipated for tumors lacking pre-infiltrated T cells, anti-PD-1 monoclonal antibody (mAb) treatment failed to delay KP tumor progression (data not shown) and did not increase KP mouse survival as defined by the Kaplan-Meier estimator (Figure 1B). Similar results were obtained for KP mice on the 129 and C57BL/6 backgrounds (data not shown).

We extended our examination to wild-type mice bearing orthotopic syngeneic KP1.9 lung adenocarcinomas harboring *Kras* and *Trp53* mutations. Anti-PD-1 treatment also failed to control tumor progression in this model (Figure 1C). Using a third mouse model, we examined whether introducing neoantigens sensitizes KP tumors to immune checkpoint therapy. We gave KP mice a Cre-based lentiviral vector containing ovalbumin (OVA) peptide sequences to produce KP-OVA mice bearing tumors expressing model OVA neoantigens (DuPage et al., 2011). These mice were treated with both anti-PD-1 and anti-cytotoxic T-lymphocyte-associated protein 4 (CTLA-4) mAbs because combined checkpoint blockade can increase response rates in cancer patients (Sharma and Allison, 2015; Postow et al., 2015; Wolchok et al., 2013). Treatment was initiated on day 133 when lung adenocarcinomas were detectable by micro-computed tomography (Figure 1D) and poorly infiltrated by CD8⁺ T cells (DuPage et al., 2011). KP-OVA tumors remained refractory to anti-PD-1 and anti-CTLA-4 mAb combination therapy (Figure 1D).

We also assessed the effects of mainstay lung cancer chemotherapeutics in KP mice. Besides cisplatin treatment, which only marginally controls KP tumor progression (Oliver et al., 2010), we evaluated paclitaxel (Ptax) and carboplatin (Carbo), which are often administered in combination because of their synergistic effects on microtubule and DNA damage, respectively. We observed that Ptax-Carbo treatment failed both to curb KP tumor progression (Figures 1E and S1D) and to extend KP mouse survival (Figure 1F). We also assessed tumor infiltration by CD8⁺ T cells in 76 tumor biopsy sections from NSCLC patients who were genotyped for *KRAS*, *TP53*, and epidermal growth factor receptor (*EGFR*) mutations. We did not detect differences in CD8⁺ T cell infiltration based on the *KRAS* or *EGFR* status of tumors; however, *TP53*-mutated tumors as well as *TP53*-*KRAS* double-mutated tumors showed significantly reduced CD8⁺ T cell infiltration compared to their nonmutated counterparts (Figures S1E and S1F). Taken together, these results indicate that the KP mouse model is relevant to explore tumors that share important features with their human counterparts and, most importantly, resist current immuno- and chemotherapeutic interventions.

Selected Chemotherapeutics Induce KP Tumor Cell Immune Phenotypes

Considering that KP tumor nodules lack T cells, we hypothesized that therapeutically reversing this phenotype might help control cancer progression. To this end, we initially tested diverse chemotherapeutic drug combinations for their ability to induce immunogenic phenotypes in various KP tumor cell lines (KP L1-3, L1-5, and L2-9) *in vitro*. These proof-of-principle studies used high mobility group box 1 (HMGB1) release as a surrogate marker for drug-induced tumor cell immunogenicity (Zitvogel et al., 2013) and evaluated Food and Drug Administration (FDA)-approved chemotherapeutics to favor clinical translatability. We found that the NSCLC chemotherapeutics docetaxel (Dtax) and Carbo, alone or in combination, failed to induce HMGB1 release by all KP tumor cell lines tested (Figure 2A). Likewise, the anthracycline mitoxantrone (Mtx), which can have immunogenic effects (Kroemer et al., 2013), did not trigger HMGB1 release by KP tumor cells, even when combined with

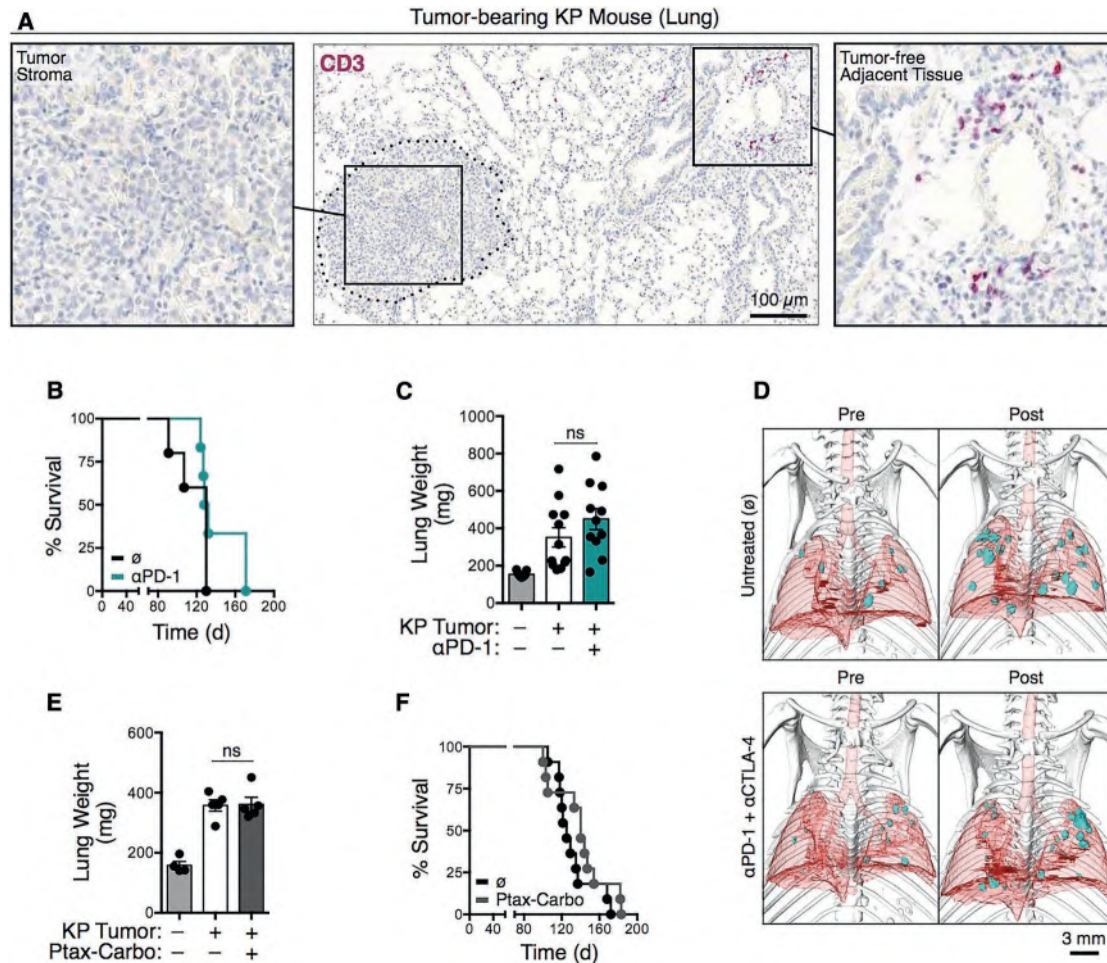


Figure 1. *Kras-Trp53*-Mutated Lung Adenocarcinomas Are Inadequately Infiltrated by T Cells and Resist Current Treatment Options

(A) Immunohistochemistry of CD3⁺ cells in KP lung tumor tissue on day 66 after tumor initiation.

(B) Survival of KP mice treated or not with anti-PD-1 (α PD-1) mAbs (n = 5–6 mice per group). Tumors were induced on day 0 by intratracheal intubation and inhalation (i.t.) of an adenovirus expressing Cre recombinase (AdCre). Mice were treated every third or fourth day with anti-PD-1 Abs intraperitoneally (i.p.) starting from day 60 to 86.

(C) Lung weight as proxy for tumor burden (Cortez-Retamozo et al., 2012) measured on day 44 in mice bearing orthotopic KP1.9 tumors and treated or not with anti-PD-1 mAbs every third or fourth day from day 25 to 42 after tumor cell injection (n = 9–12 mice per group).

(D) Micro-computed tomography of KP-OVA mice both before (day 122) and after (day 146) treatment with no antibody (\emptyset) or with anti-PD-1 and anti-CTLA-4 (α PD-1 + α CTLA-4) mAbs. Tumors were induced with a lentiviral vector containing OVA peptide sequences (LucOS) i.t. and mAb treatment was performed every second or third day from day 133 to 145.

(E and F) Lung weight (E) (n = 4–5 mice per group) and survival (F) (n = 11 mice per group) of KP mice treated or not with paclitaxel and carboplatin (Ptax-Carbo). Mice were treated once a week for 3 weeks starting on day 63 after i.t. tumor initiation and lungs analyzed 3 days after the last drug injection. For survival studies, Ptax-Carbo was injected i.p. once a week.

Results are expressed as mean \pm SEM. ns, not significant. See also Figure S1.

mafosfamide (Maf) (Figure 2B), which is the active metabolite of cyclophosphamide (Cyc) (Schiavoni et al., 2011). However, the oxaliplatin-mafosfamide (Oxa-Maf) combination stimulated HMGB1 release by all KP tumor cell lines (Figures 2A and 2B). This combination also triggered calreticulin (CRT) exposure by living KP tumor cells (Figure 2C), which is an additional marker of cell immunogenicity (Zitvogel et al., 2013). Building on these observations, we tested the combined Oxa-Cyc treatment in tumor-bearing KP mice using well-tolerated drug concentrations (Figures S2A and S2B). Unlike Ptax-Carbo, Oxa-Cyc treatment significantly increased nuclear HMGB1 staining within KP tumor

nodules (Figures 2D and S2C), a result that mirrors our in vitro findings. These data demonstrate that selected chemotherapeutics can induce immunogenic phenotypes in KP lung adenocarcinoma cells both in vitro and in vivo.

Chemotherapeutics Selected for Their Ability to Induce Immunogenicity in Tumors Delay KP Cancer Progression

KP mice sacrificed after 3 weeks of Oxa-Cyc treatment showed significantly lower tumor burden compared to Ptax-Carbo-treated or untreated mice (Figures 3A and S3A–S3C). We

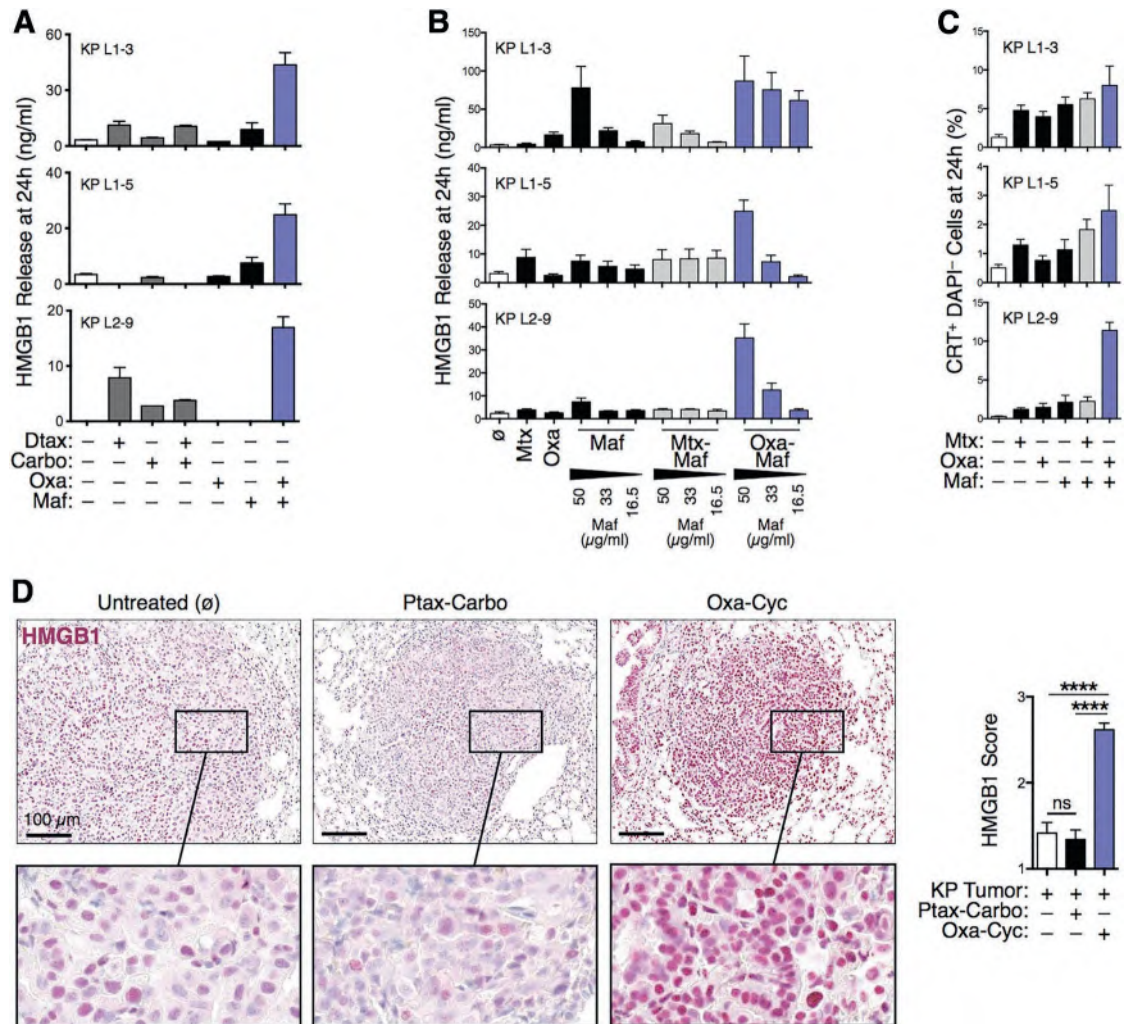


Figure 2. Selected Drugs Induce KP Tumor Cell Immune Phenotypes

(A) In vitro HMGB1 release by three KP tumor cell lines, generated from lung tissue of tumor-bearing KP mice, in response to various chemotherapeutic drug combinations as determined by ELISA ($n = 2-4$ replicates).

(B) HMGB1 release by tumor cell lines treated with mitoxantrone (4 μM), oxaliplatin (300 μM), and/or mafosamide at different concentrations (16.5, 33, or 50 $\mu\text{g/ml}$) ($n = 4$ replicates).

(C) Calreticulin exposure by tumor cell lines treated with defined drug combinations measured by flow cytometry ($n = 6$ replicates).

(D) HMGB1 immunohistochemistry (left) and scoring (right) in lung tumor nodules ($n = 39-48$) of KP mice untreated (\emptyset) or treated with Ptax-Carbo or Oxa-Cyc (see also Figure S2C for comparable images). Scale bars represent 100 μm . **** $p < 0.0001$.

Results are expressed as mean \pm SEM. Abbreviations are as follows: ns, not significant; CRT, calreticulin; Carbo, carboplatin; Cyc, cyclophosphamide; Dtax, docetaxel; Maf, mafosamide; Mtx, mitoxantrone; Oxa, oxaliplatin; Ptax, paclitaxel. See also Figure S2.

confirmed the ability of Oxa-Cyc treatment to control cancer growth in mice bearing KP1.9 tumors (Figures S3D–S3F). Because the above experiments used terminal procedures to assess tumors at different time points and in different mice, we also used in vivo MRI to monitor lung tumor volumes over time noninvasively to gain quantitative information on lung tumor progression in individual KP mice. This approach confirmed overall control of KP tumor growth during Oxa-Cyc treatment duration (Figure 3B). In contrast, Ptax-Carbo treatment showed only a limited ability to suppress cancer progression. In Oxa-Cyc-treated mice, we found that some tumor nodules progressed whereas others regressed (Figure 3B) and that tumor cell apoptosis, defined by cleaved caspase 3 staining,

increased in some but not all tumor nodules (Figure S3G). These data demonstrate the possibility of significantly altering KP tumor growth with rationally selected and clinically approved chemotherapeutics.

Drug-Induced Tumor Control Involves a Systemic Host Response

Having identified Oxa-Cyc as a model of successful treatment against KP tumors, we explored how it controlled cancer progression at a mechanistic level in vivo. First, we asked whether restricting Oxa-Cyc exposure to KP tumor cells is sufficient to alter cancer progression. To address this question, C57BL/6 mice received multiple injections of KP1.9 cells previously killed

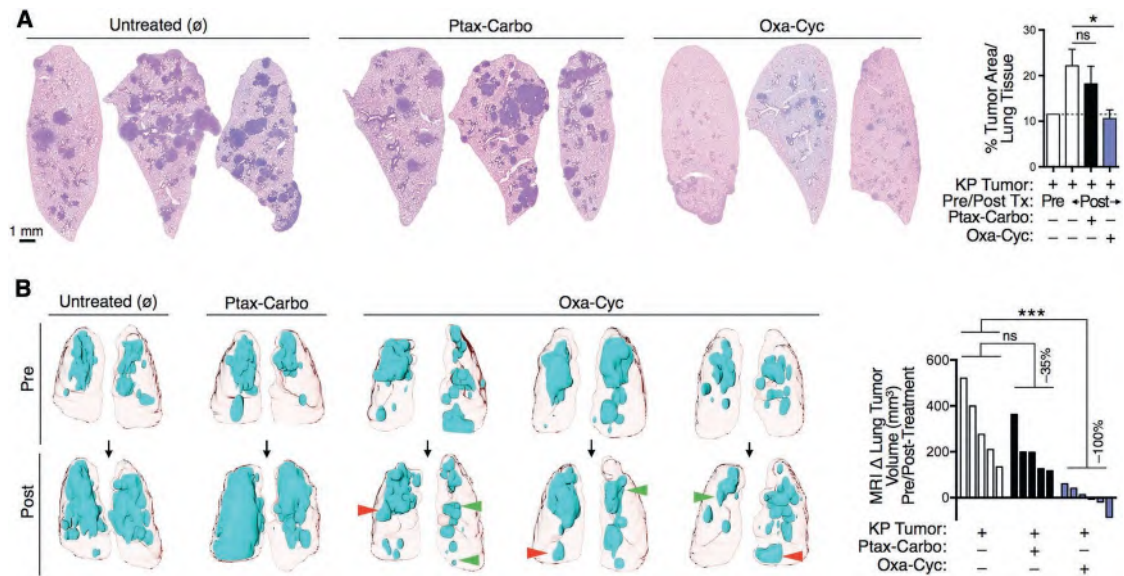


Figure 3. Drugs Selected for Their Immunogenicity Delay KP Cancer Progression

(A) Lung tumor burden identification (left) and quantification (right) by hematoxylin and eosin (H&E) staining. Mice were treated with Ptax-Carbo or Oxa-Cyc after establishment of lung adenocarcinomas for a duration of 3 weeks.

(B) Lung tumor detection by noninvasive MRI both before and after treatment as in (A) (left) and quantification of tumor progression, defined as delta tumor volume in mm³, in individual mice over time (right, n = 5–6 mice per group). Red and green arrowheads show progressing and regressing tumor areas, respectively.

Results are expressed as mean ± SEM. *p < 0.05; ***p < 0.001. Abbreviations are as follows: ns, not significant; Tx, treatment; Carbo, carboplatin; Cyc, cyclophosphamide; Oxa, oxaliplatin; Ptax, paclitaxel. See also Figure S3.

in vitro with either Oxa-Maf or Ptax-Carbo (days –8, –4, –2, 5, 12); the mice were also challenged with viable KP1.9 cells on day 0. We found that the tumors grew more slowly in mice vaccinated with cells killed with Oxa-Maf compared to mice vaccinated with tumor cells killed with Ptax-Carbo (Figure 4A). This difference highlighted that tumor control is not just a consequence of immunization with dead cells. Of interest, the vaccinations had identical effects on tumors injected either ipsi- or contralaterally, thereby further indicating systemic rather than local vaccination-induced effects. Importantly, prophylactic vaccination (i.e., Oxa-Maf-killed tumor cells injected on days –8, –4, and –2 only) was sufficient to reduce both ipsi- and contralateral tumor growth (Figure 4B). Consequently, these results indicate that Oxa-Maf-sensitized tumor cells induced systemic changes that subsequently reduced cancer progression.

Drug-Induced Tumor Control Involves Adaptive Immunity

Our next step evaluated whether Oxa-Cyc sensitization in vivo promoted an antitumor immune response. By collecting single-cell suspensions from KP mouse lungs, we found increased CD8⁺ T cell:Treg cell ratios in Oxa-Cyc-treated mice as compared to untreated or Ptax-Carbo-treated mice (Figure 4C). The increased CD8⁺ T cell:Treg cell ratio favors CD8⁺ T-cell-mediated cancer immune surveillance and is associated with beneficial outcome (Sato et al., 2005; Gao et al., 2007). In further assessing the distribution of T cells in KP mouse lungs by immunohistochemistry, we found that Oxa-Cyc treatment instigated CD3⁺ T cell infiltration within tumor nodules (Figures 4D and S4A), with some CD3⁺ cells proliferating locally as revealed by

Ki67 staining (Figure S4B). The tumor-infiltrating CD3⁺ T cells, which were absent in untreated or Ptax-Carbo-treated mice, were mostly CD8⁺ and rarely CD4⁺ (Figures 4E and S4C), thereby indicating Oxa-Cyc's ability to instigate CD8⁺ T cell infiltration into, and proliferation within, KP tumors.

Because Cyc can suppress Treg cells (Ghiringhelli et al., 2004; Lutsiak et al., 2005), Oxa-Cyc might promote antitumor responses by acting on Treg cells directly. However, our data suggested that the CD8⁺ T cell response induced by Oxa-Cyc against KP tumors preferentially follows the induction of drug-mediated tumor cell immunogenicity because Oxa-Cyc treatment increased CD8⁺ T cell:Treg cell ratios selectively in lung tumor tissue (i.e., not systemically, Figure 4F), and Treg cells (as fractions of CD3⁺ cells) were already absent from tumor nodules of untreated mice (Figure S4A). Also, lung CD8⁺ T cell:Treg cell ratios increased more in mice that received both Oxa and Cyc (Figure 4F), a result that was in accordance with our in vitro observations that inducing tumor cell immunogenic phenotypes required the drug combination (Figures 2A–2C).

To test whether therapeutically controlling KP tumor progression needs adaptive immunity, we generated *Rag2*^{–/–} KP mice in the C57BL/6 background (Figures S4D–S4F). The inability of Oxa-Cyc to suppress tumor progression in these mice (Figures 4G and S4G) favors the hypothesis that KP tumor control requires CD8⁺ T cells. Because *Rag2*^{–/–} KP mice lack both T and B cells (Figures S4E and S4F), we also investigated the influence of selective CD8⁺ T cell ablation in immunocompetent (*Rag2*^{+/+}) KP mice using CD8 depleting mAbs (Figure S4H). Oxa-Cyc failed to suppress tumor progression in CD8⁺ T-cell-depleted mice (Figure 4H), which indicated that Oxa-Cyc not only instigated

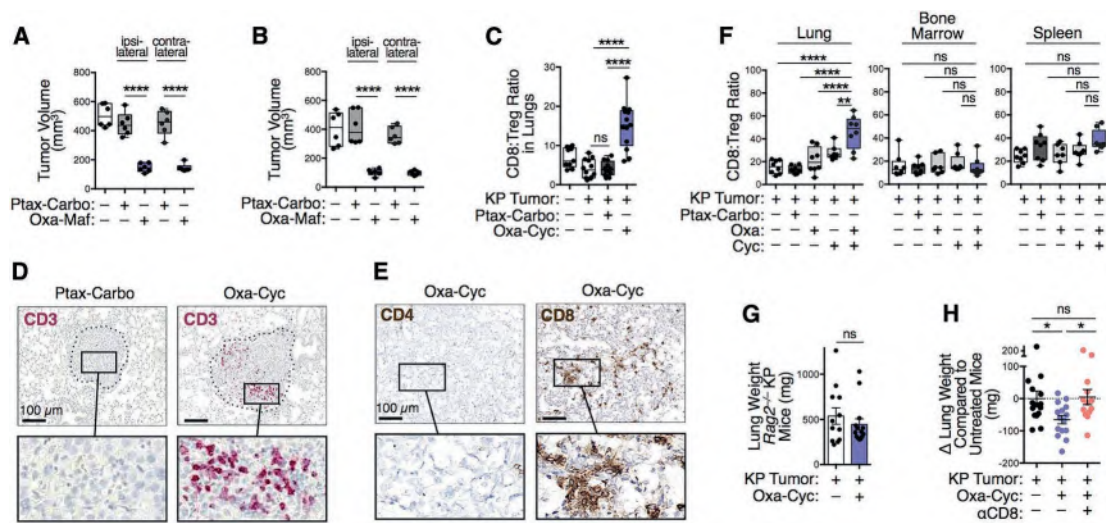


Figure 4. Drug-Induced Tumor Control Involves Adaptive Immunity

(A and B) Impact of vaccinations with Ptax-Carbo- or Oxa-Maf-killed tumor cells on growth of KP1.9 tumors injected on day 0 ipsi- or contralaterally to the vaccination sites. Mice were injected with in vitro killed tumor cells on days -8, -4, -2, 5, and 12 (A) or received only prophylactic vaccination on days -8, -4, and -2 (B). Tumor burden was analyzed on day 19 (A) or day 14 (B), respectively (n = 6 mice per group).

(C) CD8⁺ T cell:Treg cell ratio in lungs of KP mice assessed by flow cytometry at 3 weeks after treatment with Ptax-Carbo or Oxa-Cyc (n = 9–13 mice per group).

(D) CD3 immunohistochemistry of representative lung tumor sections from KP mice treated as in (C) (see Figure S4A for comparable images). Scale bars represent 100 μm.

(E) CD4 and CD8 immunohistochemistry of lung tumor tissue from Oxa-Cyc-treated KP mice (see Figure S4C for comparable images). Scale bars represent 100 μm.

(F) CD8⁺ T cell:Treg cell ratios assessed by flow cytometry in lung, bone marrow, and spleen of KP1.9 lung tumor-bearing mice left untreated or that received Ptax-Carbo, Oxa, Cyc, or Oxa-Cyc (n = 7–8 mice per group).

(G) Lung weight of *Rag2*^{-/-} KP mice treated or not with Oxa-Cyc (n = 12–14 mice per group).

(H) Lung weight of Oxa-Cyc-treated KP mice that received CD8 depleting mAbs (αCD8, n = 13–15 mice per group).

Results are expressed as mean ± SEM. *p < 0.05; **p < 0.01; ****p < 0.0001; ns, not significant. See also Figure S4.

tumor infiltration by CD8⁺ T cells but also needed these cells to control cancer growth. Tumor control in KP mice was very efficient, especially considering that this mouse model resists all conventional treatments and develops tumors that are generally viewed as non-immunogenic.

Drug-Induced Tumor Control Involves Innate Immunity

To delve deeper into drug action mechanisms, we next examined whether Oxa-Cyc-induced antitumor immunity required variables other than tumor-cell targeting and CD8⁺ T cells. We investigated innate immune cells because they are found in the KP tumor stroma (Cortez-Retamozo et al., 2012) and might be modulated by drugs to induce tumor control (Broz and Krummel, 2015; De Palma and Lewis, 2013). To uncover possible drug-induced changes on innate immune cell subsets, we collected lung tissue biopsies of KP tumor-bearing mice treated or not with Oxa-Cyc for comparative ex vivo analysis by multi-parameter flow cytometry. Furthermore, we isolated both tumor stroma biopsies and tumor-free adjacent lung tissue to assess whether drug-induced changes selectively control the immediate tumor microenvironment. By operationally dividing CD45⁺Lin⁻ myeloid cells into CD11b⁻ and CD11b⁺ cell subsets, we observed a substantial decrease in the frequency of CD11b⁻ cells in both the tumor stroma and adjacent tissue after Oxa-Cyc therapy (Figure 5A). This decrease was also observed in Ptax-Carbo-treated mice (data not shown), suggesting that this cell loss is insufficient to explain tumor control selectively in Oxa-Cyc-treated mice. In

marked contrast, Oxa-Cyc treatment significantly and selectively increased the frequency of the CD11b⁺ cell subset within the tumor stroma (Figure 5A). These findings indicate that Oxa-Cyc treatment modulates innate immune system components within the tumor microenvironment.

We further analyzed CD11b⁺ cells, and subsets thereof, and considered toll-like receptor 4 (TLR4) because it can be involved in innate immune activation and transition toward adaptive immunity in the context of drug-induced immunogenic cell death (Apetoh et al., 2007; Kroemer et al., 2013). We found that Oxa-Cyc treatment upregulated TLR4 selectively in the dendritic cell (DC)/macrophage-like subset, defined as CD11b⁺CD11c⁺Ly-6G⁻Ly-6C⁻. TLR4 upregulation occurred only within the tumor stroma and not in tumor-free adjacent tissue (Figure 5B). By comparison, the mean fluorescent intensity (MFI) of cell surface TLR4 expression was low or undetectable in CD11b⁺CD11c⁻ cells, Ly-6G⁺Ly-6C⁺ granulocytes, and Ly-6C⁺ monocyte-like cells, both in the absence and presence of Oxa-Cyc treatment (Figure 5B). We also found that CD11b⁺CD11c⁺ cells, in contrast to their CD11b⁺CD11c⁻ counterparts, upregulated the integrin CD103 (Figure 5C). CD103⁺ DC-like cells are important in regulating antitumor immunity because they have enhanced abilities to activate CD8⁺ T cells compared to CD103⁻ DCs and tumor-associated macrophages (Broz et al., 2014; Ruffell et al., 2014; Spranger et al., 2015).

To define whether TLR4⁺ cells are required for generating drug-induced KP tumor control, we examined the impact of

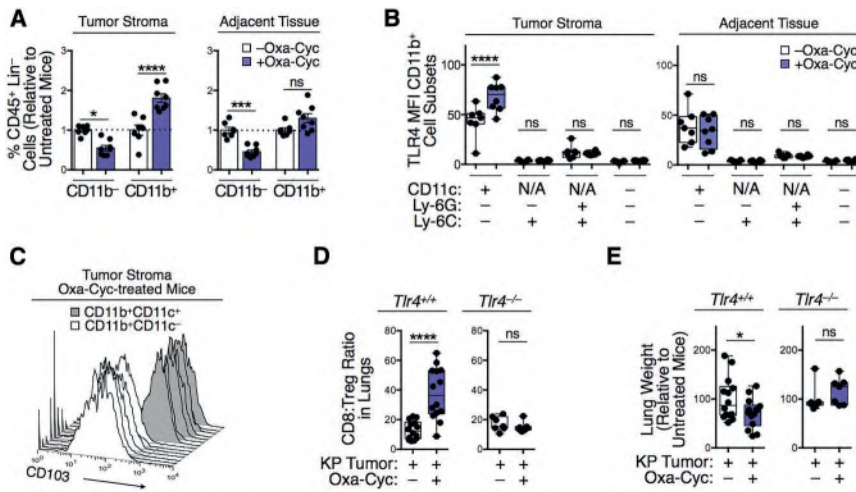


Figure 5. Drug-Induced Tumor Control Involves Innate Immunity and TLR4 Signaling

(A) CD11b⁻ and CD11b⁺ cells in lung tissue biopsies of KP mice that received Oxa-Cyc or were left untreated ($n = 7-8$ mice per group). Lung tissue biopsies of tumor and tumor-free adjacent tissues were investigated in parallel.

(B) TLR4 mean fluorescence intensity (MFI) of CD11b⁺ cell subsets in tumor and tumor-free lung tissues of Oxa-Cyc-treated or untreated KP mice ($n = 7-8$ mice per group).

(C) CD103 phenotype of CD11b⁺CD11c⁻ and CD11b⁺CD11c⁺ cells in tumor stroma of Oxa-Cyc-treated mice ($n = 7$ mice per group).

(D and E) Lung CD8⁺ T cell:Treg cell ratio (D) and lung weight (E) of KP1.9 tumor-bearing *Tlr4*^{+/+} and *Tlr4*^{-/-} mice treated or not with Oxa-Cyc ($n = 7-14$ mice per group). Lineage (Lin) defined as (B220/CD49b/CD90.2/Ter119)⁺.

Results are expressed as mean \pm SEM. * $p < 0.05$; *** $p < 0.001$; **** $p < 0.0001$; ns, not significant; N/A, not applicable.

Oxa-Cyc treatment on tumor-associated T cell responses in *Tlr4*^{-/-} mice. In contrast to their wild-type counterparts, *Tlr4*^{-/-} mice failed to increase lung CD8⁺ T cell:Treg cell ratios after Oxa-Cyc treatment (Figure 5D). Furthermore, we found that TLR4 deficiency reduced Oxa-Cyc-mediated control of KP tumor progression (Figure 5E). These data provide evidence that triggering successful antitumor T cell immunity against KP tumors with Oxa-Cyc depends on TLR4, in line with previous findings that this receptor can promote DC-mediated CD8⁺ T cell activation (Apetoh et al., 2007).

Immunogenic Chemotherapeutics Sensitize Lung Adenocarcinomas to Immune Checkpoint Therapy

With the ability to convert non-T-cell-infiltrated KP tumors into ones that display antitumor T cell immunity, we asked whether this process can be harnessed for sensitizing KP tumors to checkpoint blockade therapy. We used the KP-OVA mouse model because it is refractory to the anti-PD-1 and anti-CTLA-4 mAb combination therapy (Figure 1D) and allowed us to track CD8⁺ T cells specific for the model antigen OVA₂₅₇₋₂₆₄. We found that Oxa-Cyc treatment in these mice favored or maintained four phenotypes that are potentially associated with response to PD-1 checkpoint inhibition, namely (1) increased CD8⁺ T cell:Treg cell ratio in the lung tumor tissue (Figure 6A), (2) presence of tumor-infiltrating OVA-specific CD8⁺ T cells (Figure 6B), (3) PD-1 expression by these cells (Figure 6C), and (4) PD-L1 expression by tumor-associated host and/or tumor cells (Figure 6D).

We conducted a blinded preclinical study in which KP-OVA mice received Oxa-Cyc, anti-PD-1 + anti-CTLA-4 mAbs, or both with controls left untreated (Figure S5A). Treatments began on day 130 after tumor initiation and tumors were monitored noninvasively by high-resolution micro-computed tomography in all mice at three time points (days 122, 146, and 193) to quantify changes in tumor burden in vivo. All mice were evaluated ex vivo at day 234.

Noninvasive tumor assessment at days 122, 146, and 193 (T_0 , T_1 , and T_2) revealed that Oxa-Cyc controlled KP tumors during the first 3 weeks of treatment ($T_0 \rightarrow T_1$) when compared to un-

treated mice ($p < 0.05$) but was unable to significantly control tumors at the later time point ($T_0 \rightarrow T_2$, $p > 0.05$) (Figure 6E). Checkpoint inhibition failed to delay KP tumor progression ($T_0 \rightarrow T_1$, $p > 0.05$; $T_0 \rightarrow T_2$, $p > 0.05$). By contrast, Oxa-Cyc combined with anti-PD-1 + anti-CTLA-4 mAb treatment controlled tumor progression at both time points ($T_0 \rightarrow T_1$, $p < 0.01$; $T_0 \rightarrow T_2$, $p < 0.05$) (Figures 6E and 6F).

Postmortem evaluation at day 234 (T_3) validated the advantage of the combination treatment to suppress KP tumors durably (i.e., over 16 weeks; $p < 0.001$; Figures 6E and 6G). The combination treatment was significantly better than either Oxa-Cyc or anti-PD-1 + anti-CTLA-4 alone (Figures 6E and 6G).

Multiphoton microscopy of explanted lung tissue confirmed successful tumor control in the same mice. This approach further revealed the CD8⁺ T cells' selective ability to accumulate and remain within tumor nodules of Oxa-Cyc-treated KP-OVA mice, whether or not they received the immune checkpoint blockers (Figures 6H, S5B, and S5C). These data support the idea that tumor infiltration by CD8⁺ T cells is insufficient to durably control cancer progression but can generate effective responses to checkpoint blockade treatment.

Additionally, when using the KP1.9 tumor-bearing mouse model, we found that Oxa-Cyc treatment significantly increased overall mouse survival when combined with anti-PD-1 + anti-CTLA-4 mAbs, whereas anti-PD-1 or anti-CTLA-4 mAbs alone did not confer protection (Figure S5D). Comparisons of various combination treatments suggested that anti-PD-1 mAb treatment was mostly responsible for improving Oxa-Cyc treatment efficacy in the KP1.9 tumor-bearing mice at least 20 days after initiation of treatment (Figure S5E). Taken together, these data indicate that rationally selected immunogenic chemotherapeutics can sensitize KP lung adenocarcinomas to immune checkpoint therapy.

Immunogenic Chemotherapeutics Can Sensitize Other Tumors to Immune Checkpoint Therapy

Finally, we tested whether other immunogenic chemotherapeutics could sensitize tumors to immune checkpoint therapy. We explored MCA205 fibrosarcoma-bearing mice because they

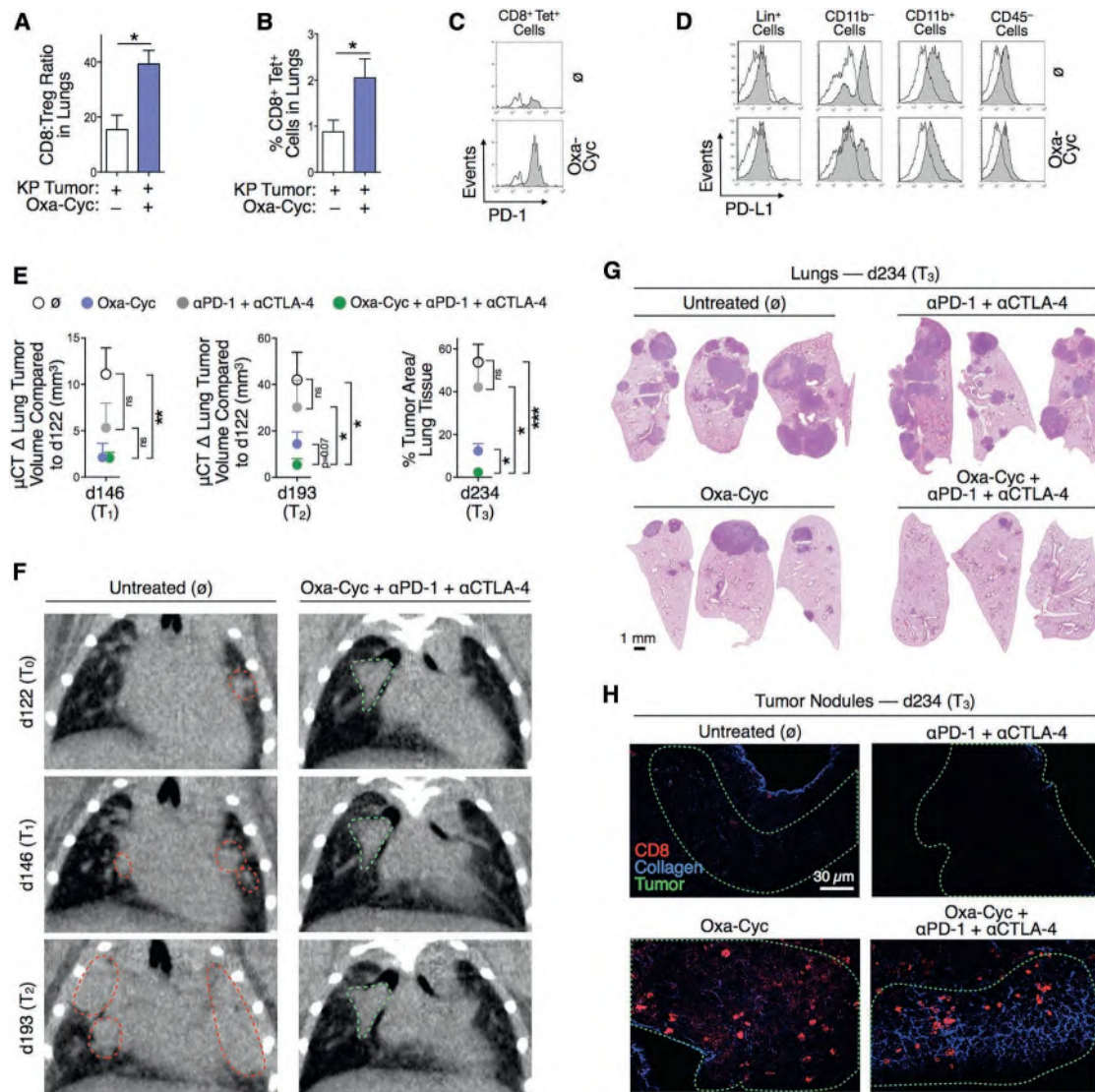


Figure 6. Drug-Induced Tumor Infiltration by CD8⁺ T Cells Sensitizes Lung Adenocarcinomas to Immune Checkpoint Therapy

(A–D) Lung CD8⁺ T cell:Treg cell ratio (A), percent of OVA-specific CD8⁺ T cells in lungs (B), PD-1 expression by these cells (C), and PD-L1 surface expression by different tumor stroma cell populations (D; white histograms are fluorescence minus one [FMO] controls) in KP-OVA mice treated or not with Oxa-Cyc ($n = 2$ –5 mice per group).

(E) Micro-computed tomography imaging (d146, d193) and ex vivo analysis (d234) of lungs of KP-OVA mice treated with Oxa-Cyc and anti-PD-1 + anti-CTLA-4 mAbs either alone or in combination ($n = 5$ mice per group). Tumors were induced with a lentiviral vector containing OVA peptide sequences (LucOS). Change in tumor volume (defined by micro-computed tomography at d146 = T₁ and d193 = T₂) and tumor area in lung tissues (defined by H&E staining at d234 = T₃) in these mice.

(F) Coronal micro-computed tomography at d122, d146, and d193 of an untreated mouse (left) or mouse that received the combination therapy (right). Dotted lines identify tumor nodules that progressed (red) or not (green).

(G) Lung tumor burden identification by H&E staining at d234 in the same mice as in (E).

(H) CD8⁺ cell (red) infiltration in KP-OVA tumors (tumor contour defined with green dashed lines, see Figure S5B for comparable images) identified by multiphoton microscopy ex vivo at d234 in the same mice. Collagen is shown in blue.

Results are expressed as mean \pm SEM. * $p < 0.05$; ** $p < 0.01$; *** $p < 0.001$; ns, not significant. See also Figure S5.

failed to respond to anti-PD-1 + anti-CTLA-4 mAbs (Figure 7A). We found that cisplatin treatment, which does not induce immunogenic cell death, failed to improve immune checkpoint blockade treatment (Figure 7A). By contrast, doxorubicin, which induces MCA205 immunogenic cell death (Zitvogel et al., 2013), significantly delayed tumor progression

when combined with anti-PD-1 + anti-CTLA-4 mAb therapy (Figure 7A).

We also investigated CT26 colon carcinoma-bearing mice, which did not respond to anti-CTLA-4 mAb therapy (Figure 7B). Oxa treatment induces immunogenic CT26 tumor cell death (Apetoh et al., 2007; Tesniere et al., 2010) and increases

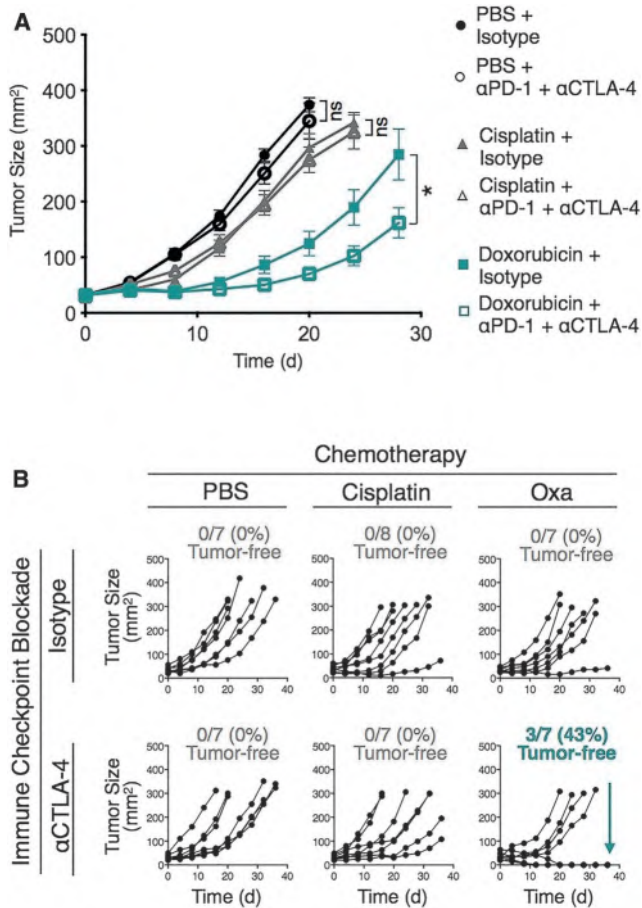


Figure 7. Immunogenic Chemotherapeutics Improve Immune Checkpoint Blockade Treatment against MCA205 Fibrosarcoma and CT26 Colon Carcinoma

(A) Tumor size measurement of MCA205 fibrosarcoma-bearing C57BL/6 mice ($n = 7-8$ per group) treated with PBS or chemotherapy (cisplatin or doxorubicin) together with anti-PD-1 + anti-CTLA-4 (α PD-1 + α CTLA-4) mAbs or isotype control mAbs. Tumor cells were injected on d-8; the chemotherapeutics were given on d0 and the mAbs on d8, 12, and 16.

(B) Tumor size measurement of CT26 colon carcinoma-bearing BALB/c mice ($n = 7-8$ per group) treated with PBS or chemotherapy (cisplatin or oxaliplatin [Oxa]) together with anti-CTLA-4 or isotype control mAbs. Tumor cells were injected on d-11; the chemotherapeutics were given on d0 and the mAbs on d8, 12, and 16. Each line represents an individual mouse.

Results are expressed as mean \pm SEM. * $p < 0.05$; ns, not significant.

CD8⁺ T cell infiltration at the tumor site (Gou et al., 2014). We found that Oxa treatment provided minimal control of CT26 tumor progression, similarly to cisplatin, which was used as a control agent (Figure 7B). Checkpoint blockade therapy with anti-CTLA-4 mAb, either as monotherapy or combined with cisplatin, was also largely ineffective. However, the Oxa + anti-CTLA-4 mAb combination was able to reject CT26 tumors in ~40% of mice analyzed (Figure 7B). These results demonstrate that our findings in the KP mouse model can be extended to other tumor types; they also indicate that tailoring chemotherapy treatments to a given tumor type might be a generalizable approach to sensitize tumors to immune checkpoint therapy.

DISCUSSION

We used genetically engineered mouse models that closely recapitulate human disease to examine whether autochthonous tumors lacking pre-infiltrated T cells can also be sensitized therapeutically to induce T-cell-mediated control of tumor progression. We investigated lung adenocarcinomas carrying common *KRAS* and/or *TP53* mutations because we identified these tumors to be inadequately infiltrated by CD8⁺ T cells in both humans and mice. In addition, we found that *Kras/Trp53* mutant tumors in mice resist current chemo- and immunotherapies even when the tumors expressed neoantigens, which are targets of successful checkpoint blockade therapy. We report that appropriately selected and clinically approved therapeutics can produce CD8⁺ T cell infiltration in otherwise non-T cell inflamed tumors and that this process inhibits cancer progression. Furthermore, the T cell response induced by immunogenic chemotherapeutics can be harnessed to sensitize lung adenocarcinomas to immune checkpoint therapy. The antitumor response triggered by the immunogenic chemotherapeutics depended on (1) direct drug actions on tumor cells, (2) host CD8⁺ T cell activation, and (3) intact TLR4 signaling.

First, Oxa-Cyc-induced effects on tumor cells alone can trigger a systemic antitumor response. Indeed, injecting tumor-bearing mice with KP1.9 tumor cells previously killed by Oxa-Maf (but not by Ptax-Carbo) efficiently inhibited tumor progression. Combined with our *in vitro* results, which showed Oxa-Cyc's ability to directly induce KP tumor cells with immunogenic phenotypes, our findings indicate that Oxa-Cyc-mediated effects on tumor cells instigate a cascade of events that ultimately lead to tumor control. Whether some immunotherapeutics might overcome the limitations of poorly immunogenic chemotherapeutics requires further study. Nonetheless, considering the importance of initial tumor cell drug targeting, it might be possible to further improve clinical outcomes by increasing chemotherapeutic load at the tumor site. This might be achieved by encapsulating drugs within nanoparticles (Peer et al., 2007) or by targeting the vasculature (Chauhan et al., 2012).

Second, the Oxa-Cyc-induced antitumor response depends on host CD8⁺ T cells: the drugs failed to control tumor progression in mice lacking these cells (*Rag2*^{-/-} KP mice as well as wild-type KP mice depleted with anti-CD8 mAbs). Another study using a genetic mammary cancer model showed that chemotherapeutics can have comparable effects against genetically engineered tumors growing in either *Rag*-competent or *Rag*-deficient mice (Ciampricotti et al., 2012). These findings suggest that chemotherapy can limit tumor progression without CD8⁺ T cells. Yet, the chemotherapeutics used in the mammary tumor models only delayed tumor growth, whereas accumulating evidence shows that potent tumor infiltration by CD8⁺ T cells might be key to durably controlling cancer (Gajewski et al., 2013; Tumei et al., 2014; Spranger et al., 2015). Our study indicates that drug-induced CD8⁺ T cell tumor infiltration can contribute to tumor control in genetic mouse models and be harnessed for checkpoint blockade therapy. These findings accord with the observation in a mouse model of castrate-resistant prostate cancer that Oxa can induce CD8⁺ T-cell-dependent tumor eradication (Shalapour et al., 2015).

Third, the drug-induced antitumor T cell response needs intact TLR4 signaling. We observed that TLR4 deficiency prevented Oxa-Cyc from increasing CD8⁺ T cell:Treg cell ratios within the tumor bed and from controlling tumor progression. Accordingly, we found that Oxa-Cyc makes dying tumor cells release HMGB1, which activates TLR4 directly (Apetoh et al., 2007). Also, systemic Oxa-Cyc treatment caused an influx of TLR4⁺ DC-like cells specifically in the tumor stroma. These tumor-infiltrating cells expressed CD103 and thus resembled DCs previously identified as critical stimulators of antitumor CD8⁺ T cell immunity (Broz et al., 2014; Ruffell et al., 2014; Spranger et al., 2015). Our results are in accordance with previous findings that TLR4 can promote DC tumor antigen cross-presentation and CD8⁺ T cell activation after immunogenic tumor cell death (Apetoh et al., 2007) and that tumor-infiltrating DCs can be key regulators of antitumor immunity (Broz et al., 2014). Although the detailed mechanisms shaping successful immune responses against KP tumors require further investigation, the aforementioned findings already provide evidence that shaping these immune responses will require a combination of variables including tumor cell targeting and both the adaptive and innate arms of the immune system. We hypothesize that Oxa-Cyc-induced enrichment of TLR4⁺ antigen-presenting cells in KP tumors precedes and facilitates the local influx of CD8⁺ T cells. TLR4 genotype (Casanova et al., 2011) and tumor-associated myeloid cell content (Broz and Krummel, 2015) can vary across individuals and/or tissues, so evaluating these innate immune variables could help select treatment options.

Checkpoint blockade therapies have yielded unprecedented clinical benefits against lung and other cancers but on their own might preferentially benefit patients whose tumors are pre-infiltrated by CD8⁺ T cells (Tumeh et al., 2014; Gajewski et al., 2013). We found that therapy-induced T cell infiltration enabled successful treatment with immune checkpoint inhibition, further indicating that appropriately selected drugs that transform “cold” tumor tissues into immunologically “hot” T-cell-rich environments can be used to sensitize tumors to immune checkpoint therapy and improve clinical outcome.

Our results provide a proof of principle that chemotherapeutics selected for their ability to induce immunogenicity in tumors (e.g., Oxa-Cyc against KP tumors, Doxorubicin against MCA205, and Oxa against CT26) provide additive or synergistic benefits when combined with immune checkpoint blockers. It will be important to explore whether and when other drugs or drug combinations can achieve similar results. For example, it is possible that Oxa alone or Ptax-Carbo also sensitize KP tumors to immune checkpoint blockade or synergize with immunotherapy against other cancers. Also, preclinical studies using an ovarian cancer graft model indicate that PD-1 blockade can improve Ptax therapy (Lu et al., 2014) and ongoing clinical trials are testing the potential of Ptax-Carbo to enhance the efficacy of immune checkpoint blocking agents against various cancer types, including NSCLC (S.V. Liu et al., 2015, ASCO Annual Meet., abstract; V. Papadimitrakopoulou et al., 2015, ASCO Annual Meet., abstract).

To achieve tumor sensitization and improved outcomes, we envision two scenarios: (1) re-evaluating the chemotherapeutics used in combination with checkpoint blockade agents to specif-

ically include drugs with the potential to induce immunogenic cell death (e.g., Oxa and Cyc as investigated for the KP lung tumor model), and (2) using precision medicine to select drugs with the ability to promote tumor cells' immunogenicity in a given patient. The first approach could provide immediate clinical benefit by expanding the proportion of cancer patients who respond to current immune checkpoint treatments. The second approach involves screening drugs for individual patients and is thus more technically challenging, but because it takes into account that different tumor genetic drivers, tissues of origin, and tumor microenvironments can profoundly modify a given drug's efficacy, this drug selection approach might benefit even more patients. The drug-induced readouts could be expanded to study various forms of cell death, including pyroptosis or necroptosis, which can also promote antitumor immunity. Regardless of the approach, drugs that are already FDA approved could be used to accelerate clinical translation.

EXPERIMENTAL PROCEDURES

Mice

Kras^{LSL-G12D/+}, *Trp53*^{fllox/fllox} (KP) mice were used as a conditional mouse model of NSCLC (Cortez-Retamozo et al., 2013). Details about all murine strains and tumor models are provided in the Supplemental Experimental Procedures. All animal experiments were approved by the Massachusetts General Hospital Subcommittee on Research Animal Care, except experiments in BALB/c and MCA205-bearing C57BL/6 mice that were approved by the Ethical Committee of the Gustave Roussy Cancer Campus (Villejuif, France).

Cell Lines

The lung adenocarcinoma cell line KP1.9 was derived from lung tumors of C57BL/6 KP mice and was kindly provided by Dr. A. Zippelius, University Hospital Basel, Switzerland. The lung adenocarcinoma cell lines KP L1-3, KP L1-5, and KP L2-9 were derived from 129 KP mouse lung tumors and all established in our laboratory. Additional information on further cell lines and cell culture conditions are detailed in the Supplemental Experimental Procedures.

Human Tumor Samples

Sections from paraffin-embedded biopsies of lung resections (n = 76) from NSCLC patients with known *KRAS* and *EGFR* gene mutation status were obtained from the Department of Pathology at Massachusetts General Hospital according to an approved institutional review board protocol (IRB 2009P001838). TP53 and CD8 immunohistochemistry were performed and evaluated blindly based on defined scoring systems as described in the Supplemental Experimental Procedures.

Micro-computed Tomography and MRI

Tumor burden was evaluated by micro-computed tomography (μ CT) or MRI in anonymized mice. Details of the imaging protocols are provided in the Supplemental Experimental Procedures.

Mouse Histology, Immunohistochemistry, and Immunofluorescence Microscopy

Histological analysis of tumor burden in mice was done on formaldehyde-fixed and paraffin-embedded lung tissues using hematoxylin and eosin (H&E) staining. Immunohistochemistry (IHC) was done on either paraffin-embedded (HMGB1, cleaved caspase-3, Ki67, CD3, CD4) or frozen (CD8) tissue sections. Detailed information regarding antibody clones and staining procedures are in the Supplemental Experimental Procedures.

Multiphoton Microscopy

Small lung pieces from tumor-bearing KP mice and tumor-free tissue were fixed, stained, and imaged with an Ultima multiphoton microscope (Prairie Technologies). Images were pre-processed in R statistical computing environment with RStudio and stitched/analyzed with Fiji software. More

information on staining procedures and image processing are described in the Supplemental Experimental Procedures.

HMGB1 and Calreticulin In Vitro Assays

The KP L1-3, KP L1-5, and KP L2-9 tumor lines were seeded in tissue culture plates before treatment with chemotherapeutic drugs for 24 hr (Dtax, 30 μ M; Carbo, 500 μ M; Oxa, 300 μ M; Maf, 16.5, 33, 50 μ g/ml; Mtx, 4 μ M). For the calreticulin assay, the cells were harvested from cell culture plates, fixed and incubated with rabbit anti-calreticulin Ab followed by anti-rabbit Alexa Fluor 488 conjugated Ab, and investigated by flow cytometry (CyAn ADP analyzer, Beckman Coulter). Detailed assay conditions are provided in the Supplemental Experimental Procedures.

In Vivo Drug Treatments

KP tumor-bearing mice were either left untreated or received chemotherapy intraperitoneally (i.p.) once a week for 3 weeks (Oxa, 2.5 mg/kg; Cyc, 50 mg/kg; Ptax, 10 mg/kg; Carbo, 10 mg/kg). BALB/c mice bearing CT26 flank tumors and MCA205 flank tumor-bearing C57BL/6 mice received one intratumoral chemotherapeutic drug injection (Oxa, 1.25 mg/kg; cisplatin, 0.25 mg/kg; Doxorubicin, 2.9 mg/kg). mAbs specific for PD-1 (clone 29F.1A12, provided by Dr. G.J. Freeman) and CTLA-4 (clone 9D9, BioXcell) were injected i.p. Details about in vivo experiments including drug treatment conditions and cell depletion strategies are provided in the Supplemental Experimental Procedures.

Recovery of Cells from Murine Tissues and Flow Cytometry

Single-cell suspensions were prepared from murine lung, spleen, and bone marrow and investigated by flow cytometry (LSRII, BD Biosciences). Where indicated, equally sized pieces of tumor stroma and corresponding tumor-free adjacent tissue were isolated separately from lungs of Oxa-Cyc-treated or untreated tumor-bearing KP mice. Details about cell recovery strategies and flow cytometry staining procedures including Ab clones and identified cell populations are in the Supplemental Experimental Procedures.

Statistics

Results were expressed as mean \pm SEM. Statistical tests included one-way ANOVA followed by Tukey's or Dunnett's multiple comparison test. When applicable, unpaired one-tailed and two-tailed Student's *t* tests using Welch's correction for unequal variances were used. Comparison of survival curves was performed with the Log-rank Mantel-Cox test. *p* values of 0.05 or less were considered to denote significance (**p* < 0.05; ***p* < 0.01; ****p* < 0.001; *****p* < 0.0001; ns, not significant).

SUPPLEMENTAL INFORMATION

Supplemental Information includes five figures and Supplemental Experimental Procedures and can be found with this article online at <http://dx.doi.org/10.1016/j.immuni.2015.11.024>.

AUTHOR CONTRIBUTIONS

C.P. and C.E. designed the study, performed experiments, analyzed data, and wrote the manuscript. S.R., M.M.-K., and T.G.H. performed immunohistochemistry and analysis. V.C.-R., C.G., F.P., T.Y., V.P.-C., A.N., Y.R., and Y.-J.L. performed experiments and generated and analyzed data. G.W. performed and analyzed murine μ CT and MRI data. Y.I. conducted tissue sectioning and slide scanning. R.O.H., G.J.F., G.K., L.Z., and R.W. provided input for research design and interpretation and edited the manuscript. M.J.P. directed the study and wrote the manuscript.

ACKNOWLEDGMENTS

The authors thank the members of the Hope Babette Tang Histology Facility at the Koch Institute Swanson Biotechnology Center for technical support. This work was supported in part by the Samana Cay MGH Research Scholar Fund (to M.J.P.), NIH grants P50-CA86355 and R01-AI084880 (to M.J.P.), U54-CA126515 (to R.W.), U54CA163125 (to G.J.F.), and U54-CA163109 and the Howard Hughes Medical Institute (to R.O.H.). C.P. was supported

by the Deutsche Forschungsgemeinschaft (DFG) PF809/1-1, C.E. by the Boehringer Ingelheim Fonds, and S.R. by the DFG RI2408/1-1.

Received: September 17, 2015

Revised: November 11, 2015

Accepted: November 11, 2015

Published: February 9, 2016

REFERENCES

- Apetoh, L., Ghiringhelli, F., Tesniere, A., Obeid, M., Ortiz, C., Criollo, A., Mignot, G., Maiuri, M.C., Ullrich, E., Saulnier, P., et al. (2007). Toll-like receptor 4-dependent contribution of the immune system to anticancer chemotherapy and radiotherapy. *Nat. Med.* **13**, 1050–1059.
- Broz, M.L., and Krummel, M.F. (2015). The emerging understanding of myeloid cells as partners and targets in tumor rejection. *Cancer Immunol. Res.* **3**, 313–319.
- Broz, M.L., Binnewies, M., Boldajipour, B., Nelson, A.E., Pollack, J.L., Erle, D.J., Barczak, A., Rosenblum, M.D., Daud, A., Barber, D.L., et al. (2014). Dissecting the tumor myeloid compartment reveals rare activating antigen-presenting cells critical for T cell immunity. *Cancer Cell* **26**, 638–652.
- Casanova, J.L., Abel, L., and Quintana-Murci, L. (2011). Human TLRs and IL-1Rs in host defense: natural insights from evolutionary, epidemiological, and clinical genetics. *Annu. Rev. Immunol.* **29**, 447–491.
- Chauhan, V.P., Stylianopoulos, T., Martin, J.D., Popović, Z., Chen, O., Kamoun, W.S., Bawendi, M.G., Fukumura, D., and Jain, R.K. (2012). Normalization of tumour blood vessels improves the delivery of nanomedicines in a size-dependent manner. *Nat. Nanotechnol.* **7**, 383–388.
- Ciampricotti, M., Hau, C.S., Doornebal, C.W., Jonkers, J., and de Visser, K.E. (2012). Chemotherapy response of spontaneous mammary tumors is independent of the adaptive immune system. *Nat. Med.* **18**, 344–346, author reply 346.
- Cortez-Retamozo, V., Etzrodt, M., Newton, A., Rauch, P.J., Chudnovskiy, A., Berger, C., Ryan, R.J., Iwamoto, Y., Marinelli, B., Gorbатов, R., et al. (2012). Origins of tumor-associated macrophages and neutrophils. *Proc. Natl. Acad. Sci. USA* **109**, 2491–2496.
- Cortez-Retamozo, V., Etzrodt, M., Newton, A., Ryan, R., Pucci, F., Sio, S.W., Kuswanto, W., Rauch, P.J., Chudnovskiy, A., Iwamoto, Y., et al. (2013). Angiotensin II drives the production of tumor-promoting macrophages. *Immunity* **38**, 296–308.
- De Palma, M., and Lewis, C.E. (2013). Macrophage regulation of tumor responses to anticancer therapies. *Cancer Cell* **23**, 277–286.
- DuPage, M., Cheung, A.F., Mazumdar, C., Winslow, M.M., Bronson, R., Schmidt, L.M., Crowley, D., Chen, J., and Jacks, T. (2011). Endogenous T cell responses to antigens expressed in lung adenocarcinomas delay malignant tumor progression. *Cancer Cell* **19**, 72–85.
- Fridman, W.H., Pagès, F., Sautès-Fridman, C., and Galon, J. (2012). The immune contexture in human tumours: impact on clinical outcome. *Nat. Rev. Cancer* **12**, 298–306.
- Gajewski, T.F., Schreiber, H., and Fu, Y.X. (2013). Innate and adaptive immune cells in the tumor microenvironment. *Nat. Immunol.* **14**, 1014–1022.
- Gao, Q., Qiu, S.J., Fan, J., Zhou, J., Wang, X.Y., Xiao, Y.S., Xu, Y., Li, Y.W., and Tang, Z.Y. (2007). Intratumoral balance of regulatory and cytotoxic T cells is associated with prognosis of hepatocellular carcinoma after resection. *J. Clin. Oncol.* **25**, 2586–2593.
- Ghiringhelli, F., Larmonier, N., Schmitt, E., Parcellier, A., Cathelin, D., Garrido, C., Chauffert, B., Solary, E., Bonnotte, B., and Martin, F. (2004). CD4+CD25+ regulatory T cells suppress tumor immunity but are sensitive to cyclophosphamide which allows immunotherapy of established tumors to be curative. *Eur. J. Immunol.* **34**, 336–344.
- Gou, H.F., Huang, J., Shi, H.S., Chen, X.C., and Wang, Y.S. (2014). Chemotherapy with oxaliplatin and interleukin-7 inhibits colon cancer metastasis in mice. *PLoS ONE* **9**, e85789.
- Gubin, M.M., Zhang, X., Schuster, H., Caron, E., Ward, J.P., Noguchi, T., Ivanova, Y., Hundal, J., Arthur, C.D., Krebber, W.J., et al. (2014). Checkpoint

- blockade cancer immunotherapy targets tumour-specific mutant antigens. *Nature* 515, 577–581.
- Herbst, R.S., Soria, J.C., Kowanzet, M., Fine, G.D., Hamid, O., Gordon, M.S., Sosman, J.A., McDermott, D.F., Powderly, J.D., Gettinger, S.N., et al. (2014). Predictive correlates of response to the anti-PD-L1 antibody MPDL3280A in cancer patients. *Nature* 515, 563–567.
- Klug, F., Prakash, H., Huber, P.E., Seibel, T., Bender, N., Halama, N., Pfirschke, C., Voss, R.H., Timke, C., Umansky, L., et al. (2013). Low-dose irradiation programs macrophage differentiation to an iNOS⁺/M1 phenotype that orchestrates effective T cell immunotherapy. *Cancer Cell* 24, 589–602.
- Kroemer, G., Galluzzi, L., Kepp, O., and Zitvogel, L. (2013). Immunogenic cell death in cancer therapy. *Annu. Rev. Immunol.* 31, 51–72.
- Lu, L., Xu, X., Zhang, B., Zhang, R., Ji, H., and Wang, X. (2014). Combined PD-1 blockade and GITR triggering induce a potent antitumor immunity in murine cancer models and synergizes with chemotherapeutic drugs. *J. Transl. Med.* 12, 36.
- Lutsiak, M.E., Semnani, R.T., De Pascalis, R., Kashmiri, S.V., Schlom, J., and Sabzevari, H. (2005). Inhibition of CD4(+)/25+ T regulatory cell function implicated in enhanced immune response by low-dose cyclophosphamide. *Blood* 105, 2862–2868.
- Olive, K.P., Jacobetz, M.A., Davidson, C.J., Gopinathan, A., McIntyre, D., Honess, D., Madhu, B., Goldgraben, M.A., Caldwell, M.E., Allard, D., et al. (2009). Inhibition of Hedgehog signaling enhances delivery of chemotherapy in a mouse model of pancreatic cancer. *Science* 324, 1457–1461.
- Oliver, T.G., Mercer, K.L., Sayles, L.C., Burke, J.R., Mendus, D., Lovejoy, K.S., Cheng, M.H., Subramanian, A., Mu, D., Powers, S., et al. (2010). Chronic cisplatin treatment promotes enhanced damage repair and tumor progression in a mouse model of lung cancer. *Genes Dev.* 24, 837–852.
- Peer, D., Karp, J.M., Hong, S., Farokhzad, O.C., Margalit, R., and Langer, R. (2007). Nanocarriers as an emerging platform for cancer therapy. *Nat. Nanotechnol.* 2, 751–760.
- Postow, M.A., Chesney, J., Pavlick, A.C., Robert, C., Grossmann, K., McDermott, D., Linette, G.P., Meyer, N., Giguere, J.K., Agarwala, S.S., et al. (2015). Nivolumab and ipilimumab versus ipilimumab in untreated melanoma. *N. Engl. J. Med.* 372, 2006–2017.
- Rizvi, N.A., Hellmann, M.D., Snyder, A., Kvistborg, P., Makarov, V., Havel, J.J., Lee, W., Yuan, J., Wong, P., Ho, T.S., et al. (2015). Cancer immunology. Mutational landscape determines sensitivity to PD-1 blockade in non-small cell lung cancer. *Science* 348, 124–128.
- Rooney, M.S., Shukla, S.A., Wu, C.J., Getz, G., and Hacohen, N. (2015). Molecular and genetic properties of tumors associated with local immune cytolytic activity. *Cell* 160, 48–61.
- Ruffell, B., Chang-Strachan, D., Chan, V., Rosenbusch, A., Ho, C.M., Pryer, N., Daniel, D., Hwang, E.S., Rugo, H.S., and Coussens, L.M. (2014). Macrophage IL-10 blocks CD8+ T cell-dependent responses to chemotherapy by suppressing IL-12 expression in intratumoral dendritic cells. *Cancer Cell* 26, 623–637.
- Sato, E., Olson, S.H., Ahn, J., Bundy, B., Nishikawa, H., Qian, F., Jungbluth, A.A., Frosina, D., Gnjjatic, S., Ambrosone, C., et al. (2005). Intraepithelial CD8+ tumor-infiltrating lymphocytes and a high CD8+/regulatory T cell ratio are associated with favorable prognosis in ovarian cancer. *Proc. Natl. Acad. Sci. USA* 102, 18538–18543.
- Schiavoni, G., Sistigu, A., Valentini, M., Mattei, F., Sestili, P., Spadaro, F., Sanchez, M., Lorenzi, S., D'Urso, M.T., Belardelli, F., et al. (2011). Cyclophosphamide synergizes with type I interferons through systemic dendritic cell reactivation and induction of immunogenic tumor apoptosis. *Cancer Res.* 71, 768–778.
- Schreiber, R.D., Old, L.J., and Smyth, M.J. (2011). Cancer immunoeediting: integrating immunity's roles in cancer suppression and promotion. *Science* 331, 1565–1570.
- Schumacher, T.N., and Schreiber, R.D. (2015). Neoantigens in cancer immunotherapy. *Science* 348, 69–74.
- Shalpour, S., Font-Burgada, J., Di Caro, G., Zhong, Z., Sanchez-Lopez, E., Dhar, D., Willmsky, G., Ammirante, M., Strasner, A., Hansel, D.E., et al. (2015). Immunosuppressive plasma cells impede T-cell-dependent immunogenic chemotherapy. *Nature* 521, 94–98.
- Sharma, P., and Allison, J.P. (2015). The future of immune checkpoint therapy. *Science* 348, 56–61.
- Spranger, S., Bao, R., and Gajewski, T.F. (2015). Melanoma-intrinsic β -catenin signalling prevents anti-tumour immunity. *Nature* 523, 231–235.
- Tesniere, A., Schlemmer, F., Boige, V., Kepp, O., Martins, I., Ghiringhelli, F., Aymeric, L., Michaud, M., Apetoh, L., Barault, L., et al. (2010). Immunogenic death of colon cancer cells treated with oxaliplatin. *Oncogene* 29, 482–491.
- Topalian, S.L., Hodi, F.S., Brahmer, J.R., Gettinger, S.N., Smith, D.C., McDermott, D.F., Powderly, J.D., Carvajal, R.D., Sosman, J.A., Atkins, M.B., et al. (2012). Safety, activity, and immune correlates of anti-PD-1 antibody in cancer. *N. Engl. J. Med.* 366, 2443–2454.
- Topalian, S.L., Drake, C.G., and Pardoll, D.M. (2015). Immune checkpoint blockade: a common denominator approach to cancer therapy. *Cancer Cell* 27, 450–461.
- Torre, L.A., Bray, F., Siegel, R.L., Ferlay, J., Lortet-Tieulent, J., and Jemal, A. (2015). Global cancer statistics, 2012. *CA Cancer J. Clin.* 65, 87–108.
- Tumeh, P.C., Harview, C.L., Yearley, J.H., Shintaku, I.P., Taylor, E.J., Robert, L., Chmielowski, B., Spasic, M., Henry, G., Ciobanu, V., et al. (2014). PD-1 blockade induces responses by inhibiting adaptive immune resistance. *Nature* 515, 568–571.
- Wolchok, J.D., Kluger, H., Callahan, M.K., Postow, M.A., Rizvi, N.A., Lesokhin, A.M., Segal, N.H., Ariyan, C.E., Gordon, R.A., Reed, K., et al. (2013). Nivolumab plus ipilimumab in advanced melanoma. *N. Engl. J. Med.* 369, 122–133.
- Zitvogel, L., Galluzzi, L., Smyth, M.J., and Kroemer, G. (2013). Mechanism of action of conventional and targeted anticancer therapies: reinstating immunosurveillance. *Immunity* 39, 74–88.

Facilitating T Cell Infiltration in Tumor Microenvironment Overcomes Resistance to PD-L1 Blockade

Haidong Tang,^{1,2} Yang Wang,^{1,2} Lukasz K. Chlewicki,¹ Yuan Zhang,¹ Jingya Guo,³ Wei Liang,³ Jieyi Wang,⁴ Xiaoxiao Wang,⁵ and Yang-Xin Fu^{2,3,*}

¹Department of Pathology and Committee on Immunology, University of Chicago, Chicago, IL 60637, USA

²Department of Pathology, University of Texas Southwestern Medical Center, Dallas, TX 75235, USA

³Chinese Academy of Science Key Laboratory for Infection and Immunity, IBP-UTSW Joint Immunotherapy Group, Institute of Biophysics, Chinese Academy of Sciences, Beijing 100101, China

⁴Oncology Biologics, AbbVie Biotherapeutics Research (ABR), 1500 Seaport Boulevard, Redwood City, CA 94063, USA

⁵Alphamab Co. Ltd., Suzhou, Jiangsu 215125, China

*Correspondence: yang-xin.fu@utsouthwestern.edu

<http://dx.doi.org/10.1016/j.ccell.2016.02.004>

SUMMARY

Immune checkpoint blockade therapies fail to induce responses in the majority of cancer patients, so how to increase the objective response rate becomes an urgent challenge. Here, we demonstrate that sufficient T cell infiltration in tumor tissues is a prerequisite for response to PD-L1 blockade. Targeting tumors with tumor necrosis factor superfamily member LIGHT activates lymphotoxin β -receptor signaling, leading to the production of chemokines that recruit massive numbers of T cells. Furthermore, targeting non-T cell-inflamed tumor tissues by antibody-guided LIGHT creates a T cell-inflamed microenvironment and overcomes tumor resistance to checkpoint blockade. Our data indicate that targeting LIGHT might be a potent strategy to increase the responses to checkpoint blockades and other immunotherapies in non-T cell-inflamed tumors.

INTRODUCTION

The Programmed Cell Death Protein 1 (also known as CD279 and PD-1) and its ligand PD-1 Ligand (PD-L1) signaling pathway is a critical immune checkpoint that functions normally to protect against autoimmunity (Keir et al., 2008; Nishimura et al., 2001). Increasing evidence has suggested that PD-1 signaling is also an important mechanism utilized by tumors to escape antitumor immune responses (Dong et al., 2002; Iwai et al., 2002; Shin and Ribas, 2015). Recent clinical trials with anti-PD-1 and PD-L1 monoclonal antibodies have shown unprecedented durable responses in some patients with a variety of cancers (Brahmer et al., 2012; Topalian et al., 2012). Unfortunately, only a minority of the total of treated patients respond to the current immuno-

therapy treatment. Thus, it has become a primary priority to identify the factors that determine the responsiveness to checkpoint blockade, and to develop strategies that could potentially increase the patient response rates (Sznol and Chen, 2013).

Some recent retrospective clinical studies have shown correlations between tumor PD-L1 expression and response to PD-1/PD-L1 checkpoint blockade therapy (Herbst et al., 2014; Topalian et al., 2012). In contrast, other studies have also suggested that the presence of tumor-infiltrating lymphocytes (TILs) is an important biomarker for predicting responses to PD-L1 blockade therapy (Tumeh et al., 2014). Interestingly, the presence of TILs has been previously shown to correlate with better patient outcomes during various antitumor therapies in multitude of cancers (Galon et al., 2006; Hwang et al., 2012; Mahmoud et al., 2011).

Significance

PD-1/PD-L1 blockade can produce positive responses in cancer patients. Most studies aiming to increase response rates to immune checkpoint blockade focus on combining PD-1/PD-L1 blockade with other checkpoint therapies for T cell activation. However, we demonstrate that increasing tumor-infiltrating T cells in unresponsive tumors can also promote responses to checkpoint blockade, and conversely, inhibiting T cell infiltration in responsive tumors can diminish the efficacy. We generated an antibody-guided LIGHT fusion protein that is able to create a T cell-inflamed tumor microenvironment. We further demonstrate that antibody-LIGHT is able to overcome tumor resistance to checkpoint blockade by increasing T cell infiltration. Our study has created a strategy that could potentially increase the response rates to checkpoint blockades in cancer patients.

However, it is commonly known that the tumor microenvironment often inhibits activated T cells from entering tumor tissues or prevents effective T cell priming for tumor control through various pathways (Gajewski et al., 2013). By using only clinical samples and data, it is difficult to dissect the relative contribution of PD-L1 and TILs for responsiveness to PD-L1 blockade; thus, proper mouse tumor models are needed for conclusive mechanism studies.

Our laboratory has previously shown that upregulation of LIGHT (which stands for “homologous to lymphotoxin, exhibits inducible expression and competes with HSV glycoprotein D for binding to herpesvirus entry mediator, a receptor expressed on T lymphocytes”) in peripheral tissues results in T cell activation and migration into non-lymphoid tissues and the formation of lymphoid-like structures, which can lead to rapid T cell-mediated tissue destruction (Lee et al., 2006). LIGHT, also known as tumor necrosis factor superfamily member 14 (TNFSF14), is one of the co-stimulatory molecules that can regulate T cell activation (Wang et al., 2009). LIGHT is predominantly expressed on immune cells, especially on the surface of immature dendritic cells (DCs) and activated T cells. Forced expression of LIGHT in tumor cells promotes the formation of lymphoid-like structures for direct T cell sequestration and activation, leading to tumor regression (Yu et al., 2004, 2007). Furthermore, adoptive transfer of LIGHT-expressing mesenchymal stem cells can enhance T cell infiltration and efficiently control tumors (Zou et al., 2012).

LIGHT is a ligand protein that can bind to two different receptors, herpesvirus entry mediator (HVEM), which is also known as tumor necrosis factor receptor superfamily member 14 (TNFRSF14) and is encoded by *TNFRSF14*, and lymphotoxin β receptor (LT β R), which is encoded by *LTBR*. The binding of LIGHT to HVEM delivers a co-stimulatory signal to T cells (Wang et al., 2009). In addition, LIGHT can bind to LT β R, which is commonly expressed on non-lymphoid cells, and is critical for the formation of secondary and tertiary lymphoid structures (Fu and Chaplin, 1999; Ware, 2005). LT β R plays a pivotal role in the formation of lymph nodes (LNs) and in the organization of distinct T cell and B cell zones in secondary lymphoid organs. Signaling via LT β R regulates the expression of various chemokines and adhesion molecules that control the migration and positioning of DCs and lymphocytes in the spleen (Cyster, 1999). Overexpression of lymphotoxin in non-lymphoid tissues is sufficient to promote functional lymphoid neogenesis (Ruddle, 1999). These activities indicate that activating LIGHT signaling might be an attractive approach to increase lymphocyte infiltration in tumor tissues. Based on these studies, we sought to test whether targeting LIGHT into tumor tissues could increase TIL numbers, and whether it could synergize with current checkpoint blockade therapies.

RESULTS

Higher T Cell Infiltration, but Not PD-L1 Level, Is Associated with Responsiveness to Checkpoint Blockade

The mechanistic studies about whether and how TILs or PD-L1 are required for a positive response to checkpoint blockades has not been completely elucidated due to the lack of proper experimental models. To understand why some PD-L1⁺ tumors

do not respond to PD-L1 blockade while other tumors do respond, we compared a series of well-established mouse tumor lines for their PD-L1 expression and responsiveness to anti-PD-L1 treatment (Table S1). Interestingly, the implanted tumor lines, such as MC38 and Ag104Ld, represent distinct models mirroring what have been observed in the clinic; specifically, MC38 and Ag104Ld both have similarly high levels of PD-L1 expression while having different responsiveness to anti-PD-L1 therapy (Figures 1A–1C and Table S1). When stimulated by interferon- γ (IFN- γ), they both upregulated PD-L1 to similar levels, indicating there was no intrinsic defects in PD-L1 expression upon stimulation in both cell lines (Figure 1A). Mice bearing MC38 tumors were able to control their tumor burdens effectively with anti-PD-L1 treatment (Figure 1B). In contrast, mice bearing Ag104Ld tumors treated with the same anti-PD-L1 did not respond to treatment and the tumor burdens were not controlled (Figure 1C). Both ex vivo MC38 and Ag104Ld tumors expressed similar levels of PD-L1, as analyzed by flow cytometry (Figure 1D). In addition, there was no significant difference of PD-L1 expression in TILs (Figures S1A–S1C). These data suggest that factors other than PD-L1 expression inside the tumor environment might be essential for responsiveness to PD-L1 blockade therapy.

To determine whether MC38 and Ag104Ld might have different tumor microenvironments that could contribute to the differences in response to checkpoint blockade therapy, we decided to examine the tumors and look for the presence of TILs. To compare the levels of lymphocyte infiltration, we collected tumor tissues and analyzed them using flow cytometry. Interestingly, MC38 tumors have much more (up to 5-fold) T cells (CD45⁺CD3⁺) than Ag104Ld tumors. Among the tumor-infiltrating T cells, the percentage of CD8⁺ T cells is also higher in MC38 (Figure 1E). Specifically, there is approximately 7- to 10-fold more CD8⁺ T cells in MC38 than in Ag104Ld. These data raise the possibility that more CD8⁺ T cells inside MC38 tumors, not seen in Ag104Ld tumors, lead to its responsiveness to anti-PD-L1. To address the role of TILs for checkpoint blockade responsiveness, we sought two strategies to test: (1) whether a reduction of TILs in MC38 will diminish its response to PD-L1 blockade, and (2) whether an increase in TILs in Ag104Ld will induce its response to PD-L1 blockade.

To address whether a higher number of TILs in MC38 is responsible for its responsiveness to PD-L1 blockade, we utilized FTY720 to block new lymphocyte infiltration. FTY720 is a small-molecule analog of sphingosine 1-phosphate (S1P). FTY720 treatment induces the internalization and degradation of S1P receptor, thereby preventing lymphocyte egress from the LNs (Thompson et al., 2010). After a single injection of FTY720, there was ~90% reduction in peripheral T cells (Figure S1D). Circulating T cell numbers gradually recovered by 4 days after injection. The concentration of FTY720 used does not induce cell death in vitro (Figures S1E–S1H). To test whether a higher number of TILs is required for the response to PD-L1 blockade, we treated mice with FTY720 after MC38 tumor inoculation. After tumors were established, mice were treated with anti-PD-L1. Strikingly, the antitumor effects of anti-PD-L1 were completely abrogated in the presence of FTY720 (Figure 1F). These data suggest that a significant number of TILs is a prerequisite for the response to PD-L1 blockade.

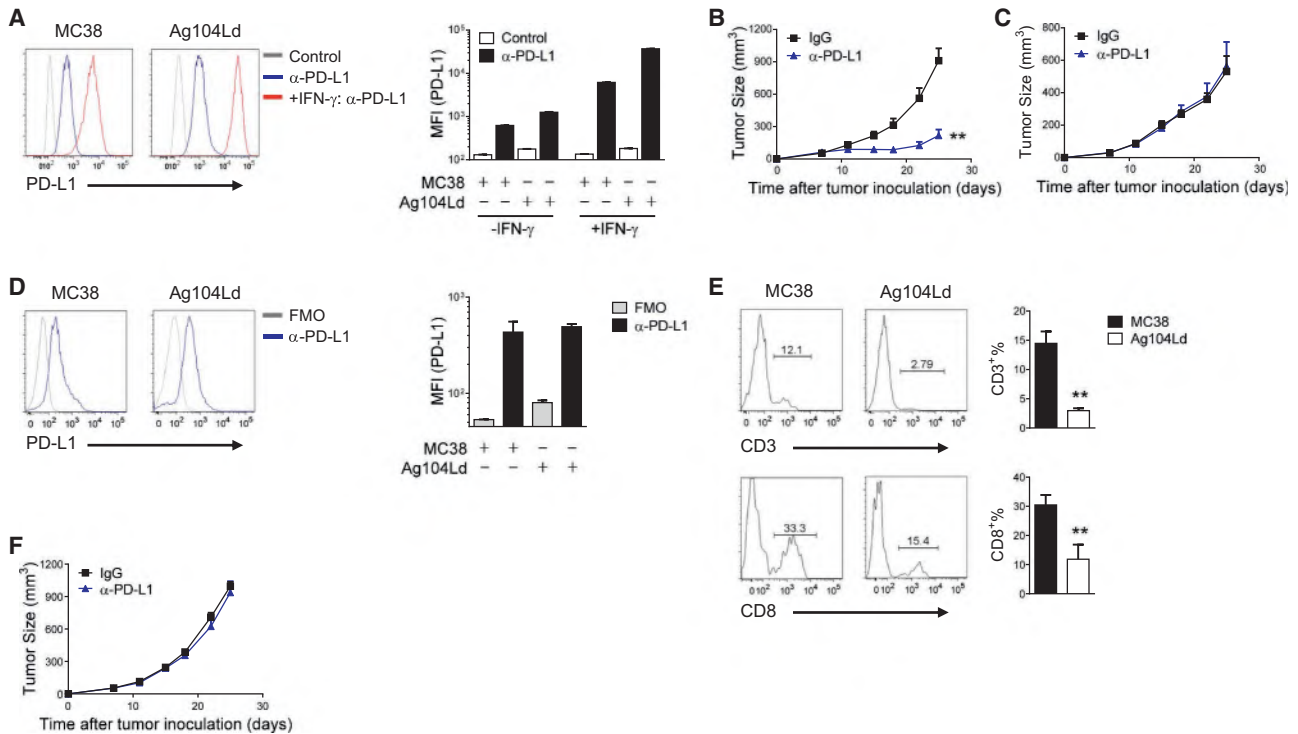


Figure 1. Significant Lymphocyte Infiltration Is Associated with Responsiveness to PD-L1 Blockade

(A) MC38 and Ag104Ld cells were treated with or without 500 U/ml IFN- γ for 24 hr then stained with anti-PD-L1. The expression levels of PD-L1 were measured by flow cytometry. Mean fluorescent intensities (MFIs) of PD-L1 staining were compared. (B) WT B6 mice were inoculated subcutaneously with 1×10^6 MC38 cells on day 0. On days 7 and 10, mice were treated with 200 μ g of anti-PD-L1 or control IgG. Tumor growth was measured and compared twice weekly. (C) B6C3F1 mice were injected subcutaneously with 1×10^6 Ag104Ld cells and treated with 200 μ g of anti-PD-L1 or control IgG on days 7 and 10. (D) Tumor tissues were collected 7 days after inoculation. PD-L1 expression levels in CD45⁺ cells were measured by flow cytometry. FMO, fluorescence minus one. (E) Tumor tissues were collected as in (D). Percentages of CD3⁺ among CD45⁺ cells (upper panel) and CD8⁺ among CD3⁺ cells (lower panel) were analyzed by flow cytometry. (F) WT B6 mice were injected subcutaneously with 1×10^6 MC38 cells on day 0 and treated with FTY720 from day 1. On days 7 and 10, mice were treated with 200 μ g of anti-PD-L1 or control IgG. Tumor growth was measured and compared twice weekly. Data indicate mean \pm SEM and are representative of two (A, B, F) or three (C, D, E) independent experiments. ** $p < 0.01$. See also Figure S1 and Table S1.

Generation and Selection of Human LIGHT Mutants that Bind to Mouse Receptors with Higher Affinities

To test our hypothesis that increased TILs in non-T cell-inflamed tumors, such as Ag104Ld, are able to induce response to PD-L1 blockade, we sought to target LIGHT signaling to increase infiltration. Initial attempts to produce recombinant LIGHT protein to target tumor tissues were not successful, since recombinant mouse LIGHT (mLIGHT) is not stable and tends to aggregate (data not shown; Del Rio et al., 2010). On the other hand, human LIGHT (hLIGHT) is more stable but fails to bind mouse receptors, and thus cannot be used in experimental mouse models. To verify the absence of cross-species binding, we performed binding experiments using a yeast-displayed version of wild-type (WT) hLIGHT that showed undetectable binding to mouse LT β R and HVEM (mLT β R and mHVEM), with positive binding to human LT β R and HVEM (hLT β R and hHVEM) (Figure 2A). To better evaluate the therapeutic efficacy of hLIGHT construct in experimental model systems, we engineered a LIGHT protein that has the capabilities of binding and activating both human and mouse receptors. HmLIGHT (human LIGHT mutant that

can effectively bind both human and mouse receptors) was selected from a random error mutagenesis library of hLIGHT using yeast surface display. Engineered mutants of hLIGHT that had increased surface expression (indicative of protein stability) and binding to both mouse and human receptors were isolated (Figure 2A). Several of these mutants have been identified. One of these mutants has been chosen for further studies due to its remarkable thermal stability (LT β R binding above 80°C, Figure 2B) and similarly higher binding affinities to both mouse and human receptors in the yeast display system. Sequencing results showed the presence of four point mutations between hmLIGHT and WT hLIGHT (Figure 2C). This stable and higher-affinity hmLIGHT may have an increased therapeutic efficacy in an immunocompetent host, with the additional benefit of being suitable for both mouse and human experimental model systems.

Production and Characterization of Antibody-LIGHT Fusion Protein In Vitro

To confirm the functionality of the sequence isolated from the yeast display system, we cloned hmLIGHT to produce

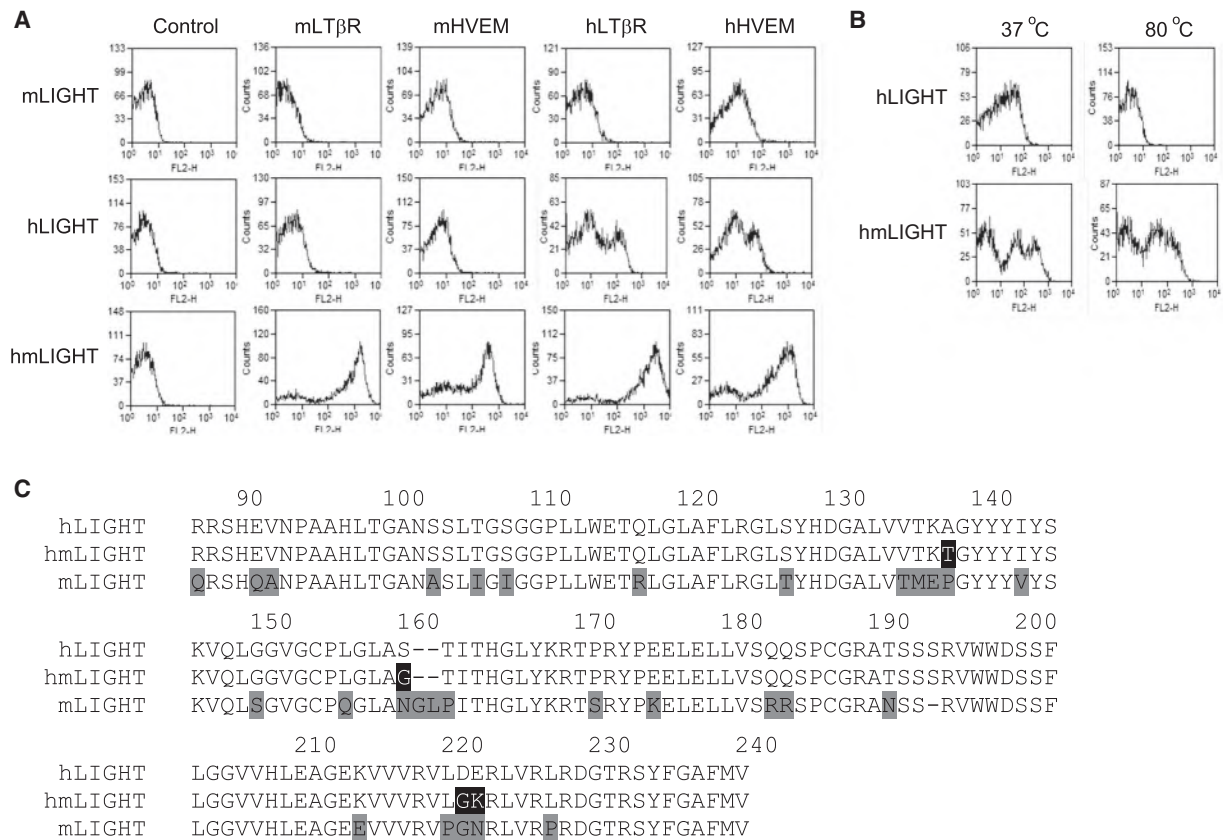


Figure 2. Engineered LIGHT Has Increased Stability and Binding Affinities to Both Human and Mouse Receptors

(A) Flow cytometry histograms of yeast-displayed mLIGHT, hLIGHT, and hmLIGHT clones. All clones were stained with the indicated ligands and analyzed by flow cytometry.

(B) Flow cytometry histograms from thermal denaturation experiments using yeast-displayed hLIGHT and hmLIGHT. Samples were heated at indicated temperatures for 30 min and stained with mLT β R.

(C) Amino acid sequence alignment of hLIGHT, mLIGHT, and hmLIGHT. Residues highlighted by black indicate the differences between hmLIGHT and hLIGHT. Differences between mLIGHT and hLIGHT are highlighted by gray.

recombinant protein. First, we confirmed that hmLIGHT was capable of binding to both human and mouse receptors in ELISA assays with great sensitivity (Figure 3A). Second, we were able to demonstrate activation of signaling, since stimulation of human T cells by hmLIGHT induced the production of IFN- γ in a dose-dependent manner (data not shown). HmLIGHT also induced the production of IFN- γ in mouse splenocytes (Figure 3B) and interleukin-6 (IL-6) in mouse embryonic fibroblast cells (Figure 3C), while hLIGHT only showed limited activity.

Given the limitations of a therapeutic that requires local delivery to patients, and that systemic injections of immune cytokine can often lead to dose-dependent side effects, we wanted to develop a system that can provide targeted delivery of LIGHT (Yang et al., 2014). To study the mechanism of targeted LIGHT delivery, we took advantage of the inherent specificities of antibody fusion proteins. We generated an anti-epidermal growth factor receptor (EGFR)-hmLIGHT fusion protein (Ab-LIGHT) to specifically target hmLIGHT to EGFR-expressing tumor tissues. To avoid aggregations, we linked together three units of hmLIGHT (3 \times hmLIGHT) using polypeptide linkers, and fused them to the N-terminal of antibody immunoglobulin G (IgG) Fc

(Figure 3D). The resulting anti-EGFR-hmLIGHT fusion protein could specifically bind to both EGFR and mLT β R/mHVEM (Figures 3E, S2A, and S2B). In vitro activities of the fusion protein were further confirmed by its ability to induce IFN- γ production in mouse splenocytes (Figure 3F). This stimulation could be abrogated by recombinant mHVEM-Ig. Furthermore, the fusion protein can specifically target to EGFR-positive tumor tissues when delivered systemically (Figure S2C). Together, these data suggest that hmLIGHT has functional capabilities to bind and specifically activate LIGHT receptors in vitro.

Targeted Delivery of LIGHT Eradicates Established Tumors

To test the activity of hmLIGHT in targeting tumors in vivo, we treated mice bearing established EGFR-expressing tumors with anti-EGFR-hmLIGHT or control antibody. Ag104Ld is a highly progressive tumor model that is resistant to most immunotherapies through unknown mechanisms (Chen et al., 1994; Melero et al., 1997; Ward et al., 1989; Wick et al., 1997; Yu et al., 2005). We hypothesized that the lack of sufficient TILs makes Ag104Ld less responsive to most immunotherapies. Strikingly,

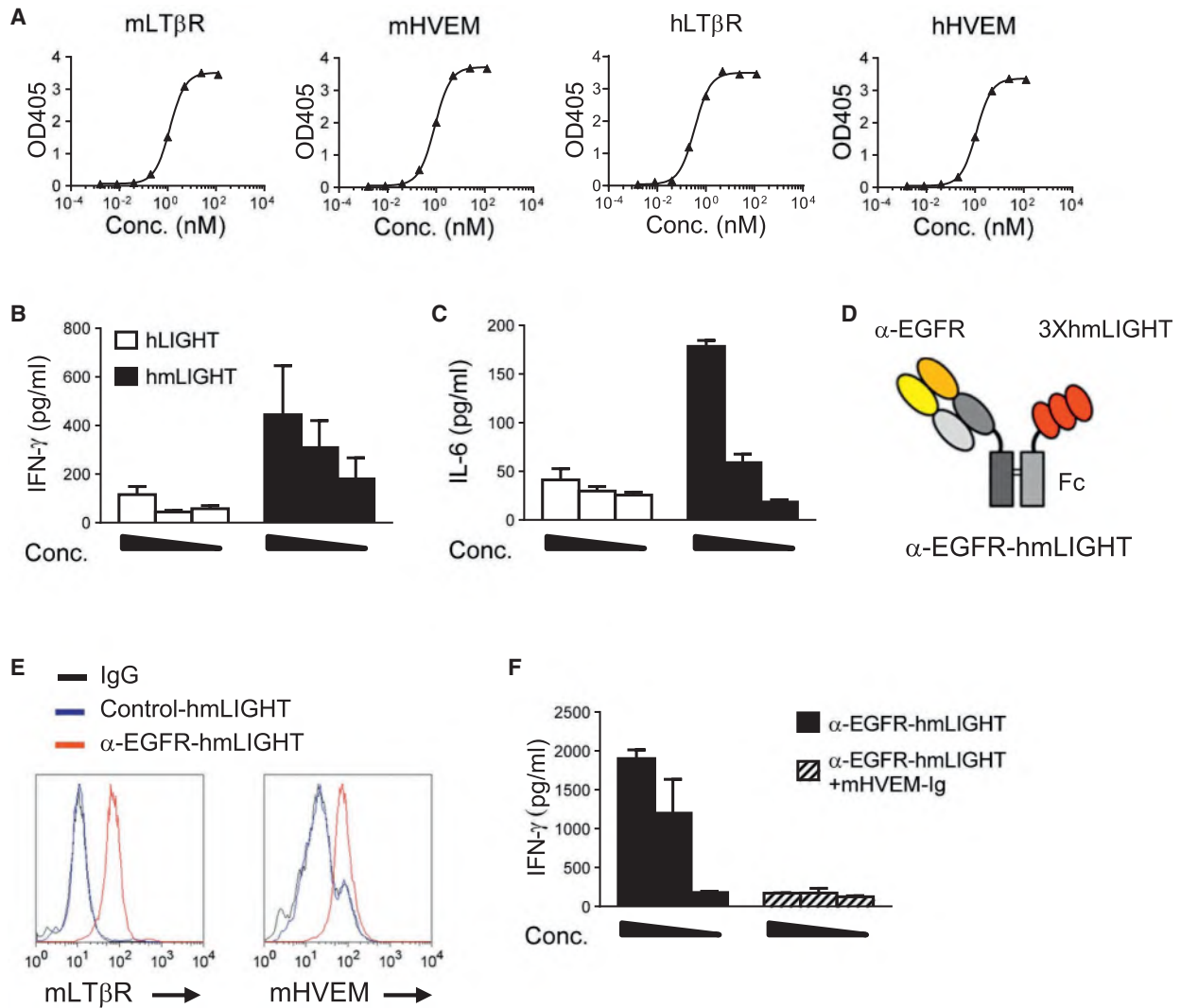


Figure 3. In Vitro Characterization of hmLIGHT Fusion Protein

(A) Binding between recombinant hmLIGHT and human/mouse LTβR/HVEM were measured by ELISA.

(B) Splenocytes from *Rag1*^{-/-} mice were stimulated with 25, 5, or 1 nM of hLIGHT or hmLIGHT for 48 hr. IFN-γ levels in culture supernatants were measured by cytometric bead array (CBA).

(C) Mouse embryonic fibroblast cells were stimulated with hLIGHT or hmLIGHT for 24 hr. IL-6 levels were measured by CBA.

(D) Schematic representation shows anti-EGFR-hmLIGHT fusion protein construction.

(E) B16-EGFR cells were incubated with anti-EGFR-hmLIGHT, followed by mLTβR or mHVEM staining. A control antibody-hmLIGHT fusion protein was used as negative control.

(F) Splenocytes from *Rag1*^{-/-} mice were pretreated with or without mHVEM-Ig fusion protein before treated with 25, 5, or 1 nM anti-EGFR-hmLIGHT for 48 hr. IFN-γ levels were measured by CBA.

Data indicate mean ± SEM and are representative of at least two independent experiments. Conc., concentration. See also Figure S2.

anti-EGFR-hmLIGHT induced complete regression in established EGFR-expressing Ag104Ld tumors, while control antibody or anti-PD-L1 alone has no effect on tumor growth (Figures 4A and 1C). No significant side effect was observed, as we did not see significant changes in either body weights or serum inflammatory cytokines (data not shown). The antitumor effects of anti-EGFR-hmLIGHT depend on EGFR-expression on tumor cells, as EGFR-negative tumor fails to respond to the treatment (data not shown). To test whether LIGHT-mediated antitumor responses result in prolonged protective T cell immunity, we rechallenged

mice that underwent complete tumor regression after anti-EGFR-hmLIGHT treatment with a lethal dose of Ag104Ld-EGFR cells. All the mice rejected the rechallenged tumor (Figure 4B). Therefore, LIGHT is able to mediate rejection of a highly progressive tumor that is traditionally thought to be resistant to immunotherapies. In addition, LIGHT allows for the generation of memory cells that can mediate protection.

When tumor cells are initially transplanted into immunocompetent hosts, massive tumor cell necrosis leads to inflammation within the first few days (Dirkx et al., 2006). Therefore, it is

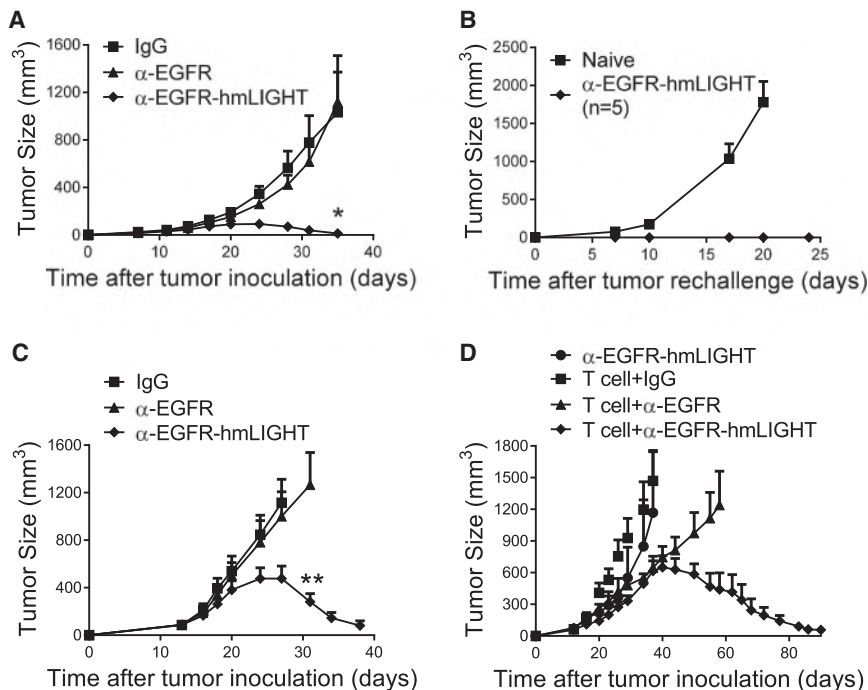


Figure 4. LIGHT Delivered to Tumor Eradicates Established Tumors

(A) B6C3F1 mice were inoculated subcutaneously with 2×10^6 Ag104Ld-EGFR cells and treated with 25 μ g of control IgG, anti-EGFR, or anti-EGFR-hmLIGHT on days 7, 9, 11, and 13. Tumor growth was measured and compared twice weekly.

(B) Two weeks after tumor eradication, mice treated with anti-EGFR-hmLIGHT from (A) were rechallenged with 1×10^7 Ag104Ld-EGFR cells.

(C) *Rag1*^{-/-} mice were inoculated subcutaneously with 1×10^6 MC38-EGFR cells, and 5×10^6 WT splenocytes were adoptively transferred on day 11. Mice were treated with 25 μ g of control IgG, anti-EGFR, or anti-EGFR-hmLIGHT on days 12, 14, 16, and 18.

(D) *Rag1*^{-/-} mice were injected subcutaneously with 1×10^6 A431 cells. OT-1 LN cells (2×10^6) were adoptively transferred on day 13. Twenty-five micrograms of control IgG, anti-EGFR, or anti-EGFR-hmLIGHT (Ab-homotrimer LIGHT from Abbvie) was administered intravenously daily from day 14 to day 18.

Data indicate mean \pm SEM. One representative result of a total of three (A and D) or two (B and C) independent experiments is shown. * $p < 0.05$, ** $p < 0.01$.

possible that this initial inflammation might artificially increase the priming and recruiting of TILs. To avoid this extra priming and infiltrations, we set up a mouse tumor model without such priming of TILs. In this model, *Rag1*^{-/-} mice were challenged with MC38-EGFR cells to allow the growth of tumor without T cell infiltration and priming. After tumors were established, WT splenocytes were transferred before immunotherapy treatment. Significantly, anti-EGFR-hmLIGHT showed superior antitumor effects over antibody control (Figure 4C).

One advantage of hmLIGHT is that it can be suitable for both human and mouse experimental models. To test the efficacy of anti-EGFR-hmLIGHT for controlling human tumor, and for possible future clinical implications, we developed a xenograft model using immune-reconstituted mice (Lee et al., 2009; Yang et al., 2013). *Rag1*^{-/-} mice were inoculated with human A431 tumor cells that were previously established from an epidermoid carcinoma patient. After tumors were established, 2 million LN cells (~50% T cells) from ovalbumin-specific class I-restricted T cell receptor (OT-1 TCR) transgenic mice were adoptively transferred. T cells from OT-1 mice have ~2% non-OT-1 T cells, some of which have the potential to recognize antigens from human tumors. A few hundred potentially specific T cells is comparable with the number of tumor-reactive T cells observed in human patients. Furthermore, among the transferred T cells, ~98% of them are OT-1-specific T cells, which can prevent the homeostatic proliferation of tumor-reactive T cells. Without T cell transfer, A431 tumors grew aggressively. In the presence of T cells, anti-EGFR-hmLIGHT treatment induced much better antitumor effects compared with anti-EGFR control (Figure 4D). The same LIGHT treatment cannot control tumor growth in the absence of LN cells, indicating LIGHT-mediated antitumor effects are T cell dependent. Taken together, these data showed that LIGHT is able to control tumor

growth in different mouse and xenograft human tumor models, and to provide long-term immunological memory.

LIGHT-Mediated Antitumor Immunity Depends on LT β R Signaling

LIGHT has two receptors, LT β R and HVEM. To further elucidate the essential contributions of LT β R and HVEM signaling in LIGHT-mediated antitumor immunity, we treated tumor-bearing *Rag1*^{-/-}; *Ltbr*^{-/-} and *Rag1*^{-/-}; *Tnfrsf14*^{-/-} mice reconstituted with T cells with anti-EGFR-hmLIGHT. Anti-EGFR-hmLIGHT fusion protein failed to control tumor growth in *Rag1*^{-/-}; *Ltbr*^{-/-} mice (Figure 5A). In contrast, anti-EGFR-hmLIGHT was able to control tumors in *Rag1*^{-/-}; *Tnfrsf14*^{-/-} mice as effectively as in *Rag1*^{-/-} mice (Figures 5B and 4C). Similar to *Ltbr*^{-/-} mice, *Rag1*^{-/-}; *Ltbr*^{-/-} mice have multiple immune abnormalities, including lack of secondary lymphoid structures (Zhu et al., 2010). To exclude the possibility that developmental defects dampen antitumor immune responses, we pretreated WT mice bearing Ag104Ld-EGFR tumors with LT β R-Ig before LIGHT treatment. The antitumor activities of anti-EGFR-hmLIGHT were completely abrogated in the presence of LT β R-Ig (Figure 5C). Consistently, depleting CD8⁺ T cells also eliminated the effects. We also determined that both MC38 and Ag104Ld tumors express similar levels of LT β R (Figure S3). Together, these results suggest that LIGHT-mediated antitumor immunity mainly depends on LT β R signaling and T cells.

Activation of LT β R signaling in non-lymphoid tissues promotes functional lymphoid neogenesis (Ruddle, 1999). To find out whether anti-EGFR-hmLIGHT activated LT β R to increase TILs, we collected and analyzed tumor tissues after fusion protein treatment. There was a 300%–500% increase of CD8⁺ T cells in tumor tissues treated with anti-EGFR-hmLIGHT as both CD3⁺ and CD8⁺ cells were significantly increased (Figure 5D). Tumor histology

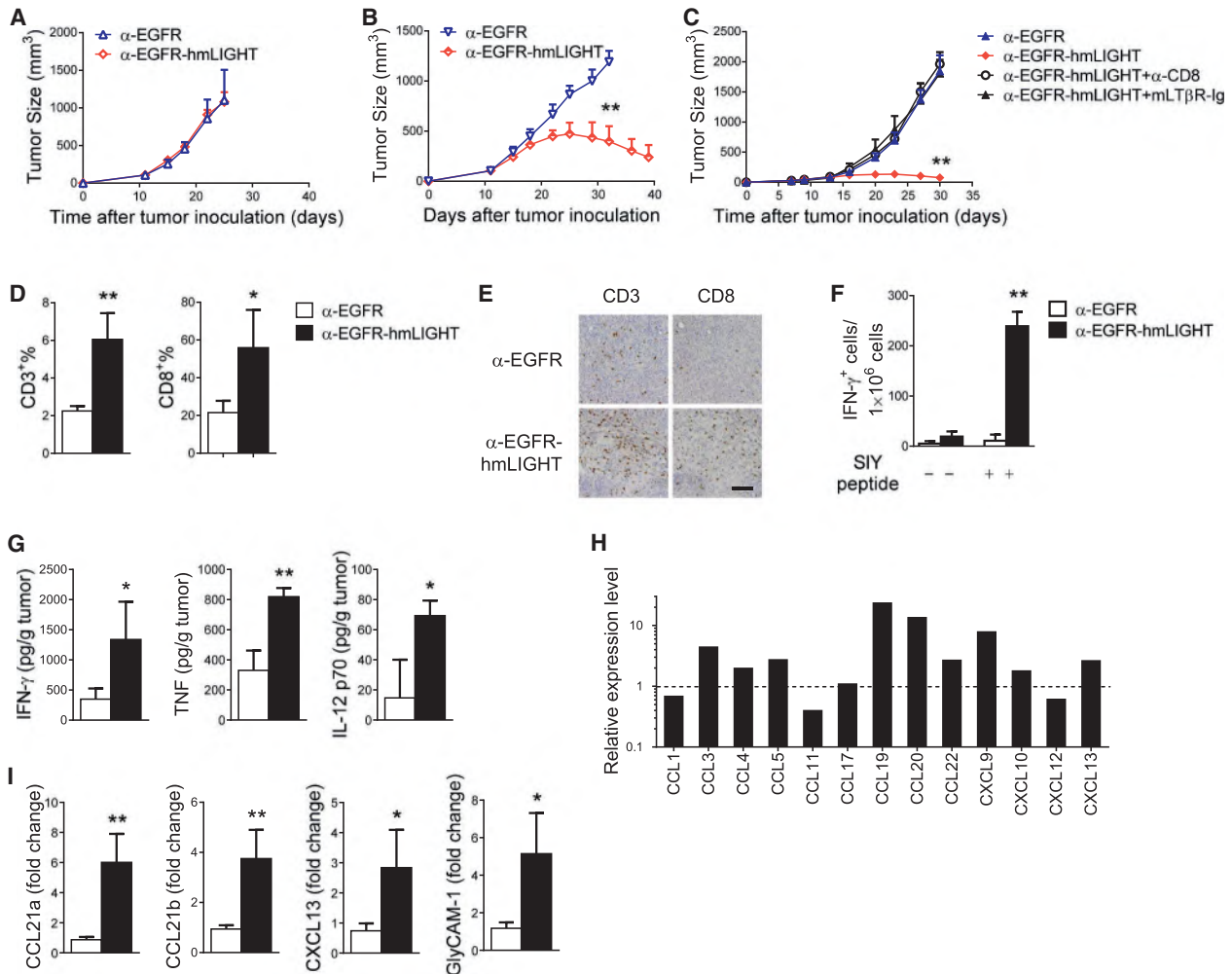


Figure 5. LIGHT-Mediated Antitumor Immunity Depends on LTβR Signaling

(A) *Rag1*^{-/-};*Ltr*^{-/-} or (B) *Rag1*^{-/-};*Tnfrsf14*^{-/-} mice were inoculated subcutaneously with 1 × 10⁶ MC38-EGFR cells. Five million splenocytes were adoptively transferred on day 11. Mice were treated with 25 μg of anti-EGFR or anti-EGFR-hmLIGHT on days 12, 14, 16, and 18. Tumor growth was measured and compared twice weekly.

(C) B6C3F1 mice were inoculated subcutaneously with 2 × 10⁶ Ag104Ld-EGFR cells and treated with 25 μg of anti-EGFR or anti-EGFR-hmLIGHT on days 7, 9, 11, and 13. LTβR-Ig (100 μg/mouse) was administered on days 4, 7, and 11. For CD8⁺ T cell depletion, mice were treated with 200 μg anti-CD8 on days 7 and 11. Tumor growth was measured and compared twice weekly.

(D–I) B6C3F1 mice were inoculated subcutaneously with 2 × 10⁶ Ag104Ld-EGFR cells and treated with 25 μg of anti-EGFR or anti-EGFR-hmLIGHT on days 7, 9, 11, and 13. Tumor tissues were analyzed on day 25. (D) Percentages of CD3⁺ among CD45⁺ cells (left) and CD8⁺ among CD3⁺ cells (right) were analyzed by flow cytometry. (E) Frozen sections of the indicated tumor tissues were stained with hematoxylin and anti-CD3 or anti-CD8. Scale bar, 100 μm. (F) Splenocytes were collected and an IFN-γ ELISPOT assay was performed with or without SIY peptide restimulation. (G) Inflammatory cytokine levels in homogenates from tumor tissues were measured by CBA. (H) RNA was isolated from tumor tissues treated with anti-EGFR or anti-EGFR-hmLIGHT. Relative expression levels of chemokines in pooled samples were measured by RT² PCR Profiler and calculated as (anti-EGFR-hmLIGHT/anti-EGFR). (I) Expressions of CCL21a, CCL21b, CXCL19, and GlyCAM-1 in individual samples were measured by qRT-PCR.

Data shown are representative of two independent experiments (A, B, C, E, F) or the pool of two independent experiments (D, G, I). Data indicate mean ± SEM. *p < 0.05, **p < 0.01. N.S., not significant. See also Figure S3 and Table S2.

showed a higher number of CD3⁺ and CD8⁺ cells after anti-EGFR-hmLIGHT treatment (Figure 5E). The increase in antigen-specific CD8⁺ T cells indicated that a sufficient number of cytotoxic T lymphocytes (CTLs) might play important roles in the rejection of tumors. To track tumor antigen-specific T cell responses, we generated an Ag104Ld-EGFR-SIY tumor cell line using the SIY peptide to mimic mutated antigens. Twelve days after the last anti-EGFR-hmLIGHT treatment, splenocytes from tumor-bearing

mice were collected and an IFN-γ ELISPOT assay was performed in the presence or absence of SIY peptides. The number of SIY-specific T cells dramatically increased after anti-EGFR-hmLIGHT treatment (Figure 5F). Inflammatory cytokine profile analysis showed that there were significant increases in the levels of IFN-γ, TNF-α, and IL-12 (Figure 5G). Taken together, these data suggest that LIGHT can not only increase TILs but also induce tumor-specific T cell responses for tumor control.

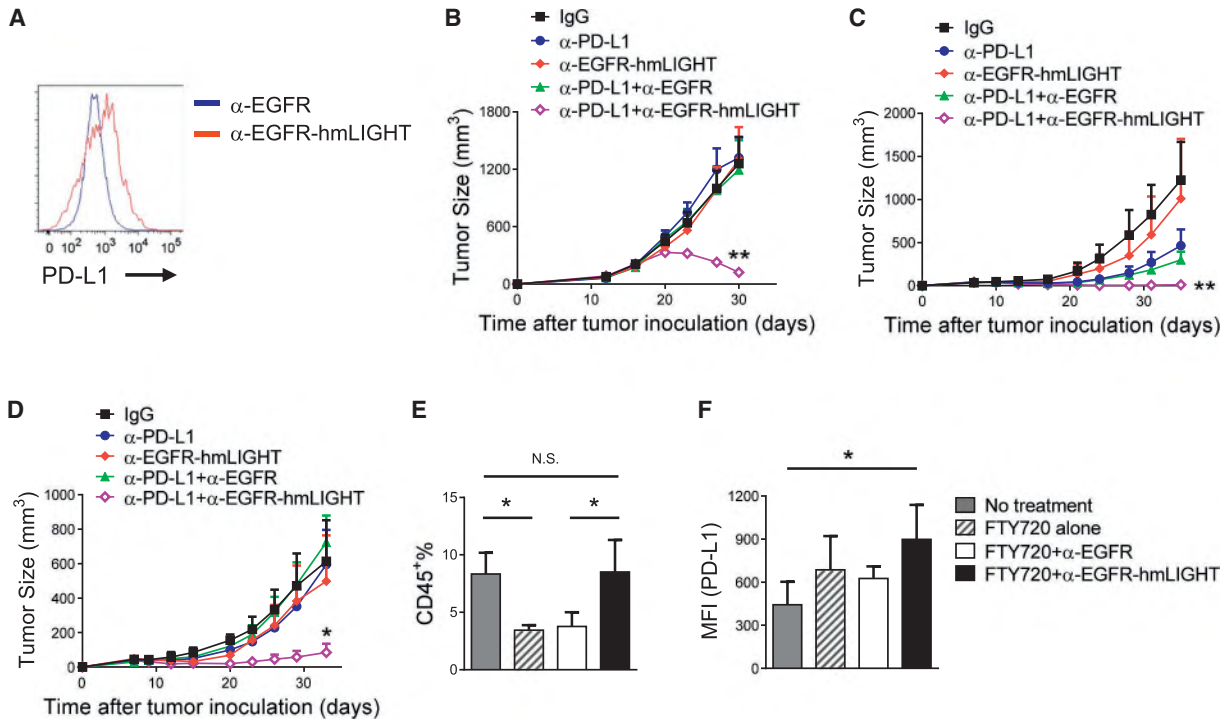


Figure 6. LIGHT Overcomes Tumor Resistance to Checkpoint Blockade

(A) B6C3F1 mice were treated as in Figure 5D. PD-L1 expression in CD45⁻ cells were compared by flow cytometry. (B) B6C3F1 mice were inoculated subcutaneously with 2×10^6 Ag104Ld-EGFR cells and treated with 25 μ g of anti-EGFR or anti-EGFR-hmLIGHT on days 14, 16, 18, and 20. A PD-L1 blocking antibody (200 μ g/mouse) was administered on days 14 and 18. Tumor growth was measured and compared twice weekly. (C) WT B6 mice were injected subcutaneously with 2×10^6 MC38-EGFR cells and treated with 25 μ g of anti-EGFR or anti-EGFR-hmLIGHT on days 7 and 9. Anti-PD-L1 (100 μ g/mouse) was administered on day 7. Tumor growth was measured and compared twice weekly. (D) WT B6 mice were inoculated subcutaneously with 2×10^6 MC38-EGFR cells and treated with FTY720 from day 1 to day 3. Twenty-five micrograms of anti-EGFR or anti-EGFR-hmLIGHT was administered on days 7, 9, 11, and 13. For PD-L1 blockade, mice were treated with 200 μ g anti-PD-L1 on days 7 and 11. (E) Mice were treated as in (D). Two days after the last treatment, tumor tissues were collected and tumor-infiltrating leukocytes (CD3⁺ among CD45⁺ cells) were measured by flow cytometry. (F) MFIs of PD-L1 staining in CD45⁻ cells were compared. Data are representative of three (A, D) or two (B) independent experiments, or the pool of two independent experiments (C, E, F). Data indicate mean \pm SEM. * $p < 0.05$, ** $p < 0.01$. N.S., not significant.

LT β R signaling induces IKK α -dependent expression of lymphoid tissue chemokines and adhesion molecules, which are able to recruit lymphocytes (Dejardin et al., 2002). To compare the chemokine expression profiles after LIGHT treatment, we isolated RNA from tumor tissues and analyzed the expression levels of chemokines by RT² Profiler PCR array. Interestingly, most of the chemokines associated with T cell trafficking were significantly upregulated after anti-EGFR-hmLIGHT treatment (Figure 5H and Table S2) (Bromley et al., 2008). To further confirm that anti-EGFR-hmLIGHT-mediated tumor rejection occurs through activation of LT β R signaling, we performed real-time PCR. The level of CCL21 was increased ~ 6 fold after anti-EGFR-hmLIGHT treatment (Figure 5I). CCL21 is a ligand for CCR7, and is important for the homing of T cells to both lymphoid and non-lymphoid tissues (Lo et al., 2003). Other LT β R-regulated chemokines, including CXCL13 and GlyCAM-1, were also upregulated. Collectively, these data suggest that LIGHT enhances the recruitment of lymphocytes into tumor tissues through LT β R activation, and can induce tumor-specific T cell responses for tumor control and rejection.

LIGHT Overcomes Tumor Resistance to Anti-PD-L1 by Increasing T Cell Infiltration

When tumors became larger, the antitumor effects of LIGHT were gradually reduced. One possibility that could explain why LIGHT treatment does not work on large tumors is due to the fact that LIGHT increases the level of IFN- γ (Figure 5G), which can also promote PD-L1 upregulation as part of the adaptive resistance mechanism (Blank et al., 2004). We hypothesized that LIGHT might trigger inhibitory signals as a negative feedback mechanism, which in turn can dampen the initial antitumor effects on large tumors. To test this notion, we treated tumor-bearing mice with anti-EGFR-hmLIGHT and CD45⁻ cells from tumors were analyzed for PD-L1 expression. Indeed, LIGHT treatment significantly increased the expression level of PD-L1 (Figure 6A). When Ag104Ld-EGFR tumors reached a size >120 mm³, anti-EGFR-hmLIGHT alone had limited effects on tumor growth (Figure 6B). Impressively, additional PD-L1 blockade following LIGHT completely eradicated tumors while PD-L1 blockade or LIGHT treatment alone failed to control tumors. The same synergistic effect was also observed in MC38-EGFR tumors

(Figure 6C). Together, these data suggest that a proper combination treatment that dampens PD-L1 inhibition while increasing new T cell infiltration can overcome checkpoint blockade resistance, thus resulting in better tumor control than either treatment alone.

Since our data showed that LIGHT is efficient in recruiting TILs, we wondered whether LIGHT is able to rescue the responsiveness to checkpoint blockade in non-T cell-inflamed tumor. To test this hypothesis, we treated MC38-EGFR tumor-bearing mice with FTY720 to block lymphocyte trafficking until 4 days before treatment. Mice were then treated with either anti-EGFR-hmLIGHT or anti-PD-L1 alone, or together (Figure 6D). Interestingly, although mice were only treated with FTY720 for the first few days, the antitumor effect of anti-PD-L1 was still completely lost. Strikingly, targeting tumor with LIGHT restored its ability to respond to anti-PD-L1 for tumor burden control (Figure 6D). Flow cytometry analysis showed that there was a significant reduction of TILs after FTY720 blockade (Figure 6E). Anti-EGFR-hmLIGHT treatment increased the number of TILs to a level comparable with that in control mice. Interestingly, LIGHT also increased the level of PD-L1. This observation could explain why LIGHT alone was not sufficient for tumor control while PD-L1 blockade with LIGHT allowed for synergistic responses (Figure 6F). Taken together, these data indicate that significant lymphocyte infiltration is critical for tumor responsiveness to checkpoint blockade immunotherapy. They also show that activation of LT β R signaling by LIGHT is able to overcome resistance to checkpoint blockade by sufficiently increasing lymphocyte infiltration to the tumor tissues.

DISCUSSION

Immune checkpoint blockade is one of the most remarkable advances in recent cancer therapy; however, objective responses are only achieved in a small proportion of patients. Both PD-L1 expression and the presence of TILs have been implicated to correlate with responses to PD-L1 blockade (Herbst et al., 2014; Topalian et al., 2012, 2015; Tumei et al., 2014). Furthermore, the relative contribution of PD-L1 on tumor cells and non-tumor cells, such as DCs, remains to be determined (Curiel et al., 2003; Herbst et al., 2014). In the current study, we showed that sufficient T cell infiltration, and not PD-L1 expression, is essential for tumor responses to checkpoint blockade. Specifically, a PD-L1⁺ tumor with an insufficient number of TILs is unresponsive to anti-PD-L1 immunotherapy. In contrast, a PD-L1⁺ tumor with a sufficient number of TILs can be well controlled by the same immunotherapy. Furthermore, prevention of T cells from entering the tumor microenvironment can transform a checkpoint blockade responsive tumor into an unresponsive tumor. Unfortunately, increasing TILs within established tumor has been very difficult. To develop approaches to effectively increase TILs, we produced an Ab-LIGHT fusion protein to specifically target LIGHT to tumor tissues. In three different tumor models, we were able to show that Ab-LIGHT therapy can control established tumors. We found that Ab-LIGHT activates LT β R signaling to induce the production of chemokines and adhesion molecules in tumor tissues. These chemokines attract lymphocyte to the local tumor tissues, thus resulting in control and rejection of tumors. Therefore, we have

developed a strategy to overcome tumor resistance to checkpoint blockade by increasing lymphocyte infiltration.

Several combination therapies have been developed to increase the response rate to checkpoint blockade (Ai and Curran, 2015). Among them, the combination with anti-PD-1 and anti-CTLA-associated antigen 4 (CTLA-4) has shown the best improvement in clinical trials (Hammers et al., 2014; Postow et al., 2015; Wolchok et al., 2013). CTLA-4 blockade induces the expansion of tumor-infiltrating T cells inside the tumor tissue, which is critical for the efficacy of combination therapy (Cha et al., 2014). However, anti-CTLA-4 might only expand T cells already present inside tumors. The antitumor effects are completely abrogated when initial lymphocyte infiltration is blocked. Specifically, blocking lymphocyte trafficking at a later time point has no effects on the synergy (Spranger et al., 2014). In significant contrast, LIGHT increases TILs by recruiting naive T cells from the periphery (Yu et al., 2004). Spontaneous tumor-infiltrating T cells in established tumors are usually exhausted or anergic due to the inhibitory microenvironment, and are difficult to be reactivated (Crespo et al., 2013). By contrast, newly recruited T cells have less chance to be suppressed and might be easier to be activated. Furthermore, recruiting naive T cells from periphery by LIGHT gives us the potential to maximize the effects of checkpoint blockade therapies in treating tumors without pre-existing lymphocyte infiltrations.

The presence of spontaneous TILs correlates with better prognosis, especially for tumor immunotherapies (Woo et al., 2015). Recently, consistent with our observations, two exceptional studies have shown that both mouse and human tumor cells can be programmed to suppress chemokine production that can limit immune infiltrates, leading to resistance to PD-1 blockade therapies (Peng et al., 2015; Spranger et al., 2015). Unfortunately, limited approaches are available to increase lymphocyte infiltration without severe side effects. IFNs have been considered as such candidates, and our laboratory has shown that an antibody-IFN- β fusion protein can synergize with PD-L1 blockade in a B16 tumor model (Yang et al., 2014). However, increased TILs were only observed in some tumor models but not in others, probably due to the multiple effects downstream of IFNs (H.T. and Y.X.F., unpublished data). B-raf inhibitors represent another candidate that could increase TILs (Wilmott et al., 2012). However, these drugs only work on B-raf mutated tumors, and side effects usually occur during treatment, both of which limit their applications (Boussemaert et al., 2013). Some viral vectors, such as adenovirus, have been shown to enhance lymphocyte infiltration and improve efficacy of adoptive T cell therapy (Tähtinen et al., 2015). Previous studies in our laboratory have used adenovirus-expressing LIGHT for tumor immunotherapy (Lee et al., 2009; Yu et al., 2007). However, such therapies usually require intratumoral injection of the virus, which is not feasible for the majority of patients. Furthermore, safety is another concern if using viral vectors (Pesonen et al., 2010). Recently, Rosa et al. have demonstrated that inhibition of dipeptidylpeptidase 4 (DPP4) preserves active chemokine CXCL10, which can lead to increased lymphocyte infiltration to tumor tissues (da Silva et al., 2015). However, combination therapy with DPP4 inhibitor and checkpoint blockade only had a marginal improvement when compare with checkpoint blockade alone (da Silva et al., 2015). Their study implies that targeting a

single chemokine may not be sufficient to recruit enough lymphocytes for complete tumor control. In fact, when comparing chemokine profiles in MC38 and Ag104Ld tumors, we found that several chemokines related to T cell trafficking, besides CXCL10, were significantly higher in MC38 (data not shown). In contrast to targeting one specific chemokine, LIGHT activates LT β R signaling in tumor tissues, which induces the expression of multiple chemokines and adhesion molecules for effective T cell recruitment to the tumor tissue (Figures 5H and 5I). The induction of multiple chemokines makes LIGHT more efficient for lymphocyte recruitment and activation.

LT β R signaling plays an important role in the organization of lymphocytes during lymphoid neogenesis (Ruddle, 1999), so it is an attractive target for modulating lymphocyte infiltration. Previous attempts have been made to activate LT β R signaling through agonist antibodies for tumor immunotherapy (Lukashev et al., 2006). However the effects were marginal, possibly due to wide expression of LT β R, which makes it difficult to specifically activate signaling in tumor tissues. Another approach to activate LT β R signaling is through engagement with LIGHT. Our laboratory has tried to produce recombinant mLIGHT protein, but it is characteristically unstable and tends to aggregate (data not shown; Del Rio et al., 2010). Human LIGHT is more stable but does not cross-react with mouse receptors. In the past, such human molecules can only be evaluated in xenograft models, which lack the adaptive immune system. However, given the roles of LIGHT on adaptive immunity, it is important to evaluate LIGHT in immunocompetent hosts. By combining the yeast surface display system and random error mutagenesis, we were able to engineer human LIGHT (hmLIGHT) to bind to both human and mouse receptors while remaining stable. We further showed that hmLIGHT is able to induce tumor regression in both mouse and human tumor models (Figure 4). Our study provides the proof of concept for the development of LIGHT for tumor immunotherapy.

Overall, our study proposes several interesting mechanisms that can be used to further cancer immunotherapy. First, our data suggest that a significant T cell-inflamed tumor microenvironment is critical for positive responses to checkpoint blockade. Blocking lymphocyte infiltration will abrogate the responsiveness in an originally anti-PD-L1 responding tumor. Second, we show that targeting LIGHT can induce antitumor immunity in both mouse and human tumor models by increasing lymphocyte infiltration. These data suggest that LIGHT, either alone or together with other immunotherapies, might be an effective strategy for cancer therapy. Third, in tumors resistant to checkpoint blockade therapy due to a lack of lymphocyte infiltration, we prove that additional LIGHT treatment can promote the efficacy of checkpoint blockade therapies. In other words, our study indicates that unresponsiveness to checkpoint blockade can be due to a lack of sufficient lymphocyte infiltration; moreover, LIGHT could be used to increase the response rates to checkpoint blockades, and other immunotherapies, in commonly found non-T cell-inflamed tumors.

EXPERIMENTAL PROCEDURES

Mice

C57BL/6J, B6C3F1, *Rag1*^{-/-}, and OT-1 CD8⁺ TCR-Transgenic mice were purchased from Jackson Laboratory. *Ltbr*^{-/-} and *Tnfrsf14*^{-/-} mice were

kindly provided by Dr. K. Pfeffer (Heinrich-Heine-Universität Dusseldorf). *Ltbr*^{-/-} and *Tnfrsf14*^{-/-} mice were crossed to *Rag1*^{-/-} mice to obtain *Rag1*^{-/-};*Ltbr*^{-/-}, and *Rag1*^{-/-};*Tnfrsf14*^{-/-} mice. All mice were maintained under specific pathogen-free conditions at the University of Chicago. Animal experiment protocols were consistent with NIH guideline. All studies were approved by the Animal Care and Use Committee of the University of Chicago.

In Vitro Evolution of Human LIGHT

Engineered hLIGHT with increased affinities to both human and mouse receptors was selected using yeast surface display as previously described (Boder and Wittrup, 1997). In brief, WT hLIGHT gene was inserted into the T7/pCT302 yeast display vector. The construct was used as template for error-prone PCR. Mutagenized PCR product and digested vector were co-electroporated into EBY100 yeast to generate libraries. The resulting library was cultured and induced for surface LIGHT expression. It was then stained by mouse/human LT β R-Ig/HVEM-Ig, followed by PE-conjugated goat anti-human IgG (Jackson Immunoresearch). Yeast clones with higher receptor binding affinities and species cross-reactivity were selected by alternating rounds of selection by flow cytometric sorting. Thermal stability was assessed by incubating yeast for 30 min at 37°C or 80°C, followed by mLT β R-Ig staining.

Tumor Growth and Treatments

1×10^6 MC38 or Ag104Ld cells were subcutaneously injected into the right flank of mice. Mice were treated intraperitoneally with 200 μ g of anti-PD-L1 (10F.9G2) on days 7 and 10. Tumor volumes were measured twice weekly and calculated as (length \times width \times height/2). To block lymphocyte trafficking, we injected mice intravenously with 25 μ g of FTY720 on day 1 after tumor inoculation. Five micrograms of FTY720 was given every day to maintain blockade. In some experiments, FTY720 was given on days 1–3 after tumor inoculation. For LIGHT treatment, 2×10^6 Ag104Ld-EGFR cells were inoculated subcutaneously into mice. Twenty-five micrograms of anti-EGFR-hmLIGHT or anti-EGFR was injected intratumorally (or intravenously when specified) at indicated time points. Mouse LT β R-Ig (100 μ g/mouse) was administered on days 4, 7, and 11. To deplete CD8 T cells, we injected mice intraperitoneally with 200 μ g of anti-CD8 (YTS 169.4.2) on days 7 and 11. For immune-reconstituted models, *Rag1*^{-/-} mice were inoculated subcutaneously with 1×10^6 MC38-EGFR or A431 cells. After tumors were established, mice were adoptively transferred with 5×10^6 WT splenocytes or 2×10^6 OT-1 LN cells before being treated with anti-EGFR-hmLIGHT.

Statistical Analysis

Mean values were compared using an unpaired Student's two-tailed t test.

SUPPLEMENTAL INFORMATION

Supplemental Information includes Supplemental Experimental Procedures, three figures, and two tables and can be found with this article online at <http://dx.doi.org/10.1016/j.ccell.2016.02.004>.

AUTHOR CONTRIBUTIONS

H.T. and Y.-X.F. designed experiments, analyzed data, and wrote the manuscript. H.T., Y.W., and L.K.C. performed experiments. J.G., W.L., J.W., and X.W. provided reagents. Y.Z. contributed to manuscript preparation. Y.-X.F. supervised the project.

ACKNOWLEDGMENTS

We thank Ting Xu for providing heterodimeric Fc sequence. We thank Xuanming Yang, Liufu Deng, Heng Ru, Wenguang Liang, and Weifeng Liu for helpful scientific discussions. This work was in part supported by the U.S. NIH through National Cancer Institute grants CA141975, grant from AbbVie, grants from the Chinese Academy of Sciences (XDA09030303), and the Chinese Ministry of Science and Technology (2012ZX10002006) to Y.X.F. H.T. is supported by the Cancer Research Institute Irvington Fellowship.

Received: August 24, 2015
 Revised: December 30, 2015
 Accepted: February 8, 2016
 Published: March 14, 2016; corrected online August 29, 2016

REFERENCES

- Ai, M., and Curran, M.A. (2015). Immune checkpoint combinations from mouse to man. *Cancer Immunol. Immunother.* *64*, 1–8.
- Blank, C., Brown, I., Peterson, A.C., Spiotto, M., Iwai, Y., Honjo, T., and Gajewski, T.F. (2004). PD-L1/B7H-1 inhibits the effector phase of tumor rejection by T cell receptor (TCR) transgenic CD8+ T cells. *Cancer Res.* *64*, 1140–1145.
- Boder, E.T., and Wittrup, K.D. (1997). Yeast surface display for screening combinatorial polypeptide libraries. *Nat. Biotechnol.* *15*, 553–557.
- Boussemaert, L., Routier, E., Mateus, C., Opletalova, K., Seville, G., Kamsu-Kom, N., Thomas, M., Vagner, S., Favre, M., and Tomasic, G. (2013). Prospective study of cutaneous side-effects associated with the BRAF inhibitor vemurafenib: a study of 42 patients. *Ann. Oncol.* *24*, 1691–1697.
- Brahmer, J.R., Tykodi, S.S., Chow, L.Q., Hwu, W.-J., Topalian, S.L., Hwu, P., Drake, C.G., Camacho, L.H., Kauh, J., and Odunsi, K. (2012). Safety and activity of anti-PD-L1 antibody in patients with advanced cancer. *N. Engl. J. Med.* *366*, 2455–2465.
- Bromley, S.K., Mempel, T.R., and Luster, A.D. (2008). Orchestrating the orchestrators: chemokines in control of T cell traffic. *Nat. Immunol.* *9*, 970–980.
- Cha, E., Klinger, M., Hou, Y., Cummings, C., Ribas, A., Faham, M., and Fong, L. (2014). Improved survival with T cell clonotype stability after anti-CTLA-4 treatment in cancer patients. *Sci. Transl. Med.* *6*, 238ra270.
- Chen, L., McGowan, P., Ashe, S., Johnston, J., Li, Y., Hellström, I., and Hellström, K. (1994). Tumor immunogenicity determines the effect of B7 costimulation on T cell-mediated tumor immunity. *J. Exp. Med.* *179*, 523–532.
- Crespo, J., Sun, H., Welling, T.H., Tian, Z., and Zou, W. (2013). T cell anergy, exhaustion, senescence, and stemness in the tumor microenvironment. *Curr. Opin. Immunol.* *25*, 214–221.
- Curiel, T.J., Wei, S., Dong, H., Alvarez, X., Cheng, P., Mottram, P., Krzysiek, R., Knutson, K.L., Daniel, B., and Zimmermann, M.C. (2003). Blockade of B7-H1 improves myeloid dendritic cell-mediated antitumor immunity. *Nat. Med.* *9*, 562–567.
- Cyster, J.G. (1999). Chemokines and cell migration in secondary lymphoid organs. *Science* *286*, 2098–2102.
- da Silva, R.B., Laird, M.E., Yatim, N., Fiette, L., Ingersoll, M.A., and Albert, M.L. (2015). Dipeptidylpeptidase 4 inhibition enhances lymphocyte trafficking, improving both naturally occurring tumor immunity and immunotherapy. *Nat. Immunol.* *16*, 850–858.
- Dejardin, E., Droin, N.M., Delhase, M., Haas, E., Cao, Y., Makris, C., Li, Z.-W., Karin, M., Ware, C.F., and Green, D.R. (2002). The lymphotoxin- β receptor induces different patterns of gene expression via two NF- κ B pathways. *Immunity* *17*, 525–535.
- Del Rio, M., Lucas, C., Buhler, L., Rayat, G., and Rodriguez-Barbosa, J. (2010). HVEM/LIGHT/BTLA/CD160 cosignaling pathways as targets for immune regulation. *J. Leukoc. Biol.* *87*, 223–235.
- Dirkx, A.E., Oude Egbrink, M.G., Wagstaff, J., and Griffioen, A.W. (2006). Monocyte/macrophage infiltration in tumors: modulators of angiogenesis. *J. Leukoc. Biol.* *80*, 1183–1196.
- Dong, H., Strome, S.E., Salomao, D.R., Tamura, H., Hirano, F., Flies, D.B., Roche, P.C., Lu, J., Zhu, G., and Tamada, K. (2002). Tumor-associated B7-H1 promotes T-cell apoptosis: a potential mechanism of immune evasion. *Nat. Med.* *8*, 793–800.
- Fu, Y.-X., and Chaplin, D.D. (1999). Development and maturation of secondary lymphoid tissues. *Annu. Rev. Immunol.* *17*, 399–433.
- Gajewski, T.F., Schreiber, H., and Fu, Y.-X. (2013). Innate and adaptive immune cells in the tumor microenvironment. *Nat. Immunol.* *14*, 1014–1022.
- Galon, J., Costes, A., Sanchez-Cabo, F., Kirilovsky, A., Mlecnik, B., Lagorce-Pagès, C., Tosolini, M., Camus, M., Berger, A., and Wind, P. (2006). Type, density, and location of immune cells within human colorectal tumors predict clinical outcome. *Science* *313*, 1960–1964.
- Hammers, H.J., Plimack, E.R., Infante, J.R., Ernstoff, M.S., Rini, B.I., McDermott, D.F., Razak, A.R., Pal, S.K., Voss, M.H., and Sharma, P. (2014). Phase I study of nivolumab in combination with ipilimumab in metastatic renal cell carcinoma (mRCC). *J. Clin. Oncol.* *32*, 5s, (suppl; abstr 4504).
- Herbst, R.S., Soria, J.-C., Kowanetz, M., Fine, G.D., Hamid, O., Gordon, M.S., Sosman, J.A., McDermott, D.F., Powderly, J.D., and Gettinger, S.N. (2014). Predictive correlates of response to the anti-PD-L1 antibody MPDL3280A in cancer patients. *Nature* *515*, 563–567.
- Hwang, W.-T., Adams, S.F., Tahirovic, E., Hagemann, I.S., and Coukos, G. (2012). Prognostic significance of tumor-infiltrating T cells in ovarian cancer: a meta-analysis. *Gynecol. Oncol.* *124*, 192–198.
- Iwai, Y., Ishida, M., Tanaka, Y., Okazaki, T., Honjo, T., and Minato, N. (2002). Involvement of PD-L1 on tumor cells in the escape from host immune system and tumor immunotherapy by PD-L1 blockade. *Proc. Natl. Acad. Sci. USA* *99*, 12293–12297.
- Keir, M.E., Butte, M.J., Freeman, G.J., and Sharpe, A.H. (2008). PD-1 and its ligands in tolerance and immunity. *Annu. Rev. Immunol.* *26*, 677–704.
- Lee, Y., Chin, R.K., Christiansen, P., Sun, Y., Tumanov, A.V., Wang, J., Chervonsky, A.V., and Fu, Y.-X. (2006). Recruitment and activation of naive T cells in the islets by lymphotoxin β receptor-dependent tertiary lymphoid structure. *Immunity* *25*, 499–509.
- Lee, Y., Auh, S.L., Wang, Y., Burnette, B., Wang, Y., Meng, Y., Beckett, M., Sharma, R., Chin, R., and Tu, T. (2009). Therapeutic effects of ablative radiation on local tumor require CD8+ T cells: changing strategies for cancer treatment. *Blood* *114*, 589–595.
- Lo, J.C., Chin, R.K., Lee, Y., Kang, H.-S., Wang, Y., Weinstock, J.V., Banks, T., Ware, C.F., Franzoso, G., and Fu, Y.-X. (2003). Differential regulation of CCL21 in lymphoid/nonlymphoid tissues for effectively attracting T cells to peripheral tissues. *J. Clin. Invest.* *112*, 1495.
- Lukashev, M., LePage, D., Wilson, C., Bailly, V., Garber, E., Lukashin, A., Ngam-ek, A., Zeng, W., Allaire, N., and Perrin, S. (2006). Targeting the lymphotoxin- β receptor with agonist antibodies as a potential cancer therapy. *Cancer Res.* *66*, 9617–9624.
- Mahmoud, S.M., Paish, E.C., Powe, D.G., Macmillan, R.D., Grainge, M.J., Lee, A.H., Ellis, I.O., and Green, A.R. (2011). Tumor-infiltrating CD8+ lymphocytes predict clinical outcome in breast cancer. *J. Clin. Oncol.* *29*, 1949–1955.
- Melero, I., Shuford, W.W., Newby, S.A., Aruffo, A., Ledbetter, J.A., Hellström, K.E., Mittler, R.S., and Chen, L. (1997). Monoclonal antibodies against the 4-1BB T-cell activation molecule eradicate established tumors. *Nat. Med.* *3*, 682–685.
- Nishimura, H., Okazaki, T., Tanaka, Y., Nakatani, K., Hara, M., Matsumori, A., Sasayama, S., Mizoguchi, A., Hiai, H., and Minato, N. (2001). Autoimmune dilated cardiomyopathy in PD-1 receptor-deficient mice. *Science* *291*, 319–322.
- Peng, D., Kryczek, I., Nagarsheth, N., Zhao, L., Wei, S., Wang, W., Sun, Y., Zhao, E., Vatan, L., and Szeliga, W. (2015). Epigenetic silencing of TH1-type chemokines shapes tumour immunity and immunotherapy. *Nature* *527*, 249–253.
- Pesonen, S., Kangasniemi, L., and Hemminki, A. (2010). Oncolytic adenoviruses for the treatment of human cancer: focus on translational and clinical data. *Mol. Pharm.* *8*, 12–28.
- Postow, M.A., Chesney, J., Pavlick, A.C., Robert, C., Grossmann, K., McDermott, D., Linette, G.P., Meyer, N., Giguere, J.K., and Agarwala, S.S. (2015). Nivolumab and ipilimumab versus ipilimumab in untreated melanoma. *N. Engl. J. Med.* *372*, 2006–2017.
- Ruddle, N.H. (1999). Lymphoid neo-organogenesis: lymphotoxin's role in inflammation and development. *Immunol. Res.* *19*, 119–125.
- Shin, D.S., and Ribas, A. (2015). The evolution of checkpoint blockade as a cancer therapy: what's here, what's next? *Curr. Opin. Immunol.* *33*, 23–35.
- Springer, S., Koblisch, H.K., Horton, B., Scherle, P.A., Newton, R., and Gajewski, T.F. (2014). Mechanism of tumor rejection with doublets of CTLA-4, PD-1/PD-L1, or IDO blockade involves restored IL-2 production

- and proliferation of CD8 (+) T cells directly within the tumor microenvironment. *J. Immunother. Cancer* 2, 3.
- Spranger, S., Bao, R., and Gajewski, T.F. (2015). Melanoma-intrinsic [bgr]-catenin signalling prevents anti-tumour immunity. *Nature* 523, 231–235.
- Sznol, M., and Chen, L. (2013). Antagonist antibodies to PD-1 and B7-H1 (PD-L1) in the treatment of advanced human cancer. *Clin. Cancer Res.* 19, 1021–1034.
- Tähtinen, S., Grönberg-Vähä-Koskela, S., Lumen, D., Merisalo-Soikkeli, M., Siurala, M., Airaksinen, A.J., Vähä-Koskela, M., and Hemminki, A. (2015). Adenovirus improves the efficacy of adoptive T-cell therapy by recruiting immune cells to and promoting their activity at the tumor. *Cancer Immunol. Res.* 3, 915–925.
- Thompson, E.D., Enriquez, H.L., Fu, Y.-X., and Engelhard, V.H. (2010). Tumor masses support naive T cell infiltration, activation, and differentiation into effectors. *J. Exp. Med.* 207, 1791–1804.
- Topalian, S.L., Hodi, F.S., Brahmer, J.R., Gettinger, S.N., Smith, D.C., McDermott, D.F., Powderly, J.D., Carvajal, R.D., Sosman, J.A., and Atkins, M.B. (2012). Safety, activity, and immune correlates of anti-PD-1 antibody in cancer. *N. Engl. J. Med.* 366, 2443–2454.
- Topalian, S.L., Drake, C.G., and Pardoll, D.M. (2015). Immune checkpoint blockade: a common denominator approach to cancer therapy. *Cancer Cell* 27, 450–461.
- Tumeh, P.C., Harview, C.L., Yearley, J.H., Shintaku, I.P., Taylor, E.J., Robert, L., Chmielowski, B., Spasic, M., Henry, G., and Ciobanu, V. (2014). PD-1 blockade induces responses by inhibiting adaptive immune resistance. *Nature* 515, 568–571.
- Wang, Y., Zhu, M., Miller, M., and Fu, Y.X. (2009). Immunoregulation by tumor necrosis factor superfamily member LIGHT. *Immunol. Rev.* 229, 232–243.
- Ward, P.L., Koeppen, H., Hurteau, T., and Schreiber, H. (1989). Tumor antigens defined by cloned immunological probes are highly polymorphic and are not detected on autologous normal cells. *J. Exp. Med.* 170, 217–232.
- Ware, C.F. (2005). Network communications: lymphotoxins, LIGHT, and TNF. *Annu. Rev. Immunol.* 23, 787–819.
- Wick, M., Dubey, P., Koeppen, H., Siegel, C.T., Fields, P.E., Chen, L., Bluestone, J.A., and Schreiber, H. (1997). Antigenic cancer cells grow progressively in immune hosts without evidence for T cell exhaustion or systemic anergy. *J. Exp. Med.* 186, 229–238.
- Wilmott, J.S., Long, G.V., Howle, J.R., Haydu, L.E., Sharma, R.N., Thompson, J.F., Kefford, R.F., Hersey, P., and Scolyer, R.A. (2012). Selective BRAF inhibitors induce marked T-cell infiltration into human metastatic melanoma. *Clin. Cancer Res.* 18, 1386–1394.
- Wolchok, J.D., Kluger, H., Callahan, M.K., Postow, M.A., Rizvi, N.A., Lesokhin, A.M., Segal, N.H., Ariyan, C.E., Gordon, R.-A., and Reed, K. (2013). Nivolumab plus ipilimumab in advanced melanoma. *N. Engl. J. Med.* 369, 122–133.
- Woo, S.-R., Corrales, L., and Gajewski, T.F. (2015). Innate immune recognition of cancer. *Annu. Rev. Immunol.* 33, 445–474.
- Yang, X., Zhang, X., Mortenson, E.D., Radkevich-Brown, O., Wang, Y., and Fu, Y.-X. (2013). Cetuximab-mediated tumor regression depends on innate and adaptive immune responses. *Mol. Ther.* 21, 91–100.
- Yang, X., Zhang, X., Fu, M.L., Weichselbaum, R.R., Gajewski, T.F., Guo, Y., and Fu, Y.-X. (2014). Targeting the tumor microenvironment with interferon- β bridges innate and adaptive immune responses. *Cancer Cell* 25, 37–48.
- Yu, P., Lee, Y., Liu, W., Chin, R.K., Wang, J., Wang, Y., Schietinger, A., Philip, M., Schreiber, H., and Fu, Y.-X. (2004). Priming of naive T cells inside tumors leads to eradication of established tumors. *Nat. Immunol.* 5, 141–149.
- Yu, P., Lee, Y., Liu, W., Krausz, T., Chong, A., Schreiber, H., and Fu, Y.-X. (2005). Intratumor depletion of CD4+ cells unmasks tumor immunogenicity leading to the rejection of late-stage tumors. *J. Exp. Med.* 201, 779–791.
- Yu, P., Lee, Y., Wang, Y., Liu, X., Auh, S., Gajewski, T.F., Schreiber, H., You, Z., Kaynor, C., and Wang, X. (2007). Targeting the primary tumor to generate CTL for the effective eradication of spontaneous metastases. *J. Immunol.* 179, 1960–1968.
- Zhu, M., Brown, N.K., and Fu, Y.-X. (2010). Direct and indirect roles of the LT β R pathway in central tolerance induction. *Trends Immunol.* 31, 325–331.
- Zou, W., Zheng, H., He, T.-C., Chang, J., Fu, Y.-X., and Fan, W. (2012). LIGHT delivery to tumors by mesenchymal stem cells mobilizes an effective antitumor immune response. *Cancer Res.* 72, 2980–2989.

Oncogenic RAS Signaling Promotes Tumor Immuno-resistance by Stabilizing PD-L1 mRNA

Matthew A. Coelho,¹ Sophie de Carné Trécesson,¹ Sareena Rana,⁷ Davide Zecchin,¹ Christopher Moore,¹ Miriam Molina-Arcas,¹ Philip East,² Bradley Spencer-Dene,³ Emma Nye,³ Karin Barnouin,⁴ Ambrosius P. Snijders,⁴ Wi S. Lai,⁵ Perry J. Blackshear,^{5,6} and Julian Downward^{1,7,8,*}

¹Oncogene Biology

²Computational Biology

³Experimental Histopathology

⁴Protein Analysis and Proteomics Laboratories

The Francis Crick Institute, 1 Midland Road, London NW1 1AT, UK

⁵Signal Transduction Laboratory, National Institute of Environmental Health Sciences, Research Triangle Park, NC 27709, USA

⁶Departments of Medicine and Biochemistry, Duke University Medical Center, Durham, NC 27703, USA

⁷Lung Cancer Group, Division of Molecular Pathology, The Institute of Cancer Research, 237 Fulham Road, London SW3 6JB, UK

⁸Lead Contact

*Correspondence: julian.downward@crick.ac.uk

<https://doi.org/10.1016/j.immuni.2017.11.016>

SUMMARY

The immunosuppressive protein PD-L1 is upregulated in many cancers and contributes to evasion of the host immune system. The relative importance of the tumor microenvironment and cancer cell-intrinsic signaling in the regulation of PD-L1 expression remains unclear. We report that oncogenic RAS signaling can upregulate tumor cell PD-L1 expression through a mechanism involving increases in PD-L1 mRNA stability via modulation of the AU-rich element-binding protein tristetraprolin (TTP). TTP negatively regulates PD-L1 expression through AU-rich elements in the 3' UTR of PD-L1 mRNA. MEK signaling downstream of RAS leads to phosphorylation and inhibition of TTP by the kinase MK2. In human lung and colorectal tumors, RAS pathway activation is associated with elevated PD-L1 expression. *In vivo*, restoration of TTP expression enhances anti-tumor immunity dependent on degradation of PD-L1 mRNA. We demonstrate that RAS can drive cell-intrinsic PD-L1 expression, thus presenting therapeutic opportunities to reverse the innately immuno-resistant phenotype of RAS mutant cancers.

INTRODUCTION

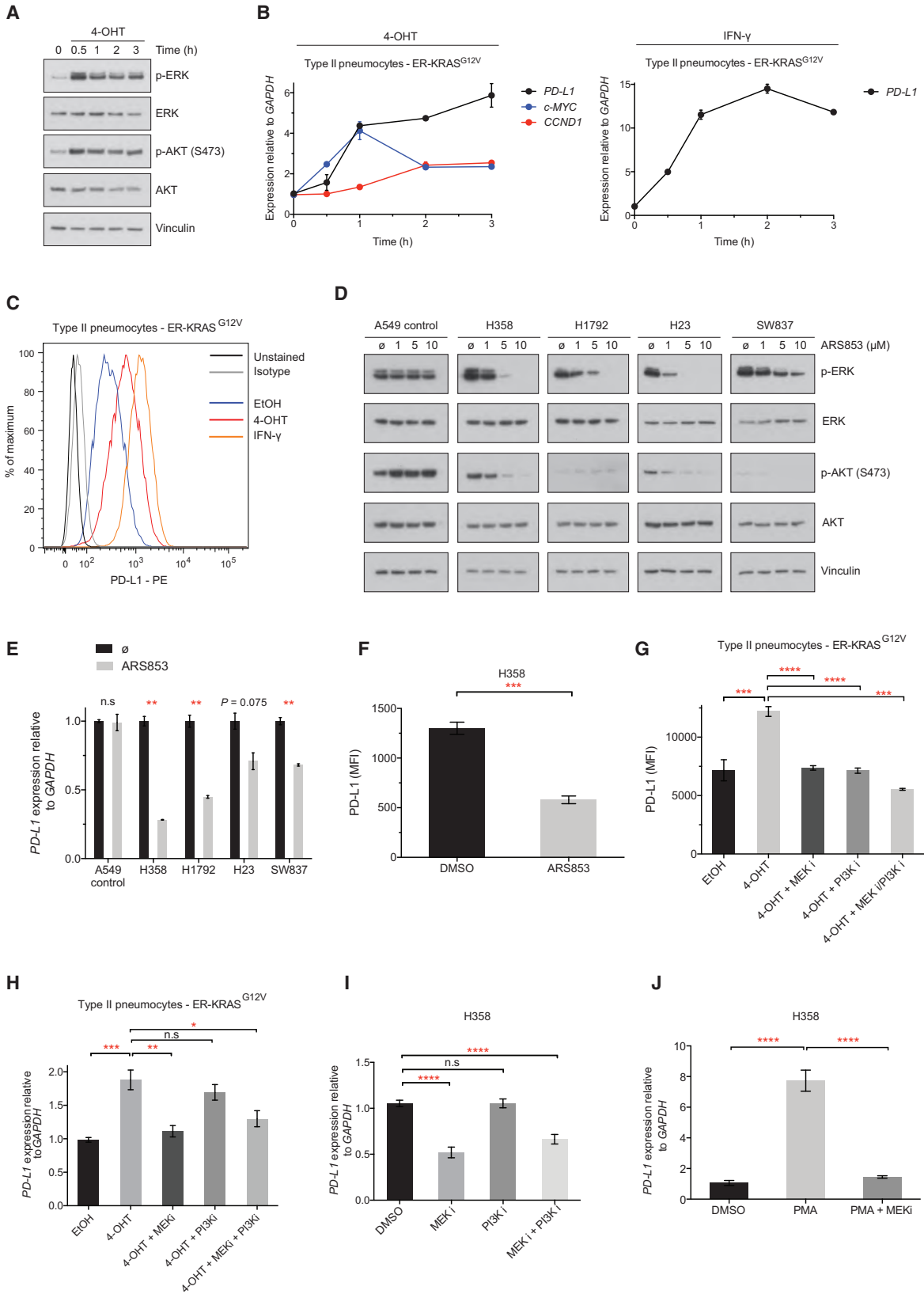
Therapeutic antibodies blocking the coinhibitory PD-1 pathway by targeting PD-L1 (programmed death 1 ligand 1, also known as B7-H1 or CD274) or its receptor, PD-1, have caused striking regressions in several malignancies in which RAS mutations are frequent driver events, including non-small cell lung cancer (NSCLC) (Herbst et al., 2014; Topalian et al., 2012) and mismatch-repair-deficient colorectal cancer (Le et al., 2015). PD-L1 is critical for limiting autoimmune-related damage to normal tissues in the context of chronic inflammation but is

also aberrantly upregulated on cancer cells in order to evade immune destruction (Pardoll, 2012). As anti-PD-1 pathway immunotherapies are effective in only a minority of cancer patients (Topalian et al., 2012), there is a great need for reliable biomarkers of patient response. To what degree tumor PD-L1 expression is prognostic of patient response to PD-1 pathway blockade remains contentious. Recent clinical trials of the anti-PD-1 antibody nivolumab report that tumor cell PD-L1 expression correlates with response to nivolumab in non-squamous but not the squamous subtype of NSCLC (Borghaei et al., 2015; Brahmer et al., 2015). Notably, non-squamous NSCLC patients with *KRAS* mutations benefited from nivolumab therapy in terms of overall survival, whereas *KRAS* wild-type patients did not (Borghaei et al., 2015). Response rate and progression-free survival was increased in NSCLC patients treated with pembrolizumab in cases where at least 50% of tumor cells were positive for PD-L1 (Garon et al., 2015). In this patient cohort, *KRAS* mutant tumors were more frequently PD-L1 positive than *KRAS* wild-type tumors.

The success of immune-checkpoint blockade is dependent on the immunogenicity of the tumor (Gubin et al., 2014; Linnemann et al., 2015; Rizvi et al., 2015), so one possible confounding factor in the use of tumor PD-L1 as a biomarker for response is the uncoupling of tumor PD-L1 expression from tumor immunogenicity. It is therefore critical to understand the signaling pathways that dictate tumor cell PD-L1 expression. The inflammatory cytokine IFN- γ is the best-characterized stimulus for PD-L1 expression, but several studies suggest that cell-intrinsic oncogenic signaling can also promote PD-L1 expression in cancer cells through epidermal growth factor receptor (EGFR), the transcription factor MYC, and the kinase AKT (Akbay et al., 2013; Casey et al., 2016; Parsa et al., 2007). Studies performed on melanoma (Jiang et al., 2013) and acute myeloid leukemia (Berthon et al., 2010) have indicated that MEK signaling is involved in upregulation of PD-L1 in some tumor cell lines, but the molecular basis of this regulation remains poorly defined.

Separately, genetic rearrangements in the 3' UTR of *CD274* (encoding PD-L1) have been found in a multitude of different cancers at low frequency and are associated with massively





(legend on next page)

increased expression of tumor PD-L1 (Kataoka et al., 2016). These results imply that control of PD-L1 expression through the *CD274* 3' UTR might contribute to immune escape in human cancers, although the underlying mechanisms of post-transcriptional regulation responsible for this effect are unclear.

In this report, we reveal that tumor cell PD-L1 expression can be driven by oncogenic RAS pathway activation by a mechanism involving post-transcriptional regulation of the stability of PD-L1 mRNA. This provides a direct mechanism whereby RAS signaling in tumor cells can provide protection from attack by the immune system.

RESULTS

Cell-Intrinsic Upregulation of PD-L1 through Oncogenic RAS Signaling

We tested the potential role of oncogenic RAS signaling in the regulation of PD-L1 expression in human epithelial cells using ER-RAS^{G12V} fusion constructs, which allow for the induction of oncogenic RAS activity with 4-hydroxytamoxifen (4-OHT) (Molina-Arcas et al., 2013). As expected, addition of 4-OHT led to the rapid activation of oncogenic KRAS signaling through MEK and PI3K (Figure 1A) and coincided with induction of MYC mRNA and CCND1 mRNA (encoding cyclin D1) in an immortalized human pneumocyte cell line derived from type II cells (Figure 1B; Kemp et al., 2008). PD-L1 mRNA was rapidly increased following stimulation of oncogenic KRAS signaling with 4-OHT, resulting in a 6-fold induction of mRNA expression after 3 hr (Figure 1B). By way of comparison with known regulators, stimulation with IFN- γ led to increases in PD-L1 mRNA in excess of 10-fold after 3 hr and both KRAS activation and IFN- γ stimulation dramatically increased PD-L1 protein expression at the cell surface after 48 hr (Figure 1C). Oncogenic HRAS signaling was also capable of inducing PD-L1 mRNA and protein expression in the immortalized breast epithelial cell line MCF10A and the *KRAS* wild-type colon carcinoma cell line HKE-3 (Figures S1A and S1B), implying that induction of PD-L1 expression by RAS is not a tissue-specific or RAS-isof orm-specific phenomenon. The induction of PD-L1 protein

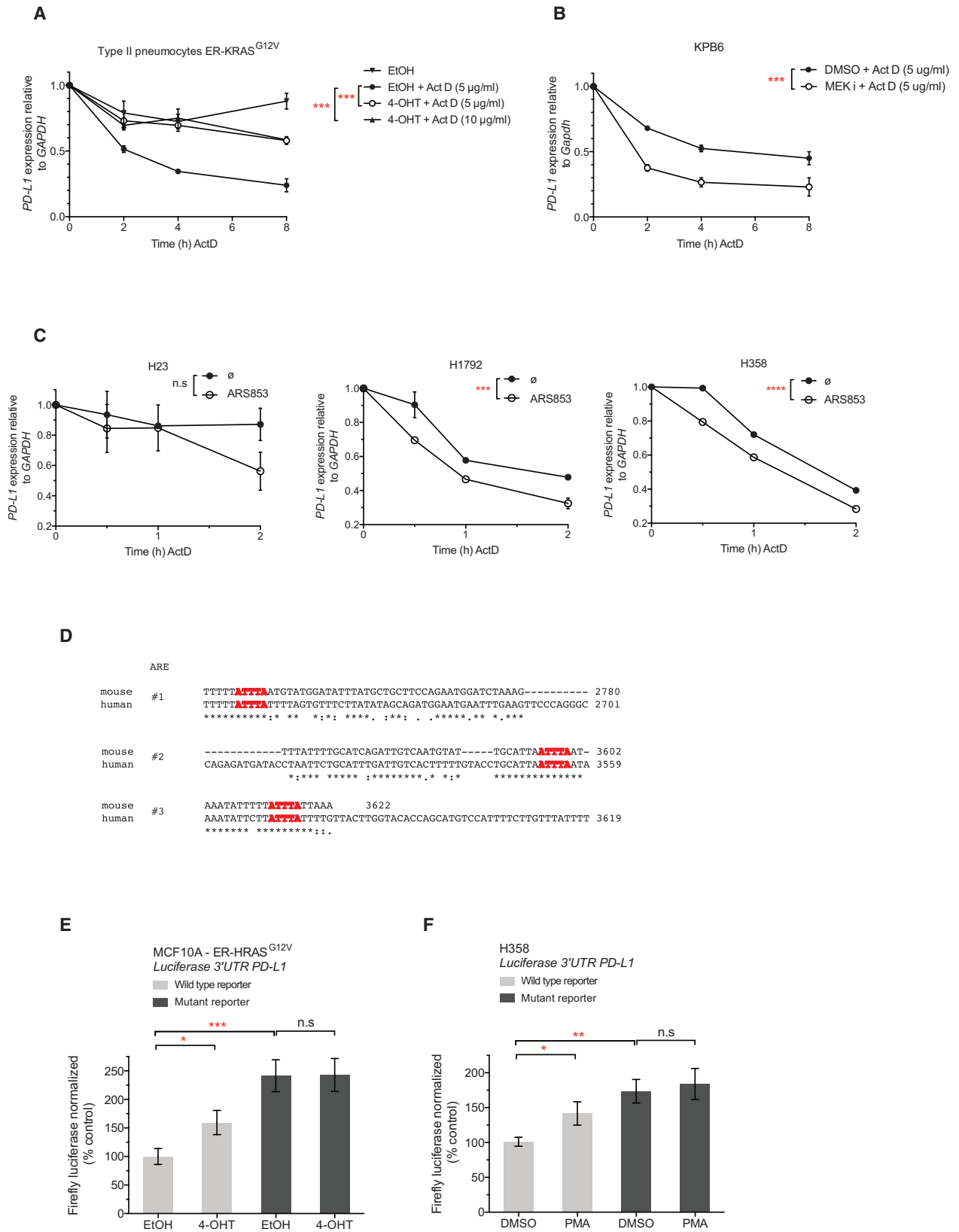
was most striking in ER-HRAS^{G12V} MCF10A cells, perhaps reflecting the low basal expression of PD-L1. Chronic RAS activation for 4 days led to more profound increases in PD-L1 protein, whereas shorter-term activation resulted in modest inductions of PD-L1 expression (Figure S1B). Importantly, 4-OHT did not induce PD-L1 expression in parental cell lines lacking ER-RAS constructs (Figure S1C).

Direct inhibition of KRAS signaling with the KRAS^{G12C}-specific inhibitor ARS853 (Lito et al., 2016; Patricelli et al., 2016) in lung and colorectal cancer cell lines harboring KRAS^{G12C} mutations led to reductions in PD-L1 mRNA expression, but not in the KRAS^{G12S} A549 control lung cancer cell line (Figures 1D and 1E). Moreover, ARS853 treatment led to significant reductions in PD-L1 surface protein expression in the *KRAS* mutant lung cancer cell line H358 (Figure 1F). To dissect which downstream effectors of RAS are responsible for regulating PD-L1 expression, we used the specific inhibitors of MEK and pan type I PI3Ks, GSK1120212 (trametinib) and GDC-0941 (pictilisib), respectively (Figure S1D). Notably, MEK and PI3K inhibitors could block RAS-induced expression of PD-L1 protein in ER-KRAS^{G12V} type II pneumocytes, either alone or in combination (Figure 1G). MEK inhibition significantly reversed KRAS-mediated PD-L1 mRNA upregulation (Figure 1H), but PI3K inhibition only reduced PD-L1 protein expression, concordant with evidence for AKT signaling increasing PD-L1 expression predominantly through activating translation of the transcript (Parsa et al., 2007). MEK inhibition, but not PI3K inhibition, reduced PD-L1 mRNA expression in H358 (Figure 1I), H23, and H1792 lung cancer cell lines (Figure S1E). Downstream of MEK, inhibition of ERK1/2 with SCH772984 potently reduced PD-L1 expression in H358 and H23 cells (Figure S1F). Furthermore, PMA, a potent chemical activator of MEK-ERK signaling via protein kinase C stimulation, markedly and rapidly increased PD-L1 expression, an effect that was largely reversed with the inhibition of MEK (Figures 1J and S1G). More extensive analysis of PD-L1 surface expression on multiple *KRAS* mutant lung cancer cell lines, both human and murine, revealed generally consistent PD-L1 downregulation after MEK and PI3K inhibition, suggesting that this regulatory pathway is of broad significance

Figure 1. Cell-Intrinsic Upregulation of PD-L1 through Oncogenic RAS Signaling

- (A) Western blotting analysis of ER-KRAS^{G12V} type II pneumocytes treated with 4-OHT in starvation medium. Phospho-ERK and phospho-AKT was measured over time to monitor RAS pathway activation. Data are representative of two independent experiments.
- (B) qPCR analysis of ER-KRAS^{G12V} type II pneumocytes treated with 4-OHT or IFN- γ in starvation medium. Mean \pm SEM of biological duplicates (n = 2) from the experiment described in (A).
- (C) Representative flow cytometry histogram of PD-L1 surface protein expression in ER-KRAS^{G12V} type II pneumocytes treated in starvation medium for 48 hr. Data are representative of two independent experiments.
- (D) Western blotting analysis of RAS signaling following 5 hr treatment with the KRAS^{G12C} inhibitor ARS853. Phospho-ERK and phospho-AKT signal reflect RAS pathway activity. Data are representative of two independent experiments.
- (E) qPCR analysis following 5 hr treatment with the KRAS^{G12C} inhibitor ARS853 (10 μ M). Mean \pm SEM of biological duplicates (n = 2) from the experiment described in (D).
- (F) Flow cytometry analysis of PD-L1 surface protein expression in H358 cells treated with ARS853 (10 μ M) for 48 hr. Mean \pm SEM of biological triplicates.
- (G) Flow cytometry analysis of PD-L1 surface protein expression in ER-KRAS^{G12V} type II pneumocytes treated in starvation medium for 24 hr. Mean \pm SEM of two independent experiments.
- (H) qPCR analysis from the experiment described in (G). Mean \pm SEM of biological triplicates pooled from two independent experiments.
- (I) qPCR analysis of H358 cells treated for 24 hr. Mean \pm SEM of two independent experiments.
- (J) qPCR analysis of H358 cells treated with PMA for 3 hr following a 30 min pre-treatment with DMSO or MEK inhibitor. Mean \pm SD of two independent experiments.

Abbreviations and quantities are as follows: MFI, mean fluorescence intensity; EtOH, ethanol vehicle; 4-OHT, 100 nM; IFN- γ , 20 ng/mL; MEK inhibitor GSK1120212, 25 nM; PI3K inhibitor GDC-0941, 500 nM; PMA, 200 nM. ****p < 0.0001, ***p < 0.001, **p < 0.01, *p < 0.05, n.s., not significant. Unpaired, two-tailed Student's t tests. See also Figure S1.



(legend on next page)

(Figure S1H). Taken together, these results suggest that oncogenic RAS signaling through MEK and PI3K is sufficient to drive PD-L1 expression.

Since RAS signaling has been implicated in reducing the expression of genes involved in the presentation of antigens by MHC class I molecules (Ebert et al., 2016; El-Jawhari et al., 2014), we analyzed the expression of antigen processing and antigen presentation machinery following oncogenic RAS activation (Figure S1I). As expected, KRAS G12V signaling led to significant decreases in expression of *TAP1*, *TAPBP*, as well as *HLA-A*, *HLA-B*, *HLA-C*, and *B2M*, suggesting that compromised antigen processing and presentation in concert with increases in PD-L1 expression may contribute to an augmented state of immunoresistance in RAS mutant tumor cells.

RAS Signaling Increases PD-L1 mRNA Stability through AU-Rich Elements in the 3' UTR

To investigate how RAS-MEK signaling regulates PD-L1 expression, we first asked whether RAS regulates PD-L1 via a transcriptional mechanism. We generated a series of luciferase reporter constructs containing promoter fragments cloned from the human *CD274* locus (Figure S2A). In all cases, the physiological stimulus IFN- γ , but not PMA, induced expression of the promoter reporter constructs in H358 cells, a cell line in which endogenous PD-L1 mRNA expression is robustly induced with PMA (Figure 1J). Incorporation of putative enhancer elements (Sumimoto et al., 2016) into the *CD274* promoter reporter constructs also failed to confer sensitivity to MAPK activation (Figure S2A), as did including predicted regulatory regions spanning the 5' of exon 1 (data not shown). Furthermore, none of the reporters showed evidence of decreased expression when H358 cells were treated with MEK inhibitor (data not shown).

Therefore, we investigated possible mechanisms of post-transcriptional regulation of PD-L1 expression by RAS. We induced oncogenic KRAS signaling with 4-OHT in ER-KRAS^{G12V} type II pneumocytes and concomitantly blocked transcription with actinomycin D. Surprisingly, we found human PD-L1 mRNA to have a short half-life, which was significantly stabilized by the induction of oncogenic KRAS signaling (Figure 2A). Moreover, murine PD-L1 mRNA also had a comparably short half-life, and the stability of the transcript in a *Kras* mutant, p53-deleted murine lung tumor cell line (KPB6), could be reduced further still when MEK was inhibited (Figure 2B), implicating KRAS-MEK signaling in the stabilization of the labile PD-L1 transcript. Consistently, direct inhibition of oncogenic KRAS signaling

with ARS853 also caused reductions in PD-L1 mRNA half-life in H23, H1792, and H358 cells (Figure 2C). However, inhibition of PI3K alone did not result in altered PD-L1 mRNA stability in KPB6 cells (Figure S2B).

Common genetic elements conferring mRNA instability include miRNA binding sites and AU-rich elements (AREs) in the 3' UTR of the transcript. The core motif for AREs is an ATTTA pentamer sequence, but functional AREs are often found in an AU-rich context, conforming to the WWATTTAWWW nonamer consensus (where W denotes an A or T) (Zubiaga et al., 1995) constituting the binding site for several AU-rich element binding proteins (AUBPs), which can subsequently recruit mRNA decay machinery (Lykke-Andersen and Wagner, 2005). For example, a canonical ARE-regulated transcript is *TNF*, which contains nine pentamer sequences in the human transcript and eight pentamers in the murine transcript. Upon inspection of the 3' UTR of PD-L1 mRNA, we noted a high number of ARE pentamers. Specifically, out of 14 ATTTA pentamer sequences in the human transcript and 11 in the murine transcript, there were 3 conserved AREs conforming to the nonamer consensus (Figure 2D).

We tested the influence of MEK inhibition on the half-life of another unstable transcript, *Tusc2* mRNA (tumor suppressor candidate 2, or *Fus1*), which does not contain AU-rich elements in the 3' UTR but is targeted by multiple miRNAs (Du et al., 2009). Although *Tusc2* mRNA had a similar half-life to PD-L1 mRNA, MEK inhibition did not influence the stability of the *Tusc2* transcript (Figure S2C), indicating that the observed post-transcriptional regulation of PD-L1 by MEK may relate to AU-rich elements in the 3' UTR. Indeed, a transcript containing functional AU-rich elements, *Ptgs2* mRNA (Cha et al., 2011), displayed a significant reduction in mRNA half-life in response to MEK inhibition (Figure S2C), reminiscent of PD-L1 mRNA.

To directly analyze the functional importance of these AREs, we constructed a luciferase reporter containing a fragment of the 3' UTR of human *CD274* containing the last six ATTTA pentamers, including the three conserved nonamer sequences. Mutation of ATTTA pentamers to ATGTA has been shown to increase the expression of ARE-containing mRNAs (Rajagopalan et al., 1995; Yang et al., 2004). Consistent with this, mutating the six ATTTA pentamer sequences to ATGTA increased expression of the PD-L1 3' UTR luciferase reporter in ER-HRAS^{G12V} MCF10A and H358 cells, suggesting that these AREs are functionally relevant for controlling the expression of PD-L1 (Figures 2E and 2F). Stimulation with 4-OHT in

Figure 2. RAS Signaling Increases PD-L1 mRNA Stability through AU-Rich Elements in the 3' UTR

(A) qPCR analysis of PD-L1 mRNA stability in ER-KRAS^{G12V} type II pneumocytes after the concomitant addition of actinomycin D (5 μ g/mL or 10 μ g/mL) and 4-OHT or vehicle added at time = 0 hr in starvation medium. Mean \pm SEM of two independent experiments. ***p < 0.0005; two-way ANOVA.

(B) qPCR analysis of PD-L1 mRNA stability in KPB6 cells after the addition of actinomycin D (5 μ g/mL) and DMSO or MEK inhibitor. Cells were pre-treated with DMSO or MEK inhibitor for 30 min before actinomycin D addition. Mean \pm SEM of two independent experiments. ***p < 0.0005; two-way ANOVA.

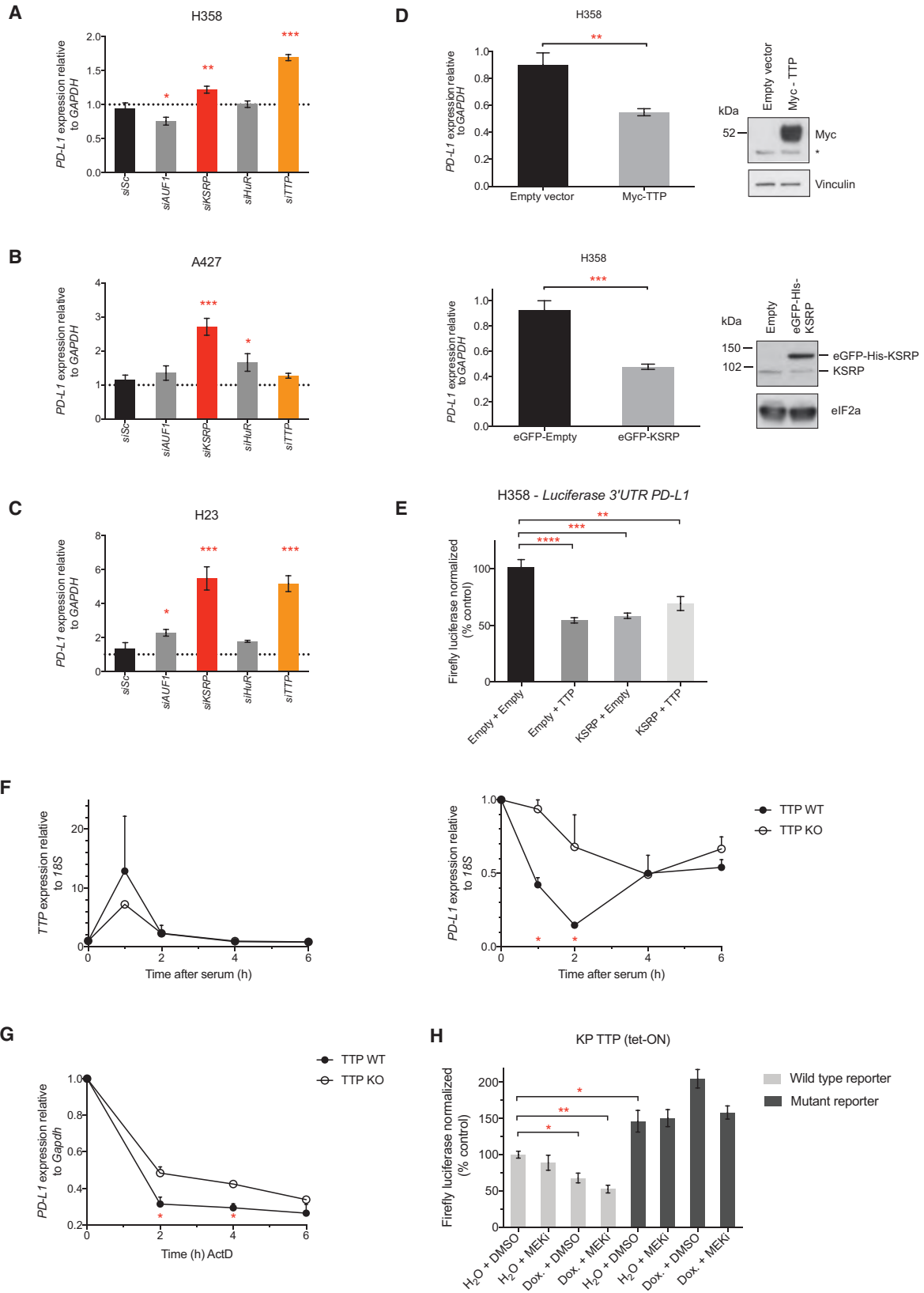
(C) qPCR analysis of PD-L1 mRNA stability after the addition of actinomycin D (5 μ g/mL) and DMSO or ARS853. Cells were pre-treated with DMSO or ARS853 for 35 min before actinomycin D addition. Mean \pm SEM of two independent experiments. ***p < 0.0005; two-way ANOVA.

(D) Sequence alignment of conserved AU-rich element ATTTA pentamer sequences (highlighted in red) in the mouse and human *CD274* 3' UTR.

(E) Normalized luciferase signal in ER-HRAS^{G12V} MCF10A cells from wild-type (ATTTA x 6) or mutant (ATGTA x 6) PD-L1 3' UTR reporters, 24 hr after treatment in starvation medium. Mean \pm SEM of three independent experiments.

(F) Normalized luciferase signal in H358 cells from wild-type (ATTTA x 6) or mutant (ATGTA x 6) PD-L1 3' UTR reporters, 6 hr after treatment. Mean \pm SEM of three independent experiments.

Abbreviations and quantities: 4-OHT, 100 nM; MEK inhibitor GSK1120212, 25 nM; PMA, 200 nM. ***p < 0.0005, **p < 0.005, *p < 0.05, n.s., not significant. Unpaired, two-tailed Student's t tests. See also Figure S2.



(legend on next page)

ER-HRAS^{G12V} MCF10A cells, or PMA in H358 cells, increased expression of the wild-type reporter, whereas the ATGTA mutant reporter was insensitive to these treatments (Figures 2E and 2F). In sum, these data suggest that AREs in the 3' UTR of PD-L1 mRNA can mediate control of PD-L1 expression by RAS-MEK signaling.

AU-Rich Element Binding Proteins TTP and KSRP Are Negative Regulators of PD-L1 Expression

To assess which AU-rich element binding proteins (AUBPs) could mediate regulation of PD-L1 expression downstream of RAS signaling, we performed a selected siRNA screen of likely candidate genes, *AUF1*, *KSRP*, *HuR*, and *TTP* (also known as tristetraprolin or *ZFP36*), in three RAS mutant lung cancer cell lines (Figures 3A–3C). Knockdown efficiency was verified in each case by qPCR (Figures S3A–S3C). siRNA-mediated knockdown of KSRP and TTP most consistently increased PD-L1 mRNA expression across the cell line panel, with the exception of A427, where knock-down of TTP did not lead to significant increases in PD-L1 mRNA levels. Overexpression of KSRP or TTP was sufficient to significantly decrease PD-L1 expression (Figure 3D) and PD-L1 3' UTR luciferase reporter expression in H358 cells (Figure 3E), corroborating our results from the siRNA screen and confirming that KSRP and TTP impart their negative regulation of PD-L1 expression through the 3' UTR. Overexpression of TTP and KSRP together did not result in additive reductions in PD-L1 expression, suggesting that they may regulate PD-L1 through the same mechanism (Figure S3D). Notably, siRNA-mediated knockdown of TTP family members, BRF-1 and BRF-2, was incapable of increasing PD-L1 expression to the extent achieved by silencing TTP expression (Figures S3E and S3F). We confirmed that TTP protein expression was reduced following knock-down in H23 and H358 cells, but this was less clear in A427 cells, which express lower levels of TTP protein (Figure S3G). Deconvolution of siRNA pools targeting TTP showed that multiple siRNAs increased expression of PD-L1 mRNA in H23 and H358 cells (Figure S3H).

We further examined the regulation of PD-L1 mRNA by TTP by using TTP wild-type (WT) and TTP knock-out (KO) MEFs. In the TTP KO MEFs, TTP mRNA is expressed but no functional TTP protein can be made due to the introduction of a premature stop codon at the endogenous locus (Lai et al., 2006; Taylor et al., 1996). Acute activation of TTP expression with serum temporally coincided with a substantial and transient decrease in PD-L1 mRNA in TTP WT MEFs, but not in the TTP KO MEFs

(Figure 3F), with PD-L1 levels recovering to near baseline at 6 hr after serum addition. Moreover, the total absence of functional TTP protein in the TTP KO MEFs increased the half-life of PD-L1 mRNA relative to TTP WT MEFs (Figure 3G).

Finally, we generated a KP6 lung cancer cell line with a tetracycline-inducible TTP transgene (TTP tet-ON). As expected, inducible expression of TTP led to reductions in wild-type PD-L1 3' UTR luciferase reporter expression, but not of the ATGTA mutant 3' UTR reporter (Figure 3H). When combined with MEK inhibition, TTP expression more robustly suppressed expression of the wild-type reporter. In sum, these data provide evidence for the negative regulation of PD-L1 mRNA expression by the AUBPs KSRP and TTP.

RAS Regulates PD-L1 Expression through TTP

To further investigate whether MEK and TTP regulate PD-L1 via a shared pathway, we silenced TTP expression using siRNAs in the context of MEK inhibition. Knock-down of TTP was largely able to rescue the decrease in PD-L1 expression caused by MEK inhibition (Figure 4A). However, the knockdown of KSRP could not rescue this phenotype, despite profound silencing of expression (Figure S4A). Furthermore, MEK inhibition significantly increased TTP mRNA expression (Figure 4A), and chronic activation of oncogenic KRAS signaling significantly decreased TTP mRNA expression (Figure 4B).

Next, we tested whether the RAS pathway regulates the activity of TTP and/or KSRP protein. Crucially, we found that endogenous levels of TTP and KSRP both co-precipitated with PD-L1 mRNA in RNA immunoprecipitation (RNA-IP) reactions from KP6 mouse lung cancer cells (Figure S4B). TTP also significantly bound to PD-L1 mRNA in H358 cells (Figure 4C). In all cases, the enrichment for the PD-L1 transcript was far greater than that of a control mRNA, GAPDH, which lacks AREs in the 3' UTR (Figures 4C and S4C). MEK inhibition did not significantly alter the occupancy of TTP or KSRP on PD-L1 mRNA, consistent with RAS regulating the activity of the AUBP, rather than the occupancy on the target mRNA.

ERK has been shown to phosphorylate (Taylor et al., 1995) and negatively regulate TTP activity and expression (Bourcier et al., 2011; Deleault et al., 2008; Essafi-Benkhadir et al., 2007; Härdle et al., 2015). Inhibition of MEK decreased phosphorylation of TTP at PXSP (ERK target-site consensus) and RXXS/T (RSK/AKT target-site consensus) motifs (Figures 4D and 4E), confirming that TTP is regulated by phosphorylation downstream of MEK signaling in cancer cells. Mutation of two of the highest

Figure 3. AU-Rich Element Binding Proteins TTP and KSRP Are Negative Regulators of PD-L1 Expression

(A–C) qPCR analysis 48 hr after transfection with siRNAs targeting AU-rich element binding proteins (AU-BPs) relative to siScrambled (siSc) control. Mean \pm SD of biological triplicates.

(D) qPCR and western blotting analysis of H358 cells 24 hr after transfection. qPCR data represent the mean \pm SD of biological triplicates and are representative of two independent experiments. *, non-specific band.

(E) Normalized luciferase signal from the wild-type, PD-L1 3' UTR reporter 24 hr after co-transfection with the indicated constructs. Mean \pm SEM of two independent experiments.

(F) qPCR analysis after serum stimulation in serum-starved TTP WT or TTP KO MEFs. Mean \pm SEM of two independent experiments.

(G) qPCR analysis of PD-L1 mRNA stability after the addition of actinomycin D (5 μ g/mL) in TTP WT or TTP KO MEFs. Mean \pm SEM of two independent experiments.

(H) Normalized luciferase signal in KP6 TTP (tet-ON) cells wild-type (ATTTA x 6) or mutant (ATGTA x 6) PD-L1 3' UTR reporters, 7 hr after treatment. Data represent the mean \pm SEM of biological triplicates and are representative of two independent experiments.

Abbreviations and quantities: MEK inhibitor, GSK1120212, 25 nM; Dox., doxycycline 1 μ g/mL. ****p < 0.0001, ***p < 0.001, **p < 0.01. Unpaired, two-tailed Student's t tests. See also Figure S3.

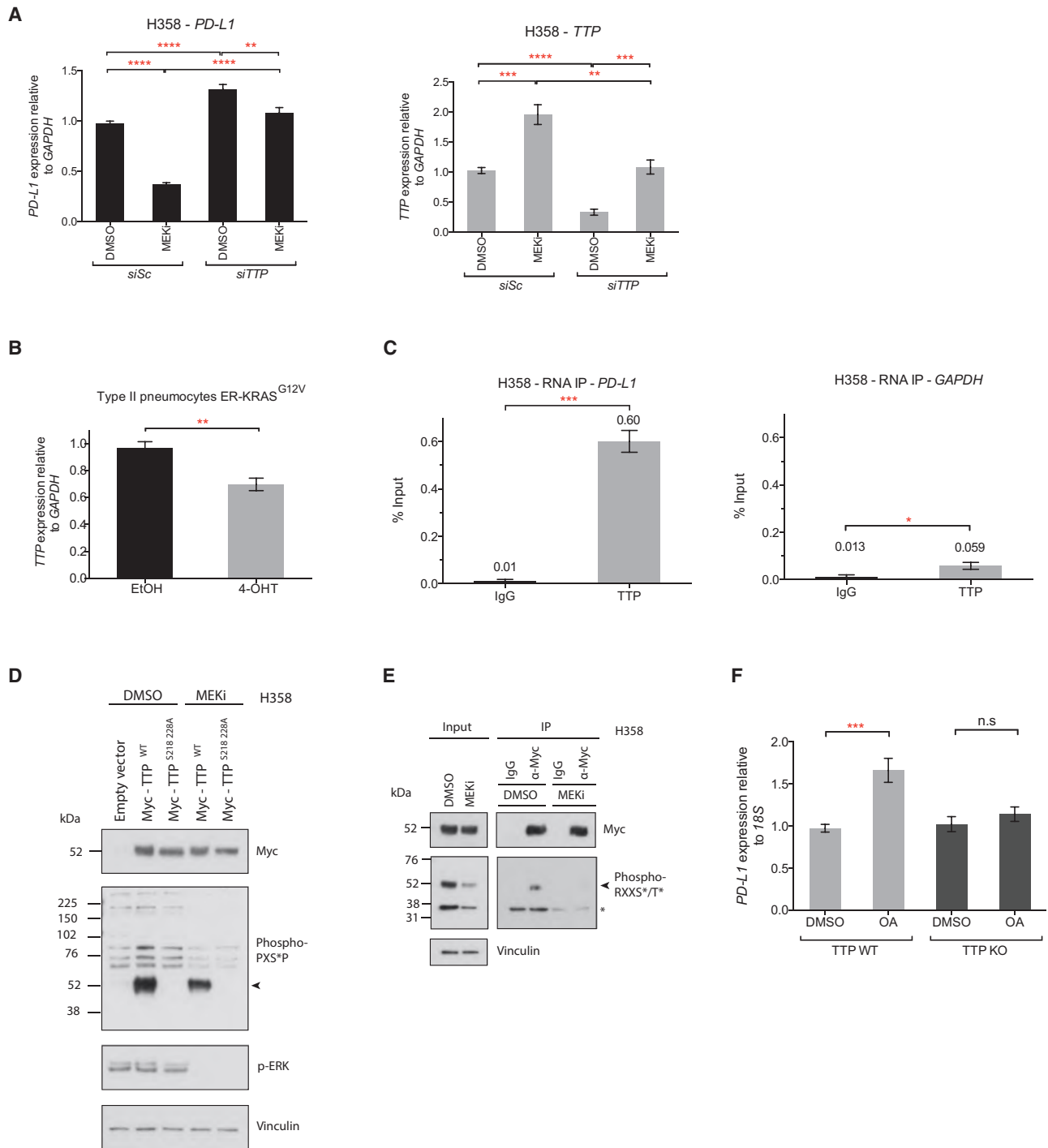


Figure 4. RAS Regulates PD-L1 Expression through TTP

(A) qPCR analysis of H358 cells following siRNA-mediated knock-down of TTP (24 hr) followed by MEK inhibition (24 hr). Mean ± SEM of two independent experiments.

(B) qPCR analysis of ER-KRAS^{G12V} type II pneumocytes treated for 24 hr in starvation medium. Mean ± SEM of three independent experiments.

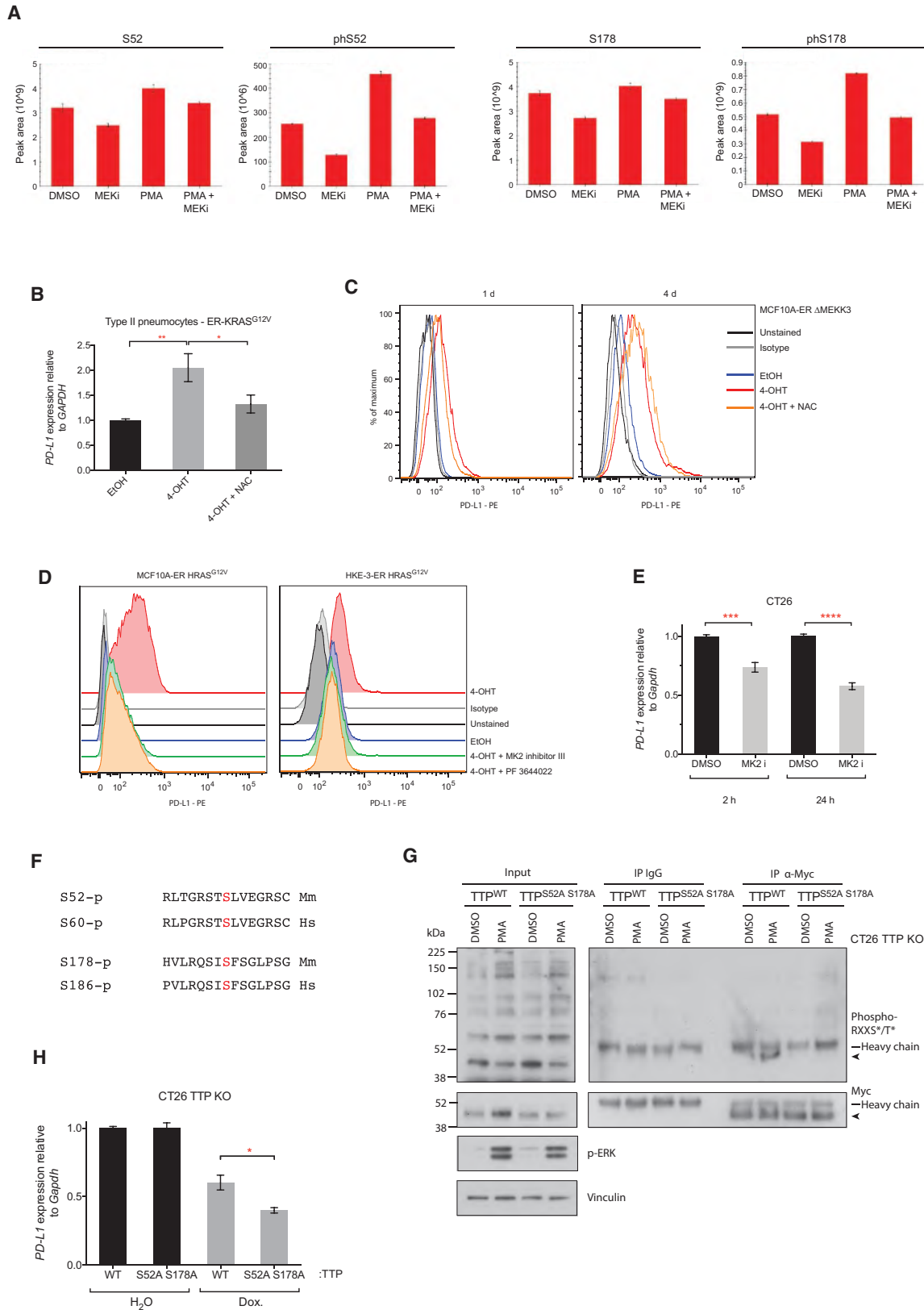
(C) qPCR analysis of RNA-IP immunoprecipitates from H358 cells. Mean ± SEM from biological triplicates.

(D) Western blotting analysis of H358 cells expressing the indicated constructs. 6.5 hr post-transfection, cells were treated with DMSO or MEK inhibitor for an additional 16 hr. Arrow indicates Myc-TTP. Data are representative of two independent experiments.

(E) Western blotting analysis of immunoprecipitations from H358 cells transfected with Myc-TTP. 6.5 hr post-transfection, cells were treated with DMSO or MEK inhibitor for an additional 16 hr. Arrow indicates Myc-TTP; * indicates co-precipitating protein. Data are representative of two independent experiments.

(F) qPCR analysis of TTP WT or TTP KO MEFs treated with okadaic acid or DMSO for 2 hr. Mean ± SEM of two independent experiments.

Abbreviations and quantities: EtOH, ethanol vehicle; 4-OHT, 100 nM; okadaic acid, OA, 1 μM; MEK inhibitor, GSK1120212, 25 nM. ****p < 0.0001, ***p < 0.001, **p < 0.01. Unpaired, two-tailed Student's t tests. See also Figure S4.



(legend on next page)

confidence predicted ERK-target residues on human TTP (S218 and S228) abrogated detection of TTP with the phospho-PXSP motif-specific antibody (Figure 4D), but the phosphosite mutant TTP (S218A 228A) did not show enhanced activity in reducing PD-L1 mRNA expression compared to wild-type TTP (data not shown), implying the involvement of other residues that are not readily detected with this antibody. Furthermore, although AKT signaling has been shown to regulate KSRP activity through phosphorylation of S193 (Díaz-Moreno et al., 2009), the KSRP S193A phosphosite mutant did not show enhanced activity in reducing PD-L1 mRNA expression compared to wild-type KSRP (Figure S4D).

Equally, the serine/threonine phosphatase PP2A has been implicated in positively regulating TTP function by reversing inhibitory phosphorylation events (Sun et al., 2007). Therefore, we tested whether inhibition of PP2A with okadaic acid (OA) would increase PD-L1 expression. OA rapidly increased PD-L1 mRNA expression in TTP WT MEFs, but not TTP KO MEFs (Figure 4F), demonstrating that PP2A activity decreases PD-L1 expression specifically through modulating TTP activity.

RAS-ROS-p38 Signaling Controls TTP Activity

To discover which residues are functionally important for regulating TTP activity downstream of RAS, we performed mass spectrometry on immunoprecipitated Myc-TTP after PMA, MEK inhibitor, or PMA and MEK inhibitor treatment. We used the *Kras* mutant, mouse colon carcinoma cell line CT26, based on its immunogenicity and sensitivity to anti-PD-L1 antibody therapy, making it suitable for downstream *in vivo* experiments. Most notably, mass spectrometry analysis revealed MEK-dependent phosphorylation of S52 and S178; PMA significantly enhanced phosphorylation of these residues, and this effect was reversed with MEK inhibition (Figures 5A and S5A and Table S1). Moreover, MEK inhibition alone was sufficient to reduce phosphorylation of these residues (Figure 5A).

S52 and S178 residues are crucial for the regulation of TTP activity through binding to 14-3-3 proteins following phosphorylation by MK2 (also known as MAPKAPK2) downstream of p38 (Chrestensen et al., 2004). Consequently, p38 signaling results in decreased TTP activity, partly through reducing the association with deadenylase machinery (Mahtani et al., 2001; Stoecklin et al., 2004). In parallel, phosphorylation of S52 and S178 stabi-

lizes TTP protein (Brook et al., 2006), which is consistent with the observed increase in abundance of total TTP peptides detected in the PMA versus the MEK inhibitor-treated condition (Figure 5A).

We reasoned that oncogenic RAS might stimulate p38 signaling through promoting the MEK-dependent accumulation of reactive oxygen species (ROS) (Nicke et al., 2005) and thus inhibit TTP function. Indeed, oncogenic RAS signaling dramatically increased intracellular ROS in MCF10A cells, and ROS levels were distinctly correlated with the extent of PD-L1 induction (Figure S5B). Furthermore, the addition of the potent antioxidant N-acetyl-L-cysteine (NAC) largely reversed the induction of PD-L1 protein by RAS (Figures 5B and S5B), collectively suggesting that ROS induction by oncogenic RAS is functionally important in driving PD-L1 expression.

Specific activation of the p38 pathway using an inducible version of the upstream kinase MEKK3 (Δ MEKK3-ER) (Figures 5C and S5C; Garner et al., 2002) was sufficient to increase PD-L1 protein expression, albeit to a lesser extent than that achieved by RAS itself. Co-treatment with NAC was considerably less effective in reversing PD-L1 induction in this context, consistent with ROS operating upstream of p38 in this pathway (Figure 5C). Moreover, inhibition of MK2 strongly reversed RAS-induced PD-L1 expression in MCF10A and HKE-3 cells (Figure 5D) and PD-L1 expression in CT26 cells, which have endogenous levels of mutant KRAS (Figure 5E). We also observed reductions in expression of PD-L1 mRNA in several NSCLC cell lines with endogenous *KRAS* mutations following treatment with NAC, reduced glutathione, or MK2 inhibitor III (Figure S5D), although we noted some heterogeneity in response between the four cell lines tested.

To directly test the functional significance of the MK2 target residues downstream of MEK pathway activation, we generated TTP knock-out CT26 cell lines using CRISPR/Cas (to obviate functional contributions from endogenous TTP) and reconstituted these cells with either a wild-type (WT) or phosphosite mutant (S52A S178A), tetracycline-inducible TTP transgene. S52 and S178 of mouse TTP are highly conserved, with S52 conforming to the RXXS/T phosphosite motif (Figure 5F). Immunoprecipitation of Myc-tagged TTP following acute MAPK activation with PMA revealed phosphorylation of WT TTP, but not of the S52A S178A mutant protein at RXXS/T sites (Figure 5G),

Figure 5. RAS-ROS-p38 Signaling Controls TTP Activity

(A) Histograms represent peak areas from extracted ion chromatograms for non-phosphorylated and phosphorylated peptides corresponding to S52 and S178 phosphosites of mouse TTP. Myc-TTP was immunoprecipitated from CT26 Myc-TTP (tet-ON) cells 1 hr after the indicated treatment. Mean \pm SD of technical triplicates. Representative of two independent biological experiments.

(B) qPCR analysis of ER-KRAS^{G12V} type II pneumocytes treated in starvation medium for 24 hr. Mean \pm SEM of four independent experiments.

(C) Representative flow cytometry histograms of PD-L1 surface protein expression in MCF10A ER- Δ MEKK3 cells treated in starvation medium for 1 day or 4 days. Data are representative of two independent experiments.

(D) Flow cytometry analysis of PD-L1 surface protein expression on ER-HRAS^{G12V} MCF10A cells (24 hr) and ER-HRAS^{G12V} HKE-3 cells (48 hr) after treatment in starvation medium. Data are representative of biological duplicates.

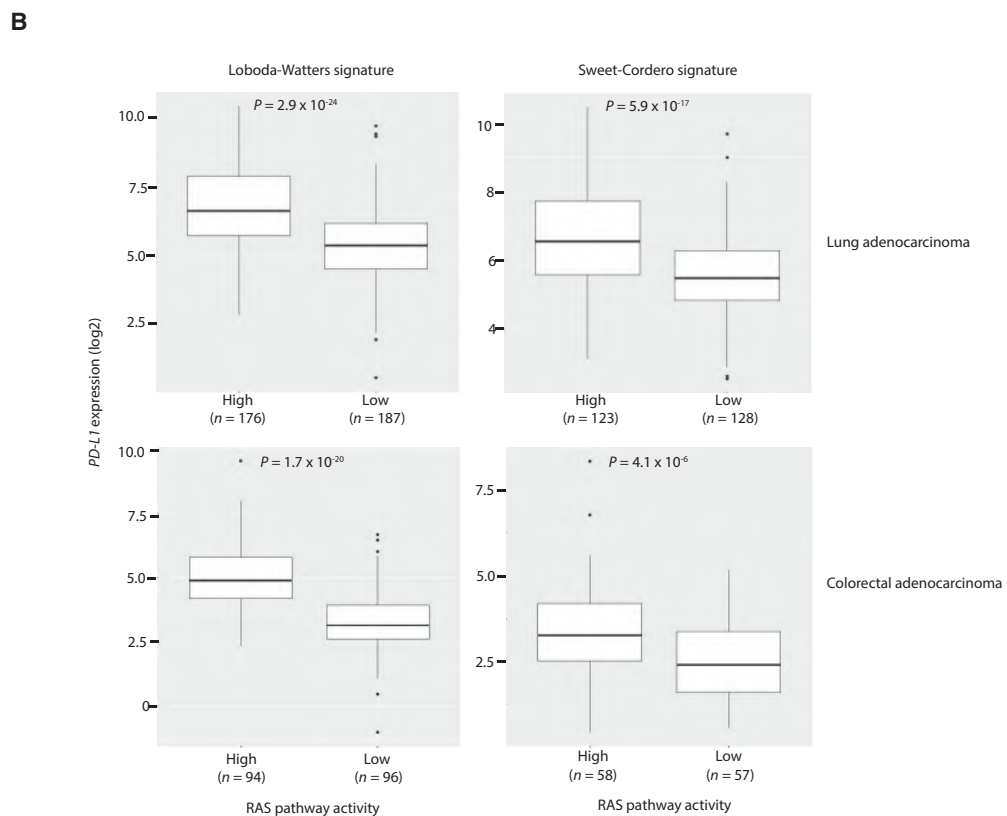
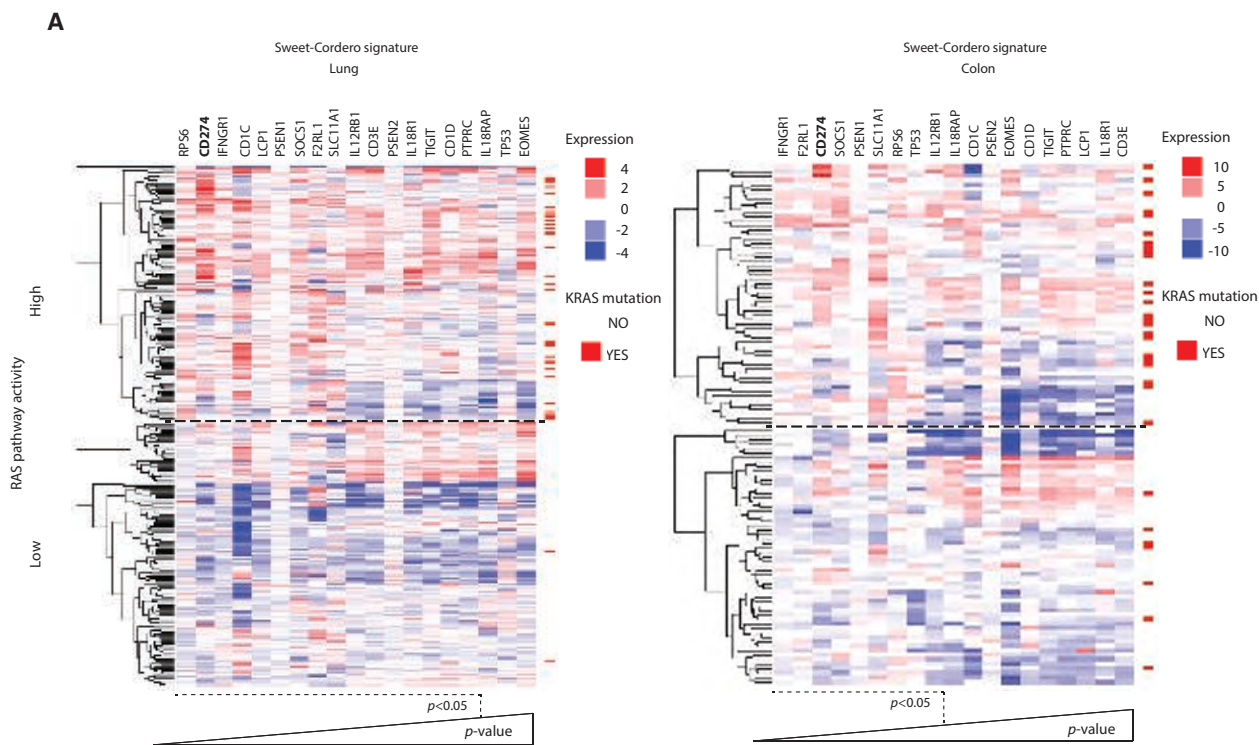
(E) qPCR analysis of CT26 cells at 2 hr or 24 hr after MK2 inhibition with PF 3644022. Mean \pm SEM of two independent experiments.

(F) Sequence alignments of the conserved phosphosites (highlighted red) targeted by MK2 in mouse (*Mm*) and human (*Hs*) TTP protein.

(G) Western blotting of immunoprecipitations from CT26 TTP KO cells harboring tet-ON, WT, or phospho mutant, Myc-TTP constructs. Cells were treated with dox. for 24 hr before the addition of PMA or DMSO for 1 hr. Arrow indicates Myc-TTP. Data are representative of two independent experiments.

(H) qPCR analysis of CT26 TTP KO cells harboring tet-ON, WT, or phospho mutant, Myc-TTP constructs, treated with dox or vehicle for 48 hr. Data represent the mean \pm SEM of two independent experiments.

** $p < 0.005$, * $p < 0.05$. Unpaired, two-tailed Student's *t* test. Abbreviations and quantities: 4-OHT, 100 nM; NAC, N-acetyl-L-cysteine, 10 mM; PMA, 200 nM; MEK inhibitor, GSK1120212, 25 nM; MK2 inhibitor PF 3644022, 1 μ M; MK2 inhibitor III, 1 μ M; dox., doxycycline, 1 μ g/mL. See also Figure S5.



(legend on next page)

verifying our findings from mass spectrometry analysis. Crucially, the S52A S178A mutant TTP had significantly enhanced activity in reducing PD-L1 mRNA expression relative to WT TTP (Figures 5H and S5E). In sum, these results suggest that a RAS-ROS-p38 signaling axis contributes to PD-L1 upregulation through phosphorylation and inactivation of TTP.

RAS Pathway Activation Is Associated with PD-L1 Upregulation in Human Cancers

To further evaluate the role of oncogenic RAS signaling in regulating PD-L1 expression in cancer, we analyzed TCGA gene expression data from patient-derived lung adenocarcinoma (LUAD) or colon adenocarcinoma (COAD) samples. To account for the effects of alternative oncogenes that can activate downstream RAS effector pathways such as EGFR, BRAF, and ALK, we used two published gene expression signatures for RAS activation (Loboda et al., 2010; Sweet-Cordero et al., 2005) to segregate patient samples into “high” and “low” RAS pathway activity based on gene expression. As expected, annotation of *KRAS* mutation status revealed a strong enrichment for *KRAS* mutant samples in the high RAS activity cohorts in both signatures (Figures 6A and S6A). We compared the expression of T cell function-related genes between high and low RAS activity cohorts and found *CD274* (encoding PD-L1) expression to be significantly increased in the high RAS pathway activity samples in LUAD (1.42 log₂-fold change) and COAD (1.17 log₂-fold change) samples, using either signature (Figures 6A, 6B, and S6A). Stromal PD-L1 and tumor PD-L1 expression appear to have independent, suppressive effects on anti-tumor immunity (Lau et al., 2017), but we noted that the expression of the pan-leukocyte marker *PTPRC* (coding for CD45) and lymphocyte marker *CD3E* were only modestly increased in the high RAS pathway activity cohort, indicating that the differential in PD-L1 expression is not likely to be solely attributable to a higher degree of leukocyte infiltration in the tumor microenvironment (Figure 6A).

Of note, *IFNGR1* was also among the most significantly enriched transcripts in the high RAS pathway activity groups. To investigate the possibility that PD-L1 may be upregulated in RAS active tumors due to regulation by IFNGR1, we induced PD-L1 expression with RAS in ER-*KRAS*^{G12V} type II pneumocytes and concomitantly blocked IFNGR1 signaling using a depleting antibody for IFN- γ or with the JAK1/2 inhibitor ruxolitinib. Although both treatments effectively reduced responses to exogenous IFN- γ , PD-L1 induction by RAS was unaffected, suggesting independence from IFN- γ -IFNGR1 signaling (Figure 6SB).

To further explore the *in vivo* relevance of TTP regulation in human cancer, we compared TTP mRNA expression in normal tissue and tumor samples by using publically available datasets. TTP mRNA was strikingly downregulated in human lung and

colon tumor samples compared to normal tissue (Figure S6C; Selamat et al., 2012; Skrzypczak et al., 2010), confirming that aberrant regulation of TTP expression is relevant in the human disease. Consistently, in FACS-sorted epithelial cells isolated from normal lung or matched tumor tissue from *Kras*^{LSL-G12D/+}; *Trp53*^{F/F} (KP) mice, TTP mRNA expression was reduced in lung tumor tissue (Figure S6D). PD-L1 mRNA expression was generally higher in tumor tissue than in normal lung but not significantly increased; however, PD-L1 protein expression was significantly elevated, perhaps reflecting the contribution from AKT in promoting PD-L1 protein expression (Figure S6E).

Restoration of Tumor Cell TTP Expression Enhances Anti-tumor Immunity

Next, we set out to directly assess the functional importance of the regulation of PD-L1 expression by TTP in tumor progression. To this end, we generated a series of stable CT26 cell lines expressing Myc-tagged mouse TTP under a tetracycline-inducible promoter (TTP tet-ON), and in addition, constitutively expressing either empty vector or mouse *Cd274* cDNA lacking the 3' UTR (PD-L1 Δ 3' UTR). TTP expression was induced upon addition of doxycycline in a dose-dependent manner (Figure 7A), resulting in decreased PD-L1 protein expression at the cell surface (Figure 7B). Overexpression of PD-L1 Δ 3' UTR rendered total PD-L1 levels effectively insensitive to TTP induction (Figure 7B). TTP transgene expression with doxycycline was also associated with a decrease in PD-L1 mRNA stability, which was comparable to that mediated by MEK inhibition in this system (Figure S7A).

To independently verify our findings in another cell line, we used MC38 tumor cells because they are known to exhibit sensitivity to PD-L1 modulation *in vivo* and show RAS pathway activation (Giannou et al., 2017). As expected, TTP was induced with doxycycline in MC38 (tet-ON) cells, leading to reductions in PD-L1 expression (Figures S7B and S7C).

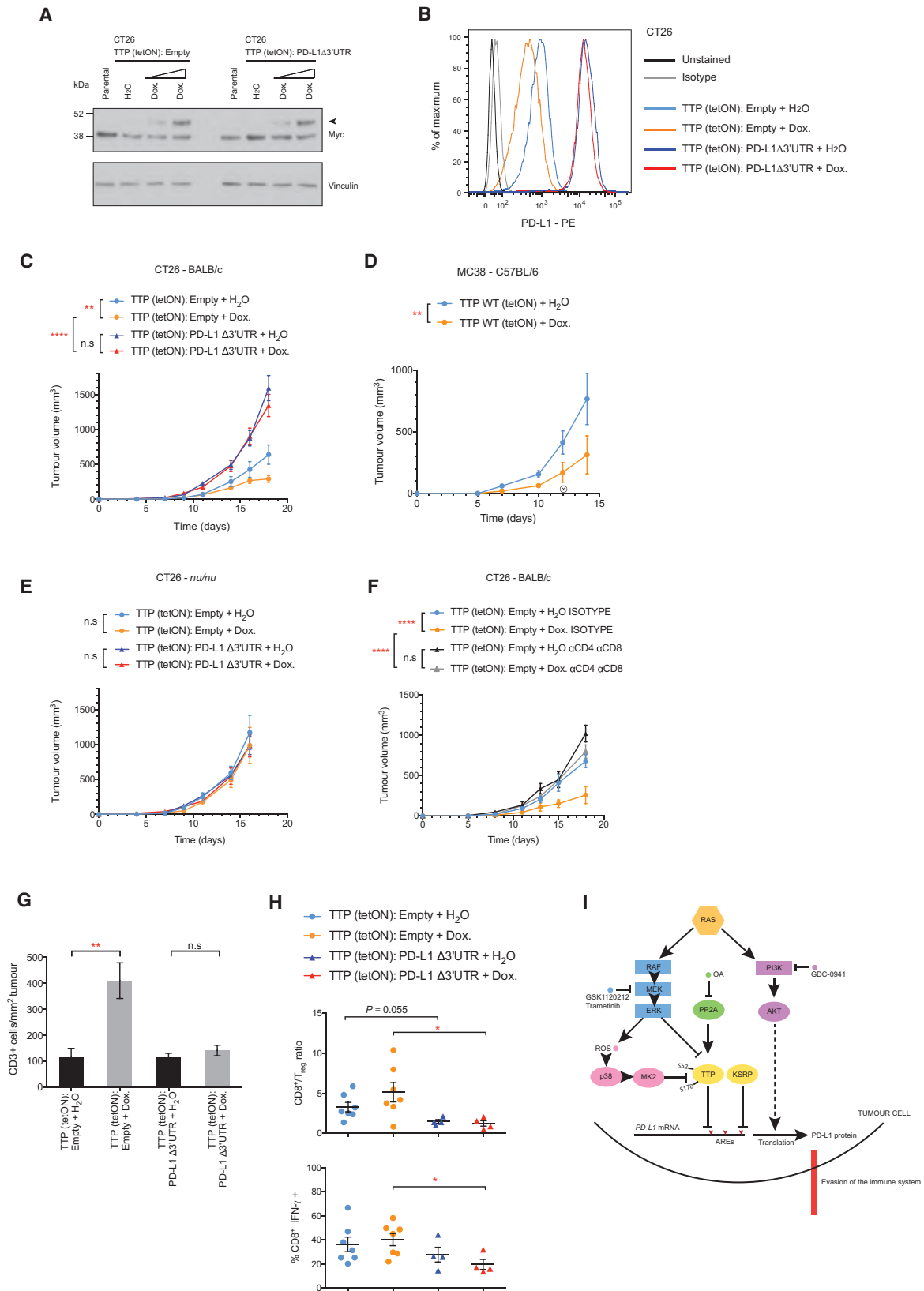
Using these engineered cell lines, we performed subcutaneous transplantation experiments in mice and monitored tumor progression. Notably, the growth rates of the stable cell lines *in vitro* did not significantly differ with the overexpression of PD-L1 Δ 3' UTR cDNA or the induction of TTP transgene expression with doxycycline (Figure S7D and S7E). However, *in vivo*, doxycycline treatment significantly reduced CT26 and MC38 tumor growth in immune-competent, syngeneic mice (Figures 7C and 7D). Strikingly, the anti-tumor effects mediated by doxycycline treatment were absent in immunocompromised *nu/nu* mice harboring CT26 tumors (Figure 7E) and in mice treated with depleting antibodies against CD8 and CD4, implying an essential contribution from the adaptive immune system to this anti-tumor response (Figure 7F). CT26 tumor cells overexpressing PD-L1 Δ 3' UTR grew faster than the empty vector cells in BALB/c mice but had no growth advantage in *nu/nu* mice. Moreover, expression of PD-L1 Δ 3' UTR was able to rescue

Figure 6. RAS Pathway Activation Is Associated with PD-L1 Upregulation in Human Cancers

(A) Heat-maps showing fold change in expression of T cell function related genes between high and low RAS pathway activity cohorts of lung adenocarcinoma (LUAD) and colon adenocarcinoma (COAD) TCGA samples. *KRAS* mutation status (codons 12, 13, and 61) is indicated for each sample. Genes are ranked in order of significance. Wald test, DESeq2.

(B) Box-and-whisker plots comparing PD-L1 mRNA expression in RAS high versus low pathway activity cohorts in LUAD and COAD using two independent RAS gene expression signatures. Wald test, DESeq2.

See also Figure S6.



(legend on next page)

much of the growth inhibition mediated by doxycycline treatment in BALB/c mice, suggesting that suppression of tumor cell PD-L1 expression is an essential component of the anti-tumor effects mediated by TTP transgene induction (Figure 7C). As expected, CT26 cells expressing a *Cd274* cDNA with the full-length, wild-type 3' UTR (PD-L1 WT 3' UTR) had considerably lower expression of PD-L1 protein than the PD-L1 Δ 3' UTR cells, but still responded to TTP induction in terms of reductions in PD-L1 expression (Figure S7F) and control of tumor growth in immune-competent mice (Figure S7G).

Consistent with a heightened anti-tumor immune response, tumors derived from mice treated with doxycycline had a greater degree of CD3⁺ lymphocyte infiltration than tumors from mice treated with vehicle, and this corresponding infiltration was abrogated in tumors derived from cells overexpressing PD-L1 Δ 3' UTR (Figures 7G and S7H). Moreover, we found higher CD8⁺/Treg cell ratios in tumors expressing the TTP transgene and higher levels of IFN- γ production by CD8⁺ tumor-infiltrating lymphocytes (TILs) derived from TTP-expressing tumors, versus PD-L1 Δ 3' UTR tumors expressing TTP (Figure 7H); however, we did not find significant differences in CD4⁺ TIL populations (data not shown).

Collectively, these data highlight the functional importance of the regulation of PD-L1 expression by TTP in tumor progression and demonstrate that this novel regulatory pathway may be exploited for the treatment of *Ras* mutant cancers. These findings support a model whereby tumor-specific suppression of TTP can foster PD-L1 upregulation, and ultimately, tumor immunoresistance (Figures 7I and S7I).

DISCUSSION

In this report, we demonstrate that oncogenic RAS signaling can increase tumor cell-intrinsic PD-L1 expression, implying that mutant RAS oncogenes can directly contribute to the evasion of immune destruction in cancer. We revealed that RAS-MEK signaling controlled expression of PD-L1, at least in part, by modulating the stability of the transcript. We showed that the mouse and human PD-L1 mRNAs were labile transcripts containing functional AU-rich elements (AREs) in the 3' UTR that permitted regulation of PD-L1 expression by RAS. Our data provide a potential explanation for the genomic struc-

tural variations in the *CD274* 3' UTR observed in human cancer (Kataoka et al., 2016). The simultaneous loss of regulation by miRNAs and AREs is likely to contribute to the high overexpression observed in tumors with complete loss of the 3' UTR. In addition, we provide a molecular basis for the tendency of *KRAS* mutant NSCLCs to be positive for PD-L1 expression (D'Incecco et al., 2015; Dong et al., 2017; Li et al., 2017; Yang et al., 2017), implying that PD-1-PD-L1 blockade may prove more successful in *RAS* mutant patients that also harbor a sufficient number of tumor antigens.

We identify TTP as a principle AU-rich element binding protein responsible for negatively regulating PD-L1 expression, consistent with a previous report identifying PD-L1 mRNA as one of a number of TTP targets in an RNA immunoprecipitation, microarray-based screen in mouse macrophages (Stoecklin et al., 2008). Mechanistically, MEK inhibition reduced PD-L1 mRNA stability, coinciding with an increase in TTP expression and reduction in phosphorylation of TTP at ERK and RSK/AKT consensus motifs. Conversely, activation of RAS and the associated ROS accumulation led to enhanced TTP phosphorylation, notably by MK2 at key inhibitory sites.

TTP transgene expression restrained tumor growth in CT26 and MC38 tumor transplantation models. This anti-tumor effect is predominantly non-cell autonomous, dependent on the adaptive immune system and suppression of tumor cell PD-L1 expression. We noted only minor reductions in tumor growth rates following TTP transgene induction in cells overexpressing PD-L1 Δ 3' UTR. TTP has been reported to have cell-autonomous tumor-suppressive roles (Rounbehler et al., 2012) and non-cell-autonomous anti-tumor effects through targeting VEGF and COX-2 mRNAs (Cha et al., 2011; Essafi-Benkhadir et al., 2007), which may contribute to some of these ostensibly PD-L1-independent effects, the magnitude of which are likely to be determined by the level of TTP overexpression in each system.

Our data extend the molecular understanding of the regulation of PD-L1 expression in cancer and highlight druggable targets to enhance anti-tumor immunity in tumors that are wild-type for the *CD274* 3' UTR. We provide evidence that pharmacological targeting of RAS, or RAS effector proteins, may elicit non-cell-autonomous anti-tumor effects in *RAS* mutant tumors. Recently, MEK inhibitors and PD-1 pathway blockade were shown to combine strongly in a mouse model of *Ras* mutant colon

Figure 7. Restoration of Tumor Cell TTP Expression Enhances Anti-tumor Immunity

(A) Western blotting analysis of CT26 Myc-TTP tet-ON cells expressing either empty vector or mouse *Cd274* cDNA lacking the 3' UTR (PD-L1 Δ 3' UTR), 24 hr after treatment (Dox., 0.1 μ g/mL or 1 μ g/mL). Arrow indicates Myc-TTP. Data are representative of two independent experiments.

(B) Representative flow cytometry histograms of PD-L1 surface protein expression in CT26 stable cells lines in (A), 72 hr after treatment (Dox., 1 μ g/mL). Data are representative of three independent experiments.

(C) Tumor growth curves for CT26-derived cell lines subcutaneously transplanted into BALB/c mice (n = 8 per group).

(D) Tumor growth curves for MC38-derived cell lines subcutaneously transplanted into C57BL/6 mice (n = 6 per group). X denotes the loss of a doxycycline-treated mouse.

(E) Tumor growth curves for CT26-derived cell lines subcutaneously transplanted into *nu/nu* mice (n = 6 per group).

(F) Tumor growth curves for CT26-derived cell lines subcutaneously transplanted into BALB/c mice (n = 4–5 per group).

For (C)–(F), data represent the mean \pm SEM from individual experiments. **p < 0.01, ****p < 0.0001, n.s., not significant; two-way ANOVA.

(G) Histological analysis of subcutaneous tumors at the end-point from the experiment described in (C), with quantification of CD3⁺ cells in 5 fields of view per mouse with 5–6 mice per group. Mean \pm SEM. **p < 0.01; unpaired, two-tailed Student's t test.

(H) Quantification of CD8⁺/Treg cell ratios and CD8⁺ IFN- γ ⁺ cells from flow cytometry analysis of tumors after 18–20 days of growth. Each data point represents data from an individual mouse; mean \pm SEM. *p < 0.05; unpaired, two-tailed Student's t test. Data are pooled from two independent experiments.

(I) Proposed molecular model. Signaling nodes that influence anti-tumor immunity and are amenable to inhibition with drugs used in this study are highlighted. S52 and S178 represent MK2 target sites and numbering corresponds to mouse TTP. OA, okadaic acid.

See also Figure S7.

carcinoma (Ebert et al., 2016; Liu et al., 2015). We anticipate that our findings will inform the development of effective combination therapies with immune checkpoint blockade in cancer.

STAR★METHODS

Detailed methods are provided in the online version of this paper and include the following:

- KEY RESOURCES TABLE
- CONTACT FOR REAGENT AND RESOURCE SHARING
- EXPERIMENTAL MODEL AND SUBJECT DETAILS
 - Cell Lines
 - *In vivo* studies
- METHOD DETAILS
 - *In vivo* studies
 - Transfections
 - Cloning, plasmids and stable cell lines
 - Flow cytometry
 - Immunoprecipitation
 - Immunohistochemistry
 - CRISPR/Cas
 - Bioinformatics
 - Mass Spectrometry
 - Western blotting
 - Luciferase assays
 - Quantitative real-time PCR (qPCR)
 - RNA-immunoprecipitation
- QUANTIFICATION AND STATISTICAL ANALYSIS

SUPPLEMENTAL INFORMATION

Supplemental Information includes seven figures and two tables and can be found with this article online at <https://doi.org/10.1016/j.immuni.2017.11.016>.

AUTHOR CONTRIBUTIONS

M.A.C. and J.D. designed the study, interpreted the results, and wrote the manuscript. M.A.C., S.C.T., and S.R. performed the biochemical experiments, D.Z. and C.M. assisted with *in vivo* studies, M.M.-A. provided reagents and conceptual advice, B.S.-D. and E.N. performed histopathological studies, S.C.T. and P.E. performed bioinformatics analyses, K.B. and A.P.S. performed mass spectrometry analyses, and W.S.L. and P.J.B. provided TTP KO and WT MEFs. All authors contributed to manuscript revision and review.

ACKNOWLEDGMENTS

We thank Charles Swanton and Caetano Reis e Sousa for helpful discussion, David Hancock and Febe Van Maldegem for critical reading of the manuscript, and science technology platforms at the Francis Crick Institute including Biological Resources, FACS, Equipment Park, Experimental Histopathology, and Cell Services. We thank Lynn McGregor and Kevan Shokat for providing ARS853. This work was supported by the Francis Crick Institute, which receives its core funding from Cancer Research UK (FC001070), the UK Medical Research Council (FC001070), and the Wellcome Trust (FC001070), and by funding to J.D. from the European Research Council Advanced Grant RASTARGET and a Wellcome Trust Senior Investigator Award (103799/Z/14/Z). This work was also supported in part by the Intramural Research Program of the National Institute of Environmental Health Sciences, NIH (W.S.L. and P.J.B.). S.C.T. was supported by a fellowship from the European Commission Marie Skłodowska-Curie Actions programme, iGEMMdev.

Received: October 14, 2016

Revised: June 6, 2017

Accepted: November 20, 2017

Published: December 12, 2017

REFERENCES

- Akbay, E.A., Koyama, S., Carretero, J., Altan, A., Tchaicha, J.H., Christensen, C.L., Mikse, O.R., Cherniack, A.D., Beachamp, E.M., Pugh, T.J., et al. (2013). Activation of the PD-1 pathway contributes to immune escape in EGFR-driven lung tumors. *Cancer Discov.* 3, 1355–1363.
- Berthon, C., Driss, V., Liu, J., Kuranda, K., Leleu, X., Jouy, N., Hetuin, D., and Quesnel, B. (2010). In acute myeloid leukemia, B7-H1 (PD-L1) protection of blasts from cytotoxic T cells is induced by TLR ligands and interferon-gamma and can be reversed using MEK inhibitors. *Cancer Immunol. Immunother.* 59, 1839–1849.
- Borghaei, H., Paz-Ares, L., Horn, L., Spigel, D.R., Steins, M., Ready, N.E., Chow, L.Q., Vokes, E.E., Felip, E., Holgado, E., et al. (2015). Nivolumab versus docetaxel in advanced nonsquamous non-small-cell lung cancer. *N. Engl. J. Med.* 373, 1627–1639.
- Bourcier, C., Griseri, P., Grépin, R., Bertolotto, C., Mazure, N., and Pagès, G. (2011). Constitutive ERK activity induces downregulation of tristetraprolin, a major protein controlling interleukin8/CXCL8 mRNA stability in melanoma cells. *Am. J. Physiol. Cell Physiol.* 301, C609–C618.
- Brahmer, J., Reckamp, K.L., Baas, P., Crinò, L., Eberhardt, W.E., Poddubskaya, E., Antonia, S., Pluzanski, A., Vokes, E.E., Holgado, E., et al. (2015). Nivolumab versus docetaxel in advanced squamous-cell non-small-cell lung cancer. *N. Engl. J. Med.* 373, 123–135.
- Brook, M., Tchen, C.R., Santalucia, T., McIlrath, J., Arthur, J.S., Saklatvala, J., and Clark, A.R. (2006). Posttranslational regulation of tristetraprolin subcellular localization and protein stability by p38 mitogen-activated protein kinase and extracellular signal-regulated kinase pathways. *Mol. Cell. Biol.* 26, 2408–2418.
- Casey, S.C., Tong, L., Li, Y., Do, R., Walz, S., Fitzgerald, K.N., Gouw, A.M., Baylot, V., Gütgemann, I., Eilers, M., and Felsner, D.W. (2016). MYC regulates the antitumor immune response through CD47 and PD-L1. *Science* 352, 227–231.
- Cha, H.J., Lee, H.H., Chae, S.W., Cho, W.J., Kim, Y.M., Choi, H.J., Choi, D.H., Jung, S.W., Min, Y.J., Lee, B.J., et al. (2011). Tristetraprolin downregulates the expression of both VEGF and COX-2 in human colon cancer. *Hepatogastroenterology* 58, 790–795.
- Chrestensen, C.A., Schroeder, M.J., Shabanowitz, J., Hunt, D.F., Pelo, J.W., Worthington, M.T., and Sturgill, T.W. (2004). MAPKAP kinase 2 phosphorylates tristetraprolin on *in vivo* sites including Ser178, a site required for 14-3-3 binding. *J. Biol. Chem.* 279, 10176–10184.
- D’Incecco, A., Andreozzi, M., Ludovini, V., Rossi, E., Capodanno, A., Landi, L., Tibaldi, C., Minuti, G., Salvini, J., Coppi, E., et al. (2015). PD-1 and PD-L1 expression in molecularly selected non-small-cell lung cancer patients. *Br. J. Cancer* 112, 95–102.
- Deleault, K.M., Skinner, S.J., and Brooks, S.A. (2008). Tristetraprolin regulates TNF TNF-alpha mRNA stability via a proteasome dependent mechanism involving the combined action of the ERK and p38 pathways. *Mol. Immunol.* 45, 13–24.
- Díaz-Moreno, I., Hollingworth, D., Frenkiel, T.A., Kelly, G., Martin, S., Howell, S., García-Mayoral, M., Gherzi, R., Briata, P., and Ramos, A. (2009). Phosphorylation-mediated unfolding of a KH domain regulates KSRP localization via 14-3-3 binding. *Nat. Struct. Mol. Biol.* 16, 238–246.
- Dong, Z.Y., Zhong, W.Z., Zhang, X.C., Su, J., Xie, Z., Liu, S.Y., Tu, H.Y., Chen, H.J., Sun, Y.L., Zhou, Q., et al. (2017). Potential predictive value of TP53 and KRAS mutation status for response to PD-1 blockade immunotherapy in lung adenocarcinoma. *Clin. Cancer Res.* 23, 3012–3024.
- Du, L., Schageman, J.J., Subauste, M.C., Saber, B., Hammond, S.M., Prudkin, L., Wistuba, I.I., Ji, L., Roth, J.A., Minna, J.D., and Pertsemelidis, A. (2009). miR-93, miR-98, and miR-197 regulate expression of tumor suppressor gene FUS1. *Mol. Cancer Res.* 7, 1234–1243.

- Ebert, P.J.R., Cheung, J., Yang, Y., McNamara, E., Hong, R., Moskalenko, M., Gould, S.E., Maecker, H., Irving, B.A., Kim, J.M., et al. (2016). MAP kinase inhibition promotes T cell and anti-tumor activity in combination with PD-L1 checkpoint blockade. *Immunity* 44, 609–621.
- El-Jawahri, J.J., El-Sherbiny, Y.M., Scott, G.B., Morgan, R.S., Prestwich, R., Bowles, P.A., Blair, G.E., Tanaka, T., Rabbitts, T.H., Meade, J.L., and Cook, G.P. (2014). Blocking oncogenic RAS enhances tumour cell surface MHC class I expression but does not alter susceptibility to cytotoxic lymphocytes. *Mol. Immunol.* 58, 160–168.
- Essafi-Benkhadir, K., Onesto, C., Stebe, E., Moroni, C., and Pagès, G. (2007). Tristetraprolin inhibits Ras-dependent tumor vascularization by inducing vascular endothelial growth factor mRNA degradation. *Mol. Biol. Cell* 18, 4648–4658.
- Garner, A.P., Weston, C.R., Todd, D.E., Balmanno, K., and Cook, S.J. (2002). Delta MEKK3:ER* activation induces a p38 alpha/beta 2-dependent cell cycle arrest at the G2 checkpoint. *Oncogene* 21, 8089–8104.
- Garon, E.B., Rizvi, N.A., Hui, R., Leigh, N., Balmanoukian, A.S., Eder, J.P., Patnaik, A., Aggarwal, C., Gubens, M., Horn, L., et al.; KEYNOTE-001 Investigators (2015). Pembrolizumab for the treatment of non-small-cell lung cancer. *N. Engl. J. Med.* 372, 2018–2028.
- Giannou, A.D., Marazioti, A., Kanellakis, N.I., Giopanou, I., Lilis, I., Zazara, D.E., Ntaliarda, G., Kati, D., Armenis, V., Giotopoulou, G.A., et al. (2017). NRAS destines tumor cells to the lungs. *EMBO Mol. Med.* 9, 672–686.
- Gubin, M.M., Zhang, X., Schuster, H., Caron, E., Ward, J.P., Noguchi, T., Ivanova, Y., Hundal, J., Arthur, C.D., Krebber, W.J., et al. (2014). Checkpoint blockade cancer immunotherapy targets tumour-specific mutant antigens. *Nature* 515, 577–581.
- Hall, M.P., Huang, S., and Black, D.L. (2004). Differentiation-induced colocalization of the KH-type splicing regulatory protein with polypyrimidine tract binding protein and the c-src pre-mRNA. *Mol. Biol. Cell* 15, 774–786.
- Härdle, L., Bachmann, M., Bollmann, F., Pautz, A., Schmid, T., Eberhardt, W., Kleinert, H., Pfeilschifter, J., and Mühl, H. (2015). Tristetraprolin regulation of interleukin-22 production. *Sci. Rep.* 5, 15112.
- Herbst, R.S., Soria, J.C., Kowanetz, M., Fine, G.D., Hamid, O., Gordon, M.S., Sosman, J.A., McDermott, D.F., Powderly, J.D., Gettinger, S.N., et al. (2014). Predictive correlates of response to the anti-PD-L1 antibody MPDL3280A in cancer patients. *Nature* 515, 563–567.
- Jiang, X., Zhou, J., Giobbie-Hurder, A., Wargo, J., and Hodi, F.S. (2013). The activation of MAPK in melanoma cells resistant to BRAF inhibition promotes PD-L1 expression that is reversible by MEK and PI3K inhibition. *Clin. Cancer Res.* 19, 598–609.
- Kataoka, K., Shiraiishi, Y., Takeda, Y., Sakata, S., Matsumoto, M., Nagano, S., Maeda, T., Nagata, Y., Kitanaka, A., Mizuno, S., et al. (2016). Aberrant PD-L1 expression through 3'-UTR disruption in multiple cancers. *Nature* 534, 402–406.
- Kemp, S.J., Thorley, A.J., Gorelik, J., Seckl, M.J., O'Hare, M.J., Arcaro, A., Korchev, Y., Goldstraw, P., and Tetley, T.D. (2008). Immortalization of human alveolar epithelial cells to investigate nanoparticle uptake. *Am. J. Respir. Cell Mol. Biol.* 39, 591–597.
- Lai, W.S., Parker, J.S., Grissom, S.F., Stumpo, D.J., and Blackshear, P.J. (2006). Novel mRNA targets for tristetraprolin (TTP) identified by global analysis of stabilized transcripts in TTP-deficient fibroblasts. *Mol. Cell. Biol.* 26, 9196–9208.
- Lau, J., Cheung, J., Navarro, A., Lianoglou, S., Haley, B., Totpal, K., Sanders, L., Koeppen, H., Caplazi, P., McBride, J., et al. (2017). Tumour and host cell PD-L1 is required to mediate suppression of anti-tumour immunity in mice. *Nat. Commun.* 8, 14572.
- Le, D.T., Uram, J.N., Wang, H., Bartlett, B.R., Kemberling, H., Eyring, A.D., Skora, A.D., Luber, B.S., Azad, N.S., Laheru, D., et al. (2015). PD-1 blockade in tumors with mismatch-repair deficiency. *N. Engl. J. Med.* 372, 2509–2520.
- Li, D., Zhu, X., Wang, H., and Li, N. (2017). Association between PD-L1 expression and driven gene status in NSCLC: A meta-analysis. *Eur. J. Surg. Oncol.* 43, 1372–1379.
- Linnemann, C., van Buuren, M.M., Bies, L., Verdegaal, E.M.E., Schotte, R., Calis, J.J.A., Behjati, S., Velds, A., Hilkmann, H., Atmioui, D.E., et al. (2015). High-throughput epitope discovery reveals frequent recognition of neo-antigens by CD4+ T cells in human melanoma. *Nat. Med.* 21, 81–85.
- Lito, P., Solomon, M., Li, L.S., Hansen, R., and Rosen, N. (2016). Allele-specific inhibitors inactivate mutant KRAS G12C by a trapping mechanism. *Science* 351, 604–608.
- Liu, L., Mayes, P.A., Eastman, S., Shi, H., Yadavilli, S., Zhang, T., Yang, J., Seestaller-Wehr, L., Zhang, S.Y., Hopson, C., et al. (2015). The BRAF and MEK inhibitors dabrafenib and trametinib: effects on immune function and in combination with immunomodulatory antibodies targeting PD-1, PD-L1, and CTLA-4. *Clin. Cancer Res.* 21, 1639–1651.
- Loboda, A., Nebozhyn, M., Klinghoffer, R., Frazier, J., Chastain, M., Arthur, W., Roberts, B., Zhang, T., Chenard, M., Haines, B., et al. (2010). A gene expression signature of RAS pathway dependence predicts response to PI3K and RAS pathway inhibitors and expands the population of RAS pathway activated tumors. *BMC Med. Genomics* 3, 26.
- Lykke-Andersen, J., and Wagner, E. (2005). Recruitment and activation of mRNA decay enzymes by two ARE-mediated decay activation domains in the proteins TTP and BRF-1. *Genes Dev.* 19, 351–361.
- Mahtani, K.R., Brook, M., Dean, J.L., Sully, G., Saklatvala, J., and Clark, A.R. (2001). Mitogen-activated protein kinase p38 controls the expression and posttranslational modification of tristetraprolin, a regulator of tumor necrosis factor alpha mRNA stability. *Mol. Cell. Biol.* 21, 6461–6469.
- Molina-Arcas, M., Hancock, D.C., Sheridan, C., Kumar, M.S., and Downward, J. (2013). Coordinate direct input of both KRAS and IGF1 receptor to activation of PI3 kinase in KRAS-mutant lung cancer. *Cancer Discov.* 3, 548–563.
- Nicke, B., Bastien, J., Khanna, S.J., Warne, P.H., Cowling, V., Cook, S.J., Peters, G., Delpuech, O., Schulze, A., Berns, K., et al. (2005). Involvement of MINK, a Ste20 family kinase, in Ras oncogene-induced growth arrest in human ovarian surface epithelial cells. *Mol. Cell* 20, 673–685.
- Pardoll, D.M. (2012). The blockade of immune checkpoints in cancer immunotherapy. *Nat. Rev. Cancer* 12, 252–264.
- Parsa, A.T., Waldron, J.S., Panner, A., Crane, C.A., Parney, I.F., Barry, J.J., Cachola, K.E., Murray, J.C., Tihan, T., Jensen, M.C., et al. (2007). Loss of tumor suppressor PTEN function increases B7-H1 expression and immunoresistance in glioma. *Nat. Med.* 13, 84–88.
- Patricelli, M.P., Janes, M.R., Li, L.S., Hansen, R., Peters, U., Kessler, L.V., Chen, Y., Kucharski, J.M., Feng, J., Ely, T., et al. (2016). Selective inhibition of oncogenic KRAS output with small molecules targeting the inactive state. *Cancer Discov.* 6, 316–329.
- Rajagopalan, L.E., Burkholder, J.K., Turner, J., Culp, J., Yang, N.S., and Malter, J.S. (1995). Granulocyte-macrophage colony-stimulating factor mRNA stabilization enhances transgenic expression in normal cells and tissues. *Blood* 86, 2551–2558.
- Rizvi, N.A., Hellmann, M.D., Snyder, A., Kvistborg, P., Makarov, V., Havel, J.J., Lee, W., Yuan, J., Wong, P., Ho, T.S., et al. (2015). Cancer immunology. Mutational landscape determines sensitivity to PD-1 blockade in non-small cell lung cancer. *Science* 348, 124–128.
- Rounbehler, R.J., Fallahi, M., Yang, C., Steeves, M.A., Li, W., Doherty, J.R., Schaub, F.X., Sanduja, S., Dixon, D.A., Blackshear, P.J., and Cleveland, J.L. (2012). Tristetraprolin impairs myc-induced lymphoma and abolishes the malignant state. *Cell* 150, 563–574.
- Selamat, S.A., Chung, B.S., Girard, L., Zhang, W., Zhang, Y., Campan, M., Siegmund, K.D., Koss, M.N., Hagen, J.A., Lam, W.L., et al. (2012). Genome-scale analysis of DNA methylation in lung adenocarcinoma and integration with mRNA expression. *Genome Res.* 22, 1197–1211.
- Skrzypczak, M., Goryca, K., Rubel, T., Paziewska, A., Mikula, M., Jarosz, D., Pachlewski, J., Oledzki, J., and Ostrowski, J. (2010). Modeling oncogenic signaling in colon tumors by multidirectional analyses of microarray data directed for maximization of analytical reliability. *PLoS ONE* 5, 5.
- Stoecklin, G., Stubbs, T., Kedersha, N., Wax, S., Rigby, W.F., Blackwell, T.K., and Anderson, P. (2004). MK2-induced tristetraprolin:14-3-3 complexes

- prevent stress granule association and ARE-mRNA decay. *EMBO J.* **23**, 1313–1324.
- Stoecklin, G., Tenenbaum, S.A., Mayo, T., Chittur, S.V., George, A.D., Baroni, T.E., Blakeshear, P.J., and Anderson, P. (2008). Genome-wide analysis identifies interleukin-10 mRNA as target of tristetraprolin. *J. Biol. Chem.* **283**, 11689–11699.
- Sumimoto, H., Takano, A., Teramoto, K., and Daigo, Y. (2016). RAS-mitogen-activated protein kinase signal is required for enhanced PD-L1 expression in human lung cancers. *PLoS ONE* **11**, e0166626.
- Sun, L., Stoecklin, G., Van Way, S., Hinkovska-Galcheva, V., Guo, R.F., Anderson, P., and Shanley, T.P. (2007). Tristetraprolin (TTP)-14-3-3 complex formation protects TTP from dephosphorylation by protein phosphatase 2a and stabilizes tumor necrosis factor- α mRNA. *J. Biol. Chem.* **282**, 3766–3777.
- Sweet-Cordero, A., Mukherjee, S., Subramanian, A., You, H., Roix, J.J., Ladd-Acosta, C., Mesirov, J., Golub, T.R., and Jacks, T. (2005). An oncogenic KRAS2 expression signature identified by cross-species gene-expression analysis. *Nat. Genet.* **37**, 48–55.
- Taylor, G.A., Thompson, M.J., Lai, W.S., and Blakeshear, P.J. (1995). Phosphorylation of tristetraprolin, a potential zinc finger transcription factor, by mitogen stimulation in intact cells and by mitogen-activated protein kinase in vitro. *J. Biol. Chem.* **270**, 13341–13347.
- Taylor, G.A., Carballo, E., Lee, D.M., Lai, W.S., Thompson, M.J., Patel, D.D., Schenkman, D.I., Gilkeson, G.S., Broxmeyer, H.E., Haynes, B.F., and Blakeshear, P.J. (1996). A pathogenetic role for TNF α in the syndrome of cachexia, arthritis, and autoimmunity resulting from tristetraprolin (TTP) deficiency. *Immunity* **4**, 445–454.
- Topalian, S.L., Hodi, F.S., Brahmer, J.R., Gettinger, S.N., Smith, D.C., McDermott, D.F., Powderly, J.D., Carvajal, R.D., Sosman, J.A., Atkins, M.B., et al. (2012). Safety, activity, and immune correlates of anti-PD-1 antibody in cancer. *N. Engl. J. Med.* **366**, 2443–2454.
- Yang, N.S., Wang, J.H., and Turner, J. (2004). Molecular strategies for improving cytokine transgene expression in normal and malignant tissues. *Gene Ther.* **11**, 100–108.
- Yang, H., Chen, H., Luo, S., Li, L., Zhou, S., Shen, R., Lin, H., and Xie, X. (2017). The correlation between programmed death-ligand 1 expression and driver gene mutations in NSCLC. *Oncotarget* **8**, 23517–23528.
- Zubiaga, A.M., Belasco, J.G., and Greenberg, M.E. (1995). The nonamer UUAUUUAUU is the key AU-rich sequence motif that mediates mRNA degradation. *Mol. Cell. Biol.* **15**, 2219–2230.

Distinct Cellular Mechanisms Underlie Anti-CTLA-4 and Anti-PD-1 Checkpoint Blockade

Spencer C. Wei,^{1,*} Jacob H. Levine,² Alexandria P. Cogdill,^{1,3} Yang Zhao,⁴ Nana-Ama A.S. Anang,¹ Miles C. Andrews,³ Padmanee Sharma,^{5,6} Jing Wang,⁴ Jennifer A. Wargo,^{3,6,7} Dana Pe'er,² and James P. Allison^{1,6,8,*}

¹Department of Immunology, The University of Texas MD Anderson Cancer Center, Houston, TX 77030, USA

²Computational and Systems Biology Program, Sloan Kettering Institute, New York, NY 10065, USA

³Department of Surgical Oncology, The University of Texas MD Anderson Cancer Center, Houston, TX 77030, USA

⁴Department of Bioinformatics and Computational Biology, The University of Texas MD Anderson Cancer Center, Houston, TX 77030, USA

⁵Department of Genitourinary Medical Oncology, The University of Texas MD Anderson Cancer Center, Houston, TX 77030, USA

⁶Parker Institute for Cancer Immunotherapy, The University of Texas MD Anderson Cancer Center, Houston, TX 77030, USA

⁷Department of Genomic Medicine, The University of Texas MD Anderson Cancer Center, Houston, TX 77030, USA

⁸Lead Contact

*Correspondence: scwei@mdanderson.org (S.C.W.), jallison@mdanderson.org (J.P.A.)

<http://dx.doi.org/10.1016/j.cell.2017.07.024>

SUMMARY

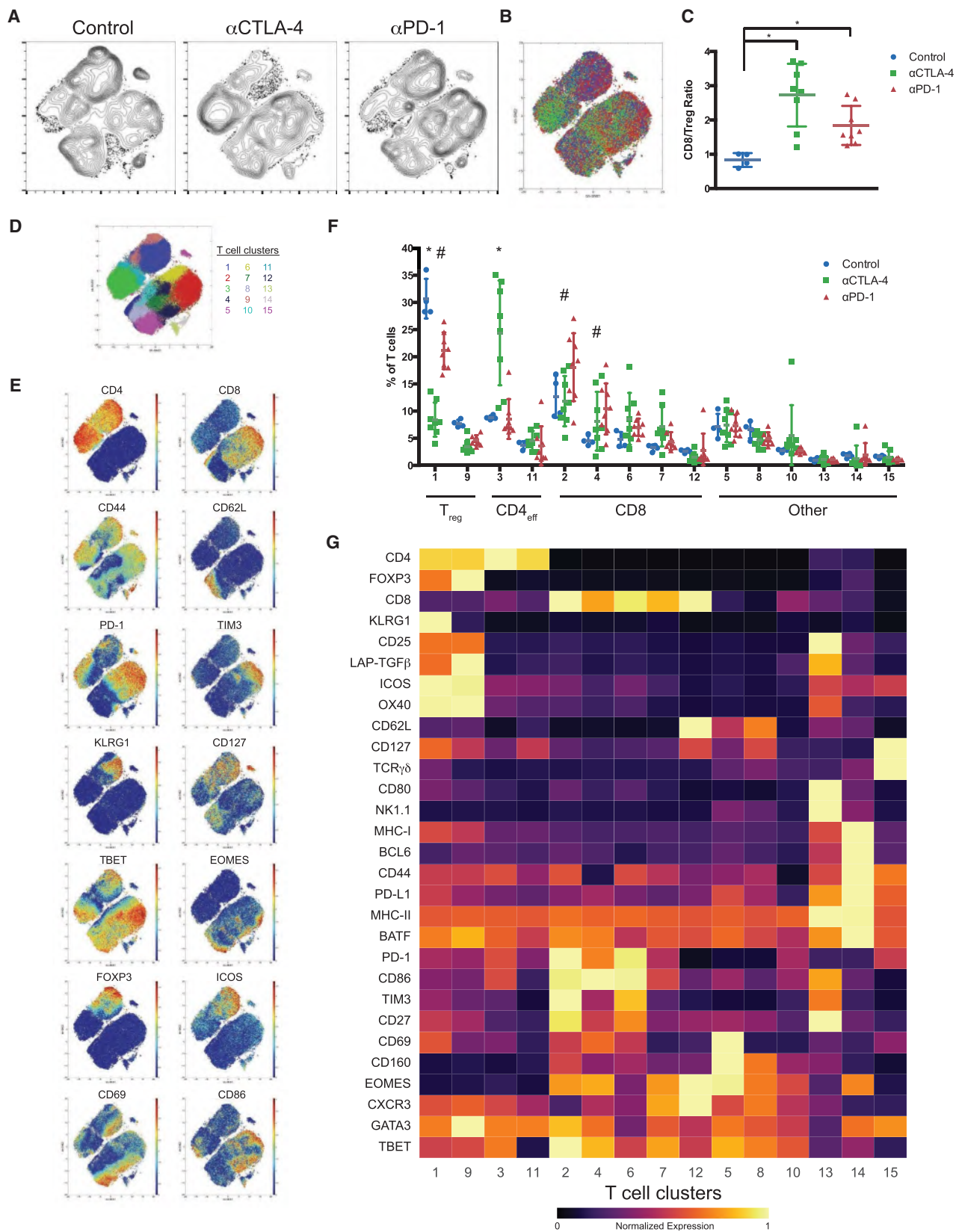
Immune-checkpoint blockade is able to achieve durable responses in a subset of patients; however, we lack a satisfying comprehension of the underlying mechanisms of anti-CTLA-4- and anti-PD-1-induced tumor rejection. To address these issues, we utilized mass cytometry to comprehensively profile the effects of checkpoint blockade on tumor immune infiltrates in human melanoma and murine tumor models. These analyses reveal a spectrum of tumor-infiltrating T cell populations that are highly similar between tumor models and indicate that checkpoint blockade targets only specific subsets of tumor-infiltrating T cell populations. Anti-PD-1 predominantly induces the expansion of specific tumor-infiltrating exhausted-like CD8 T cell subsets. In contrast, anti-CTLA-4 induces the expansion of an ICOS⁺ Th1-like CD4 effector population in addition to engaging specific subsets of exhausted-like CD8 T cells. Thus, our findings indicate that anti-CTLA-4 and anti-PD-1 checkpoint-blockade-induced immune responses are driven by distinct cellular mechanisms.

INTRODUCTION

Immunotherapy is assuming a role as a pillar of cancer treatment, but the remarkable immune-mediated responses are limited to a minority of patients. Immune-checkpoint blockade (ICB) is able to elicit durable responses in a fraction of cancer patients. For example, 22% of advanced-melanoma patients treated with anti-CTLA-4 have durable responses extending beyond 10 years (Hodi et al., 2010; Schadendorf et al., 2015). Similarly, blockade of the PD-1/PD-L1 signaling axis is also sufficient to induce significant responses in multiple tumor types (Brahmer et al., 2012; Topalian et al., 2012). Despite such

tremendous clinical progress, we still lack a detailed understanding of the fundamental mechanisms that underlie anti-CTLA-4- and anti-PD-1-induced tumor immune rejection, which is necessary for the improvement of current therapies and for the rational design of combination therapy approaches. The aspects of the host immune response and the tumor intrinsic properties that define therapeutic sensitivity to ICB therapy remain to be elucidated (Sharma and Allison, 2015; Topalian et al., 2015). Despite evidence that tumor properties such as mutational load (Hugo et al., 2016; McGranahan et al., 2016) and genetic lesions (Gao et al., 2016; Spranger et al., 2015; Zaretsky et al., 2016) can influence therapeutic response to ICB, we do not fully understand why different tumor types display such a range of therapeutic sensitivity. Conceptually, such differences could arise because different tumor types elicit fundamentally distinct immune responses or, alternatively, because the magnitude of host immune responses varies between different tumor types.

A critical unresolved question is whether anti-tumor immune responses induced by anti-CTLA-4 and anti-PD-1 antibodies are mediated through distinct, non-redundant mechanisms. A wealth of studies have demonstrated that CTLA-4 and PD-1 attenuate T cell activation through distinct mechanisms (Pardoll, 2012). CTLA-4 is upregulated immediately following TCR ligation and outcompetes CD28 for B7 ligand binding, thus attenuating positive costimulation by CD28 (Krummel and Allison, 1995; Walunas et al., 1994). PD-1 is induced later during T cell activation and, upon engagement with PD-L1 or PD-L2, attenuates TCR signaling via recruitment of tyrosine phosphatases (Chemnitz et al., 2004; Freeman et al., 2000; Latchman et al., 2001). In addition to utilizing distinct molecular mechanisms of action, CTLA-4 and PD-1 attenuate T cell activity through mechanisms that are separated spatially and temporally. Whereas CTLA-4 primarily attenuates T cell activation in the priming phase through cell intrinsic and extrinsic mechanisms, PD-1 primarily attenuates T cell activity in peripheral tissues through cell intrinsic mechanisms (Pardoll, 2012; Walker and Sansom, 2011). This distinction is highlighted by the fact that the cellular sources of the ligands of PD-1 and CTLA-4 are different and serve different physiological functions. Thus, we hypothesized that anti-CTLA-4- and



(legend on next page)

anti-PD-1-induced anti-tumor immune responses are mediated by distinct cellular mechanisms.

To address this hypothesis, we utilized mass cytometry to comprehensively profile the immune infiltrates of solid tumors following ICB. Mass cytometry allows for the interrogation of more than 40 analytes at single-cell resolution and enables systematic identification of complex cellular populations using high-dimensional analyses (Newell and Cheng, 2016; Tanner et al., 2013). Mass-cytometry-driven approaches have been utilized to characterize cellular processes including hematopoiesis, immune-cell differentiation, and leukemic disease progression (Bendall et al., 2011; Spitzer and Nolan, 2016) and, more recently, to analyze the immune infiltrates of solid tumors (Chevrier et al., 2017; Lavin et al., 2017; Leelatian et al., 2017; Spitzer et al., 2017). Here, we leverage mass cytometry to comprehensively characterize the cellular mechanisms of ICB in human melanoma and murine syngeneic transplantable tumor models. Comparisons of murine tumor models indicate that the phenotypes of infiltrating T cell populations and mechanisms of ICB are tumor-type independent. Both anti-PD-1 and anti-CTLA-4 only target a subset of tumor-infiltrating T cell populations, inducing the expansion of exhausted-like CD8 T cells. Notably, anti-CTLA-4 but not anti-PD-1 modulates the CD4 effector compartment, specifically inducing the expansion of an ICOS⁺ Th1-like CD4 effector subset. Together, these pre-clinical and clinical analyses indicate that anti-tumor immune responses induced by CTLA-4 and PD-1 blockade are driven by distinct cellular mechanisms.

RESULTS

Identification of Checkpoint-Blockade-Responsive MC38 Tumor-Infiltrating T Cell Subsets

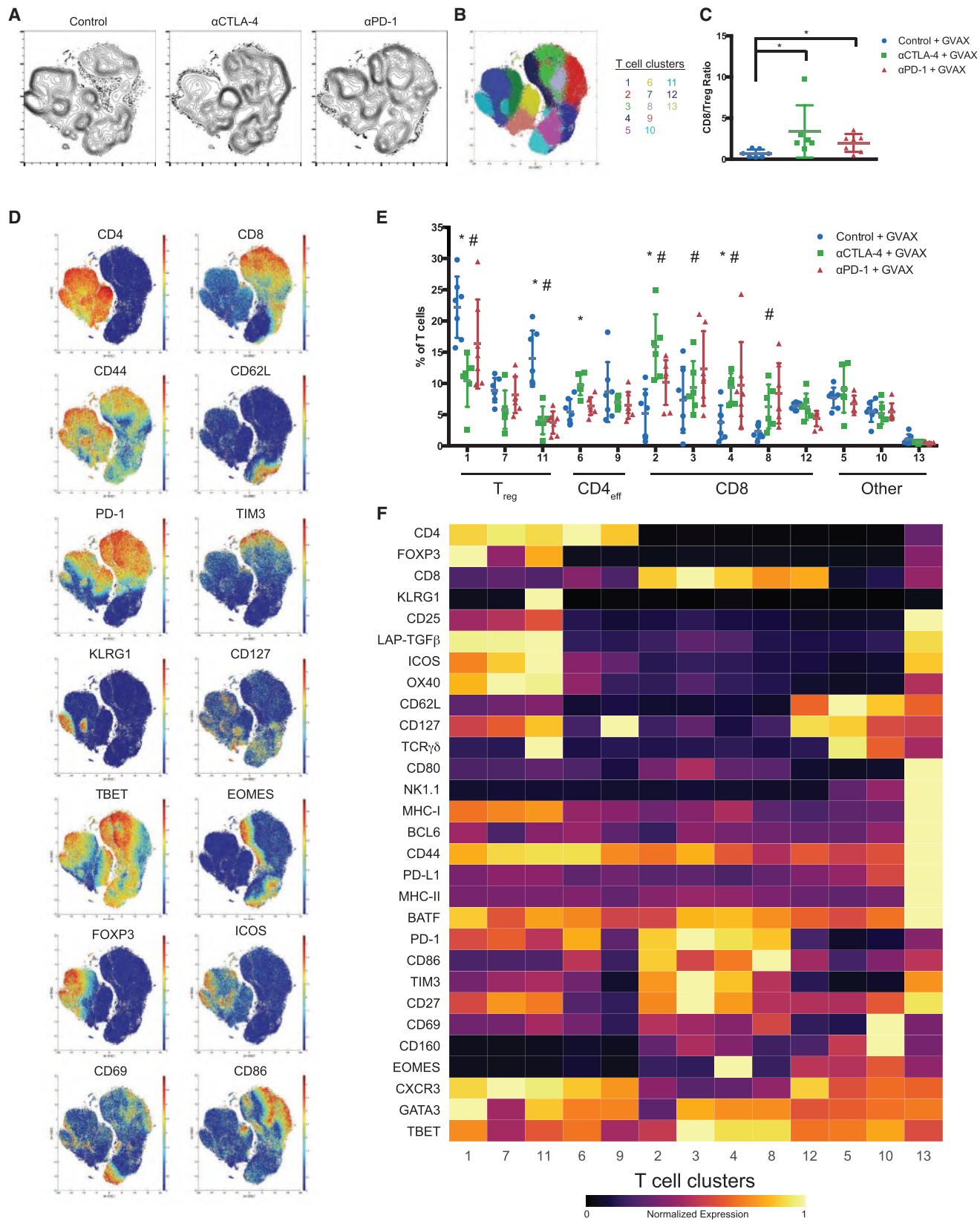
To identify ICB-responsive tumor-infiltrating T cell populations, we profiled tumors by mass cytometry and utilized a well-validated data-driven unsupervised clustering approach to classify cellular populations (Levine et al., 2015; Melchiotti et al., 2017; Shekhar et al., 2016). We further validated this approach for quantitative *de novo* classification of tumor-infiltrating lymphocyte (TIL) populations using spike-in experiments (Figure S1; STAR Methods). To comprehensively characterize tumor-infiltrating T cell populations, we designed a staining panel with 33 surface and 10 intracellular markers. This panel included non-T cell lineage markers (e.g., CD11b, CD11c, CD19), T cell differentiation and activation markers (e.g., PD-1, ICOS, TIM3, KLRG1, CD127), and importantly, T cell lineage transcription factors

(e.g., TBET, EOMES, GATA3, BCL6, ROR γ T, FOXP3). Using this approach, we analyzed immunogenic MC38 colorectal tumors from mice treated with anti-CTLA-4 or anti-PD-1. To enable analysis of TILs, we empirically defined a tumor inoculation dose and treatment schedule (using standard antibody dosages) such that tumors were not completely rejected at time of analysis despite induction of an effective immune response. Treatment was initiated only after tumors became palpable and thus also more closely reflected the clinical context. We focused our analyses on the T cell compartment given our current understanding of CTLA-4 and PD-1 biology, the design of our staining panel, and analyses of the total CD45⁺ compartment (Figure S1). Analysis of the T cell compartment revealed dramatic population shifts in response to anti-CTLA-4 and anti-PD-1 (Figures 1A and 1B). These observations are consistent with an increase in CD8/T_{reg} ratio following both treatments, as determined by manual gating analyses and reflect the induction of an effective immune response by ICB (Figure 1C).

To gain a more in-depth understanding of the mechanisms that underlie ICB, we generated a high-resolution map of phenotypically defined tumor-infiltrating T cell populations using unsupervised clustering. 15 distinct MC38 tumor-infiltrating T cell clusters of >0.5% relative frequency were identified, including 5 CD8, 2 T_{reg}, and 2 CD4 effector clusters (Figures 1D–1F). This approach focused specifically on tumor-infiltrating populations, and thus many canonical T cell subsets present in other tissues would not be expected present (e.g., naive); as such, this represents an extensive catalog of infiltrating T cell subsets. Notably, ICB did not modulate the frequency of any NKT, $\gamma\delta$ T cell, or low frequency (<0.5%) clusters. Thus, we focused our analyses on CD4 and CD8 T cell subsets, which displayed a range of activation and exhaustion phenotypes (Figure 1G). Both anti-CTLA-4 and anti-PD-1 treatment led to an expansion of CD8 T cells; however, not all CD8 T cell subsets expanded following ICB. Surprisingly, a phenotypically exhausted PD-1^{hi}TIM3⁺ population expanded the most among CD8 populations (Figure 1F). To address whether T cell expansion results from increased proliferation or infiltration, we assessed short-term incorporation of 5-iodo-deoxyuridine (IdU). ICB-responsive CD8 clusters incorporated IdU, suggesting that these cells are proliferating within the tumor microenvironment (TME) (Figure S1). Given the timing of IdU treatment and retention of IdU in daughter cells, this approach may detect extratumoral-blasting T cells that subsequently infiltrate the tumor, in addition to cells proliferating within the TME. Nonetheless, these observations indicate that ICB-sensitive T cells retain proliferative capacity even after multiple rounds of

Figure 1. Identification of Checkpoint-Blockade-Responsive MC38 Tumor-Infiltrating T Cell Populations

(A) Density t-SNE plots of an equal number of CD3e⁺ MC38 tumor-infiltrating T cells from each treatment group.
 (B) Overlaid t-SNE plot displaying equal number of events from each treatment group (control, blue; anti-CTLA-4, green; anti-PD-1, red).
 (C) Plot of CD8/T_{reg} ratios displayed on a per-mouse basis with mean \pm SD (*p < 0.05, unpaired t test).
 (D) t-SNE plot of MC38 infiltrating T cells overlaid with color-coded clusters.
 (E) t-SNE plot of infiltrating T cells overlaid with the expression of selected markers.
 (F) Frequency of T cell clusters displayed on a per-mouse basis with mean \pm SD (*, control versus anti-CTLA-4; #, control versus anti-PD-1; p < 0.05, Dunnett's multiple comparison). T cell compartments are denoted including CD8, T_{reg}, and CD4 effector (CD4_{eff}).
 (G) Heatmap displaying normalized marker expression of each T cell cluster. Representative data from three independent experiments is shown. See also Figure S1 and STAR Methods.



(legend on next page)

therapy and that ICB leads to the expansion of only specific intratumoral T cell subsets.

We next assessed the effect of ICB on CD4 T cell populations. Within the T_{reg} compartment, two clusters were identified that are largely distinguished by KLRG1 expression (Figure 1G). Relative T_{reg} frequency decreased following both anti-PD-1 and anti-CTLA-4, consistent with a shift between effector and regulatory T cell populations (Quezada et al., 2006). The magnitude of this decrease was greater following CTLA-4 blockade, consistent with findings that treatment with anti-CTLA-4 leads to intratumoral T_{reg} depletion in murine tumor models (Selby et al., 2013; Simpson et al., 2013). Two CD4 effector T cell subsets were identified in the TME, and both display an activated phenotype but differ in their expression of key markers including PD-1 and TBET (Figure 1G). Most notably, treatment with anti-CTLA-4 but not anti-PD-1 was associated with a significant expansion of a TBET⁺ Th1-like CD4 effector subset (Figure 1F). This population was proliferative but to a lesser degree than other clusters (Figure S11). We denote this subset as distinct from canonical Th1 cells because of expression of PD-1 and ICOS, which are defining characteristics of T follicular helper (TFH) cells, despite expression of TBET but not BCL6 (Th1- and TFH-lineage transcription factors, respectively). Neither therapy led to an expansion of un-skewed activated CD4 effectors. These observations suggest that specific T cell subsets are targeted by ICB and that anti-CTLA-4 leads to expansion of CD4 effector T cells.

Identification of Checkpoint-Blockade-Responsive B16BL6 Tumor-Infiltrating T Cell Subsets

We then sought to determine whether these findings reflect a generalizable mechanism of ICB responses. For this purpose, we performed similar experiments in the poorly immunogenic B16BL6 melanoma model to contrast the relatively high immunogenicity of MC38, allowing us to distinguish ICB response phenomena from tumor-type-specific observations. Due to low baseline T cell tumor infiltration and the lack of response to anti-CTLA-4 monotherapy (van Elsas et al., 1999), we treated mice with a single dose of the GVAX tumor vaccine in order to boost overall T cell infiltration. As in the MC38 system, we empirically defined the B16BL6 tumor inoculate and treatment schedule (using standard antibody dosages) such that tumors were not completely rejected at time of analysis despite induction of an effective immune response. Analysis of CD45⁺ TILs revealed significant therapy-induced changes in immune composition (Figure S2). We focused our analyses on the T cell compartment to identify ICB-responsive T cell populations.

Reflective of induction of an effective immune response, significant shifts in T cell populations in the TME were observed following treatment with anti-CTLA-4 and anti-PD-1 (Figures 2A and 2B), which mirrored an increase in CD8/ T_{reg} ratio as determined by manual gating (Figure 2C). Clustering identified 13 clusters of frequency greater than 0.5% including 5 CD8, 3 T_{reg} , 2 CD4 effector, NKT, and $\gamma\delta$ T cell clusters (Figures 2D and 2E). ICB did not affect the frequencies of any NKT, $\gamma\delta$ T cell, or low-frequency subsets. Remarkably, despite analysis of a different tumor type, time point of tumor progression, and the addition of a GM-CSF-expressing tumor vaccine, the T cell clusters identified in B16BL6 tumors were nearly identical to those identified in MC38 tumors. Of the five identified CD8 clusters, only a subset were responsive to ICB with PD-1⁺TIM3⁺ exhausted CD8 T cells expanding the most (Figures 2E and 2F). Of the three T_{reg} subsets identified, two contracted significantly following ICB. These populations differ primarily in their expression of KLRG1, with KLRG1⁺ T_{reg} decreasing in relative frequency most dramatically. Of the two CD4 effector populations identified, both displayed an activated CD44⁺CD62L^{lo} phenotype but were distinguished by expression of PD-1, CD127, and TBET (Figure 2F). Notably, the frequency of TBET⁺ Th1-like CD4 effector T cells increased following anti-CTLA-4 but not anti-PD-1 (Figure 2E). Thus, as observed in MC38 tumors, both anti-CTLA-4 and anti-PD-1 induce the expansion of specific T cell subsets and differentially affect CD4 effector T cells.

MC38 and B16BL6 Tumor-Infiltrating T Cell Populations Are Fundamentally Similar

The remarkable similarity in T cell populations identified by unsupervised clustering in MC38 and B16BL6 tumors suggests that the mechanisms governing responses to ICB are tumor-type independent. Conceptually, this implies that the same types of T cells are involved in anti-tumor T cell responses to different tumor types, at least in the context of transplantable murine tumor models. To explicitly address this possibility, we analyzed the multivariate profiles of infiltrating T cell populations from MC38 and B16BL6 tumors simultaneously in order to identify any significant associations between T cell phenotype and tumor type. Projecting these phenotypes into the coordinate axes defined by their principal components, we asked whether the distributions along each component differed significantly between MC38- and B16BL6-derived T cell populations (STAR methods). In other words, we asked whether any of the phenotypic variance among all T cell populations observed in all treatments (independent of frequency) was attributable to the tumor-model source.

Figure 2. Identification of Checkpoint-Blockade-Responsive B16BL6 Tumor-Infiltrating T Cell Populations

- (A) Density t-SNE plots of an equal number of CD3e⁺ B16BL6 tumor-infiltrating T cells from each treatment group.
 (B) t-SNE plot of infiltrating T cells overlaid with color-coded clusters.
 (C) Plot of CD8/ T_{reg} ratios displayed on a per-mouse basis with mean \pm SD (* p < 0.05, unpaired t test).
 (D) t-SNE plot of tumor-infiltrating T cells overlaid with the expression of selected markers.
 (E) Frequency of T cell clusters displayed on a per-mouse basis with mean \pm SD (*, control versus anti-CTLA-4; #, control versus anti-PD-1; p < 0.05, Dunnett's multiple comparison).
 (F) Heatmap displaying normalized marker expression of each T cell cluster. Representative data from three independent experiments is shown. See also Figure S2.

Comparison along each principal-component axis revealed that MC38 and B16BL6 tumor-infiltrating T cell subpopulations are phenotypically indistinguishable (Figure 3; Table S1A). The distribution of T cell subpopulations derived from MC38 and B16BL6 tumors did not differ along 38 of 39 principal components, which together explain 95% of the variance of the data (Table S1A). In the one case where a significant difference was detected (PC6), the discrepancy was attributable to contaminating CD19⁺ subpopulations in several MC38 samples and likely represents a technical artifact rather than a biological effect. This analysis indicates that there is no association between tumor model and the vast majority of phenotypic variance among the T cells identified in these models. This observation is confirmed visually by the overlap of MC38- and B16BL6-derived T cell populations plotted on biaxial pairs of the largest principal-component projections (Figure 3).

Thus, the multivariate phenotypes of T cell subsets from MC38 and B16BL6 tumors are quantitatively similar. This finding is striking given the use of the GVAX tumor vaccine only with the B16BL6 model and the difference in immunogenicity of these models. Consistent with MC38 being highly immunogenic and B16BL6 being poorly immunogenic, MC38 has more than 2-fold more nonsynonymous single-nucleotide variants (SNV) than B16BL6 (2,327 and 1,107, respectively; Table S1B). These data indicate that the types of T cells that infiltrate transplantable murine tumors are tumor-type independent and suggest that differences in immunogenicity between tumor types arise due to tumor intrinsic properties that modulate the magnitude (e.g., subset frequency), but not type, of anti-tumor T cell responses. Combined with the observation that similar T cell subsets are regulated in response to ICB in both tumor models, this suggests that the cellular mechanisms of CTLA-4 and PD-1 blockade are tumor-type independent.

Identification of B16BL6-Infiltrating T Cell Populations that Correlate with Tumor Growth

We then sought to identify T cell populations whose frequencies correlate with tumor growth to gain insight into their functional relevance. For this purpose, we leveraged our B16BL6 datasets and combined three independent biological replicate cohorts, which together displayed a robust response to ICB (Figures 4A and 4B). Using a metaclustering approach, in which populations first identified at the individual mouse level using PhenoGraph are then allowed to merge across cohorts (STAR Methods), 14 T cell populations were identified. The phenotypes and responses of these subsets to ICB were consistent with findings from single cohort analyses. Because ICB only modulated the frequencies of CD4 and CD8 T cell subsets, we focused our analyses on the 10 metaclusters within these compartments (Figures 4C, 4D, and S3). Expectedly, the frequency of major T_{reg} subsets correlated positively with tumor growth (Figures 4E and S3). The two major T_{reg} populations are primarily distinguished by KLRG1 expression, with the frequency of KLRG1⁺ T_{reg} (MC4) correlating more strongly with tumor growth than KLRG1⁻ T_{reg} (MC0) or manually gated T_{reg} (Figure S3; Tables S2A and S2B). Whether this difference reflects differences in functionality or response to ICB is unclear; however, both sub-

sets significantly correlated with tumor growth, suggesting that both retain suppressive activity.

Surprisingly, the frequency of only two of the four tumor-infiltrating CD8 T cell subsets negatively correlated with tumor growth (Figure 4E). These populations displayed an activated phenotype and increased frequencies following anti-CTLA-4 and anti-PD1 treatment (Figures 4C and 4D). Metacluster 2 (MC2) displayed a PD-1⁺TIM3^{lo}TBET⁺EOMES⁻ phenotype, while metacluster 10 (MC10) displayed a PD-1^{hi}TIM3⁺TBET⁺EOMES⁺ phenotype. The frequency of a third CD8 population (MC13), which displayed a PD-1^{hi}TIM3⁺TBET⁺EOMES⁻ exhausted phenotype, did not correlate with tumor growth (Table S2A). Thus, subtle multivariate phenotypic differences between metaclusters 2, 10, and 13 distinguish T cell populations that significantly differ in their correlation with tumor growth, which likely reflects functional differences between these populations. Moreover, these data suggest that fully exhausted non-terminally differentiated T cells (MC13) may not contribute significantly to tumor rejection in the context of ICB, at least during later stages of response. In contrast, less-exhausted non-terminally differentiated (MC2) and fully exhausted terminally differentiated (MC10) appear to provide the bulk of the functional anti-tumor T cell response.

Unexpectedly, the frequency of a non-proliferative CD44⁺CD62L⁺PD-1⁻ CD8 T cell subset, metacluster 11 (MC11), positively correlated with tumor growth (Figure 4E; Table S2A). This population may be tumor-irrelevant central memory CD8 T cells, raising the possibility that infiltration of antigen-irrelevant CD8 T cells is not only ineffective but may in fact dampen the anti-tumor immune response. In terms of the proliferative capacity of effective CD8 T cell subsets, MC10 incorporated IdU at almost four times the rate of MC2 (Figure S3C). In contrast, despite being highly proliferative, the frequency of MC13 does not correlate with tumor growth. This suggests that high proliferative capacity of CD8 T cells in the TME during later stages of responses to ICB is neither necessary nor sufficient for effective anti-tumor responses. Whether effective CD8 T cell subsets of low (MC2)- and high (MC10)-proliferative capacity contribute through distinct functions remains unclear.

The two CD4 effector T cell metaclusters identified include a PD-1^{hi}TBET⁺ Th1-like subset (MC3) and a PD-1^{lo}CD44^{int}CD127^{int} subset (MC5). Only the frequency of MC3 negatively correlated with tumor growth (Figure 4E; Table S2A). Notably, this correlation is driven by the specific expansion of this population following anti-CTLA-4 treatment. Interestingly, the Th1-like population displayed a low proliferation rate in both B16BL6 and MC38 tumor models (Figures S1 and S3), raising the possibility that modulation of this population by anti-CTLA-4 may primarily occur at earlier time points or in secondary lymphoid organs. Together, these data indicate that only specific populations of tumor-infiltrating CD4 and CD8 T cells mediate responses to ICB and suggest that the quantification of these phenotypically defined T cell subsets will provide improved predictive value compared to assessment of bulk compartments (e.g., CD8 T cells).

These findings reinforce the notion that data-driven multivariate analyses enable unbiased comprehensive cellular classification and robust *de novo* discovery of biologically relevant

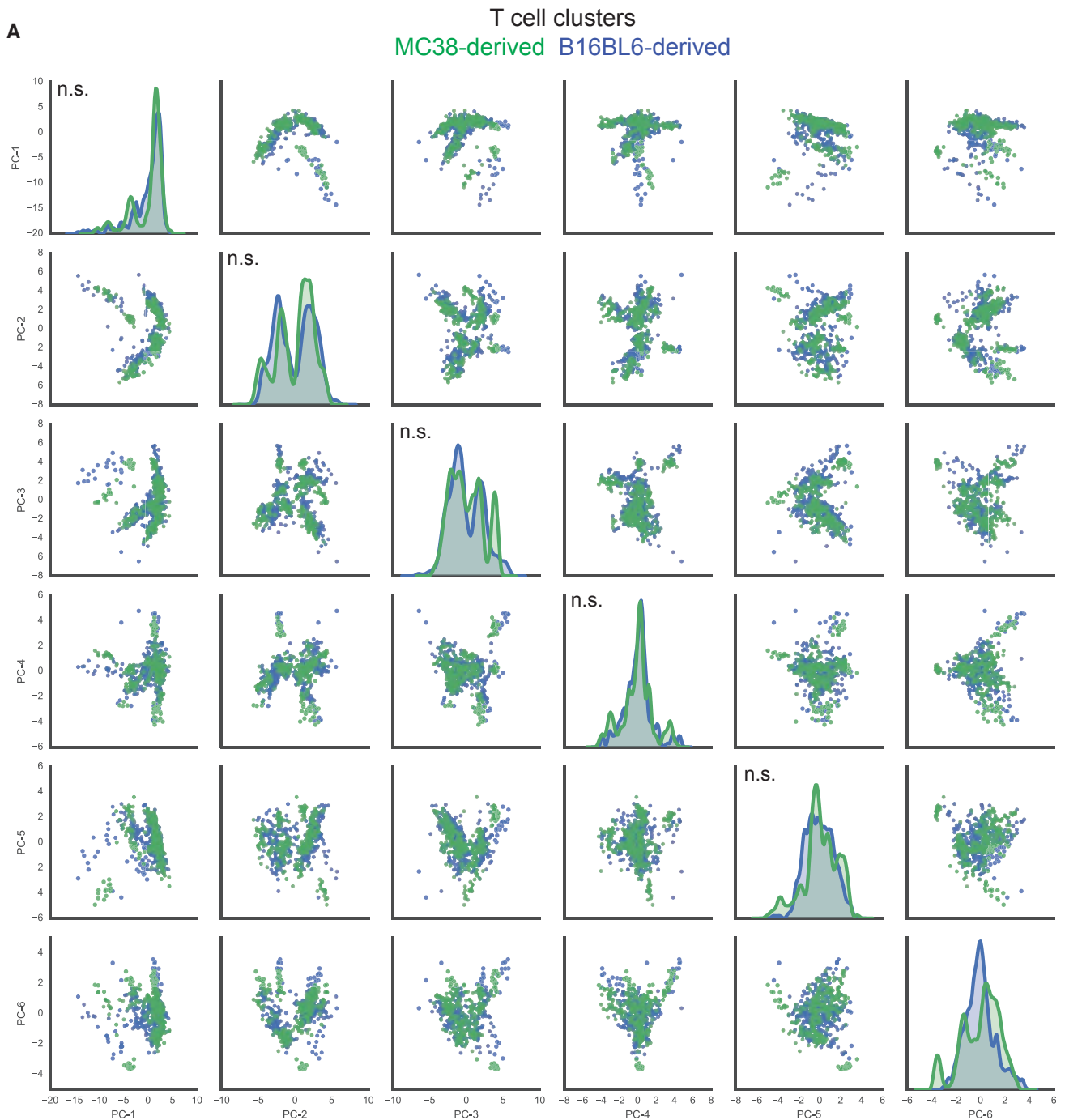
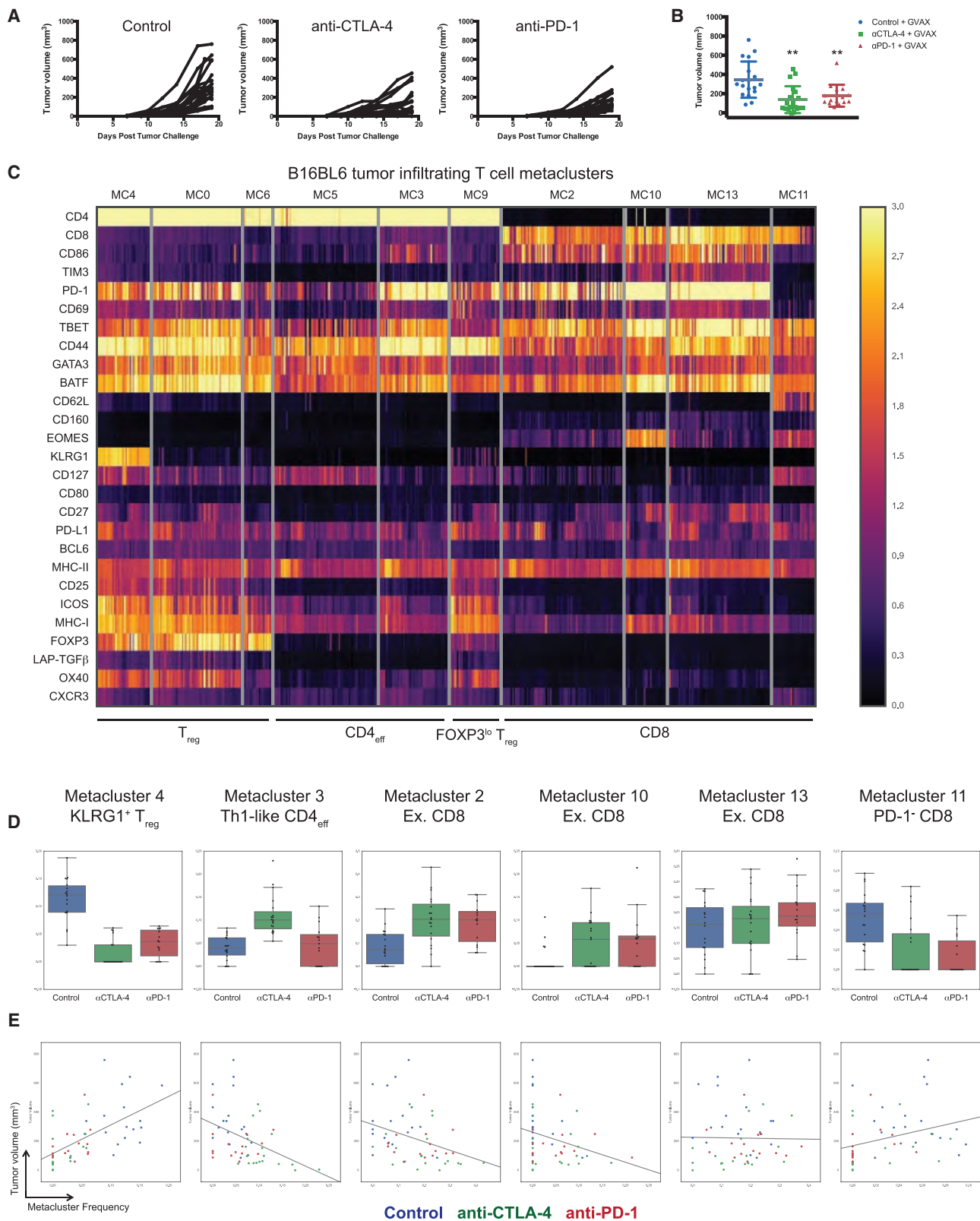


Figure 3. B16BL6 and MC38 Tumor-Infiltrating T Cell Populations Are Quantitatively Similar

(A) PCA was applied to T cell clusters identified on a per-mouse basis from MC38 and B16BL6 mass cytometry datasets. Projections of MC38 and B16BL6 infiltrating T cell clusters on to the first six principal components (PC), which together account for 78% of the phenotypic variance, are displayed in a pair-wise fashion (MC38, green; B16BL6, blue). Univariate distributions of T cell clusters along each of the first six principal components are displayed along the diagonal. The Kolmogorov-Smirnov test was applied to test whether distributions of MC38- and B16BL6-derived T cell clusters along each PC are different (n.s., not significant).

See also Table S1.



(legend on next page)

populations. It is important to note that while we ascribe key phenotypic features to identified clusters (Figure 4; Table S2A), quantitative multivariate analyses provide vastly improved subset assignment compared to manual gating. We sought to determine whether the insights provided by high-dimensional analyses would enable approximation of these subsets by manual gating. Using a limited number of key parameters derived from multivariate analyses, manual gating is able to discriminate relevant T cell subsets, albeit with significantly reduced fidelity (Figure S3E; Table S2B). Consistent with the importance of lineage transcription factors for robust subset identification, expression of TBET but not individual surface markers was sufficient to identify CD4 effector subpopulations that significantly negatively correlate with tumor growth.

Differential Transcriptional Regulation in Tumor-Infiltrating CD4 T Cells following Anti-CTLA-4 and Anti-PD-1 Checkpoint Blockade

Next, we investigated whether anti-CTLA-4 and anti-PD-1 induce different transcriptional changes in tumor-infiltrating CD4 T cells, as has been observed in CD8 T cells in preclinical and clinical contexts (Das et al., 2015; Gubin et al., 2014). Gene-expression analyses of MC38 tumor-infiltrating ICOS⁺ CD4 T cells revealed significant, but largely non-overlapping, transcriptional responses induced by anti-CTLA-4 and anti-PD-1 (Figure S4). Of the top 15 cellular pathways regulated by each treatment, only 3 were shared. Mitochondrial and oxidative phosphorylation pathways were among the most significantly modulated by anti-PD-1, consistent with findings that these pathways can restrict T cell activity in the TME (Bensch et al., 2016; Gubin et al., 2014). CTLA-4 blockade led to an engagement of largely distinct pathways, which included pathways involved in cell-cycle regulation. These observations indicate that anti-CTLA-4 and anti-PD-1 induce differential transcription effects in tumor-infiltrating CD4 T cells and support the paradigm that these therapies act through distinct mechanisms.

Anti-CTLA-4 and Anti-PD-1 Therapies Modulate Specific T Cell Populations in Human Melanoma

Finally, we sought to determine whether distinct cellular mechanisms also underlie anti-CTLA-4 and anti-PD-1 tumor rejection in humans. Using a similarly designed human T cell mass cytometry panel, we analyzed surgically resected melanoma tumors from patients being treated with ipilimumab (ipi), anti-PD-1 (nivolumab, nivo; or pembrolizumab, pembro), or ipi plus nivo (Table S3). This approach enables direct interrogation of tumor-infiltrating T cell populations that may not be fully represented in peripheral blood. t-SNE analysis revealed striking differences between normal donor blood and tumor-infiltrating T cells, as

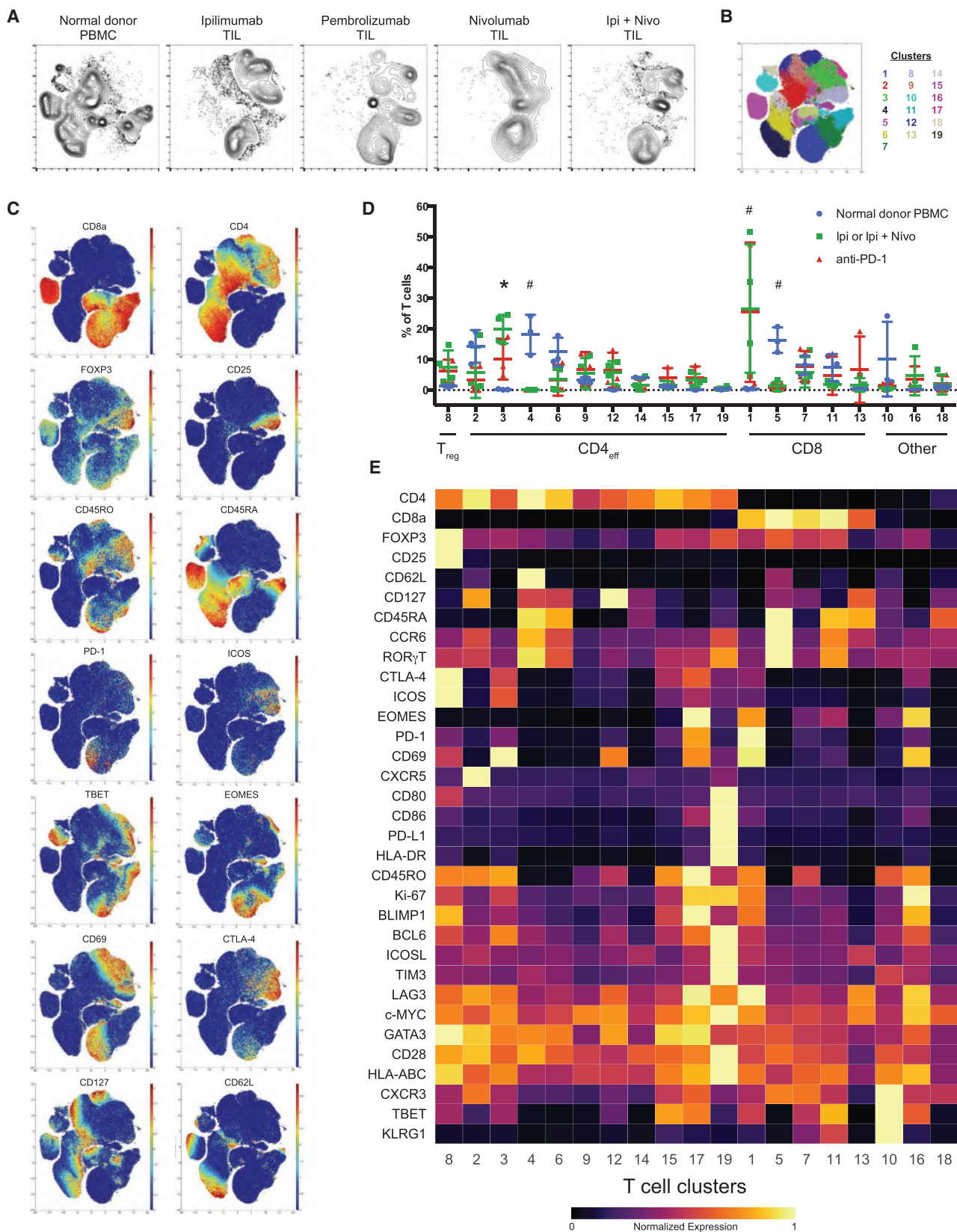
well as treatment-specific effects (Figures 5A–5C and S5). To more deeply interrogate the effects of anti-CTLA-4 therapy, we compared samples from patients being treated with ipi (alone or in combination with nivo) or anti-PD-1 monotherapy. This approach enabled more robust statistical analyses given the rarity of ipi monotherapy tumor samples in the current landscape of standard of care therapy for patients with metastatic melanoma. Unsupervised clustering of tumor and normal donor blood samples identified 19 distinct T cell subsets, including 5 CD8 and 11 CD4 clusters (Figures 5D and 5E; STAR Methods). The increased number of T cell subsets compared to our murine TIL data likely reflects the identification of canonical subsets in blood that are not present in tumors and as such would be absent from our preclinical analyses. Consistent with this notion, naive T cell subsets were specific to blood, while many of the T cell subsets were observed at similar frequencies in normal donor blood and tumors.

Surprisingly, of the 19 T cell subsets identified, only 2 were significantly expanded in ICB-treated tumors compared to normal donor blood. Although most melanoma-infiltrating T cell subsets were actively proliferating, only clusters 1 and 3 significantly expanded, suggesting that they are functionally distinguished by as yet unidentified mechanisms (Figure S5D). The CD8 T cell population expanded in ICB-treated tumors displayed a CD45RO⁺PD-1⁺TBET⁺EOMES⁺ phenotype (Figure 5E, cluster 1); analogous to the exhausted-like terminally differentiated CD8 T cell subset identified in murine tumor models as important for tumor rejection. The CD4 T cell population expanded in ICB-treated tumors displayed a CD45RO⁺ICOS⁺PD-1^{lo}TBET⁺ effector phenotype (Figure 5E, cluster 3), analogous to the activated Th1-like CD4 effector subset identified in murine tumor models that expands in response to CTLA-4 blockade but not PD-1 blockade.

Notably, the only ICB-treatment-specific effect observed was an increased frequency of Th1-like T cells in melanomas treated with anti-CTLA-4 compared to those treated with anti-PD-1 (Figure 5D, cluster 3). Thus, remarkably, despite the presence of confounding variables (e.g., diverse treatment histories) and small sample size, these analyses suggest that anti-CTLA-4 and anti-PD-1 therapies modulate only specific tumor-infiltrating T cell subsets and that anti-CTLA-4 induces a more robust CD4 effector response—observations consistent with our preclinical findings. Future studies are needed to validate these findings in a larger patient cohort and to determine whether the discrepancy in the number of ICB-responsive CD8 T cell subsets in mouse and human tumors reflects a difference in underlying biology or rather a technical aspect of our analyses. In both mouse and human, the CD4 effector response is defined by expansion of an ICOS⁺ TBET⁺ Th1-like subset. Notably, despite

Figure 4. Identification of B16BL6 Tumor-Infiltrating T Cell Populations that Correlate with Tumor Growth

- (A) B16BL6 tumor growth curves in each treatment group.
 (B) Final tumor volume in each treatment group displayed on a per-mouse basis with mean \pm SD (**, control versus treatment, $p < 0.01$, unpaired t test).
 (C) Metaclustering analysis of B16BL6 tumor-infiltrating T cell clusters. Two-way hierarchical clustering of T cell metaclusters and individual parameters displayed as a heatmap. Only CD4 and CD8 T cell metaclusters are displayed.
 (D) The frequencies of T cell metaclusters in individual mice plotted as a fraction of total tumor-infiltrating T cells and displayed as a boxplot.
 (E) The frequencies of T cell metaclusters in individual mice plotted as a function of B16BL6 tumor volume with linear regression best-fit lines displayed.
 See also Figure S3 and Table S2.



(legend on next page)

qualitative (e.g., CD44 versus CD45RO) and quantitative (e.g., levels of ICOS and PD-1) differences in phenotypic profiles of T cells infiltrating human and murine tumors, unsupervised clustering enabled robust detection of biologically analogous populations (Figures S5E and S5F). Together, these data indicate that the cellular mechanisms of CTLA-4 and PD-1 blockade are distinct and that the hallmarks of these mechanisms are largely conserved between mouse and human.

DISCUSSION

Here, we systematically classify tumor-infiltrating T cells from murine tumor models and human melanomas in the context of ICB using mass cytometry and unsupervised analyses. These studies provide insight into several key concepts: (1) ICB only induces the expansion of specific tumor-infiltrating T cell subsets, (2) PD-1 blockade primarily induces expansion of exhausted-like tumor-infiltrating CD8 T cells, (3) CTLA-4 blockade induces expansion of ICOS⁺ Th1-like CD4 effector as well as exhausted-like CD8 T cells, (4) the frequency of only specific tumor-infiltrating CD4 and CD8 T cell populations correlates with tumor growth, and (5) the phenotypes of tumor-infiltrating T cell subsets in different transplantable murine tumor models are fundamentally similar.

Together, these observations indicate that anti-CTLA-4- and anti-PD-1-induced anti-tumor responses are driven by distinct cellular mechanisms, primarily differing on the expansion of the CD4 effector compartment induced by anti-CTLA-4. Given that we profiled anti-tumor immune responses in the context of partial regression by design, it remains to be determined whether the same mechanisms mediate complete tumor rejection in the context of resolution of antigen burden. The similarity of findings in the MC38 and B16BL6 systems despite analyses of different time points (2 and 10 days after treatment, respectively) suggests that these mechanisms persist and may be independent of the phase of tumor rejection. Our findings are consistent with clinical observations that increased CD8, but not CD4, T cell activity is associated with anti-PD-1 therapy in melanoma (Daud et al., 2016) and also consistent with the fundamental understanding that PD-1 and CTLA-4 attenuate T cell activation through distinct molecular and cellular mechanisms. It is likely that dual engagement of these distinct cellular mechanisms underlies, at least in part, the enhanced efficacy of combination anti-CTLA-4 and anti-PD-1 therapy that has been observed in preclinical and clinical contexts (Curran et al., 2010; Wolchok et al., 2013).

Additional mechanistic investigation of anti-CTLA-4 and anti-PD-1 is also warranted. For example, the necessity and suffi-

ciency of specific ICB-responsive tumor-infiltrating T cell subsets identified in our study remains to be definitively tested. Furthermore, recent studies have shown that anti-PD-1 therapy leads to a dynamic expansion of proliferating PD-1⁺ CD8 T cells in peripheral blood of melanoma and lung cancer patients (Huang et al., 2017; Kamphorst et al., 2017). Whether expansion of ICB-responsive exhausted-like CD8 T cells is driven by therapeutic engagement of peripheral or tumor-infiltrating populations is unknown. Furthermore, the degree to which anti-tumor T cell subsets are equally represented in tumor and peripheral blood remains unclear. Analyses of paired tumor and blood samples from patients being treated with ICB therapy may provide critical insight into these issues. Examination of additional parameters, such as costimulatory molecules, may offer additional clarity by providing an even finer resolution catalog of T cell subsets, as in recent analyses of renal cell carcinoma (Chevrier et al., 2017).

It remains unclear what functionally distinguishes ICB-responsive and nonresponsive CD8 T cell populations. ICB-responsive subsets may represent the bulk of tumor-antigen specific T cells or, alternatively, represent a functionally distinct subset thereof. Distinguishing between these possibilities may inform the development of therapeutic strategies. Likewise, future studies are required to determine whether ICB-responsive CD8 T cell subsets are functionally as well as phenotypically exhausted and, moreover, whether they are functionally distinct from each other. The maintenance of PD-1 on responsive CD8 T cells despite prolonged anti-PD-1 therapy suggests that PD-1 blockade is sufficient to reinvigorate these populations but not to reprogram them into a non-exhausted state, consistent with epigenetic regulation (Pauken et al., 2016).

Although our findings indicate that CTLA-4 blockade induces an expansion of tumor-infiltrating Th1-like CD4 T cells, the definitive source (anatomical and temporal) and precise function of this expansion remain open questions. It is possible that expansion of specific tumor-infiltrating T cell subsets in response to ICB results from engagement of distinct progenitor populations in secondary lymphoid organs, analogous to findings in viral models (Im et al., 2016). With respect to function, it is tempting to speculate that expansion of Th1-like CD4 effectors by anti-CTLA-4 improves anti-tumor responses by enhancing CD8 infiltration, cytolytic CD8 activity, and T cell memory formation. Addressing these possibilities is of great interest given that expansion of ICOS⁺ CD4 T cells following ipi treatment has been observed in multiple tumor types (Chaput et al., 2017; Chen et al., 2009; Liakou et al., 2008), that expansion of ICOS⁺ CD4 T cells is associated with overall survival following ipi therapy (Carthon et al., 2010), and that genetic loss of *Icos* attenuates the efficacy of anti-CTLA-4 in preclinical tumor models (Fan

Figure 5. Identification of Checkpoint-Blockade-Responsive Tumor-Infiltrating T Cell Populations in Human Melanoma

(A) Density t-SNE plots of CD3⁺ tumor-infiltrating T cells from melanoma patients being treated with indicated ICB therapies and T cells from normal donor peripheral blood.

(B) t-SNE plot of total T cells from all samples overlaid with color-coded clusters.

(C) t-SNE plots of total T cells from all samples overlaid with the expression of selected markers.

(D) Frequency of T cell clusters displayed on a per-sample basis with mean \pm SD (*, ipi/ipi plus nivo versus anti-PD-1; #, anti-PD-1 and ipi/ipi plus nivo versus normal PBMC; $p < 0.05$, Tukey's multiple comparison).

(E) Heatmap displaying normalized marker expression of T cell clusters.

See also Figure S5 and Table S3.

et al., 2014). Our findings suggest that expansion of the CD4 effector compartment by anti-CTLA-4 differentiates its mechanism of action from that of PD-1 blockade. Such insights will inform the rational design of combinatorial approaches, particularly given the fundamental understanding that CD4 help is critical for the development of robust T cell responses, as well as recent findings that CD4 T cells are critical for effective immunotherapy (Spitzer et al., 2017).

In conclusion, we comprehensively profiled T cells in preclinical and clinical tumor samples using a mass-cytometry-based systems approach. We identify specific tumor-infiltrating T cell populations that expand in response to ICB and demonstrate that anti-PD-1 and anti-CTLA-4 operate through distinct cellular mechanisms. These findings highlight the utility of unsupervised systems-based analyses for in-depth mechanistic investigation.

STAR★METHODS

Detailed methods are provided in the online version of this paper and include the following:

- KEY RESOURCES TABLE
- CONTACT FOR REAGENT AND RESOURCE SHARING
- EXPERIMENTAL MODELS AND SUBJECT DETAILS
 - Cell lines
 - Inbred mice strains
 - *In vivo* murine tumor experiments
 - Human subjects
- METHOD DETAILS
 - Mass cytometry antibodies
 - Mass cytometry analysis of murine tumors
 - Synthetic tumor spike-in experiments
 - Mass cytometry analysis of human melanoma tumors
 - RNA-seq of murine tumor infiltrating T cells
 - Whole-exome sequencing of murine cell lines
- QUANTIFICATION AND STATISTICAL ANALYSIS
 - Analysis of murine tumor mass cytometry datasets
 - Principal component analysis of mass cytometry data
 - Metaclustering of B16BL6 infiltrating T cells
 - Analysis of human melanoma mass cytometry datasets
 - Analysis of RNaseq expression data
 - Whole-exome sequencing data analysis
 - Statistical Analyses
- DATA AND SOFTWARE AVAILABILITY
 - Mass cytometry datasets
 - RNaseq dataset
 - Whole-exome sequencing of murine cell lines
 - Metaclustering of mass cytometry data

SUPPLEMENTAL INFORMATION

Supplemental Information includes five figures and four tables and can be found with this article online at <http://dx.doi.org/10.1016/j.cell.2017.07.024>.

AUTHOR CONTRIBUTIONS

S.C.W. and J.P.A. conceived the project and wrote the manuscript. S.C.W. performed experiments. J.H.L. developed computational approaches for

mass cytometry data analysis. N.A.S.A. provided technical assistance. S.C.W., J.H.L., and Y.Z. analyzed data. A.P.C, M.C.A., and J.A.W. acquired and annotated clinical samples. S.C.W., J.H.L., J.W., P.S., J.A.W., D.P., and J.P.A. interpreted data. All authors contributed to the revision of the manuscript.

ACKNOWLEDGMENTS

We thank Duncan Mak for expert advice and technical assistance with mass cytometry analysis. Mass cytometry and cell sorting were performed at the MDACC Flow Cytometry and Cellular Imaging Core Facility, which is in part funded by NCI Cancer Center Support Grant (CCSG) P30CA016672. Sequencing was performed at the MDACC Sequencing and Microarray Facility, which is also in part funded by P30CA016672(SMF). This work was supported by a grant from Cancer Prevention and Research Institute of Texas (CPRIT) to J.P.A. (R1203), the MDACC CCSG Bioinformatics Shared Resource (P30CA016672 39), NIH grants to D.P. (DP1-HD084071 and R01CA164729), and a MSK Cancer Center Support Grant/Core Grant to D.P. (P30CA008748). S.C.W. is an MDACC Odyssey postdoctoral fellow. J.P.A. and P.S. are co-directors, and J.A.W. is a member of the Parker Institute for Cancer Immunotherapy. P.S. has consulted for AstraZeneca, Amgen, GlaxoSmithKline (GSK), and Bristol-Myers Squibb (BMS). P.S. serves on the scientific advisory boards for Jounce, Neon, Constellation, and Kite. P.S. is a co-founder of Jounce Therapeutics. P.S. received funding on NIH R01CA163793. M.C.A. has attended speakers' bureau with travel support from BMS and MSD. J.A.W. has received honoraria from speakers' bureau of Dava Oncology, BMS, and Illumina and is an advisory board member for GSK, Novartis, and Roche/Genentech. J.P.A. is a co-founder of Jounce and Neon Therapeutics, is an advisory board member for Jounce, Neon, Amgen, and Kite Pharmaceuticals, and has received royalties from intellectual property licensed to BMS and Merck.

Received: February 8, 2017

Revised: May 10, 2017

Accepted: July 14, 2017

Published: August 10, 2017

REFERENCES

- Amir, el-A.D., Davis, K.L., Tadmor, M.D., Simonds, E.F., Levine, J.H., Bendall, S.C., Shenfeld, D.K., Krishnaswamy, S., Nolan, G.P., and Pe'er, D. (2013). viSNE enables visualization of high dimensional single-cell data and reveals phenotypic heterogeneity of leukemia. *Nat. Biotechnol.* **31**, 545–552.
- Behbehani, G.K., Bendall, S.C., Clutter, M.R., Fantl, W.J., and Nolan, G.P. (2012). Single-cell mass cytometry adapted to measurements of the cell cycle. *Cytometry A* **81**, 552–566.
- Bendall, S.C., Simonds, E.F., Qiu, P., Amir, A.D., Krutzik, P.O., Finck, R., Bruggner, R.V., Melamed, R., Trejo, A., Ornatsky, O.I., et al. (2011). Single-cell mass cytometry of differential immune and drug responses across a human hematopoietic continuum. *Science* **332**, 687–696.
- Bengsch, B., Johnson, A.L., Kurachi, M., Odorizzi, P.M., Pauken, K.E., Attanasio, J., Stelekati, E., McLane, L.M., Paley, M.A., Delgoffe, G.M., and Wherry, E.J. (2016). Bioenergetic insufficiencies due to metabolic alterations regulated by the inhibitory receptor PD-1 are an early driver of CD8⁺ T cell exhaustion. *Immunity* **45**, 358–373.
- Brahmer, J.R., Drake, C.G., Wollner, I., Powderly, J.D., Picus, J., Sharfman, W.H., Stankevich, E., Pons, A., Salay, T.M., McMiller, T.L., et al. (2010). Phase I study of single-agent anti-programmed death-1 (MDX-1106) in refractory solid tumors: safety, clinical activity, pharmacodynamics, and immunologic correlates. *J. Clin. Oncol.* **28**, 3167–3175.
- Brahmer, J.R., Tykodi, S.S., Chow, L.Q., Hwu, W.J., Topalian, S.L., Hwu, P., Drake, C.G., Camacho, L.H., Kauh, J., Odunsi, K., et al. (2012). Safety and activity of anti-PD-L1 antibody in patients with advanced cancer. *N. Engl. J. Med.* **366**, 2455–2465.

- Carthon, B.C., Wolchok, J.D., Yuan, J., Kamat, A., Ng Tang, D.S., Sun, J., Ku, G., Troncoco, P., Logothetis, C.J., Allison, J.P., and Sharma, P. (2010). Preoperative CTLA-4 blockade: tolerability and immune monitoring in the setting of a presurgical clinical trial. *Clin. Cancer Res.* *16*, 2861–2871.
- Chaput, N., Lepage, P., Coutzac, C., Soularue, E., Le Roux, K., Monot, C., Boselli, L., Routier, E., Cassard, L., Collins, M., et al. (2017). Baseline gut microbiota predicts clinical response and colitis in metastatic melanoma patients treated with ipilimumab. *Ann. Oncol.* *28*, 1368–1379.
- Chemnitz, J.M., Parry, R.V., Nichols, K.E., June, C.H., and Riley, J.L. (2004). SHP-1 and SHP-2 associate with immunoreceptor tyrosine-based switch motif of programmed death 1 upon primary human T cell stimulation, but only receptor ligation prevents T cell activation. *J. Immunol.* *173*, 945–954.
- Chen, H., Liakou, C.I., Kamat, A., Pettaway, C., Ward, J.F., Tang, D.N., Sun, J., Jungbluth, A.A., Troncoco, P., Logothetis, C., and Sharma, P. (2009). Anti-CTLA-4 therapy results in higher CD4+ICOShi T cell frequency and IFN-gamma levels in both nonmalignant and malignant prostate tissues. *Proc. Natl. Acad. Sci. USA* *106*, 2729–2734.
- Chevrier, S., Levine, J.H., Zanotelli, V.R.T., Silina, K., Schulz, D., Bacac, M., Ries, C.H., Ailles, L., Jewett, M.A.S., Moch, H., et al. (2017). An immune atlas of clear cell renal cell carcinoma. *Cell* *169*, 736–749.e718.
- Curran, M.A., Montalvo, W., Yagita, H., and Allison, J.P. (2010). PD-1 and CTLA-4 combination blockade expands infiltrating T cells and reduces regulatory T and myeloid cells within B16 melanoma tumors. *Proc. Natl. Acad. Sci. USA* *107*, 4275–4280.
- Das, R., Verma, R., Sznol, M., Boddupalli, C.S., Gettinger, S.N., Kluger, H., Callahan, M., Wolchok, J.D., Halaban, R., Dhodapkar, M.V., and Dhodapkar, K.M. (2015). Combination therapy with anti-CTLA-4 and anti-PD-1 leads to distinct immunologic changes in vivo. *J. Immunol.* *194*, 950–959.
- Daud, A.I., Loo, K., Pauli, M.L., Sanchez-Rodriguez, R., Sandoval, P.M., Taravati, K., Tsai, K., Nosrati, A., Nardo, L., Alvarado, M.D., et al. (2016). Tumor immune profiling predicts response to anti-PD-1 therapy in human melanoma. *J. Clin. Invest.* *126*, 3447–3452.
- Fan, X., Quezada, S.A., Sepulveda, M.A., Sharma, P., and Allison, J.P. (2014). Engagement of the ICOS pathway markedly enhances efficacy of CTLA-4 blockade in cancer immunotherapy. *J. Exp. Med.* *211*, 715–725.
- Freeman, G.J., Long, A.J., Iwai, Y., Bourque, K., Chernova, T., Nishimura, H., Fitz, L.J., Malenkovich, N., Okazaki, T., Byrne, M.C., et al. (2000). Engagement of the PD-1 immunoinhibitory receptor by a novel B7 family member leads to negative regulation of lymphocyte activation. *J. Exp. Med.* *192*, 1027–1034.
- Gao, J., Shi, L.Z., Zhao, H., Chen, J., Xiong, L., He, Q., Chen, T., Roszik, J., Bernatchez, C., Woodman, S.E., et al. (2016). Loss of IFN- γ pathway genes in tumor cells as a mechanism of resistance to anti-CTLA-4 therapy. *Cell* *167*, 397–404.e9.
- Gubin, M.M., Zhang, X., Schuster, H., Caron, E., Ward, J.P., Noguchi, T., Ivanova, Y., Hundal, J., Arthur, C.D., Krebber, W.J., et al. (2014). Checkpoint blockade cancer immunotherapy targets tumour-specific mutant antigens. *Nature* *515*, 577–581.
- Hodi, F.S., O'Day, S.J., McDermott, D.F., Weber, R.W., Sosman, J.A., Haanen, J.B., Gonzalez, R., Robert, C., Schadendorf, D., Hassel, J.C., et al. (2010). Improved survival with ipilimumab in patients with metastatic melanoma. *N. Engl. J. Med.* *363*, 711–723.
- Huang, A.C., Postow, M.A., Orlowski, R.J., Mick, R., Bengsch, B., Manne, S., Xu, W., Harmon, S., Giles, J.R., Wenz, B., et al. (2017). T-cell invigoration to tumor burden ratio associated with anti-PD-1 response. *Nature* *545*, 60–65.
- Hugo, W., Zaretsky, J.M., Sun, L., Song, C., Moreno, B.H., Hu-Lieskovan, S., Berent-Maoz, B., Pang, J., Chmielowski, B., Cherry, G., et al. (2016). Genomic and transcriptomic features of response to anti-PD-1 therapy in metastatic melanoma. *Cell* *165*, 35–44.
- Im, S.J., Hashimoto, M., Gerner, M.Y., Lee, J., Kissick, H.T., Burger, M.C., Shan, Q., Hale, J.S., Lee, J., Nasti, T.H., et al. (2016). Defining CD8+ T cells that provide the proliferative burst after PD-1 therapy. *Nature* *537*, 417–421.
- Kamphorst, A.O., Pillai, R.N., Yang, S., Nasti, T.H., Akondy, R.S., Wieland, A., Sica, G.L., Yu, K., Koenig, L., Patel, N.T., et al. (2017). Proliferation of PD-1+ CD8 T cells in peripheral blood after PD-1-targeted therapy in lung cancer patients. *Proc. Natl. Acad. Sci. USA* *114*, 4993–4998.
- Koboldt, D.C., Zhang, Q., Larson, D.E., Shen, D., McLellan, M.D., Lin, L., Miller, C.A., Mardis, E.R., Ding, L., and Wilson, R.K. (2012). VarScan 2: somatic mutation and copy number alteration discovery in cancer by exome sequencing. *Genome Res.* *22*, 568–576.
- Krummel, M.F., and Allison, J.P. (1995). CD28 and CTLA-4 have opposing effects on the response of T cells to stimulation. *J. Exp. Med.* *182*, 459–465.
- Latchman, Y., Wood, C.R., Chernova, T., Chaudhary, D., Borde, M., Chernova, I., Iwai, Y., Long, A.J., Brown, J.A., Nunes, R., et al. (2001). PD-L2 is a second ligand for PD-1 and inhibits T cell activation. *Nat. Immunol.* *2*, 261–268.
- Lavin, Y., Kobayashi, S., Leader, A., Amir, E.D., Elefant, N., Bigenwald, C., Remark, R., Sweeney, R., Becker, C.D., Levine, J.H., et al. (2017). Innate immune landscape in early lung adenocarcinoma by paired single-cell analyses. *Cell* *169*, 750–765.e717.
- Leelatian, N., Doxie, D.B., Greenplate, A.R., Mobley, B.C., Lehman, J.M., Sinnaeve, J., Kauffmann, R.M., Werkhaven, J.A., Mistry, A.M., Weaver, K.D., et al. (2017). Single cell analysis of human tissues and solid tumors with mass cytometry. *Cytometry B Clin. Cytom.* *92*, 68–78.
- Levine, J.H., Simonds, E.F., Bendall, S.C., Davis, K.L., Amir, A.D., Tadmor, M.D., Litvin, O., Fienberg, H.G., Jager, A., Zunder, E.R., et al. (2015). Data-driven phenotypic dissection of AML reveals progenitor-like cells that correlate with prognosis. *Cell* *162*, 184–197.
- Li, H., and Durbin, R. (2009). Fast and accurate short read alignment with Burrows-Wheeler transform. *Bioinformatics* *25*, 1754–1760.
- Liakou, C.I., Kamat, A., Tang, D.N., Chen, H., Sun, J., Troncoco, P., Logothetis, C., and Sharma, P. (2008). CTLA-4 blockade increases IFN-gamma-producing CD4+ICOShi cells to shift the ratio of effector to regulatory T cells in cancer patients. *Proc. Natl. Acad. Sci. USA* *105*, 14987–14992.
- McGranahan, N., Furness, A.J., Rosenthal, R., Ramskov, S., Lyngaa, R., Saini, S.K., Jamal-Hanjani, M., Wilson, G.A., Birkbak, N.J., Hiley, C.T., et al. (2016). Clonal neoantigens elicit T cell immunoreactivity and sensitivity to immune checkpoint blockade. *Science* *351*, 1463–1469.
- Mei, H.E., Leipold, M.D., and Maecker, H.T. (2016). Platinum-conjugated antibodies for application in mass cytometry. *Cytometry A* *89*, 292–300.
- Melchioni, R., Gracio, F., Kordasti, S., Todd, A.K., and de Rinaldis, E. (2017). Cluster stability in the analysis of mass cytometry data. *Cytometry A* *91*, 73–84.
- Newell, E.W., and Cheng, Y. (2016). Mass cytometry: blessed with the curse of dimensionality. *Nat. Immunol.* *17*, 890–895.
- Pardoll, D.M. (2012). The blockade of immune checkpoints in cancer immunotherapy. *Nat. Rev. Cancer* *12*, 252–264.
- Pauken, K.E., Sammons, M.A., Odorizzi, P.M., Manne, S., Godec, J., Khan, O., Drake, A.M., Chen, Z., Sen, D.R., Kurachi, M., et al. (2016). Epigenetic stability of exhausted T cells limits durability of reinvigoration by PD-1 blockade. *Science* *354*, 1160–1165.
- Pounds, S., and Morris, S.W. (2003). Estimating the occurrence of false positives and false negatives in microarray studies by approximating and partitioning the empirical distribution of p-values. *Bioinformatics* *19*, 1236–1242.
- Quezada, S.A., Peggs, K.S., Curran, M.A., and Allison, J.P. (2006). CTLA4 blockade and GM-CSF combination immunotherapy alters the intratumor balance of effector and regulatory T cells. *J. Clin. Invest.* *116*, 1935–1945.
- Schadendorf, D., Hodi, F.S., Robert, C., Weber, J.S., Margolin, K., Hamid, O., Patt, D., Chen, T.T., Berman, D.M., and Wolchok, J.D. (2015). Pooled analysis of long-term survival data from phase II and phase III trials of ipilimumab in unresectable or metastatic melanoma. *J. Clin. Oncol.* *33*, 1889–1894.
- Selby, M.J., Engelhardt, J.J., Quigley, M., Henning, K.A., Chen, T., Srinivasan, M., and Korman, A.J. (2013). Anti-CTLA-4 antibodies of IgG2a isotype enhance antitumor activity through reduction of intratumoral regulatory T cells. *Cancer Immunol. Res.* *1*, 32–42.
- Sharma, P., and Allison, J.P. (2015). The future of immune checkpoint therapy. *Science* *348*, 56–61.

- Shekhar, K., Lapan, S.W., Whitney, I.E., Tran, N.M., Macosko, E.Z., Kowalczyk, M., Adiconis, X., Levin, J.Z., Nemesh, J., Goldman, M., et al. (2016). Comprehensive classification of retinal bipolar neurons by single-cell transcriptomics. *Cell* *166*, 1308–1323.e1330.
- Simpson, T.R., Li, F., Montalvo-Ortiz, W., Sepulveda, M.A., Bergerhoff, K., Arce, F., Roddie, C., Henry, J.Y., Yagita, H., Wolchok, J.D., et al. (2013). Fc-dependent depletion of tumor-infiltrating regulatory T cells co-defines the efficacy of anti-CTLA-4 therapy against melanoma. *J. Exp. Med.* *210*, 1695–1710.
- Spitzer, M.H., Carmi, Y., Reticker-Flynn, N.E., Kwek, S.S., Madhireddy, D., Martins, M.M., Gherardini, P.F., Prestwood, T.R., Chabon, J., Bendall, S.C., et al. (2017). Systemic immunity is required for effective cancer immunotherapy. *Cell* *168*, 487–502.e415.
- Spitzer, M.H., and Nolan, G.P. (2016). Mass cytometry: single cells, many features. *Cell* *165*, 780–791.
- Spranger, S., Bao, R., and Gajewski, T.F. (2015). Melanoma-intrinsic β -catenin signalling prevents anti-tumour immunity. *Nature* *523*, 231–235.
- Tanner, S.D., Baranov, V.I., Ornatsky, O.I., Bandura, D.R., and George, T.C. (2013). An introduction to mass cytometry: fundamentals and applications. *Cancer Immunol. Immunother.* *62*, 955–965.
- Topalian, S.L., Drake, C.G., and Pardoll, D.M. (2015). Immune checkpoint blockade: a common denominator approach to cancer therapy. *Cancer Cell* *27*, 450–461.
- Topalian, S.L., Hodi, F.S., Brahmer, J.R., Gettinger, S.N., Smith, D.C., McDermott, D.F., Powderly, J.D., Carvajal, R.D., Sosman, J.A., Atkins, M.B., et al. (2012). Safety, activity, and immune correlates of anti-PD-1 antibody in cancer. *N. Engl. J. Med.* *366*, 2443–2454.
- Van der Auwera, G.A., Carneiro, M.O., Hartl, C., Poplin, R., Del Angel, G., Levy-Moonshine, A., Jordan, T., Shakir, K., Roazen, D., Thibault, J., et al. (2013). From FastQ data to high confidence variant calls: the Genome Analysis Toolkit best practices pipeline. *Curr Protoc Bioinformatics* *43*, 11.10.11–33.
- van der Maaten, L., and Hinton, G.E. (2008). Visualizing high-dimensional data using t-SNE. *J. Mach. Learn. Res.* *9*, 2579–2605.
- van Elsas, A., Hurwitz, A.A., and Allison, J.P. (1999). Combination immunotherapy of B16 melanoma using anti-cytotoxic T lymphocyte-associated antigen 4 (CTLA-4) and granulocyte/macrophage colony-stimulating factor (GM-CSF)-producing vaccines induces rejection of subcutaneous and metastatic tumors accompanied by autoimmune depigmentation. *J. Exp. Med.* *190*, 355–366.
- Walker, L.S., and Sansom, D.M. (2011). The emerging role of CTLA4 as a cell-extrinsic regulator of T cell responses. *Nat. Rev. Immunol.* *11*, 852–863.
- Walunas, T.L., Lenschow, D.J., Bakker, C.Y., Linsley, P.S., Freeman, G.J., Green, J.M., Thompson, C.B., and Bluestone, J.A. (1994). CTLA-4 can function as a negative regulator of T cell activation. *Immunity* *1*, 405–413.
- Wang, K., Li, M., and Hakonarson, H. (2010). ANNOVAR: functional annotation of genetic variants from high-throughput sequencing data. *Nucleic Acids Res.* *38*, e164.
- Wolchok, J.D., Kluger, H., Callahan, M.K., Postow, M.A., Rizvi, N.A., Lesokhin, A.M., Segal, N.H., Ariyan, C.E., Gordon, R.A., Reed, K., et al. (2013). Nivolumab plus ipilimumab in advanced melanoma. *N. Engl. J. Med.* *369*, 122–133.
- Zaretsky, J.M., Garcia-Diaz, A., Shin, D.S., Escuin-Ordinas, H., Hugo, W., Hu-Lieskovan, S., Torrejon, D.Y., Abril-Rodriguez, G., Sandoval, S., Barthly, L., et al. (2016). Mutations associated with acquired resistance to PD-1 blockade in melanoma. *N. Engl. J. Med.* *375*, 819–829.

Tumor and Microenvironment Evolution during Immunotherapy with Nivolumab

Nadeem Riaz,^{1,2,3,15} Jonathan J. Havel,^{1,15} Vladimir Makarov,^{1,3,15} Alexis Desrichard,^{1,15} Walter J. Urba,⁴ Jennifer S. Sims,^{1,3} F. Stephen Hodi,⁵ Salvador Martín-Algarra,⁶ Rajarsi Mandal,⁷ William H. Sharfman,⁸ Shailender Bhatia,⁹ Wen-Jen Hwu,¹⁰ Thomas F. Gajewski,¹¹ Craig L. Slingluff, Jr.,¹² Diego Chowell,^{1,3} Sviatoslav M. Kendall,^{1,3} Han Chang,¹³ Rachna Shah,¹ Fengshen Kuo,³ Luc G.T. Morris,^{3,7} John-William Sidhom,¹⁴ Jonathan P. Schneck,¹⁴ Christine E. Horak,¹³ Nils Weinhold,^{2,*} and Timothy A. Chan^{1,2,3,16,*}

¹Human Oncology and Pathogenesis Program, Memorial Sloan Kettering Cancer Center, New York, NY 10065, USA

²Department of Radiation Oncology, Memorial Sloan Kettering Cancer Center, New York, NY 10065, USA

³Immunogenomics and Precision Oncology Platform, Memorial Sloan Kettering Cancer Center, New York, NY 10065, USA

⁴Earle A. Chiles Research Institute, Providence Cancer Center, Portland, OR 97213, USA

⁵Department of Medical Oncology, Dana-Farber Cancer Institute, Boston, MA 02215, USA

⁶Medical Oncology, Clínica Universidad de Navarra, Instituto de Investigación Sanitaria de Navarra, 31008 Pamplona, Spain

⁷Department of Surgery, Memorial Sloan Kettering Cancer Center, New York, NY 10065, USA

⁸Sidney Kimmel Comprehensive Cancer Center, Johns Hopkins University School of Medicine, Baltimore, MD 21287, USA

⁹Fred Hutchinson Cancer Research Center, University of Washington, Seattle, WA 98105, USA

¹⁰Department of Melanoma Medical Oncology, University of Texas MD Anderson Cancer Center, Houston, TX 77030, USA

¹¹Department of Medicine, Section of Hematology/Oncology, University of Chicago, Chicago, IL 60637, USA

¹²Department of Surgery and University of Virginia Cancer Center, University of Virginia School of Medicine, Charlottesville, VA 22908, USA

¹³Bristol-Myers Squibb, Princeton, NJ 08648, USA

¹⁴Department of Biomedical Engineering, Johns Hopkins University School of Medicine, Baltimore, MD 21205, USA

¹⁵These authors contributed equally

¹⁶Lead Contact

*Correspondence: weinholn@mskcc.org (N.W.), chant@mskcc.org (T.A.C.)

<https://doi.org/10.1016/j.cell.2017.09.028>

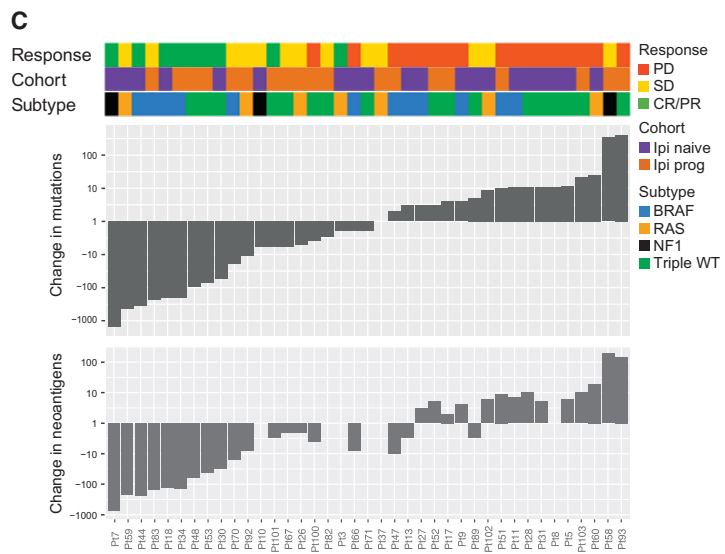
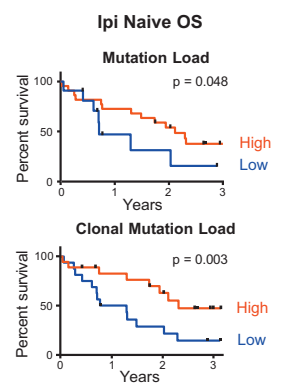
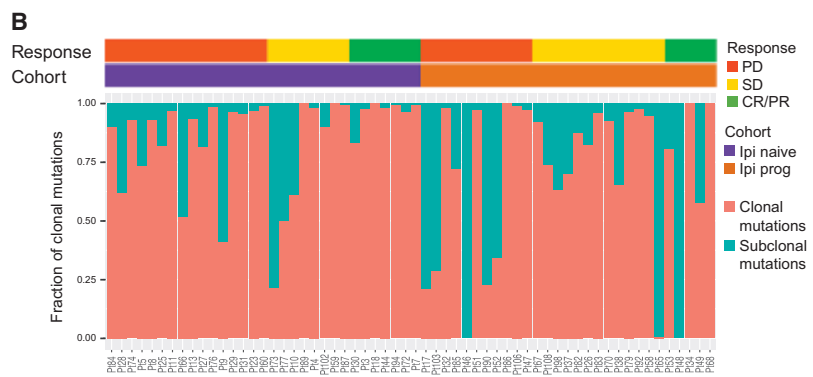
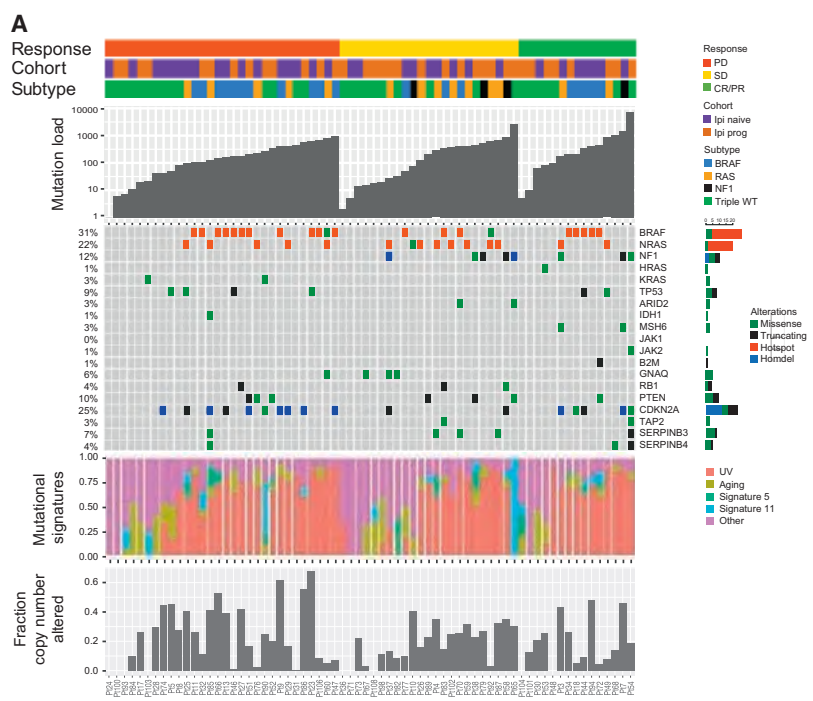
SUMMARY

The mechanisms by which immune checkpoint blockade modulates tumor evolution during therapy are unclear. We assessed genomic changes in tumors from 68 patients with advanced melanoma, who progressed on ipilimumab or were ipilimumab-naïve, before and after nivolumab initiation (CA209-038 study). Tumors were analyzed by whole-exome, transcriptome, and/or T cell receptor (TCR) sequencing. In responding patients, mutation and neoantigen load were reduced from baseline, and analysis of intratumoral heterogeneity during therapy demonstrated differential clonal evolution within tumors and putative selection against neoantigenic mutations on-therapy. Transcriptome analyses before and during nivolumab therapy revealed increases in distinct immune cell subsets, activation of specific transcriptional networks, and upregulation of immune checkpoint genes that were more pronounced in patients with response. Temporal changes in intratumoral TCR repertoire revealed expansion of T cell clones in the setting of neoantigen loss. Comprehensive genomic profiling data in this study provide insight into nivolumab's mechanism of action.

INTRODUCTION

Immune checkpoint inhibitors have demonstrated improved overall survival (OS) and progression-free survival (PFS) in the treatment of many different tumor types (Brahmer et al., 2015; Ferris et al., 2016; Hodi et al., 2016; Motzer et al., 2015; Robert et al., 2015). The underlying genomic features of a tumor can contribute to its response to checkpoint blockade, and increased tumor mutation load associates with survival benefits from both anti-CTLA-4 and anti-PD-1 therapy in multiple malignancies (Hugo et al., 2016; Le et al., 2015; Rizvi et al., 2015; Rosenberg et al., 2016; Snyder et al., 2014; Van Allen et al., 2015). High tumor mutation load may increase the probability of generating immunogenic neoantigens, which facilitate recognition of a tumor as foreign (Riaz et al., 2016a; Schumacher and Schreiber, 2015). Thus, tumors with a high number of clonal neoantigens may be more likely to elicit effective immune responses (McGranahan et al., 2016).

Features of the tumor microenvironment (TME) also associate with response to checkpoint inhibitor therapy. Expression of PD-L1 in the TME associates with clinical response to anti-PD-1/PD-L1 therapies in multiple tumor types (Herbst et al., 2014; Topalian et al., 2012). Baseline levels of tumor-infiltrating CD8⁺ T cells correlate with the likelihood of response and may increase during therapy in responding, but not progressing, tumors (Topalian et al., 2016; Tumei et al., 2014). Further, the location of CD8⁺ T cells at the invasive margin of tumors may indicate an effective immune response (Chen et al., 2016; Spranger et al.,



(legend on next page)

2015; Tumei et al., 2014). The TME may limit extravasation of effector T cells into the tumor, diminish T cell expansion, or reduce the viability of tumor-infiltrating lymphocytes (TILs) (Joyce and Fearon, 2015).

How checkpoint inhibitor-mediated immune activation modulates the mutational landscape of the tumor and the TME remains poorly understood. To characterize genomic changes, we performed comprehensive genomic analyses on melanoma samples pre- and post-nivolumab (Nivo; anti-PD-1 agent) therapy.

RESULTS

Genomic Characteristics of Tumors before Nivo Treatment

Pre-therapy biopsies from 68 patients were assessed by whole-exome sequencing (WES) at 150× (mean depth: 168; range: 121–237) (Table S1). Thirty-five patients had previously progressed on ipilimumab (Ipi) therapy (Ipi-P); 33 patients were Ipi-naïve (Ipi-N) (Table S2). In the patients with WES data, rates of response (RECIST v1.1-defined complete response [CR] or partial response [PR]) to Nivo were comparable in Ipi-N (21%) and Ipi-P (22%) patients. Median mutation load in the patient cohort was 183 mutations (range: 1–7,360; interquartile range: 44–433) (Tables S2 and S3) and did not differ significantly between Ipi-N and Ipi-P patients (Figure 1A). Mutational subtypes of melanoma as defined by The Cancer Genome Atlas (TCGA) (Cancer Genome Atlas Network, 2015) did not differ in response to Nivo. There were more triple wild-type (WT) patients in the Ipi-P cohort than the Ipi-N cohort (57% versus 33%, $p = 0.06$; Fisher's exact test) (Figure 1A).

Tumor and Clonal Mutation Load Are Associated with OS and Response in Nivo-Treated Ipi-N Patients

Tumor mutation load associated with OS in Ipi-N but not Ipi-P patients (Figures 1B and S1A), and Ipi-P patients tended to have lower numbers of clonal mutations ($p = 0.08$) (Figure S1B). Stratification of patients by the number of clonal mutations improved the ability to predict survival and response of Ipi-N but not Ipi-P patients (Figures 1B, S1C, and S1D). Mutation signatures may play a role in response to checkpoint blockade in NSCLC (Rizvi et al., 2015). However, here, no relationship between the proportion of mutations due to any of the known melanoma mutation signatures (e.g., UV or aging) (Alexandrov et al., 2013), and response to therapy was observed (Figure 1A).

No single gene mutations were significantly associated with response or resistance to therapy. *SERPINB3/B4* gene mutations in melanoma samples associate with response to anti-CTLA-4 therapy (Riaz et al., 2016b), and here, five of six patients

with *SERPINB3/B4* mutations had disease control (CR/PR or stable disease [SD]), however, this was not statistically significant, likely due to small numbers ($p = 0.21$; Fisher's exact test). One patient with PR had a frameshift alteration in *B2M* with corresponding loss of heterozygosity, alterations previously associated with acquired resistance to anti-PD-1 therapy (Zaretsky et al., 2016). *JAK1* and *JAK2* mutations were not associated with resistance in this cohort (Figure 1A). No recurrent copy-number alterations as determined by TCGA associated with response; nor did copy-number alterations in interferon (IFN) genes on chromosome 9p (Figures S1E and S1F). However, the frequency of global genomic instability (Davoli et al., 2017) associated with OS in Ipi-P but not Ipi-N patients (Figure S1G).

Evolution of Tumors during Nivo Treatment

To determine if Nivo therapy affects tumor mutation load and intratumor heterogeneity, WES was performed on a subset ($n = 41$) of paired pre- and on-therapy biopsy samples (Table S4). Significant differences between pre- and on-therapy biopsies correlated with response ($p = 5.87 \times 10^{-5}$; Mann-Whitney test for CR/PR versus progressive disease [PD]) (Figures 1C, S1H, and S1I). Among Ipi-N and Ipi-P responders, a reduction in mutation and neoantigen load was observed 4 weeks after initiation of Nivo, perhaps consistent with immunoediting (Tables S5A and S5B). To ensure that these observations were not solely due to changes in tumor purity after therapy, further deep sequencing (300×) was performed on responding tumors. In each case, many of the mutations seen in the pre-therapy samples were still detectable in on-therapy samples (Figures S2A–S2C). The proportion of mutations that remained detectable varied depending on response: the mean fraction of variants in on-therapy samples was 19% for CR/PR (range: 1%–99%), 82% for SD (range: 2%–140%), and 101% for PD (range: 33%–205%) (values >100% indicate additional mutations beyond those in pre-therapy samples were detected). Power calculations, assuming a global 5-fold decrease in the variant allele frequency on-therapy (see STAR Methods), demonstrated that the magnitude in change of mutation load could not be explained by changes in tumor purity alone (Figures S2D–S2F). There were four cases of focal loss of *CDKN2A* that appeared in on-therapy samples, all in patients with PD. In three of these patients, chromosome 9p deletions also included the nearby IFN gene cluster.

Subsequently, we examined association of changes in the clonal compositions of paired pre- and on-therapy tumor samples with response. The fraction of tumor cells carrying a variant (cancer cell fraction [CCF]) in both pre- and on-therapy samples was estimated (see STAR Methods) (Roth et al., 2014). The temporally related changes that occurred in the clonal

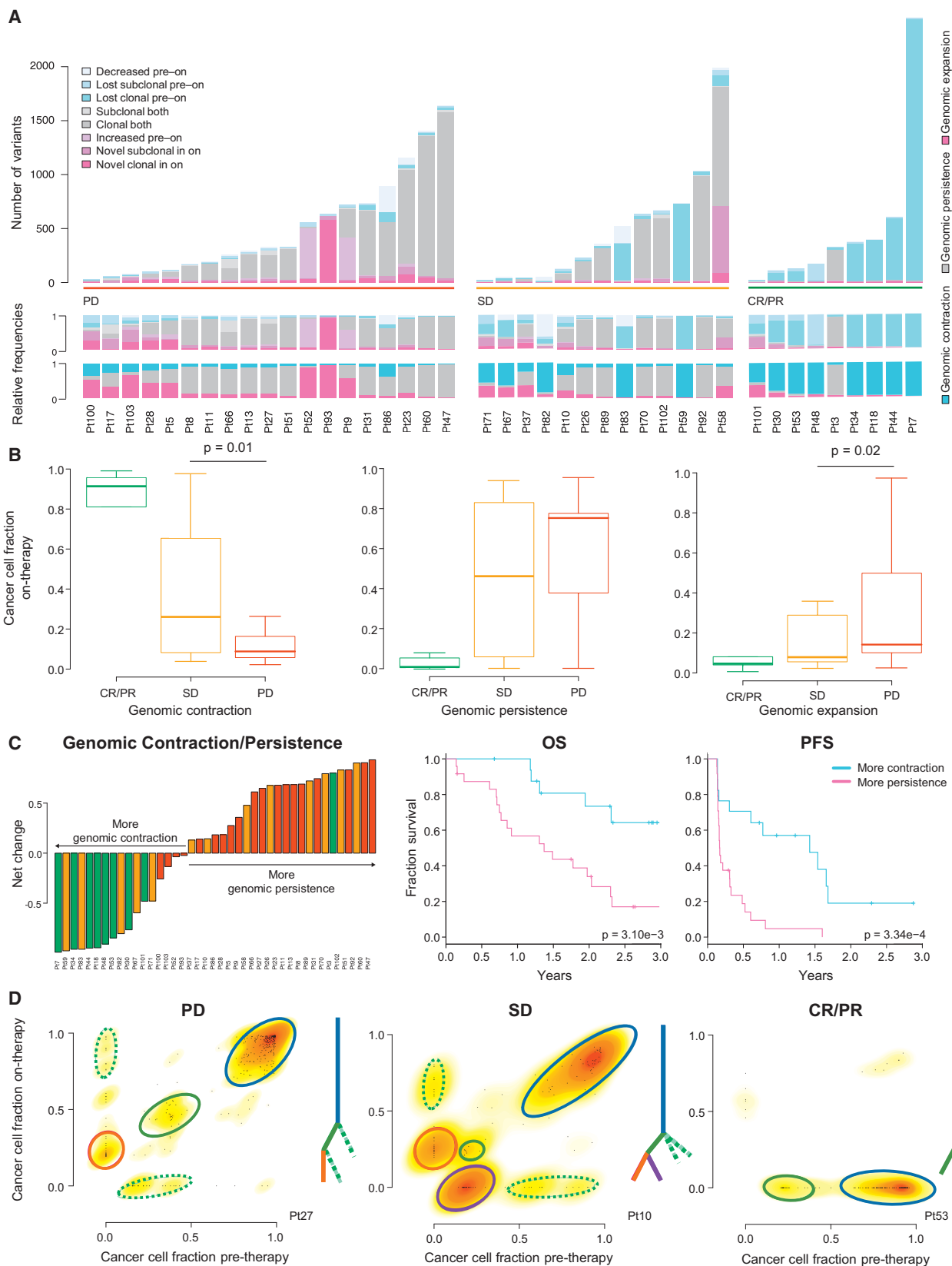
Figure 1. Genomic Features and Sculpting of the Tumor Mutational Landscape by Immunotherapy

(A) Baseline genomic characteristics of melanoma tumors from patients treated with immune checkpoint therapy. An OncoPrint image of WES data for the cohort sorted by response group (CR/PR, SD, PD). The OncoPrint displays genes recurrently mutated in melanoma and genes that have been recently associated with response to therapy.

(B) Left: Analysis of clonality in pre-therapy samples identifies a trend toward more subclonal mutations in Ipi-P patients ($p = 0.08$; Mann-Whitney test; see also Figure S1A). Right: OS in Ipi-N patients by mutation load (high mutation load defined as >100 mutations) and clonal mutation load.

(C) Waterfall plot of change in mutation (non-synonymous) and putative neoantigen load between pre-therapy biopsy and cycle 1, day 29 on-therapy biopsy by response status.

See also Tables S1–S5.



(legend on next page)

composition of tumors differed between response groups. Patients with CR/PR had high frequencies of tumor clonal and subclonal variants that decreased in prevalence after Nivo therapy and, in many cases, were not detected on-therapy (mutational contraction) (Figure 2A; STAR Methods). The relative frequencies of single nucleotide variations (SNVs) undergoing mutational contraction were significantly lower in patients with PD than SD ($p = 0.01$). In addition, the relative frequencies of novel SNVs detectable on-therapy were significantly higher on a per-sample basis in patients with PD than SD ($p = 0.02$), consistent with presumed mutational expansion and/or genetic drift (Figure 2B). Net genomic changes (defined as the difference of variants representing mutational contraction and mutational persistence [see STAR Methods]) per sample strongly associated with response and OS, and this metric was superior to the temporal change in mutation load in predicting response (Figure 2C). Tumors from patients with SD were identified as an intermediate molecular phenotype between those with CR/PR and PD: 26% (5 of 19) of PD samples had >50% of SNVs with variant gain (SD: 0 of 13), while 38% (5 of 13) of SD samples had >50% of SNVs under variant loss (PD: 0 of 19) (Figure 2A).

Excluding patient 3, all patients with CR/PR consistently lost one or more clones on-therapy; conversely, patients with SD and PD gained novel sets of mutations on-therapy (Figures 2A and 2D). For example, patient 27 (PD) and patient 10 (SD) both had a dominant clone, at least one smaller subclone at initiation of therapy, and the emergence of a novel subclone in the on-therapy sample. In addition, patient 10 had a subclone that was lost after treatment (Figure 2D). Losses were more common in patients with SD than PD. On aggregate, novel subclonal variants were often due to mutational signature 11, which has previously been associated with melanoma and exposure to temozolomide (Alexandrov et al., 2013) and in this setting, suggests that a specific type of repair process becomes dysfunctional due to immunotherapy-mediated stress (Figure S2G).

Transcriptome Analysis and Changes during Treatment Pre-therapy Expression Analysis Identified Pre-existing Immune Programs in Responders and Expression Footprints of “Hot” versus “Cold” Tumors Based on Prior Immunotherapy Exposure

Baseline transcriptional programs using RNA sequencing (RNA-seq) were characterized, and associations with clinical response were investigated ($n = 45$) (Table S4). Analysis of differentially expressed genes (DEGs) between patients with CR/PR and PD identified 189 DEGs ($q < 0.20$) (Figure 3A). Highly expressed

genes were immune-related, which suggests pre-existing immune recognition of the tumor; however, Gene Ontology (GO) analysis using the Reactome database only identified high-level categories such as T cell activation and lymphocyte aggregation as enriched ($q < 0.1$) (Figure S3A). Notably, this group included *IL17RE*, *IL17RC*, and *FGFR3* (Table S6A), which modulate the immune environment (Sweis et al., 2016). Next, pre-existing signatures of immune response were evaluated by immune deconvolution (see STAR Methods). A pre-existing immunologically active or “hot tumor” environment was observed in all Ipi-P patients with CR/PR, whereas variable immunological activity was observed in Ipi-N patients with CR/PR (Figures 3B and S3B). No association between the previously reported IPRES gene signature and response was seen in this cohort or in another cohort previously described (Hugo et al., 2016) (Figure S3C).

On-Therapy Genomic Contraction Phenotype Correlated with Pre-existing Immunity in Responders

We hypothesized that a molecular phenotype of response, such as tumor genomic contraction/persistence, ascertained at an early time-point, such as 4 weeks (Figure 2C), may more strongly correspond to underlying biological changes than would clinical assessments of response. Differential gene expression analysis between patients who had genomic contraction and genomic persistence was performed to examine pre-existing differences in immunity pre-therapy. In the cohort of 26 patients with paired WES and RNA-seq, 695 DEGs were observed ($q < 0.10$) (Figure 3C; Table S6B), of which 565 had a fold change greater than two. Clustering analysis of all patients and other checkpoint-blockade-treated cohorts demonstrated that this set of immune-related genes stratified patient survival (Figure 3D).

Gene set enrichment analysis demonstrated enrichment of genes involved in PD-1 signaling, co-stimulation of the CD28 family, downstream T cell receptor (TCR) signaling, interferon (IFN)- γ , and interleukin (IL)-2 signaling ($q < 0.1$) (Figure S3D). Although PD-1 signaling was enriched, neither *PDCD1* (PD-1) nor *CD274* (PD-L1) were differentially expressed. However, components of the TCR immunological synapse were enriched (e.g., *CD3D/E/G*, *PTPN6*, *CD247*, *CD28*, *CD86*). Notably, several HLA class II alleles were differentially regulated between the two groups in addition to genes associated with PI3K- γ signaling by G protein-coupled receptors (Figures S3D and S3E).

On-Therapy Analysis of Tumor Transcriptome

We subsequently hypothesized that anti-PD-1 therapy can induce tumor transcriptional and microenvironmental sculpting associated with response and therefore evaluated how the expression landscape of melanoma is altered during Nivo

Figure 2. Changes in Tumor Clonal Composition after Treatment with Nivo Therapy

(A) Changes in CCF of mutations (synonymous and non-synonymous, clonal/subclonal) from pre- to on-therapy samples. Similar CCFs in both pre- and on-therapy samples (genomic persistence) in gray, increased CCF or novel in on-therapy samples (genomic expansion) in pink, and decreased CCF/lost in on-therapy samples (genomic contraction) in blue.

(B) Lost mutations indicating genomic contraction were ubiquitous in CR/PR samples, and significantly more frequent in patients with SD than PD. Persistent mutations were less common in samples without response and not significantly different between patients with SD and PD. Variant gains (genomic expansion) were significantly more frequent in patients with PD than SD. Data are presented as median and interquartile range (IQR).

(C) Left: Waterfall plot of net change between fraction of mutations representing genomic contraction and genomic persistence. Right: OS and PFS by genomic contraction and genomic persistence ($p = 0.003$; log-rank test and $p = 3.34 \times 10^{-4}$; log-rank test, respectively).

(D) Changes of CCF in representative cases from patients with CR/PR (patient 53), SD (patient 10) and PD (patient 27). Tree diagrams illustrate the relationships between the clones. Colored lines and circles denote specific clones.

See also Figure S2 and Tables S4 and S5.

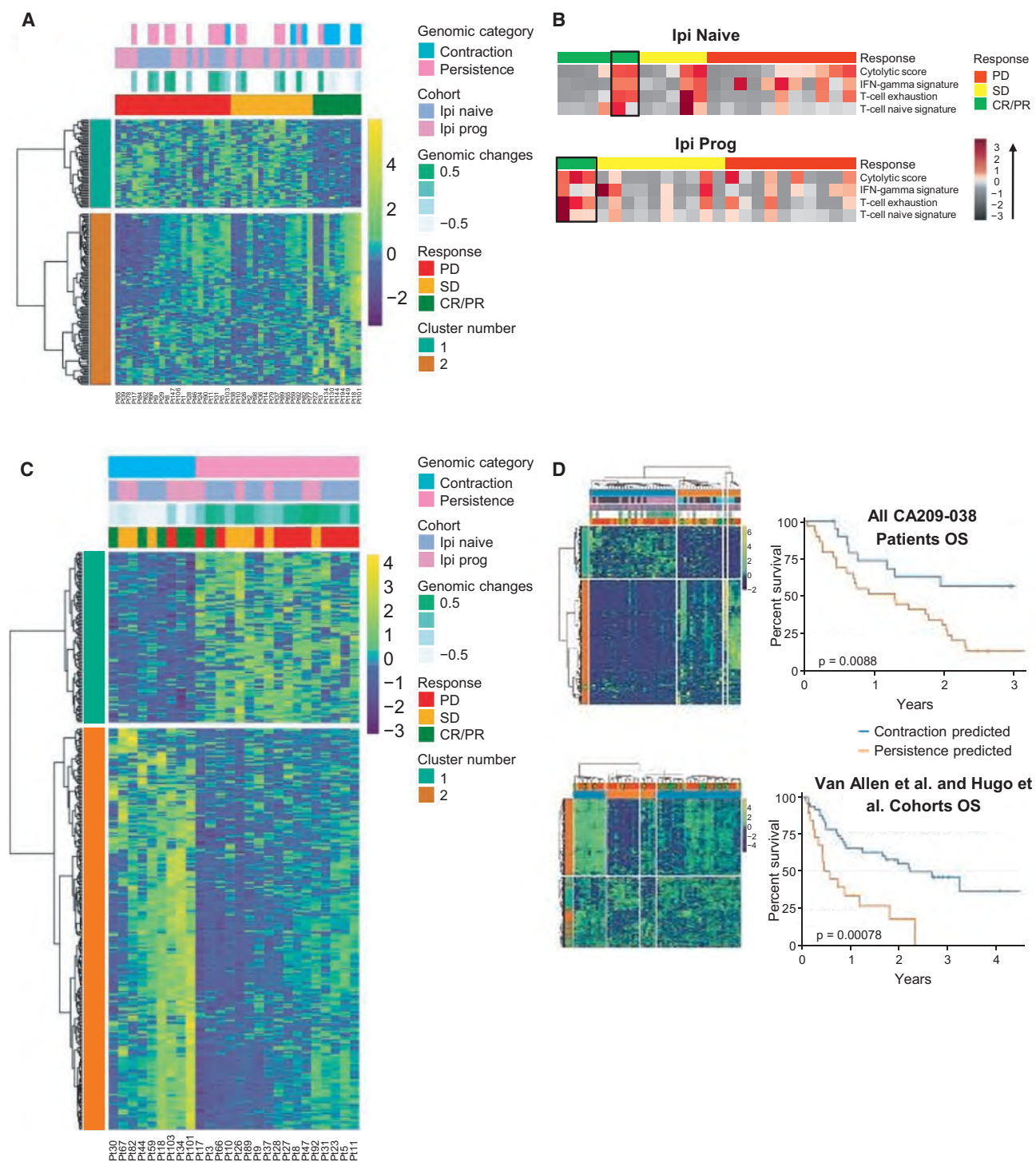


Figure 3. Pre-therapy Tumor Gene Expression Analysis

(A) Hierarchical clustering analysis of DEGs in tumors from pre-therapy biopsies.

(B) Heatmap associations of gene expression signatures in the Ipi-P and Ipi-N cohorts.

(C) Analysis of DEGs in tumors with genomic contraction versus those with genomic persistence ($n = 26$).

(D) Left: Clustering of the entire cohort of patients ($n = 45$) by DEGs identified in (C) clusters patients into two groups in entire cohort and into four groups in combined Hugo et al. (2016) and Van Allen et al. (2015) cohorts. Right: Long-term OS associates with clustered groups of patients from the entire cohort and from the combined Hugo et al. (2016) and Van Allen et al. (2015) cohorts.

See also Figure S3 and Tables S4 and S6.

therapy. To identify expression changes indicative of a “pharmacologic response” to Nivo, expression of genes that significantly change on-therapy, regardless of response, were analyzed. 475 DEGs were identified in on-therapy samples ($q < 0.20$) (Figure 4A; Table S6C), most of which were associated with immune regulation as determined by ingenuity pathway analysis (IPA) (Figure S4A). Many immune checkpoint genes increased in expression, regardless of response to therapy, including *PDCD1* (PD-1), *CD274* (PD-L1), *CTLA-4*, *CD80* (CTLA-4-L), *ICOS*, *LAG3*, and *TNFRSF9* (4-1BB).

Matched pre- and on-therapy samples were examined to determine whether relative differences in gene expression changes on-therapy could distinguish between patients whose disease was controlled and patients with PD. 2670 DEGs were identified between pre- and on-therapy samples of responders and non-responders ($q < 0.20$) (Figure 4B; Table S6D). Upregulated genes in responders involved a broader spectrum of immune-related genes than genes solely identified in pre-therapy samples (Figures S4B and S4C) including additional checkpoint-related genes (*TNFRSF4* [OX40], *TIGIT*, *HAVCR2* [TIM-3], and *C10orf54* [VISTA]) and genes involved in lymphocyte activation, chemotaxis and cytokine signaling, and immune cytolytic activity, consistent with previous findings (Das et al., 2015). Downregulated genes in responders involved pathways related to tumor growth, including neural and melanin pathways, cell-cycle regulation, mitotic division, and translation (Figure 4C). Significantly more immune-related genes were selectively upregulated in responders than in non-responders ($p = 6.17 \times 10^{-3}$ and $p = 4.61 \times 10^{-4}$ for depletion in the inflammatory response and cytokine-mediated signaling pathways from GO, respectively).

Changes in immune subpopulations between pre-therapy and on-therapy samples were assessed by immune-deconvolution analysis (see STAR Methods) and numerous changes in immune response among different tumors were observed. An increase in number of CD8⁺ T cells and NK cells, and a decrease in M1 macrophages, was associated with response to therapy (Figure 4D).

T Cell Repertoire Analysis and Immune Checkpoint Therapy

How Nivo therapy influences T cell repertoires was examined by analysis of changes in intratumoral T cell abundance, activation, and diversity. We also evaluated how these anti-PD-1-induced changes are affected by prior immunotherapy exposure. To study the dynamics of T cell infiltration and repertoire diversity in response to Nivo, next-generation deep sequencing of TCR β -chain complementarity determining regions (CDR3s) (TCR-seq) was performed on tumor samples pre- and 4 weeks post-Nivo initiation ($n = 34$) (Table S4). From these nucleotide sequences, the repertoire of amino acid motifs that determine the specificity of antigen-binding and their relative abundances were tabulated (see STAR Methods). Due to the limited number of samples for which TCR-seq data were available, we grouped patients as those with benefit (CR, PR, and SD) or no benefit (PD).

Changes in T Cell Tumor Infiltration and Activation Associated with Prior Treatment Status and Clinical Response

The fraction of TILs present within each tumor (the proportion of sample that is infiltrated by lymphocytes) was assessed by both

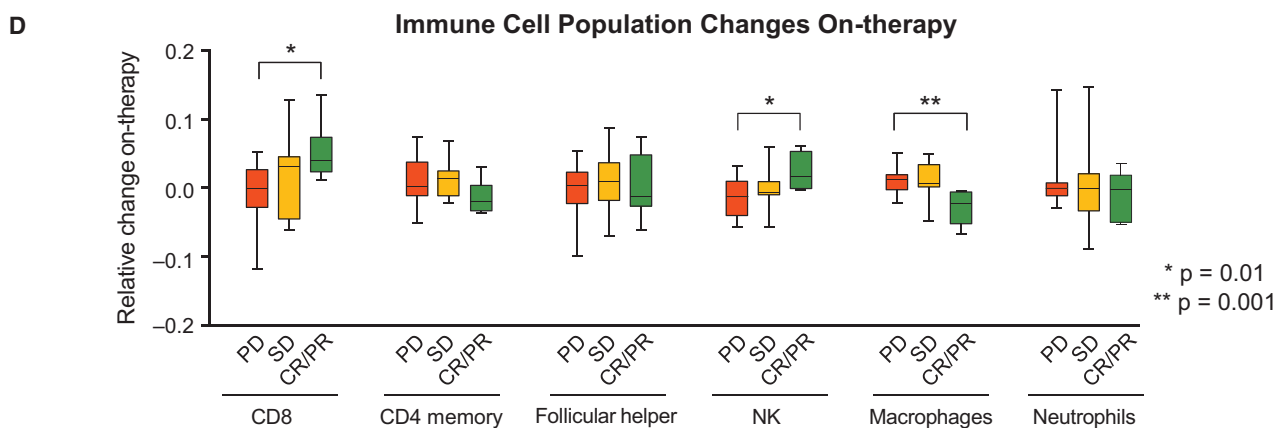
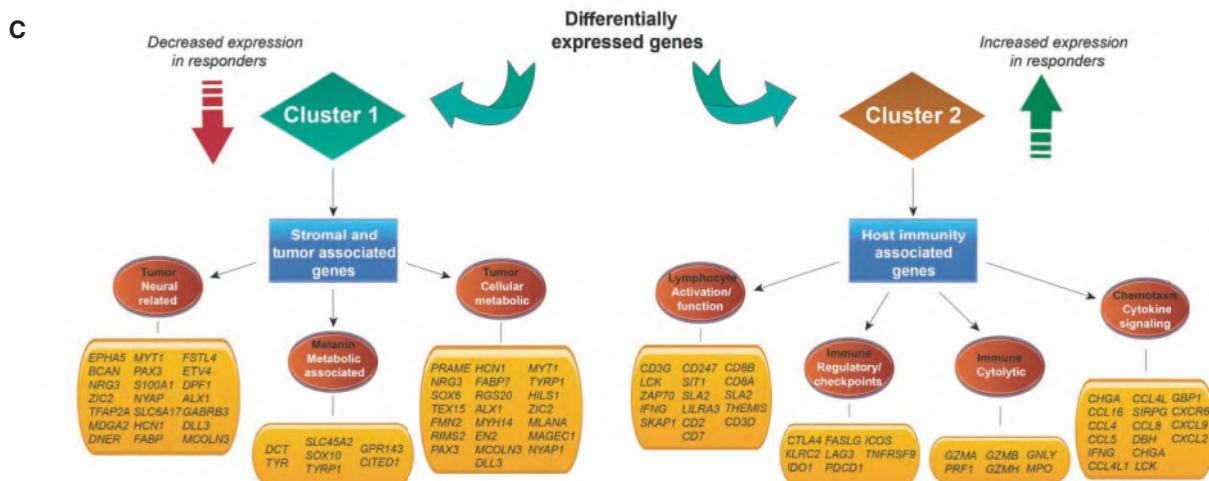
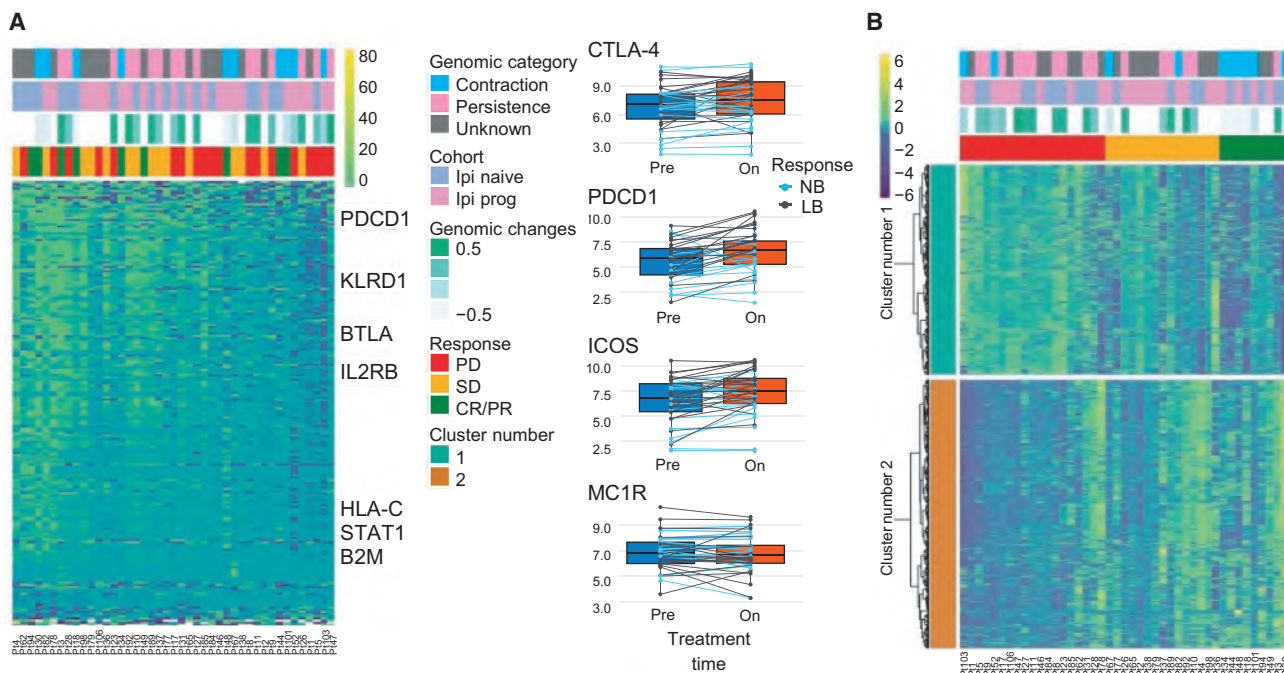
TCR-seq and immunohistochemical (IHC) staining for CD3 on mostly non-overlapping cohorts of patients (Table S4). By both approaches, an increase in the fraction of TILs upon Nivo therapy was significantly greater among benefiting than non-benefiting patients in the Ipi-N, but not Ipi-P, cohort (TCR-seq, $p = 0.040$; IHC, $p = 0.023$). Despite the differences in T cell infiltration, increased cytolytic pathway genes (Rooney et al., 2015) as measured by RNA-seq were associated with benefit in both Ipi-P and Ipi-N cohorts ($p = 0.043$ and $p = 0.005$) (Figure 5A). Notably, there was no significant difference in TIL abundance pre-therapy between patients with benefit and no benefit, or between Ipi-N and Ipi-P cohorts (Figure S5A).

On-Therapy Changes in Intratumoral T Cell Repertoire Diversity Associated with Response Differently in Ipi-P and Ipi-N Patients

The diversity of the CDR3 repertoire can be characterized by the Shannon entropy metric, which has two components: the number of unique CDR3s (richness) and their equality of distribution (evenness) (see STAR Methods). Pre-therapy, no significant difference in either of these metrics was observed between cohorts or response status (Figures S5B and S5C). On-therapy, the median fold change in the number of unique CDR3 sequences (richness) was significantly associated with benefit in Ipi-P but not Ipi-N patients ($p = 0.016$ versus $p = 0.489$) (Figure 5B). In contrast, the median change in T cell evenness on-therapy was associated with benefit in Ipi-N but not Ipi-P patients ($p = 0.036$ versus $p = 0.594$) (Figure 5B).

To refine interpretation of these findings with respect to the antigen-binding properties of the TCR repertoire, the diversity of the CDR3 amino acid sequences encoded by a single VJ cassette combination was analyzed individually for every observed VJ combination (see STAR Methods). Notably, a significant decrease in median CDR3 evenness per VJ group on-therapy was observed in Ipi-N but not Ipi-P patients ($p = 0.006$ versus $p = 0.600$) (Figures 5C and 5D) and in benefiting but not non-benefiting patients ($p = 0.003$ versus $p = 0.636$) (Figures 5D and 5E). When stratified by both prior treatment status and response, the fold change in CDR3 richness per VJ combination was associated with benefit in Ipi-P but not Ipi-N patients ($p = 0.014$ versus $p = 0.287$) (Figure S5E), while a significant decrease in CDR3 evenness per VJ pair was observed in Ipi-N but not Ipi-P benefiting patients ($p = 0.020$ versus $p = 0.131$) (Figure S5D). These results, derived from CDR3 subsets grouped by VJ combination, are mostly consistent with the trends of bulk CDR3 populations (Figure 5B). This suggests, due to association with CDR3 amino acid sequences rather than VJ cassette identities, that T cell population diversity dynamics are driven substantially by antigen recognition.

To visualize these changes in CDR3 diversity within each VJ combination, CDR3 evenness per VJ versus number of CDR3s per VJ were plotted for every VJ cassette group pre- and on-therapy as kernel density plots (Figure 5D). In the Ipi-N cohort, rightward shifts along the x axis represent increases in CDR3 richness per VJ combination on-therapy, and downward shifts along the y axis represent decreases in CDR3 evenness per VJ combination on-therapy. Notably, the shifts in evenness and richness per VJ are less prominent in the Ipi-P cohort.



(legend on next page)

Integrated T Cell Abundance and Diversity Metrics Associated with Response

Due to the diversity of the TCR repertoire in circulating blood (Zarnitsyna et al., 2013), increased T cell infiltration is usually concomitant with an increase in the observed diversity of that TIL repertoire. To understand whether the changes observed in the TIL CDR3 repertoires during Nivo therapy were primarily a function of the degree of infiltration or were due to clonotype distribution changes, indicative of selection and expansion of T cell clonotypes, the minimum percentage of unique CDR3 sequences accounting for 90% of the sequencing reads (D90) was calculated for each TIL sample. D90 is an indicator of evenness in which lower values indicate a more skewed distribution. While the evenness of most Ipi-P TIL repertoires did not change on-therapy, evenness varied widely among Ipi-N patients (Figure 5E). D90 value versus the level of TIL infiltration showed that in Ipi-N patients, disease control was greater among patients with lower TIL D90, including several with low TIL infiltration, such as patients 10, 89, and 94 (Figure 5E). This likely reflects the expansion of specific clonal populations in Nivo responders. This behavior contrasted with that of the Ipi-P cohort, in which high fractional TIL levels during Nivo therapy were a strong indicator of disease control, but CDR3 diversity varied relatively little (Figures 5E and S5A). Furthermore, usage of CD8-associated V-segments (Emerson et al., 2013) was significantly correlated with response ($p = 0.005$; ordinal regression), while CD4-associated V-segments were not ($p = 0.329$; ordinal regression) (Figure 5F).

Integrative Analysis of Tumor and T Cell Dynamics Changes in T Cell Diversity Associate with Tumor Neoantigen Landscape

We next assessed how the underlying T cell clonal dynamics related to the clonal dynamics of the tumor. Changes in T cell repertoire evenness were directly proportional to changes in the fraction of clonal mutations in patients with CR/PR and PD. Notably, there was a trend for a positive relationship in responders ($p = 0.07$) but a negative relationship in patients with PD ($p = 0.08$) (Figure 6A). Furthermore, in patients with CR/PR, we detected a linear relationship between the number of expanded T cell clones and the number of neoantigens that became undetectable on-therapy ($p = 0.03$) (Figure 6B; Table S5B). Notably, this relationship was not observed in patients with SD or PD, suggesting a qualitative difference in the T cell response in these tumors. Similar results were obtained when considering clonal mutations that became undetectable on-therapy, pre-therapy mutation load, or genomic contraction/persistence cases, supporting the view that T cell expansion is related to the underlying genetic profile of the tumor (Figures S6A–S6C).

Selective Depletion of Antigenic Mutations On-Therapy in Responding Patients

To investigate whether mutations that became undetectable on-therapy were more likely to be neoantigens or missense mutations than nonantigenic or synonymous mutations, the ratios of mutations that produce predicted neoantigens to those that do not were compared between mutations detected solely on-therapy and those detected solely pre-therapy. We hypothesized that the ratio of neoantigen-producing mutations would be higher pre-therapy versus on-therapy in patients with an active immune response, indicating selective pressure against the generation of antigenic mutations. Patients with CR/PR had lower neoantigen ratios on-therapy than patients with PD ($p = 0.03$; Wilcoxon rank-sum test), and patients with SD had a borderline association ($p = 0.11$; Wilcoxon rank-sum test) (Figures 6C and S6D).

To evaluate the possibility of selective depletion of putative neoantigens within each individual patient, the pre-therapy number of neoantigens per synonymous mutation was determined, and the expected number of neoantigens on-therapy was computed using the measured number of on-therapy synonymous mutations (see STAR Methods). In patients with CR/PR, the observed number of neoantigens was lower than the expected value ($p < 0.05$) (Figure S6E), suggesting that T cells were effective in eliminating tumor cells expressing immunogenic neoantigens.

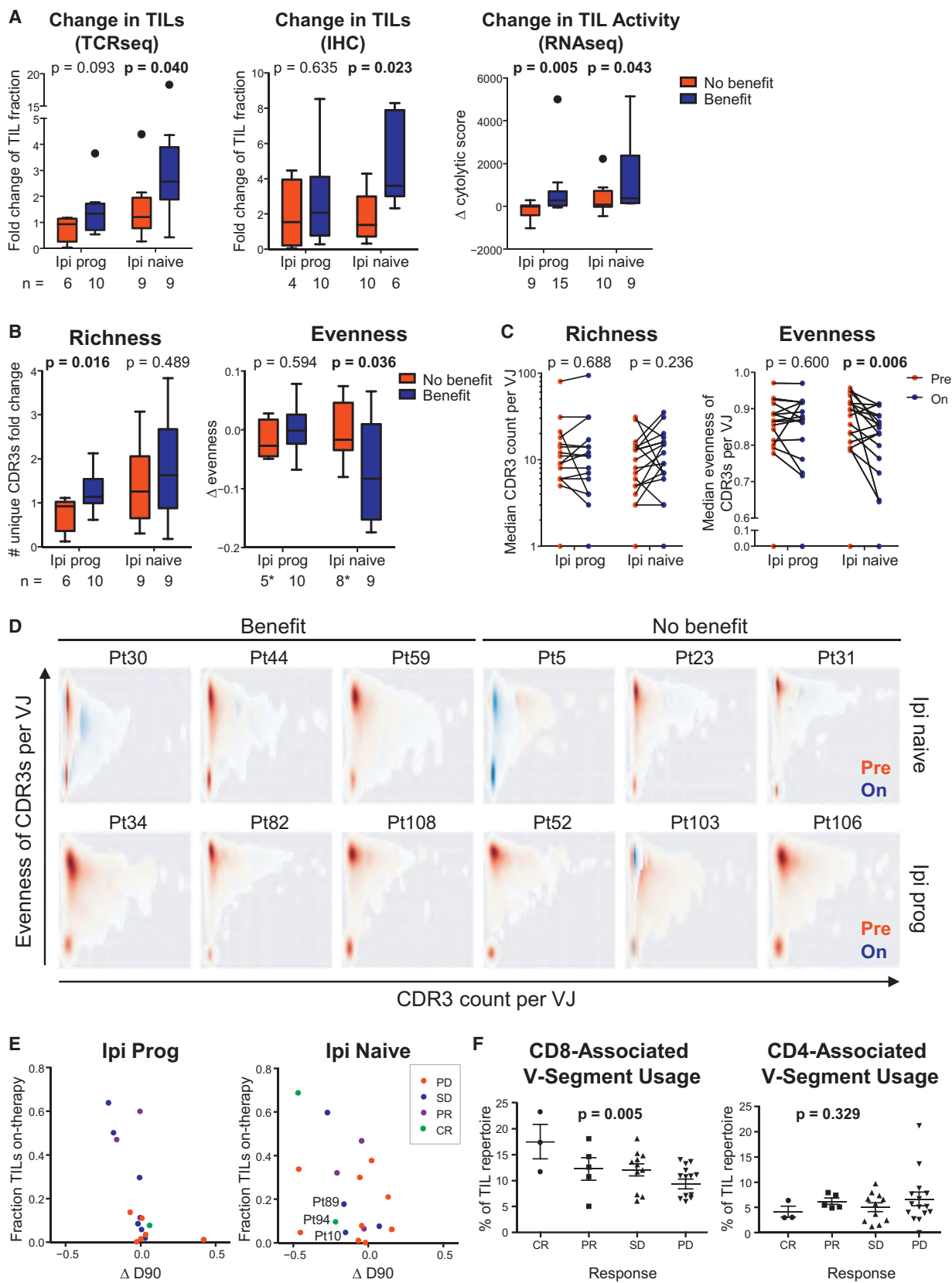
DISCUSSION

Previous reports indicate that increased tumor mutation load is associated with response to immune checkpoint therapy and that this relationship improves with assessment of clonality (McGranahan et al., 2016; Rizvi et al., 2015; Snyder et al., 2014). We observed an association of pre-therapy tumor mutation load and clonal mutation load with survival and response; however, this observation was limited to the Ipi-N subset of patients, consistent with previous findings (Weber et al., 2016a). Ipi-P patients had significantly more subclonal mutations present, and neither of these genomic markers correlated with response to therapy in these patients. These findings suggest that current biomarkers used to determine which patients will respond to immunotherapy may be more useful for Ipi-N patients than Ipi-P patients, although larger studies will be necessary to confirm these findings.

After 4 weeks of Nivo therapy, we observed a marked decrease in detectable mutations among patients with CR/PR and a moderate decrease in patients with SD. Clonality analysis identified that Nivo therapy affects the evolutionary landscape of tumors in patients with CR/PR, leading to the collapse of whole clonal populations, while in patients with SD, Nivo may shift the landscape in favor of specific subclones. Notably, in several

Figure 4. Changes in Gene Expression following Nivo Therapy

(A) Left: Analysis of ratio of DEGs and selected genes between pre- and on-therapy samples. Right: Examples of genes that change after initiation of Nivo. (B) Analysis of changes in gene expression (on-therapy compared with pre-therapy) that are altered in tumors that respond or do not respond to Nivo. (C) Graphical illustration of key pathways differentially expressed in (B). (D) Immune deconvolution of RNA-seq data comparing pre- and on-therapy samples. Data are presented as median and IQR. See also Figure S4 and Tables S4 and S6.



(legend on next page)

patients with SD, some subclones became undetectable while others remained. In addition, we demonstrated genomic evidence of effective immune elimination of tumor cells containing non-synonymous mutations and neoantigens on-therapy in responding patients as a group and in a subset of responding patients individually. Moreover, T cell clones expanded in proportion to the number of neoantigenic mutations that became undetectable on-therapy. These observations agree with evidence of immune-mediated genetic loss of patient-specific mutations, such as after adoptive T cell therapy (Verdegaal et al., 2016). Our genetic data are consistent with immunoediting and are derived from a larger group of patients than previously studied (Verdegaal et al., 2016). However, we cannot make definitive conclusions due to computational limitations, namely, unambiguous identification of specific neoantigens driving this effect.

Therapy-induced clonal evolution has been reported following other cancer therapies such as cytotoxic treatments in glioblastoma (GBM) and chronic lymphocytic leukemia, and our observation of *CDKN2A* loss in four patients with PD agrees with reported changes in GBM tumors at progression (Johnson et al., 2014; Landau et al., 2015). The appearance of new mutations on-therapy could represent genetic drift, or alternatively, could be consistent with a model in which certain subclonal populations are selected under immunologic pressure. However, on-therapy expression analysis indicates that an immune ignorance or immune exclusion mechanism of resistance is likely operative rather than the evolution of an intrinsic genetic mechanism mediating resistance. The early collapse in clonal populations among responding patients is consistent with previous findings (Landau et al., 2015; Wang et al., 2016) and suggests that clonal composition undergoes significant changes after cytotoxic therapy. Our results may potentially be affected by variation in the anatomic location from which the tissue was taken, by intratumoral heterogeneity, and by decreased purity in on-therapy biopsies. However, biopsies targeted the same site and, although purity did decrease on-therapy, the magnitude of change was not large enough to explain observations herein.

Expression analysis of pre-therapy tumor samples identified a small set of upregulated immune-related genes in responders, consistent with prior reports demonstrating an IFN- γ signature associated with response (Taube et al., 2012, 2015). However, these expression changes were only marginally predictive of response. It is notable that consistent with previous findings (Larkin et al., 2017; Weber et al., 2016b) of patients who received prior immunotherapy, only those with PD-L1-expressing or

immunologically “hot tumors” appeared to respond whereas significant responses were observed among PD-L1 low to no expression subgroups among Ipi-N patients. These findings may again be limited due to the size of the cohort but, like mutation load and tumor clonality, suggest that the importance of a “hot tumor” may depend on prior therapy received.

Surprisingly, stratification based on a molecular phenotype of response (i.e., genomic contraction/persistence) demonstrated a more pronounced difference in pre-existing immunity between molecular responders and non-responders. Genes differentially expressed between groups could predict survival in other patients in this dataset and in other immunotherapy-treated cohorts, signifying their biologic relevance and suggesting that delays in clinical response may be secondary to immune infiltration (Wolchok et al., 2009). This highlights the difficulty in relying solely on clinical and radiographic response to understand the underlying biologic mechanisms of response to therapy in human tumors. Notably, this analysis identified numerous HLA class II genes, along with other genes, as differentially expressed and this is similar to a recently reported signature indicating differences in regulation of macrophages (Kaneda et al., 2016). Changes in macrophages on-therapy also associated with clinical response (Figure 4D), suggesting that macrophages may play an important role in response (Gordon et al., 2017).

Analysis of on-therapy expression changes revealed marked upregulation of a multitude of immune pathways that were more pronounced in responding patients and included additional checkpoints and a broader set of DEGs than previously reported (Chen et al., 2016). Some of these newly identified gene products may be considered as candidate targets for future combination immunotherapy trials. Most patients with PD had minimal immune response on-therapy, and differential gene analysis did not identify a dominant or single method of tumor-intrinsic immune evasion, suggesting an immune ignorance or immune exclusion mechanism rather than an adaptive resistance mechanism (Salerno et al., 2016; Spranger et al., 2013) (Figure 4B). In contrast, many patients with SD appeared to have modest immune response induction, suggesting that an adaptive mechanism of resistance may have a more important role in these patients (Taube et al., 2012, 2015).

Increased cytolytic activity, indicative of T cell activation, associated with response. Both cytolytic activity and response were observed at similar rates regardless of prior immune therapy exposure. However, analysis of T cell repertoires suggested that anti-PD-1 response is associated with different patterns of T cell

Figure 5. T Cell Infiltrate and Repertoire Association with Response to Nivo

Due to the reduced number of cases with paired TCR-seq data, patients with CR/PR and SD were grouped as having “benefit,” and patients with PD were considered to have “no benefit.”

(A) Change in TIL abundance and activity as measured by multiple methods (DNA-based TCR-seq, IHC, and RNA-based cytolytic score). Data are presented as median and IQR.

(B) Change in richness and evenness of intratumoral T cell repertoires. *Two outliers were removed per Grubbs’ test, $\alpha = 0.1$ (see the STAR Methods). Data are presented as median and IQR.

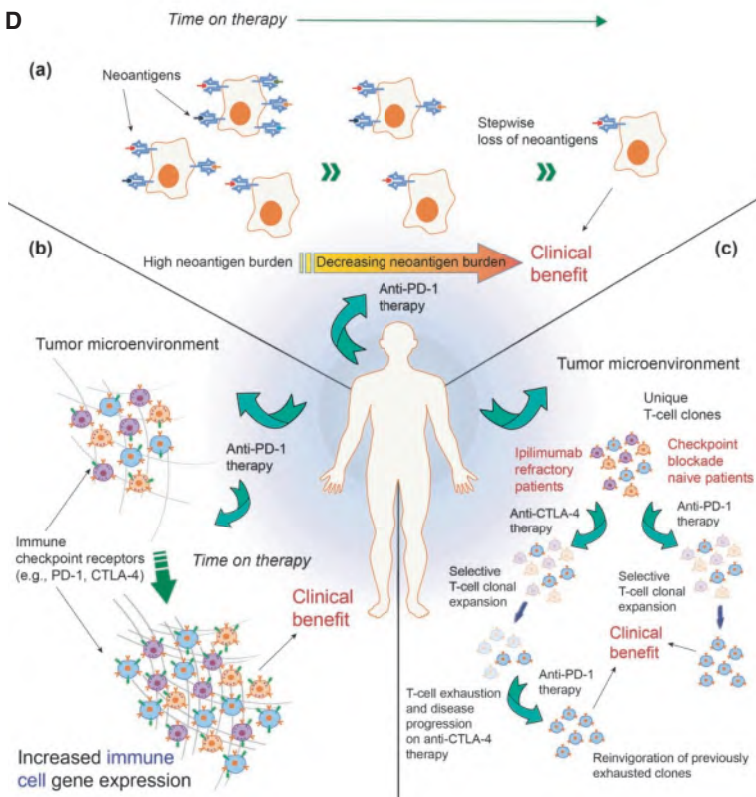
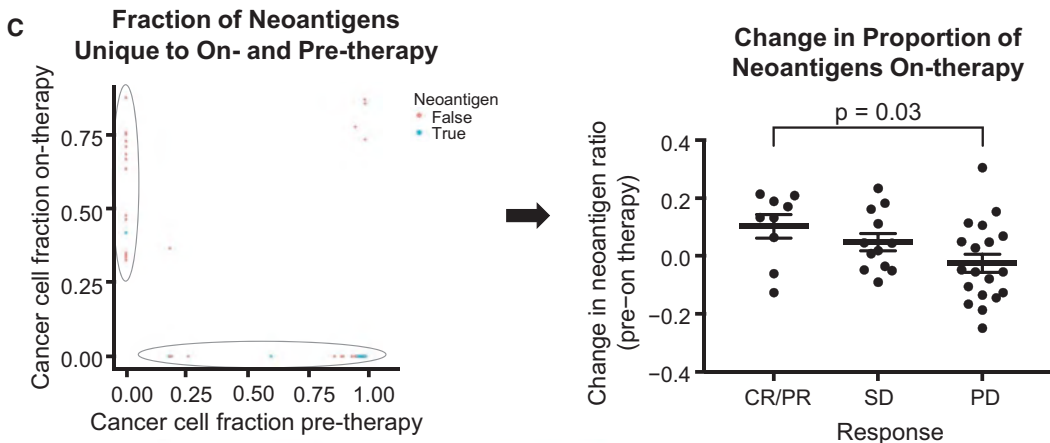
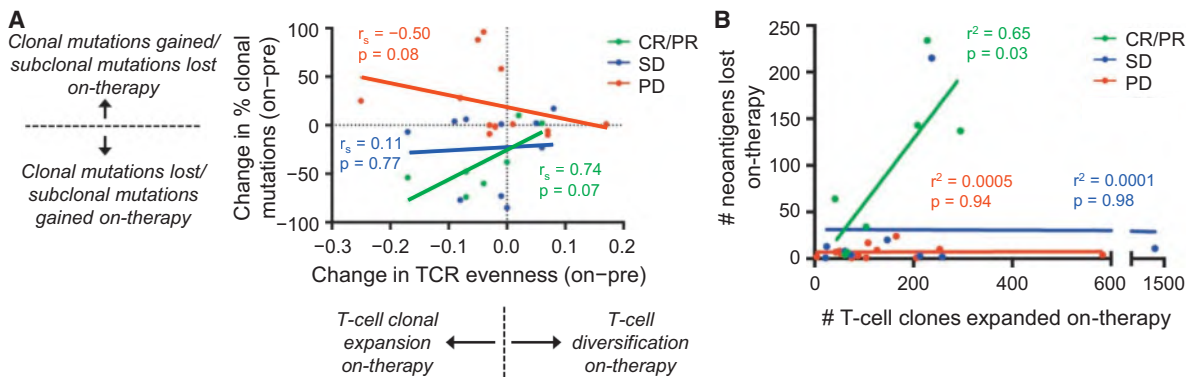
(C) Median richness and evenness of CDR3s per VJ combinations pre-therapy and on-therapy (see also Figure S6E).

(D) Kernel density plots of CDR3 evenness versus number of unique CDR3s for every observed VJ pair in selected patients.

(E) Comparison of on-therapy TIL levels with changes in T cell repertoire evenness (D90, defined as the minimum fraction of total unique CDR3 sequences that constitutes 90% of all sequencing reads).

(F) Fraction of on-therapy TCR repertoire utilizing V-segments associated with CD8 or CD4 T cells. Data are presented as mean \pm SEM.

See also Figure S5 and Table S4.



(legend on next page)

diversity dynamics in Ipi-N versus Ipi-P patients. We infer that decreased evenness without a significant change in the total number of CDR3s (richness) observed in Ipi-N responders is consistent with expansion and accumulation of specific T cell clonotypes in response to the detection of tumor antigens. We speculate that TILs of Ipi-P patients may represent a binding repertoire already differentially selected by the tumor antigenic landscape during Ipi treatment but subsequently exhausted through PD-1/PD-L1 signaling. The predictive value of exhaustion marker expression for responsiveness in Ipi-P but not Ipi-N patients is consistent with this model (Figure 3B). Thus, we speculate that in Ipi-P patients, anti-PD-1 therapy functions mainly by alleviating exhaustion among the extant distribution of TIL clonotypes, while in Ipi-N patients, anti-PD-1 therapy facilitates selective intra-tumoral expansion of tumor-reactive clonotypes (Figure 6D).

We hypothesize that changes in T cell repertoire diversity are associated with anti-PD-1-induced tumor clonal architecture changes, reflecting the cytolytic anti-tumor effect of expanded tumor antigen-specific T cell clonotypes. Of note, changes in T cell repertoire evenness were directly proportional to changes in the fraction of clonal mutations in responders and patients with PD. There was a trend for a positive and negative relationship in responders and non-responders, respectively, suggesting that in responders, as T cell clones expand, clonal mutations are targeted and eliminated. Possible explanations for the negative relationship in non-responders include: (1) T cell clonotypes that expand may target subclonal mutations instead of clonal mutations, resulting in a futile T cell response (Figure S6F), or (2) decreased T cell repertoire evenness could be due to clonal expansion of regulatory T cells, which may enhance an immunosuppressive environment.

In conclusion, we performed extensive immunogenomic analyses on melanoma samples treated with anti-PD-1 therapy and characterized how tumor genomic and microenvironmental features changed over time. Assessment of the genomic landscape on-therapy demonstrated clonal evolution consistent with therapy-dependent immunoediting. T cell repertoire analysis identified that T cell clonotypes expand in proportion to the number of neoantigens that become undetectable in responding patients. Gene expression analysis revealed the changing transcriptional and microenvironmental alterations induced by anti-PD-1 therapy and identified a broad spectrum of immune checkpoint-related genes that were upregulated. These data have important implications for understanding the mechanism of action of checkpoint inhibitors and for the design of future immune checkpoint blockade trials. Based on our observations, we propose a model of tumor evolution and its microenvironment in response to anti-PD-1 therapy (Figure 6D). Lastly, we provide an interactive visualization of the data contained herein at <http://www.ioexplorer.org>.

STAR★METHODS

Detailed methods are provided in the online version of this paper and include the following:

- KEY RESOURCES TABLE
- CONTACT FOR REAGENT AND RESOURCE SHARING
- EXPERIMENTAL MODEL AND SUBJECT DETAILS
- METHOD DETAILS
 - Whole-Exome Sequencing
 - Neoantigen Analysis
 - Copy-Number Analysis
 - Tumor Clonality Analysis
 - RNA Sequencing
 - TCR β -Chain Sequencing and Analysis
 - Immunohistochemistry
 - Tumor Purity Assessment
- QUANTIFICATION AND STATISTICAL ANALYSIS
 - Statistics and Survival Analysis
- DATA AND SOFTWARE AVAILABILITY

SUPPLEMENTAL INFORMATION

Supplemental Information includes six figures and six tables and can be found with this article online at <https://doi.org/10.1016/j.cell.2017.09.028>.

AUTHOR CONTRIBUTIONS

Funding Acquisition, T.A.C.; Conceptualization, T.A.C., N.R., C.E.H., and W.J.U.; Clinical Trial Implementation and Accrual, W.J.U., F.S.H., S.M.-A., W.H.S., S.B., W.-J.H., T.F.G., C.L.S., and C.E.H.; Investigation and Formal Analysis, N.R., V.M., and S.M.K.; Analysis of Pre- and On-therapy Changes in Mutation Load and Clonality, N.W., V.M., and N.R.; Neoantigen Analysis, D.C., V.M., N.R., and J.J.H.; Analysis of RNA-Seq Data, A.D., F.K., H.C., R.M., and N.R.; Exome-Seq Data from Pre-therapy Samples, V.M., L.G.T.M., S.M.K., R.S., and N.R.; Analysis of TCR-Seq Data, J.J.H., J.S.S., J.-W.S., and J.P.S.; Writing – Original Draft, N.R., J.J.H., A.D., N.W., and T.A.C.; Writing – Review & Editing, all authors; Supervision, N.W. and T.A.C.

ACKNOWLEDGMENTS

We first thank each patient and their families for participation in this study. This work was funded by Bristol-Myers Squibb, the Pershing Square Sohn Cancer Research Foundation (T.A.C.), the PaineWebber Chair (T.A.C.), Stand Up 2 Cancer (T.A.C.), the Memorial Sloan Kettering Cancer Center (core grant 5P30 CA008748-50), and the STARR Cancer Consortium (T.A.C.). S.B. reports grants from Abraxis, Amgen, Bionomics, Bristol-Myers Squibb, EMD Serono, Immune Design, Immunogen, Merck, NantKwest, and OncoSec, and personal fees from Genentech. T.A.C. is a co-founder of Gritstone Oncology and reports research grants from Bristol-Myers Squibb. H.C. and C.E.H. are full-time employees and stock shareholders of Bristol-Myers Squibb. T.F.G. reports grants from Bristol-Myers Squibb, Incyte, Merck, Ono, Genentech, and Seattle Genetics, personal fees from AbbVie, Aduro, Bayer, Jounce Therapeutics, Merck,

Figure 6. T Cells Expand in Proportion to Depletion of Neoantigens

(A) Changes in T cell population distribution (i.e., evenness) and changes in tumor mutation clonality by response. (B) Relationship between the number of predicted neoantigens lost and the number of T cell clones expanded on-therapy. (C) Neoantigen ratios (mutations predicted to generate neoantigens per mutations not predicted to generate neoantigens) from mutations solely identified in pre-therapy samples compared with those identified solely in on-therapy samples. Data are presented as mean \pm SEM. (D) Graphical model depicting changes during anti-PD-1 therapy. (a) Changes in mutations and neoantigens during therapy. (b) Changes in TCR repertoire depend on exposure to prior immunotherapy. (c) Changes in immune landscape and checkpoints during therapy. See also Figure S6 and Table S5.

and Genentech, and is a stock shareholder of Jounce Therapeutics. J.J.H. reports that spouse is a full-time employee of Regeneron Pharmaceuticals. F.S.H. reports grants from Bristol-Myers Squibb and personal fees from Bristol-Myers Squibb, EMD Serono, Genentech, Merck, and Novartis. W.-J.H. reports grants from Bristol-Myers Squibb, GlaxoSmithKline, MedImmune, and Merck, and personal fees from Merck. F.K. and V.M. report grants from Bristol-Myers Squibb. S.M.-A. reports personal fees from Bristol-Myers Squibb and Merck. L.G.T.M. reports personal fees from Merck. N.R. reports grants from Bristol-Myers Squibb, and personal fees from MedImmune. J.P.S. reports grants and personal fees from, and is a stock shareholder of, NexImmune. W.H.S. reports grants from Bristol-Myers Squibb and Merck and personal fees from Bristol-Myers Squibb, Castle Biosciences, Merck, and Novartis. C.L.S. reports grants from Merck and Polynoma, personal fees from Immatics, and is a patent holder for the University of Virginia. W.J.U. reports grants and personal fees from Bristol-Myers Squibb and MedImmune and personal fees from Green Peptide and eTheRNA. Medical writing and editorial assistance provided by Amrita Dervan, MSc, and Jay Rathi, MA, of Spark Medica (US), funded by Bristol-Myers Squibb.

Received: February 17, 2017

Revised: July 11, 2017

Accepted: September 18, 2017

Published: October 12, 2017

REFERENCES

- Alexandrov, L.B., Nik-Zainal, S., Wedge, D.C., Aparicio, S.A., Behjati, S., Biankin, A.V., Bignell, G.R., Bolli, N., Borg, A., Borresen-Dale, A.L., et al.; Australian Pancreatic Cancer Genome Initiative; ICGC Breast Cancer Consortium; ICGC MML-Seq Consortium; ICGC PedBrain (2013). Signatures of mutational processes in human cancer. *Nature* 500, 415–421.
- Arnaud-Haond, S., Duarte, C.M., Alberto, F., and Serrão, E.A. (2007). Standardizing methods to address clonality in population studies. *Mol. Ecol.* 16, 5115–5139.
- Arstila, T.P., Casrouge, A., Baron, V., Even, J., Kanellopoulos, J., and Kourilsky, P. (1999). A direct estimate of the human alphabeta T cell receptor diversity. *Science* 286, 958–961.
- Brahmer, J., Reckamp, K.L., Baas, P., Crinò, L., Eberhardt, W.E., Poddubskaya, E., Antonia, S., Pluzanski, A., Vokes, E.E., Holgado, E., et al. (2015). Nivolumab versus docetaxel in advanced squamous-cell non-small-cell lung cancer. *N. Engl. J. Med.* 373, 123–135.
- Cancer Genome Atlas Network (2015). Genomic classification of cutaneous melanoma. *Cell* 161, 1681–1696.
- Carlson, C.S., Emerson, R.O., Sherwood, A.M., Desmarais, C., Chung, M.W., Parsons, J.M., Steen, M.S., LaMadrid-Herrmannsfeldt, M.A., Williamson, D.W., Livingston, R.J., et al. (2013). Using synthetic templates to design an unbiased multiplex PCR assay. *Nat. Commun.* 4, 2680.
- Carter, S.L., Cibulskis, K., Helman, E., McKenna, A., Shen, H., Zack, T., Laird, P.W., Onofrio, R.C., Winckler, W., Weir, B.A., et al. (2012). Absolute quantification of somatic DNA alterations in human cancer. *Nat. Biotechnol.* 30, 413–421.
- Chen, P.L., Roh, W., Reuben, A., Cooper, Z.A., Spencer, C.N., Prieto, P.A., Miller, J.P., Bassett, R.L., Gopalakrishnan, V., Wani, K., et al. (2016). Analysis of immune signatures in longitudinal tumor samples yields insight into biomarkers of response and mechanisms of resistance to immune checkpoint blockade. *Cancer Discov.* 6, 827–837.
- Chiappinelli, K.B., Strissel, P.L., Desrichard, A., Li, H., Henke, C., Akman, B., Hein, A., Rote, N.S., Cope, L.M., Snyder, A., et al. (2015). Inhibiting DNA methylation causes an interferon response in cancer via dsRNA including endogenous retroviruses. *Cell* 162, 974–986.
- Cibulskis, K., Lawrence, M.S., Carter, S.L., Sivachenko, A., Jaffe, D., Sougnez, C., Gabriel, S., Meyerson, M., Lander, E.S., and Getz, G. (2013). Sensitive detection of somatic point mutations in impure and heterogeneous cancer samples. *Nat. Biotechnol.* 31, 213–219.
- Dako (2016). PD-L1 IHC 28-8 pharmDx. https://www.accessdata.fda.gov/cdrh_docs/pdf15/P150027c.pdf.
- Das, R., Verma, R., Sznol, M., Boddupalli, C.S., Gettinger, S.N., Kluger, H., Callahan, M., Wolchok, J.D., Halaban, R., Dhodapkar, M.V., and Dhodapkar, K.M. (2015). Combination therapy with anti-CTLA-4 and anti-PD-1 leads to distinct immunologic changes in vivo. *J. Immunol.* 194, 950–959.
- Davoli, T., Uno, H., Wooten, E.C., and Elledge, S.J. (2017). Tumor aneuploidy correlates with markers of immune evasion and with reduced response to immunotherapy. *Science* 355, eaaf8399.
- DeWitt, W.S., Emerson, R.O., Lindau, P., Vignali, M., Snyder, T.M., Desmarais, C., Sanders, C., Utsugi, H., Warren, E.H., McElrath, J., et al. (2015). Dynamics of the cytotoxic T cell response to a model of acute viral infection. *J. Virol.* 89, 4517–4526.
- Dobin, A., Davis, C.A., Schlesinger, F., Drenkow, J., Zaleski, C., Jha, S., Batut, P., Chaisson, M., and Gingeras, T.R. (2013). STAR: ultrafast universal RNA-seq aligner. *Bioinformatics* 29, 15–21.
- Emerson, R., Sherwood, A., Desmarais, C., Malhotra, S., Phippard, D., and Robins, H. (2013). Estimating the ratio of CD4+ to CD8+ T cells using high-throughput sequence data. *J. Immunol. Methods* 391, 14–21.
- Ferris, R.L., Blumenschein, G., Jr., Fayette, J., Guigay, J., Colevas, A.D., Licitra, L., Harrington, K., Kasper, S., Vokes, E.E., Even, C., et al. (2016). Nivolumab for recurrent squamous-cell carcinoma of the head and neck. *N. Engl. J. Med.* 375, 1856–1867.
- Fisher, S., Barry, A., Abreu, J., Minie, B., Nolan, J., Delorey, T.M., Young, G., Fennell, T.J., Allen, A., Ambrogio, L., et al. (2011). A scalable, fully automated process for construction of sequence-ready human exome targeted capture libraries. *Genome Biol.* 12, R1.
- Gordon, S.R., Maute, R.L., Dulken, B.W., Hutter, G., George, B.M., McCracken, M.N., Gupta, R., Tsai, J.M., Sinha, R., Corey, D., et al. (2017). PD-1 expression by tumour-associated macrophages inhibits phagocytosis and tumour immunity. *Nature* 545, 495–499.
- Herbst, R.S., Soria, J.C., Kowanzet, M., Fine, G.D., Hamid, O., Gordon, M.S., Sosman, J.A., McDermott, D.F., Powderly, J.D., Gettinger, S.N., et al. (2014). Predictive correlates of response to the anti-PD-L1 antibody MPDL3280A in cancer patients. *Nature* 515, 563–567.
- Hodi, F.S., Kluger, H., Sznol, M., Carvajal, R., Lawrence, D., Atkins, M., Powderly, J., Sharfman, W., Puzanov, I., Smith, D., et al. (2016). Abstract CT001: durable, long-term survival in previously treated patients with advanced melanoma (MEL) who received nivolumab (NIVO) monotherapy in a phase I trial. *Cancer Res.* 76, CT001–CT001.
- Hugo, W., Zaretsky, J.M., Sun, L., Song, C., Moreno, B.H., Hu-Lieskovan, S., Berent-Maoz, B., Pang, J., Chmielowski, B., Cherry, G., et al. (2016). Genomic and transcriptomic features of response to anti-PD-1 therapy in metastatic melanoma. *Cell* 165, 35–44.
- Johnson, B.E., Mazor, T., Hong, C., Barnes, M., Aihara, K., McLean, C.Y., Fouse, S.D., Yamamoto, S., Ueda, H., Tatsuno, K., et al. (2014). Mutational analysis reveals the origin and therapy-driven evolution of recurrent glioma. *Science* 343, 189–193.
- Joyce, J.A., and Fearon, D.T. (2015). T cell exclusion, immune privilege, and the tumor microenvironment. *Science* 348, 74–80.
- Kaneda, M.M., Messer, K.S., Ralainirina, N., Li, H., Leem, C.J., Gorjestani, S., Woo, G., Nguyen, A.V., Figueiredo, C.C., Foubert, P., et al. (2016). PI3K γ is a molecular switch that controls immune suppression. *Nature* 539, 437–442.
- Koboldt, D.C., Zhang, Q., Larson, D.E., Shen, D., McLellan, M.D., Lin, L., Miller, C.A., Mardis, E.R., Ding, L., and Wilson, R.K. (2012). VarScan 2: somatic mutation and copy number alteration discovery in cancer by exome sequencing. *Genome Res.* 22, 568–576.
- Landau, D.A., Tausch, E., Taylor-Weiner, A.N., Stewart, C., Reiter, J.G., Bahlo, J., Kluth, S., Bozic, I., Lawrence, M., Böttcher, S., et al. (2015). Mutations driving CLL and their evolution in progression and relapse. *Nature* 526, 525–530.
- Larkin, J., Minor, D., D'Angelo, S., Neyns, B., Smylie, M., Miller, W.H., Jr., Gutzmer, R., Linette, G., Chmielowski, B., Lao, C.D., et al. (2017). Overall

- survival in patients with advanced melanoma who received nivolumab versus investigator's choice chemotherapy in CheckMate 037: a randomized, controlled, open-label phase III trial. *J. Clin. Oncol.* <https://doi.org/10.1200/JCO.2016.71.8023>.
- Larson, D.E., Harris, C.C., Chen, K., Koboldt, D.C., Abbott, T.E., Dooling, D.J., Ley, T.J., Mardis, E.R., Wilson, R.K., and Ding, L. (2012). SomaticSniper: identification of somatic point mutations in whole genome sequencing data. *Bioinformatics* 28, 311–317.
- Le, D.T., Uram, J.N., Wang, H., Bartlett, B.R., Kemberling, H., Eyring, A.D., Skora, A.D., Luber, B.S., Azad, N.S., Laheru, D., et al. (2015). PD-1 blockade in tumors with mismatch-repair deficiency. *N. Engl. J. Med.* 372, 2509–2520.
- Love, M.I., Huber, W., and Anders, S. (2014). Moderated estimation of fold change and dispersion for RNA-seq data with DESeq2. *Genome Biol.* 15, 550.
- McGranahan, N., Favero, F., de Bruin, E.C., Birkbak, N.J., Szallasi, Z., and Swanton, C. (2015). Clonal status of actionable driver events and the timing of mutational processes in cancer evolution. *Sci. Transl. Med.* 7, 283ra54.
- McGranahan, N., Furness, A.J., Rosenthal, R., Ramskov, S., Lyngaa, R., Saini, S.K., Jamal-Hanjani, M., Wilson, G.A., Birkbak, N.J., Hiley, C.T., et al. (2016). Clonal neoantigens elicit T cell immunoreactivity and sensitivity to immune checkpoint blockade. *Science* 351, 1463–1469.
- Morris, L.G., Riaz, N., Desrichard, A., Şenbabaoğlu, Y., Hakimi, A.A., Makarov, V., Reis-Filho, J.S., and Chan, T.A. (2016). Pan-cancer analysis of intratumor heterogeneity as a prognostic determinant of survival. *Oncotarget* 7, 10051–10063.
- Motzer, R.J., Escudier, B., McDermott, D.F., George, S., Hammers, H.J., Srinivas, S., Tykodi, S.S., Sosman, J.A., Procopio, G., Plimack, E.R., et al.; CheckMate 025 Investigators (2015). Nivolumab versus everolimus in advanced renal-cell carcinoma. *N. Engl. J. Med.* 373, 1803–1813.
- Newman, A.M., Liu, C.L., Green, M.R., Gentles, A.J., Feng, W., Xu, Y., Hoang, C.D., Diehn, M., and Alizadeh, A.A. (2015). Robust enumeration of cell subsets from tissue expression profiles. *Nat. Methods* 12, 453–457.
- Nielsen, M., Lundegaard, C., Wornig, P., Lauemøller, S.L., Lamberth, K., Buus, S., Brunak, S., and Lund, O. (2003). Reliable prediction of T-cell epitopes using neural networks with novel sequence representations. *Protein Sci.* 12, 1007–1017.
- Riaz, N., Morris, L., Havel, J.J., Makarov, V., Desrichard, A., and Chan, T.A. (2016a). The role of neoantigens in response to immune checkpoint blockade. *Int. Immunol.* 28, 411–419.
- Riaz, N., Havel, J.J., Kendall, S.M., Makarov, V., Walsh, L.A., Desrichard, A., Weinhold, N., and Chan, T.A. (2016b). Recurrent SERPINB3 and SERPINB4 mutations in patients who respond to anti-CTLA4 immunotherapy. *Nat. Genet.* 48, 1327–1329.
- Rizvi, N.A., Hellmann, M.D., Snyder, A., Kvistborg, P., Makarov, V., Havel, J.J., Lee, W., Yuan, J., Wong, P., Ho, T.S., et al. (2015). Cancer immunology. Mutational landscape determines sensitivity to PD-1 blockade in non-small cell lung cancer. *Science* 348, 124–128.
- Robert, C., Long, G.V., Brady, B., Dutriaux, C., Maio, M., Mortier, L., Hassel, J.C., Rutkowski, P., McNeil, C., Kalinka-Warzocho, E., et al. (2015). Nivolumab in previously untreated melanoma without BRAF mutation. *N. Engl. J. Med.* 372, 320–330.
- Robins, H.S., Campregher, P.V., Srivastava, S.K., Wacher, A., Turtle, C.J., Kahsai, O., Riddell, S.R., Warren, E.H., and Carlson, C.S. (2009). Comprehensive assessment of T-cell receptor beta-chain diversity in alphabeta T cells. *Blood* 114, 4099–4107.
- Rooney, M.S., Shukla, S.A., Wu, C.J., Getz, G., and Hacohen, N. (2015). Molecular and genetic properties of tumors associated with local immune cytolytic activity. *Cell* 160, 48–61.
- Rosenberg, J.E., Hoffman-Censits, J., Powles, T., van der Heijden, M.S., Balar, A.V., Necchi, A., Dawson, N., O'Donnell, P.H., Balmanoukian, A., Loriot, Y., et al. (2016). Atezolizumab in patients with locally advanced and metastatic urothelial carcinoma who have progressed following treatment with platinum-based chemotherapy: a single-arm, multicentre, phase 2 trial. *Lancet* 387, 1909–1920.
- Rosenthal, R., McGranahan, N., Herrero, J., Taylor, B.S., and Swanton, C. (2016). DeconstructSigs: delineating mutational processes in single tumors distinguishes DNA repair deficiencies and patterns of carcinoma evolution. *Genome Biol.* 17, 31.
- Roth, A., Khattra, J., Yap, D., Wan, A., Laks, E., Biele, J., Ha, G., Aparicio, S., Bouchard-Côté, A., and Shah, S.P. (2014). PyClone: statistical inference of clonal population structure in cancer. *Nat. Methods* 11, 396–398.
- Salerno, E.P., Bedognetti, D., Mauldin, I.S., Deacon, D.H., Shea, S.M., Pinczewski, J., Obeid, J.M., Coukos, G., Wang, E., Gajewski, T.F., et al. (2016). Human melanomas and ovarian cancers overexpressing mechanical barrier molecule genes lack immune signatures and have increased patient mortality risk. *Oncolimmunology* 5, e1240857.
- Saunders, C.T., Wong, W.S., Swamy, S., Becq, J., Murray, L.J., and Cheetham, R.K. (2012). Strelka: accurate somatic small-variant calling from sequenced tumor-normal sample pairs. *Bioinformatics* 28, 1811–1817.
- Schumacher, T.N., and Schreiber, R.D. (2015). Neoantigens in cancer immunotherapy. *Science* 348, 69–74.
- Shen, R., and Seshan, V.E. (2016). FACETS: allele-specific copy number and clonal heterogeneity analysis tool for high-throughput DNA sequencing. *Nucleic Acids Res.* 44, e131.
- Sims, J.S., Grinshpun, B., Feng, Y., Ung, T.H., Neira, J.A., Samanamud, J.L., Canoll, P., Shen, Y., Sims, P.A., and Bruce, J.N. (2016). Diversity and divergence of the glioma-infiltrating T-cell receptor repertoire. *Proc. Natl. Acad. Sci. USA* 113, E3529–E3537.
- Six, A., Mariotti-Ferrandiz, M.E., Chaara, W., Magadan, S., Pham, H.P., Lefranc, M.P., Mora, T., Thomas-Vaslin, V., Walczak, A.M., and Boudinot, P. (2013). The past, present, and future of immune repertoire biology - the rise of next-generation repertoire analysis. *Front. Immunol.* 4, 413.
- Snyder, A., Makarov, V., Merghoub, T., Yuan, J., Zaretsky, J.M., Desrichard, A., Walsh, L.A., Postow, M.A., Wong, P., Ho, T.S., et al. (2014). Genetic basis for clinical response to CTLA-4 blockade in melanoma. *N. Engl. J. Med.* 371, 2189–2199.
- Spranger, S., Spaapen, R.M., Zha, Y., Williams, J., Meng, Y., Ha, T.T., and Gajewski, T.F. (2013). Up-regulation of PD-L1, IDO, and T(regs) in the melanoma tumor microenvironment is driven by CD8(+) T cells. *Sci. Transl. Med.* 5, 200ra116.
- Spranger, S., Bao, R., and Gajewski, T.F. (2015). Melanoma-intrinsic β -catenin signalling prevents anti-tumour immunity. *Nature* 523, 231–235.
- Sweis, R.F., Spranger, S., Bao, R., Paner, G.P., Stadler, W.M., Steinberg, G., and Gajewski, T.F. (2016). Molecular drivers of the non-T-cell-inflamed tumor microenvironment in urothelial bladder cancer. *Cancer Immunol. Res.* 4, 563–568.
- Taube, J.M., Anders, R.A., Young, G.D., Xu, H., Sharma, R., McMiller, T.L., Chen, S., Klein, A.P., Pardoll, D.M., Topalian, S.L., and Chen, L. (2012). Colocalization of inflammatory response with B7-h1 expression in human melanocytic lesions supports an adaptive resistance mechanism of immune escape. *Sci. Transl. Med.* 4, 127ra37.
- Taube, J.M., Young, G.D., McMiller, T.L., Chen, S., Salas, J.T., Pritchard, T.S., Xu, H., Meeker, A.K., Fan, J., Cheadle, C., et al. (2015). Differential expression of immune-regulatory genes associated with PD-L1 display in melanoma: implications for PD-1 pathway blockade. *Clin. Cancer Res.* 21, 3969–3976.
- Topalian, S.L., Hodi, F.S., Brahmer, J.R., Gettinger, S.N., Smith, D.C., McDermott, D.F., Powderly, J.D., Carvajal, R.D., Sosman, J.A., Atkins, M.B., et al. (2012). Safety, activity, and immune correlates of anti-PD-1 antibody in cancer. *N. Engl. J. Med.* 366, 2443–2454.
- Topalian, S.L., Taube, J.M., Anders, R.A., and Pardoll, D.M. (2016). Mechanism-driven biomarkers to guide immune checkpoint blockade in cancer therapy. *Nat. Rev. Cancer* 16, 275–287.
- Tumeh, P.C., Harview, C.L., Yearley, J.H., Shintaku, I.P., Taylor, E.J., Robert, L., Chmielowski, B., Spasic, M., Henry, G., Ciobanu, V., et al. (2014). PD-1 blockade induces responses by inhibiting adaptive immune resistance. *Nature* 515, 568–571.

- Van Allen, E.M., Miao, D., Schilling, B., Shukla, S.A., Blank, C., Zimmer, L., Sucker, A., Hillen, U., Foppen, M.H.G., Goldinger, S.M., et al. (2015). Genomic correlates of response to CTLA-4 blockade in metastatic melanoma. *Science* *350*, 207–211.
- Verdegaal, E.M., de Miranda, N.F., Visser, M., Harryvan, T., van Buuren, M.M., Andersen, R.S., Hadrup, S.R., van der Minne, C.E., Schotte, R., Spits, H., et al. (2016). Neoantigen landscape dynamics during human melanoma-T cell interactions. *Nature* *536*, 91–95.
- Wang, J., Cazzato, E., Ladewig, E., Frattini, V., Rosenbloom, D.I., Zairis, S., Abate, F., Liu, Z., Elliott, O., Shin, Y.J., et al. (2016). Clonal evolution of glioblastoma under therapy. *Nat. Genet.* *48*, 768–776.
- Weber, J., Horak, C., Hodi, F.S., Chang, H., Woods, D., Sanders, C., Robins, H., and Yusko, E. (2016a). Baseline tumor T cell receptor (TCR) sequencing analysis and neo antigen load is associated with benefit in melanoma patients receiving sequential nivolumab and ipilimumab. *Ann. Oncol.* *27*, 10470.
- Weber, J., Gibney, G., Kudchadkar, R., Yu, B., Cheng, P., Martinez, A.J., Kroeger, J., Richards, A., McCormick, L., Moberg, V., et al. (2016b). Phase I/II study of metastatic melanoma patients treated with nivolumab who had progressed after ipilimumab. *Cancer Immunol. Res.* *4*, 345–353.
- Wei, L., Liu, L.T., Conroy, J.R., Hu, Q., Conroy, J.M., Morrison, C.D., Johnson, C.S., Wang, J., and Liu, S. (2015). MAC: identifying and correcting annotation for multi-nucleotide variations. *BMC Genomics* *16*, 569.
- Wolchok, J.D., Hoos, A., O'Day, S., Weber, J.S., Hamid, O., Lebbé, C., Maio, M., Binder, M., Bohnsack, O., Nichol, G., et al. (2009). Guidelines for the evaluation of immune therapy activity in solid tumors: immune-related response criteria. *Clin. Cancer Res.* *15*, 7412–7420.
- Yau, C. (2013). OncoSNP-SEQ: a statistical approach for the identification of somatic copy number alterations from next-generation sequencing of cancer genomes. *Bioinformatics* *29*, 2482–2484.
- Yoshihara, K., Shahmoradgoli, M., Martínez, E., Vegesna, R., Kim, H., Torres-García, W., Treviño, V., Shen, H., Laird, P.W., Levine, D.A., et al. (2013). Inferring tumour purity and stromal and immune cell admixture from expression data. *Nat. Commun.* *4*, 2612.
- Yu, G., Wang, L.G., Han, Y., and He, Q.Y. (2012). clusterProfiler: an R package for comparing biological themes among gene clusters. *OMICS* *16*, 284–287.
- Zaretsky, J.M., Garcia-Diaz, A., Shin, D.S., Escuin-Ordinas, H., Hugo, W., Hu-Lieskovan, S., Torrejon, D.Y., Abril-Rodriguez, G., Sandoval, S., Barthly, L., et al. (2016). Mutations associated with acquired resistance to PD-1 blockade in melanoma. *N. Engl. J. Med.* *375*, 819–829.
- Zarnitsyna, V.I., Evavold, B.D., Schoettle, L.N., Blattman, J.N., and Antia, R. (2013). Estimating the diversity, completeness, and cross-reactivity of the T cell repertoire. *Front. Immunol.* *4*, 485.

Inactivation of Interferon Receptor Promotes the Establishment of Immune Privileged Tumor Microenvironment

Kanstantsin V. Katlinski,^{1,7} Jun Gui,^{1,7} Yuliya V. Katlinskaya,¹ Angelica Ortiz,¹ Riddhita Chakraborty,¹ Sabyasachi Bhattacharya,¹ Christopher J. Carbone,¹ Daniel P. Beiting,² Melanie A. Gironde,³ Amy R. Peck,³ Ellen Puré,¹ Priya Chatterji,⁴ Anil K. Rustgi,⁴ J. Alan Diehl,⁵ Constantinos Koumenis,⁶ Hallgeir Rui,³ and Serge Y. Fuchs^{1,8,*}

¹Department of Biomedical Sciences, Mari Lowe Center for Comparative Oncology, School of Veterinary Medicine, University of Pennsylvania, Philadelphia, PA 19104, USA

²Department of Pathobiology, School of Veterinary Medicine, University of Pennsylvania, Philadelphia, PA 19104, USA

³Department of Pathology, Medical College of Wisconsin, Milwaukee, WI 53226, USA

⁴Division of Gastroenterology, Department of Medicine, Perelman School of Medicine, University of Pennsylvania, Philadelphia, PA 19104, USA

⁵Department of Biochemistry, Hollings Cancer Center, Medical University of South Carolina, Charleston, SC 29425, USA

⁶Department of Radiation Oncology, Perelman School of Medicine, University of Pennsylvania, Philadelphia, PA 19104, USA

⁷Co-first author

⁸Lead Contact

*Correspondence: syfuchs@upenn.edu

<http://dx.doi.org/10.1016/j.ccell.2017.01.004>

SUMMARY

Refractoriness of solid tumors, including colorectal cancers (CRCs), to immunotherapies is attributed to the immunosuppressive tumor microenvironment that protects malignant cells from cytotoxic T lymphocytes (CTLs). We found that downregulation of the type I interferon receptor chain IFNAR1 occurs in human CRC and mouse models of CRC. Downregulation of IFNAR1 in tumor stroma stimulated CRC development and growth, played a key role in formation of the immune-privileged niche, and predicted poor prognosis in human CRC patients. Genetic stabilization of IFNAR1 improved CTL survival and increased the efficacy of the chimeric antigen receptor T cell transfer and PD-1 inhibition. Likewise, pharmacologic stabilization of IFNAR1 suppressed tumor growth providing the rationale for upregulating IFNAR1 to improve anti-cancer therapies.

INTRODUCTION

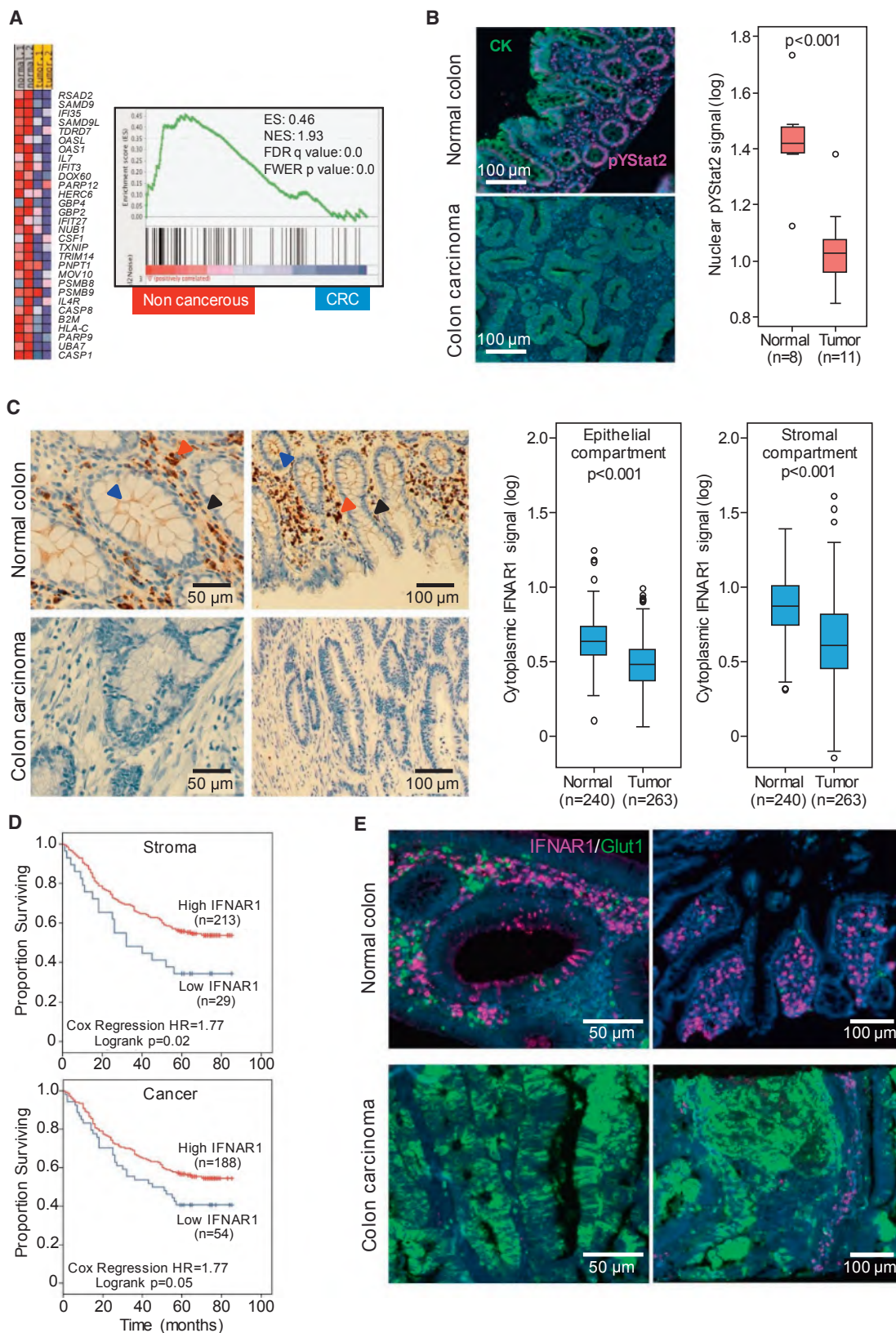
The presence of tumor-specific T cells in the blood of cancer patients, the “Hellström paradox” (Hellström et al., 1968), suggests that, although developing cancers are able to induce a comprehensive immune response, tumors can progress by hindering anti-tumor effector cells (Klemm and Joyce, 2015; Quail and Joyce, 2013). However, recent success in cancer immunotherapy indicates that augmentation of the immune response can improve prognosis. As such, current approaches

to cancer immunotherapy focus on increasing either tumor antigen presentation (via vaccines) or the number of tumor-specific CD8⁺ cytotoxic T lymphocytes (CTLs) (via chimeric antigen receptors [CARs] therapy and other types of adoptive transfer) or enhancing CTL activities (via checkpoint inhibition; reviewed in Rosenberg and Restifo, 2015; Sharma and Allison, 2015).

Regrettably, the majority of patients with solid tumors, including colorectal cancers (CRCs), are refractory to these treatments (Brahmer et al., 2012; Gilham et al., 2012; Topalian

Significance

Understanding the mechanisms by which solid tumors suppress anti-tumor immunity is critical for success of immune therapies. Here we demonstrate that tumor microenvironment factors-induced downregulation of type I interferon receptor IFNAR1 is a central mechanism underlying the ability of the tumor microenvironment to undermine the viability of cytotoxic T cells and to generate intra-tumoral immune-privileged niches devoid of these cells. Means to prevent the loss of IFNAR1 eliminate these niches, inhibit tumor growth, and increase the efficacy of immunotherapies utilizing checkpoint inhibitors or chimeric antigen receptor T cells. These findings delineate a mechanism of localized intra-tumoral immune suppression and prompt the development of IFNAR1-stabilizing agents for use in anti-cancer immune therapies.



(legend on next page)

et al., 2012). Solid tumors evade anti-cancer immune control by establishing immune-privileged niches within the tumor micro-environment (TME). Diverse cellular and acellular (e.g., deficit of oxygen and nutrients) TME elements reduce proliferation, viability, or activity of intra-tumoral CTLs thereby inhibiting their anti-tumor effector function (Fearon, 2014; Joyce and Fearon, 2015; Zhou et al., 2014). Indeed, the apparent exclusion of CTLs from CRC is associated with a poor prognosis (Chiba et al., 2004; Galon et al., 2006; Naito et al., 1998) while, conversely, increased accumulation of CTLs within tumors is associated with a favorable outcome (Talmadge et al., 2007). Delineating the mechanisms that prevent CTL accumulation within the TME remains a major challenge in understanding the immunosuppressive properties of the TME and increase the efficacy of immunotherapies (Joyce and Fearon, 2015).

Studies modeling sarcomas and melanomas in mice lacking the IFNAR1 chain of type I interferon (IFN) receptor suggest that endogenous IFNs contribute to anti-tumor immunity via stimulating specific CD8 α^+ lineage dendritic cells (DCs) to cross-present antigen to CTLs (Diamond et al., 2011; Fuertes et al., 2011; Hildner et al., 2008). IFNs also provide a “third signal” to stimulate the clonal expansion of CD8 $^+$ T cells (Aichele et al., 2006; Curtsinger et al., 2005; Hervas-Stubbs et al., 2010) and increase the viability of activated anti-viral CD8 $^+$ T lymphocytes (Crouse et al., 2014; Kolumam et al., 2005; Wang et al., 2012; Xu et al., 2014) and tumor-specific CTLs (Hiroishi et al., 2000). These reports are consistent with the long-known anti-tumorigenic effects of IFN (Platanias, 2005; Trinchieri, 2010; Zitvogel et al., 2015). Nevertheless, given that tumorigenesis readily proceeds in IFNAR1-competent mice and humans, it is apparent that cancers manage to overcome the effects of endogenous IFN through a poorly understood mechanism.

Cell surface IFNAR1 levels are critical for all IFN effects (Fuchs, 2013; Uze et al., 2007). These levels are controlled by IFNAR1 ubiquitination and degradation facilitated by the SCF- β Trcp E3 ligase, which binds to IFNAR1 phosphorylated on Ser535 (Ser526) in mouse IFNAR1; (Kumar et al., 2003). Phosphorylation of these serine residues can be triggered in vitro by stimuli characteristic for the TME such as unfolded protein response (Liu et al., 2009), oxygen or nutrient deficit (Bhattacharya et al., 2013), vascular endothelial growth factor (Zheng et al., 2011), and inflammatory cytokines (Huangfu et al., 2012). Here we aimed to characterize the status of IFNAR1 and IFN signaling in CRC tumors and to determine the importance of IFNAR1 downregulation in establishing the intra-tumoral immune-privileged niche.

RESULTS

IFNAR1 Levels and Signaling Are Reduced in the TME

Global expression profiling within hypoxic areas of transplanted tumors revealed a decrease in expression of the immune response genes (Marotta et al., 2011). We also noted a suppression of the IFN-signaling signature in hypoxic tumor areas characterized by TME stress (Figures S1A and S1B). Importantly, mining of datasets from patients with CRC (Rohr et al., 2013) revealed a decrease in IFN-induced gene expression in tumors compared with benign colorectal tissues from the same patients (Figure 1A). In addition, compared with normal colorectal tissues, tumors exhibited markedly decreased levels of nuclear phosphorylated STAT2 (Figure 1B), which is a downstream effector of IFN signaling (Platanias, 2005). These results suggest that IFN signaling is inhibited in human CRC tumors.

TME-associated stress stimuli such as nutrient/oxygen deficit can cause a loss of IFNAR1 protein in vitro (Bhattacharya et al., 2013). Although comparable *IFNAR1* mRNA expression was reported in CRC and normal colorectal tissues (Rohr et al., 2013), we noted dramatic differences in IFNAR1 protein levels. IFNAR1 was detected in all normal human colon cell types including epithelial cells (especially at their apical surface), stromal fibroblasts, and infiltrating immune cells. However, all cell types within human colorectal adenocarcinomas exhibited partial or complete loss of IFNAR1 (Figures 1C and S1C). For these samples, IFNAR1 levels in the cancer cell compartment and in the stromal compartment positively correlated ($r = 0.700$, $p < 0.001$; $n = 263$). Importantly, downregulation of IFNAR1 in either stromal or cancer cell compartments of human CRC tumors were associated with poor prognosis (Figure 1D). Furthermore, whereas many cells expressed high levels of IFNAR1 in normal human colon, those few IFNAR1-positive cells found in colon carcinomas were spatially segregated from the tumor areas, which were positive for GLUT1, a marker of TME stress (Figures 1E and S1D). These data collectively suggest that TME conditions in human CRC prompt IFNAR1 downregulation and suppress IFN signaling.

Downregulation of IFNAR1 in the Stromal Compartment Stimulates Colorectal Tumorigenesis

Guided by these data in human patients, we sought to determine the role of partial loss of IFNAR1 using murine CRC models. Notably, downregulation of IFNAR1 protein observed in human CRC (Figure 1C) was faithfully recapitulated in the mouse model of inflammatory colorectal carcinogenesis induced by treatment with azoxymethane and dextran sodium sulfate (AOM-DSS). The

Figure 1. IFNAR1 Levels and Signaling Are Reduced in Colorectal Adenocarcinomas

(A) Heatmap and gene set enrichment analysis (GSEA) of IFN signaling pathway genes of the transcriptome profiles of human normal colon and matched CRC tissues (from Rohr et al., 2013). ES, enrichment score; NES, non-enrichment score; FDR, false discovery rate; FWER, family-wise error rate.

(B) Representative immunofluorescent analysis of phospho-Tyr-STAT2 (red) and pan-cytokeratin (CK, green) in normal and malignant colon tissues counterstained with DAPI (blue). Boxplot showing nuclear pTyr-Stat2 levels in representative normal ($n = 8$) and cancer ($n = 11$) cases indicates median (dark line), 25%–75% range (box), minimum and maximum values (whiskers), and individual scatterplot values (circles) overlaying the boxplot.

(C) Representative chromogen immunohistochemistry analysis of IFNAR1 in normal and malignant colon. Arrows point to IFNAR1-positive fibroblasts (black), epithelial cells (blue), and immune cells (red). Boxplots as in (B) show cytoplasmic IFNAR1 expression levels in the epithelial (left) or stromal (right) compartments of malignant colon and adjacent normal tissue.

(D) Kaplan-Meier plot of cases of colorectal adenocarcinomas based on levels of cytoplasmic IFNAR1.

(E) IFNAR1 (red)- and GLUT1 (green)-positive cells in normal and malignant human colon tissues. See also Figure S1.

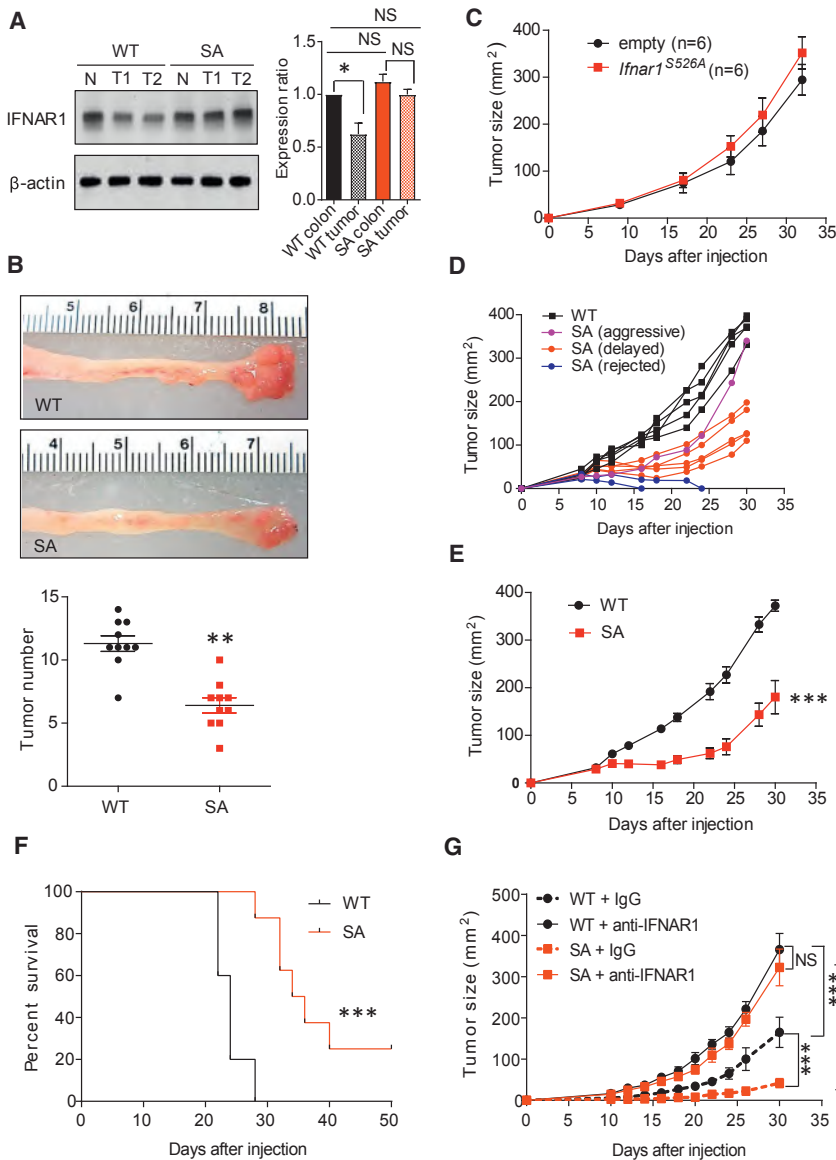


Figure 2. Downregulation of IFNAR1 in the Stromal Compartment Stimulates Colorectal Tumorigenesis

(A) Immunoblot analysis of IFNAR1 immunoprecipitated from the whole-tissue lysates prepared from normal colon or AOM-DSS-induced tumors from WT and SA mice. The IFNAR1/ β -actin (loading control) signal relative ratios calculated from six mice for each group (WT colon taken as 1.0 and shown as mean \pm SD) are depicted on the right. Henceforth asterisks: * p < 0.05; ** p < 0.01; *** p < 0.001. NS, not significant.

(B) Representative images and quantification of colorectal tumors in mice of indicated genotypes at day 70 after treatment with AOM-DSS.

(C) Growth of MC38mRFP cells that received GFP or IFNAR1^{S526A}-GFP constructs after subcutaneous injection into WT mice (mean \pm SEM, n = 6).

(D) Subcutaneous growth of individual MC38 tumors in WT and SA mice.

(E) A representative experiment demonstrating the average size of MC38 tumors growing in WT (n = 5) and SA (n = 8) mice (mean \pm SEM).

(F) Kaplan-Meier analysis of the survival of MC38 tumor-bearing WT and SA mice from (E).

(G) Effect of anti-IFNAR1 neutralizing antibodies on MC38 tumor growth in WT and SA mice (mean \pm SEM, n = 5–6 for each of two experiments).

See also Figure S2.

observed decrease in levels of IFNAR1 protein (Figures 2A and S2A) but not *Ifnar1* mRNA (Figure S2B) in AOM-DSS-induced colorectal tumors suggested an increased IFNAR1 degradation within tumors. Therefore, we next used *Ifnar1*^{S526A} mice (henceforth “SA”), previously shown to be deficient in IFNAR1 ubiquitination and degradation (Bhattacharya et al., 2014). SA mice treated with AOM-DSS sustained high levels of IFNAR1 protein (Figures 2A and S2A) and mRNA for IFN-stimulated and inflammatory genes (Figure S2C) relative to wild-type (WT) mice. Importantly, AOM-DSS treatment induced fewer tumors in SA mice (Figure 2B), indicating that downregulation of IFNAR1 contributes to efficient colorectal tumorigenesis.

In a transplantation model, tumors formed in WT mice by MC38 colon adenocarcinoma cells expressed lower levels of IFNAR1 compared with these cells cultured in vitro (Figure S2D), demonstrating that the MC38 tumor model re-capitulates the IFNAR1 loss observed in human CRC. To determine the impor-

tance of IFNAR1 downregulation in the malignant cell compartment, we next aimed to restore IFNAR1 levels in MC38 cancer cells. Previous studies in fibrosarcomas and mammary adenocarcinomas demonstrated a tumor-suppressive effect of the IFN signaling in malignant cells (Bidwell et al., 2012; Sistigu et al., 2014). We also reported that expression of the *Ifnar1*^{S526A} allele in *Ifnar1*-null mouse melanoma cell line delays growth of these tumors (Katlinskaya et al., 2016). However, expression of the *Ifnar1*^{S526A} allele

in MC38mRFP cells did not affect their ability to form tumors in WT mice (Figures 2C, S2E, and S2F), indicating that the cell-autonomous anti-tumorigenic effects of IFNAR1 expression and IFN signaling might be cell or tumor type specific.

To determine the role of IFNAR1 downregulation in the stromal compartment, we inoculated WT or SA mice with MC38 cells (Figure S2G). While WT mice readily supported tumor growth, very few of MC38 tumors grew aggressively in SA mice (Figure 2D). Notably, most of these tumors were either rejected or exhibited a delayed growth (Figures 2D, 2E, and S2H) resulting in a prolonged survival (Figure 2F) in SA mice, suggesting an important role of downregulation of stromal IFNAR1 in tumorigenesis. Indeed, injection of IFNAR1-neutralizing antibodies further stimulated MC38 tumor growth in WT mice and dramatically rescued tumor growth in SA hosts (Figure 2G). These results indicate that efficient tumor growth requires downregulation of IFNAR1 levels primarily in the non-malignant cells.

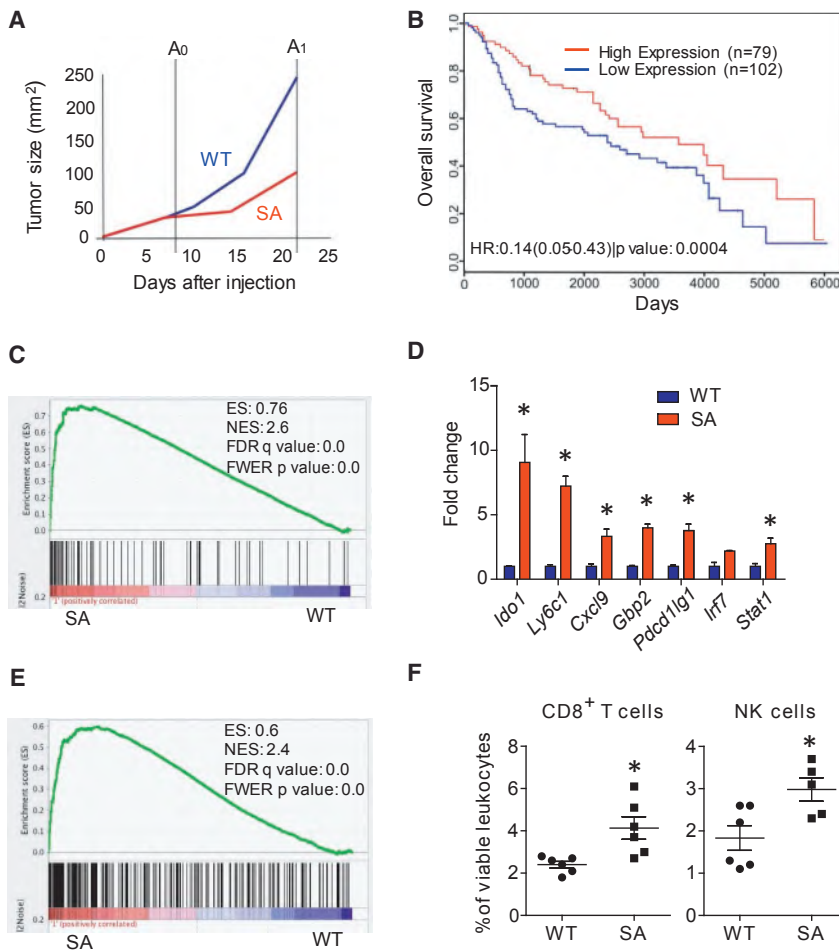


Figure 3. Alterations of Gene Expression Associated with IFNAR1 Downregulation Correlate with Local Immunosuppression and with a Poor Prognosis in CRC Patients

(A) Schematic representation of MC38 tumor growth in WT and SA mice. Time points of harvesting tumors of comparable (A0) and disparate (A1) size are indicated.

(B) Survival of adjusted for stage CRC patients (GEO: GSE41258) harboring the expression pattern of 30 selected genes similar to MC38 that grew either in WT (blue) or in SA (red) mice.

(C) GSEA results of the IFN- α/β signaling pathway in tumors harvested at day 9 (time point A0) and used for RNA isolation and microarray analysis.

(D) qPCR analysis of the indicated genes expressed in WT and SA tumors.

(E) GSEA results for the immune system process in tumors harvested at A0.

(F) Percent of NK and CD8⁺ T cells (relative to CD45⁺ cells) infiltrating MC38 tumors in WT and SA mice.

Data are shown as mean \pm SEM from five to six tumors.

See also Figure S3 and Table S1.

Alterations of Gene Expression Associated with IFNAR1 Downregulation Correlate with Local Immunosuppression and Poor Prognosis in CRC Patients

We next profiled the gene expression associated with IFNAR1 downregulation (in tumors with WT stroma) or stabilized IFNAR1 (in tumors with SA stroma). Notably, at an early time point after MC38 transplantation (A0, Figure 3A), the stromal compartments from tumors of comparable size that arose in WT or SA mice already differed in their gene expression patterns (Table S1). While most of differentially expressed genes (e.g., *Irf7*, *Ifit2*, *Mx2*, *Usp18*, etc.) are well known to be induced by IFN, others (*Clec7a*, *Sdc3*) have not been previously reported as bona fide IFN-regulated genes in global expression studies (Mostafaei et al., 2016; Rusinova et al., 2013), suggesting that downregulation of IFNAR1 in the context of a growing tumor may elicit a more complex response than merely an IFN-signaling suppression. Specifically, the status of a set of 30 genes whose expression was increased in the stroma of early mouse SA tumors compared with WT ones (Table S1) was associated with impaired tumor progression in SA mice (Figures 2D, 2E, and S2H).

More importantly, this gene expression profile was also predictive of a better prognosis in two separate stage-adjusted co-

hort of human CRC patients (Figures 3B and S3A). Furthermore, dramatic suppression of the IFN-induced genes (Figures 3C and 3D) correlated with subsequent aggressive tumor growth (Figure 2D) was seen in early WT (but not SA) tumors. These data suggest that IFNAR1 downregulation and the ensuing alterations in gene expression contribute to CRC progression and appear to be predictive of disease outcome in human CRC patients.

Additional comparison of WT and SA gene expression patterns revealed a suppressed immune pathway in early WT tumors (Figures 3D and 3E) pointing to the immune system as a putative target of IFNAR1 downregulation. At later time points, when tumors in WT mice became larger than tumors in SA mice (A1, Figure 3A), we noted a similar suppression of IFN signaling and in the signature of immune genes in WT tumors (Figures S3B and S3C). These results indicate that decreased IFNAR1 levels in the stromal compartment may determine both the immunosuppressive capacity and growth potential of the tumor.

Prompted by gene expression data we assessed the levels of immune cells in WT and SA mice burdened with MC38 tumors. Compared with SA mice, spleens from WT mice contained somewhat greater overall levels of CD11b⁺Ly6G⁺ cells; however, we did not detect significant differences in the frequencies of splenic natural killer (NK) cells or T cells (Figure S3D) that would be characteristic of generalized immunosuppression in tumor-bearing WT animals. Conversely, analysis of tumor-infiltrating leukocyte subsets revealed significantly reduced frequencies of CD8⁺ T cells, NK cells, and Ly6C^{hi}Ly6G⁻ cells in tumors from WT animals compared with tumors from SA mice (Figures 3F and S3E). This result indicates that downregulation of IFNAR1 within WT tumors is associated with a localized intra-tumoral

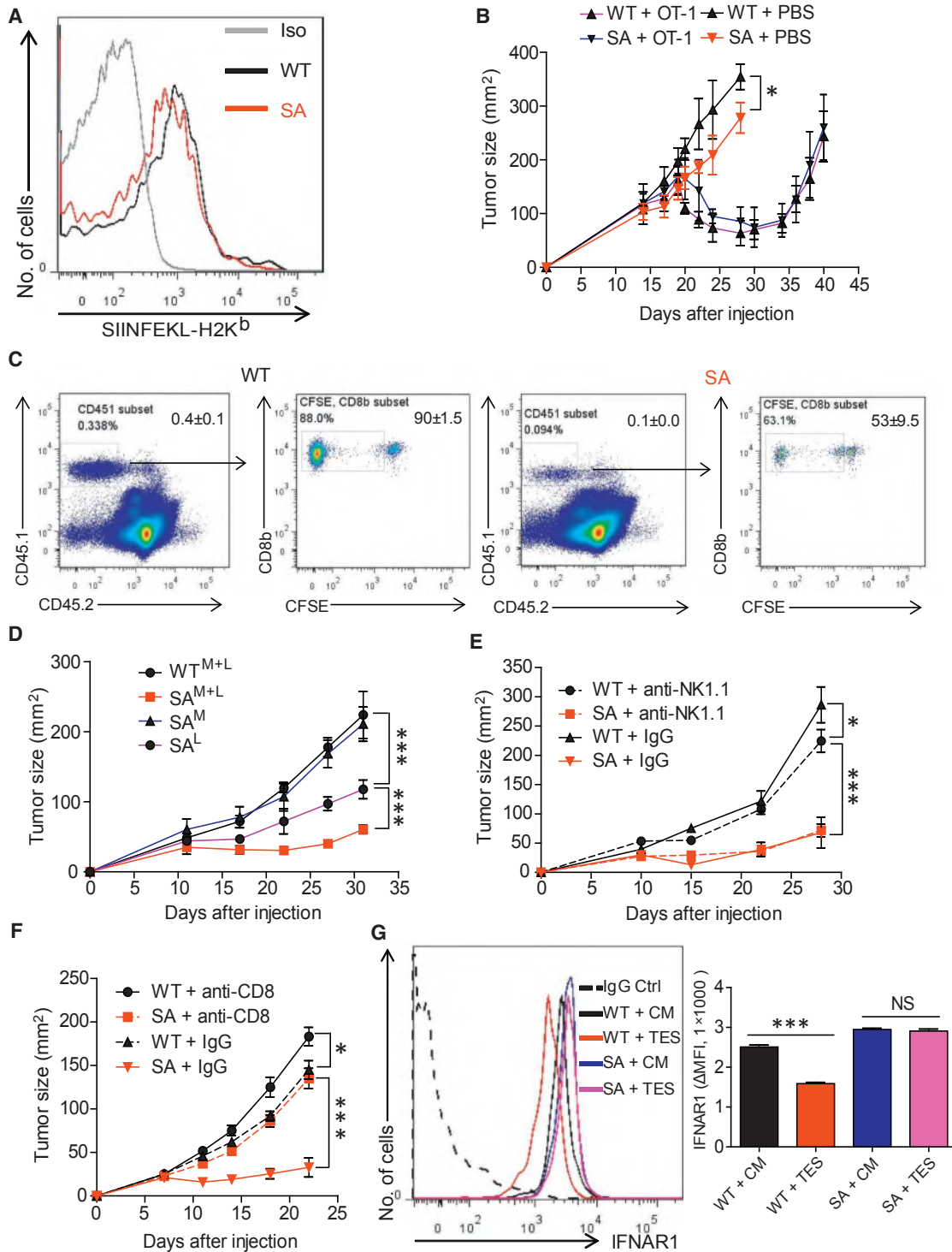


Figure 4. Downregulation of IFNAR1 on CTLs Promotes Tumor Growth

(A) Representative fluorescence-activated cell sorting (FACS) analysis of levels of MHC-I-complexed OVA peptide on the surface of intra-tumoral CD45⁺MHC-II⁺CD103⁺CD11c⁺ DCs isolated from the MC38OVA tumors grown in *Rag1*^{-/-} mice harboring WT or SA IFNAR1.

(B) Growth of MC38-OVA tumors in *Rag1*^{-/-} mice harboring WT or SA IFNAR1 after adoptive transfer of WT OT-1 T cells injected on day 18 after tumor inoculation.

(C) Representative flow cytometry analysis of the percentage (left panels) and proliferation (right panels) of CD8⁺CD45.1⁺ at day 7 in the spleens from WT and SA mice after adoptive transfer of naive carboxyfluorescein succinimidyl ester (CFSE)-labeled OT-1 T cells at day 0 and subsequent challenge with MC38OVA cells at day 1.

(legend continued on next page)

immunosuppression, resulting in reduced CTL accumulation within the TME.

Downregulation of IFNAR1 in CTLs Contributes to Development of the Immunosuppressive TME in CRC

Previous studies of sarcomas and melanomas grown in WT or *Ifnar1* knockout mice suggested a critical role of IFN in the ability of specific CD8 α ⁺ lineage DCs to cross-present antigen to the CD8⁺ cytotoxic lymphocytes and highlighted the critical role of these DCs in anti-tumor immune protection (Diamond et al., 2011; Fuertes et al., 2011; Hildner et al., 2008). We did not observe changes in the overall frequency of intra-tumoral CD11b⁺ CD11c⁺ MHC-II⁺ CD103⁻, CD11c⁺ MHC-II⁺ CD8 α ⁺, or CD11c⁺ MHC-II⁺ CD103⁺ DCs between MC38 tumors that grew in WT and SA mice (Figure S3E). DCs isolated from WT or SA mice exhibited a similar efficacy in direct antigen presentation (Figure S4A) as well as in cross-presentation of tumor antigens (Figure S4B), indicating that reduced tumorigenesis in SA mice cannot be readily explained by an increased antigen presentation capacity.

We next transplanted MC38 tumor cells ectopically expressing ovalbumin (OVA) (MC38OVA) into immune-deficient *Rag1*^{-/-} mice that harbored either WT or SA IFNAR1. Dendritic cells (CD45⁺ MHC-II⁺CD103⁺ CD11c⁺) isolated from either WT or SA tumors presented comparable levels of MHC-I-complexed OVA peptide (Figure 4A). Consistent with these data, adoptive transfer of WT OVA-specific OT-1 CTLs into these *Rag1*^{-/-} mice resulted in an initial decrease in tumor volume (followed by subsequent re-growth of tumors) regardless of IFNAR1 status (Figure 4B).

We next injected WT or SA mice with naive OT-1 T cells followed by challenge with MC38OVA and subsequent assessment of numbers and proliferation of splenic OT-1 CD8⁺ T cells 6 days later. Under these conditions, even less CTL proliferation was seen in the SA hosts compared with WT mice (Figure 4C), further indicating that the tumor growth defect observed in SA mice is unlikely to depend on increased antigen presentation by SA DCs.

We next generated mixed bone marrow chimeras in which myeloid and/or lymphoid cells from either WT or SA animals were used to reconstitute bone marrow in lethally irradiated WT mice (Diamond et al., 2011). These chimeric mice harbored comparable numbers of myeloid and lymphoid cells and the expected IFNAR1 levels on these cells in the spleen (Figure S4C). A dramatic suppression of MC38 tumor growth observed in chimeras that received both lymphoid and myeloid cells from SA donors ("SA^{M+L}," Figures 4D and S4D) was indicative of the critical importance of IFNAR1 downregulation in the bone marrow-derived cells. Relative to this group, only a slight acceleration of tumorigenesis was seen in mice that received WT myeloid cells and SA lymphocytes ("SA^L"). This result indicates that, while

there is a role for IFNAR1 expressed on myeloid cells, maintaining the levels of IFNAR1 on lymphocytes appears to be critical for tumor growth suppression.

Indeed, while depletion of NK cells in SA mice did not alter growth of MC38 tumors (Figures 4E and S4E), depletion of CD8⁺ cells notably stimulated tumor growth in SA animals (Figures 4F and S4F). We next sought to determine whether IFNAR1 can be downregulated specifically on the intra-tumoral CD8⁺ T cells. Incubation of WT (but not SA) CD8⁺ T cells with the tumor explant supernatant (Figure 4G) or MC38 cell-conditioned medium (Figure S4G) robustly downregulated IFNAR1 cell surface levels. Together with notably lower levels of IFNAR1 on the surface of CD3⁺CD8⁺ WT (but not SA) cells isolated from tumors compared with those isolated from spleens (Figure S4H), these data suggest that tumor conditions trigger downregulation of IFNAR1 on the surface of CTLs and that this downregulation contributes to aggressive tumorigenesis.

The majority of cells expressing high levels of IFNAR1 in normal human colon were CD3⁺ cells (Figure S5A). Importantly, in human CRC tissues, most IFNAR1-positive T lymphocytes were peripheral to the tumor and very few of them were found inside human tumors (Figures 5A and S5B). Whereas these low numbers of CTLs found in human CRC could be recapitulated in MC38 tumors grown in WT mice, a greater absolute and relative number of the CD3⁺CD8⁺ CTLs was found within tumors developed in SA animals (Figures 3F and 5B). Consistent with this result, mouse SA tumors exhibited a prominent T cell gene expression signature (Figure 5C) and particularly high levels of mRNA of genes indicative of T cell effector function including *Ifng* and *Gzmb* (Figure S5C), as well as increased levels of IFN- γ and granzyme B proteins in MC38 tumor lysates (Figure S5D). Likewise, greater levels of *Ifng* mRNA expression were also observed in SA tumors induced by AOM-DSS treatment compared with WT tumors (Figure S2C). These results suggest that reduced accumulation of CTLs (indicative of immune-privileged niche) in CRC is associated with IFNAR1 downregulation.

Accordingly, studies involving adoptive transfer of CD8⁺ T cells into *Rag1*^{-/-} mice burdened with MC38OVA tumors revealed a greater intra-tumoral accumulation of CTLs derived from SA OT-1 mice compared with CTLs from WT OT-1 animals (Figure 5D). These results suggest that the status of IFNAR1 on CTLs determines their ability to accumulate within tumors. These findings in human and mouse tumors collectively indicate that the IFNAR1 downregulation on CTLs that occurs within CRC tumors prevents CTL accumulation, thereby establishing a local immune-privileged TME.

Given that little, if any, difference was detected in proliferation of SA and WT CD8⁺ T lymphocytes activated in vitro (Figure S5E) or isolated from tumor-bearing mice (Figure S5F), we next focused on other mechanisms that could explain preferential

(D) Growth of MC38 tumors in *Rag1*^{-/-} mice that received bone marrow containing WT or SA myeloid and lymphoid cells (WT^{M+L} and SA^{M+L}), WT myeloid and SA lymphoid cells (SA^L), or WT lymphoid and SA myeloid cells (SA^M).

(E) MC38 tumor growth in WT or SA mice treated with anti-NK.1.1 or immunoglobulin G (IgG) control antibodies.

(F) MC38 tumor growth in WT or SA mice treated with anti-CD8 or IgG control antibodies.

(G) Representative FACS analysis and quantification (n = 4, each in triplicate) of IFNAR1 levels on the surface of CD3⁺ CD8⁺ cells isolated from WT or SA spleens and incubated in vitro with control medium (CM) or tumor explant supernatant (TES) for 2 hr. NS, not significant.

Data depicted as mean \pm SEM (n = 4–6); similar results were obtained in at least two independent experiments.

See also Figure S4.

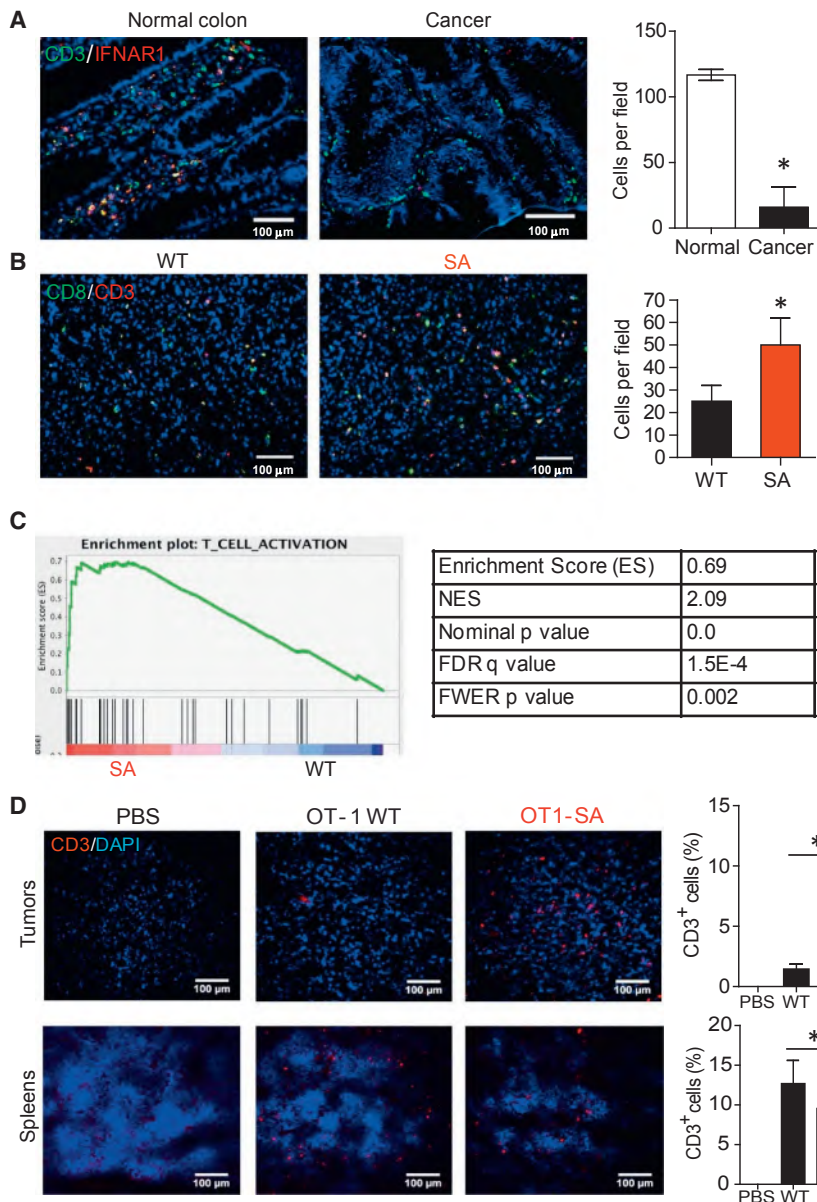


Figure 5. Downregulation of IFNAR1 in CTLs Contributes to Development of the Immunosuppressive Tumor Microenvironment in CRC

(A) Representative immunofluorescent analysis and quantification of IFNAR1^{hi}CD3⁺ T cell infiltration of human normal colon and CRC. Tissue sections were stained with antibodies against IFNAR1 (red) and CD3 (green) and contrasted with DAPI (blue). At least 20 randomly chosen fields from each of eight patient samples for each group were quantified.

(B) Representative immunofluorescent analysis and quantification of CD3⁺CD8⁺ T cell infiltration of MC38 tumors from WT and SA mice. Tumor sections were stained with anti-CD3 (red) and -CD8 (green) antibodies and contrasted with DAPI (blue). At least 20 randomly chosen fields from each of five tumor samples were quantified.

(C) GSEA results of the T cell activation gene signature in WT and SA tumors.

(D) Representative immunofluorescent analysis of T cells found in the spleens or MC38OVA tumors grown in *Rag1*^{-/-} mice after treating these mice with PBS or adoptive transfer of WT or SA OT-1 T cells (2×10^7 per mouse). Data are depicted as the percentage of CD3⁺ cells among all DAPI-stained cells and are representative of at least 20 random fields scored from tissues of four mice.

Data are shown as mean \pm SEM.

See also Figure S5.

CTL accumulation in tumors of SA mice. Cancer-associated fibroblasts positive for the fibroblast activation protein (FAP) produce CXCL12 chemokine that prevents intra-tumoral CTL buildup in a mouse pancreatic cancer model (Feig et al., 2013). Intriguingly, activated SA and WT CTLs exhibited a similar chemotaxis toward CXCL12 or CXCL9 (Figure S5G), suggesting that retaining IFN signaling may not necessarily increase the migratory abilities of CTLs.

Downregulation of IFNAR1 on CTLs Undermines Their Survival within the TME

IFN promotes survival of anti-viral CTLs by protecting them from killing by NK cells (Crouse et al., 2014; Xu et al., 2014). Depletion of NK cells in *Rag1*^{-/-} mice indeed increased the total number of transferred T cells but did not affect a greater viability of SA T cells compared with WT T cells (Figure S6). Given this result

and the observation that NK depletion did not alter tumorigenesis in either WT or SA mice (Figure 4E), we focused on other mechanisms by which downregulation of IFNAR1 may affect anti-tumor CTLs. Antigen-exposed SA CTLs cultured in vitro maintained greater levels of IFNAR1, the mRNA, and the protein levels for the anti-apoptotic regulator, B cell lymphoma-extra large (Bcl-XL), and lower levels of cleaved caspase-3 compared with WT CTLs (Figures 6A and S7A). Accordingly, a decrease in cell viability was more pronounced in WT cells than in SA cells under these conditions (Figure 6B). Importantly, while pre-treatment with interleukin-2 (IL-2) increased the viability of WT CTLs, neutralizing the IL-2 receptor using anti-CD25 antibody undermined the survival of SA CTLs (Figure 6B). We further found that SA CTLs produced notably more IL-2 (Figure S7B) and expressed greater levels of IL-2R α mRNA and protein compared with WT cells (Figures S7C and S7D). Thus, it is likely that downregulation of IFNAR1 promotes death of activated CTLs by attenuating the pro-survival effects of the IL-2 pathway.

Activated SA OT-1 CTLs exhibited greater viability than WT OT-1 CTLs when these cells were simultaneously injected in a 1:1 ratio intravenously or directly into the MC38OVA tumors grown in *Rag1*^{-/-} mice (Figures 6C and 6D). This result suggests that stabilization of IFNAR1 on antigen-specific CTLs improves their survival within the tumors. To further corroborate this possibility, we used the CAR-based approach that involved the

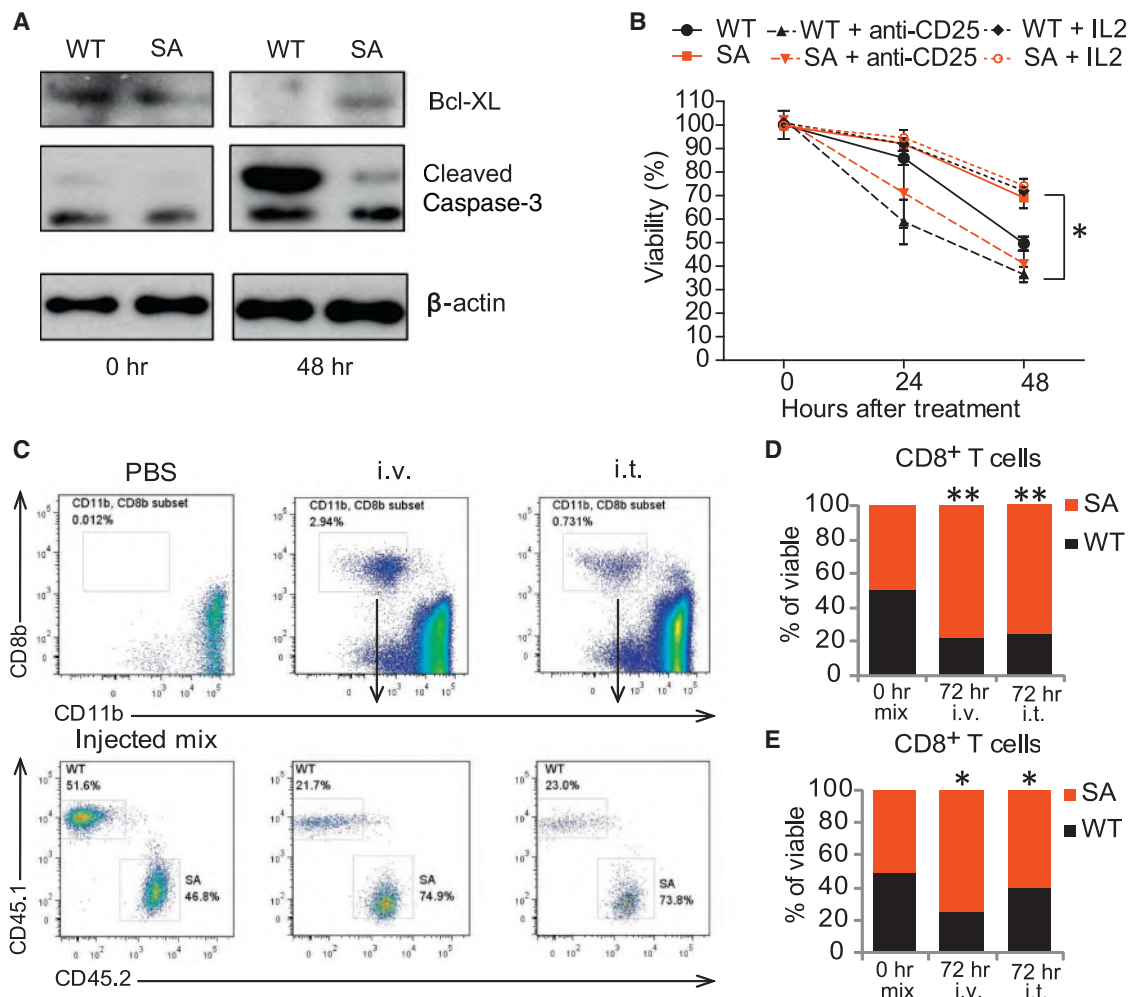


Figure 6. Downregulation of IFNAR1 on Cytotoxic T Lymphocytes Undermines their Survival within the TME

(A) Immunoblot analysis of Bcl-XL, cleaved caspase-3 levels, and β -actin (loading control) in splenocytes from WT and SA OT-1 mice activated with SIINFEKL peptide (0.5 μ g/mL for 48 hr) and then cultured for indicated times.

(B) Viability of activated CD3⁺CD8⁺ cells in the presence of medium supplemented or not with either IL-2 (100 U/mL) or anti-CD25 antibody (100 μ g/mL), as indicated, was determined by flow cytometry analysis after the indicated times. Mean \pm SD (triplicates per mouse spleen, average from three mice) are shown. Asterisks denote statistical significance ($p < 0.05$) between WT and SA, between WT and WT treated with IL-2, and between SA and SA treated with anti-CD25 antibody.

(C) Flow cytometry analysis of the fraction of viable OT-1 WT (CD45.1) or SA (CD45.2) CTLs in the MC38OVA tumors 72 hr after intravenous (i.v.) injection (1:1 ratio) or directly into the tumors (i.t.) of *Rag1*^{-/-} mice bearing MC38OVA tumors.

(D) Quantitation of the experiments shown in (C) (mean percentage of viable cells from tumors from three to five mice). Similar results were obtained in at least two independent experiments.

(E) Quantitation of flow cytometry analysis of the fraction of viable FAP-CAR EGFP⁺ WT (CD45.1) or EGFP⁺ SA (CD45.2) CTLs in the MC38 tumors 72 hr after i.v. injection (1:1 ratio) or directly into the tumors (i.t.) of WT MC38 tumor-bearing mice. Data are shown as the mean percentage of viable cells ($n = 5$). See also Figures S6 and S7.

introduction of the CAR against FAP (FAP-CAR [Wang et al., 2014]) into WT or SA CTLs. We generated FAP-CAR T cells separately from WT or SA lymphocytes, and then mixed these cells in equal parts prior to adoptive transfer (as a 1:1 mixture) into MC38 tumor-bearing WT mice (Figure S7E). Regardless of the route of administration (intra-tumoral or intravenous), a greater fraction of SA cells was found in the tumor 3 days later (Figures 6E and S7F). These results suggest that TME-induced downregulation of IFNAR1 on CTLs compromises the viability of these CTLs inside tumors.

Downregulation of IFNAR1 in CTLs Limits the Efficacy of Anti-cancer Therapies

We next examined the importance of IFNAR1 downregulation in modulating the efficacy of adoptive CTL transfer-based immunotherapy. Adoptive transfer of WT OT-1 lymphocytes into *Rag1*^{-/-} mice bearing MC38OVA tumors was much less efficient in sustained suppression of tumor growth and prolonging animal survival compared with SA OT-1 cells (Figures 7A and 7B). Furthermore, FAP-CAR CTLs prepared from SA cells exhibited a substantially greater therapeutic effect against MC38 tumors

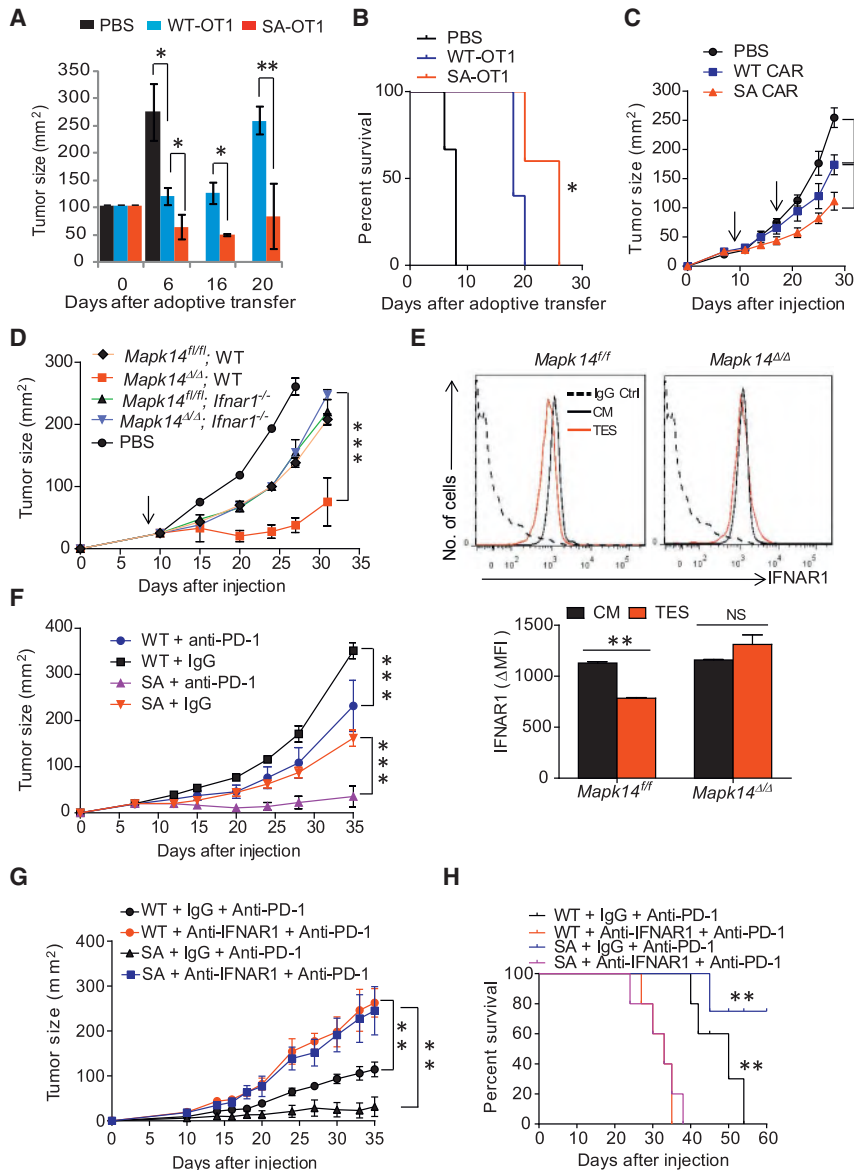


Figure 7. Downregulation of IFNAR1 in CTLs Limits the Efficacy of Immunotherapies

(A) Anti-tumor effects of adoptively transferred OT-1-SA and OT-1 WT T cells in MC38OVA tumor-bearing *Rag1*^{-/-} described in Figure 5D. (B) Kaplan-Meier analysis of survival of MC38 tumor-bearing mice from (A). (C) Anti-tumor effects of IFNAR1 WT and IFNAR1 SA FAP-CAR T cells (time of administration indicated by arrow) in MC38 tumor-bearing mice. (D) Growth of MC38 tumors in WT mice that received PBS or FAP-CAR T cells harboring indicated status of *Mapk14* and *Ifnar1* shown. (E) Cell surface IFNAR1 levels on CD3⁺CD8⁺ splenocytes of the indicated genotype treated with TES or CM for 2 hr. Representative FACS and quantitation (below) are shown. (F) Anti-tumor effect of anti-PD-1 antibody administration in WT mice and SA mice bearing MC38. (G) Effect of IFNAR1 neutralization on the efficacy of anti-PD-1 treatment of WT or SA mice bearing MC38 tumors. (H) Kaplan-Meier analysis of survival of MC38 tumor-bearing mice from (G). Data shown as mean \pm SEM (n = 3–5) from each of at least two to three independent experiments.

ablation of *Ifnar1*, suggesting that most (if not all) effects of p38 α deletion depend on sustained IFNAR1 signaling within CTLs (Figure 7D). Together with the inability of CTLs lacking p38 α to downregulate IFNAR1 in response to an in vitro treatment with the tumor explant supernatant (Figure 7E), these data provide genetic evidence suggesting that tumor-derived factors-induced p38 α -dependent downregulation of IFNAR1 on the surface of CTLs limits the efficacy of CAR-based therapeutics in solid tumors.

Intriguingly, a fraction of MC38 tumors that did not get rejected in SA mice eventually reached a larger size (A1, Figure 3A). Whereas SA tissues retained a greater immune response and robust IFN signatures, there was also a notable increase in expression of the PD-L1/CD274 checkpoint molecule (Figure S3C). Accordingly, treatment with the anti-PD-1 antibody at a dose that only slightly delayed MC38 tumor growth in WT mice caused a robust therapeutic effect leading to a stable disease in SA mice (Figure 7F). Importantly, anti-PD-1 therapy was notably less efficient in suppressing tumor growth (Figure 7G) and improving animal survival (Figure 7H) in SA mice that also received anti-IFNAR1 neutralizing antibody. These data collectively suggest that downregulation of IFNAR1 undermines the efficacy of checkpoint-targeted immunotherapeutics against solid tumors.

relative to FAP-CAR WT CTLs (Figure 7C). The magnitude of these effects is probably underappreciated because the SA allele may inhibit proliferation of CAR CTLs (data not shown), and FAP-CAR SA cells used in these experiments were likely to partially suppress IFN signaling downstream of the receptor.

To overcome this problem we sought to acutely stabilize IFNAR1 via inducible ablation of p38 α , a kinase potentially involved in the ligand-independent downregulation of IFNAR1 (Bhattacharya et al., 2011). We prepared FAP-CAR T cells from the splenocytes of mice harboring floxed *Mapk14* (a gene that encodes p38 α), either *Ifnar1*^{+/+} (WT) or *Ifnar1*^{-/-} alleles, and either no Cre or inducible *Ubc9-Cre*^{ERT2}. These FAP-CAR T cells were treated with 4-hydroxytamoxifen and then injected into WT mice burdened with MC38 tumors. As seen from Figure 7D, inactivation of p38 α in IFNAR1-expressing FAP-CAR CTLs (*Mapk14* ^{Δ/Δ} WT) dramatically increased the anti-tumor efficacy of these cells. Importantly, this increased effect could be negated by concurrent

We noted a greater phosphorylation of p38 α in lysates from MC38 tumors relative to cultured MC38 cells (Figure 8A), consistent with activation of p38 α by TME stress. Accordingly, we next examined whether downregulation of IFNAR1 can be reversed

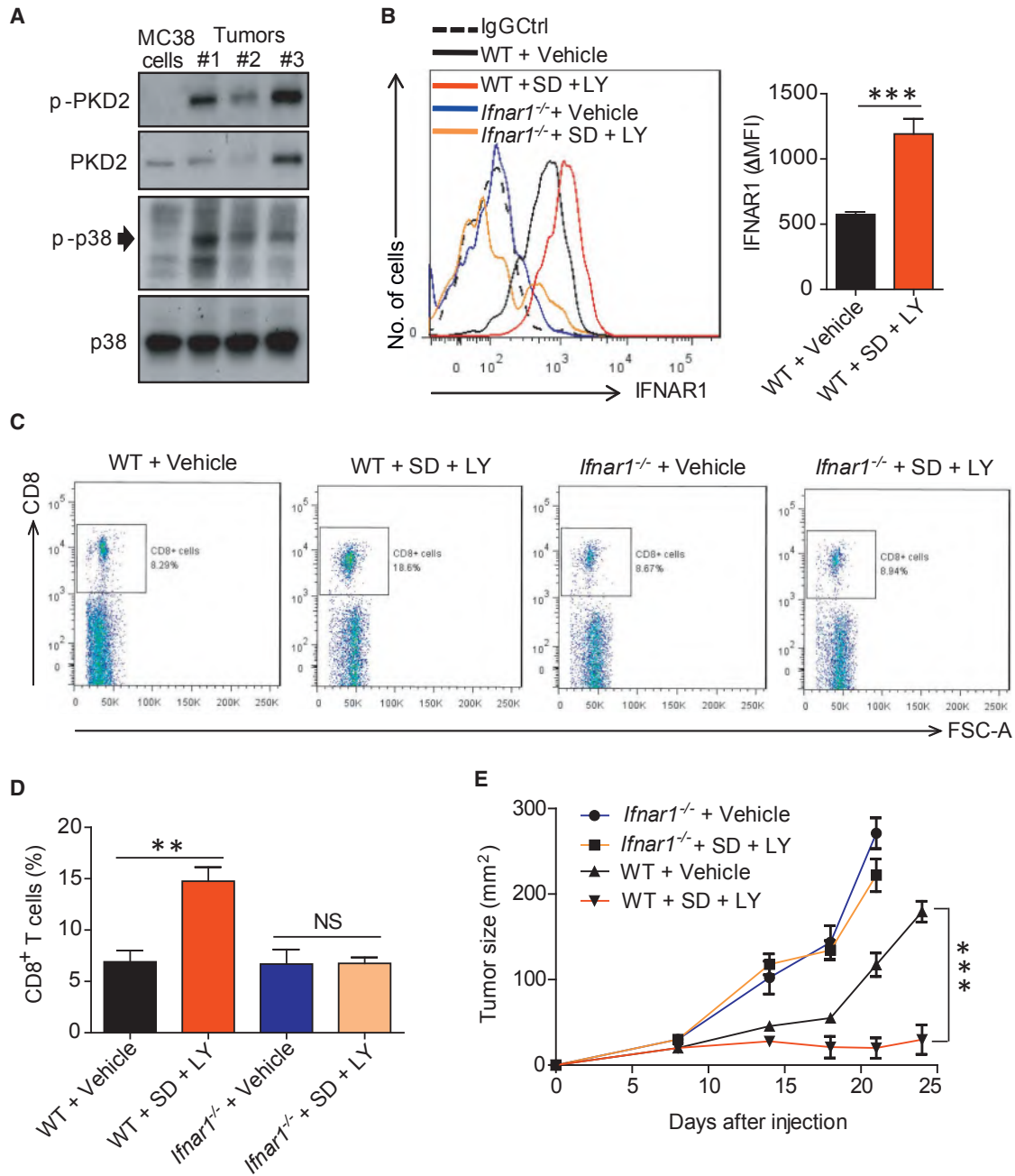


Figure 8. Pharmacologic Stabilization of IFNAR1 Disrupts Immune-Privileged Niche and Elicits a Therapeutic Effect against Tumors

(A) Immunoblot analysis of phosphorylation and levels of p38 α and PKD2 kinases in cultured MC38 cells and MC38 tumors.

(B) Levels of cell surface IFNAR1 on tumor-infiltrating CD3⁺CD8⁺ cells isolated from MC38 tumors grown in WT or *Ifnar1*-null mice treated with kinase inhibitors as indicated. Representative FACS and quantification are shown.

(C) Frequency of CD8⁺ T cells (% of CD45⁺ cells) isolated from MC38 tumors grown in WT or *Ifnar1*-null mice treated with kinase inhibitors as indicated.

(D) Quantification of results shown in (C).

(E) Anti-tumor effect of SD-208 and LY2228820 administered to *Ifnar1*^{-/-} and WT mice bearing MC38 tumors as described in the Experimental Procedures.

Data are shown as mean \pm SEM (n = 5 from each of three independent experiments).

See also Figure S8.

by pharmacologic means. To this end, we attempted to stabilize IFNAR1 using the p38 inhibitor LY2228820 (LY). Given that some TME factors such as vascular endothelial growth factor can also downregulate IFNAR1 via activating protein kinase-2

(PKD2) (Zheng et al., 2011), and that PKD2 activity was indeed increased in MC38 tumors compared with cultured MC38 cells (Figure 8A), we combined the p38 inhibitor with SD-208 (SD), a PKD inhibitor.

The combination of these small molecules (LY + SD) prevented tumor explant supernatant-induced downregulation of IFNAR1 on CTLs *in vitro* (Figure S8A). Furthermore, *in vivo* treatment with this combination (which was well tolerated by tumor-bearing mice, Figure S8B), led to a notable increase in the overall levels of IFNAR1 within tumors (Figure S8C) and specifically of cell surface IFNAR1 levels on intra-tumoral CD3⁺CD8⁺ cells (Figure 8B). Remarkably, administration of LY + SD robustly increased numbers of CTLs found inside MC38 tumors that grew in WT but not in *Ifnar1*^{-/-} mice (Figures 8C, 8D, S8D, and S8E), suggesting that inhibition of p38 and PKD disrupts the immune-privileged niche within the TME in an IFNAR1-dependent manner.

Consistent with an important role of IFNAR1 downregulation in the stimulation of tumorigenesis, treatment with these kinase inhibitors dramatically suppressed growth of MC38 tumors in WT mice, but not in mice lacking *Ifnar1* (Figure 8E), indicating that stimulation of IFNAR1 signaling is a major mechanism underlying the immune-reactivating and anti-tumorigenic effects of these agents. In all, these results provide a proof of principle for pharmacologic stabilization of IFNAR1 as the means to attenuate local immunosuppression within tumors and to suppress tumor growth.

DISCUSSION

Delineating the mechanisms that impose localized immune suppression within the TME is essential for improving the efficacy of immunotherapeutics in solid tumors. Here we present evidence that links the TME stress-driven downregulation of IFNAR1 to the reduced viability of intra-tumoral CTLs and the ensuing establishment of an immune-privileged niche in CRC tumors. A decrease in IFNAR1 levels and expression of IFN-inducible genes found in human CRC tumors and recapitulated in mouse tumors is associated with the establishment of a localized niche virtually void of CTLs, as well as with robust tumor growth and poor prognosis. Downregulation of IFNAR1 specifically in CTLs induced by tumor-associated factors inhibits CTL viability and undermines the efficacy of immune therapies. Conversely, genetic or pharmacologic stabilization of IFNAR1 disrupts the immune-privileged niche, suppresses tumor growth, and increases the efficacy of CAR T cell therapy and immune checkpoint inhibitors.

These findings suggest that IFNAR1 downregulation contributes to the development and progression of CRC. While not arguing against additional role of IFNAR1 in IFN-modulated regulation of antigen presentation and activation of DCs (Diamond et al., 2011; Fuertes et al., 2011; Hildner et al., 2008), stromal resistance to tumor-induced angiogenesis (Zheng et al., 2011) and other processes, our current results strongly indicate that IFNAR1 downregulation on intra-tumoral CTLs contributes to the establishment of immune-privileged TME by undermining CTL survival. These results are consistent with an important role of IFN as an activation signal for T cells (Curtsinger et al., 2005) and the observation that insufficient “third signal” contributes to the inhibition of CTLs in solid tumors (Curtsinger et al., 2007). It appears that downregulation of IFNAR1 on CTL negatively affects responses of these CTLs to IL-2 pro-survival signals and, accordingly, stimulates pro-apoptotic pathways, although other mechanisms cannot be ruled out. Regardless of the exact

mechanisms, the data presented here argue for the development of therapeutic strategies aimed to stabilize IFNAR1 and improve CTL viability within solid tumors.

Our results specifically emphasize the importance of IFNAR1 downregulation on CTLs. Given the importance of these cells in anti-tumor immunity against diverse malignant lesions, it is likely that downregulation of IFNAR1 in the stromal compartment may stimulate growth and progression of other cancer types. Indeed, we have recently demonstrated that loss of IFNAR1 stimulates growth of transplanted melanomas (Katlinskaya et al., 2016). Overall, our data are consistent with intra-tumoral IFN production being linked with CTL generation and viability (Hiroishi et al., 2000), observations that IFN may act to improve the effect of adoptive transfer of CTLs (Hervas-Stubbs et al., 2012), and with recent finding that a specific CAR design, which serendipitously increased IFN signaling in CTLs, evoked an augmented therapeutic effect (Zhao et al., 2015). Nevertheless, our results do not rule out additional putative cellular targets (e.g., interleukin-10-expressing Treg cells; Stewart et al., 2013) and additional mechanisms by which elimination of IFNAR1 and suppression of IFN signaling can further contribute to localized immunosuppression and stimulation of solid tumors growth.

Previous studies utilizing chemically induced and transplantable sarcomas and melanomas in IFNAR1 knockouts have identified specific CD8 α ⁺ DCs as targets of protective role of IFN against tumors (Diamond et al., 2011; Fuertes et al., 2011; Hildner et al., 2008). Functional defects of *Ifnar1*-null DCs reported in these studies are consistent with an important role of IFNAR1 in the maturation of DCs (Le Bon and Tough, 2002; Santini et al., 2009). We did not observe an increase in antigen presentation in SA mice. Furthermore, SA DCs might have a survival disadvantage given that elimination of IFNAR1 plays an important role in preserving the viability of IFN-expressing DCs exposed to inducers of pathogen recognition receptor signaling (Qian et al., 2011). Future use of SA animals in sarcoma and melanoma models is likely to reveal additional information on the relative contribution of IFNAR1 status in DCs and other leukocytes to anti-tumor immunity.

Genetic and pharmacologic studies described here provide a proof of principle for a focus on stabilization of IFNAR1 to increase the efficacy of immunotherapies against CRC and possibly other solid tumors. Whereas the mechanisms underlying the therapeutic effect of p38/PKD inhibitors are likely to be mediated by many cell types (in addition to CTLs), it is noteworthy that these inhibitors still act in an IFNAR1-dependent manner. In addition to targeting p38 and PKD kinases responsible for phosphorylation of IFNAR1 leading to recruitment of the SCF- β Trcp E3 ligase, it might be possible to inhibit this class of ligases. Cullin-dependent ligases (including SCF- β Trcp) can be targeted by inhibiting the NEDD9-activating enzyme; its selective inhibitor, MLN4924, is currently under clinical trials in solid tumors (Sarantopoulos et al., 2015). Additional studies on combining IFNAR1-stabilizing regimens with diverse immunotherapeutic approaches are currently in progress.

EXPERIMENTAL PROCEDURES

A detailed description of the procedures utilized in this work can be found in the Supplemental Experimental Procedures. Use of pre-existing human

archival de-codified and de-identified CRC tissue arrays, previously collected under informed consent, and samples that could not be directly or indirectly linked to individual human subjects was exempt from institutional review. All animal experiments were approved by the Institutional Animal Care and Use Committee (IACUC) of the University of Pennsylvania and were carried out in accordance with the IACUC guidelines. All mice were on the C57BL/6 background and had water ad libitum and were fed regular chow. Mice were maintained in a specific pathogen-free facility in accordance with American Association for Laboratory Animal Science guidelines. Littermate animals from different cages were randomly assigned into the experimental groups. These randomized experimental cohorts were either co-housed or systematically exposed to the bedding of other groups to ensure equal exposure to the microbiota of all groups. Statistical analysis was performed using Microsoft or GraphPad Prism 7 software. Unpaired Student's *t* test was used for the comparison between two groups. One-way ANOVA or two-way ANOVA analysis followed by the Bonferroni post hoc test were used for the multiple comparisons. Repeated-measure two-way ANOVA (mixed-model) followed by the Bonferroni post hoc test was used for the analysis of tumor growth curve. A value of $p < 0.05$ was considered significant.

Data from the global expression profiling studies were collected with Illumina BeadStudio 3.1.1.0 software, and statistical analyses were conducted on the IlluminaGUI R-package. Gene sets from microarray data were analyzed for overlap with curated datasets (C5, H) in the MSigDB using the web interface available at <http://www.broadinstitute.org/gsea/msigdb/index.jsp>. The raw data have been deposited at NCBI (GEO: GSE76889).

For AOM-DSS colorectal carcinogenesis, co-housed experimental mice were intraperitoneally injected with 10 mg/kg azoxymethane (Sigma). A week later, they were supplied with tap water containing 2.5% dextran sodium sulfate (TdB Consultancy) for 7 days followed by 14 days of regular water. This cycle was repeated three times and mice were killed 2 weeks after the end of the last DSS cycle or at the end of 10 weeks. Colons were harvested, washed of feces with Dulbecco's PBS, and slit open longitudinally to count tumors. Tumors were flash frozen in liquid nitrogen or embedded into optimal cutting temperature medium for subsequent analysis.

SUPPLEMENTAL INFORMATION

Supplemental Information includes Supplemental Experimental Procedures, eight figures, and one table and can be found with this article online at <http://dx.doi.org/10.1016/j.ccell.2017.01.004>.

AUTHOR CONTRIBUTIONS

S.Y.F., K.V.K., J.G., E.P., H.R., C.K., and J.A.D. designed the research; K.V.K., J.G., A.O., Y.V.K., R.C., C.J.C., S.B., D.P.B., M.G., A.R.P., P.C., and A.K.R. performed the experiments and interpreted the data; S.Y.F., K.V.K., J.G., E.P., H.R., C.K., and J.A.D. wrote the manuscript with the help of all authors.

ACKNOWLEDGMENTS

This work was supported by the NIH/NCI PO1 CA165997 grant (to J.A.D., C.K., and S.Y.F.), and RO1 CA092900 (to S.Y.F. and H.R.). Additional support from NIH/NCI T32 CA009140 (to K.V.K.) is also appreciated. We thank Ze'ev Ronai, Mark J. Smyth, Melissa Wong, Yibin Wang, Susan Weiss, and Susan Ostrand-Rosenberg for reagents, Sandra Pellegrini, Mathias Müller, Birgit Strobl, and the members of Gabrielovich, Fuchs, Diehl, Koumenis, Pear, and Minn labs for critical suggestions.

Received: May 23, 2016

Revised: September 15, 2016

Accepted: January 9, 2017

Published: February 13, 2017

REFERENCES

Aichele, P., Unsoeld, H., Koschella, M., Schweier, O., Kalinke, U., and Vucikuj, S. (2006). CD8 T cells specific for lymphocytic choriomeningitis virus require type I IFN receptor for clonal expansion. *J. Immunol.* *176*, 4525–4529.

Bhattacharya, S., Qian, J., Tzimas, C., Baker, D.P., Koumenis, C., Diehl, J.A., and Fuchs, S.Y. (2011). Role of p38 protein kinase in the ligand-independent ubiquitination and down-regulation of the IFNAR1 chain of type I interferon receptor. *J. Biol. Chem.* *286*, 22069–22076.

Bhattacharya, S., HuangFu, W.C., Dong, G., Qian, J., Baker, D.P., Karar, J., Koumenis, C., Diehl, J.A., and Fuchs, S.Y. (2013). Anti-tumorigenic effects of type 1 interferon are subdued by integrated stress responses. *Oncogene* *32*, 4214–4221.

Bhattacharya, S., Katlinski, K.V., Reichert, M., Takano, S., Brice, A., Zhao, B., Yu, Q., Zheng, H., Carbone, C.J., Katlinskaya, Y.V., et al. (2014). Triggering ubiquitination of IFNAR1 protects tissues from inflammatory injury. *EMBO Mol. Med.* *6*, 384–397.

Bidwell, B.N., Slaney, C.Y., Withana, N.P., Forster, S., Cao, Y., Loi, S., Andrews, D., Mikeska, T., Mangan, N.E., Samarajiva, S.A., et al. (2012). Silencing of Irf7 pathways in breast cancer cells promotes bone metastasis through immune escape. *Nat. Med.* *18*, 1224–1231.

Brahmer, J.R., Tykodi, S.S., Chow, L.Q., Hwu, W.J., Topalian, S.L., Hwu, P., Drake, C.G., Camacho, L.H., Kauh, J., Odunsi, K., et al. (2012). Safety and activity of anti-PD-L1 antibody in patients with advanced cancer. *N. Engl. J. Med.* *366*, 2455–2465.

Chiba, T., Ohtani, H., Mizoi, T., Naito, Y., Sato, E., Nagura, H., Ohuchi, A., Ohuchi, K., Shiiba, K., Kurokawa, Y., and Satomi, S. (2004). Intraepithelial CD8+ T-cell-count becomes a prognostic factor after a longer follow-up period in human colorectal carcinoma: possible association with suppression of micrometastasis. *Br. J. Cancer* *91*, 1711–1717.

Crouse, J., Bedenikovic, G., Wiesel, M., Ibberson, M., Xenarios, I., Von Laer, D., Kalinke, U., Vivier, E., Jonjic, S., and Oxenius, A. (2014). Type I interferons protect T cells against NK cell attack mediated by the activating receptor NCR1. *Immunity* *40*, 961–973.

Curtsinger, J.M., Valenzuela, J.O., Agarwal, P., Lins, D., and Mescher, M.F. (2005). Type I IFNs provide a third signal to CD8 T cells to stimulate clonal expansion and differentiation. *J. Immunol.* *174*, 4465–4469.

Curtsinger, J.M., Gerner, M.Y., Lins, D.C., and Mescher, M.F. (2007). Signal 3 availability limits the CD8 T cell response to a solid tumor. *J. Immunol.* *178*, 6752–6760.

Diamond, M.S., Kinder, M., Matsushita, H., Mashayekhi, M., Dunn, G.P., Archambault, J.M., Lee, H., Arthur, C.D., White, J.M., Kalinke, U., et al. (2011). Type I interferon is selectively required by dendritic cells for immune rejection of tumors. *J. Exp. Med.* *208*, 1989–2003.

Fearon, D.T. (2014). The carcinoma-associated fibroblast expressing fibroblast activation protein and escape from immune surveillance. *Cancer Immunol. Res.* *2*, 187–193.

Feig, C., Jones, J.O., Kraman, M., Wells, R.J., Deonarine, A., Chan, D.S., Connell, C.M., Roberts, E.W., Zhao, Q., Caballero, O.L., et al. (2013). Targeting CXCL12 from FAP-expressing carcinoma-associated fibroblasts synergizes with anti-PD-L1 immunotherapy in pancreatic cancer. *Proc. Natl. Acad. Sci. USA* *110*, 20212–20217.

Fuchs, S.Y. (2013). Hope and fear for interferon: the receptor-centric outlook on the future of interferon therapy. *J. Interferon Cytokine Res.* *33*, 211–225.

Fuertes, M.B., Kacha, A.K., Kline, J., Woo, S.R., Kranz, D.M., Murphy, K.M., and Gajewski, T.F. (2011). Host type I IFN signals are required for antitumor CD8+ T cell responses through CD8[alpha]+ dendritic cells. *J. Exp. Med.* *208*, 2005–2016.

Galon, J., Costes, A., Sanchez-Cabo, F., Kirilovsky, A., Mlecnik, B., Lagorce-Pages, C., Tosolini, M., Camus, M., Berger, A., Wind, P., et al. (2006). Type, density, and location of immune cells within human colorectal tumors predict clinical outcome. *Science* *313*, 1960–1964.

Gilham, D.E., Debets, R., Pule, M., Hawkins, R.E., and Abken, H. (2012). CAR-T cells and solid tumors: tuning T cells to challenge an inveterate foe. *Trends Mol. Med.* *18*, 377–384.

Hellström, I., Hellström, K.E., Pierce, G.E., and Yang, J.P. (1968). Cellular and humoral immunity to different types of human neoplasms. *Nature* *220*, 1352–1354.

- Hervas-Stubbis, S., Riezu-Boj, J.I., Gonzalez, I., Mancheno, U., Dubrot, J., Azpilicueta, A., Gabari, I., Palazon, A., Aranguren, A., Ruiz, J., et al. (2010). Effects of IFN- α as a signal-3 cytokine on human naive and antigen-experienced CD8(+) T cells. *Eur. J. Immunol.* **40**, 3389–3402.
- Hervas-Stubbis, S., Mancheno, U., Riezu-Boj, J.I., Larraga, A., Ochoa, M.C., Alignani, D., Alfaro, C., Morales-Kastresana, A., Gonzalez, I., Larrea, E., et al. (2012). CD8 T cell priming in the presence of IFN- α renders CTLs with improved responsiveness to homeostatic cytokines and recall antigens: important traits for adoptive T cell therapy. *J. Immunol.* **189**, 3299–3310.
- Hildner, K., Edelson, B.T., Purtha, W.E., Diamond, M., Matsushita, H., Kohyama, M., Calderon, B., Schraml, B.U., Unanue, E.R., Diamond, M.S., et al. (2008). Batf3 deficiency reveals a critical role for CD8 α + dendritic cells in cytotoxic T cell immunity. *Science* **322**, 1097–1100.
- Hiroishi, K., Tuting, T., and Lotze, M.T. (2000). IFN- α -expressing tumor cells enhance generation and promote survival of tumor-specific CTLs. *J. Immunol.* **164**, 567–572.
- Huangfu, W.C., Qian, J., Liu, C., Liu, J., Lokshin, A.E., Baker, D.P., Rui, H., and Fuchs, S.Y. (2012). Inflammatory signaling compromises cell responses to interferon alpha. *Oncogene* **31**, 161–172.
- Joyce, J.A., and Fearon, D.T. (2015). T cell exclusion, immune privilege, and the tumor microenvironment. *Science* **348**, 74–80.
- Katinskaya, Y.V., Katinski, K.V., Yu, Q., Ortiz, A., Beiting, D.P., Brice, A., Davar, D., Sanders, C., Kirkwood, J.M., Rui, H., et al. (2016). Suppression of type I interferon signaling overcomes oncogene-induced senescence and mediates melanoma development and progression. *Cell Rep* **15**, 171–180.
- Klemm, F., and Joyce, J.A. (2015). Microenvironmental regulation of therapeutic response in cancer. *Trends Cell Biol.* **25**, 198–213.
- Kolumam, G.A., Thomas, S., Thompson, L.J., Sprent, J., and Murali-Krishna, K. (2005). Type I interferons act directly on CD8 T cells to allow clonal expansion and memory formation in response to viral infection. *J. Exp. Med.* **202**, 637–650.
- Kumar, K.G., Tang, W., Ravindranath, A.K., Clark, W.A., Croze, E., and Fuchs, S.Y. (2003). SCF(HOS) ubiquitin ligase mediates the ligand-induced down-regulation of the interferon-alpha receptor. *EMBO J.* **22**, 5480–5490.
- Le Bon, A., and Tough, D.F. (2002). Links between innate and adaptive immunity via type I interferon. *Curr. Opin. Immunol.* **14**, 432–436.
- Liu, J., HuangFu, W.C., Kumar, K.G., Qian, J., Casey, J.P., Hamanaka, R.B., Grigoriadou, C., Aldabe, R., Diehl, J.A., and Fuchs, S.Y. (2009). Virus-induced unfolded protein response attenuates antiviral defenses via phosphorylation-dependent degradation of the type I interferon receptor. *Cell Host Microbe* **5**, 72–83.
- Marotta, D., Karar, J., Jenkins, W.T., Kumanova, M., Jenkins, K.W., Tobias, J.W., Baldwin, D., Hatzigeorgiou, A., Alexiou, P., Evans, S.M., et al. (2011). In vivo profiling of hypoxic gene expression in gliomas using the hypoxia marker EF5 and laser-capture microdissection. *Cancer Res.* **71**, 779–789.
- Mostafavi, S., Yoshida, H., Moodley, D., LeBoite, H., Rothamel, K., Raj, T., Ye, C.J., Chevrier, N., Zhang, S.Y., Feng, T., et al. (2016). Parsing the interferon transcriptional network and its disease associations. *Cell* **164**, 564–578.
- Naito, Y., Saito, K., Shiiba, K., Ohuchi, A., Saigenji, K., Nagura, H., and Ohtani, H. (1998). CD8+ T cells infiltrated within cancer cell nests as a prognostic factor in human colorectal cancer. *Cancer Res.* **58**, 3491–3494.
- Platanias, L.C. (2005). Mechanisms of type-I- and type-II-interferon-mediated signalling. *Nat. Rev. Immunol.* **5**, 375–386.
- Qian, J., Zheng, H., Huangfu, W.C., Liu, J., Carbone, C.J., Leu, N.A., Baker, D.P., and Fuchs, S.Y. (2011). Pathogen recognition receptor signaling accelerates phosphorylation-dependent degradation of IFNAR1. *PLoS Pathog.* **7**, e1002065.
- Quail, D.F., and Joyce, J.A. (2013). Microenvironmental regulation of tumor progression and metastasis. *Nat. Med.* **19**, 1423–1437.
- Rohr, C., Kerick, M., Fischer, A., Kuhn, A., Kashofer, K., Timmermann, B., Daskalaki, A., Meinel, T., Drichel, D., Borno, S.T., et al. (2013). High-throughput miRNA and mRNA sequencing of paired colorectal normal, tumor and metastasis tissues and bioinformatic modeling of miRNA-1 therapeutic applications. *PLoS One* **8**, e67461.
- Rosenberg, S.A., and Restifo, N.P. (2015). Adoptive cell transfer as personalized immunotherapy for human cancer. *Science* **348**, 62–68.
- Rusinova, I., Forster, S., Yu, S., Kannan, A., Masse, M., Cumming, H., Chapman, R., and Hertzog, P.J. (2013). Interferome v2.0: an updated database of annotated interferon-regulated genes. *Nucleic Acids Res.* **41**, D1040–D1046.
- Santini, S.M., Lapenta, C., Santodonato, L., D'Agostino, G., Belardelli, F., and Ferrantini, M. (2009). IFN-alpha in the generation of dendritic cells for cancer immunotherapy. *Handb. Exp. Pharmacol.* **295–317**.
- Sarantopoulos, J., Shapiro, G.I., Cohen, R.B., Clark, J.W., Kauh, J.S., Weiss, G.J., Cleary, J.M., Mahalingam, D., Pickard, M.D., Faessel, H.M., et al. (2015). Phase I study of the investigational NEDD8-activating enzyme inhibitor Pevonedistat (TAK-924/MLN4924) in patients with advanced solid tumors. *Clin. Cancer Res.* **22**, 847–857.
- Sharma, P., and Allison, J.P. (2015). The future of immune checkpoint therapy. *Science* **348**, 56–61.
- Sistigu, A., Yamazaki, T., Vacchelli, E., Chaba, K., Enot, D.P., Adam, J., Vitale, I., Goubar, A., Baracco, E.E., Remedios, C., et al. (2014). Cancer cell-autonomous contribution of type I interferon signaling to the efficacy of chemotherapy. *Nat. Med.* **20**, 1301–1309.
- Stewart, C.A., Metheny, H., Iida, N., Smith, L., Hanson, M., Steinhagen, F., Leighty, R.M., Roers, A., Karp, C.L., Muller, W., and Trinchieri, G. (2013). Interferon-dependent IL-10 production by Tregs limits tumor Th17 inflammation. *J. Clin. Invest.* **123**, 4859–4874.
- Talmadge, J.E., Donkor, M., and Scholar, E. (2007). Inflammatory cell infiltration of tumors: Jekyll or Hyde. *Cancer Metastasis Rev.* **26**, 373–400.
- Topalian, S.L., Hodi, F.S., Brahmer, J.R., Gettinger, S.N., Smith, D.C., McDermott, D.F., Powderly, J.D., Carvajal, R.D., Sosman, J.A., Atkins, M.B., et al. (2012). Safety, activity, and immune correlates of anti-PD-1 antibody in cancer. *N. Engl. J. Med.* **366**, 2443–2454.
- Trinchieri, G. (2010). Type I interferon: friend or foe? *J. Exp. Med.* **207**, 2053–2063.
- Uze, G., Schreiber, G., Piehler, J., and Pellegrini, S. (2007). The receptor of the type I interferon family. *Curr. Top. Microbiol. Immunol.* **316**, 71–95.
- Wang, Y., Swiecki, M., Cella, M., Alber, G., Schreiber, R.D., Gilfillan, S., and Colonna, M. (2012). Timing and magnitude of type I interferon responses by distinct sensors impact CD8 T cell exhaustion and chronic viral infection. *Cell Host Microbe* **11**, 631–642.
- Wang, L.C., Lo, A., Scholler, J., Sun, J., Majumdar, R.S., Kapoor, V., Antzis, M., Cotner, C.E., Johnson, L.A., Durham, A.C., et al. (2014). Targeting fibroblast activation protein in tumor stroma with chimeric antigen receptor T cells can inhibit tumor growth and augment host immunity without severe toxicity. *Cancer Immunol. Res.* **2**, 154–166.
- Xu, H.C., Grusdat, M., Pandya, A.A., Polz, R., Huang, J., Sharma, P., Deenen, R., Kohrer, K., Rahbar, R., Diefenbach, A., et al. (2014). Type I interferon protects antiviral CD8+ T cells from NK cell cytotoxicity. *Immunity* **40**, 949–960.
- Zhao, Z., Condomines, M., van der Stegen, S.J., Perna, F., Kloss, C.C., Gunset, G., Plotkin, J., and Sadelain, M. (2015). Structural design of engineered costimulation determines tumor rejection kinetics and persistence of CAR T cells. *Cancer Cell* **28**, 415–428.
- Zheng, H., Qian, J., Carbone, C.J., Leu, N.A., Baker, D.P., and Fuchs, S.Y. (2011). Vascular endothelial growth factor-induced elimination of the type 1 interferon receptor is required for efficient angiogenesis. *Blood* **118**, 4003–4006.
- Zhou, P., Shaffer, D.R., Alvarez Arias, D.A., Nakazaki, Y., Pos, W., Torres, A.J., Cremasco, V., Dougan, S.K., Cowley, G.S., Elpek, K., et al. (2014). In vivo discovery of immunotherapy targets in the tumour microenvironment. *Nature* **506**, 52–57.
- Zitvogel, L., Galluzzi, L., Kepp, O., Smyth, M.J., and Kroemer, G. (2015). Type I interferons in anticancer immunity. *Nat. Rev. Immunol.* **15**, 405–414.

Light your way.

Get the full picture with trusted tumor immune response results from our in-house validated antibodies.

When it comes to your tumor immune response research, blind spots are unacceptable. Independent testing has demonstrated that 75% of antibodies in today's market are non-specific or simply do not work at all.* But at Bethyl, we've manufactured and validated every antibody we make on site to ensure target specificity and sensitivity. All to guarantee our antibodies will function as designed in your assay 100% of the time. More than 10,000 independent citations over the past 15 years have proven that, at Bethyl, we put a lot in every drop.

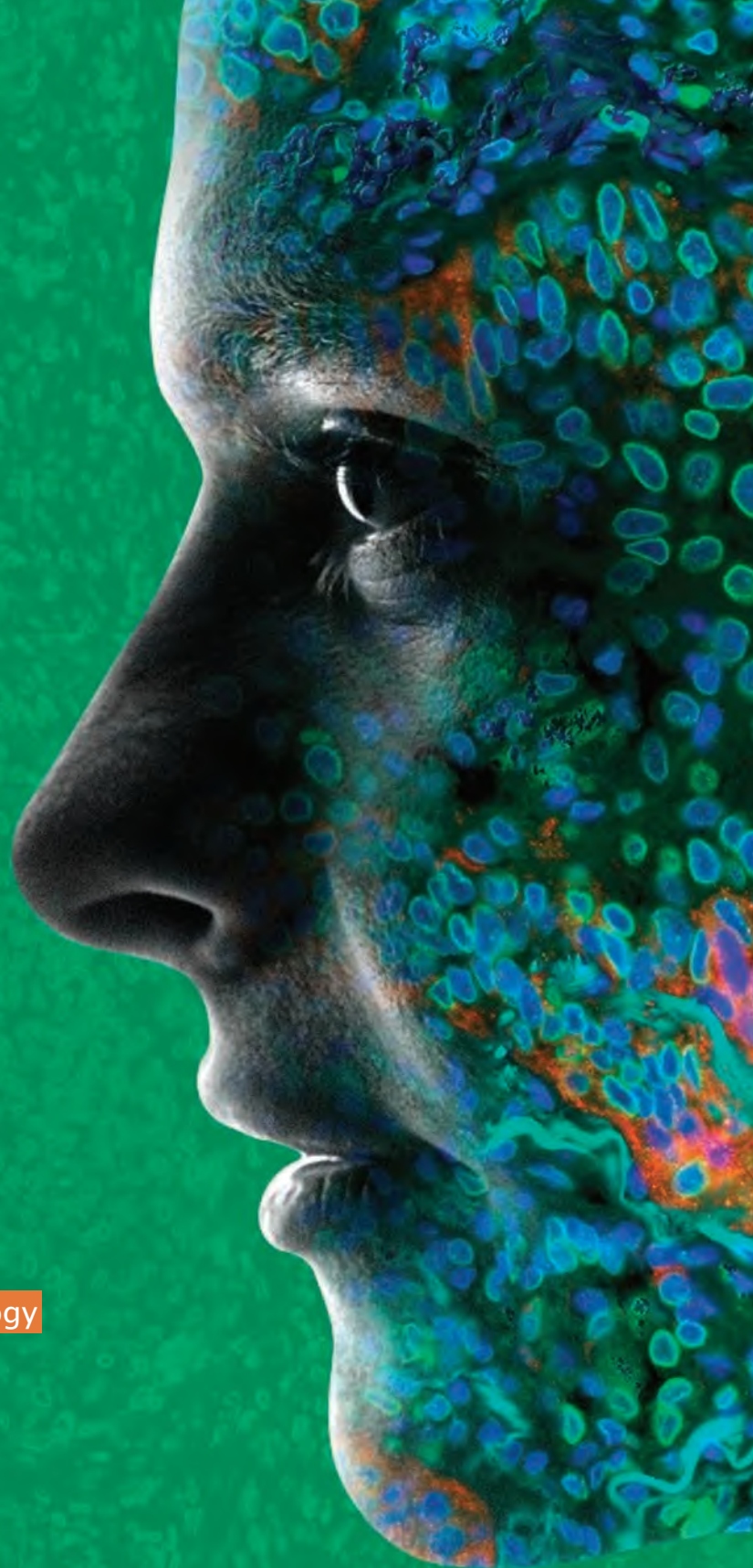
See our data at bethyl.com/immuno-oncology

**Weller, MG, Analytical Chemistry Insights:11, 21-27 (2016).*

Antibodies shown: Rabbit anti-PD-L1 (red, A700-020) & Lamin-A/C (green, A303-430A) in FFPE lung.
©2018 Bethyl Laboratories, Inc. All rights reserved.

BETHYL
LABORATORIES, INC

Really Good Antibodies





Make your big idea bright.

Use our bulk antibody manufacturing & processing services to deliver consistent results on a larger scale.

When your ideas are big, it's important that your antibodies consistently perform. For more than 40 years, we've focused on manufacturing high quality antibodies in bulk. From antiserum generation to large-scale conjugation, preparative work to the final product, you can count on our big bulk capabilities to elevate big discoveries. At Bethyl, we put a lot in every drop.

Find your reliable bulk partner
at [bethyl.com/bulkabs](https://www.bethyl.com/bulkabs)

Antibody shown: Rabbit anti-KIF14 (IHC-00475)
in formaldehyde-fixed HeLa cells.
©2018 Bethyl Laboratories, Inc. All rights reserved.

Ignite your breakthrough.

Ensure reproducible results with antibodies that are 100% guaranteed to work.

Every great discovery requires a bold approach and reliable tools. With each cell-labeling experiment, you can trust in our more than 40 years of experience in antibody manufacturing and on site validation. You need antibodies with performance that exceeds the 50% failure rate common in the industry.* That's why, from polyclonals to recombinant rabbit monoclonal abs, we guarantee 100% target specificity and sensitivity to help you continue moving toward your next breakthrough. Our antibodies have been trusted in over 10,000 independent citations in the last 15 years. Because at Bethyl, we put a lot in every drop.

See our data at bethyl.com/breakthrough

**Weller, MG, Analytical Chemistry Insights:11, 21-27 (2016).*

Antibodies shown: Rabbit anti-CD3e recombinant monoclonal (yellow, A700-016) & mouse anti-CD23 monoclonal (red, A500-017A) in FFPE lymphnode.
©2018 Bethyl Laboratories, Inc. All rights reserved.

BETHYL
LABORATORIES, INC

Really Good Antibodies

